EFFECTIVE STRESS STRENGTH OF CLAYS EVALUATED FROM PIEZOCONE AND FLAT DILATOMETER TESTS

A Dissertation
Presented to
The Academic Faculty

by

Zhongkun “Frankie” Ouyang

In Partial Fulfillment
of the Requirements for the Degree
Doctor of Philosophy in the
School of Civil and Environmental Engineering

Georgia Institute of Technology
May 2019

EFFECTIVE STRESS STRENGTH OF CLAYS EVALUATED FROM PIEZOCONE AND FLAT DILATOMETER TESTS

Approved by:

Dr. Paul W. Mayne, Advisor
School of Civil and Environmental Engineering
Georgia Institute of Technology

Dr. J. David Frost
School of Civil and Environmental Engineering
Georgia Institute of Technology

Dr. Susan E. Burns
School of Civil and Environmental Engineering
Georgia Institute of Technology

Dr. Sheng Dai
School of Civil and Environmental Engineering
Georgia Institute of Technology

Dr. Robert Bachus
Geosyntec Consultants
Kennesaw, GA

Dr. Zhigang Peng
School of Earth and Atmospheric Science
Georgia Institute of Technology

Date Approved: March 08th ,2019

To the most loving and caring parents,

Kang Peng and Xu Ou

ACKNOWLEDGMENTS

It all started back on August 23rd, 2013 when I first landed in Atlanta, GA and admitted as a graudate student in School of Civil and Environmental Engineering of Georgia Tech. Indebted to my mentor, thesis supervisor, research advisor, and my friend: Prof. Paul W. Mayne, I soon became a Graduate Research Assistant in the In-Situ Testing Group and worked on a project funded by Fugro during my Master program and after that he provided me another opportunity to pursue my Ph.D research. His knowledgeable insights into geotechnical engineering have broadened my horizons and helped me overcome my research challenges. Great acknowledgment is due for his sincere support, valuable guidance, motivation, constructive comments throughout the course of this study. Dr. Mayne pushed my boundaries and helped me become a better researcher, writer, speaker and presenter. Also, I learned how to be a person of "OCD" (yes, Obsessive-Compulsive Disorder, not Overconsolidation Difference) by always being strict to details in research and paper writing.

I would also like to express my gratitude and appreciation to my guidance committee members: Dr. J. David Frost, Dr. Susan E. Burns, Dr. Sheng Dai, Dr. Robert Bachus and Dr. Zhigang Peng for their constructive feedback and valuable advices that enhanced the quality and the value of the presented research. I am also thankful to all other faculty members that I have been luckily interacted with in geosystems group and provided me with the needed knowledge through interesting challenging courses that helped me better understand and appreciate the merits of geotechnical engineering, including Dr. Santamarina, Dr. Arson, Dr. Huang, and Dr. Assimaki.

I would also like to thank the staff at the CEE Department who have helped me a lot and made the journey easier: Robert Simon, Daniela Estrada, Ellen Cormack, Jenny Eaton, Jenny Freeman, and Mike Anderson. I would like to particularly thank Andrew Udell and his crew from the shop (Blake Baklini and Billy Plum) for their efforts in restoring the Georgia Tech cone truck and the anchorage system and help in designing and manufacturing the rod rack.

I am thankful to all the past and present members of GeoSociety for bringing happiness during my time at Tech. I always enjoyed those talks and discussions with our GeoSociety family members comining from all over the world with different cultures and backgrounds. I would like to particularly thank my office mate, Egyptian brother Dr. Shehab Agaiby for his amazing friendship, calm spirit, supportive personality and for being my true companion at Georgia Tech. I would also like to thank Ms. Qidi Sun for proofreading the manuscript.

I also like to express my gratitude to my sponsors throughout the years I spent at Georgia Tech: ConeTec Investigations of Richmond, BC, Design House Consultancy of Dubai and Fugro. I would also like to express my thanks to the School of Civil and Environmental engineering, College of Engineering, and the Anne Robinson Clough fund for graciously providing me with travel grants and sufficient funds to cover my expenses for the international conferences I have participated in.

Finally, and most importantly, I am deeply indebted to my family. I would like to express my sincere gratitude to my parents, Kang Peng and Xu Ou, for raising me up and guarding me with born optimism and confidence. 爸爸妈妈我爱你们！荣誉属于你们！

TABLE OF CONTENTS

LIST OF TABLES

LIST OF FIGURES

SUMMARY

During geotechnical site investigations involving clay deposits, results from piezocone penetration tests (CPTu) and flat plate dilatometer tests (DMT) are traditionally interpreted using a total stress analysis, and consequently the evaluation focuses on the undrained shear strength (s_u). In actuality, the fundamental strength of clays is really governed by effective stress conditions, specifically the effective stress friction angle (ϕ') which is required for stress path analyses, critical state soil mechanics (CSSM), and the prediction of pore pressures during construction using finite element analyses.

This research program offers the interpretation of ϕ' from in-situ CPTu data for clays and clayey silts of normally consolidated (NC) to lightly-overconsolidated (LOC) to intact overconsolidated (OC) and fissured OC clays. Towards this purpose, an existing effective stress limit plasticity developed in Norway is modified, applied, and statistically verified by examining several databases (lab chamber tests, centrifuge models, and 110+ field case records) involving clay soils subjected to both CPTu and triaxial compression tests (TC).

This research program also establishes a nexus between CPTu and DMT in soft to firm clays through spherical cavity expansion (SCE) theory, thus provides a means for evaluating ϕ' in clays using DMT data. Two databases are prepared: (a) results from 49 clay sites to validate the CPT-DMT link; and (b) results from another 46 clay deposits with companion DMT-TC information. Finally, an effort is undertaken to assess the undrained rigidity index (I_R) of soft to firm clays from DMT data which can evaluate s_u, yield stress, and coefficient of consolidation based on a hybrid SCE-CSSM analytical approach.

CHAPTER 1. INTRODUCTION

1.1 Background and Motivation

Geotechnical site characterization, or "geocharacterization", is of vital importance prior to the design and construction of all civil engineering works in the ground and involves buildings, bridges, excavations, offshore windmills, oil platforms, water reservoirs, dams, and embankments. In addition to delineating the soil stratigraphy, geocharacterization involves the study of soil and rock behavior and requires quantification of a reasonably good number of different engineering parameters. The assessment of these *geoparameters* and subsurface information is achieved by either rotary drilling, sampling, and laboratory tests, or alternatively using in-situ tests, or both, coupled with supplementary information obtained from geophysical testing. Of particular interest in soils is the geocharacterization of soil strength, including clays, silts, sands, and mixed soils, because it controls the stability of the ground and capacity of foundations, slopes, and embankments.

The traditional approach to site investigation is to advance soil borings by augering and rotary drilling methods to obtain samples for laboratory testing (Mayne et al. 2002). Tests on undisturbed samples of high quality are needed for performing hydro-mechanical type laboratory tests in providing evaluations of geoparameters that are necessary for analysis of bearing capacity of shallow and deep foundations, embankment and foundation settlements, time rate-of-consolidation, slope stability, and dynamic problems, such as liquefaction, deformations, and performance. Because of the many complexities in soil behavior, a large number of geoparameters have been defined to capture the various

nuances in the representation of the stress-strain-strength and flow characteristics of the ground, including: undrained shear strength (s_u), effective stress friction angle (ϕ'), effective cohesion intercept (c'), compressibility parameters (C_c, C_s), preconsolidation stress (σ_p'), geostatic stress state (K_0), hydraulic conductivity (k), coefficient of consolidation (c_v), overconsolidation ratio (OCR), elastic moduli (E', E_u, G', G_u, K', D'), creep (C_α), and strain rate behavior, as well as other aspects. However, difficulties in obtaining thin-walled tubes coupled with soil disturbance due to extraction, transportation, extrusion, trimming, moisture losses, and stress-release effects result in laboratory specimens of mediocre quality, perhaps not truly representative of field conditions. Moreover, individual laboratory tests are expensive, require long testing times, and provide only a limited number of discrete point values at select locations.

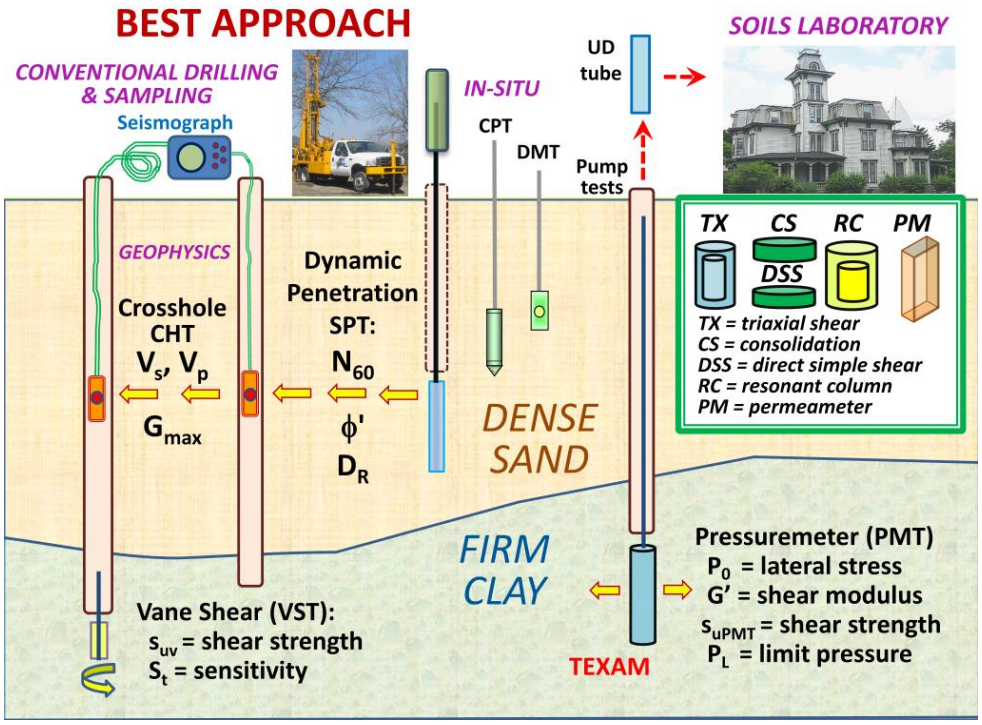

Figure 1.1. Best practice for geotechnical site characterization of soils includes: rotary drilling, sampling, and lab testing coupled with geophysics and in-situ probings

In contrast, in-situ methods obtain measurements of the soil in its own natural environment under ambient anisotropic and geostatic stress states. In-situ testing is fast, continuous, and provides results for immediate use in evaluation and analysis. Thus, the optimal site characterization program involves a series of soil borings with sampling, complemented by a series of in-situ tests and laboratory reference testing, as illustrated by Figure 1.1.

For general soil investigations involving geostratification and subsurface site exploration, two popular in-situ devices which offer economic benefits and expediency are the piezocone penetration test (CPTu) and the flat plate dilatometer test (DMT), consequently, these have become widely adopted in practice in many geologic settings. Both CPTu and DMT can be used in soft to firm to hard clays and silts, and loose to dense sands, therefore applicable to many geologic settings situated in soil formations and deposits.

1.1.1 TSA versus ESA

1.1.1.1 Undrained Shear Strength of Clays from Total Stress Analysis (TSA)

Undrained shear strength (s_u) is undeniably one of the most sought after geoparameters when it comes to the evaluation of the clay strength based on total stress analysis (TSA). Undrained shear strength is often measured in the laboratory using triaxial tests, or by direct simple shear testing, and determined by in-situ testing such as field vane, pressuremeter and/or the piezocone penetration test. The triaxial test can be used to assess the effects of consolidation stresses and overconsolidation on the undrained strength. The apparatus, sample preparation, and test procedures for triaxial testing can be found in

ASTM standards (ASTM (2011) D4767) or other recognized equivalent guidelines (e.g., Bishop and Henkel 1962; Germaine and Germaine 2009; Lade 2016). From laboratory triaxial test results, the undrained shear strength of clays is often taken as the maximum shear stress (τ_{max}) on the stress-strain curve, as illustrated by Figure 1.2. Additional discussion on various strength modes of undrained shear strength of clays is given in later sections of this chapter.

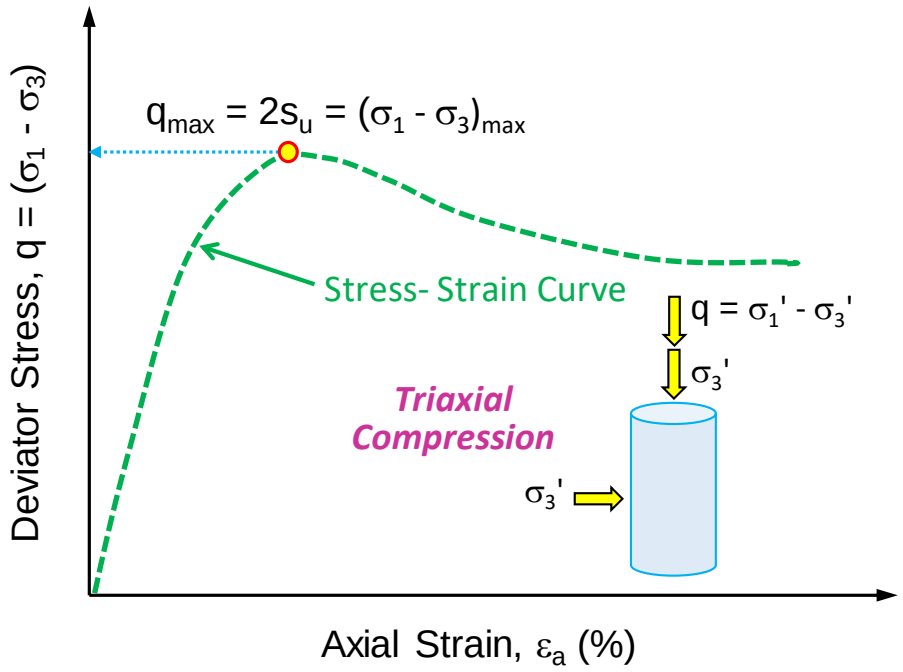

Figure 1.2. Schematic stress-strain curve of soil in triaxial compression test

1.1.1.2 Principle of Effective Stress and Effective Strength Envelope from Triaxial Test

Terzaghi (1925) observed that soil behavior is controlled by effective stresses and established the famous "principle of effective stress" in which the effective stress (σ') acting on a soil is calculated from two components, total stress (σ) and porewater pressure (u) according to:

$$\sigma' = \sigma - u \quad [1.1]$$

As evidenced within the framework of critical state soil mechanics (CSSM), the fundamental strength of clays is represented by the effective stress strength angle, ϕ' (Hvorslev 1960; Schofield & Wroth 1968; Wood 1990; Diaz-Rodriguez et al. 1992; Leroueil & Hight, 2003; Mayne et al. 2009; Holtz et al. 2010). However, in terms of the common Mohr-Coulomb strength criterion, there are two strength parameters: ϕ' = effective friction angle and c' = effective cohesion intercept, where shear stress τ and the effective normal stress σ' are expressed in the following formula:

$$\tau = c' + \sigma' \tan\phi' \quad [1.2]$$

Prior to 1960's, in the laboratory, the effective strength parameters of soils were normally determined by direct shear tests (ASTM D 3080). Following the release of *The Triaxial Test* by Bishop & Henkel (1962), geotechnical laboratories quickly adopted the more versatile triaxial test, since it offered direct control of vertical and lateral effective stresses, drainage conditions, and measurement of porewater pressures. During a triaxial test, a soil specimen confined by a rubber membrane is placed in a chamber. An all-around confining stress (σ_3) is applied to the specimen by means of chamber fluid (consolidation stage). An added deviator stress ($\Delta\sigma = q = \sigma_1 - \sigma_3$) is then applied to the specimen in the axial direction to cause failure ($\Delta\sigma = \Delta\sigma_f$ at failure), which is called the shearing stage. Drainage from the specimen can either be allowed or prevented, depending on the desired test conditions. There are three primary triaxial tests conducted in the laboratory, each allowing the soil response for different engineering applications to be observed. There are:

- Unconsolidated Undrained test (UU)

- Consolidated Drained test (CD)
- Consolidated Undrained test (CU)

The UU is a fast and simple test but has conflicting issues as it is marred by sample disturbance effects, since no reconsolidation phase is permitted, and the shearing phase is run rather quickly, thus affected by strain rate effects. In fact, Ladd & DeGroot (2003) and others have recommended the discontinuation of UU tests for stability problems involving soft clays.

For the CD and CU types, loading can be either in compression or extension (Lade 2016). The most common type of triaxial test in geotechnical practice is the consolidated undrained triaxial compression (TC) mode, as it allows both TSA and ESA. That is, the recorded data permit an evaluation of both s_u and the effective stress parameters, ϕ' and c'. During the test, the following quantities are measured:

1. Confining stress (σ_3)
2. Deviator load
3. Vertical (or axial) deformation
4. Volume change (ΔV) or pore water pressure (Δu)

These measurements constitute the test data from which other quantities can be derived (e.g., deviator stress $q = \sigma_1 - \sigma_3$, axial strain ε_a. and volumetric strain ε_v). The measured porewater pressure (Δu) can be plotted against the axial strain ε_a to reflect the evolution of the excess porewater developed in the test, and the deviator stress q can be plotted against the mean effective stress $p' = (\sigma_1' + 2\sigma_3')/3 = [(\sigma_1 - \Delta u) + 2(\sigma_3 - \Delta u)]/3$ to

construct the effective stress paths towards the determination of the effective stress strength parameters (ϕ' and c') of a given soil specimen. Figure 1.3a shows a schematic plot of the deviator stress q versus the mean effective stress p' and the effective stress friction angle ϕ' can be determined by solving M_c = slope of the frictional envelope at failure under triaxial compression, where $M_c = \frac{6 \cdot \sin\phi'}{3 - \sin\phi'}$. Such presentation of deviator stress q versus the mean effective stress p' is called the Cambridge q - p' space and popularized by the Cambridge soil mechanics group (Schofield & Wroth 1968; Mayne et al. 2009).

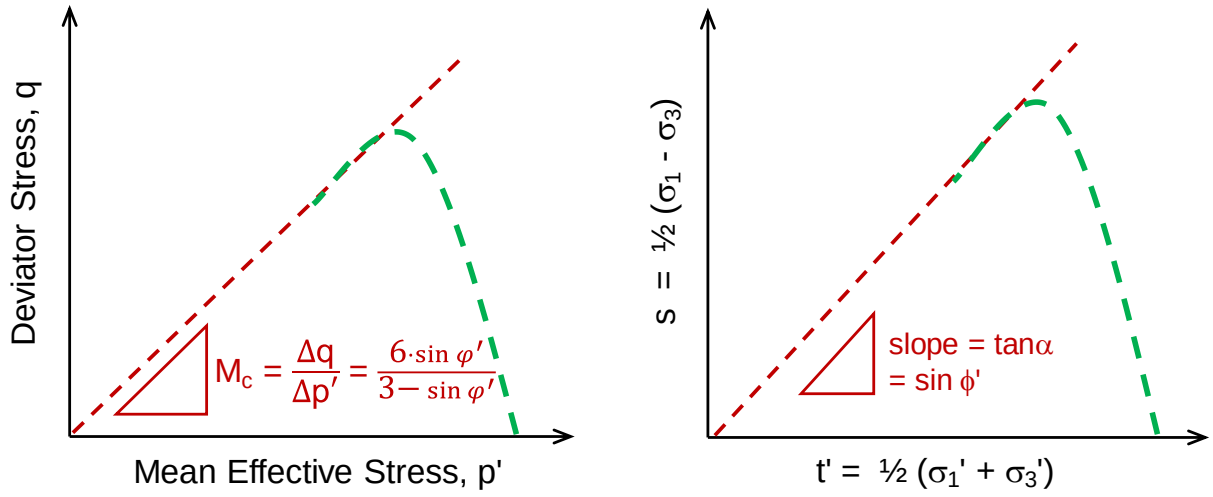

Figure 1.3. Schematic effective stress path of a consolidated undrained triaxial compression test expressed in (a): Cambridge q-p' diagram, and (b): MIT t'-s diagram

Alternatively, the measurements from triaxial test can be expressed in term of shear stress $s = (\sigma_1 - \sigma_3)/2$ and $t' = (\sigma_1' + \sigma_3')/2 = [(\sigma_1 - \Delta u) + (\sigma_3 - \Delta u)]/2$. This employment of the t'-s diagram has been popularized largely by the MIT soil mechanics group (Lambe 1964, Lambe & Whitman 1979, and Wood 1990). The relationships between the Cambridge q - p' diagram and the MIT t' - s diagram can be found in Lade (2016). In the

MIT t′ - s diagram, the effective stress friction angle ϕ' can calculated using the following equation:

$$\sin\phi' = \tan\alpha \qquad [1.3]$$

where α is the slope of the failure envelope on the MIT t′-s diagram, shown by Figure 1.3b.

The interpretation of ϕ' can be evaluated on the basis of different criteria, including (a) maximum deviator stress (q_{max}); (b) maximum obliquity or maximum principal effective stress ratio, $(\sigma'_1/\sigma'_3)_{max}$ (where σ'_1 and σ'_3 are the major and minor principal effective stresses, respectively); or (c) value taken at large strains, normally at 15% axial strain, or in some cases, at 20% strain. The third criterion is sometimes interpreted as the value corresponding to critical state (ϕ'_{cs}). The effective stress friction angle ϕ' determined from both Cambridge q-p′ diagram MIT t′-s diagram by Figure 1.3 are taken at large strains, or at the end of the stress path, which can be interpreted as the value corresponding to critical state (ϕ'_{cs}). For soft inorganic clays of low sensitivity, the various criteria often provide comparable values of ϕ' when interpreting data from triaxial tests.

Figure 1.4 shows a schematic yield envelope for natural clays which is centered about the stress line for K_0 normal consolidation in the MIT t′ - s diagram and anchored by the yield stress (σ'_p) or preconsolidation stress of the clays. Here the shape of the yield envelope is controlled by the effective stress friction angles (ϕ') of the clays. The concept of yield in soft clays have been explored by Diaz-Rodriguez et al. (1992), based on a study of 50 clays and the full range of effective stress friction angles (ϕ') measured on natural clays ranges from 17° to 43°. Figure 1.5 shows a summary plot of ϕ' of selected clays with

their corresponding yield envelopes and confirmed the relationship among the shape of yield envelopes, the yield stress (σ'_p) of the clays and the effective stress friction angles (ϕ') of the clays. It is observed that the position of the upper part of the yield envelope, above the ϕ'_{NC} line, changes with the value of the friction angle.

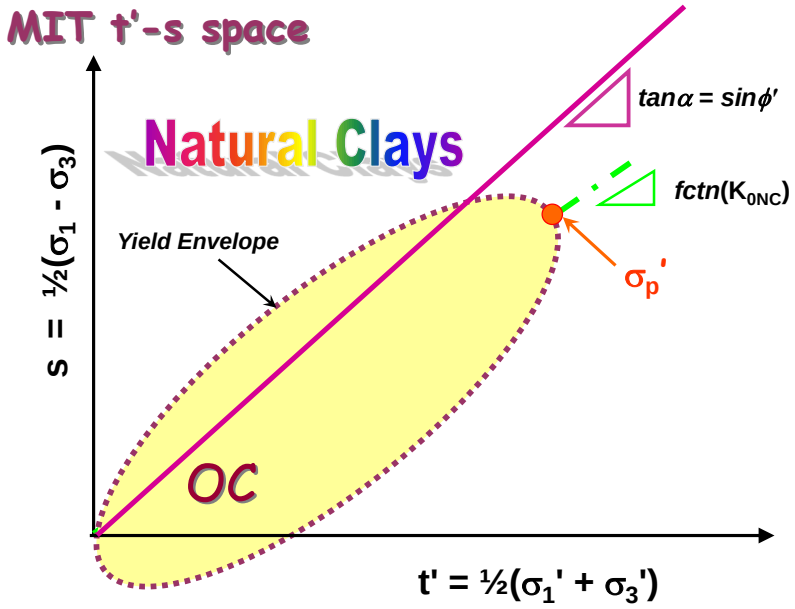

Figure 1.4. Schematic yield envelope of natural clays in MIT t′-s diagram

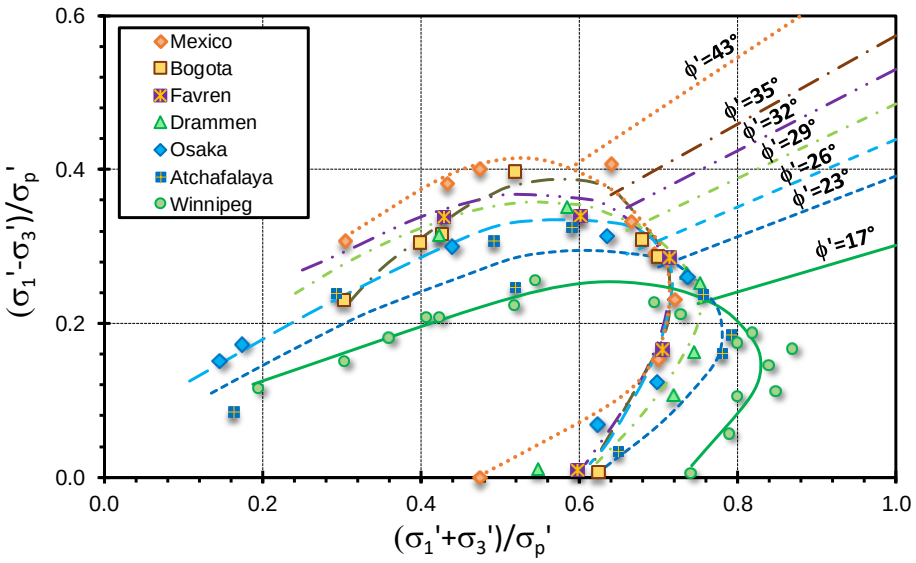

Figure 1.5. Observed range of ϕ′ and corresponding yield envelopes for various natural clays (modified from Diaz-Rodriguez et al. 1992).

The parameter c' indicates the existence of tensile strength, which is characteristic of rocks and cemented soils, particularly those of great age (i.e. Cretaceous, Eocene) and certain mineralogical constituency (e.g. carbonates, calcareous components). Figure 1.6 shows the corresponding definition of the cohesion intercept c' and effective stress friction angle ϕ′ in three different stress spaces: τ-σ′ of Mohr - Coulomb criterion, Cambridge q - p′ diagram and the MIT t′ - s diagram.

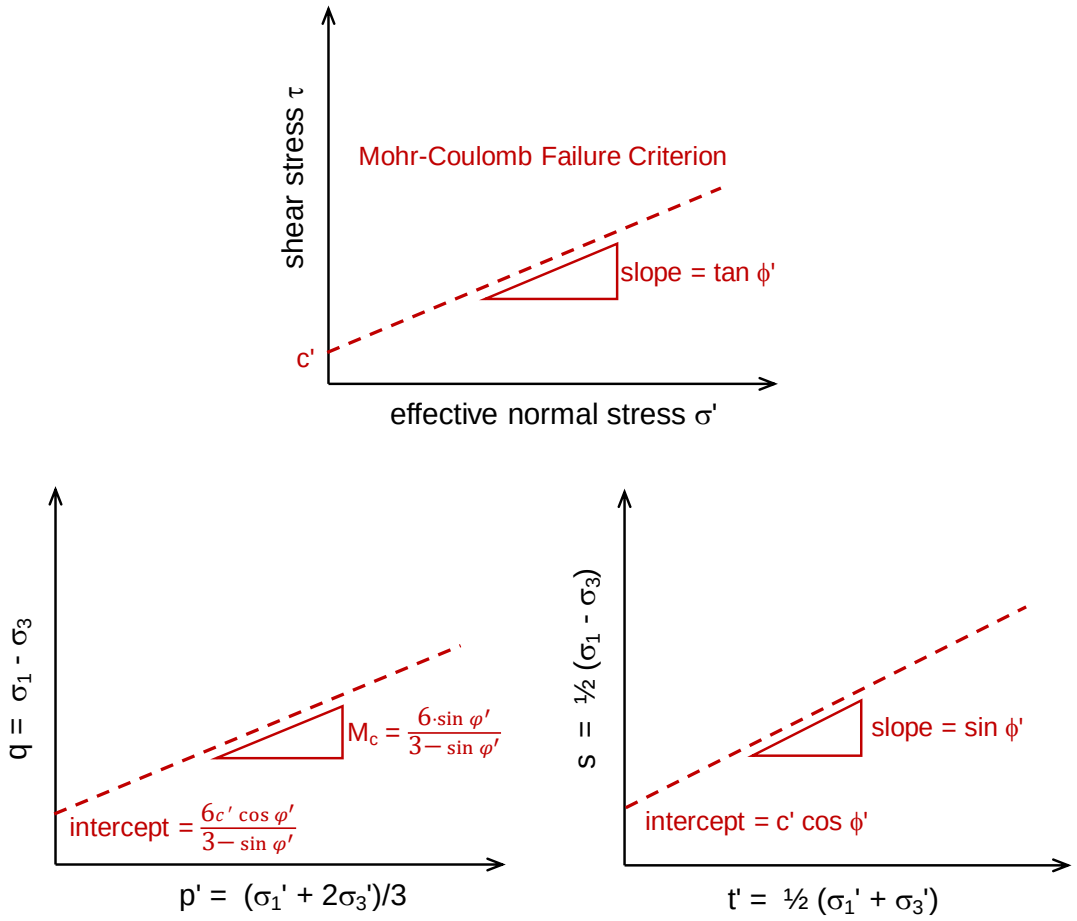

Figure 1.6. Interpretation of effective stress strength parameters c' and ϕ′ in: (a) τ-σ′ space, (b) Cambridge q - p′ diagram, and (c) MIT t′ - s diagram.

More often, however, soils are uncemented and it is found that c' = 0 applies to the majority of soils, including normally consolidated (NC) to lightly overconsoldiated (LOC) soft clays, silts, and loose sands which are recent deposits of Holocene age (Leroueil & Hight 2003; Mesri & Abdel-Ghaffar 1993; Lade 2016). These uncemented sediments are normally composed of common minerals such as kaolin, illite, quartz, silica, feldspar, and chlorite. Even for overconsolidated clays, only a small value of c′ is appropriate (Lade 2016). Mayne & Stewart (1988) suggested around c′ = 4% of the soils' preconsoldiation

stress (σ'_p) and Larsson (1997) recommended such ratio to be 3%. Casey (2014) conducted laboratory study on Resedimented Boston Blue Clay and interpreted an $c'/\sigma'_p \approx 0.03$,

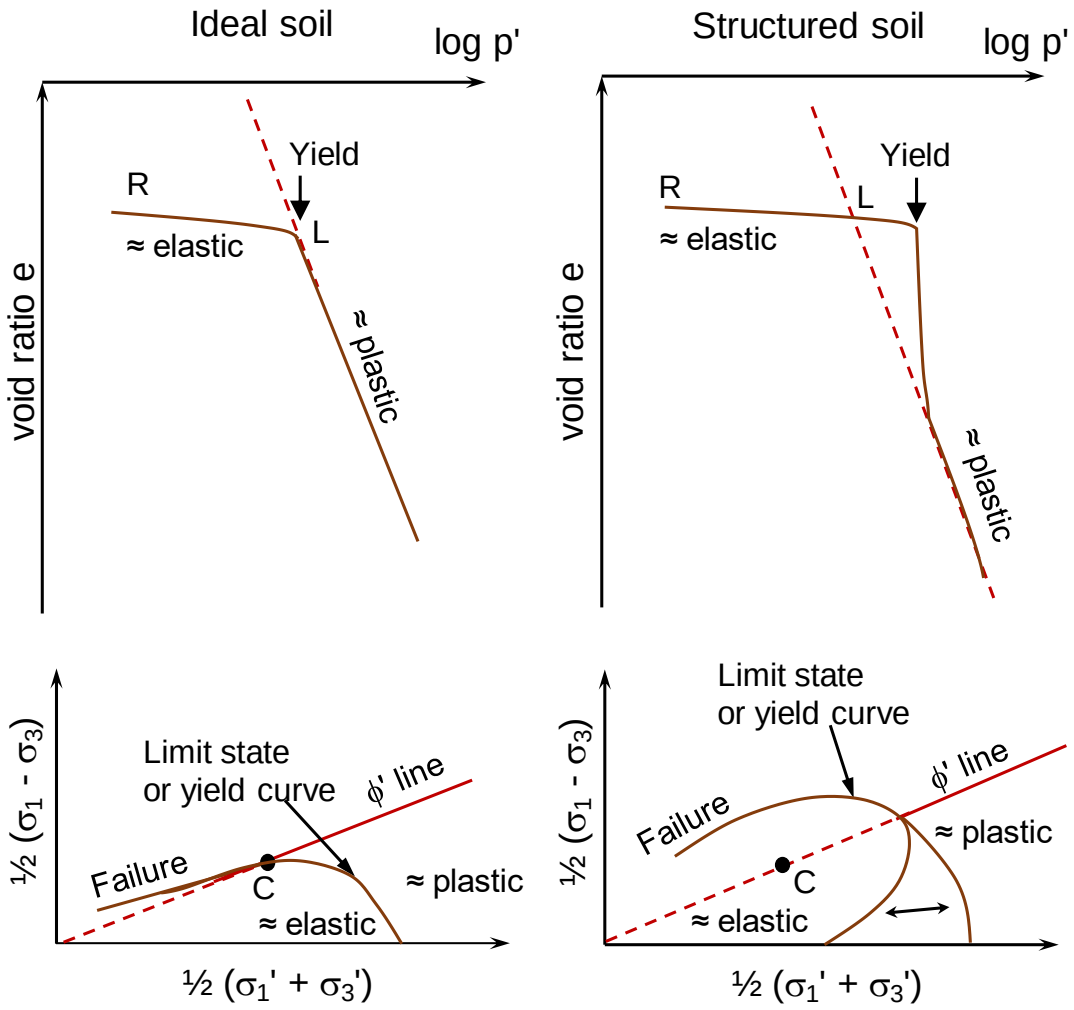

Figure 1.7. Schematic behaviour of ideal and structured soils (modified after Leroueil 1992)

In actuality, an observed value of c' may in fact be a manifestation of that portion of the yield surface that extends above the frictional envelope as illustrated by Figure 1.7, such that c' = 0 also applies to many if not most OC clays (Leroueil & Hight 2003; Mayne 2016). Thus, for soft to firm clays that are normally-consolidated (NC) to lightly-

overconsolidated (LOC), the adoption of c' = 0 is a reasonable assumption for many sedimentary deposits encountered during site investigation.

1.1.1.3 Modes of Undrained Shear Strength and Influence from Sample Disturbance

As described earlier, the undrained shear strength of clays is taken as the maximum shear stress (τ_{max}) on the stress-strain curve in laboratory testing from undisturbed samples. However, due to the complex effects of anisotropy, strain rate, direction of loading, and boundary conditions, it is not possible to assign a single value of s_u for a given clay. Instead, a family of s_u values must be considered, including shear in compression and extension under various modes. The various strength modes can be evaluated by laboratory tests on intact, undisturbed soil samples, for instance: anisotropically-consolidated triaxial compression and extension (CAUC and CAUE), plane strain compression and extension (PSC and PSE), as well as simple shear (SS), direct simple shear (DSS), torsional shear (TS), and other modes (e.g., CIUC, true triaxial, hollow cylinder, directional shear, etc.). The relationship among triaxial compression mode, triaxial extension mode and the direct simple shear mode and the failure plane for a typical slip surface in the field is demonstrated by Figure 1.8.

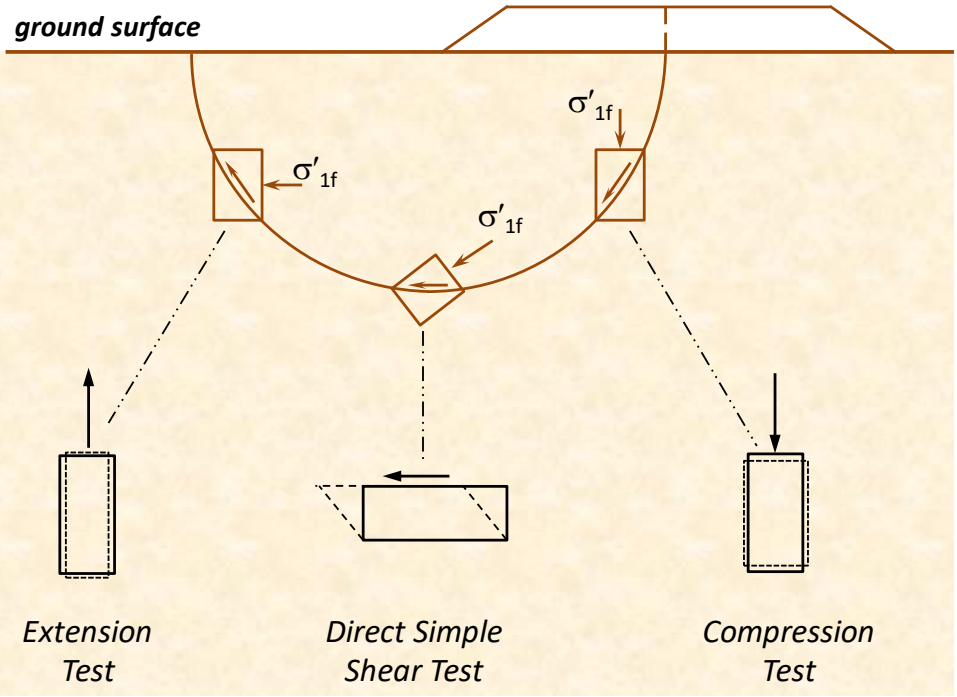

Figure 1.8. Relationship between laboratory tests and shear modes in the field (adopted from Terzaghi, Peck, and Mesri, 1996)

While undrained shear strength may vary greatly with the orientation of the failure plane, Ladd and DeGroot (2003) note that the undrained shear strength measured in direct simple shear is approximately equal to the average of the undrained shear strengths measured in triaxial compression, triaxial extension and direct simple shear for most normally consolidated and lightly overconsolidated fine-grained soils. Constitutive soil models help in establishing a general hierarchy of the test modes. For instance, the Wroth-Prevost hybrid model establishes the model order in terms of normalized undrained shear strength to effective overburden stress for normally-consolidated (NC) clays: $S=s_u/\sigma_{vo}'$, as shown by Figure 1.9. In this framework, the values of S for various modes are expressed as functions of effective stress friction angle ϕ' of the clays. Kulhawy & Mayne (1990),

Ladd & DeGroot (2003), Karlsrud et al. (2005), and others have also verified the general hierarchy of the strength modes through laboratory testing on natural clays.

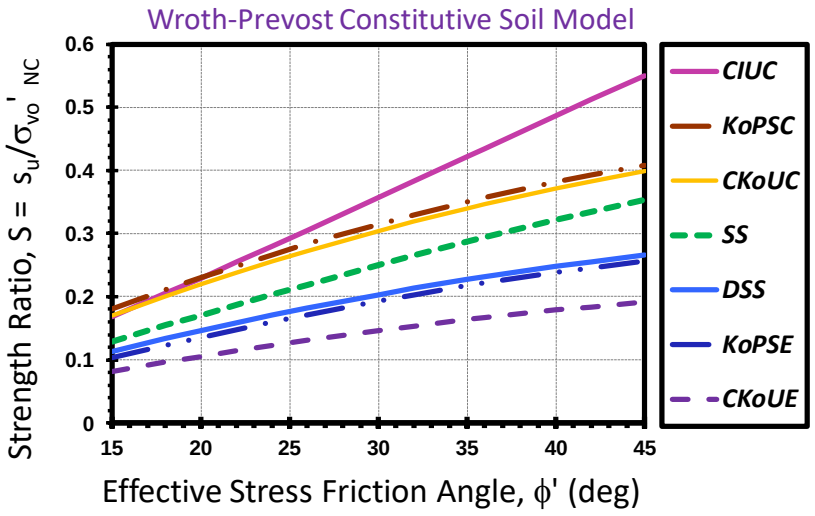

Figure 1.9. Normalized strength ratios for various shearing modes for Wroth-Prevost hybrid constitutive soil model (after Mayne 2008)

In the laboratory, the value of undrained shear strength is also largely affected by the quality the samples tested. For soft clays and silts, the issue of sample disturbance is of paramount concern and depends on the drilling procedures, type of sampler, extraction, level of stress relief, sealing methods, transport, storage time, moisture conditions, tube extrusion of specimens, mounting, and laboratory care (Ladd & DeGroot 2003). Research studies by Tanaka (2000) comparing six different samplers in three soft clays found that the quality depended upon inside and outside diameter of the tube, sampler design, wall thickness, cutting angle, piston geometry, and other details. Generally, the highest quality specimens showed more pronounced peaks with higher s_u values, greater post-peak softening, and stiffer stress-strain responses during undrained compression loading than samples of inferior quality.

The effects of sample quality are illustrated by the anisotropically-consolidated triaxial compression (CAUC) test results presented below. Figure 1.10a shows results from three specimens on Lierstranda clay from 6.1 m depths, the peak s_u are reported as 30kPa (block sample), 24kPa (sample from larger 75-mm tube) and 22kPa (sample from small 54-mm tube). However, all three effective stress paths observed in Figure 1.10b join the same effective stress strength envelope represented by c' = 0 and ϕ' = 34.4º.

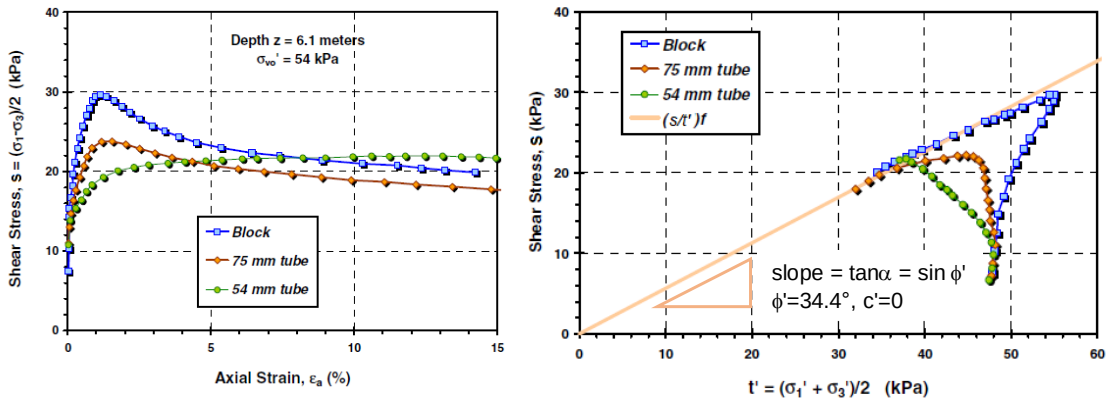

Figure 1.10. Sample disturbance effects for CAUC triaxial compression tests on Lierstranda clay showing (a) undrained stress-strain-strength response; (b) effective stress paths (data from Lunne et al. 2006)

A recent study by Amundsen & Thakur (2017) also investigated the effects of sample disturbance on strength parameters of normally consolidated to lightly overconsolidated Tiller clay in Norway. Block samples and 54mm piston samples are taken in boreholes and were stored in stainless tubes. The top and bottom of the tubes were sealed with a rubber plug and rubber cups. The samples were transported about 12 km away to the laboratory, where they were stored in a humid room with a constant temperature of 4°C for a period up to five months. From Figure 1.11a, it is observed that the block sample subjected to anisotropically-consolidated triaxial compression (CAUC) test immediately

after taken out of boreholes exhibit the highest normalized deviator stress ratio ((σ_1-σ_3)/σ_{v0}'=1.09) and the deviator stress ratio for 54mm piston samples decrease from 0.87 (tested immediately after sampling) to 0.7 (stored for 1 month), and to 0.6 (stored for 5 months). Notably, the effective stress paths for the Tiller clay site converge to the same effective stress envelope, as evident in Figure 1.11b, with an interpreted effective friction angle value of 34.1° and c′ = 0. The important findings here can be stated: (1) undrained shear strength in triaxial compression (s_{uTC}) is significantly affected by sample disturbance; (2) the effective friction angle (ϕ') is essentially not affected by disturbance effects; and (3) For soft to firm clays that are normally-consolidated (NC) to lightly-overconsolidated (LOC), the cohesion intercept c' is found to be 0.

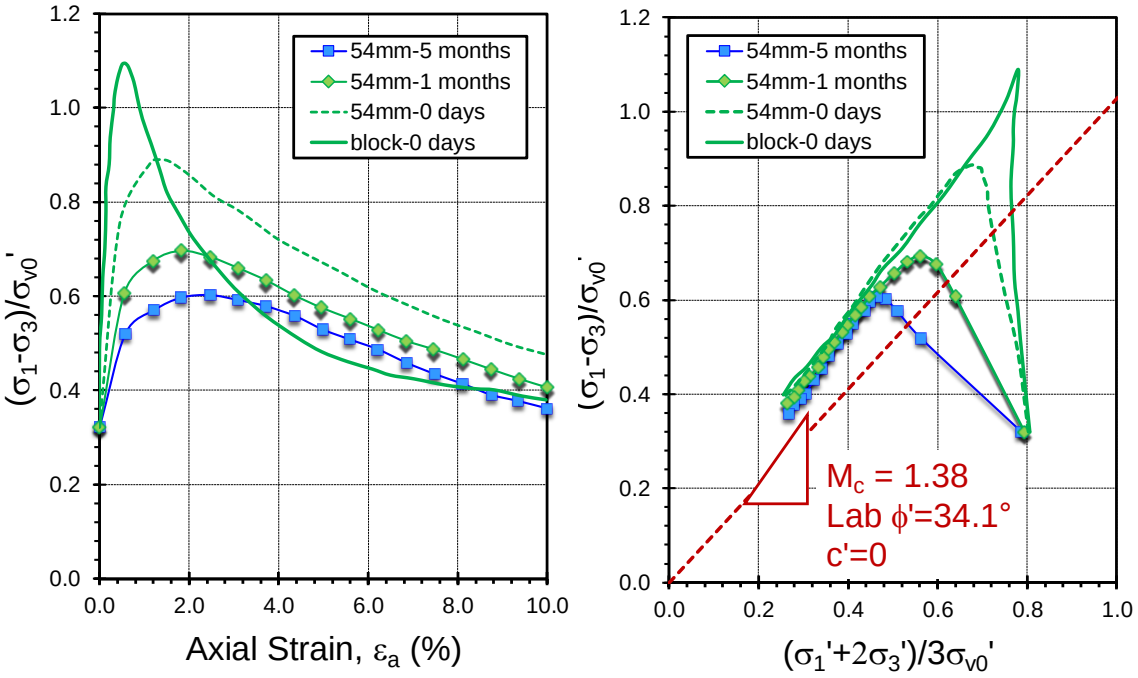

Figure 1.11. Sample disturbance effects for CAUC triaxial compression tests on Tiller clay showing (a) undrained stress-strain response; (b) effective stress paths (data from Amundsen & Thakur 2017)

Amundsen & Thakur (2017) further state that sample quality, storage time, and testing time between sampling and shearing appreciably affect the magnitude of preconsolidation stress, and constrained modulus. However, the magnitude of the effective stress friction angle was little affected by these same factors.

1.2 Piezocone Penetration Testing (CPTu)

Piezocone testing (CPTu) involves the (vertical) pushing of an instrumented probe into the soil at a constant rate of penetration of 20 mm/s to collect data with depth. For the standard CPTu, a modern electronic penetrometer contains load cells and pressure transducers to obtain three separate readings with depth: cone tip resistance (q_c), sleeve friction (f_s), and penetration porewater pressure at the shoulder position (u_2). Readings are generally taken at 1 or 2 second intervals, thus data are essentially continuous. The measured q_c is converted to total cone tip resistance (q_t) using $q_t = q_c + (1 - a_{net}) \cdot u_2$, where a_{net} is defined as net area ratio (Campanella and Robertson 1988).

A schematic diagram illustrating the piezocone penetration test is presented in Figure 1.12. Details concerning CPTu equipment, field test procedures, and reporting of acquired data are given by ASTM D 5778 and Lunne et al. (1997). Interpretative methods for assessing the stratigraphy, soil types, and selected geoparameters are covered by Mayne (2007), Schnaid (2009), and Robertson & Cabal (2016).

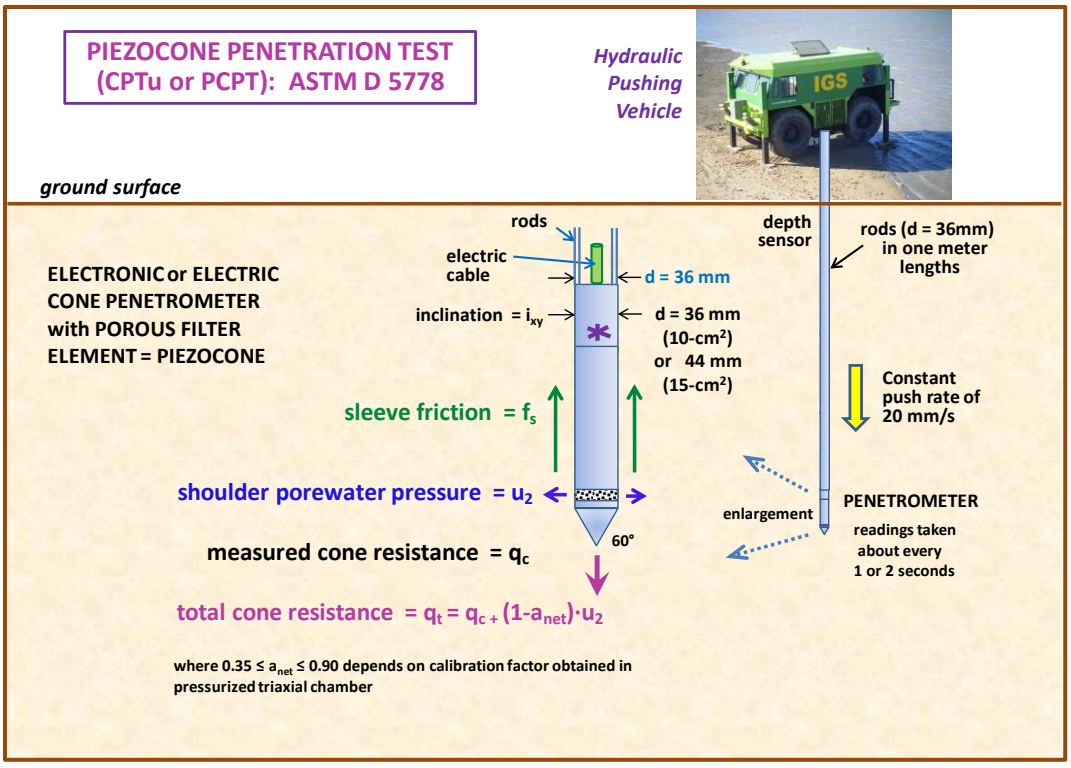

Figure 1.12. Illustration of the cone penetration test with porewater pressure measurements, termed piezocone testing (CPTu)

For soil type identification, simple "rules of thumb" rely on one or more of the cone readings, where a reference cone resistance value q_t = 5 MPa should be identified. When the measured q_t > 5 MPa, the results imply clean sands; whereas when q_t < 5 MPa the readings suggest clays. For the friction sleeve, it is convenient to plot this in terms of friction ratio, FR = f_s/q_t (%). As such, clean sands are identified by FR < 1%, whereas insensitive clays exhibit FR > 4%.

In order to account for depth effects on the readings, stress-normalized CPT parameters have been defined by Lunne, et al. (1997) as follows:

$$Q = (q_t - \sigma_{v0}) / \sigma_{v0}' \qquad [1.4]$$

$$F = 100 \cdot f_s / (q_t - \sigma_{v0}) \qquad [1.5]$$

To better identify the soil type, it is convenient to use the CPT material index, I_c which is defined (Robertson & Wride, 1998):

$$I_c = \sqrt{\{3.47 - \log(Q)\}^2 + \{1.22 + \log(F)\}^2} \quad [1.6]$$

The aforementioned stress normalization for tip resistance (Q) directly with effective overburden stress works well in soft clays and silts, however in sands the stress normalization is proportional to the square root of effective stress, probably due to particle grain crushing or breakage effects. In this case, a modified normalized cone tip resistance has been defined as (Robertson 2009):

$$Q_{tn} = \frac{q_t - \sigma_{vo}}{\sigma_{atm}} \cdot \left(\frac{\sigma_{atm}}{\sigma'_{vo}}\right)^n \quad [1.7]$$

where σ_{atm} = 1 atmosphere $\approx$ 1 bar = 100 kPa and the exponent n is varying with soil type, with typical values of 1.0 in the general case of clays (I_c > 2.95), n = 0.75 for silty soils, and n = 0.5 for clean sands (I_c < 2.05). The exponent n is a function of the material index I_c which in turn is dependent on the modified normalized cone tip resistance ($Q = Q_{tn}$). Therefore, an iterative approach is needed to find the appropriate exponent n to identify the CPT material index using:

$$n = 0.381 \cdot (I_c) + 0.05 \cdot (\sigma_{v0}'/\sigma_{atm}) - 0.15 \quad [1.8]$$

A common means to classify the soil type is using empirical soil behavioral type (SBT) charts as proposed by Robertson et al. (1986). The original 12-zone SBT system has been updated and modified to a 9-zone classification scheme. The SBT number is determined by plotting the CPTu data in terms of Q_{tn} versus F. According to Robertson (2009), basic clay is found in zone 3 while "hourglass" sands form zone 6, guidelines for

the modified SBTn classifications are identified in Table 1.1. For the scope of this study, the focus will be on clayey materials (mostly Zone 3).

Table 1.1. Soil Behavioral Type and Zone Number as defined by CPTu Material Index, I_c

Soil Classification	SBT Zone	Range CPT Material Index I_c
Stiff sand and clays	8 and 9	(see note 1)
Sands with gravels	7	$I_c < 1.31$
Sands: clean to silty	6	$1.31 < I_c < 2.05$
Sandy mixtures	5	$2.05 < I_c < 2.60$
Silty mixtures	4	$2.60 < I_c < 2.95$
Clays	3	$2.95 < I_c < 3.60$
Organic soils	2	$I_c > 3.60$
Sensitive soils	1	(see note 2)

Notes:

1. Zone 8 ($1.4 < F < 4.5$ %) and Zone 9 ($F > 4.5$ %) and following criterion:

$$Q_{tn} \geq \frac{1}{0.006 \cdot (F - 0.9) - 0.004 \cdot (F - 0.9)^2 - 0.002}$$

2. Sensitive soils of zone 1 identified when $Q < 12 \exp(-1.4 \cdot F)$

1.2.1 Profiling strength of clays by piezocone testing

In clays, piezocone penetration tests (CPTu) have routinely been used for evaluating the profile of undrained shear strength (s_u) with depth. Clays and clayey silts are characterized as fine-grained soils having low permeabilities with $k < 10^{-7}$ m/s. Therefore, at the standard CPTu advancement rate of 20 m/s, the soil behaves in an undrained condition, corresponding to a state of constant volume. However, at slower rates, a partially-drained or even fully-drained condition can be achieved in clays, resulting in volume changes within the soil matrix.

Numerous theoretical solutions for the CPTu interpretation of s_u are based on various frameworks, such as bearing capacity theory (Terzaghi 1925), cavity expansion theory (Vesic 1975, 1977, Yu 1993), analytical and numerical approaches (Ladanyi 1967, Lu et al. 2004, Walker & Yu 2006, Liyanapathirana 2016), and strain path theory (Baligh 1985, Teh & Houlsby 1991, Whittle 1992).

The most common CPTu interpretation of the undrained shear strength is utilizing the net cone resistance (q_t-σ_{v0}), as represented by the following formula:

$$s_u = (q_t-\sigma_{v0})/N_{kt} \quad [1.9]$$

where N_{kt} is the cone bearing factor for corrected cone tip resistance q_t.

Agaiby (2018) provided a summary of some 23 expressions for the cone bearing factor N_{kt}, whose determination ranges from theoretical, experimental, numerical, and/or statistical relationships, including bearing capacity theory, spherical cavity expansion theory, strain path method, and finite element modelling. For a given deposit, the appropriate choice of N_{kt} should be made on the basis of site-specific calibration of the CPTu with selective laboratory testing (e.g., triaxial testing, vane shear, simple shear) performed on high quality undisturbed samples of the soil.

Based on past experience, it has been found that the operational value of N_{kt} ranges from around 8 to 16 corresponding to the triaxial compression mode for intact soft to firm clays (Lunne et al. 2005, Low et al. 2010, and Mayne & Peuchen 2018). A representative mean value of N_{kt} = 11.8 can be assigned to soft to firm intact clays corresponding to the CAUC triaxial mode (Mayne et al. 2015). For differing shearing modes, other operational values of N_{kt} must be used. For instance, Low et al. (2010) found a mean N_{kt} = 13.6 for the

laboratory average strength (s_{uAVE}) from triaxial compression, direct simple shear, and triaxial extension (range: $10.6 \leqslant N_{kt} \leqslant 17.4$), which is close to the direct simple shear mode (s_{uDSS}). For calibration with the field vane (s_{uv}), they determined N_{kt} averages 13.3 with a range $10.8 \leqslant N_{kt} \leqslant 19.9$. In contrast, for overconsolidated and fissured clays, Powell & Quarterman (1988) showed that a much higher N_{kt} factor ($20 < N_{kt} < 30$) was necessary to match reference values of s_u obtained from laboratory triaxial compression tests and field plate load test results.

Another avenue to calculate undrained shear strength from CPTu readings is the use of the measured excess porewater pressures ($\Delta u = u_2 - u_0$) using the form:

$$s_u = (u_2 - u_0)/N_{\Delta u} \qquad [1.10]$$

where $N_{\Delta u}$ = cone bearing factor for excess porewater pressures.

For the triaxial compression mode, Lunne (2010) recommends a tentative value of $N_{\Delta u} = 6$ for preliminary offshore site investigation work and/or initial estimates until calibrated with laboratory tests on undisturbed samples. From an independent study, Low et al. (2010) indicate a mean value of $N_{\Delta u} = 5.88$, while a separate study by Mayne, Peuchen, & Baltoukas (2015) found a representative $N_{\Delta u} = 6.5$.

Another option for assessing s_u in clays is via the effective cone resistance (Lunne et al., 1997):

$$s_u = (q_t - u_2)/N_{ke} \qquad [1.11]$$

where N_{ke} is a cone bearing factor averaging about 8.0 in soft-firm clays (Mayne et al. 2015).

1.2.2 CPTu Effective Stress Solution for Clays

While a total stress analysis (TSA) is most commonly adopted for CPTu in geotechnical practice, an effective stress analysis (ESA) is preferred in order to permit a more fundamental assessment of soil behavior, including the quantification of ϕ' in clays. TSA only requires one measurement in order to assess s_u. In the laboratory, the evaluation of ϕ' in clays requires either drained triaxial tests ($\Delta u = 0$), or undrained shear tests with porewater pressure measurements. During CPTu, soft to firm to stiff intact clays will exhibit excess porewater pressures during penetration tests ($\Delta u > 0$, where $\Delta u = u_2 - u_0$). In fact, the CPTu measures both q_t and u_2 during advancement, thus has to potential for determining both s_u and ϕ' in soft-firm clays.

1.2.2.1 Empirical effective stress approach for CPTu

A semi-empirical approach was proposed by Keaveny (1985) and Keaveny & Mitchell (1986) to interpret the effective stress strength parameters (c', ϕ') of clays from CPTu data. This method requires an initial estimate of a series of geoparameters for the soil under investigation, including: rigidity index (I_R), lateral stress coefficient (K_0), and Skempton's pore pressure parameter at failure from triaxial tests (A_f). The sequence of these empirically-based relationships in the interpretation procedure seems to be a major difficulty with this approach. Errors in an early stage of the interpretation will be transmitted to the next stage, and the results may be misleading. The necessary input parameters have to be determined in an extensive laboratory program, and the empirical relationships are hence abundant. Sandven (1990) examined the Keaveny & Mitchell's

method using CPTu data from six Norwegian clays and found significant discrepancies between laboratory and empirically determined parameters.

1.2.2.2 Theoretical effective stress approach for CPTu

An effective stress limit plasticity solution that utilizes the total cone resistance (q_t) and measured shoulder porewater pressure (u_2) has been developed by the Norwegian Institute of Technology (NTH), as detailed by Janbu & Senneset (1974), Senneset et al. (1982), Senneset & Janbu (1985), Senneset et al. (1989), Sandven (1990), Sandven & Watn (1995), and Sandven et al. (2015, 2016).

Janbu & Senneset (1974) proposed an effective stress limit plasticity solution for the CPTu towards the evaluation of ϕ' during probe penetration. In this approach, the cone resistance number (N_m) is defined as

$$N_m = \frac{N_q - 1}{1 + N_u B_q} = \frac{q_t - \sigma_{v0}}{\sigma'_{v0} + a'} \quad [1.12]$$

where $B_q = (u_2 - u_0)/q_{net}$ is the normalized pore-water pressure parameter, u_0 is the hydrostatic porewater pressure, $q_{net} = q_t - \sigma_{v0}$ is the net cone resistance, σ_{v0} is the initial vertical stress, σ'_{v0} is the initial vertical effective stress, $a' = c' \cot\phi'$ is the effective attraction, and c' is the effective cohesion intercept. The tip bearing capacity factor, N_q, and the pore-water pressure bearing factor, N_u, are given by (Senneset et al. 1989).

$$N_q = K_p \cdot exp[(\pi - 2\beta) \cdot tan\phi'] \quad [1.13]$$

$$N_u = 6 \cdot tan\phi'(1 + tan\phi') \quad [1.14]$$

$$K_p = (1 + sin\phi')/(1 - sin\phi') \quad [1.15]$$

where K_p is the passive lateral stress coefficient and is the angle of plastification ($-40° < \beta < +30°$) that defines the size of the failure zone (Senneset & Janbu 1985).

The full solution allows for an interpretation of a paired set of effective stress Mohr–Coulomb strength parameters (effective cohesion intercept, c', and ϕ') for all soil types, including: sands, silts, and clays, as well as mixed soils (Sandven 1990; Mayne 2016). The parameter N_q is the tip bearing capacity factor from limit plasticity solutions that is well known for pile foundations. For the case where $\beta = 0°$, N_q is identical to the classical solution for a deep foundation (i.e., Terzaghi equation). The parameter N_u is a porewater pressure bearing factor (Senneset et al. 1989).

When $a' = c' = 0$, the parameter N_m is identical to the normalized cone tip resistance, $N_m=Q = (q_t - \sigma_{v0})/\sigma'_{v0}$, that is used extensively in CPTu interpretations (Lunne et al. 1997; Mayne 2007a; Robertson 2009). Thus, a relationship between ϕ' and the cone parameters ($N_m=Q$ and B_q) can be expressed as a single equation:

$$N_m = Q = \frac{tan^2(45°+\phi'/2)exp(\pi tan\phi')-1}{1+6tan\phi'(1+tan\phi')B_q} \quad [1.16]$$

which is shown graphically in Figure 1.13.

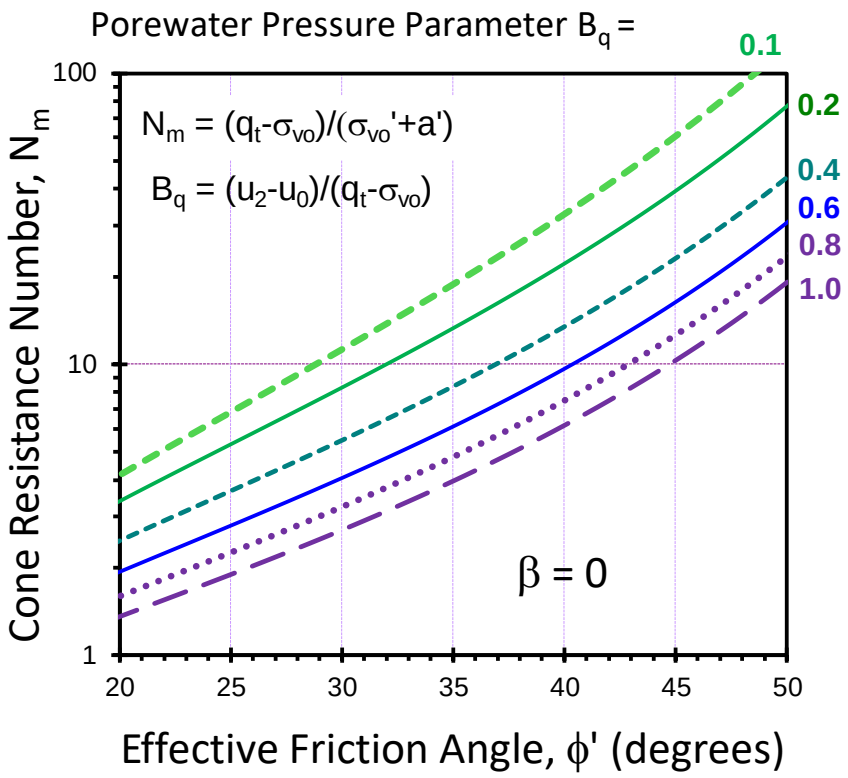

Figure 1.13. NTH method for evaluating ϕ′ from CPTu in silts and clays.

While the NTH method received some attention in applications for seven Norwegian clays (Sandven 1990; Sandven & Watn 1995), four clays in the North Sea (Lunne et al. 1985), two Swedish clays (Larsson & Mulabdic 1991), clay from Texas (Sellountou et al. 2004), and Egyptian clay (Hamza & Shahien 2009), it appears that little recognition has been acknowledged by geotechnical practitioners and researchers in the rest of the world.

A primary goal of this research effort was undertaken to collect data from a wide assortment of different clay deposits from across the planet where reference values of ϕ' were available from benchmark triaxial compression tests and the clays had also been tested by CPTu at the same elevations, thus allowing for a validation and verification of

the NTH solution in assessing ϕ'. The review included compilations of data from series of laboratory chamber deposits, centrifuge testing, and natural clay field test sites.

1.3 Flat Plate Dilatometer Test (DMT)

The flat plate dilatometer test (DMT) was developed in Italy (Marchetti 1980) and quickly gained popularity among both practitioners in the geoengineering profession and academicians in geotechnical research who were seeking new and improved methods for site exploration. The DMT involves pushing a flat blade and inflating a flexible membrane to obtain two pressure readings at set vertical depth intervals. The DMT is a quick, reliable, and robust in-situ test that investigates subsurface characteristics and allows for the interpretation of geoparameters in an efficient, economic, and expedient manner along the soil profile.

A diagram illustrating the flat plate dilatometer test (DMT) is presented in Figure 1.14. The flat dilatometer has a high-strength stainless-steel blade that is pushed into the ground at depth increments of either 20 or 30 cm using common field equipment, i.e., drill rigs or hydraulic pushing rigs. The blade has a flat 60-mm diameter circular steel membrane mounted flush on one side, which determines two separate pressure readings at each depth by inflating the membrane with nitrogen gas on the side of the pushing blade. A pressure read-out box at the ground surface is used to obtain the two pressure readings that include: (1) A-pressure, which is required to simply begin to move the membrane against the soil, and (2) B-pressure, which is required to move the center of the membrane 1.1 mm against the soil. Per ASTM D6635-15, the A and B readings must be corrected by the values of ΔA and ΔB, which are determined by calibration, to account for membrane stiffness and

are eventually converted to p_0 (contact pressure) and p_1 (expansion pressure) readings according to the following equations:

$$p_0 = 1.05(A + \Delta A) - 0.05(B - \Delta B) \quad [1.17]$$

$$p_1 = B - \Delta B \quad [1.18]$$

Details concerning the DMT equipment, field test procedures, and interpretations are given by Marchetti (1980) and ASTM D6635-15, *Standard Test Method for Performing the Flat Dilatometer Test (DMT).* Updates to the test are discussed by Mayne et al. (2002), Marchetti et al. (2006) and Marchetti (2015).

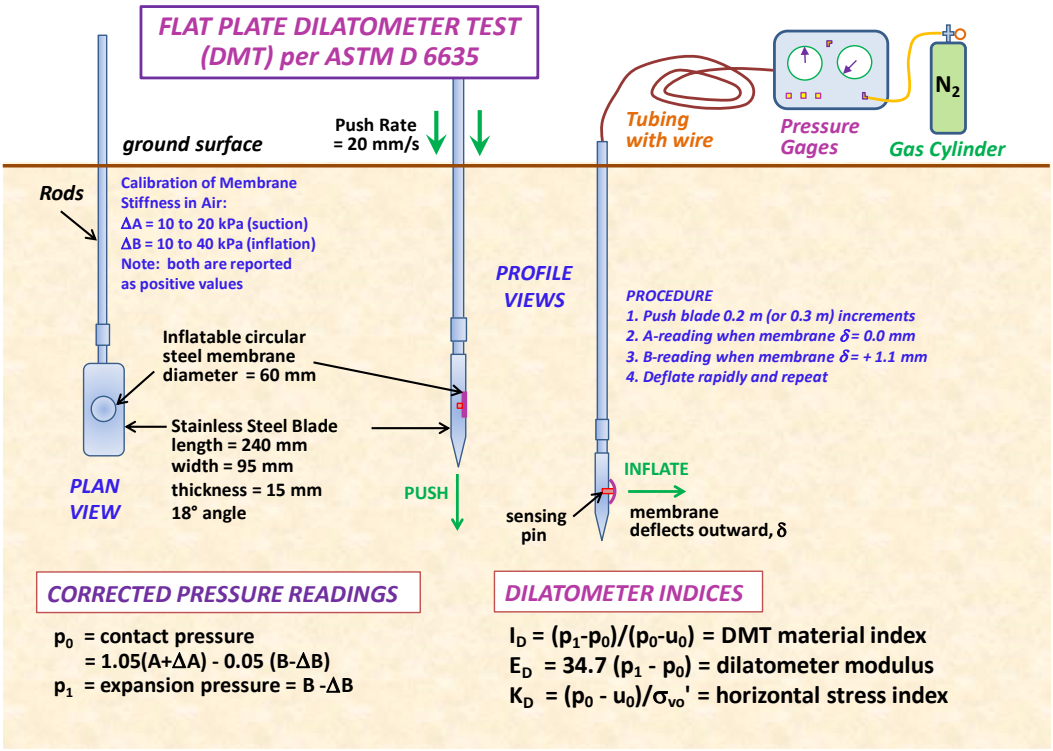

Figure 1.14. Illustration of the flat plate dilatometer test (DMT)

The two dilatometer pressures, p_0 and p_1, are combined with the hydrostatic water pressure, u_o, to provide three index parameters: (a) material index I_D, (b) horizontal stress

index K_D, and (c) dilatometer modulus E_D. These were developed by Marchetti (1980) to provide information on the stratigraphy, soil types, and the evaluation of soil parameters. Hydrostatic water pressure (u_0) can be evaluated based on available groundwater table information. The material index, I_D, is related to the soil classification and is presented as:

$$I_D = (p_1 - p_0) / (p_0 - u_0) \quad [1.19]$$

Soil type can be identified by the approximate criteria: clay: $0.1 < I_D < 0.6$, silt: $0.6 < I_D < 1.8$, and sand: $1.8 < I_D < 10$. In general, I_D provides a reasonable soil description with depth from DMT data.

The horizontal stress index, K_D, is defined as:

$$K_D = (p_0 - u_0)/\sigma'_{v0} \quad [1.20]$$

The value of K_D provides the basis for assessing several soil parameters. In NC clays having no aging, structure, or cementation, the value of $K_D \approx 2$. The K_D profile is similar in shape to the OCR profile with depth, hence can be used to better understand the soil deposit and its stress history, strength, and in-situ geostatic state of stress (Marchetti 1980, Jamiolkowski et al. 1988, Leonards & Frost 1988).

The dilatometer modulus E_D is obtained from the measured p_0 and p_1 within the theory of elasticity. For the 60 mm membrane diameter and required 1.1 mm displacement, it is found that (Marchetti 1980):

$$E_D = 34.7(p_1 - p_0) \quad [1.21]$$

1.3.1 Existing DMT relationships with clay total stress and effective stress strength parameters

The DMT can evaluate a wide variety of geotechnical parameters, such as soil type, unit weight (γ_t), overconsolidation ratio (OCR), undrained shear strength (s_u) of clays, effective friction angle in sands (ϕ'), constrained modulus (D′ or M′), lateral stress coefficient (K_0), and coefficient of consolidation (c_v), as well as provide an assessment of liquefaction potential in seismic areas underlain by sandy soils (Marchetti 2015).

The following correlation between normalized undrained shear strength and lateral stress index was initially proposed by Marchetti (1980) for cohesive soils ($I_D < 1.2$):

$$s_u/\sigma_{v0}' = 0.22\ (0.5K_D)^{1.25} \qquad [1.22]$$

Since then, various researchers have come up with modifications of the above semi-empirical correlation of the undrained shear strength with the DMT data based on local experience and geomaterial data (Lacasse & Lunne 1982, Su et al. 1993, Iwasaki & Kamei 1994, Kamei & Iwasaki 1995,) Schmertmann (1991) suggested an experimental trend between the undrained shear strength of clays and the DMT contact pressure p_0 and the hydrostatic porewater pressure u_0:

$$s_u = (p_0-u_0)/10 \qquad [1.23]$$

Mayne & Martin (1998) summarized a partial listing of comparative and correlative studies for the flat dilatometer. However, there is no existing method with regard to the effective stress strength parameters of clays using DMT data.

1.4 Contributions of This Research

When CPTu and DMT soundings are advanced into clays and fine-grained soils with low permeability characteristics at the standard push rate of 20 mm/s, the interpretation by geotechnical engineers traditionally centers around a total stress analysis, and consequently, the evaluation of strength is focused on the undrained shear strength (s_u). As noted earlier, the fundamental strength of most soft to firm clays is really governed by effective stress conditions, specifically the effective stress friction angle, ϕ', as detailed by laboratory triaxial stress path testing (i.e., Lambe & Whitman 1979; Leroueil & Hight 2003), critical state soil mechanics (Schofield & Wroth 1968; Wood 1990; Mayne et al 2009), and FEM numerical modeling (Whittle et al. 1994; Yi et al. 2012).

This program offers the interpretation of the effective stress friction angle of fine-grained soils from in-situ testing data from piezocone penetration test (CPTu) with focus on the clays and clayey materials of normally consolidated (NC) to overconsolidated nature (OC), fissured clays with high overconsolidation ratio (HOC) using a modified NTH limit plasticity theory. Evaluations have been made within an effective stress framework, specifically utilizing concepts from critical state soil mechanics (CSSM). In addition, work by Keaveny & Mitchell (1986) and Baligh (1984) show that triaxial compression mode dominates at the cone tip, as demonstrated by Figure 1.15.

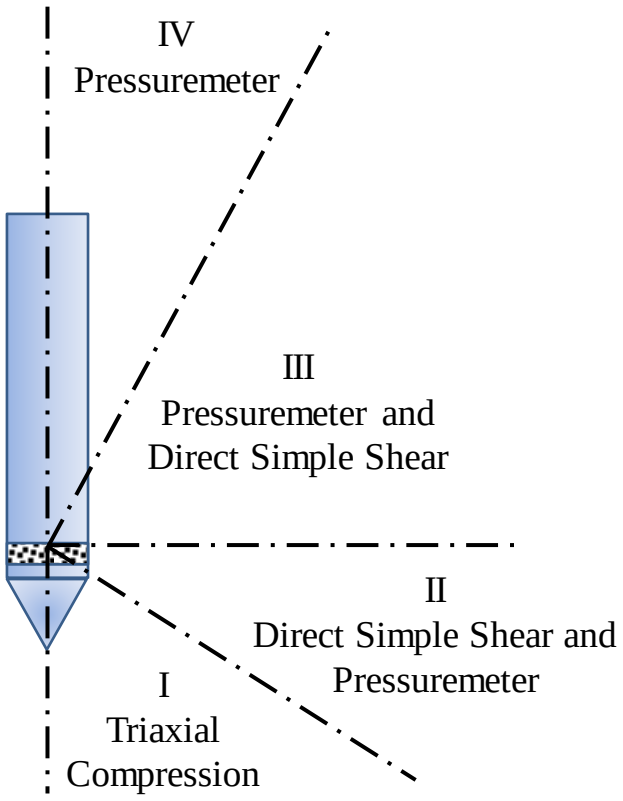

Figure 1.15. Predominant failure modes around an advancing cone penetrometer (modified after Keaveny & Mitchell 1986)

Thus, the effective stress strength parameters of fine-grained soils determined from laboratory triaxial compression type mode under undrained loading (i.e., constant volume) with porewater pressure measurements taken during shearing tests are adopted as the benchmark reference for the calibration of effective stress strength parameters evaluated by CPTu. These included isotropically consolidated (undrained triaxial compression CIUC), K_0-consolidated CK_0UC, as well as general anisotropic (undrained consolidated anisotropic CAUC) types.

This research program also develops a nexus between the cone penetration test (CPTu) and the flat dilatometer test (DMT) for clays. This theoretical nexus is established

based on spherical cavity expansion (SCE) theory. Traditionally, the evaluation of clay strength by DMT focuses only on total stress parameters, specifically the undrained shear strength (s_u). Yet, despite its relevance and importance, the effective stress friction angle (ϕ') of clays has not been conventionally determined using DMT readings. This nexus between CPTu and DMT provides a means for evaluating the effective friction angle of clays from the DMT using the NTH limit plasticity solution. For most geotechnical projects, the full suite of drilling & sampling, laboratory, and in-situ testing cannot be implemented because of time and costs. Depending upon the nature of geologic setting and level of the proposed construction, perhaps only a select number of lab tests (i.e., index, consolidation, triaxial, permeability) and one or two of the basic in-situ tests (i.e., CPTu, DMT) can be implemented. Thus, a better understanding and a link between two in-situ testing provides additional confidence for the practitioners in terms of adoption of various field investigation techniques.

A new analytical approach based on a modification of a hybrid spherical cavity expansion theory-critical state soil mechanics is established and combining the nexus between the CPTu and DMT allows the direct assessment of undrained rigidity index (I_R) of soft clay from DMT data which finds value in evaluating undrained shear strength, yield stress, and coefficient of consolidation, as well as applications involving foundation bearing capacity.

1.5 Research Outline and Thesis Structure

The thesis is divided into ten more chapters, as listed below:

- Chapter 2 - *Review of Clay Chamber Deposits Subjected to Standard and Miniature Piezocone Tests.* Series of chamber tests containing manufactured clay deposits that were tested using miniature or standard size piezocone penetrometers were reviewed and compiled from research programs conducted at Cornell University, Cambridge University/UK, Louisiana State University, Purdue, Oxford, Sheffield, Sangmyung, University of Western Australia, and the Swedish Geotechnical Institute. Details on the artificial clay deposits, chamber sizes, confining stresses, penetration rates, and penetrometer sizes are reviewed in this chapter. The calibration chamber tests were conducted mainly on normally consolidated to lightly overconsolidated kaolin specimens or kaolin-sand mixtures, with a few tests on overconsolidated clays. The task was made to evaluate the ability of piezocone tests in assessing the effective friction angle (ϕ') and undrained shear strength (s_u) of kaolin and kaolin-sand mixtures where laboratory triaxial results (CAUC) were used as the reference benchmark values for comparison. This chapter was published as:

  Ouyang, Z., Mayne, P.W. and Sharp, J. (2016). Review of clay chamber tests using miniature cone and piezocone penetrometers, *Proc. GeoVancouver 2016, (69th Canadian Geotechnical Conference)*, Canadian Geotechnical Society: www.cgs.ca

- Chapter 3 - *Interpretation of Effective Stress Friction Angle (ϕ') in Centrifuge Clays Deposits from Mini-CPTu Soundings.* The NTH is further calibrated to evaluate the effective stress friction angle (ϕ') for clayey soils subjected to CPTu in centrifuge model testing. Results from previously-conducted in-flight mini-piezocone tests conducted by various research institutes were compiled for study, including readings taken from 13 series

of centrifuge chamber tests on artificially prepared clays, mainly kaolin and kaolinitic-silica mixtures. Effective stress friction angles primarily from companion triaxial compression tests (CAUC and/or CIUC) on these soils were adopted as the benchmark values to verify the reasonableness of the NTH method in assessing ϕ' at constant penetration rates corresponding to undrained conditions. This chapter was published as:

> Ouyang, Z. and Mayne, P.W. (2018). Calibration of NTH method for friction angle using centrifuge CPTUs in clays. *Proceedings, 4th International Symposium on Cone Penetration Testing,* (CPT'18, Delft), CRC Press/Balkema: 491-498. www.cpt18.org

- Chapter 4 – *Effective Friction Angle of Clays and Silts from Field Piezocone Penetration Tests*. The NTH solution is applied to evaluate the effective stress friction angle (ϕ′) for undrained conditions for a variety of normally-consolidated (NC) to lightly-overconsolidated (LOC) fine-grained soils ranging from natural lean to plastic clays and clayey silts from marine, alluvial, lacustrine, deltaic, and glaciofluvial origins. Data from 105 clay sites are compiled to examine the field CPTu-interpreted (ϕ′) values in comparison with laboratory benchmark values obtained from CAUC and/or CIUC triaxial compression tests made on undisturbed samples. An approximate inversion of the theoretical solution is developed to allow profiles of ϕ′ to be evaluated directly with depth. Five well-documented case studies in Illinois, Louisiana, South Carolina, Ireland, and Massachusetts are presented to illustrate the application of the solution. This chapter was published as:

> Ouyang, Z. and Mayne, P.W. (2018). Effective friction angle of clays and silts from cone piezocone penetration tests. *Canadian Geotechnical Journal*. 55(9):

1230–1247, doi:10.1139/cgj-2017-0451. *Note: selected as "Editor's Choice paper for 2018"

- Chapter 5 - *CPTu Twitch Test Data Evaluated Using NTH Limit Plasticity Solution*. The NTH approach is examined for compatibility for a variety of soils subjected to variable rate penetration tests covering undrained to partially-drained to fully-drained conditions, a.k.a., twitch testing. Data from 23 series of twitch tests reported by geotechnical research groups are compiled into three categories, including: (a) field CPTu soundings, (b) laboratory 1-g chamber tests, and (c) centrifuge model tests. It is observed that the effective stress friction angle of clays, silty clays, sandy clays, and other fine-grained soils is consistent with the NTH solution, regardless of the probe push rate. For 16 of the twitch test series, where benchmark friction angles from conventional laboratory triaxial testing were available, the NTH CPTu solution compares well. Example case studies from reported twitch CPTu test series are presented to illustrate the NTH procedures in variable penetration rate CPTu. Results from this chapter are prepared to be published in Ouyang & Mayne (2019) – *in preparation*.
- Chapter 6 - *Effective Friction Angle of Soft to Firm Clays from Flat Dilatometer Tests.* A solution using spherical cavity expansion theory is used to interrelate measurements taken by piezocone penetration tests (CPTu) and flat plate dilatometer tests (DMT) in soft to firm clays. Data from 27 clay sites are shown to confirm simple links that express the CPTU net resistance and excess porewater pressure in terms of the DMT contact pressure and expansion pressure. As a result, the derived nexus is explored for evaluating the effective friction angle of soft to firm clays from DMT data using the NTH limit plasticity solution. Two well-documented case studies are presented to illustrate the

reasonable prediction of the effective friction angle in comparison with laboratory anisotropically consolidated undrained compression triaxial tests on undisturbed samples. This chapter was published as:

> Ouyang, Z. and Mayne, P.W. (2017). Effective friction angle of soft to firm clays from flat dilatometer tests. *Geotechnical Engineering*. Vol. 170 (2) Proc. Institution of Civil Engineers, London: 137-147.

- Chapter 7 - *Spherical Cavity Expansion Nexus Between CPTu and DMT in Soft-Firm Clays.* Using cavity expansion solutions for undrained penetration, a theoretical link is established between the cone tip resistance (q_t) and shoulder porewater pressure (u_2) from cone penetration tests (CPTu) in soft to firm clays and the measured contact pressure (p_0) and expansion pressure (p_1) obtained from adjacent flat plate dilatometer tests (DMT). In-situ data from paired CPTu-DMT soundings in a variety of clay deposits are used to support and validate the links. This permits an exchange of interpretations between the two tests, offering a complementary extension of methodologies. Specifically, the established solution using effective stress limit plasticity theory for the assessment of ϕ' in clays from piezocone testing is extended to DMT readings for this purpose. Data from 3 clays are presented as applied case studies: Sandpoint, Idaho; Washington DC; and Evanston, Illinois. This chapter was published as:

> Ouyang, Z. and Mayne, P.W. (2017). Spherical cavity expansion nexus between CPTu and DMT in soft-firm clays. *Proceedings of the 19th International Conference on Soil Mechanics and Geotechnical Engineering*, Vol. 1, Korean Geotechnical Society, Seoul: 631-634. www.issmge.org

• Chapter 8 - *Effective Stress Strength Parameters of Clays from DMT*. An established NTH effective stress limit plasticity solution for piezocone penetration tests (CPTu) in clay for evaluating the effective stress friction angle (ϕ') is extended to flat plate dilatometer tests (DMT) readings. A nexus between CPTu and DMT is built through spherical cavity expansion solutions for undrained penetration to link the cone tip resistance (q_t) and shoulder porewater pressure (u_2) from CPTu to the measured DMT contact pressure (p_0) and expansion pressure (p_1) in soft to firm intact clays that are normally consolidated (NC) to lightly overconsolidated (LOC). Field data from paired sets of CPTu-DMT soundings in 49 clay deposits are used to validate the links. Various soils ranging from lean to plastic clays and clayey silts from marine, alluvial, lacustrine, deltaic, and glaciofluvial origins are subjected to flat DMTs, and the measurements are utilized to evaluate the effective stress friction angle (ϕ'). Data from 46 clays are compiled to examine the DMT-interpreted ϕ' values in comparison with laboratory benchmark ϕ' values obtained from either CAUC or CIUC triaxial compression tests made on high-quality samples. An approximate inversion of the theoretical solution is also derived to allow ϕ' profiles to be determined with depth. Four well-documented DMT examples, including natural clay sites and chamber test series are presented to illustrate the NTH procedures in DMT. This chapter was published as:

> Ouyang, Z. and Mayne, P.W. (2018). Effective stress strength parameters of clays from DMT. *ASTM Geotechnical Testing Journal*. Vol. 41, No. 5: 851-867: https://doi.org/10.1520/GTJ20170379. ISSN 0149-6115.

• Chapter 9 - *Evaluating Rigidity Index, OCR, and s_u from Dilatometer Data in Soft to Firm Clays.* In geotechnics, rigidity index is defined as the ratio of shear modulus to shear strength ($I_R = G/\tau_{max}$) and serves as an important input parameter for analyses

involving bearing capacity, pile driving, porewater pressure generation, and dissipation problems. In this chapter, a nexus between CPTu and DMT is explored to interpret the undrained rigidity index of soft to firm clays using DMT data. A hybrid formulation of spherical cavity expansion and critical state soil mechanics (SCE-CSSM) is utilized for obtaining the operational undrained I_R from the flat plate dilatometer test (DMT). This value of rigidity index in useful in evaluating the profiles of overconsolidation ratio (OCR) and undrained shear strength (s_u) of soft to firm clays within the same SCE-CSSM framework. Two case studies covering clays with different geologies from the UK and USA are used to demonstrate the effectiveness of the proposed methodology for obtaining I_R, OCR, and s_u. This chapter is published as:

> Ouyang, Z. and Mayne, P. W. (2019). Evaluating rigidity index, OCR, and s_u from dilatometer data in soft to firm clays. *Proceedings, 16th Panamerican Conference on Soil Mechanics and Geotechnical Engineering*, Cancun. Mexican Geotechnical Society, (in review): www.issmge.org

- Chapter 10 - *Modified NTH Method for Assessing the Effective Friction Angle of Normally-Consolidated and Overconsolidated Clays from Piezocone Tests.* The NTH effective stress limit plasticity solution provides a theoretical evaluation of the effective stress friction angle (ϕ') for soft to firm normally-consolidated (NC) to lightly-overconsolidated clays (LOC) from piezocone penetrometer tests (CPTu). A modified NTH method using the equivalent stress concept is detailed to allow the evaluation of effective stress friction angle for overconsolidated (OC) clays. The solution requires a knowledge of the soil stress history, specifically the overconsolidation ratio (OCR) and

volumetric strain potential, $\Lambda = 1 - C_s/C_c$. A wide variety of clays have now been calibrated using this approach, including measured CPTu and triaxial data collected from six categories: (a) laboratory chamber tests in NC clays; (b) centrifuge testing in NC clays; (c) centrifuge tests in OC clays; (d) field CPTu in natural NC-LOC clays, (e) field CPTu in OC intact clays with OCR > 2.5, and (f) field CPTu in OC fissured clays. Results from compiled databases are statistically shown to validate the CPTu-interpreted ϕ' values in comparison with laboratory benchmark values obtained from CAUC and CIUC triaxial tests. Case studies of CPTu soundings conducted in the aforementioned categories are presented to elaborate the application of the NTH solution. This chapter is published as:

> Ouyang, Z. and Mayne, P.W. (2019). Modified NTH method for assessing the effective friction angle of normally-consolidated and overconsolidated clays from piezocone tests. *ASCE Journal of Geotechnical and Geoenvironmental Engineering* (accepted for publication by ASCE JGGE on 03 Feb 2019: GTENG-7251R2)

- Chapter 11 - *Limitations and Discussion of the modified NTH solution*

Discussions on the modified NTH solution regarding statistical analysis of the modified NTH solution on evaluating the effective stress friction angle ϕ' of clays and comparison of the results from the modified NTH solution. Limitations of both laboratory testing and field testing on the interpreted value of ϕ' are also illustrated. Variability of different size piezocones on affecting interpretation results is elaborated. In the end, special considerations for organic soils, sensitive clays, soils with differing mineralogy and plasticity, and structured geomaterials are also given.

- Chapter 12 - *Conclusions and Future Work.*

A summary of the findings and conclusions are presented in this final chapter. Recommended tasks for fure research on the improvements in CPTu and DMT interpretation are presented.

At the end of the dissertation, five appendices are compiled presenting the experience regarding field testing at Georgia Tech W-21 Test Site, triaxial laboratory testing at Geotechnical Lab, Golder Associate Inc, and raw data from laboratory CIUC/CAUC/CK_0UC tests and field CPTu and/or DMT as follows:

- Appendix A - Field testing at Georgia Tech W-21 parking lot
- Appendix B - Laboratory triaxial testing at Geotechnical lab, Golder Associate Inc. Atlanta, GA
- Appendix C - Raw data from investigated piezocone penetration tests
- Appendix D - Raw data from investigated flat plate dilatometer tests
- Appendix E - Raw data from laboratory CIUC/CAUC/CK_0UC triaxial tests

CHAPTER 2. REVIEW OF CLAY CHAMBER TESTS USING MINIATURE CONE AND PIEZOCONE PENETROMETERS

2.1 Introduction

Calibration chamber tests are widely used to establish relationships between in-situ test measurements and the engineering properties of soils. These relationships can be analytical, theoretical, numerical, or empirical in their formulation. This chapter involves the interpretation of chamber test results obtained using miniature cone penetration tests (CPT) that were conducted into prepared clay deposits at 1-g scale testing. A total of 11 chamber test series mainly containing manufactured kaolinitic type clay deposits were collected from nine different research institutes. Readings from the miniature cone/piezocone penetrometers were compiled including the total cone tip resistance (q_t) and penetration porewater pressure (u_2). Where available, additional basic geo-parameters were tabulated for the clays, including: plasticity index, water content, overconsolidation ratio, and other indices.

The CPT results are utilized to explore the interpretation of the effective stress friction angle (ϕ') using the NTH method. In addition, the CPT results are evaluated to provide the undrained shear strength (s_u) via classical bearing capacity solutions. Results are compared to values from the triaxial compression (TC) test as the reference laboratory mode to show the validity of these approaches. In some cases, a conversion of measured undrained shear strength (e.g., vane shear test) to an equivalent triaxial compression (TC) value was necessary.

2.2 Miniature Cone and Piezocone Chamber Test

Kaolinitic clay or mixed clay-sand specimens in this study were prepared and tested in calibration chambers. Typically, the specimens would be mixed as a slurry and consolidated in a calibration chamber, in many respects similar to a large triaxial cell or consolidometer. The chambers were constructed of either steel or plastic circular walled shells. Both fixed and flexible wall chambers have been used in these studies. In many cases, the effective confining stresses can be maintained using pressurized systems and special entry ports on the top plate of the chamber to permit penetrometer testing. For the majority of the soils studied in this chapter, the stress histories applied in the chamber tests focused on normally consolidated (NC) or lightly-overconsolidated (LOC) clay deposits, although in some cases, experimental studies were varied to investigate overconsolidated states (e.g., Nyirenda 1988; Mayne 1992; Kurup et al. 1994).

Table 2.1 shows the summary information from each of the research institutes that conducted the chamber tests, the specific clay types used in creating soil deposits, and the data reference sources. Table 2.2 shows the geotechnical index parameters of the clay deposits under investigation, such as water content, liquid limit, plasticity index, and overconsolidation ratio. The water contents of the investigated soils ranged from 30% to 120% and the plasticity index varied around 6% to 35%.

Each of the aforementioned chamber deposits of clays at various institutes were tested using miniature cone and/or piezocone penetrometers. For the latter, u_2 measurements were taken at the cone shoulder, as per ASTM D 5778 standards, to allow the determination of total cone resistance (q_t). Table 2.3 lists the details about the chamber

sizes, penetrometer probe dimensions, and the corresponding penetration rates that were used in these test series.

Boundary effects due to relative sizes of the mini-cone penetrometers with respect to the calibration chamber size may exist. However, little guidance exists to resolve this potential uncertainty.

Table 2.1. Clay chamber series reviewed in Chapter 2

Institute No.	Clay type	Reference
1. Cambridge U	Gault Clay	Almeida & Parry(1985)
2. Oxford U	Kaolin	May (1987)
3. Oxford U	kaolin	Nyirenda (1989)
4. Cornell U	Kaolin-silica	Mayne (1993)
5. LSU	K-50[1]	Kurup et al (1994)
6. Univ. Sheffield	Kaolin	Hird & Sangtian (2004) *
7. Purdue U	K-18[2]	Kim (2005)
8. Sangmyung U	K-33[3]	Kim & Tumay (2007)
9. SGI	Partille Clay	Lofroth (2008)
10.UWA	K-100[4]	Suzuki (2015)
11.UWA	K-25[5]	Suzuki (2015)

Notes:

LSU = Louisiana State University;

SGI = Swedish Geotechnical Institute;

UWA = University of Western Australia

[1]50% Kaolin+50% Edgar fine sand

[2]18% Kaolinite Clay and 82% Jumun sand

[3]33% Kaolin+67% Sand

[4]100% Kaolin

[5]25% Kaolin+75% Sand

*Additional reference from Rossato et al. (1992)

Table 2.2. Geotechnical parameters of tested clays in chapter 2

No.	Clay type	*Geotechnical Parameters*			
		w_n (%)	LL (%)	I_p (%)	OCR
1	Gault Clay	89	60	35	1.0
2	Speswhite Kaolin	120	66	33	1.0
3	Speswhite kaolin	120	66	35	1.4
4	Cornell Clay	30	33	11	6+
5	K-50[1]	60	30	14	1.0
6	Speswhite Kaolin	120	61	31	1.3
7	K-18[2]	28	35	16	1.2
8	K-33[3]	40	20	6	1.0
9	Partille Clay	48	52	31	1.0
10	K-100[4]	110	55	29	1.0
11	K-25[5]	40	20	6	1.0

Notes:

See notes in Table 2.1

Table 2.3. Chamber sizes and penetrometer information in chapter 2

No.	Clay type	*Dimensions of Chambers & Probes*		
		Chamber size (D*H in mm)	Cone Diameter, d (mm)	Probe Push Rate
1	Gault Clay	850 * 870	12.7	4 mm/s
2	Speswhite Kaolin	1001 * 1850	25.2	25 mm/s
3	Speswhite kaolin	1001 * 1850	11.3	25 mm/s
4	Cornell Clay	1370 * 2130	23.3	16 mm/s
5	K-50[1]	525 * 815	11.3	20 mm/s
6	Speswhite Kaolin	252 * 160	11.3	20 mm/s
7	K-18[2]	1200 * 1000	11.3	20 mm/s
8	K-33[3]	525 * 815	11.3	20 mm/s
9	Partille Clay	125 * 280	11.3	0.5 mm/s
10	K-100[4]	150 * 390	10.0	20 mm/s
11	K-25[5]	150 * 390	10.0	20 mm/s

Notes:

See notes in Table 2.1

2.3 Clay Friction Angle from Piezocone Penetration Test in Chamber Model

For evaluating soil behavior type, stress history, and other geo-parameters, the normalized cone resistance Q has been found valuable (e.g., Nyirenda 1988; Robertson 1990; Mayne 2007):

$$Q = (q_t - \sigma_{vo})/\sigma_{vo}' = q_{net}/\sigma_{vo}' \quad [2.1]$$

Similarly, the excess porewater pressures ($\Delta u = u_2 - u_0$) are useful when normalized:

$$B_q = \Delta u/q_{net} \quad [2.2]$$

2.3.1 Effective Friction Angle of Clays and Silts

Clays and silts will exhibit excess porewater pressures during penetration tests ($B_q > 0$). The effective stress limit plasticity solution developed at the Norwegian Institute of Technology (NTH) and detailed by Sandven and Watn (1995) provides a theoretical solution towards the evaluation of ϕ' for undrained penetration. In this approach, a cone resistance number (N_m) is defined as:

$$N_m = \frac{N_q - 1}{1 + N_u \cdot B_q} = \frac{q_t - \sigma_{vo}}{\sigma_{vo}' + a'} \quad [2.3]$$

where $a' = c' \cdot \cot \phi'$ = effective attraction term, c' = apparaent or effective cohesion intercept, $N_q = K_p \cdot \exp[(\pi - 2\beta) \cdot \tan\phi']$ = tip bearing capacity factor, $K_p = (1+\sin\phi')/(1-\sin\phi')$ is the passive lateral stress coefficient, β= angle of plastification (-40º to +30º) that defines the size of the failure zone around the cone tip, and $N_u = 6 \tan\phi' (1+ \tan\phi')$ = porewater pressure bearing factor.

The full solution allows for an interpretation of a paired set of effective stress Mohr-Coulomb strength parameters (c' and ϕ') for all soil types: sands, silts and clays, as well as mixed soils (Senneset et al. 1989). For the case where $\beta = 0$ (e.g., Terzaghi equation), the relationship for ϕ' in terms of N_m and B_q is presented in the following graphic form (Figure

2.1). In addition, when a′= c′= 0, the parameter N_m is identical to the normalized cone tip resistance, thus: $N_m = Q = q_{net}/\sigma_{vo}'$.

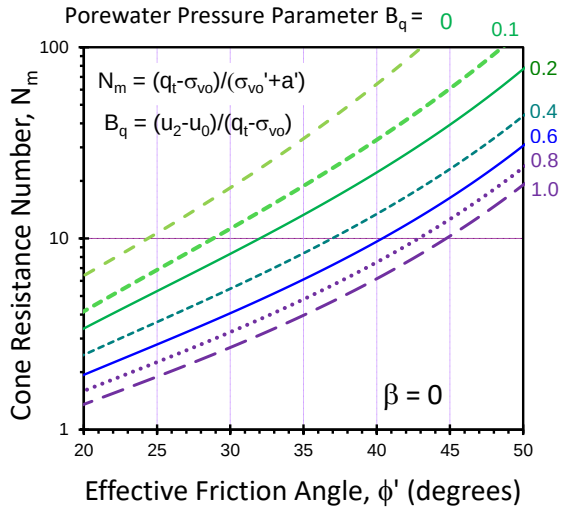

Figure 2.1. NTH Method for evaluating ϕ′ in silts and clays (modified after Sandven & Watn 1995)

Based on Equation [2.3], one can also establish a relationship between the cone resistance number Q and the normalized pore water pressure B_q in terms of effective stress friction angle ϕ′, and the paired Q-Bq for the 11 series of soft clays in this chapter are plotted and shown by Figure 2.2. Again, for this study, the solutions discussed are for a plastification angle β = 0.

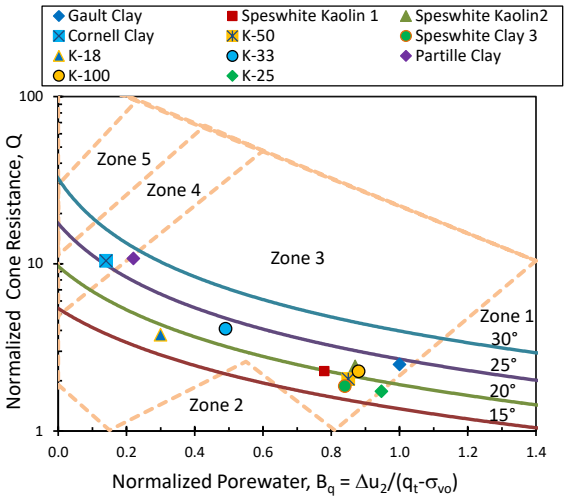

Figure 2.2. Chart for Soil Behavior Type (SBT) with superimposed dots from NTH method (modified after Robertson 1990)

An interesting finding is that it is completely compatible with the 9-zone soil behaviour type charts (Robertson, 1990, 1991). Therefore, a series of theoretical lines representing various values of effective stress friction angle ϕ' could be implemented into the soil behaviour type chart. The series of the friction angle lines cover from 15° to 30°.

The corresponding normalized pore water pressure B_q and cone resistance number Q values of the clays under investigation in this study are plotted on the Q-B_q chart to show the ranges of the soil types and effective stress friction angle ϕ'. Most of the soils under investigation fall within zone 3 and the soils could then be characterized as "clays and silty clays". The exception is the 50/50 kaolin-silica mix from Cornell which used a very fine silica (i.e., sand that is silt sized).

2.3.2 NTH Approximate method

In the original NTH solution, N_m is found as the slope by plotting q_{net} vs. σ_{vo}'. The parameter B_q can be taken as the slope of Δu vs. q_{net}.

Alternatively, Mayne (2005) derived an approximate NTH solution for obtaining ϕ' in soft to firm clays ($c' = 0$ and $\beta = 0$):

$$\phi' = 29.5\ B_q^{0.121}\ [0.256 + 0.336\ B_q + \log Q] \qquad [2.4]$$

Here, ϕ' is expressed as a function of B_q and Q. The lines in Figure 2.3 correspond to the approximation while the dots are derived from the theoretical solution. The above equation is valid for the following ranges when: $1 \leqslant OCR \leqslant 2.5$, $20^o \leqslant \phi' \leqslant 45^o$ and $0.05 \leqslant B_q \leqslant 1.0$.

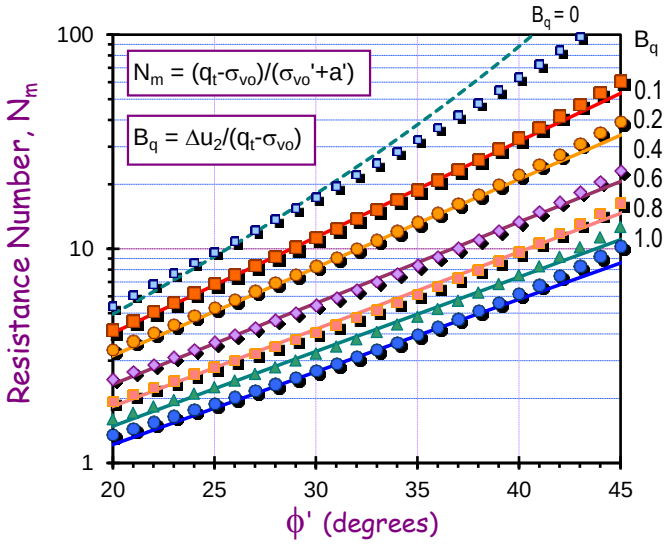

Figure 2.3. Approximate NTH Method for evaluating ϕ' (after Mayne 2005)

Using the chamber mini-cone and piezocone tip resistances (q_t) and porewater pressure readings (u_2), the NTH approximate equation is used for calculating the effective friction angle ϕ' and listed in Table 2.4. These values are compared with the measured laboratory triaxial test friction angles, also given in Table 2.4. The lab measured friction angles ϕ' of the clay soils are plotted against the NTH predicted ϕ', as shown in Figure 2.4. A value $\beta = -5°$ gave an excellent fit.

Table 2.4. Laboratory measured triaxial friction angles and NTH parameters from the mini-CPTu soundings

No.	Clay type	*Triaxial and CPTu Parameters*			
		Lab ϕ′	B_q	Q	NTH ϕ′ (deg)
1	Gault Clay	27.3	1.0	2.50	28.3
2	Speswhite Kaolin	23.0	0.78	2.28	25.1
3	Speswhite kaolin	25.0	0.87	2.43	27.1
4	Cornell Clay	31.5	0.14	10.4	30.7
5	K-50[1]	23.0	0.85	2.04	24.6
6	Speswhite Kaolin	22.0	0.84	1.85	23.3
7	K-18[2]	23.0	0.30	3.76	23.8
8	K-33[3]	26.0	0.49	4.08	27.9
9	Partille Clay	30.0	0.20	10.8	32.4
10	K-100[4]	24.0	0.88	2.27	26.3
11	K-25[5]	25.0	0.95	1.73	23.8

Note: assumes β=0°

An interesting aspect of kaolin clays is that the mineral form exhibits low frictional characteristics, while kaolin-sand mixtures have higher friction angles that are more consistent with natural clays (Rossato et al. 1992). The effective ϕ' for pure kaolins and kaolinites varies around 20° to 23°. Kaolin mixtures with fine silica and other sands give higher friction angles in the ranges of 27° to 33°, that are more or less common values of many natural clays (Leroueil & Hight 2003; Mayne 2012).

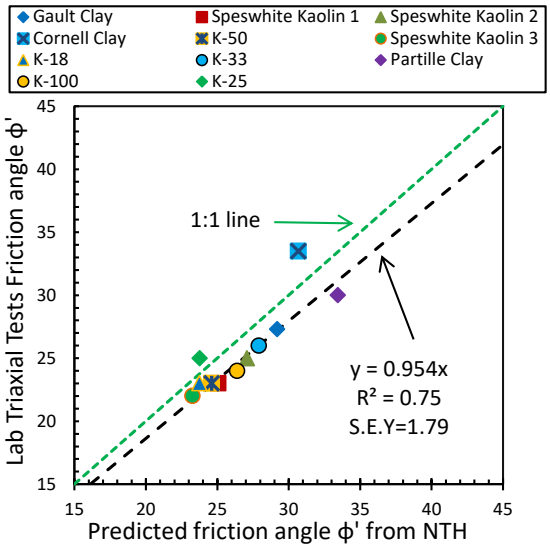

Figure 2.4. Lab Triaxial ϕ′ Versus NTH ϕ′ from CPTu

2.4 Undrained Shear Strength

Undrained shear strength s_u is not a unique parameter for a given clay, but depends upon the shearing mode, confining stress level, anisotropic stress state, strain rate, and other factors. The type of laboratory test mode for reference must be established so that consistent results are obtained.

2.4.1 Triaxial Compression Strength

In this chapter, the reference value for s_u is determined from undrained triaxial compression tests that are anisotropically consolidated (CAUC or CK_0UC), designated s_{uc}. Since some of the chamber test series used other testing for their reference values, a conversion was required for some of those s_u values to an equivalent CAUC mode.

Values from isotropically consolidated triaxial compression tests (CIUC) are only slightly higher than CAUC tests, generally 2 to 15% (Mayne 2012). The undrained shear strength in direct simple shear is approximately 70% of the strength in triaxial compression, thus: $s_{uDSS}/s_{uCAUC} = 0.7$ (Mayne 1985). For vane shear tests, Chandler (1988) showed that the undrained shear strength can be correlated with the CK_0UC strength through the following equation:

$$s_u(\text{vane})/s_u(CK_0UC) = 0.55 + 0.008\ I_p \qquad [2.5]$$

where the plasticity index (I_p) is in percent.

2.4.2 CPTu evaluation of undrained shear strength

For CPTu, the classical means to evaluate the undrained shear strength is in terms of the bearing capacity expression (Lunne et al. 1985):

$$s_u = \frac{q_t - \sigma_{v0}}{N_{kt}} = \frac{q_{net}}{N_{kt}} \quad [2.6]$$

where q_{net} = net cone resistance, N_{kt} = cone bearing factor, and σ_{v0} = total overburden stress. Values of N_{kt} have been reported to vary between 8 and 30 in actual practice (Lunne et al. 1997). Several factors, such as plasticity, stress history, stiffness, sensitivity, degree of fissuring, and fabric are known to be the causes for such wide variations.

For soft to firm normally-consolidated (NC) to lightly overconsolidated (LOC) clays, the cone factor N_{kt} has been shown to be about 12 ± 2 for the triaxial compression mode, based on recent studies (e.g. Low et al. 2010; Mayne et al. 2015).

Undrained shear strengths of the investigated soils of this research came from different modes (CAUC, direct simple shear, field vane shear test). They are converted to triaxial compression using the aforementioned approaches to set up a benchmark for comparison. The specific reference value used for each chamber series and the converted equivalent value to triaxial compression mode is listed in Table 2.5. The N_{kt} cone factor has been backcalculated by plotting the net cone resistance q_{net} against the laboratory undrained shear strength in triaxial compression (or converted back to the triaxial compression mode), as shown by Figure 2.5.

Table 2.5. Summary of undrained shear strengths of the clays for backcalculating the cone factor N_{kt}

No.	Clay type	*Undrained shear strength*	
		Measured s_u from original test mode (kPa)	Equivalent s_{uc} for triaxial compression mode (kPa)
1	Gault Clay	25.4[b]	30.6
2	Speswhite Kaolin	87.0[a]	87.0
3	Speswhite kaolin	132.0[a]	132.0
4	Cornell Clay	12.0[a]	12.0
5	K-50[1]	65.0[a]	65.0
7	K-18[2]	62.1[a]	32.1
9	Partille Clay	17.0[b]	21.3
10	K-100[4]	12.6[c]	18.1
11	K-25[5]	9.9[c]	14.2

[a]undrained shear strength from triaxial compression test

[b]undrained shear strength from vane shear test

[c]undrained shear strength from simple shear test

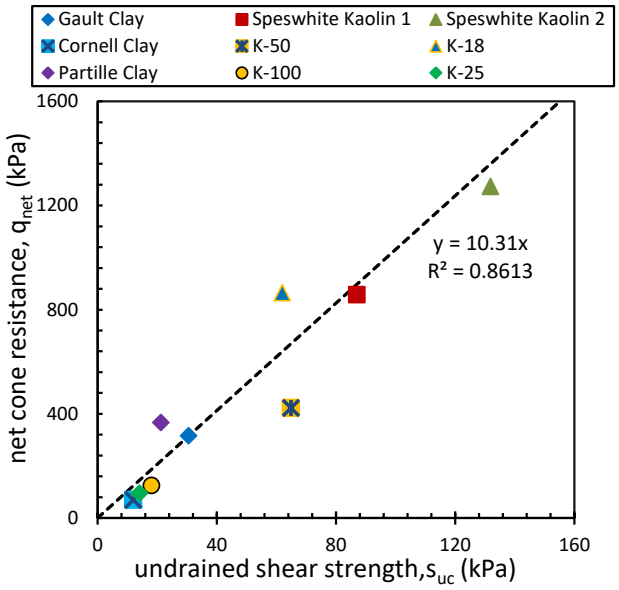

Figure 2.5. Net cone resistance q_{net} versus lab undrained shear strength s_{uc} in triaxial compression mode.

With piezocone tests, a second evaluation of undrained shear strength can be found from the measured excess porewater pressures (e.g., Lunne et al. 1997):

$$s_u = \frac{\Delta u}{N_{\Delta u}} = \frac{u_2 - u_0}{N_{\Delta u}} \qquad [2.7]$$

where $N_{\Delta u}$ = bearing factor. For natural soft to firm normally-consolidated NC-LOC clays, the cone factor $N_{\Delta u}$ has been shown to be about 6.5 ± 1.5 for the triaxial compression mode, based on recent studies (e.g. Low et al. 2010; Mayne et al. 2015).

The CPT chamber test series was used to prepare the plot of Δu versus s_u for the equivalent triaxial compression mode, with findings given in Figure 2.6. The regression slope provides the overall mean value of $N_{\Delta u}$ = 7.7 which is within the expected range.

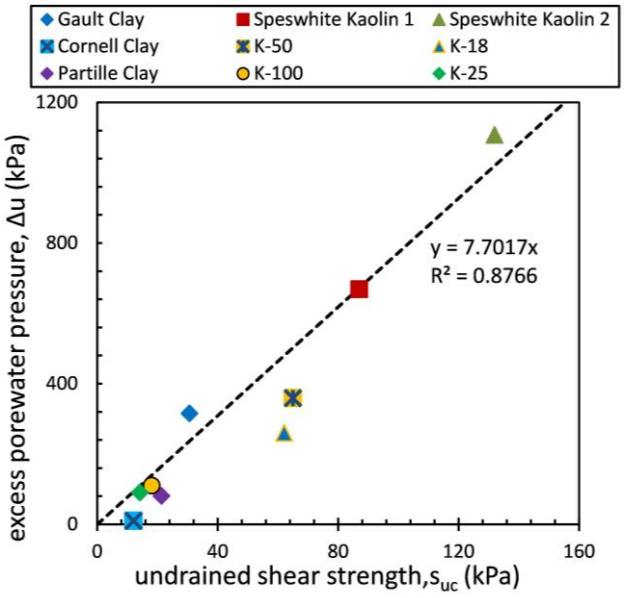

Figure 2.6. Chamber CPTu excess porewater pressure Δu versus lab s_{uc} in triaxial compression mode.

2.5 Conclusions

This chapter involves a review of cone/piezocone test data from calibration chamber tests on prepared clay deposits, mainly on kaolin based geomaterials. The chamber tests were conducted mainly on normally consolidated to lightly over-

consolidated kaolinites or kaolin-sand mixtures, with some tests including overconsolidated clays.

The effective stress limit plasticity solution developed at the Norwegian Institute of Technology (NTH) was adopted to evaluate the effective friction angle ϕ' of the clay soils under investigation which gave reasonable agreement (slight overprediction) when compared to laboratory ϕ' from triaxial tests. A further examination on the undrained shear strength (s_u) using the miniature cone data revealed that the backcalculated cone factor N_{kt} = 10.3 and $N_{\Delta u}$ = 7.7 could be adopted to predict the strength in triaxial compression mode.

CHAPTER 3. INTERPRETATION OF EFFECTIVE STRESS FRICTION ANGLE (ϕ') IN CLAYS USING CENTRIFUGE CPTU DATA

3.1 Introduction

The use of laboratory testing and artificially-prepared soils helps mitigate the issues of inherent variability and scatter from natural soil deposits when evaluating results from field tests. Also, it is possible to minimize the uncertainty involved in interpreting in-situ test results by verifying, in a calibration chamber, any analytical, theoretical numerical, or empirical relationship between a measured quantity and the reference soil parameters (Ouyang et al. 2016).

This chapter illustrates the interpretation of ϕ' from clays in centrifugal model chamber tests containing artificially-prepared soils under various accelerations and subjected to mini-piezocone penetration tests (CPTu). Results from a total of 13 centrifuge model test series on manufactured clayey soils, mainly kaolinitic clay deposits and silica-kaolin mixtures are investigated.

The data are taken from in-flight mini-piezocone penetrometer testing at constant penetration rates, as well as a few variable penetration rate tests (twitch testing). The total cone tip resistance (q_t) and penetration porewater pressure (u_2) at the shoulder position from the miniature penetrometers were recorded. Details on centrifuge model test dimensions, accelerations, piezocone diameters, test rate and soil parameters such as moisture content, liquid limit, plasticity index, and stress history were reviewed and tabulated.

The interpretation of the effective stress friction angle ϕ′ from CPTu is carried out using NTH limit plasticity solution from the Norwegian Institute of Technology (Senneset et al. 1989, Senneset & Janbu 1985). The evaluated effective stress friction angle ϕ′ from the centrifuge CPTu soundings are compared with benchmark values primarily obtained from laboratory CAUC and/or CIUC triaxial tests on the corresponding soils to examine the validity of the solution.

3.2 Centrifuge Model Testing

3.2.1 Principles of centrifuge modelling

The geotechnical centrifuge is a useful tool to study the mechanical behaviour of soils for very large physical structures in order to allow modelling at large strains where failure is too costly to conduct at full scale (Schofield 1980). The centrifuge applies an increased gravitational acceleration to small-scale physical models to produce identical self-weight stresses in the model that simulate those in the prototype. Thus, results from the centrifuge model tests can be utilized to validate and calibrate analytical and/or numerical methods. Details on the principles and operations of the centrifuge, scaling laws, equipment, and procedures are given by Springman et al. (2010).

3.2.2 Geomaterials used in centrifuge tests

The centrifuge series reviewed in this study were collected from laboratory programs established at the University of Western Australia, Cambridge University, National University of Singapore, University of Colorado Boulder, and Zhejiang University, which have different equipment, acceleration capacities, and dimensions.

For this study, the focus was on clayey type soils and the geomaterials that were subjected to centrifuge modelling are mainly kaolinitic type clay deposits and silica-kaolin and or clay-sand mixtures which are prepared initially as a slurry and then consolidated in the model chambers. For the majority of the soils studied in this paper, the stress histories applied in the chamber tests focused on normally consolidated (NC) to lightly-overconsolidated (LOC) clay deposits. A special series of tests by Cinicioglu et al. (2006) investigated a range of tests with $1 \leqslant$ OCRs $\leqslant 150$, where OCR = σ'_p / σ'_{vo} = overconsolidation ratio.

Table 3.1 shows the summary information on the centrifuge series including accelerations, clay types, and their data reference sources.

Table 3.1. Centrifuge model test series reviewed in chapter 3

No.	a_g	Clay type	Reference
1	100	Kaolin 1	Teh et al (2007)
2	100	Sandy Kaolin	Teh et al (2006)
3	160	Kaolin 2	Schneider (2008)
4	110	Kaolin 3	Mahmoodzadeh & Randolph (2014)
5	160	Kaolin 4	Randolph & Hope (2004)
6	100	Pisa Clay 1	Burland et al (2003) (1)
7	100	Pisa Clay 2	Burland et al (2003) (1)
8	100	Pisa Clay 3	Burland et al (2003) (1)
9	150	Speswhite Kaolin	Cinicioglu et al. (2006) (2)
10	30	Clayey Sand	Zhou et al (2014)
11	50	Silica flour	Silva & Bolton (2005)
12	100	K75-S25(3)	Fitzgerald (2009)
13	75	China Kaolin	Esquivel and Silva (2000)

NOTES:

a_g = centrifuge acceleration in g's, where 1 g = 9.8 m/s^2

(1) Additional data from Jamiolkowski & Pepe (2001)

(2) Additional information from Cinicioglu et al. (2007)

(3) Mixture of 75% kaolin + 25% sand

Table 3.2 illustrates the geotechnical index parameters for each clay deposit which was prepared, such as water content, liquid limit, plasticity index, and overconsolidation ratio. The initial water contents (w_n) of the soils before the consolidation stage ranged from 30% to 136%, the liquid limit (LL) was between 27% to 80%, and the plasticity index (PI) varied around 2% to 35%.

Table 3.2. Geotechnical parameters of the clayey soils in the centrifuge series

No.	Clay type	Indices			
		w_n (%)	LL (%)	PI (%)	OCR
1	Kaolin 1*	120	61	27	1.0
2	Sandy Kaolin	120	80	35	1.0
3	Kaolin 2	120	61	34	1.0
4	Kaolin 3*	120	61	27	1.0
5	Kaolin 4*	120	61	27	1.0
6	Pisa Clay 1	88	71	29	1.6
7	Pisa Clay 2	88	52	24	1.2
8	Pisa Clay 3	88	56	23	1.1
9	Speswhite Kaolin	136	53	21	1.0
10	Clayey Sand	NA	NA	27	1.0
11	Silica flour	31	27	2	NA
12	K75-S25	92	46	22	NA
13	China Kaolin	106	53	21	1.0

*Note: same type of kaolin used

3.2.3 Mini-piezocone penetration tests in centrifuge

Each of the soil deposits was tested using miniature piezocone penetrometers. Most of the probes had a diameter of d=10mm, except the penetrometers adopted by Zhou et al (2014) and Silva & Bolton (2005) where d=12mm, and Cinicioglu et al. (2006) used a mini cone with d=11.3 mm. The equivalent prototype depth was calculated as the product of the model depth times the acceleration.

Two sets of CPTu test series are analyzed to observe the influence of penetration rate: (a) inflight penetration with a constant push rate test, and (b) a limited series of twitch tests with variable penetration rates. Table 3.3 lists the details about the centrifuge chamber sizes (rectangular shape chamber/cylindrical chamber), penetrometer probe dimensions, and the corresponding penetration rates that were adopted for analysis in these test series.

A non-dimensional velocity parameter $V = v \cdot d/c_v$, where v= push rate, d = cone diameter and c_v = coefficient of consolidation has been defined to determine the drainage regime of the soils during testing (DeJong et al 2013, Randolph & Hope 2004), where a V>30 indicates undrained penetration. For most of the centrifuge testing series investigated in this paper, it is believed that the geomaterial undergo undrained penetration process, except for the twitch test series studied in the later section of the paper, which simulate different drainage regimes.

Table 3.3. Chamber sizes and penetrometer information

Soil No.	Equipment and Test Parameters			
	Chamber size [(1)]	d (mm)	v (mm/s)	V
1	650·390·340	10	1	64
2	500·370[(2)]	10	2.5	40
3	650·390·325	10	3	630
4	650·390·325	10	0.0045 to 1	160[(3)]
5	650·390·325	10	1	120
6	850·400[(2)]	10	1	NA
7	850·400[(2)]	10	1	NA
8	850·400[(2)]	10	1	NA
9	606·537[(2)]	11.3	20	400
10	730·350·300	12	1	NA
11	850·400[(2)]	12	2 to 8	>40
12	650·390·325	10	1	62
13	NA	12.7	NA	NA

[(1)] Rectangular chamber: Length · Width · Height (mm)

[(2)] Cylindrical chamber: Diameter · Height (mm)

[(3)] V varies from 1 to 160 based on different push rate

3.3 Effective Friction Angle from Centrifuge CPTu

Soft to firm to stiff intact clays will exhibit excess porewater pressures during penetration tests ($\Delta u > 0$). An effective stress limit plasticity solution from NTH was derived for the CPTu (Senneset & Janbu 1985) towards the evaluation of ϕ' during undrained penetration. The full solution allows for an interpretation of a paired set of effective stress Mohr-Coulomb strength parameters (c' and ϕ') for all soil types, including: sands, silts and clays, as well as mixed soils (Sandven 1990).

Ouyang et al. (2016) reviewed data from 11 series of 1-g clay chamber tests using miniature cone and piezocone penetrometers and found that the NTH solution gave good evaluations of ϕ' for prepared deposits of clays, mostly having used kaolin and/or kaolinite-sand mixtures in these testing programs. In a larger study, Ouyang and Mayne (2018) helped to verify the limit plasticity NTH solution by calibrating the theory with data from 105 field sites underlain by natural clays and clayey silts that were subjected to both field CPTu and laboratory triaxial testing.

For the specific case ($c' = 0$, $\beta = 0°$), a closed-form version of the analytical solution was derived for calculating the effective stress friction angle ϕ' for clays, silty clays, and clayey silts in the following mathematical format:

$$Q = \frac{\tan^2(45° + \phi'/2) \cdot \exp(\pi \cdot \tan\phi') - 1}{1 + 6 \cdot \tan\phi' \cdot (1 + \tan\phi) \cdot B_q} \qquad [3.1]$$

where the original NTH cone resistance number (N_m) is equal to $Q = q_{net}/\sigma_{v0}'$ = normalized cone tip resistance, and $B_q = \Delta u/q_{net}$ = porewater pressure parameter, $q_{net} = q_t - \sigma_{v0}$ = net cone resistance, and $\Delta u = u_2 - u_0$ = measured excess porewater pressure.

A full inversion of Equation [3.1] is not possible, yet an approximate solution can be developed over an expected range of effective stress friction angles ($20^o \leqslant \phi' \leqslant 45^o$) and limited values of porewater pressure parameter ($0.05 \leqslant B_q \leqslant 1.0$):

$$\phi' \approx 29.5° \cdot B_q^{0.121} [0.256+0.336 \cdot B_q + \log Q] \qquad [3.2]$$

The approximate expression is compared with the actual closed-form analytical solution in Figure 3.1 and seen to be in reasonable agreement over the specified ranges of ϕ' and B_q. The solution applies to NC nad LOC clays where OCR$\leqslant$ 2.5.

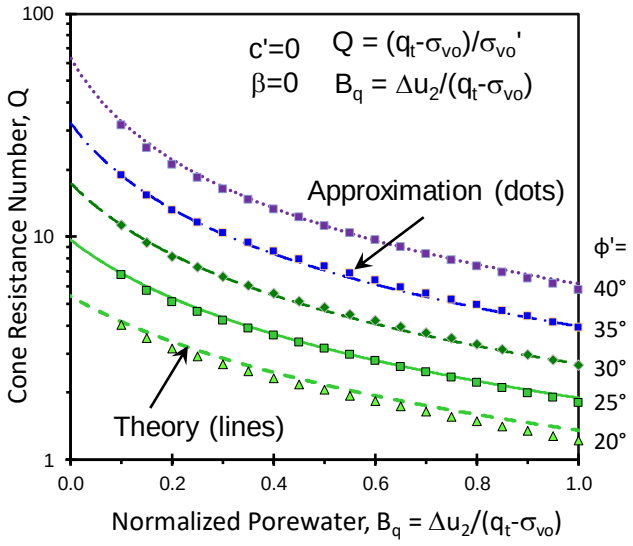

Figure 3.1. NTH method for evaluating ϕ' from CPTu in intact clays and clayey silts using approximate and exact solutions

3.4 Application of NTH in Centrifuge Series

Most of the data from in-flight mini-piezocone tests in centrifuge series were taken at constant rates of penetration. In a few special series, termed "twitch tests", the piezocone series recorded the penetration readings at variable rates of penetration. Selected examples are presented in the following subsections to illustrate the application of the NTH method.

3.4.1 Constant rate piezocone testing in centrifuge

Centrifuge testing on kaolin (Soil ID No. 3) was performed using the beam centrifuge at the University of Western Australia (UWA). The clay samples were prepared in 325 mm high strong boxes with plan dimensions of 390mm by 650mm. Normally-consolidated kaolinitic clay having a liquid limit of 61%, plasticity index of 34%, and initial water con-tent of around 55% to 70% was prepared as slurry and consolidated. Afterwards, the deposit was subjected to an acceleration of 160g and inflight piezo-cone tests made with a constant probe push rate of 3 mm/s. Miniature piezocone penetration test were conducted using a 10mm diameter penetrometer with a 60degree tip angle, which has a polypropylene filter element behind the 1 mm high cone shoulder to measure u_2. The cone did not have a friction sleeve (Schneider 2008).

Figure 3.2 illustrates the profiles of the net cone resistance ($q_{net} = q_t - \sigma_{vo}$) and the excess pore water pressures ($\Delta u = u_2 - u_0$) measured during the centrifuge piezocone penetration test. The corresponding profiles of cone resistance number Q and normalized porewater pressure B_q are also shown in Figure 3.2.

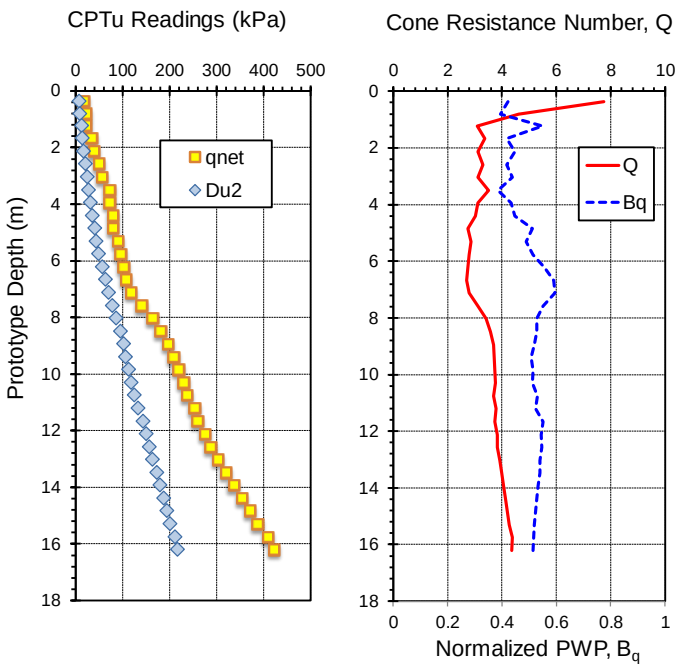

Figure 3.2. Profiles of q_{net}, Δu, Q and B_q in NC kaolin in centrifuge testing (data from Schneider 2008)

The input parameters Q and B_q for calculating the friction angle ϕ' using the NTH solution can also be found by the following process. The cone resistance number Q is found as the slope from plotting net cone resistance q_{net} vs. effective overburden stress σ'_{v0}, as illustrated in Figure 3.3 . In this example, we force the line through the origin (assuming c' =0) to obtain Q =3.88. By the same token, the normalized porewater parameter B_q is determined as the slope of measured excess porewater pressure $\Delta u = (u_2-u_0)$ versus net cone resistance q_{net}, giving the value of $B_q = 0.53$ for this sounding, as indicated by Figure 3.4. The paired Q-B_q are the input for friction angle calculation and according to Figure 3.1, and the evaluated ϕ' from the CPTu sounding is $\phi' = 28.3°$. This value compares well with a measured value of $\phi' = 28.6°$ obtained from laboratory direct simple shear test (DSS) on the same soil, as confirmed by Figure 3.5.

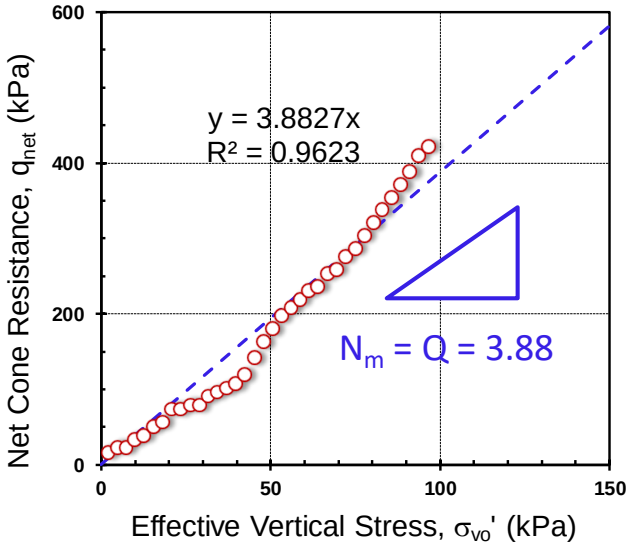

Figure 3.3. Derivation of the cone resistance number Q for kaolin 2 (data from Schneider 2008)

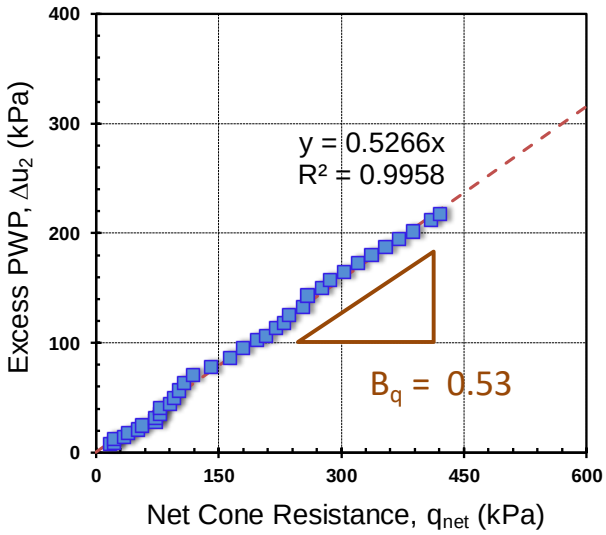

Figure 3.4. Derivation of porewater pressure parameter B_q for kaolin 2 (data from Schneider 2008)

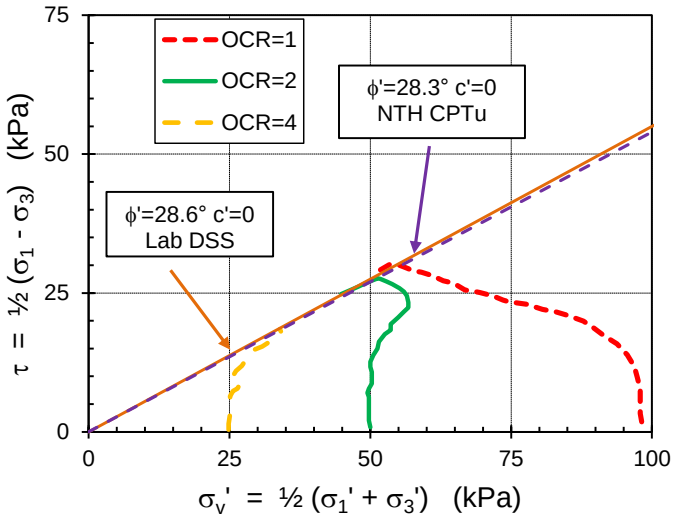

Figure 3.5. Comparison of NTH evaluated effective friction angle ϕ' from CPTu with lab DSS (data from Schneider 2008)

3.4.2 CPTu twitch tests in110g acceleration centrifuge models

A special series of CPTu soundings that are conducted at variable penetration rates are termed twitch tests (Randolph 2004; DeJong et al. 2013). Twitch testing is known to influence the measured magnitudes of cone resistance q_t and porewater pressure u_2 and was devised to study the quantify the effects of partial drainage, viscous behavior, and dissipation response of soils (Randolph & Hope 2004). In low permeability soils, by varying the CPTu penetration rate during centrifuge testing, one can monitor the consolidation conditions from undrained to partially-drained to fully drained. In this case study, a series of centrifuge CPTu of various probe push rates on normally consolidated kaolin under an acceleration of 110g were done by UWA to examine the sensitivity of the NTH method in evaluating ϕ'.

As reported by Mahmoodzadeh and Randolph (2014), a commercial dry kaolin (clay ID No. 4 in Table 3.1) was mixed under a vacuum at an initial water content of 120%

before being placed above a sand drainage layer in the centrifuge strongbox. Consolidation was applied in steps with the final sample height recorded at 230mm and corresponding to a prototype depth of 25.3m.

Penetration rates for these six twitch test series varied from 1 mm/s to 0.0045 mm/s and the effect of the testing rate on the interpretation of the soil parameters were analyzed. The change of the penetration rate could indicate the change of the drainage condition during the penetration for the kaolin clays subjected to CPTu, with the fastest rate of 1 mm/s to be undrained penetration and the lowest rate 0.0045 mm/s to be drained. Table 3.4 lists the information about the twitch testing ID, the corresponding penetration rate, the net cone resistance q_{net} at the final test depth, the excess porewater pressure Δu at the final test depth, the cone resistance number Q, the normalized porewater pressure parameter B_q and the evaluated ϕ' using the NTH approximate solution. It is observed that the magnitude of Q increases and B_q decreases as the penetration rate decreases (undrained to drained). However, when the paired sets of Q and B_q are plotted on the NTH solution chart given by Figure 3.6, they all follow the same friction angle contour ($\phi' = 23°$), indicating agreement with the NTH solution for effective stress penetration.

Table 3.4. Measured q_{net} and Δu plus derived B_q and Q from CPTu centrifuge twitch testing on kaolin (data from Mahmoodzadeh & Randolph 2014)

ID	v (mm/s)	q_{net} (kPa)	Δu (kPa)	B_q	Q	NTH ϕ'
PC-1	1	207	146	0.71	2.0	22.2°
PC-2	0.45	249	148	0.59	2.4	22.9°
PC-3	0.15	300	126	0.42	2.8	22.6°
PC-4	0.045	405	71	0.18	3.8	21.4°
PC-5	0.015	495	28	0.06	4.7	19.7°
PC-6	0.0045	501	9	0.02	4.7	19.0°

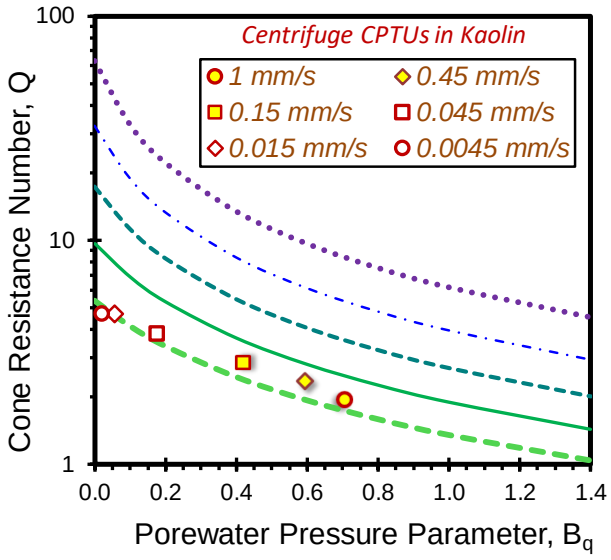

Figure 3.6. NTH CPTu evaluated ϕ' for kaolin subjected to centrifuge twitch testing (data from Mahmoodzadeh & Randolph 2014)

3.5 Database Summary

For all 13 series of CPTu centrifuge tests at constant penetration rates, Table 3.5 provides the individual cone resistance number (Q) and normalized porewater pressure readings (B_q) with their corresponding NTH effective friction angle ϕ′ and the measured benchmark ϕ′ from laboratory testing.

Table 3.5. Laboratory measured friction angles and NTH parameters from the centrifuge CPTu soundings

No.	Clay type	Lab and CPTu Parameters			
		Lab ϕ′	B_q	Q	NTH ϕ′
1	Kaolin 1	23.0°	0.18	5.35	25.1°
2	Sandy Kaolin	23.0°	0.29	3.73	23.5°
3	Kaolin 2	28.6°*	0.54	3.9	28.3°
4	Kaolin 3	23.0°	0.71	2.0	22.2°
5	Kaolin 4	23.0°	0.57	2.43	23.0°
6	Pisa Clay 1	23.5°	0.34	3.95	25.0°
7	Pisa Clay 2	28.0°	0.71	3.16	28.1°
8	Pisa Clay 3	27.0°	0.59	3.1	26.2°
9	Speswhite Kaolin	25.2°	0.92	1.87	24.4°
10	Clayey Sand	31.0°	0.05	20	32.3°
11	Silica flour	36.6°	0.01	100	37.1°
12	K75-S25	25.0°	0.37	4.22	26.4°
13	China Kaolin	23.0°	0.45	3.46	25.0°

Notes:

(a) lab reference ϕ' from triaxial compression tests

(b) *from lab DSS tests shown in Figure 3.5

Figure 3.7 presents a summary plot for the measured laboratory friction angle values versus the CPTu-determined values from centrifuge tests. Two sets of statistical measures were made on the data set, including: (a) arithmetic statistics, and (b) regression statistics, as indicated on the figure. The measured laboratory ϕ' cover the range from 23.2° to 36.6° and the CPTu-evaluated ϕ' values range from 20.8° to 37.1°. From the arithmetic measures, the ratio of measured/evaluated values ranges from 0.91 to 1.10 with an overall mean of 1.0 and standard deviation = 0.05, giving a corresponding COV (coefficient of variation) = 0.05. From the regression evaluations of laboratory vs. field values, the slope m = 0.99 with a coefficient of determination of r^2 = 0.908 and standard error of the Y-estimate SEY = 1.15 for a best fit line. The above statistics generally support that the NTH method gives a reasonable evaluation of the effective friction angle when compared with the laboratory reference value.

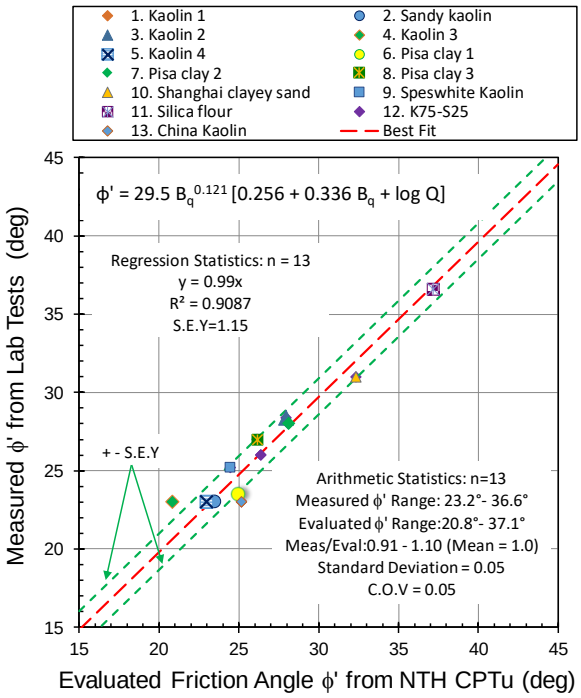

Figure 3.7. Comparison of laboratory benchmark measured ϕ' versus NTH-evaluated ϕ' from centrifuge CPTu series

3.6 Conclusions

Data from 13 series of in-flight mini-piezocone penetrometer tests in centrifuge deposits were reviewed for verifying the NTH limit plasticity solution (Sandven 1990; Senneset et al. 1989) in assessing the effective friction angle of normally consolidated to lightly over-consolidated clays and clayey silts. The majority of artificially-prepared deposits of clays included kaolinites or kaolin-sand mixtures. Primarily, the friction angle ϕ' from laboratory triaxial compression tests served as the reference benchmark value. Results from constant penetration rate CPTu soundings gave good agreement with laboratory determined ϕ'. In addition, one series of CPTu twitch tests on kaolin clay at variable rates showed that as the behavior varied from undrained to partially drained to fully drained, the changes in Q and B_q correspondingly followed the same ϕ' contours established by the NTH solution.

CHAPTER 4. EFFECTIVE FRICTION ANGLE OF CLAYS AND SILTS FROM FIELD PIEZOCONE PENETRATION TESTS

4.1 Introduction

The piezocone penetration test (CPTu) is a quick in situ test that permits the delineation of soil stratigraphy and the interpretation of geo-parameters with depth in an efficient, economic, and expedient manner. Details concerning the CPTu equipment, field test procedures, and interpretations are given by Lunne et al. (1997), Mayne (2007), and Schnaid (2009).

The piezocone penetration test provides three separate readings with depth, including uncorrected cone tip resistance (q_c), sleeve friction (f_s), and pore-water pressure at the shoulder (u_2). The measured q_c is converted to total cone tip resistance (q_t) using $q_t = q_c + (1 - a_{net}) \cdot u_2$, where a_{net} is defined as net area ratio (Campanella and Robertson 1988). The piezocone can evaluate a wide variety of geotechnical parameters, such as soil behavioral type (SBT), unit weight (γ_t), overconsolidation ratio (OCR), undrained shear strength (s_u) of clays, effective stress friction angle in sands (ϕ'), Young's modulus (E), lateral stress coefficient (K_0), and coefficient of consolidation (c_v), as well as an assessment of liquefaction potential (Robertson 2009).

For the CPTu, an effective stress limit plasticity solution has been developed for the evaluation of the effective stress friction angle (ϕ') for drained to undrained penetration for a variety of soils ranging from sands to silts to clays, as documented by the Norwegian Institute of Technology (NTH) and detailed by Janbu and Senneset (1974), Senneset and Janbu (1985), Senneset et al. (1989), Sandven (1990), and Sandven and Watn (1995). While the NTH solution has been used in Norway and parts of Sweden for some time, little

appreciation and application has been acknowledged in other countries. Thus, the intent of this chapter is fourfold: (i) review the procedures for assessing ϕ', (ii) introduce an approximate version of this solution, (iii) present several case study examples, and (iv) provide a collection of data from a number of worldwide sites to compare reference values from laboratory triaxial tests with values of ϕ' interpreted from corresponding CPTu soundings.

All triaxial tests were of the compression type mode under undrained loading (i.e., constant volume) with pore-water pressure measurements taken during shearing. These included isotropically consolidated (undrained triaxial compression, CIUC), K_0-consolidated, CK_0UC), as well as general anisotropic (undrained consolidated anisotropic, CAUC) types. Triaxial data from 47 different clays tested by both CK_0UC (or CAUC) and CIUC modes showed that the magnitude of ϕ' was similar; i.e., ϕ' (CK_0UC or CAUC) = 0.96 ϕ' (CIUC) with r2 = 0.923 and a standard error of the Y estimate (S.E.Y.) = 2.0° (Kulhawy and Mayne 1990). The reported ϕ' for these clays ranged from 18° to 42°. Generally, the value of ϕ' was defined at maximum deviatoric stress; however, in some cases an alternative definition (e.g., maximum obliquity, large strain, critical state) was utilized (Lade 2016). Also, in several circumstances, ϕ' was reported by the source, but the actual criterion used was not documented. Additional discussion on the choice of this criterion is given in a later section of this chapter.

4.2 Effective Stress Limit Plasticity Solution

Soft to firm to stiff intact clays will exhibit excess porewater pressure during penetration tests ($\Delta u > 0$, where $\Delta u = u_2 - u_0$). Janbu and Senneset (1974) proposed an effective stress limit plasticity solution for the CPTu towards the evaluation of ϕ' for undrained penetration. In this approach, the cone resistance number (N_m) is defined as

$$N_m = \frac{N_q - 1}{1 + N_u B_q} = \frac{q_t - \sigma_{v0}}{\sigma'_{v0} + a'} \quad [4.1]$$

where $B_q = (u_2 - u_0)/q_{net}$ is the normalized pore-water pressure parameter, u_0 is the hydrostatic porewater pressure, $q_{net} = q_t - \sigma_{v0}$ is the net cone resistance, σ_{v0} is the initial vertical stress, σ'_{v0} is the initial vertical effective stress, $a' = c' \cot\phi'$ is the effective attraction, and c' is the effective cohesion intercept. The tip bearing capacity factor, N_q, and the pore-water pressure bearing factor, N_u, are given by (Senneset et al. 1989).

$$N_q = K_p exp[(\pi - 2\beta) tan\phi'] \quad [4.2]$$

$$N_u = 6 tan\phi'(1 + tan\phi') \quad [4.3]$$

$$K_p = (1 + sin\phi')/(1 - sin\phi') \quad [4.4]$$

where K_p is the passive lateral stress coefficient and is the angle of plastification ($-40° < \beta < +30°$) that defines the size of the failure zone (Senneset and Janbu 1985).

The full solution allows for an interpretation of a paired set of effective stress Mohr–Coulomb strength parameters (effective cohesion intercept, c', and ϕ') for all soil types, including: sands, silts, and clays, as well as mixed soils (Sandven 1990; Mayne 2016). The parameter N_q is the tip bearing capacity factor from limit plasticity solutions that is well known for pile foundations. For the case where $\beta = 0°$, N_q is identical to the classical solution for a deep foundation (i.e., Terzaghi equation). The parameter N_u is a pore-water pressure bearing factor (Senneset et al. 1989). The NTH analytical model was calibrated by Sandven (1990) using data from six onshore and one offshore clay from Norway, as well as supported by finite element simulation.

When $a' = c' = 0$, the parameter N_m is identical to the normalized cone tip resistance, $Q = (q_t - \sigma_{v0})/\sigma'_{v0}$, that is used extensively in CPTu interpretations (Lunne et al. 1997;

Mayne 2007; Robertson 2009). Thus, a relationship between ϕ' and the cone parameters (Q and B_q) can be expressed as a single equation:

$$Q = \frac{tan^2(45°+\phi'/2)exp(\pi tan\phi')-1}{1+6tan\phi'(1+tan\phi')B_q} \quad [4.5]$$

which is shown graphically in Figure 4.1.

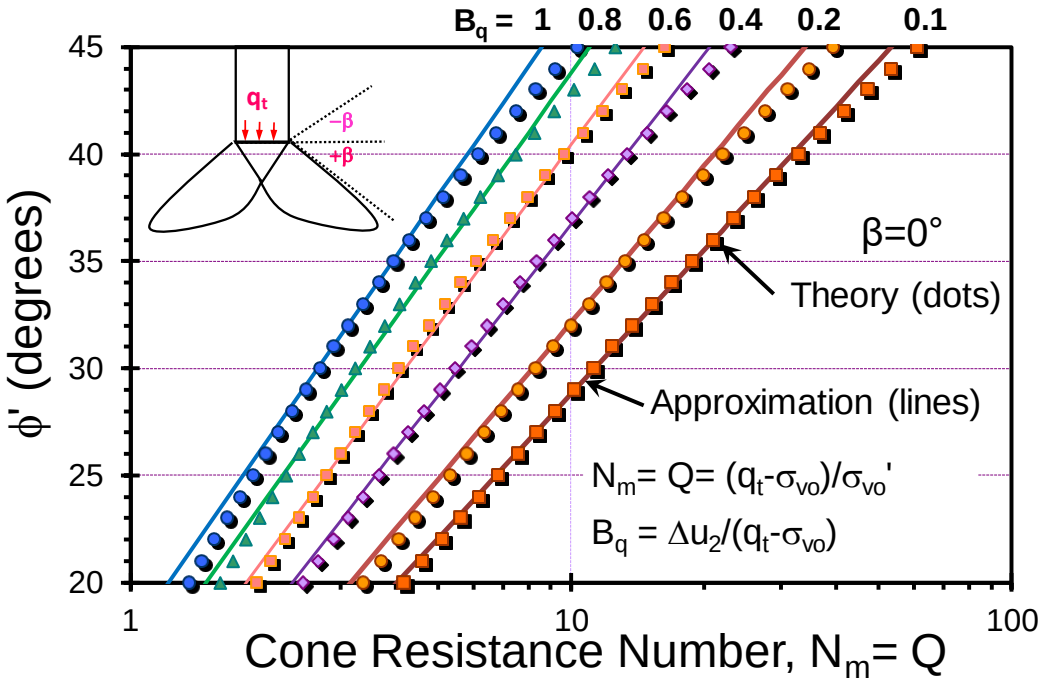

Figure 4.1. NTH method for evaluating ϕ' from CPTu in silts and clays.

A full inversion of Equation [4.5] is not possible, yet an approximate solution (Mayne 2007) can be developed over the ranges shown in parentheses for effective stress friction angles ($20° \leqslant \phi' \leqslant 45°$) and the normalized pore-water pressure parameter ($1 \leqslant OCR \leqslant 2.5$, $0.05 \leqslant B_q \leqslant 1.0$):

$$\phi' \approx 29.5{B_q}^{0.121}(0.256 + 0.336B_q + logQ) \quad [4.6]$$

The approximate solution is also presented in Figure 4.1 and can be seen to be in good agreement with the theoretical values over the specified limiting values of ϕ' and B_q.

4.3 Angle of Plastification

The plastification angle (β) in the NTH model is a means to adjust the size of the failure region in the vicinity of the penetrometer tip. With a positive value of β, a smaller region of zone is realized; whereas a negative β indicates a larger zone. This is analogous to the state parameter, ψ, that is used in critical state soil mechanics to represent drained soil behavior: $\psi > 0$ is characteristic of loose sands that tend to show a volumetric decrease, versus dilative soil behavior that exhibits an increase in volumetric strain and is represented by $\psi < 0$ (Robertson 2016). As such, a theoretical value of $\psi = 0$ is indicative of no volume, V, change ($\Delta V/V_0 = 0$, where V_0 is the initial volume), and thus is characteristic of undrained loading at constant volume. This provides the basis for starting with a set value of $\beta = 0$ for the following developments. Additional discussion on variable β values is given towards the end of this chapter.

In early presentations of the NTH solution (e.g., Senneset and Janbu 1985), it was suggested that values were associated with soil types. For clays, the range indicated was approximately $0° \leqslant \beta \leqslant +15°$ and other ranges were assigned to silts and sands. Later, Sandven (1990) re-evaluated data in soft–firm clays and suggested the range $-10° \leqslant \beta \leqslant +10°$. However, both studies were based on limited data, mainly from the North Sea and Norway, the latter also known for having sensitive to quick deposits.

4.4 Triaxial-Piezocone Database

A special database was compiled from 105 natural deposits of clay, silty clay, and clayey silt that were subjected to both field CPTu and laboratory triaxial compression tests, as documented in Table 4.1. These sites primarily comprise soft to firm clays and silts that have varying degrees of overconsolidation ratio (OCR), yet the majority were normally consolidated (NC) to lightly overconsolidated (LOC) with $1 < OCR < 2.5$. Geologic origins

of these soils include marine, alluvial, estuarine, glacial, deltaic, and lacustrine. The specific names of these sites, their locations, and their corresponding reference sources that reported the piezocone and triaxial data are noted in Table 4.1. The CPTu input parameters Q and B_q needed for the NTH analysis and the mean values of laboratory-measured water content, plasticity, and benchmark ϕ' results are also given.

Plasticity characteristics of these fine-grained soils ranged widely from very lean to highly plastic (4% < PI < 113%, where PI is the plasticity index). The mean value of PI was 38.9%, which has a standard deviation (S.D.) of 23.3%. Water contents ranged from 20% to 160% with a mean = 61.6% and S.D. = 31.2. Effective friction angles from triaxial tests ranged from 20.2° to 45.1°, with a mean value $\phi' = 31.6°$ and S.D. = 4.5°, determining a coefficient of variation (COV) = 0.145. The NTH solution using CPTu data gave a mean value $\phi' = 32.2°$ (assumed $\beta = 0°$ and $a' = 0$) and S.D. = 4.4°, determining a COV = 0.135, therefore indicating an overall very slight overestimation. Corresponding sensitivities that were reported generally were in the range of 2–8, indicating low to medium sensitive soils, except several high-sensitivity clays in eastern Canada and Scandinavia.

Table 4.1. List of clay sites subjected to laboratory triaxial and in situ piezocone penetration tests (CPTu) for NTH calibration study

Site name	Location	Soil description	Depth range (m)	Mean w_n (%)	Mean PI (%)	Total unit weight (kN/m^3)	CPTu Q	CPTu B_q	NTH ϕ' (°)	Triaxial ϕ' (°)[a]	References
17th St Canal	Louisiana	Alluvium	4-12	45	20	18.0	3.51	0.33	23.5	22.0*	Seed et al. (2006) (2008)
Adriatic shelf	Italy	Marine Clay	0-35	65	15	17.0	4.50	0.55	31.3	33.5	Sultan et al. (2008)
Agnesburg	Norway	Marine Clay	5-32	45	24	15.1	4.00	0.75	31.6	32.0	Åhnberg (1995)
Amazon River	Brazil	Alluvial Clay	5-45	70	50	16.0	3.92	0.74	31.2	31.5	Sandroni et al. (2015)
Amherst	Massachusetts	Lacustrine Varved Clay	5-11	48	15	17.1	5.50	0.70	34.8	31.7*	DeGroot & Lutenegger (2003); Sambhandharaska (1977)
Anacostia NAS	Washington, DC	Soft Alluvial Clay	5-18	65	32	15.9	7.60	0.54	36.0	35.1	Mayne (1987)
Ariake	Japan	Soft Marine Clay	4-17	106	68	13.5	5.18	0.55	31.7	32.0	Watabe et al. (2003)
Athlone	Ireland	Laminated Clay	6-12	41	35	18.0	5.70	0.40	30.3	26.0	Long et al. (2001)
Bäckebol	Sweden	Soft Inorganic Clay	4-12	60	45	16.5	5.13	0.58	32.1	30.0*	Larsson & Mulabdić (1991)
Ballina	Australia	Soft Estuarine Clay	3-11	107	66	14.1	3.61	0.68	29.3	32.0	Pineda et al. (2014); Kelly et al. (2017)
Bangkok	Thailand	Soft Marine Clay	4-9	74	61	15.4	3.33	0.77	29.6	27.4	Tanaka et al. (2001)

Table 4.1. List of clay sites subjected to laboratory triaxial and in situ piezocone penetration tests (CPTu) for NTH calibration study (continued)

Site name	Location	Soil description	Depth range (m)	Mean w_n (%)	Mean PI (%)	Total unit weight (kN/m^3)	CPTu Q	CPTu B_q	NTH ϕ' (°)	Triaxial ϕ' (°)[a]	References
Baton Rouge[c]	Louisiana	Stiff OC Deltaic Clay	5-12	32	33	18.5	14.3	0.02	28.1	28.5	Chen & Mayne (1994)
Barra da Tijuca	Brazil	Soft Marine Clay	2-18	160	105	13.0	2.80	0.60	25.1	28.0	Marcio et al. (2013); Macedo (2004)
Baytown[c]	Texas	Stiff OC Clay	2-15	22	31	19.8	40.00	0.01	31.5	28.2	Stuedlein et al. (2012)
BBC Saugus	Massachusetts	Glaciomarine Clay	10-30	41	24	17.5	5.85	0.57	33.5	33.4	Whittle et al. (2001)
Belfast	Ireland	Soft Clayey Silt	1-8	54	46	15.1	5.20	0.47	33.4	33.5	Lehane (2003)
Berthierville	Québec	Sensitive Leda Clay	8-24	47	16	18.0	4.20	0.55	29.2	28.0	Demers (2001)

Table 4.1. List of clay sites subjected to laboratory triaxial and in situ piezocone penetration tests (CPTu) for NTH calibration study (continued)

Site name	Location	Soil description	Depth range (m)	Mean w_n (%)	Mean PI (%)	Total unit weight (kN/m^3)	CPTu Q	CPTu B_q	NTH ϕ' (°)	Triaxial ϕ' (°)[a]	References
Bogota	Colombia	Soft Plastic Clay	5-24	108	96	13.6	7.00	0.50	34.4	35.0	Diaz-Rodriguez et al. (1992)
Bonneville	Utah	Soft Lacustrine Clay	2-15	36	22	18.3	5.40	0.65	33.7	32.3	Bay et al. (2005), Garner (2007)
Bothkennar	Scotland	Soft Estuarine Clay	3-11	61	40	16.5	5.74	0.64	34.4	34.0	Hight et al. (2003); Nash et al. (1992)
Brent Cross[c]	United Kingdom	Fissured London Clay	6-11	30	50	19.4	15.00	0.01	23.6	21.0	Hight et al. (2003)
Broadback	Québec	Sensitive Clay	2-11	38	10	19.5	4.90	0.52	30.6	31.0	Demers (2001)

Table 4.1. List of clay sites subjected to laboratory triaxial and in situ piezocone penetration tests (CPTu) for NTH calibration study (continued)

Site name	Location	Soil description	Depth range (m)	Mean w_n (%)	Mean PI (%)	Total unit weight (kN/m^3)	CPTu Q	CPTu B_q	NTH ϕ' (°)	Triaxial ϕ' (°)[a]	References
Burswood	Australia	Soft Estuarine Clay	4-12	79	66	14.5	4.70	0.58	30.9	29.0	Low et al. (2011)
Busan	South Korea	Soft Marine Clay	5-25	65	33	16.5	4.44	0.43	27.9	27.2	Chung et al. (2012)
Can Tho	Vietnam	Soft Alluvial Clay	2-25	58	38	16.3	4.60	0.59	30.9	36.0	Takemura et al. (2006)
CF-Mining Hardee	Florida	NC Phosphatic Clay	5-10	107	113	17.5	4.40	0.35	26.4	26.0	Wissa et al. (1983) (1991)
Cooper River	South Carolina	Stiff Calcareous Clay	2-25	40	25	18.7	17.20	0.54	45.8	45.0	Camp et al. (2002)
Drammen	Norway	Sensitive Marine Clay	5-25	52	28	16.6	5.77	0.61	34.0	34.2	Lunne & Lacasse (1999); Lunne et al. (1997)

Table 4.1. List of clay sites subjected to laboratory triaxial and in situ piezocone penetration tests (CPTu) for NTH calibration study (continued)

Site name	Location	Soil description	Depth range (m)	Mean w_n (%)	Mean PI (%)	Total unit weight (kN/m^3)	CPTu Q	CPTu B_q	NTH ϕ' (°)	Triaxial ϕ' (°)[a]	References
Eidsvoll	Norway	Silty Clay	5-15	33	20	15.6	3.16	0.98	31.9	30.5	Karlsrud et al. (1996)
Fucino	Italy	Soft Carbonate Clay	5-30	78	60	15.1	5.12	0.78	35.1	34.0	Soccodato (2002)
Gloucester Test Site 1	Ontario	Sensitive Leda Clay	5-17	70	27	15.8	4.45	0.99	37.0	39.0	McQueen et al. (2015); Landon (2007); Bozozuk (1972)
Gotaleden	Sweden	Inorganic Clay	5-35	60	NA	17.0	5.74	0.41	30.5	30.0	Persson (2004)
Grande-Baleine	Québec	Sensitive Clay	2-22	35	15	18.0	3.06	0.83	29.4	29.0	Demers (2001)
Grandes-Bergeronnes	Québec	Sensitive Clay	2-24	43	25	19.0	5.50	0.56	32.6	30.0	Demers (2001)

Table 4.1. List of clay sites subjected to laboratory triaxial and in situ piezocone penetration tests (CPTu) for NTH calibration study (continued)

Site name	Location	Soil description	Depth range (m)	Mean w_n (%)	Mean PI (%)	Total unit weight (kN/m^3)	CPTu Q	CPTu B_q	NTH ϕ' (°)	Triaxial ϕ' (°)[a]	References
Gulf of Guinea	Offshore Ghana, West Africa	Soft Marine Clay	4-30	65	40	14.4	3.10	0.92	30.9	32.2	Ozkul (2013)
Gulf of Guinea-1	West Africa	Soft Marine Clay	1-10	130	90	13.1	10.0	0.43	37.3	40.6	Sjursen et al. (2006)
Gulf of Guinea-2b	West Africa	Soft Marine Clay	2-20	135	88	13.2	5.20	0.60	32.5	34.0	Sjursen et al. (2006)
Hachirogata Clay	Japan	Soft Marine Clay	2-40	115	70	13.3	3.90	0.76	31.5	33.0	Tanaka (2006)
Haga	Norway	OC Stiff Clay	1-8	20	15	20	6.43	0.75	37.5	33.5	Lunne et al. 1986; Andersen & Stenhamar (1982)
Hamilton AFB	California	Soft Bay Mud	2-14	95	45	13.7	4.20	0.58	29.7	29.5	Bonaparte et al. (1979); Masood et al. (1988)

Table 4.1. List of clay sites subjected to laboratory triaxial and in situ piezocone penetration tests (CPTu) for NTH calibration study (continued)

Site name	Location	Soil description	Depth range (m)	Mean w_n (%)	Mean PI (%)	Total unit weight (kN/m^3)	CPTu Q	CPTu B_q	NTH ϕ' (°)	Triaxial ϕ' (°)[a]	References
Hilleren	Norway	Marine Clay	5-25	35	18	18.8	2.81	1.32	34.4	30.8	Long et al. (2009)
Hong Kong[b]	China	Marine Clay	1-8	95	55	14.8	4.20	0.90	34.4	31.4	So (2009), Koutsoftas et al. (1987)
Houma[b]	Louisiana	Soft Empire Clay	10-40	46	54	17.3	2.50	0.62	21.1	20.2	Azzouz & Baligh (1981); Waxse (2008)
Kreuzlingen	Switzerland	Soft Lacustrine Clay	2-15	35	24	18.0	3.57	0.63	28.5	27.4*	Amman & Heil (1997); Messerklinger & Springman (2003)
Kurihama	Japan	Soft Marine Clay	5-30	98	61	15.2	3.58	0.60	28.0	29.6	Tanaka (1995)

Table 4.1. List of clay sites subjected to laboratory triaxial and in situ piezocone penetration tests (CPTu) for NTH calibration study (continued)

Site name	Location	Soil description	Depth range (m)	Mean w_n (%)	Mean PI (%)	Total unit weight (kN/m^3)	CPTu Q	CPTu B_q	NTH ϕ' (°)	Triaxial ϕ' (°)[a]	References
Laminaria	Timor Sea	Marine Clay	15-45	68	31	15.9	6.80	0.75	38.2	37.0	Sjursen et al. (2006)
La Baie	Québec	Sensitive Clay	2-35	40	22	18.0	9.20	0.50	37.6	37.0	Demers (2001)
Les-Cedres	Québec	Sensitive Clay	2-26	70	30	18.0	4.00	0.60	30.5	25.0	Demers (2001)
Lianyungang	China	Soft Marine Clay	2-11	60	40	15.8	2.51	0.88	27.6	27.1	Liu et al. (2011)
Louiseville	Québec	Sensitive Leda Clay	2-13	72	42	15.6	8.73	0.64	39.5	40.7	Leroueil et al. (2003)
Lower Pentre	United Kingdom	Alluvial clayey Silt	15-35	29	28	19.2	5.27	0.31	27.7	28.0	Lambson et al. (1993); Powell & Lunne (2005)

Table 4.1. List of clay sites subjected to laboratory triaxial and in situ piezocone penetration tests (CPTu) for NTH calibration study (continued)

Site name	Location	Soil description	Depth range (m)	Mean w_n (%)	Mean PI (%)	Total unit weight (kN/m^3)	CPTu Q	CPTu B_q	NTH ϕ' (°)	Triaxial ϕ' (°)[a]	References
Lower Troll	North Sea	Marine Clay	18-45	23	13	20.0	5.14	0.63	32.9	31.0	Uzelli et al. (2006); Lunne et al. (2006)
Luva	Norway	Marine Clay	5-40	60	38	16.3	7.14	0.61	36.5	36.5	Lunne et al. (2012)
Madingley[c]	United Kingdom	OC fissured Gault clay	2-15	30	45	19.0	20.00	0.01	26.4	26.0*	Lunne and Powell (1986)
Madison	Indiana	Marl Clay	4-11	55	30	16.0	5.60	0.60	33.4	31.0	El Howayek et al. (2015)
Mark Clark Bridge	South Carolina	Calcareous Cooper Marl	2-30	36	28	18.5	18.20	0.55	46.7	45.0	Camp (2008), personal communication

Table 4.1. List of clay sites subjected to laboratory triaxial and in situ piezocone penetration tests (CPTu) for NTH calibration study (continued)

Site name	Location	Soil description	Depth range (m)	Mean w_n (%)	Mean PI (%)	Total unit weight (kN/m^3)	CPTu Q	CPTu B_q	NTH ϕ' (°)	Triaxial ϕ' (°)[a]	References
Marquette Interchange	Wisconsin	OC organic silt	2-25	24	20	19.5	7.00	0.30	30.6	31.0	Soleimanbeigi (2013); Schneider & Hotstream (2011)
Maskinongé	Québec	Sensitive Clay	5-20	80	30	15.3	4.99	0.73	34.1	35.0	Demers and Leroueil (1999)
Massueville	Québec	Sensitive Clay	2-26	65	15	16.0	4.80	0.65	32.4	31.0	Demers (2001)
Matagami	Québec	Sensitive Clay	4-12	65	40	17.0	4.50	0.65	31.6	29.0	Demers (2001)
McDonald Farm	British Columbia	Soft Clayey Silt	2-25	55	66	16.7	5.20	0.80	35.6	36.5	Robertson et al. (1992)
Mexico City	Mexico	Soft Lacustrine Clay	2-30	150	9	13.0	5.04	0.31	27.3	27.0	Cruz &Mayne (2006)

Table 4.1. List of clay sites subjected to laboratory triaxial and in situ piezocone penetration tests (CPTu) for NTH calibration study (continued)

Site name	Location	Soil description	Depth range (m)	Mean w_n (%)	Mean PI (%)	Total unit weight (kN/m^3)	CPTu Q	CPTu B_q	NTH ϕ' (°)	Triaxial ϕ' (°)[a]	References
Newbury	Massachusetts	Glaciomarine Clay	2-12	45	24	17.5	8.56	0.57	38.0	37.3	Landon (2007)
Nice	France	Soft offshore clay	11-55	75	38	16.0	6.60	0.43	32.5	34.0	Sultan et al. (2004) Dan et al. (2007)
Niger Delta	Nigeria	Soft Deltaic Clay	2-30	150	110	12.2	5.80	0.58	33.5	36.0	Sultan et al. (2007)
Norrköping	Sweden	Soft Inorganic Clay	2-12	66	42	15.7	5.05	0.66	33.1	33.5*	Larsson & Mulabdić (1991)
North Charleston	South Carolina	Soft Silty Clay	2-25	95	65	14.2	5.50	0.54	32.2	31.0	Camp (2011), personal communication

Table 4.1. List of clay sites subjected to laboratory triaxial and in situ piezocone penetration tests (CPTu) for NTH calibration study (continued)

Site name	Location	Soil description	Depth range (m)	Mean w_n (%)	Mean PI (%)	Total unit weight (kN/m^3)	CPTu Q	CPTu B_q	NTH ϕ' (°)	Triaxial ϕ' (°)[a]	References
Northwestern University	Illinois	Soft Lacustrine Clay	11-20	20	12	21.0	3.05	0.79	28.8	28.3*	Mayne (2006); Chung & Finno (1992)
Nykirke	Norway	Firm Organic Clay	4-14	22	23	20.0	6.56	0.80	38.5	36.4	Powell & Lunne (2006)
Offshore West Africa	Africa	Offshore Marine Clay	2-30	72	46	16.0	5.50	0.66	34.2	31.0	Velosa et al. (2013)
Onsøy	Norway	Soft Marine Clay	4-19	64	41	15.9	3.50	0.81	30.8	32.0	Lunne et al. (2003)
Os	Norway	Glaciomarine Silt	2-11	28	12	19.6	4.00	0.65	28.6	34.0	Long et al. (2010)
Osaka Bay	Japan	Firm Marine Clay	100-250	49	95	16.7	3.80	0.80	31.7	30.6	Tanaka et al. (2003) Yashima et al. (1998)

Table 4.1. List of clay sites subjected to laboratory triaxial and in situ piezocone penetration tests (CPTu) for NTH calibration study (continued)

Site name	Location	Soil description	Depth range (m)	Mean w_n (%)	Mean PI (%)	Total unit weight (kN/m^3)	CPTu Q	CPTu B_q	NTH ϕ' (°)	Triaxial ϕ' (°)[a]	References
Patterson	Louisiana	Soft Alluvial Atchafalaya Clay	2-30	48	28	17.2	3.92	0.23	22.9	20.2	Donaghe & Townsend (1978); SESI (2006)
Perniö	Finland	Soft Glacial Clay	2-11	88	60	14.7	3.60	0.71	29.8	27.8	Lehtonen (2015)
Pisa	Italy	Alluvial Deposit	5-20	31	30	18.7	5.82	0.50	32.3	34.0	LoPresti et al. (2003)
Port-Cartier	Quebec	Sensitive	2-18	45	16	18.0	5.68	0.77	36.3	35.0	Demers (2001)
Port Huron	Michigan	Firm Silty Clay	7-28	20	21	20.4	5.61	0.32	28.6	28.0	Chen & Mayne (1994)
Porto Tolle	Italy	Firm NC Silty Clay	6-28	35	26	18.2	4.20	0.52	28.7	29.0	Hansbo et al. (1981)

Table 4.1. List of clay sites subjected to laboratory triaxial and in situ piezocone penetration tests (CPTu) for NTH calibration study (continued)

Site name	Location	Soil description	Depth range (m)	Mean w_n (%)	Mean PI (%)	Total unit weight (kN/m^3)	CPTu Q	CPTu B_q	NTH ϕ' (°)	Triaxial ϕ' (°)[a]	References
Queensborough	UK	Soft Estuary Clay	1-12	78	65	15.6	5.00	0.60	32.1	35.0	Jardine (2003)
Recife	Brazil	Soft Organic Clay	8-25	123	69	15.6	4.69	0.68	32.5	31.8	Danziger (2007)
Islais Creek	California	Soft Bay Mud	5-34	66	41	15.5	4.10	0.75	31.9	32.0	Hunt et al. (2002); Pestana et al. (2002)
Sandpoint	Idaho	Soft clayey Silt	2-30	66	41	15.9	4.30	0.75	32.5	32.3	Fellenius et al. (2004)
Santa Cruz	Brazil	Soft Organic Clay	2-8	100	60	13.9	6.80	0.55	34.9	33.4	Hosseinpour et al. (2017)
Sarapuí	Brazil	Soft organic Clay	5-11	135	65	13.2	4.03	0.70	31.0	29.5	Almeida et al. (2003); Danziger (2007)

Table 4.1. List of clay sites subjected to laboratory triaxial and in situ piezocone penetration tests (CPTu) for NTH calibration study (continued)

Site name	Location	Soil description	Depth range (m)	Mean w_n (%)	Mean PI (%)	Total unit weight (kN/m^3)	CPTu Q	CPTu B_q	NTH ϕ' (°)	Triaxial ϕ' (°)[a]	References
Singapore	Singapore	Marine Clay	2-28	55	50	16.0	3.72	0.67	29.6	27.0	Cao (2003)
St. Alban	Québec	Soft Sensitive Clay	3-8	76	28	14.8	4.00	0.46	27.2	27.0	Demers (2001)
St. Hilaire	Québec	Sensitive NC Clay	2-22	45	40	17.0	5.05	0.76	34.7	36.0	LaFleur et al (1988)
St. Hyacinthe	Québec	Sensitive Clay	6-15	70	30	17.5	4.60	0.68	32.3	31.0	Demers (2001)
St. Jean Vianney[c]	Québec	OC Sensitive Clay	1-6	30	23	19.0	24.00	0.52	46.8	44.4	Demers (2001)
St. Jude	Québec	Soft Leda Clay	5-35	39	20	18.0	5.13	0.71	34.0	35.0	Locat et al. (2011)
St. Monique	Québec	Sensitive Leda Clay	5-40	80	52	15.5	6.41	0.66	36.0	37.0	Locat (2012)

Table 4.1. List of clay sites subjected to laboratory triaxial and in situ piezocone penetration tests (CPTu) for NTH calibration study (continued)

Site name	Location	Soil description	Depth range (m)	Mean w_n (%)	Mean PI (%)	Total unit weight (kN/m^3)	CPTu Q	CPTu B_q	NTH ϕ' (°)	Triaxial ϕ' (°)[a]	References
St. Polycarpe	Québec	Sensitive Clay	2-20	75	40	16.0	4.00	0.66	30.3	27.0	Demers (2001)
St. Thuribe	Québec	Sensitive Clay	2-30	36	10	18.5	4.00	0.74	31.5	32.0	Demers (2001)
Tanjung Bin	Malaysia	Marine Clay	2-25	80	60	14.5	5.34	0.20	25.5	23.0	Lam (2016)
Taranto[c]	Italy	Hard OC Clay	2-20	25	20	20.0	6.00	0.40	30.9	28.0*	Jamiolkowski et al. (1985); Bruzzi & Battaglio (1987)
Teg	Sweden	Organic Clay	2-22	55	NA	17.0	6.10	0.40	31.0	30.0	Larsson et al (2007)
Tiller	Norway	Sensitive Marine Clay	2-20	30	6	18.7	4.16	0.81	33.0	32.7	Gylland et al. (2013); Sandven (1990)

Table 4.1. List of clay sites subjected to laboratory triaxial and in situ piezocone penetration tests (CPTu) for NTH calibration study (continued)

Site name	Location	Soil description	Depth range (m)	Mean w_n (%)	Mean PI (%)	Total unit weight (kN/m^3)	CPTu Q	CPTu B_q	NTH ϕ' (°)	Triaxial ϕ' (°)[a]	References
Tokyo Bay	Japan	Soft Marine Clay	5-35	46	25	17.0	3.18	0.70	28.1	27.5	Takesue (2001)
Torp	Sweden	Soft Sensitive Clay	10-40	48	29	17.5	6.14	0.38	30.8	30.0	Larsson and Åhnberg (2003)
Torpa	Sweden	Glacio-Marine Clay	2-12	70	44	15.8	6.62	0.63	35.9	35.9	Lofroth (2012)
Upper Troll	North Sea	Offshore Marine Clay	2-18	60	40	17.0	4.49	0.63	31.3	32.0	Uzielli et al. (2006); Lunne et al. (2006)
Vagverket	Sweden	Stiff Clay	5-15	25	20	19.2	17.20	0.10	34.1	35.0*	Larsson (1997)
Wauwill	Switzerland	Soft Lacustrine Clay	2-30	50	30	16.8	3.80	0.80	31.7	27.0*	Springman et al. (1999)

Table 4.1. List of clay sites subjected to laboratory triaxial and in situ piezocone penetration tests (CPTu) for NTH calibration study

(continued)

Site name	Location	Soil description	Depth range (m)	Mean w_n (%)	Mean PI (%)	Total unit weight (kN/m^3)	CPTu Q	CPTu B_q	NTH ϕ' (°)	Triaxial ϕ' (°)[a]	References
Yorktown Formation[c]	Virginia	Stiff Carbonate Sandy Clay	2-16	31	4	19.0	35.00	0.4	40.9	38.0	Mayne (1998)

Notes:

a. Effective stress friction angle from either CAUC or CIUC triaxial test defined at the maximum shear stress, otherwise asterisk* notes another criterion at either maximum obliquity or large strain.

b. Type 1 face or tip (u_1) porewater pressure readings converted to equivalent Type 2 shoulder (u_2) readings based on Chen & Mayne (1994).

c. Overconsolidated clays and fissured clays are excluded from the analysis

4.5 Triaxial Testing

For the data considered, the value of ϕ' was obtained from triaxial compression (TC) tests, either isotropically and/or anisotropically consolidated undrained laboratory triaxial tests (CIUC, CK0UC, and/or CAUC) on undisturbed samples to establish the benchmark friction angle. Test procedures generally followed ASTM standards (ASTM (2011) D4767) or other recognized equivalent guidelines (e.g., Bishop and Henkel 1962; Germaine and Germaine 2009; Lade 2016). The interpretation of ϕ' can be evaluated on the basis of different criteria, including (a) maximum deviator stress (q_{max}); (b) maximum obliquity or maximum principal effective stress ratio, $(\sigma'_1/\sigma'_3)_{max}$ (where σ'_1 and σ'_3 are the major and minor principal effective stresses, respectively); or (c) value taken at large strains, normally at 15% axial strain, or in some cases, at 20% strain. The third criterion is sometimes interpreted as the value corresponding to critical state (ϕ'_{cs}).

For illustrative purposes, a representative effective stress path from triaxial compression tests on silty clay at the Port of Anchorage, Alaska, is presented in Figure 4.2. The effective friction angle is interpreted based on three different criteria, i.e., q_{max}, maximum obliquity, and 15% strain. As evident, the three values of ϕ' are close to each other, with $\phi'=30°$ at q_{max}, $\phi'=31°$ at maximum obliquity, and $\phi'=29.3°$ at large strains.

The value of ϕ' at q_{max} is a commonly used criterion, while ϕ' at $(\sigma'_1/\sigma'_3)_{max}$ - termed maximum obliquity — is also quite valid (Bishop and Henkel 1962). For soft inorganic clays of low sensitivity, the various criteria often provide comparable values of ϕ' when interpreting data from CAUC and (or) CIUC tests. The use of the q_{max} criterion is primarily associated with the definition of the total strength parameter (i.e., undrained shear strength, s_u) whereas the $(\sigma'_1/\sigma'_3)_{max}$ choice is more suited to effective stress envelopes (Lade 2016). As most geoengineers focus on an interpretation of s_u from CPTu data, this is why many

of the ϕ′ data herein have been defined by that criterion, even though the definition at $(\sigma'_1/\sigma'_3)_{max}$ may be a better choice. Additional discussion of this topic is given later.

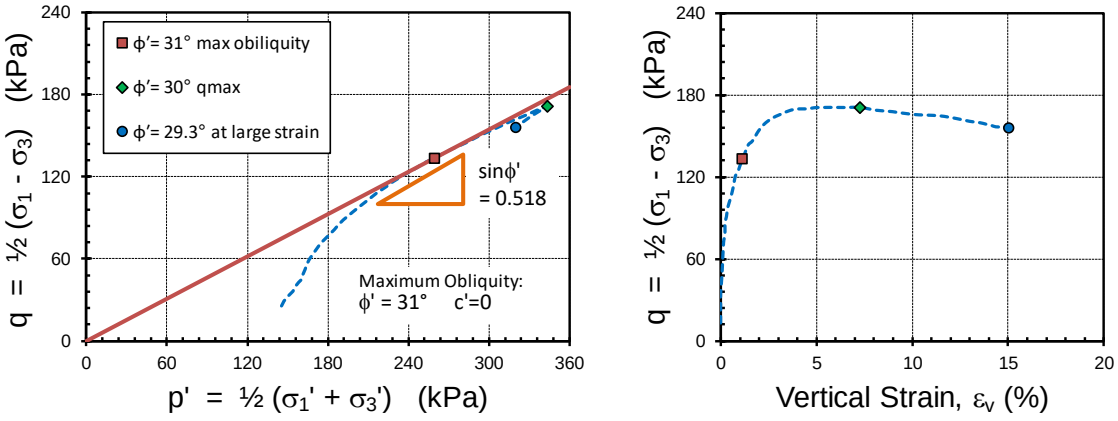

Figure 4.2. Laboratory triaxial test stress path showing different criteria for evaluating ϕ′ for clay at Anchorage, Alaska (modified from Willman et al. 2016).

Based on a study of 17 clays by Diaz-Rodriguez et al. (1992), the full range of effective stress friction angles (ϕ′) measured on natural clays ranges from 17° to 43°. Figure 4.3 shows a summary plot of ϕ′ of selected clays with their corresponding yield envelopes that are anchored by their yield stress (σ'_p) or preconsolidation stress. A study of friction angles from a large grouping of worldwide clays (n = 453) showed that the mean value ϕ′ = 28.6° ± 5.1° (Mayne 2013). As such, the reported ranges of ϕ′ from triaxial tests compiled in this study were in the range 20.2° < ϕ′ < 45.1°, thus comparable to other studies on this topic and representative of natural clay characteristics.

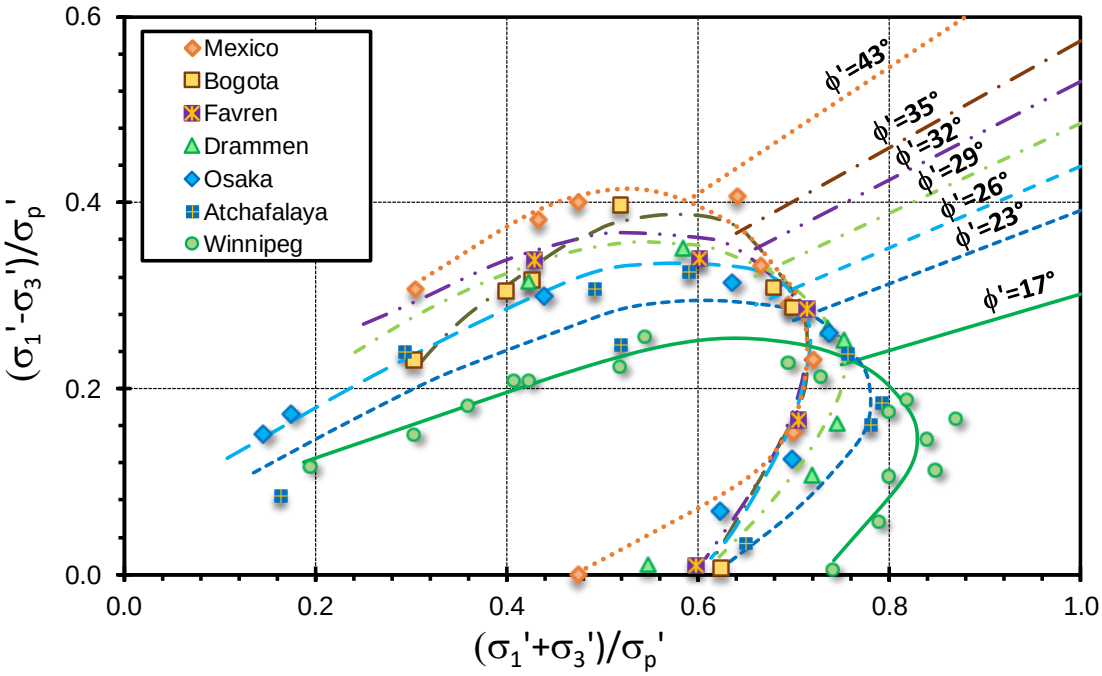

Figure 4.3. Observed range of ϕ′ and corresponding yield envelopes for various natural clays (modified from Diaz-Rodriguez et al. 1992).

A recent study by Amundsen and Thakur (2017) investigated the effects of sample disturbance on soft clay parameters. It was found that sample quality, storage time, and testing time between sampling and shearing appreciably affect the magnitude of preconsolidation stress, undrained shear strength, and constrained modulus. However, ϕ′ was little affected by these same factors.

For this study, the effective cohesion intercept has been taken as zero (c′ = 0) because the vast majority of clays considered are NC to LOC with low OCRs. Even for overconsolidated clays, a small value of c′ is appropriate (Lade 2016). If a value of c′ is necessary, the ratio $c'/\sigma'_p \approx 0.03$ can be used (Mayne 2016). Also, a means of extracting c′ from the CPTu data is also viable from the NTH solution (Sandven 1990).

4.6 Piezocone Testing

All sites were tested using either electric (analog) or electronic (digital) cone penetrometers with measurements of q_c and u_2, and in most cases, fs readings with depth. Field test procedures followed either ASTM standards (ASTM (2012) D5778) or an equivalent test method (Lunne et al. 1997). The total cone tip resistances (qt) have all been corrected for pore-water pressure effects (Campanella and Robertson 1988; Schnaid 2009), which requires the shoulder pore-water pressure (u_2). In most cases, the full depth of CPTu sounding was available as a digital file or was re-digitized to make accessible the q_t and u_2 readings that corresponded to the same elevations at the undisturbed samples for triaxial tests that were taken.

As the NTH method requires normalized parameters (Q and B_q), this also necessitated values of soil unit weight (as reported in Table 1) and depth to the groundwater table. In a few cases where information was insufficient, the groundwater depth could be inferred by assuming $u_2 \approx u_0$ (where u_0 is the hydrostatic porewater pressure) in a given sand layer either above or below the clay layer of interest. In a few cases where the unit weights were not provided, they were estimated from cone penetration test (CPT) results (Mayne 2014).

The depths of CPTs ranged between 5 and 50 m, except one exceptionally deep sounding at Osaka, Japan, that exceeded 240 m. The soundings terminated at a mean depth of 17 m with S.D. = 3.8 m. For 94% of the sites, the normalized Q ranged from 2.5 to 18.2 with a mean of 5.35 and S.D. = 2.58. The corresponding values of B_q varied from 0.11 to 0.99 with a mean of 0.62 and S.D. = 0.18. The 6% of sites that were excluded from these

statistics were (i) overconsolidated stiff clays and fissured clays including Yorktown, St. Jean Vianney, Baton Rouge, Baytown, Brent Cross, Madingely, Taranto that showed high Q and low Bq and (ii) a sensitive Hilleren clay site in Norway that exhibited a rather high Bq of 1.32. In addition, for the clay at Hong Kong, the piezocone soundings were obtained with pore-water pressures taken at the tip position (u_1), therefore a conversion was made by taking 80% of the u_1 readings to obtain an equivalent u_2 reading, as discussed by Chen and Mayne (1994).

4.7 Case Study

Five case studies are presented to show the reasonableness of interpreting effective friction angles in soft to firm clays using CPTu results in conjunction with the NTH solution.

4.7.1 Northwestern University, Illinois

The national geotechnical experimental site at Northwestern University (NWU) in Evanston, Illinois, is underlain by a 10mthick sand layer over 12 m of soft Chicago clay, which overlie other deeper soil layers. A variety of in situ and laboratory tests have been conducted here to investigate the properties of the clay soils (Finno et al. 2000). Figure 4.4 shows a representative portion of a CPTu sounding in the soft clay from 10 to 22 m depths with respective q_t, f_s, and u_2 values obtained using the Georgia Tech cone truck (Mayne 2007a). The soft clay under investigation has a mean unit weight of 20 kN/m^3, water content of 20%, liquid limit of 38%, and PI = 12%.

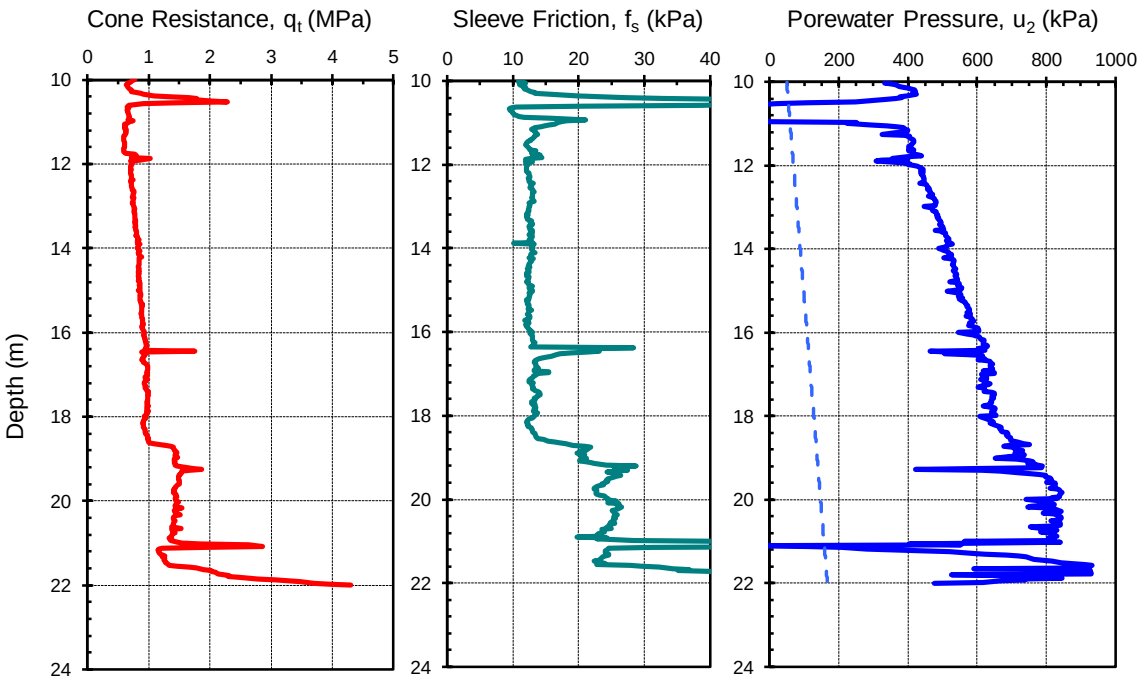

Figure 4.4. CPTu sounding at Northwestern University, Illinois.

The procedure for determining the cone resistance number (N_m = Q) is found as the slope from plotting net cone resistance versus effective overburden stress, as illustrated in Figure 4.5a. In this example, the line through the origin is forced (assuming c′= 0) to obtain Q = 3.05. By the same token, the pore–water parameter B_q is determined as the slope of measured $\Delta u = (u_2 - u_0)$ versus q_{net}, giving the value of B_q = 0.79 for the NWU site, as indicated in Figure 4.5b. These values are inputs to the solution chart in Figure 4.6, indicating ϕ' =28.8° for the soft Chicago clay. The NTH interpreted ϕ' is then compared with the laboratory value of ϕ' obtained from a series of CAUC triaxial tests conducted on undisturbed samples of these soft clays (Figure 4.7), as reported by Finno and Chung (1992) and Chung and Finno (1992). Results from the NTH method match well with the laboratory data.

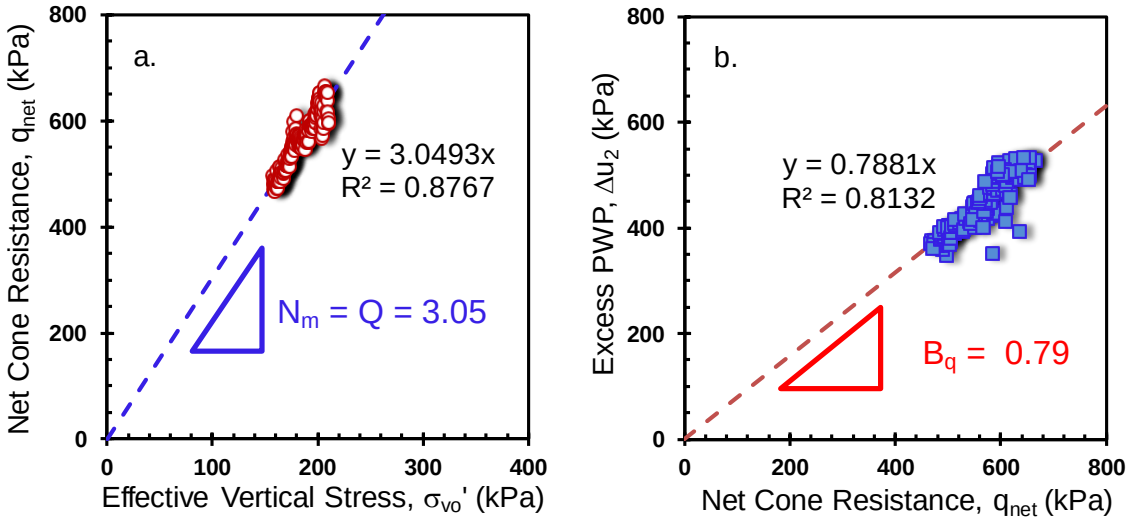

Figure 4.5. NTH post-processing of CPTu data at NWU for determination of (a) Q and (b) pore-water pressure parameter, B_q.

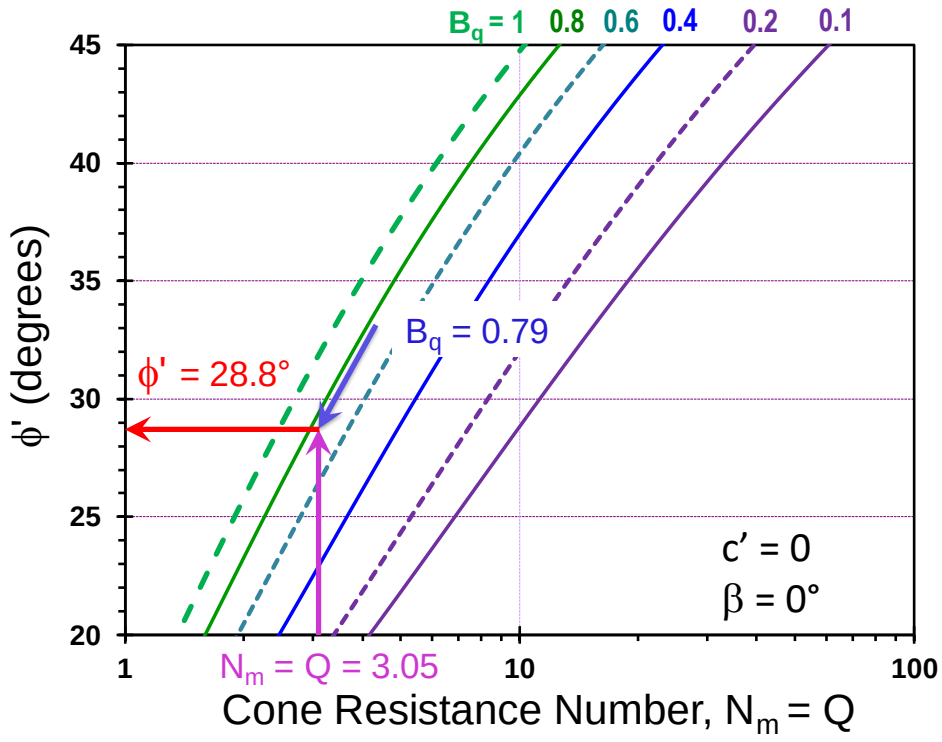

Figure 4.6. Evaluating ϕ′ from CPTu results at NWU site using NTH procedure.

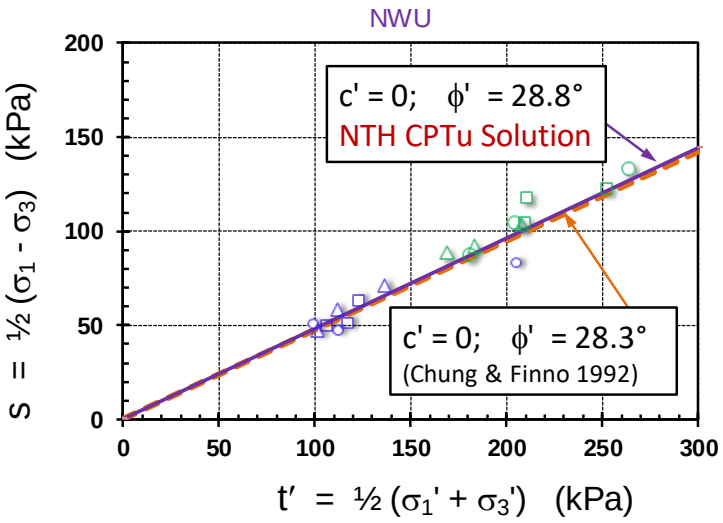

Figure 4.7. Comparison between laboratory triaxial tests showing ϕ' at q_{max} and NTH friction angle from CPTu at NWU site. (Note: triaxial results from Chung and Finno 1992).

The profiles of Q and B_q with depth from the CPTu data are presented in Figure 4.8.Here it can be seen that the approximate NTH solution gives results in agreement with the laboratory triaxial tests.

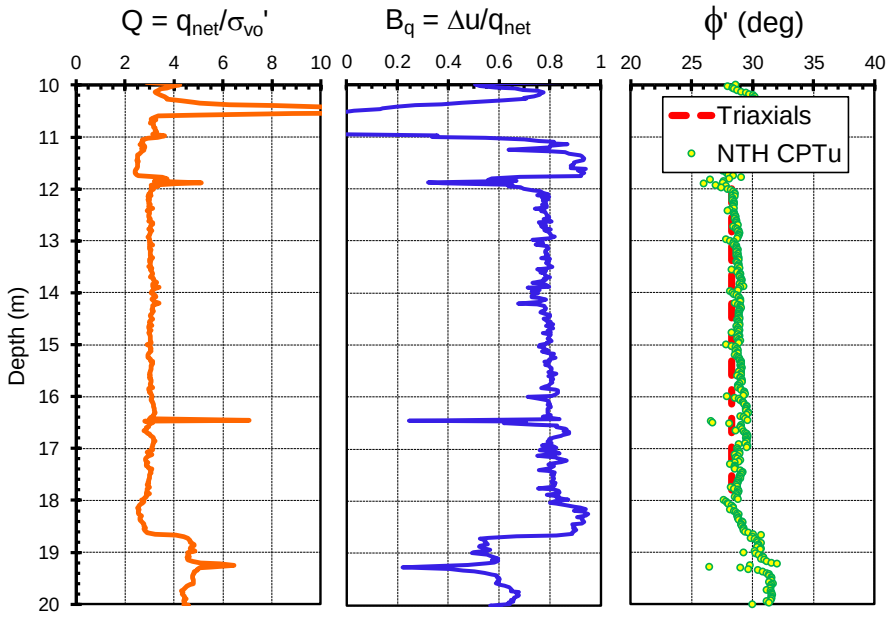

Figure 4.8. Profiles of resistance number (Q), normalized pore-water pressure (B_q), and evaluated ϕ' profile at NWU site.

4.7.2 Empire and Houma, Louisiana

Soft soils consisting of inorganic to organic clays with silty and sandy seams exist in the lower part of southern Louisiana. These geomaterials are found to exhibit low frictional characteristics and low OCRs, often less than 2. For instance, at depths of 35 - 45 m, the soft Empire clay in southern Louisiana has a low ϕ' of around 18° - 23° from laboratory triaxial test series reported by MIT (Azzouz and Baligh 1984). Similarly, CAUC and CIUC data on the Atchafalaya clay of southern Louisiana show that this clay also exhibits an $\phi' \approx 20°$ (Donaghe and Townsend 1978).

Figure 4.9 shows a representative 45m deep CPTu sounding from a dockside project in Houma, Louisiana. A sounding at the Empire site is also available; however, this utilized a type 1 piezocone so that only an approximate correction of q_c would be possible and assumptions would have to be made in converting u_1 to u_2 for input into the NTH method. Both the Empire and Houma soft plastic clays share similar engineering behavior, and the soft Louisiana clay studied here has a mean unit weight of 17.3 kN/m^3, water content of around 46%, average liquid limit of 76%, and a PI averaging 54%. The NTH approximate solution shows a deep profile of clay with ϕ' values superimposed from laboratory triaxial tests. These values from both laboratory triaxial and field piezocone testing in these southern Louisiana clays are seen to be at the low end of observed ϕ' values for natural clays.

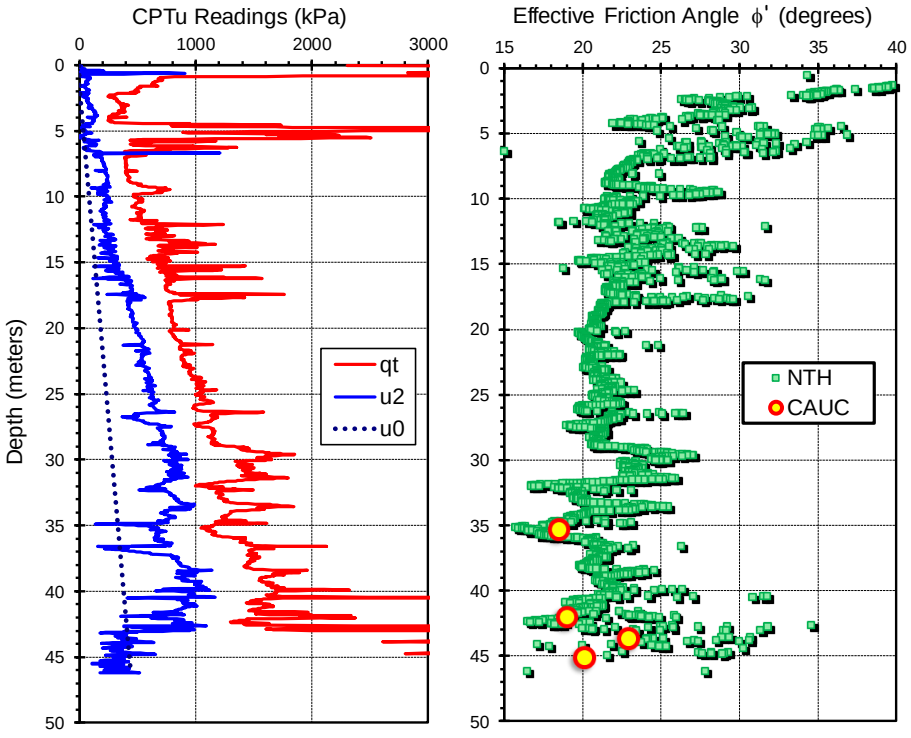

Figure 4.9. Profiles of CPTu sounding and NTH evaluated ϕ′ profile at Houma, Louisiana (laboratory data from nearby Empire clay reported by Azzouz and Baligh 1984).

4.7.3 Cooper Marl, Charleston, South Carolina

Geotechnical studies for the Arthur Ravenel Bridge over the Cooper River and Mark Clark Bridge in Charleston, South Carolina, required extensive field and laboratory studies for the design of large piling foundations and seismic concerns (Camp 2004). At depths exceeding 15–20 m lies a marine deposit of highly structured calcareous sandy clay, locally called the Cooper Marl. Many series of undrained triaxial compression (CIUC) tests with porewater pressure measurements were performed on the Cooper Marl by several consulting groups and testing firms, with over 100 triaxial tests completed. Results indicate that ϕ′ generally ranges from 40° to 46° with a mean ϕ′ = 43° (Camp et al. 2002a, 2002b). The calcareous clay studied at the Arthur Ravenel Bridge site has a mean unit weight of

18.7 kN/m^3, water content averaging 40%, and calcium carbonate content between 60% and 80%.

A total of 50 SCPTu soundings were completed for this bridge project. A representative CPTu sounding of over 53 m deep is adopted to evaluate the ϕ' at the site (Mayne 2005). Utilizing the approximate NTH Equation [4.6], the derived profile of ϕ' is presented in Figure 4.10. As evident, the NTH method successfully captures the high frictional characteristics with $\phi' \approx 44°$ for the Cooper Marl, comparable to the laboratory triaxial series.

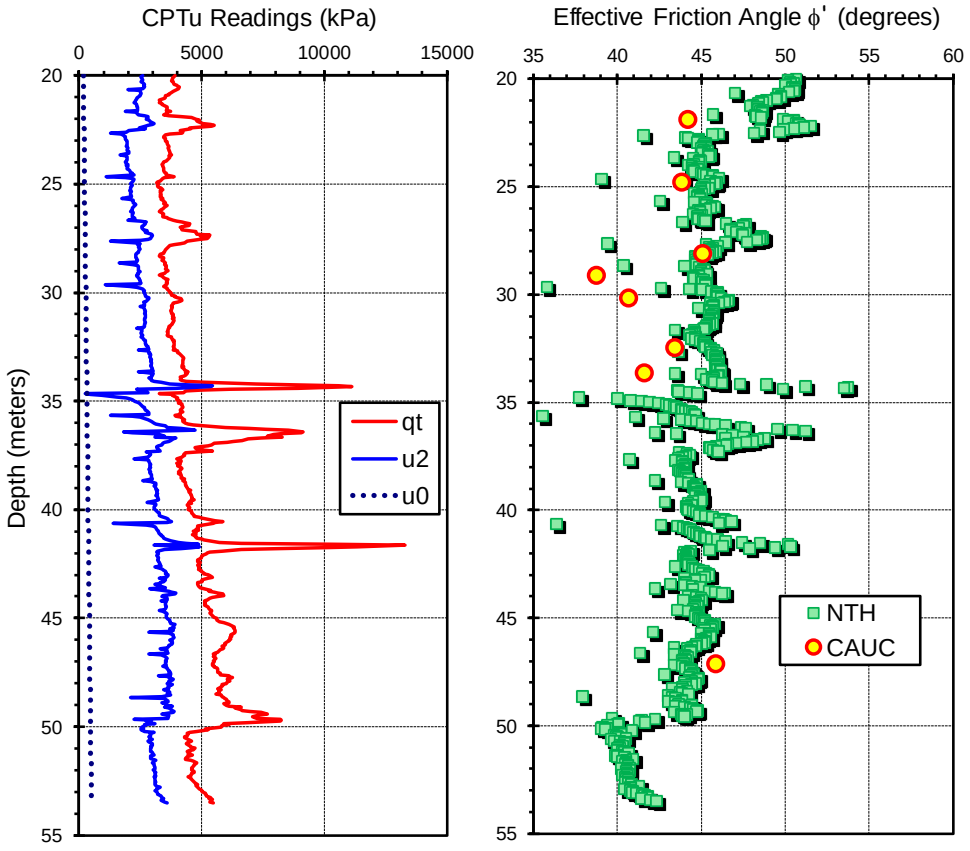

Figure 4.10. Profiles of CPTu sounding and NTH evaluated ϕ' profile at Cooper River, South Carolina (laboratory and field data from Camp 2004).

4.7.4 Belfast, Ireland

An experimental test site in Belfast, Northern Ireland, is underlain by shallow fill and topsoil that overlies a deposit of soft estuarine clayey silt to a depth of approximately 8.5 m. The water table resides at a depth of 1.4 m. The silt, which is known locally as "sleech", was laid down over the past 3000 years in water depths of between about 3 and 9 m (Lehane 2003). The soft soil layer has a mean unit weight of 15.1 kN/m^3, water content averaging about 54%, and PI = 46%. Geonor piston samples were collected for high quality specimens for laboratory testing using both CK0UC and CIUC tests. The laboratory ϕ' from 15 CIUC/CAUC tests on the clayey silt averages around $\phi' = 33.5°$. A representative CPTu sounding that was advanced to 8 m evaluated an ϕ' profile based on the approximate NTH equation, as shown in Figure 4.11. Notably, the values from the CPTu and triaxial tests compare generally well over a range of depths.

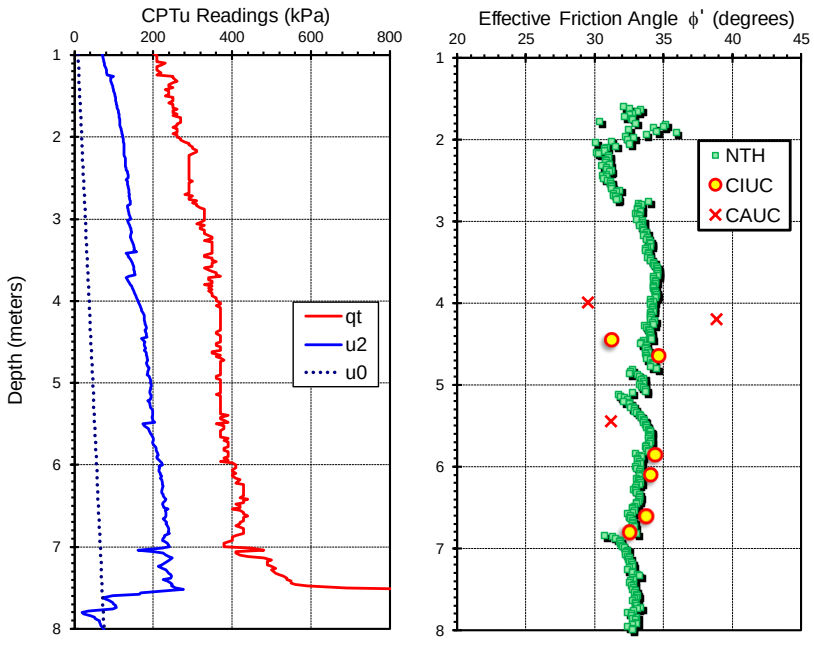

Figure 4.11. Profiles of CPTu sounding and NTH evaluated ϕ' profile at Belfast, Ireland (laboratory data from Lehane 2003).

4.7.5 Newbury, Massachusetts

Boston Blue clay (BBC) is a glacial marine deposit that exists in the greater Boston area due to deposition from glacial melt water (Landon 2007). The BBC at Newbury, Massachusetts, consists of a 12 m thick clay deposit located near the surface that exhibits an overconsolidated crust and low OCR layer at depth. The groundwater table was located 1.7 m below ground level. In situ seismic piezocone penetration tests (SCPTu) were performed to obtain soil stratigraphic information. High-quality Sherbrooke block sampling and piston tube sampling were conducted at the site and experimental test site and trimmed specimens were subsequently laboratory tested to characterize effective stress paths and strength envelopes (Landon 2007). Beneath the crust, representative qt and u2 profiles at the site from depths of between 5 and 12 m are shown in Figure 4.12. The soft to firm clay at this site has a mean unit weight of 17.5 kN/m^3, average water content of 45%, and PI = 24%. The average ϕ' values from CAUC tests on piston and Sherbrooke samples at each of four sampling depths generally hover at about $\phi' = 36.5°$ and the corresponding profile is in good agreement with the NTH profile obtained using CPTu data.

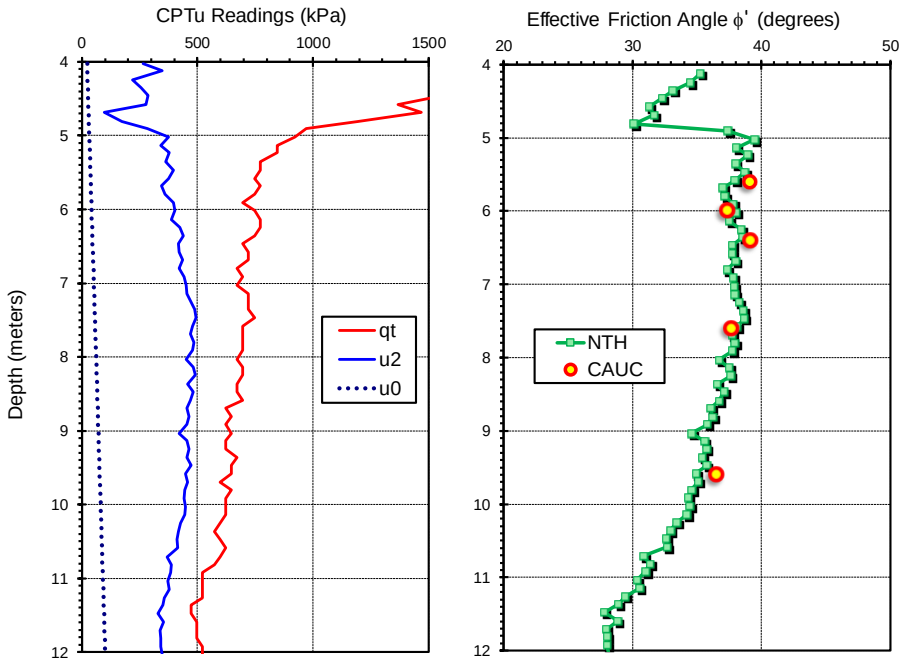

Figure 4.12. Profiles of CPTu sounding and NTH evaluated ϕ′ profile at Newbury, Massachusetts (laboratory and field data from Landon 2007).

4.8 Database Summary

The legend for the database on 98 clay sites listed in Table 4.1 is given in Figure 4.13 where each site is represented by a unique symbol by both shape and color. Figure 4.14 presents a summary plot for the measured laboratory triaxial test values versus the CPTu-determined values via the NTH solution. Two sets of statistical measures were made on the dataset, including (i) arithmetic statistics and (ii) regression statistics, as indicated in the figure. The measured laboratory ϕ′ values cover the full range from 20.2° to 45.0° and the CPTu-evaluated ϕ′ from 22.9° to 46.8°. From the arithmetic measures, the ratio of measured/evaluated values ranges from 0.88 to 1.16 with an overall mean of 0.98 and S.D. = 0.06, giving a corresponding COV = 0.06. From the regression evaluations of laboratory versus field values, the regression slope = 0.99 with a coefficient of determination, r^2 =

0.8035 and S.E.Y. = 1.81. These statistics generally support that the NTH method gives a reasonable evaluation of the ϕ' when referenced to the laboratory triaxial compression test as the benchmark value.

Figure 4.13. Legend of 98 soft to firm clay and silts sites under investigation in this study.

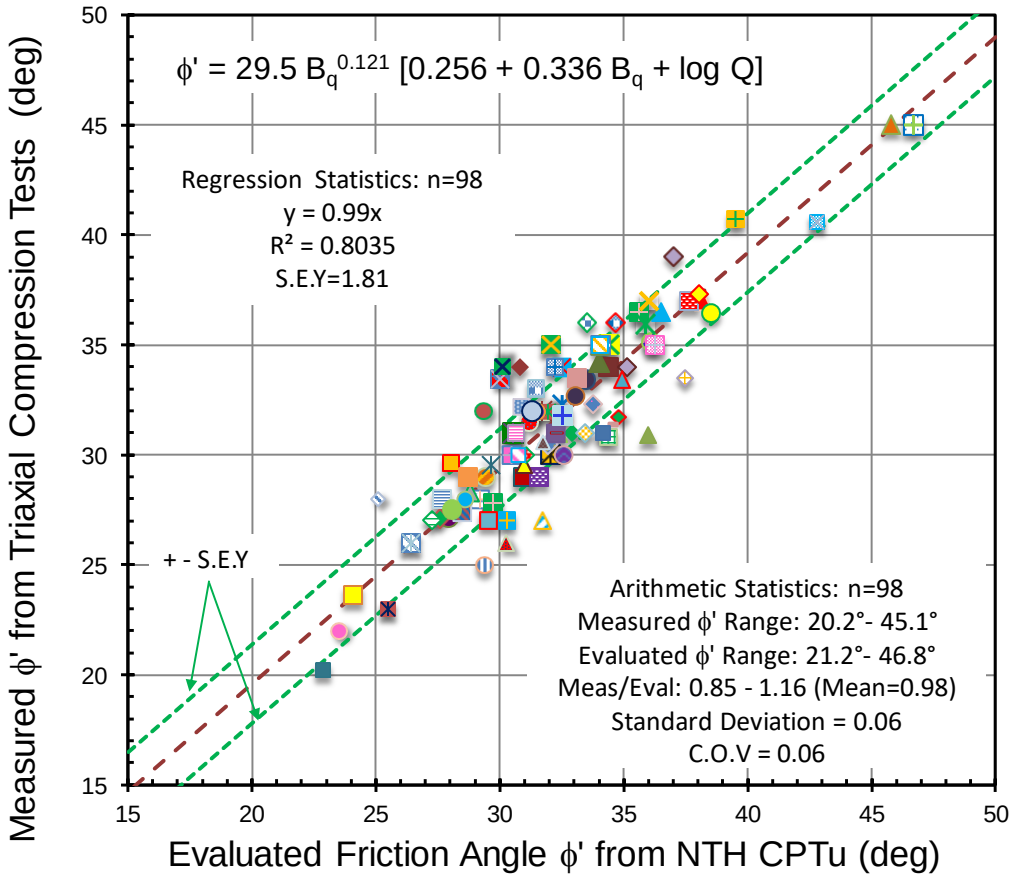

Figure 4.14. Summary plot of laboratory-measured triaxial friction angle ϕ′ versus CPTu-determined values via the NTH solution for 98 sites in this study.

4.9 Discussion of the limitation of the NTH method

While established as a versatile approach to CPT interpretation in soils, several limitations and qualifications can be made regarding the evaluation of ϕ′ in clays and fine-grained soils. These discussions are separated into the two main categories of testing for this project; namely, field piezocone results and laboratory triaxial tests.

4.9.1 Piezocone results

For the NTH to produce reliable ϕ′ profiles in clays, quality measurements of q_t and u_2 are required. Therefore, results depend upon proper procedures for saturation of the

porous filter element and cone cavities during preparation in the field (Campanella and Robertson 1988; Lunne et al. 1997). In certain geologic settings, an upper crustal layer of desiccated soils and (or) vadose zone comprising unsaturated soils may cause desaturation of the filter element, thus rendering the u_2 readings inaccurate. Insufficiently high vacuum applied during filter preparation and (or) use of various saturating fluids (water, glycerine, silicone oils) may also adversely affect the pore-water pressure readings. The magnitude of total (or corrected) q_t also depends upon the u_2 reading. Thus, care should be implemented in properly obtaining and maintaining saturation throughout the CPTu measurements.

In soils that are either fissured or heavily overconsolidated, it is common to obtain negative u_2 readings with corresponding $B_q < 0$ (Campanella et al. 1986; Mayne et al. 1990). As noted by Sandven (1990; section 5.2.1.4), "the NTH method cannot directly accommodate negative B_q values," so therefore should not be applied to such materials, except perhaps from an academic point of view.

4.9.2 Triaxial test interpretation

Results from triaxial compression tests with porewater pressure measurements can be interpreted in light of different criteria, as detailed by Lade (2016). The two most common criteria are (i) ϕ' at peak stress, or $(\sigma_1 - \sigma_3)_{max}$ (where σ_1 and σ_3 are the major and minor principal stresses, respectively); and (ii) ϕ' at maximum principal stress ratio, or $(\sigma'_1/\sigma'_3)_{max}$. Additional discussions with criteria defined at large strains, constant volume, and critical state can also be made, but are beyond the scope of this research scope.

For triaxial tests on Edgar plastic kaolinite, Lade (2016) reports $\phi' = 27.8°$ for both the $(\sigma_1 - \sigma_3)_{max}$ and $(\sigma'_1/\sigma'_3)_{max}$ criteria. Of course, with reconstituted clays or remoulded soils, this observation is well documented (Bishop and Henkel 1962). For natural clays tested at stresses higher than their natural preconsolidation stress, the value of ϕ' corresponding to s_u often exhibits a value about 3°–5° less than ϕ'at maximum obliquity (e.g., Bjerrum and Simons 1960; Koutsoftas and Ladd 1985). Yet, the higher consolidation stresses have forced this NC state. In reality, natural clays are rarely NC in situ because various geoenvironmental factors have caused a quasi-preconsolidation that can be due to ageing, groundwater changes, diagenesis, temperature fluctuations, and other influences. Excluding a few of overconsoldiated stiff clay and fissured clay sites in the database (i.e., Baytown, Baton Rouge, Madingley, Brent Cross, St. Jean Vianney, Yorktown, and Taranto), the remaining 98 sites exhibit a mean OCR = 1.53 with S.D. = 1.23. Therefore, the bulk of the data are from LOC clays and clayey silts. Soft to firm LOC clays, such as Anacostia (Mayne 1987), Swiss clay (Springman et al. 1999), Sarapui (Almeida and Marques 2003), Nykirke (Powell and Lunne 2005), Luva (Lunne et al. 2012), Tiller (Amundsen and Thakur 2017), Chicago (Finno and Chung 1992), and other clays all show essentially the same $\phi'$for both the q_{max} and $(\sigma'_1/\sigma'_3)_{max}$ criteria. For the Bothkennar soft clay, Hight et al. (2003) reported a value of $\phi' = 34°$ at q_{max} on natural samples that correspond well to drained and undrained triaxial tests on reconstituted samples; whereas, at large strains and maximum obliquity, higher values with $\phi' \approx 41°$ are observed.

In a few cases, a stress history and normalized soil engineering properties (SHANSEP) procedure was used and this may have resulted in differences in reported ϕ'

values (Jardine et al. 2003; Bay et al. 2005). In other cases, the value of ϕ' at q_{max} represents a lower bound, such as the Ballina clay site where Kelly et al. (2017) showed that the NTH method more closely aligns with ϕ' at constant volume ($\phi' \approx 29.5°$) whereas the peak values are much higher, averaging around 35.7°. Similar results are observed for the soft clay at Burswood (Low et al. 2011).

As noted previously, in many cases, the cited source of data did not report the criterion used to define ϕ', nor was the effective stress path or set of stress–strain curves and pore-water pressure data provided, so a re-interpretation and (or) comparison of ϕ' by various criteria could not be performed. In any event, it is believed that the values of ϕ' contained herein are lower bound values and consequently the NTH method provides a conservative evaluation.

4.10 Conclusions

Application of an effective stress limit plasticity theory detailed by Sandven (1990) and Senneset et al. (1989) enables the development of an approximate closed-form solution ($\beta = 0°$, $c' = 0$) for evaluating the effective stress friction angle (ϕ') in soft to firm clays, silty clays, and clayey silts from in situ piezocone measurements, specifically the cone resistance (q_t) and pore-water pressure (u_2). The approximation has restricted ranges ($20° \leqslant \phi' \leqslant 45°$ and $0.05 \leqslant B_q \leqslant 1.0$) which correspond to expected values characteristic of natural inorganic clays of low to medium sensitivity.

Data from five case studies are presented to illustrate application of the methodology, including (i) soft lean Chicago clay, (ii) soft plastic Louisiana clays with low

frictional characteristics, (iii) stiff Cooper marl with high frictional qualities, (iv) soft clayey silt, and (v) firm marine clay. Paired data from 105 natural clays, which included both laboratory triaxial tests (CK_0UC, CAUC or CIUC) and field CPTu soundings, were compiled to validate the NTH solution. The data show that the methodology provides statistically sound results for CPTu testing conducted in insensitive and inorganic clays with corresponding ϕ' values in the range $20° \leqslant \phi' \leqslant 45°$.

CHAPTER 5. CPTU TWITCH TEST DATA EVALUATED USING NTH LIMIT PLASTICITY SOLUTION

5.1 Introduction

During CPTu, the standard penetration rate of 20 mm/s is established by ASTM, CEN, and ISO standards and considered to generate a fully-drained condition in sands and fully-undrained behavior in clays of low permeability. However, these drainage conditions are not likely to exist in intermediate soils (silts, clayey sands, sandy silts, residual soils, etc.) whose soil response can be expected to be lie between that of sands and clays. Therefore, the behavior of intermediate soils at the standard penetration rate is likely to be partially-drained, or partly-undrained.

It is well-recognized that the penetration resistance q_t varies with the push rate (Lunne et al. 1997; Randolph 2004; DeJong et al. 2012). For many soft to firm soils, the penetration resistance increases as the velocity decreases due to local consolidation around the penetrometer tip (Suzuki 2015). Research has also shown that viscous effects at higher velocities in the undrained region may lead to gains in penetration resistance with increasing velocity (Kim et al 2008, Randolph and Hope 2004). However, the effect of various soil characteristics on cone penetration resistance and the measured porewater pressures from CPTu for any given drainage condition remains unclear and beckons the need for additional experimentation and research studies.

5.2 Variable Penetration Rate CPTu

The most direct approach to study the transition region from undrained to partially drained response is to conduct penetration tests at different rates in the same soil. A special type of CPTu called "twitch testing" has been developed by varying the penetration rate and measuring the resistance readings under different drainage conditions (Randolph 2004). To compare relative readings taken at different rates, a non-dimensional velocity parameter (V) has been defined by Finnie & Randolph (1994):

$$V = v \cdot d/c_v \quad [5.1]$$

where v is the test rate, d is the probe diameter, and c_v is the coefficient of consolidation of soil tested.

Variable rate testing has been applied to field vane, CPTu, T-bar, and ball penetrometer tests (Randolph 2004). For CPTu, Finnie & Randolph (1994) suggested transition points of $V < 0.01$ for drained response, and $V > 30$ to ensure undrained response. Randolph & Hope (2004) presented data from mini-piezocone tests conducted in normally consolidated kaolin in centrifuge chambers where rates of penetration varied from 3 mm/s to 0.005 mm/s. For convenience, the CPTu results can be presented in terms of dimensionless parameters:

Normalized cone resistance $Q = q_{net}/\sigma'_{v0}$ [5.2]

Normalized porewater pressure $B_q = \Delta u_2/q_{net}$ [5.3]

where $q_{net} = (q_t - \sigma_{v0})$ is the net cone tip resistance and $\Delta u_2 = (u_2 - u_0)$ is the excess porewater pressure.

Additionally, Schneider et al (2008) proposed an alternative normalized excess porewater pressure:

$$U = \Delta u_2 / \sigma'_{v0} \qquad [5.4]$$

Note that the two porewater pressure parameters are related via: $B_q = U/Q$.

Jaeger et al (2010) conducted centrifuge model tests using a miniature piezocone in an artificial mixed soil called K25-S75 (25% kaolin and 75% sand) under variable penetration rates. The variations of Q and U with normalized penetration rate (V) are presented in Figure 5.1. It is observed that the measured Q decreases with V, while in contrast, the measured value of U increases with V. Both relationships can be characterized empirically by hyperbolic functions and the corresponding expressions are given by Jaeger et al (2010). When V < 0.1, essentially drained behavior is observed (U ≈ 0), while undrained response is defined when V > 30.

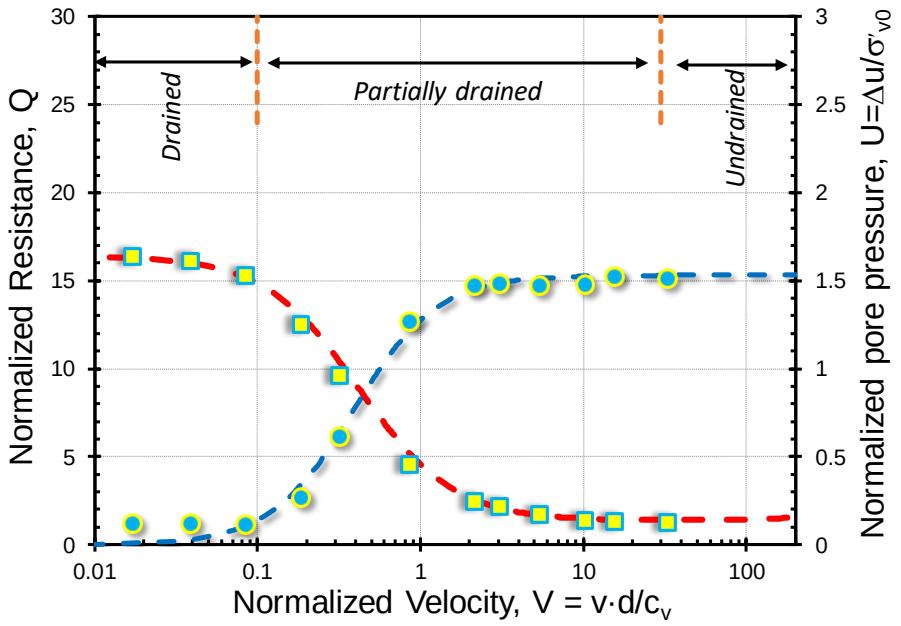

Figure 5.1. Effect of penetration rate on centrifuge piezocone measurements in 25-75 kaolin-sand mix (data from Jaeger et al 2010)

5.3 Effective Stress Limit Plasticity Solution

An effective stress limit plasticity solution for piezocone penetration tests has been developed at the Norwegian Institute of Technology (NTH), where the derivations are provided by Senneset et al. (1985, 1989), Sandven (1990), and Sandven & Watn (1995). The general solution for c' = 0 is given by:

$$Q = \frac{\tan^2(45° + \varphi'/2) \cdot \exp[(\pi - 2\beta) \cdot \tan\varphi'] - 1}{1 + 6 \cdot \tan\varphi' \cdot (1 + \tan\varphi) \cdot B_q} \qquad [5.5]$$

For drained penetration, Mayne (2006) applied the solution to a CPTu database where 13 sands had been subjected to special and expensive undisturbed sampling that permitted triaxial compression testing and the determination of the operational ϕ' for each sand. As sands more or less exhibit CPTu porewater pressures that are hydrostatic: $u_2 \approx u_0$, then $B_q = 0$ and the resulting simplified expression for drained penetration is simply:

$$q_t/\sigma_{v0}' = \tan^2(45° + \phi'/2) \cdot \exp[(\pi\text{-}2\beta) \cdot \tan\phi'] \qquad [5.6]$$

The calibration required the assessment of the angle of plastification (β) which controls the size of the failure region around the penetrometer tip. For contractive soils, $\beta > 0$ and the soil volume decreases, whereas in dilative sands, $\beta < 0$ and a volumetric increase is noted, analogous to the state parameter for sands (ψ). For sands, it was found that the angle β tracked inversely with shear rigidity (G_0/σ_{vo}') where $G_0 = \rho_t \cdot V_s^2$ is the small-strain shear modulus, ρ_t = total soil mass density, and V_s = shear wave velocity.

In the case of fine-grained soils where permeability is low, CPTu generates excess porewater pressures and generally $B_q > 0$, thus termed undrained penetration. This

corresponds to the case where volumetric strains are zero, hence β = 0. As such, Ouyang & Mayne (2018) condensed the formulation for ϕ' in terms of normalized cone parameters (Q and B_q) which can be expressed for the case c' = 0:

$$Q = \frac{\tan^2(45° + \phi'/2) \cdot \exp(\pi \cdot \tan\phi') - 1}{1 + 6 \cdot \tan\phi' \cdot (1 + \tan\phi) \cdot B_q} \qquad [5.7]$$

A full inversion of the above equation is not possible, yet an approximate solution for undrained penetration has been developed over the following range of effective stress friction angles ($20^o \leq \phi' \leq 45^o$) and limiting values of the porewater pressure parameter ($0.05 \leq B_q \leq 1.0$) that applies to soft to firm claus with OCR < 2.5:

$$\phi' = 29.5 \cdot B_q^{0.121} [0.256 + 0.336 \cdot B_q + \log Q] \qquad [5.8]$$

The closed-form analytical solution and the approximate algorithm are both presented graphically in Figure 5.2.

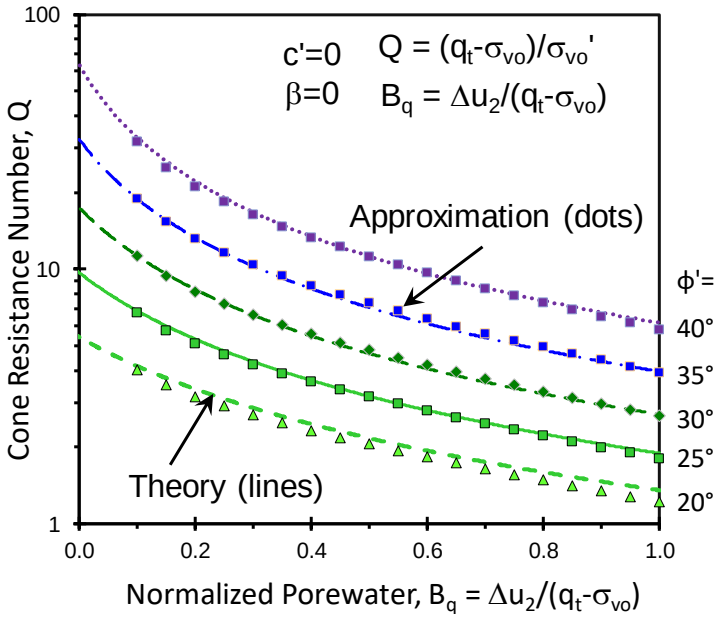

Figure 5.2. NTH method for evaluating ϕ' in soils from CPTu using approximate and exact solutions

In prior efforts, results from CPTu soundings conducted at the standard penetration rate of 20 mm/s in the field were examined with data collected from 105 clay sites (Chapter 4). The data were compiled to verify the ability of the NTH solution to match interpreted ϕ' values with those obtained by conventional laboratory triaxial tests, confirming reasonable agreement. In a parallel study, results from eleven series of 1-g chamber model tests in kaolin and clay-sand mixtures that were subjected to mini-piezocone penetration tests were also reviewed (Chapter 2). That study validated that the NTH method successfully evaluates the effective stress friction angles of clayey soils in comparison with laboratory CIUC and CAUC benchmark reference values. A third dataset involving thirteen centrifuge series of clays was also investigated (Chapter 3). Here, mini-CPTu data obtained during undrained penetration in centrifuge deposits of kaolin, clay, and clay-sand mixtures were reviewed that also showed that reasonable evaluations of ϕ' were obtained from the NTH solution.

5.4 Twitch CPTu database

The intent of this chapter is to extend the application of the NTH method from CPTu tests made at the standard penetration rate of 20mm/s to data collected at variable penetration rates, i.e., twitch testing. This study further allows an examination on the interpretation of the effective stress friction of different geomaterials by NTH method under different drainage conditions.

It is well-established that the effective stress friction angle is a fundamental soil property and should not be affected by drainage conditions. This fact is an underlying basis in effective stress path analyses (Lambe & Whitman 1979; Lade 2016) and the framework

of critical state soil mechanics (Schofield & Wroth 1968; Mayne et al. 2009; Holtz et al. 2011). Many laboratory programs involving a combination of undrained and drained triaxial tests have provided a unique value for the effective ϕ' of a given clay (e.g., Bjerrum and Simons 1960, Amerasinghe & Parry 1975, Leroueil & Hight 2003). For instance, results from series of undrained triaxial (CAUC, CAUE) and drained triaxial (CADC, CADE) tests, conducted in both compression and extension modes, performed on the well-documented soft Bothkennar clay in the UK are shown in Figure 5.3 indicating the effective stress strength is adequately represented by: c' = 0 and ϕ' = 34° (Allman & Atkinson 1992).

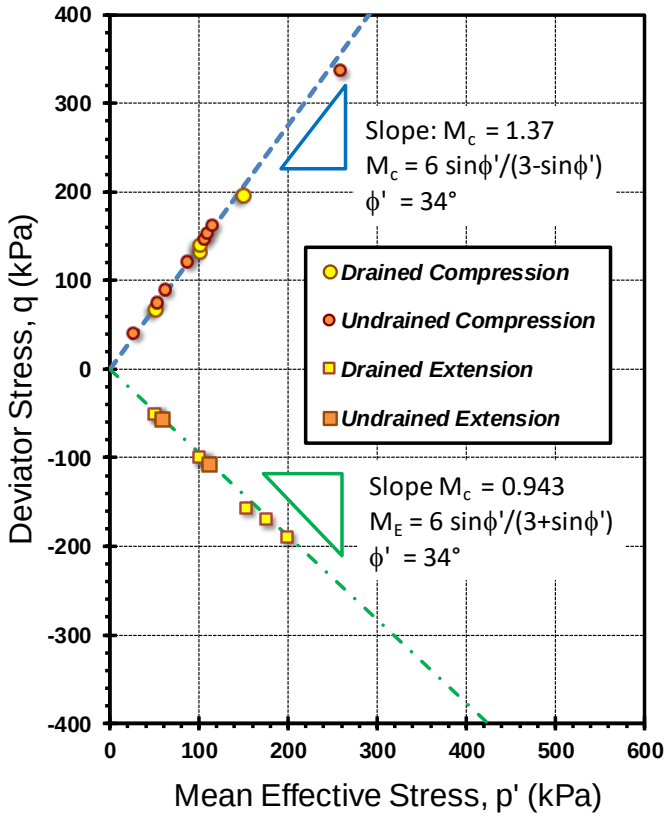

Figure 5.3. Effective strength envelope for soft Bothkennar clay, Scotland (data from Allman & Atkinson, 1992)

For this study, a special database was compiled from 20 different series of twitch CPTu tests reported in the geotechnical literature and research reports. The data can be categorized into three groups, including: (a) twelve series of CPTu field twitch tests, (b) three laboratory 1-g chamber series of twitch tests, and (c) five series of mini-CPTu centrifuge twitch tests. The soils tested by CPTu ranged from soft to firm clays, clayey silts, and silts, to silty and clayey sands. The individual soil test series, their locations, and reference sources who reported the piezocone data and laboratory results (where available) are noted in Table 5.1

All soils were tested using either electric (analog) or electronic (digital) cone penetrometers with corresponding recorded measurements of q_c and u_2. In many cases, the sleeve friction (f_s) was also reported, yet not included herein. The total cone tip resistances (q_t) have all been corrected for porewater effects, as detailed by Lunne et al. (1997) using the porewater pressure (u_2) measured at the shoulder position.

Generally, measured values of normalized cone resistance Q in the database increase as the penetration rates decrease (from undrained to partially drained to drained) whereas the normalized porewater pressure B_q follow an opposite trend. The measured porewater pressures from the piezocone soundings were generally larger than the hydrostatic pressure: $u_2 > u_0$ for all the clay to silty geomaterials with normalized velocity $V > 0.1$, inducing excess porewater pressure representing undrained to partially drained condition. In contrast, u_2 values are close to u_0 (i.e., B_q approaching 0) when the normalized velocity $V < 0.1$, indicating essentially drained penetration.

Figure 5.4 shows the distribution of the Q and B_q parameters from all twitch tests where each test series is represented by a different symbol. All the field series of twitch tests are shown using colored square/diamond dots, whereas the centrifuge series of model twitch tests are represented by circle dots and the series of 1-g chamber tests are indicated by square dots with crosses.

As the penetration rate decreases, the value of Q increases and corresponding B_q decreases. For each of the twitch test series, despite the variable rates of testing, the paired set of measured Q and B_q are observed to follow a consistent friction angle contour, as established by the NTH solution. This gives proof that the value of effective stress friction angle for a given geomaterial is independent of the drainage conditions, thus is a soil property. The value of ϕ' is applicable to the soil itself, regardless of whether the conditions are undrained, partially-drained, or fully-drained.

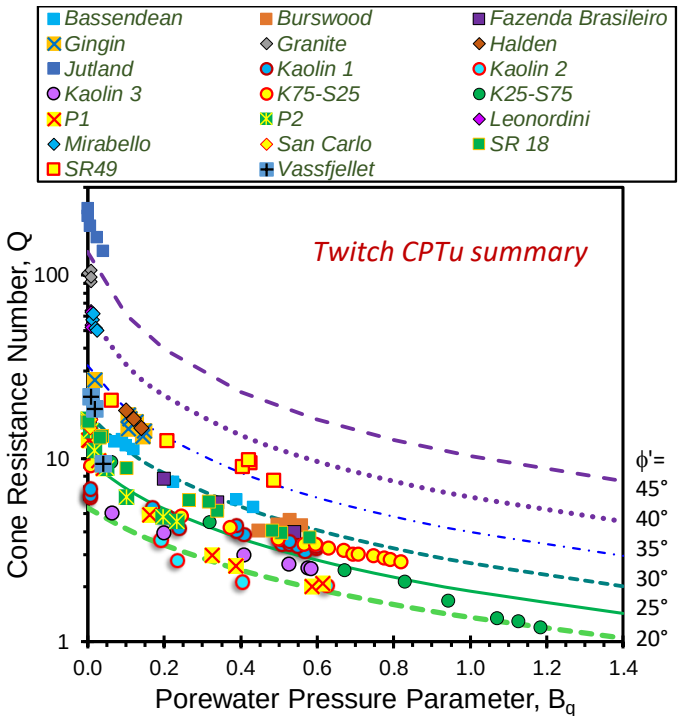

Figure 5.4. Summary of data from 20 twitch test series within the context of the NTH solution for assessing friction angle

Table 5.1. List of twitch test series evaluated by NTH CPTu solution

Site Name	Location/Institute	Description	Push rates (mm/s)	Mean w_n (%)	Mean PI (%)	Mean γ_t (kN/m^3)	CPTu		NTH ϕ' (deg)	Lab ϕ' (deg)	Reference Source
							Q	B_q			
Bassendean	Australia	Alluvial Clays	0.002-20	72	27	16.0	12.4-5.5	0.07-0.45	29.3	28.0[1]	Suzuki (2015)
Burswood	Australia	Alluvial Clays	0.0001-20	71	41	15.5	3.3-3.0	0.45-0.56	30.1	31.0	Suzuki (2015)
Frazenda Brasileiro	Brazil	Tailings Dam	1.5-20	NA	NA	18.5	7.7-4.0	0.2-0.54	29.4	31.0	Dienstmann et al (2018)
Gingin	Australia	Mine Tailings	0.2-20	NA	10	17.2	26.8-13.1	0.02-0.15	33.4	NA	Suzuki (2015)
Granite	California	Sands with fines	0.2-20	NA	NA	18.0	100-90	<0.01	37	NA	Krage et al (2014)
Halden	Norway	Low plasticity Silts	2-320	27	10	19.0	18.3-14.7	0.1-0.15	34.5	35.0	Paniagua et al (2016)
Jutland	Denmark	Sandy Silts	0.5-60	NA	NA	15.0	200-130	0.0-0.4	40.0	NA	Poulsen et al (2013)
Kaolin 1	UWA Centrifuge	Kaolin	0.003-3	120	34	16.2	6.8-3.4	0.01-0.5	26.5	28.0	Schneider (2008)
Kaolin 2	UWA Centrifuge	Kaolin	0.0003-1.0	120	27	16.1	6.8-2.0	0.01-0.63	21.4	21.0	Mahmoodzadeh & Randolph (2014)
Kaolin 3	UWA Centrifuge	Kaolin	0.01-3.0	120	27	16.1	5.1-2.5	0.06-0.58	23.1	23.0	Randolph & Hope (2004)
K75-S25	PSU Centrifuge	25% Sand+75% Kaolin	0.004-3.0	92	22	15.7	9.0-2.74	0.01-0.82	27.2	27.0	Fitzgerald (2009)

Table 5.1. List of twitch test series evaluated by NTH CPTu solution (continued)

Site Name	Location/Institute	Description	Push rates (mm/s)	Mean w_n (%)	Mean PI (%)	Mean γ_t (kN/m^3)	CPTu		NTH ϕ'	Lab ϕ'	Reference Source
							Q	B_q	(deg)	(deg)	
K25-S75	UCD Centrifuge	75% Sand+25% Kaolin	0.003-3.0	NA	9.5	18.2	16.4-1.2	0.01-1.42	27.9	28.0	Jaeger et al (2010)
P1	Purdue Chamber Test	75% Sand+25% Kaolin	0.01-20	33	NA	NA	12.6-2.1	0.01-0.61	22.0	NA	Kim (2005)
P2	Purdue Chamber Test	82% Sand+18% Kaolin	0.01-20	35	NA	NA	16.3-4.6	0.01-0.23	23.1	NA	Kim (2005)
Lenordini	California	Sands with fines	0.02-20	NA	NA	18.0	64-52	<0.01	35.0	NA	Krage et al (2014)
Mirabello	Italy	Silty Sands	10-130	NA	NA	19.0	61.7-49.9	<0.02	35.3	34.0	Garcia-Martinez (2014)
San Carlo	Italy	Silty Sands	10-80	NA	NA	19.0	21.9-14.7	<0.01	25.0	NA	Garcia-Martinez (2014)
SR 18	Indiana	Silty Clays	0.05-20	28.1	16.1	16.7	8.8-3.7	0.01-0.58	29.2	29.0[2]	Kim et al (2008)
SR 49	Indiana	Clayey Silts	0.01-20	23	9	17.7	20.7-9.9	0.06-0.42	35.5	35.0[2]	Kim et al (2008)
Vassifjellet	Norway Chamber Test	Non-plastic Silts	0.06-50	22	NA	19.2	21.9-9.4	0.01-0.04	31.0	32.0	Paniagua et al (2016)

Table 5.1. List of twitch test series evaluated by NTH CPTu solution (continued)

Note:

NA= not available

1. Suzuki (2015) adopted 28° in his thesis as the lab reference for evaluation of the piezocone dissipation tests.
2. The friction angles were estimated based on the plasticity index (Bjerrum & Simons, 1960; Kanji, 1974)

5.5 Case Studies

Three case studies are presented to show the reasonableness of interpreting effective friction angles using CPTu results in conjunction with the NTH solution under standard and variable penetration rates.

5.5.1 Standard penetration rate field CPTu in offshore clays, Troll, North Sea

Results of CPTu in soft clay at the offshore Troll site in the North Sea are utilized to illustrate the application and ability of the NTH method at the standard penetration rate of 20 mm/s. Extensive in-situ and laboratory testing programs have been conducted at the Troll gas field site, including field vane, piezocone, and pressuremeter tests, complemented by laboratory index, one-dimensional consolidation, and triaxial tests (Amundsen et al. 1985, Lunne et al. 2007, and Uzielli et al. 2007). The site shows two distinct clay layers. From the seabed to 16 m depth lies an upper high plasticity clay deposit of medium sensitivity ($\gamma_t \approx 16.8$ kN/m^3 and PI ≈ 37), which is underlain by a lower lean clay deposit of low sensitivity ($\gamma_t \approx 20.3$ kN/m^3 and PI ≈ 19) that extends beyond the termination depth of the sounding at 45 m. Consolidation testing indicated OCRs ≈ 1.5 for both clay layers.

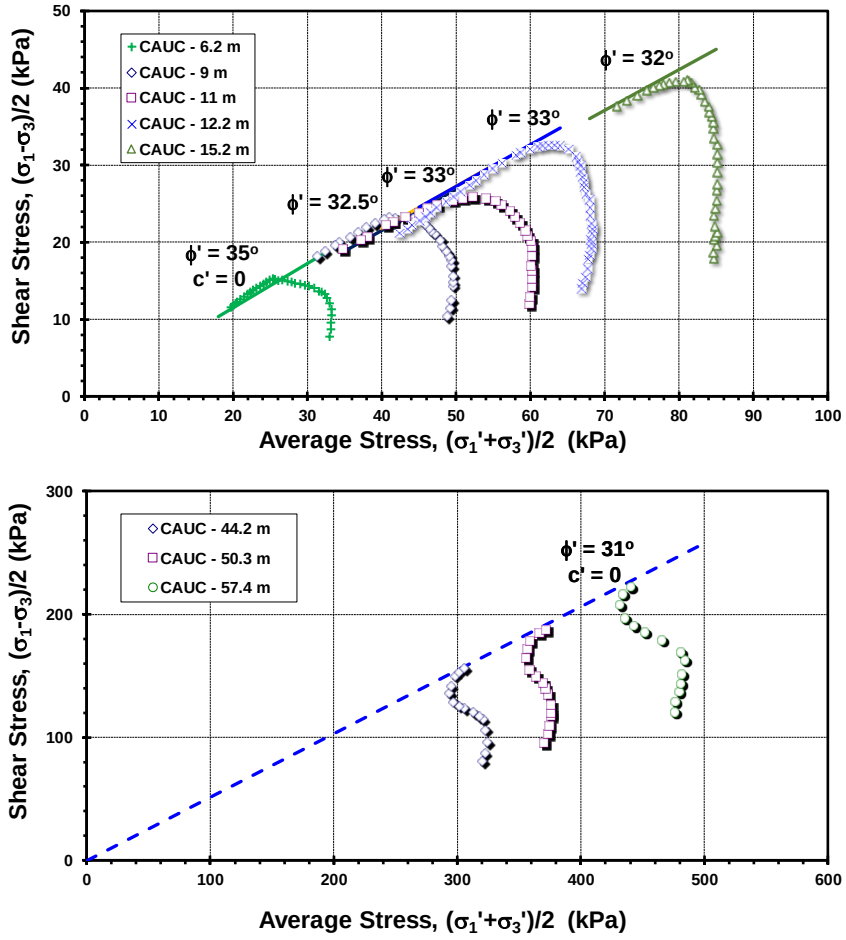

Figure 5.5. Stress paths from CAUC triaxial tests on (a) Upper Troll marine clays, and (b) Lower Troll Marine clays (data from Lunne et al. 2007)

Figure 5.5a shows the effective stress paths from five anisotropically consolidated undrained triaxial compression tests (CAUC) in the upper clay. Figure 5.5b shows three CAUC tests for the lower clay. Taken together, it is observed that the interpreted effective stress friction angle decreases with depth, starting from around $\phi' = 35°$ at 6 m to about $\phi' = 31°$ at depths below 44 below the seafloor.

Figure 5.6a shows a representative CPTu sounding at the site (Lunne et al. 2007). The calculated Q and B_q from CPTu measurements are put into the NTH solution, with

Figure 5.5b showing the CPTu profile of ϕ' with depth. It is quite evident that the results compare well with the benchmark reference friction angles obtained from the laboratory triaxial test series presented in Figure 5.5.

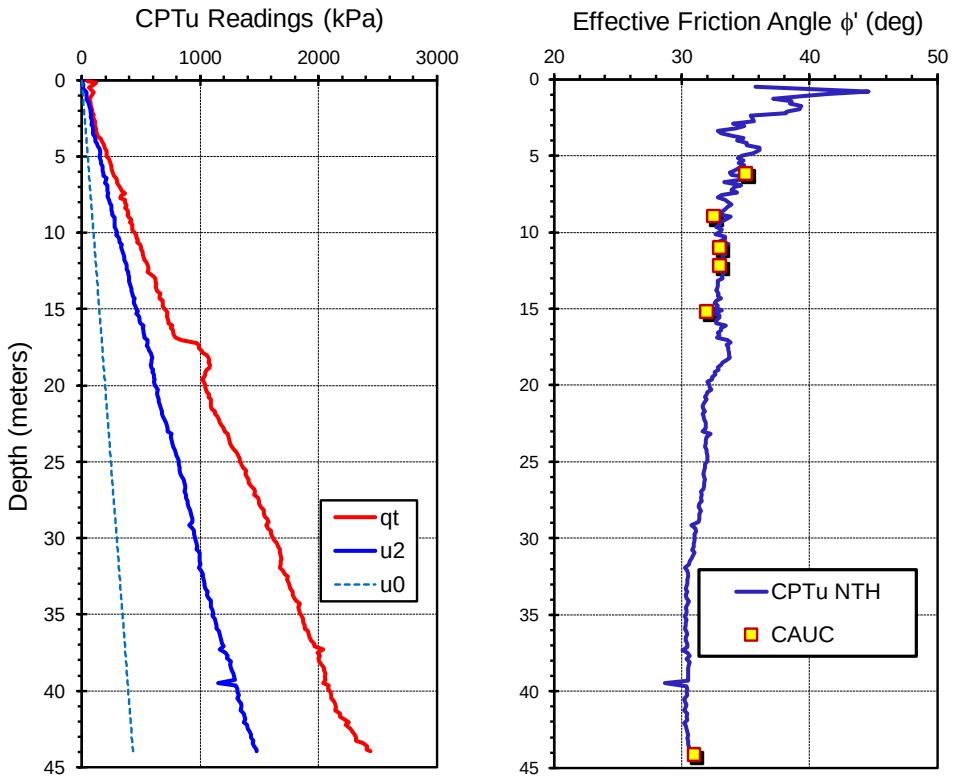

Figure 5.6. (a): Representative CPTu sounding at the Troll clay site, and (b): Profile of NTH interpreted friction angle with reference ϕ' from triaxial tests

5.5.2 Centrifuge model CPTu twitch tests on normally consolidated kaolin

Data from mini-CPTu twitch tests in centrifuge deposits of kaolin at the University of Western Australia are used here to examine the NTH solution at variable rates. Details on the testing program are provided by Mahmoodzadeh and Randolph (2014) who indicate the following properties for the normally-consolidated kaolin: initial water content, w_n = 120%, LL = 61; PL = 27%, G_s = 2.60, and ϕ_{cs}' = 23°. Centrifuge tests were performed using the 1.8-m-radius beam centrifuge which has a maximum payload of 200 kg at an

acceleration of 200g (Randolph et al. 1991). The centrifuge strongbox dimensions are 650 x 390 mm in plan with a height of 325 mm. Mini-CPTu soundings were performed using a 10-mm diameter piezocone with a 60° tip angle and load cell for obtaining the q_t readings and a 1.5-mm-thick polypropylene filter element positioned behind the cone shoulder for measuring u_2.

Tests were conducted in normally consolidated kaolin clay under an acceleration of 110g, and the penetration rates varied from 1 to 0.015 mm/s to ensure capturing the entire range of flow conditions, from undrained to partially drained to fully drained. Piezocone data were collected at various penetration rates and key data for each twitch test and deduced parameters are given in Table 5.2. Specifically, the normalized value of Q for each twitch test rate is found by plotting q_{net} versus σ_{vo}', as shown by Figure 5.7. Similarly, the B_q value for each rate is found from a graph of Δu_2 versus q_{net}, as indicated in Figure 5.8. As evident by the figures, the value of Q generally increases while the corresponding value of B_q decreases as the push rate slows down.

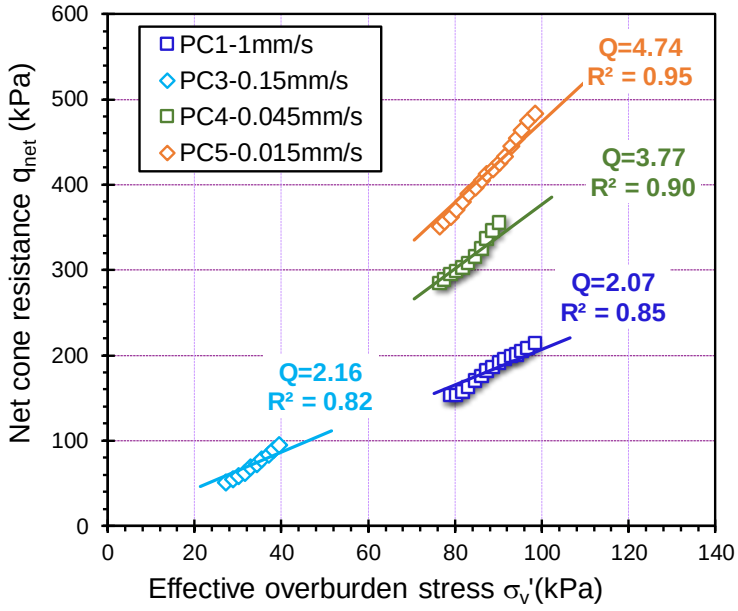

Figure 5.7. Evaluation of cone resistance number Q for mini-CPTu twitch tests in centrifuge deposits of kaolin (data from Mahmoodzadeh and Randolph 2014)

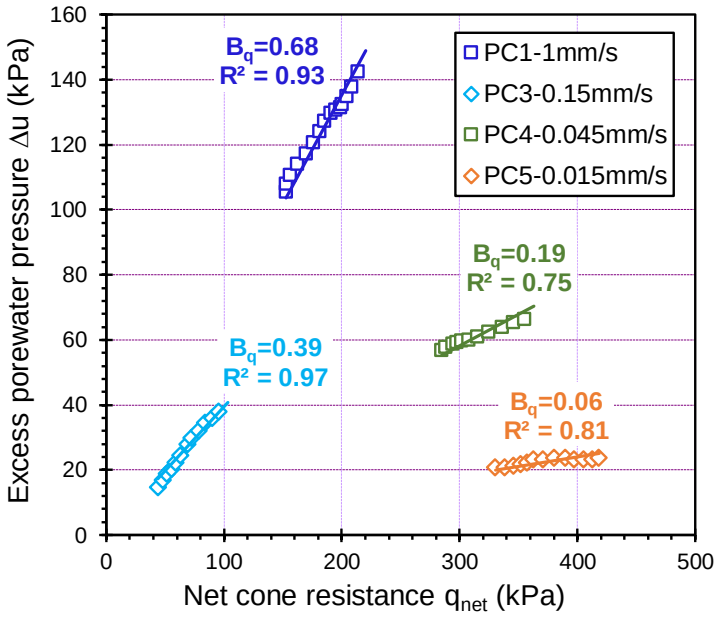

Figure 5.8. Evaluation of porewater pressure parameter B_q for mini-CPTu twitch tests in centrifuge deposits of kaolin (data from Mahmoodzadeh and Randolph 2014)

Table 5.2 . Summary of key data for each piezocone penetration test (data from Mahmoodzadeh and Randolph 2014)

Piezocone test ID*	Laboratory testing and mini-CPTu Parameters				
	Push Rate (mm/s)	V	B_q	Q	NTH ϕ' (°)
PC1	1	78.5	0.68	2.07	22.1
PC3	0.15	11.8	0.39	2.16	19.1
PC4	0.045	3.5	0.19	3.5	21.6
PC5	0.015	1.2	0.06	4.74	20.0

Note: *raw sounding data for tests PC2 and PC6 conducted at push rate of 0.45mm/s and 0.0045mm/s are not provided in the reference, thus are not included herein.

The paired set of Q and B_q for each test series are the input of the NTH solution that can be used to calculate the effective stress friction angle for NC kaolin clays, and the resulting friction angles are plotted on Figure 5.9. Despite the different penetration rates, the NTH method outputs a very consistent and low friction angle ranging between 19.1° and 22.1°, averaging $\phi' = 20.7°$, which is slightly less than the reported value of $\phi' = 23°$ by the UWA team (Mahmoodzadeh and Randolph 2014). Note that triaxial results for Speswhite kaolin reported by Univ. of Colorado (Peric et al 1988) gave $\phi' = 20°$ and CIUC triaxial tests run at Oxford University gave $\phi' = 20.7°$ (Smith 1993), much closer in agreement to the NTH findings.

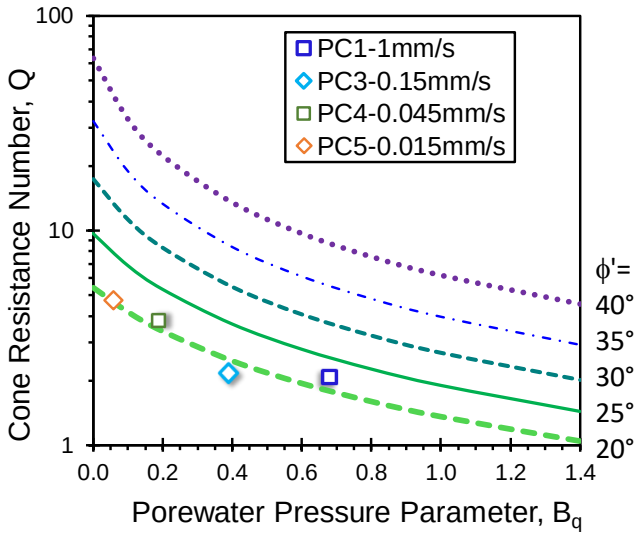

Figure 5.9. NTH evaluated of ϕ′ of kaolin under CPTu twitch test (data from Mahmoodzadeh and Randolph 2014)

5.5.3 Field twitch CPTu in clayey silts at SR18 and SR48, Indiana

A series of field CPTu twitch tests were conducted in clayey silts to silty clays at two Indiana sites that were selected by Purdue University (Kim 2005; Kim et al. 2008). The CPTu soundings were performed at standard penetration rates and slower rates to allow identification of the transitions from undrained to partially-drained, and in some cases, fully-drained conditions. The applied rates ranged from 20 to 0.01 mm/s. Site 1 was located on the west side of a bridge on State Road 18 (SR18) in Carroll County, Indiana. Site 2 is located on State Road 49 (SR49) in Jasper County, Indiana. Details on the soil stratigraphy and geoparameters for each site are given by Kim (2005). The SR 18 site has around 71.5% silt and 24% clay at z=7.4 to 8.4 meters, and the natural water content is about 28.1%, LL=35.1, and PI=16.1. The SR49 site has 64% silt and 21% clay at z=13 to 14 meters, with the natural water content ≈ 23%, LL=21, and PI=9%. The effective stress friction angles for the soils at the two sites were not reported, but they are estimated to be 29° and 35°,

respectively, based on plasticity index correlations (Bjerrum & Simons, 1960; Kanji, 1974).

The paired Q and B_q values under variable penetration rates provide the input for the NTH solution and the evaluated friction angles of ϕ' for SR18 and SR49 are plotted on Figure 5.10. It can be observed that for both sites, the normalized porewater pressure B_q reached 0.1 when the penetration rate is at the slowest, which corresponds nearly to the fully-drained condition. For penetration rates in the range between 20 and 0.2 mm/s, penetration occurred under undrained to partially-drained conditions. Kim et al (2008) report that the transition from undrained to partially drained conditions occurred at a penetration rate of around 0.1 mm/s, considering the observed changes in q_t and u_2 readings. As shown by Figure 5.10, the NTH solution again successfully captures the frictional behavior of the soils, regardless of the penetration rates.

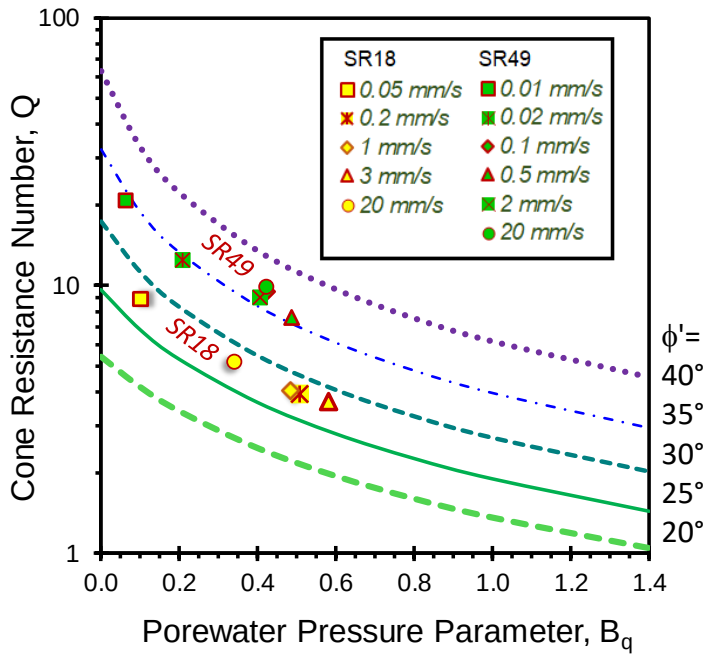

Figure 5.10. Evaluation of ϕ' from field CPTu twitch tests at Indiana field sites SR18 and SR49 based on NTH solution (data from Kim et al 2008)

5.6 CPTu Twitch Test Database Summary

A summary plot of laboratory ϕ' values versus the CPTu-determined ϕ' via the NTH solution with variable drainage conditions is presented in Figure 5.11. The NTH solutions are applied to 13 soils subjected to CPTu under different penetration rates. Each soil is represented by a unique symbol in both shape and color. For all twitch test series, the effective stress friction angle at undrained conditions (V>30) is represented by solid green circles, partially drained conditions are shown by brown squares (0.1<V<30), and drained conditions by hollow blue circles (V<0.1). Two sets of statistical measures were made on the data set, including: (a) arithmetic statistics, and (b) regression statistics, as indicated on the figure. The measured laboratory values of ϕ' cover the full range from 21.0° to 35.0°and the CPTu-evaluated ϕ' from 21.4° to 35.4°. From the arithmetic measures, the ratio of measured/evaluated values ranges from 0.88 to 1.05 with an overall mean of 1.0 and the standard deviation = 0.04, with corresponding COV (coefficient of variation) = 0.04. From the regression evaluations of lab vs. field, the regression slope = 1.01 with a coefficient of determination of R^2 = 0.877 and standard error of the Y-estimate of SEY = 1.24. The above statistics general support that the NTH method gives a reasonable evaluation of the effective friction angle when referenced to the lab triaxial test as the benchmark value.

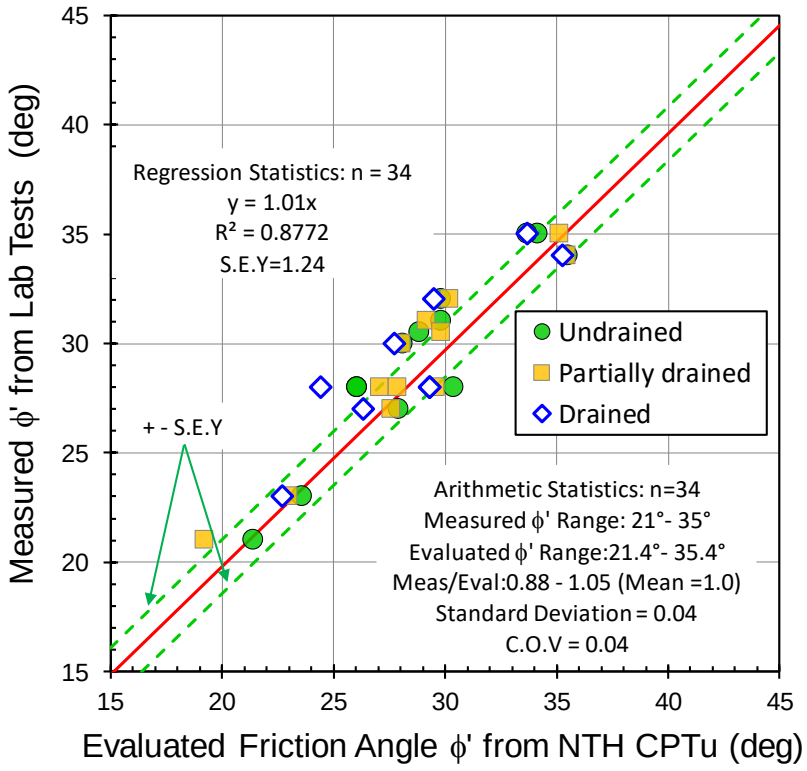

Figure 5.11. Summary plot of laboratory triaxial measured friction angle ϕ′ versus effective friction angle ϕ′ from CPTu under different drainage conditions

As shown by the above case studies and summary of CPTu twitch test data in Figure 5.11, the NTH solution is relatively insensitive to drainage conditions and the evaluated friction angles from the CPTu data under different drainage conditions can be represented by a mean friction angle for all drainage conditions. Figure 5.12 shows the average evaluated friction angle from CPTu twitch tests on each series via NTH solution plotted in comparison with the CIUC or CAUC triaxial reference benchmark value of ϕ'.

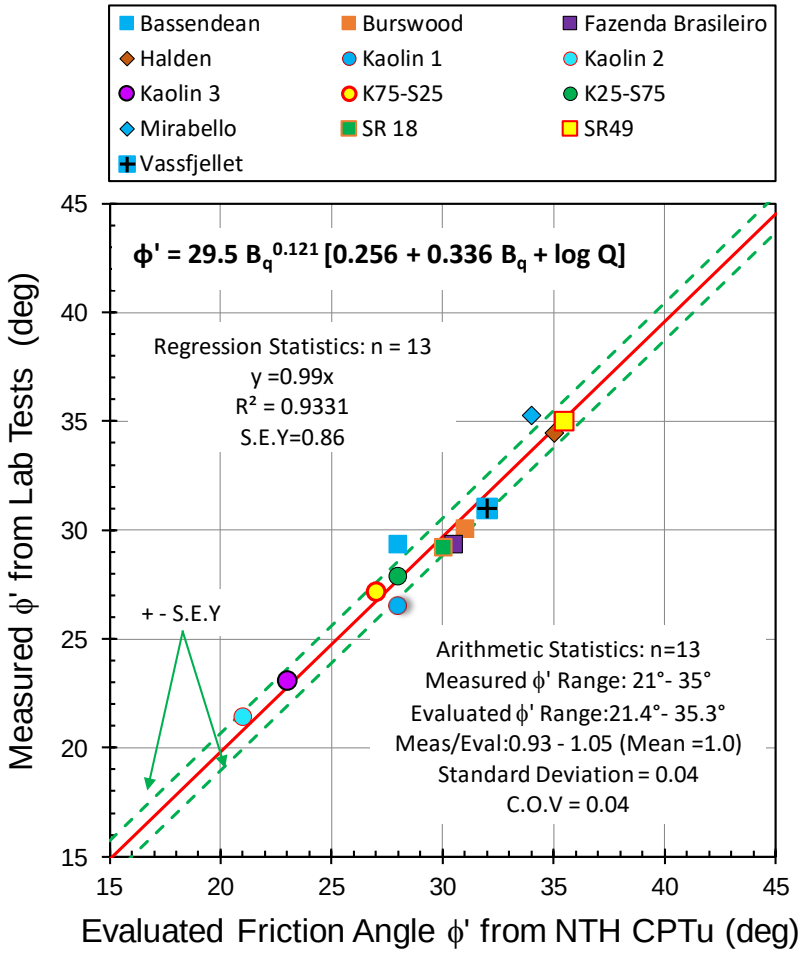

Figure 5.12. Summary plot of laboratory measured triaxial friction angle ϕ′ versus CPTu interpreted ϕ′ (taken as the average value from twitch test series)

5.7 Discussion on Transition Between Drainage Conditions

As established by ASTM, CEN, and ISO standards, the current standard test rate of CPTu is set as 20mm/s, which corresponds to an undrained penetration process for clays and drained penetration for sands. However, for practical implementation, to accurately assess whether partial drainage has happened during standard testing, the transition between different drainage conditions should be determined. The drained condition can be achieved by conducting the test at a very slow rate or through performing and evaluating dissipation tests following penetration at the standard rate of 20mm/s, and the drained

condition is reached when the normalized parameter B_q reaches or approaches zero.

DeJong et al (2012) provided a field decision chart shown by Figure 5.13 that facilitates a simple and efficient evaluation of drained, partially-drained, or undrained penetration rates with a 10 cm^2 penetrometer. During a dissipation test made following the standard rate of 20 mm/s, if the measured time to reach 50% consolidation (t_{50}) is greater than about 100 seconds, undrained conditions prevail during penetration and the corresponding c_{vh} (coefficient of consolidation) is less than about 0.3 cm^2/s. Fully drained conditions occur when u_2 is equal to the hydrostatic water pressure (u_0) and then c_{vh} > 30 cm^2/s. Intermediate conditions with partial drainage can exist when t_{50} < 100 s. If partial drainage had occurred at the standard penetration rate and either drained or undrained results are desired, then the penetration rate necessary to establish drained or undrained conditions can be determined on site.

Of additional note, Robertson (2009) updated the SBT (soil behavior type) using CPTu readings under standard rate of 20mm/s in an effort to improve the application of CPTu for identifying various soil parameters over a wide range. Recommendations were provided to identify transitions zones between drained and undrained using the rate of change of the CPT material index (I_c) near the boundary value of 2.60. The definition of I_c and its corresponding interpretations were given in details by Robertson (2009), in which a modified normalized cone tip resistance Q_{tn} has been defined as:

$$Q_{tn} = \frac{q_t - \sigma_{vo}}{\sigma_{atm}} \cdot \left(\frac{\sigma_{atm}}{\sigma'_{vo}}\right)^n \qquad [5.9]$$

where σ_{atm} = 1 atmosphere $\approx$ 1 bar = 100 kPa and the exponent n is varying with soil type, with typical values of 1.0 in the general case of clays (I_c > 2.95), n = 0.75 for silty soils,

and n = 0.5 for clean sands (I_c < 2.05). The exponent n is a function of the material index I_c which in turn is dependent on the modified normalized cone tip resistance ($Q = Q_{tn}$). Therefore, an iterative approach is needed to find the appropriate exponent n to identify the CPT material index using:

$$n = 0.381 \cdot (I_c) + 0.05 \cdot (\sigma_{v0}'/\sigma_{atm}) - 0.15 \quad [5.10]$$

Furthermore, Schneider (2008) proposed a modified classification chart for CPTu readings and assessed CPTu data in Q-U* space also under 20mm/s and provided a new framework compared to traditional Q-B_q space to identify sands, silts and clays, or soil types.

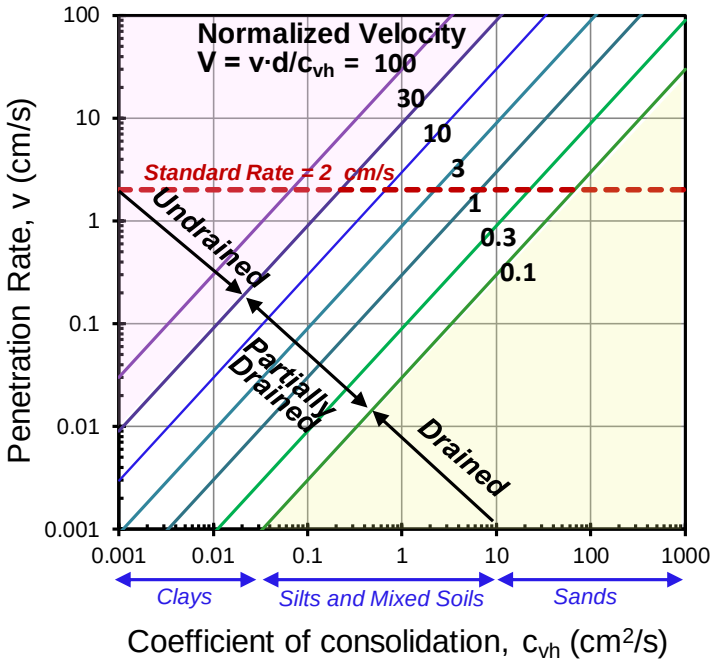

Figure 5.13. Field decision chart for 10 cm^2 cone penetrometer presenting relation between coefficient of consolidation, penetration velocity, and normalized velocity. (modified after DeJong et al 2012)

5.8 Conclusions

An established effective stress limit plasticity solution for obtaining effective stress friction angles (ϕ') from CPTu in a variety of soils is applied to data obtained in variable rate testing, i.e. twitch tests. This permits an evaluation of ϕ' under undrained to partially-drained to fully-drained conditions. Compiled data from 20 CPTu twitch test series are taken from the geotechnical literature according to three groupings: (a) field tests on natural soils; (b) 1-g laboratory chamber tests; and (c) mini-CPTu in centrifuge model tests. All results more or less show that the NTH solution for ϕ' is constant and independent of penetration rate, providing a consistent output, regardless of drainage conditions. Where available, benchmark ϕ' results from CIUC and CAUC triaxial compression tests were used to verify the CPTu ϕ' values from the NTH solution, obtaining reasonable statistical results. As ϕ' is a fundamental soil property of soils, it follows from effective stress analyses, critical state soil mechanics, and most FEM soil constitutive models that indeed its value would be a soil property and therefore constant for a given soil deposit, regardless of whether drained, partially-drained, and/or drained soil conditions were prevailing.

CHAPTER 6. EFFECTIVE STRESS FRICTION ANGLE OF SOFT TO FIRM CLAYS FROM FLAT DILATOMETER

6.1 Introduction

Both the flat plate dilatometer test (DMT) and piezocone penetration test (CPTu) are relatively fast in-situ tests that permit the delineation of soil stratigraphy and the interpretation of geoparameters in an efficient, economic, and expedient manner with depth. Of special interest herein is the interpretation of DMT data taken in soft to firm clays within the context of an effective stress framework to evaluate the friction angle (ϕ').

6.1.1 Flat plate dilatometer

The flat plate dilatometer test (DMT) consists of pushing a flat blade into the ground at regular 0.2-m vertical depth intervals and laterally expanding a 60-mm diameter flexible steel membrane with nitrogen to obtain two readings at each elevation, including: the contact pressure (p_0) and expansion pressure (p_1). Details concerning the DMT equipment, test procedures, and interpretation are detailed by Marchetti (1980) and Marchetti et al. (2001).

6.1.2 Piezocone penetrometer

The piezocone penetration test (CPTu) involves pushing a highly-instrumented electronic probe vertically into the ground at 20 mm/s to collect three continuous readings with depth, including: cone tip resistance (q_t), sleeve friction (f_s) and porewater pressure at the shoulder (u_2). Details concerning the CPTu equipment, field test procedures, and

interpretations are given by Lunne et al. (1997) and Mayne (2007). The penetrometer utilizes load cells and pressure transducers to obtain readings at approximate depth intervals of 0.02 m.

6.1.3 Geoparameter interpretation

During site investigations, the combination of these two in-situ tests can be a nice complement in defining the geotechnical parameters of the subsurface environment. The piezocone penetration test provides three separate readings with depth, whereas the flat dilatometer test gives two readings during the field procedure. Both tests have been utilized to evaluate a wide variety of geotechnical parameters, such as: soil behavioral type (SBT), unit weight (γ_t) overconsolidation ratio (OCR), undrained shear strength (s_u) of clays, effective friction angle in sands (ϕ'), Young's modulus (E), lateral stress coefficient (K_0), and coefficient of consolidation (c_v), as well as an assessment of liquefaction potential of sands. The interpretation procedures for each test have been developed separately and on the basis of different principles, including analytical, theoretical, empirical, and statistical means.

Normally, for clay soils, a total stress analysis is adopted and the geotechnical engineer seeks an interpretation of the undrained shear strength (s_u). For the CPTu, the normal means for assessing s_u is from a bearing capacity expression, such as $s_u = q_{net}/N_{kt}$ where the factor N_{kt} is found by: (a) calibration with laboratory strength tests, (b) theoretical factors derived from analytical or numerical solutions; and/or (c) assumed value based on past experience for the type of clay encountered. With regards to the latter, for a triaxial compression mode, values of $N_{kt} = 12$ are reported for soft-firm inorganic and insensitive

clays; 10 for sensitive clays; 14 for overconsolidated intact clays; and 20+ for fissured OC clays (Mayne & Peuchen, 2018). For the flat dilatometer, an empirical correlation for s_u was given by Marchetti (1980) using the horizontal stress index, $K_D = (p_0-u_0)/\sigma_{vo}'$, which corresponded to a simple shear mode, although a number of other approaches have been reported (Mayne & Martin 1998).

Alternatively, an effective stress limit plasticity solution has been established towards the evaluation of the effective stress friction angle ϕ' for undrained conditions for CPTu data obtained in a variety of soils ranging from sands to silts to clays, as developed at the Norwegian Institute of Technology (NTH) and detailed by Senneset et al. (1989) and Sandven & Watn (1995). Current interpretative procedures (Marchetti 2015) for the DMT have not included a method for evaluating ϕ' in clays. Therefore, a CPTu-DMT link was established herein using cavity expansion theory to explore a means for this purpose. One advantage of assessing ϕ' is that it applies to both drained and undrained behavior of clay, thus is more fundamental in its role as soil property, rather than a soil parameter.

6.2 Effective Stress Limit Plasticity Solution

Soft to firm intact clays exhibit excess porewater pressures during penetration tests ($\Delta u > 0$). At the Norwegian Institute of Technology (NTH, now called Norwegian University of Science & Technology, NTNU), Senneset et al. (1989) derived an effective stress limit plasticity solution for the CPTu towards the evaluation of ϕ′ for undrained penetration of clays and clayey silts. In this approach, a cone resistance number (N_m) is defined as:

$$N_m = \frac{N_q - 1}{1 + N_u \cdot B_q} = \frac{q_t - \sigma_{vo}}{\sigma_{vo}' + a'} \quad [6.1]$$

where $B_q = \Delta u/q_{net}$ = normalized porewater pressure parameter, $a' = c' \cdot \cot\phi'$ =effective attraction and c' = effective cohesion intercept. The tip bearing capacity factor (N_q) and the porewater pressure bearing factor N_u are given by (Sandven 1990):

$$N_q = K_p \cdot \exp[(\pi - 2\beta) \cdot \tan\phi'] \quad [6.2]$$

$$N_u = 6 \cdot \tan\phi' (1 + \tan\phi') \quad [6.3]$$

$$K_p = (1 + \sin\phi')/(1 - \sin\phi') \quad [6.4]$$

where K_p is the passive lateral stress coefficient, β= angle of plastification ($-40^o < \beta < +30^o$) that defines the size of the failure zone around the tip.

The full solution allows for an interpretation of a paired set of effective stress Mohr-Coulomb strength parameters (c′ and ϕ′) for all soil types: sands, silts and clays, as well as mixed soils (Sandven 1990). The parameter N_q is the tip bearing capacity factor from limit plasticity solutions, commonly used for end bearing resistances in pile foundations.

For the case where $\beta = 0^o$, the expression for N_q is identical to the classical solution for a deep foundation given by Terzaghi (1925). The parameter N_u is a porewater pressure bearing factor, not recognized by the more classical limit plasticity solutions. The resulting relationships for ϕ′ in terms of N_m and parametric values of B_q are presented in graphical form in Figure 6.1. Note that when $a' = c' = 0$, the parameter N_m is identical to the normalized cone tip resistance $Q_t = \frac{q_t - \sigma_{vo}}{\sigma_{vo}'}$ that is used extensively in CPTu interpretations, particularly applicable to soft to firm clays (Lunne et al., 1997).

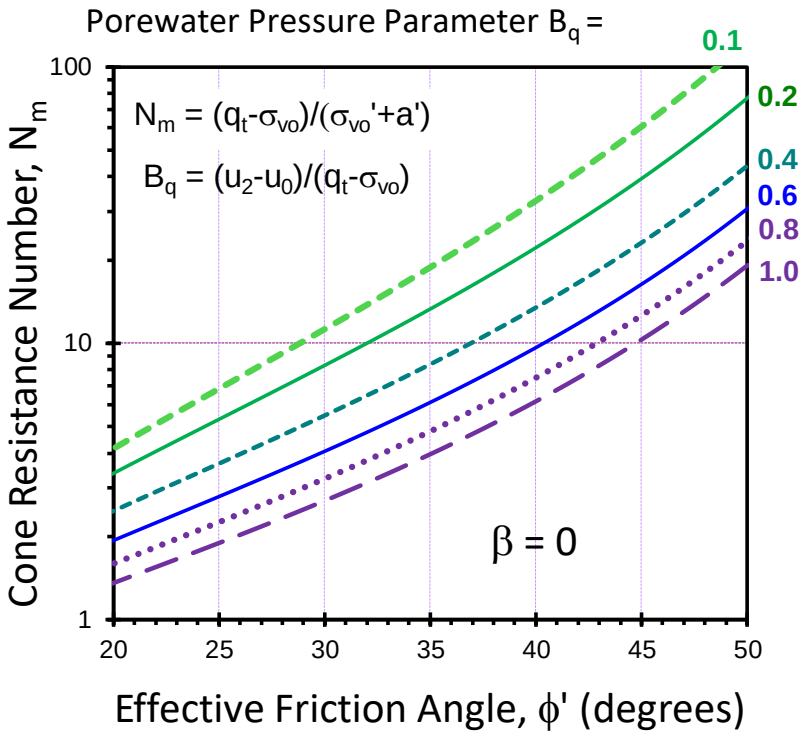

Figure 6.1. NTH method for evaluating ϕ′ from CPTUs in silts and clays

6.3 CPTu-DMT link from spherical cavity expansion theory

For CPTu results, the undrained shear strength (s_u) is most often evaluated in terms of the net total cone tip resistance ($q_{net} = q_t - \sigma_{vo}$). If the relevant mode of undrained shear strength corresponds to that for triaxial compression (s_u), then:

$$s_u = \frac{q_{net}}{N_{kt}} \qquad [6.5]$$

where N_{kt} = bearing factor for net tip resistance. The spherical cavity expansion (SCE) solution formulated by Vesić (1977) gives:

$$N_{kt} = 4/3 \cdot [\ln(I_R) + 1] + \pi/2 + 1 \qquad [6.6]$$

where $I_R = G/s_u$ =rigidity index and G = shear modulus. Therefore, the net cone resistance from the piezocone can be expressed as:

$$q_{net} = s_u \cdot \{ 4/3 \cdot [\ln(I_R) + 1] + \pi/2 + 1\} \quad [6.7]$$

In a similar manner, the undrained shear strength can alternatively be expressed in terms of the excess porewater pressures during penetration ($\Delta u = u_2 - u_0$):

$$s_u = \frac{\Delta u}{N_{\Delta u}} \quad [6.8]$$

where $N_{\Delta u}$ = bearing factor for excess porewater pressures. Here, SCE provides the bearing factor expression as:

$$N_{\Delta u} = 4/3 \cdot \ln (I_R) \quad [6.9]$$

which addresses changes in the mean stress at constant soil volume.

The standard position of the porewater pressure measurements obtained by the piezocone is at the shoulder (u_2), as detailed by Lunne et al. (1997) and Mayne (2007). The measured excess porewater pressures (Δu_2) in fact is comprised of two components: (a) changes in octahedral stress changes and (b) shear-induced pressures because of clay–steel interface interactions (Burns and Mayne, 2002). However, for young to aged normally-consolidated (NC) to lightly-overconsolidated (LOC) clays with $1 < OCR < 2$, the shear-induced portion is rather small compared with the octahedral portion and considered to be less than 20% of the total Δu (Baligh, 1986; Mayne, 1991). Therefore, considering only the former component is predominant in soft to firm NC-LOC clays, the excess porewater pressure measured by the piezocone can be expressed:

$$\Delta u = u_2 - u_0 = s_u \cdot 4/3 \cdot \ln (I_R) \quad [6.10]$$

For soft to firm intact clays, Mayne & Bachus (1989) and Mayne (2006) showed that the contact pressures (p_0) measured by the flat dilatometer tests (DMT) are very similar

in magnitude to that of the porewater pressures (u_2) measured by piezocone tests, specifically:

$$p_0 \approx u_2 \quad [6.11]$$

Therefore Equation [6.10] can also be expressed in the following manner:

$$\Delta u_{2(CPTu)} = u_2 - u_0 = \Delta u_{DMT} = p_0 - u_0 = s_u \cdot 4/3 \cdot \ln(I_R) \quad [6.12]$$

6.4 CPTu-DMT Database

A special database was compiled from 27 clay sites that were subjected to side-by-side CPTu and DMT soundings, as documented in Table 1. These sites are all comprised of soft to firm clays and silts that are normally- to lightly overconsolidated soils having 1 < OCRs < 2. Origins of these clays vary from marine, alluvial, estuarine, glacial, to lacustrine. Reference sources reporting the piezocone and dilatometer data are noted in Table 1. The plasticity characteristics range widely from lean to highly plastic (11% <PI<100%). As per the general concept that $u_2 = p_0$, the direct link between measured excess porewater pressure (Δu) from the CPTu and net contact pressure ($p_0 - u_0$) from the DMT given by Equation [6.12] seems to be validated, as shown by Figure 6.2, where data from the clay sites are plotted.

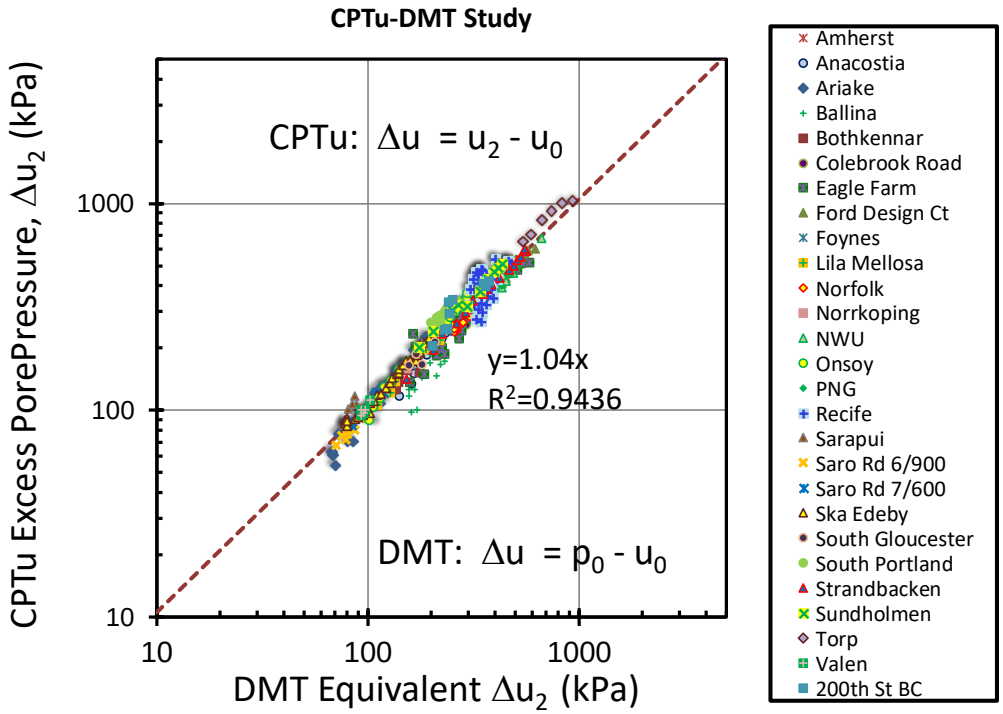

Figure 6.2. Excess porewater pressure from CPTu versus DMT-equivalent Δu

6.5 Equivalent net resistance from DMT

The SCE solution provides the magnitude of change in horizontal stress (Vesic 1972):

$$\Delta\sigma_h = s_u \cdot 4/3 \cdot [\ln(I_R)+1] \quad [6.13]$$

The increase in radial stress can be interpreted to relate directly to the DMT expansion pressure (p_1), specifically the net expansion pressure ($p_1 - u_0$) as expressed:

$$\Delta\sigma_h = p_1 - u_0 \quad [6.14]$$

Therefore, the undrained shear strength can be represented as:

$$s_u = (p_1 - u_0)/\{4/3 \cdot [\ln(I_R)+1]\} \quad [6.15]$$

Substituting the SCE terms from Equation [6.12], [6.13] and [6.14] gives an expression of the rigidity index from the dilatometer as:

$$\ln(I_R) = (p_0 - u_0)/(p_1 - p_0) \quad [6.16]$$

A further combination of Equation [6.15] and [6.16] into Equation [6.7] gives an equivalent net cone tip resistance (q_{net}) in terms of dilatometer readings as:

$$q_{netDMT} = 2.93 \cdot p_1 - 1.93 \cdot p_0 - u_0 \qquad [6.17]$$

The above euqation gives a new approach that expresses the q_{net} resistance as an equivalent value obtained from the flat dilatometer test pressures. This approach is shown to work very well for soft-firm NC-LOC clays (1<OCR<2), as evidenced by Figure 6.3 using the data obtained from the 27 soft clay sites cited in Table 6.1.

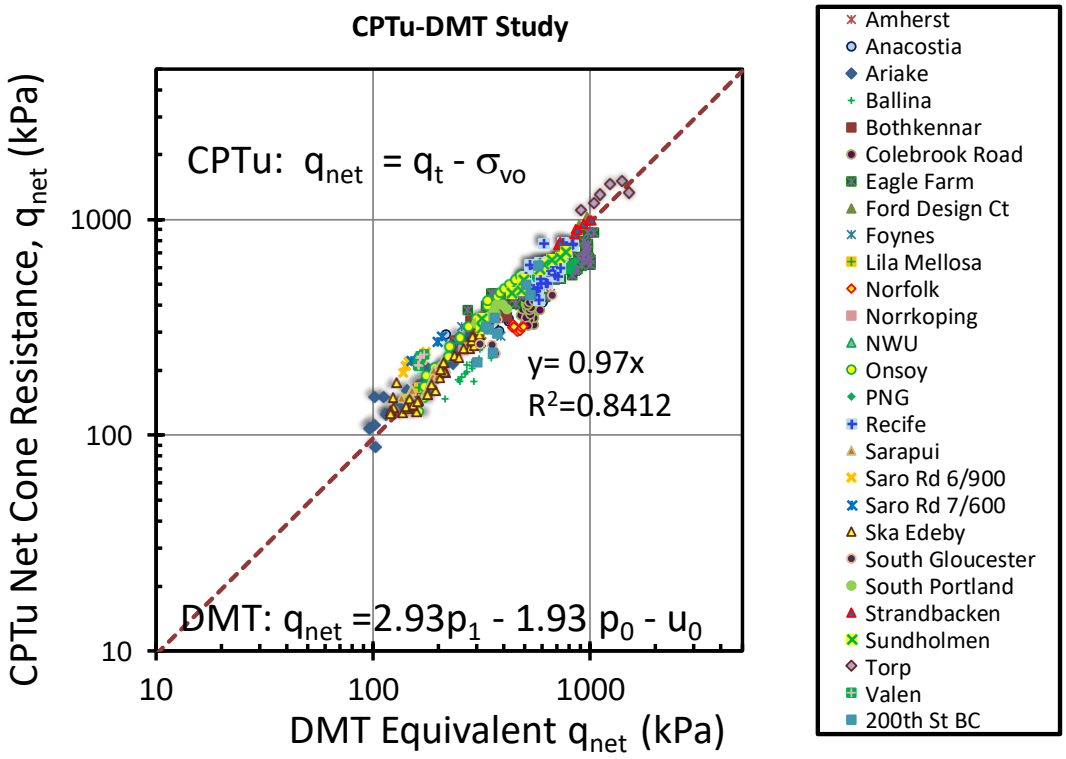

Figure 6.3. Net cone resistance q_{net} from CPTu versus DMT-equivalent q_{net}

The piezocone penetration test (CPTu) provides both q_{net} and Δu readings at each elevation which are needed in the NTH method for obtaining ϕ' in clays and silts. With the aforementioned links now given by Equation [6.12] and [6.17], the flat dilatometer test

(DMT) readings p_0 and p_1 can now be used to obtain the necessary parameters q_{net} and Δu for input into the NTH method.

Based on the above derivations, one can establish an equivalent DMT expressions giving the equivalent values for cone resistance number (N_m) and porewater pressure parameter (B_q):

$$\text{DMT-equivalent } N_m = q_{net}/\sigma_{vo}' = (2.93p_1 - 1.93p_0 - u_0)/\sigma_{vo}' \quad [6.18]$$

$$\text{DMT-equivalent } B_q = \Delta u/q_{net} = (p_0 - u_0)/(2.93p_1 - 1.93p_0 - u_0) \quad [6.19]$$

Table 6.1. List of soft to firm clay sites subjected to both piezocone penetration tests (CPTu) and flat dilatometer tests (DMT)

Site Name and Location	Clay Type	Depth (m)	Reference Source
Amherst, Massachusetts	Lacustrine Varved	5-11	Hegazy (1998)
Anacostia, Washington, DC	Alluvial Organic	5-18	Mayne (1987)
Ariake, Japan	Marine	4-17	Watabe et al (2003)
Ballina, Australia	Estuarine	3-11	Pineda et al (2014)
Bothkennar, Scotland	Estuarine	3-11	Hight et al. (2003)
Colebrook Road, BC	Sensitive	8-24	Crawford & Campanella (1991)
Eagle Farm, Australia	Estuarine	5-20	McConnell (2015)
Ford Design Center, Illinois	Lacustrine	7-19	Mayne (2006)
Foynes, Ireland	Alluvial	5-12	Carroll and Long (2012)
PNG, Australia	Estuarine	6-26	McConnell (2015)
Lilla Mellösa, Sweden	Plastic	2-11	Larsson & Mulabdic (1991)
Norfolk, Virginia	Marine	7-14	Cargill (2015)
Norrköping, Sweden	Varved	2-12	Larsson & Mulabdic (1991)
Northwestern Univ, Illinois	Lacustrine	11-20	Mayne (2006)
Onsøy, Norway	Marine	4-1 9	Lunne et al. (2003)

Table 6.1. List of soft to firm clay sites subjected to both piezocone penetration tests (CPTu) and flat dilatometer tests (DMT) (continued)

Site Name and Location	Clay Type	Depth (m)	Reference Source
Recife, Brazil	Organic	8-25	Danziger (2007)
Sarapui, Brazil	Organic	5-11	Almeida et al. (2003); Danziger (2007)
Särö Rd 6/900, Sweden	Organic	2-7	Larsson & Mulabdic (1991)
Särö Rd 7/600, Sweden	Organic	2-7	Larsson & Mulabdic (1991)
Skå Edeby, Sweden	Glacial	2-11	Larsson & Mulabdic (1991)
South Gloucester, Ontario	Sensitive Marine	5-17	McRostie and Crawford (2001)
South Portland, Maine	Marine	5-17	Roche (2006)
Strandbacken, Sweden	Glaciomarine	3-21	Larsson and Ahnberg (2003)
Sundholmen, Sweden	Marine	5-19	Larsson and Ahnberg (2003)
Torp, Sweden	Glaciomarine	10-40	Larsson and Ahnberg (2003)
Vålen, Sweden	Sensitive organic	3-7	Larsson & Mulabdic (1991)
200th Street, BC	Sensitive	7-16	Cruz (2009)

6.6 Case Studies

Two case studies are presented to illustrate the application of the NTH solution and show the reasonableness of evaluating effective friction angles in soft clays using DMT results.

6.6.1 Onsøy, Norway

Onsøy clay is a thick deposit of highly uniform normally- to lightly overconsolidated soft marine clay that serves as a national geotechnical test site in Norway. A wide range of in situ tests and different laboratory tests has been conducted to investigate the properties of the clay material at Onsøy (Lunne et al., 2003). Figure 6.4 shows a representative DMT sounding to 20 m depth with corrected pressures p_0 and p_1 at the site, along with the material index: $I_D = (p_1-p_0)/(p_0-u_0)$, dilatometer modulus: $E_D=34{\cdot}7(p_1-p_0)$ and horizontal stress index: $K_D = (p_0-u_0)/\sigma'_{vo}$ (Lacasse & Lunne 1982). Based on evaluation of the soil behavioral type, which relies on the material index I_D (Marchetti, 1980), the soil is characterised as clay.

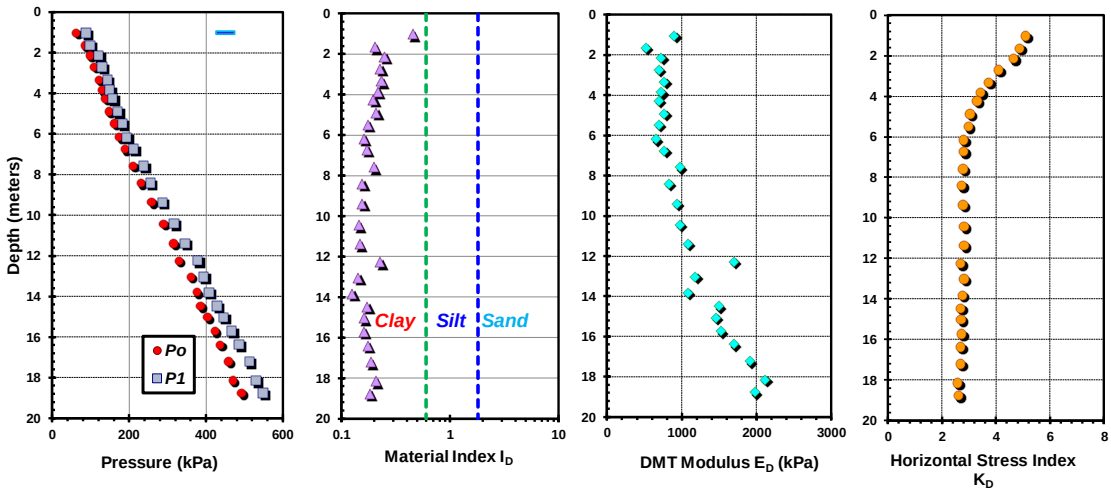

Figure 6.4. DMT profiles for soft Onsøy clay (data from Lunne et al., 2003)

The procedure for determining the DMT-equivalent resistance $N_{mDMT} = Q_{DMT}$ is found from the slope of a plotting equivalent net cone resistance against effective overburden stress, as illustrated in Figure 6.5(a). In this example, the line was forced through the origin (assuming $c' = 0$) to obtain $N_{mDMT}=4.1$. By the same token, the DMT-equivalent porewater parameter $B_{q\text{-}DMT}$ is determined as the slope of Δu_{DMT} versus q_{netDMT}, giving the DMT-equivalent porewater parameter $B_{qDMT} = 0{\cdot}66$ for the Onsøy site, as indicated in Figure 6.5(b). These values are inputs to the solution chart in Figure 6.6, showing an effective friction angle $\phi' = 31°$ for the Onsøy clay.

In Figure 6.7, the NTH-interpreted ϕ' is compared with the laboratory value of the effective stress friction angle (taken at maximum deviator stress) from anisotropically consolidated undrained compression (CAUC) triaxial tests conducted on block samples taken over a range of depths at the site, as reported by Lacasse et al. (1985). The results from the DMT-equivalent NTH method match quite well with the lab stress path data.

In lieu of the separate plots for N_m and B_q given in Figure 6.5, Mayne (2005) derived an approximate NTH friction angle equation for soft to firm clays with $c' = 0$ and assuming $\beta = 0$, which is shown in graphical format in Figure 6.8 and given by the following mathematical expression:

$$\phi' = 29.5\, B_q^{0.121}\, [0.256 + 0.336\, B_q + \log N_m] \qquad [6.20]$$

The above equation is applicable when: $1 \leqslant OCR \leqslant 2.5$, $20^o \leq \phi' \leq 45^o$ and $0.05 \leq B_q \leq 1.0$.

Figure 6.9 presents the DMT equivalent N_m and B_q profiles with depth, as well as the approximate NTH friction angle profile, by adopting Equation [6.18] and [6.19] into

analysis. Again, the approximate NTH friction angle equation compares very well with the laboratory triaxial stress path results interpreted at maximum deviator stress.

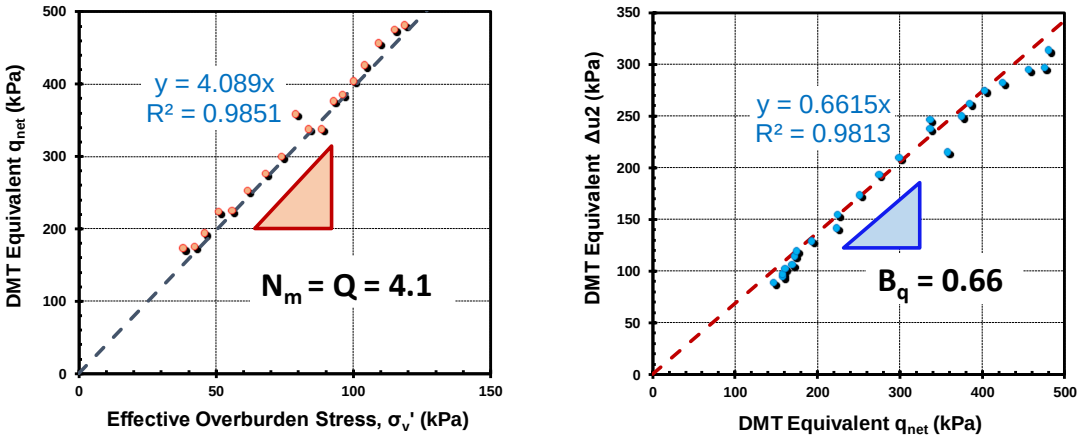

Figure 6.5. NTH post-processing of DMT data at Onsøy for determination of (a) DMT-equivalent N_m and (b) DMT-equivalent porewater pressure Bq

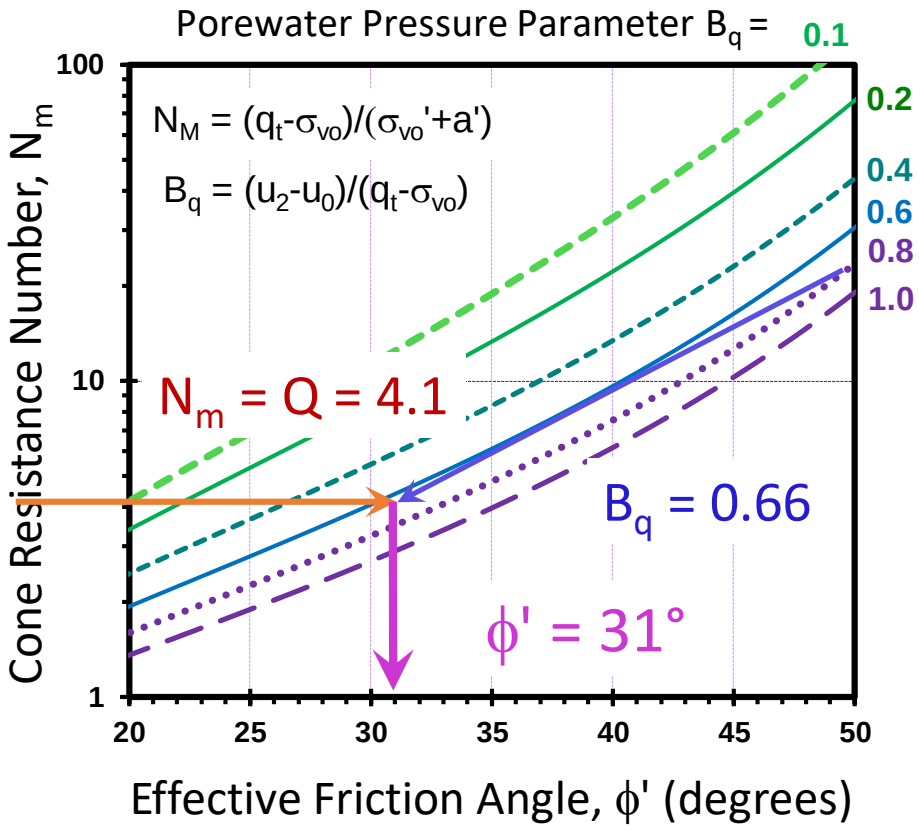

Figure 6.6. Evaluating ϕ′ from DMT results at Onsøy clay site

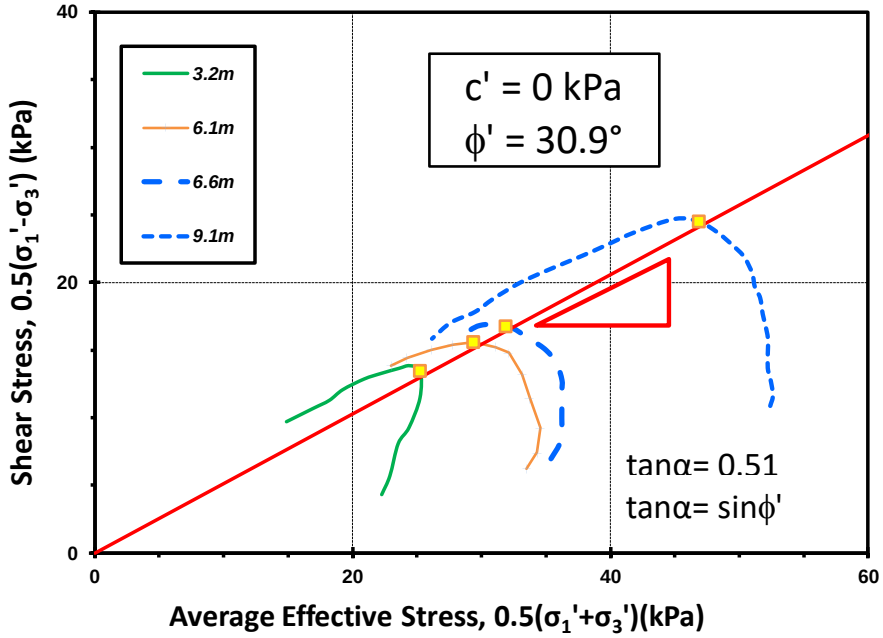

Figure 6.7. Laboratory triaxial tests on Onsøy clay showing effective stress friction angle defined at q_{max} (data from Lunne et al. 2003)

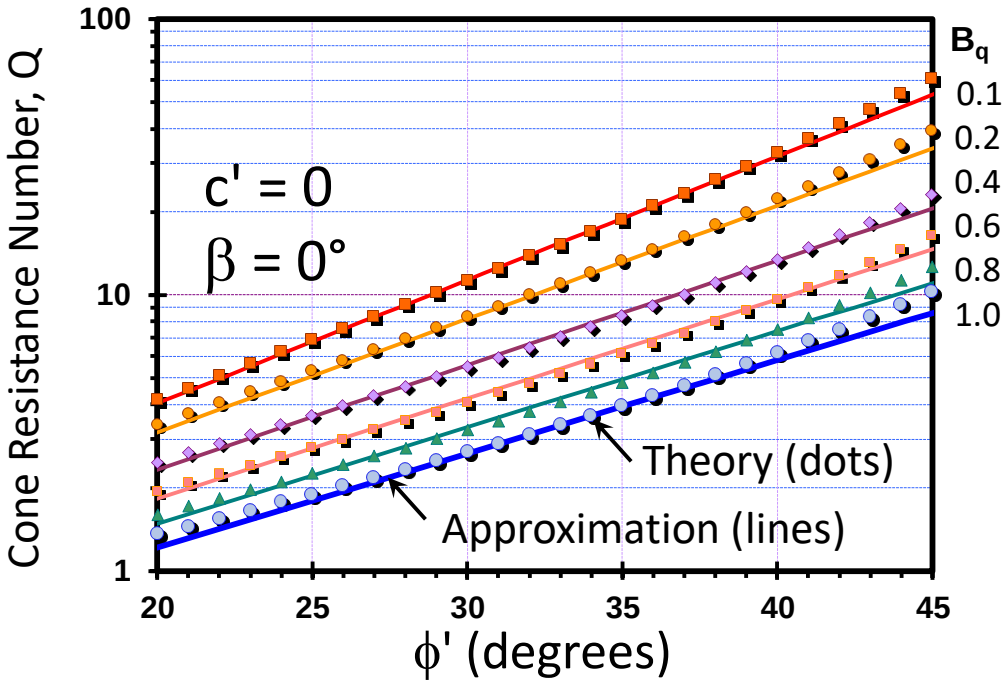

Figure 6.8. Approximate NTH expression for evaluating ϕ′ in clays (after Mayne, 2007)

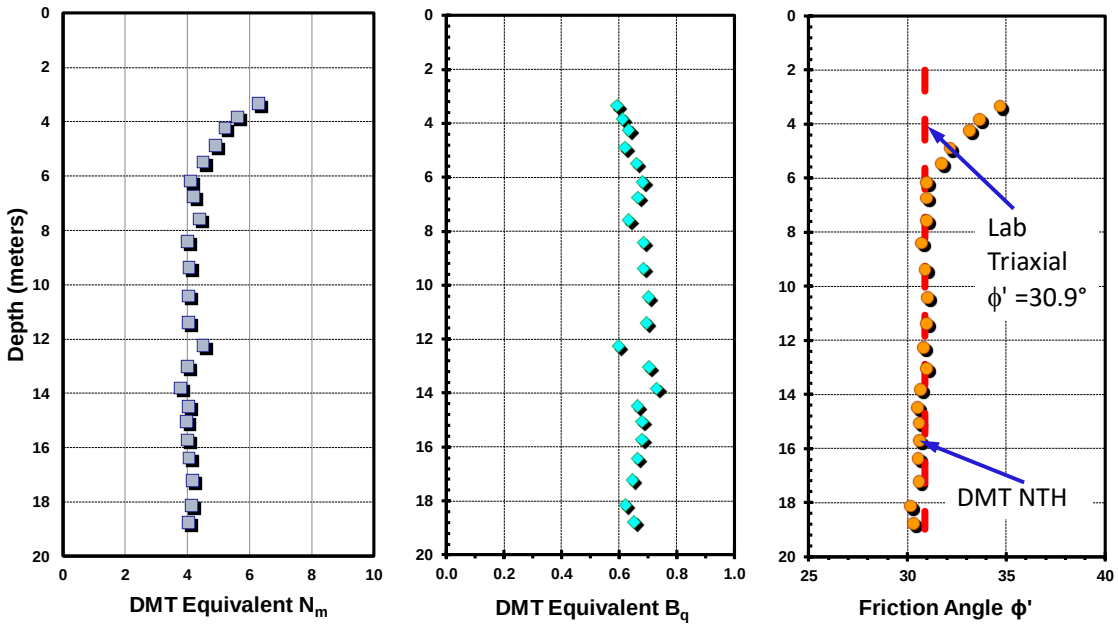

Figure 6.9. Profiles of DMT-equivalent resistance number (N_m), DMT-equivalent normalized porewater pressure (B_q) and evaluated ϕ' profile at Onsøy soft clay

6.6.2 Bothkennar, Scotland

Bothkennar soft clay is a lightly- to normally-consolidated estuarine soft clay in Scotland which serves as a national test site in the United Kingdom (Hight et al. 1992, 2003; Nash et al. 1992). The water table at the site is relatively shallow, typically on the order of 1 m deep. Representative DMT readings and derived parameters at the site are shown in Figure 6.10.

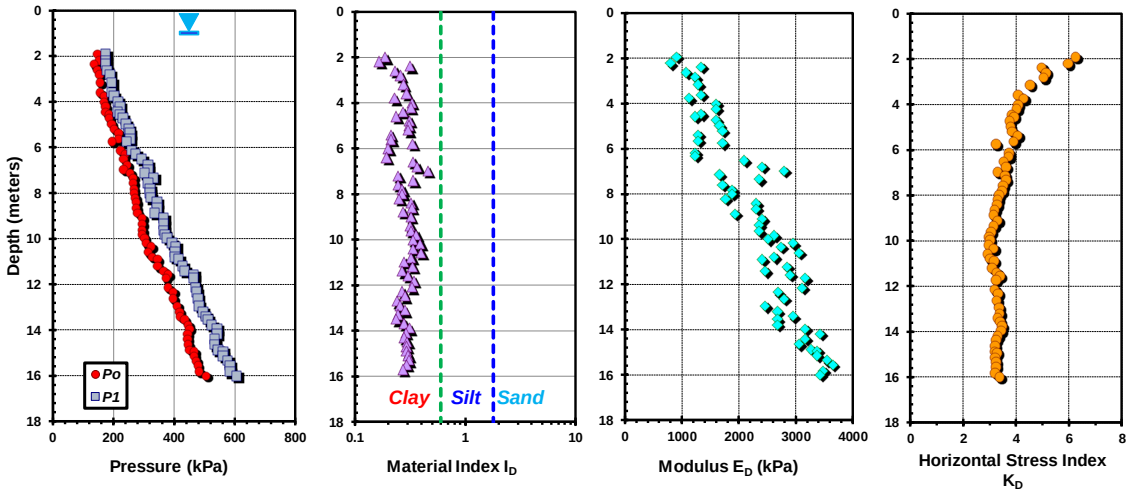

Figure 6.10. DMT profiles for soft Bothkennar clay (data from Hight et al., 2003)

Based on the aforementioned analyses, the post-processing of DMT data to obtain the equivalent N_{mDMT} = 5.93 and $B_{q\text{-}DMT}$ = 0.56 are presented in Figure 6.11. The NTH interpretation of the friction angle is presented in Figure 6.12 which outputs a value of effective friction angle of ϕ' = 34º for the soft clay. This compares well with laboratory CAUC triaxial data at maximum deviator stress which gives a friction angle ϕ' = 33.9º and the corresponding stress paths are shown in Figure 6.13. Finally, Figure 6.14 shows the profile of interpreted effective friction angle from the approximate NTH equation and good to excellent agreement with the mean laboratory friction angle.

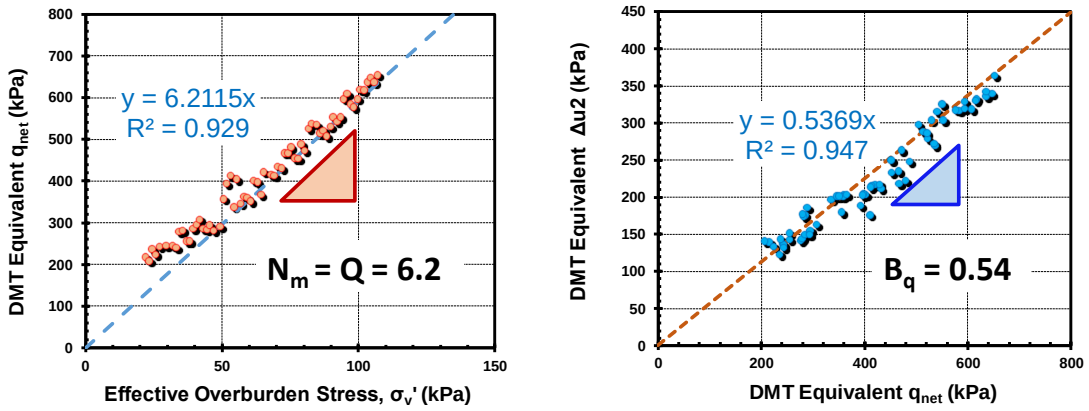

Figure 6.11. NTH post-processing of DMT data at Bothkennar

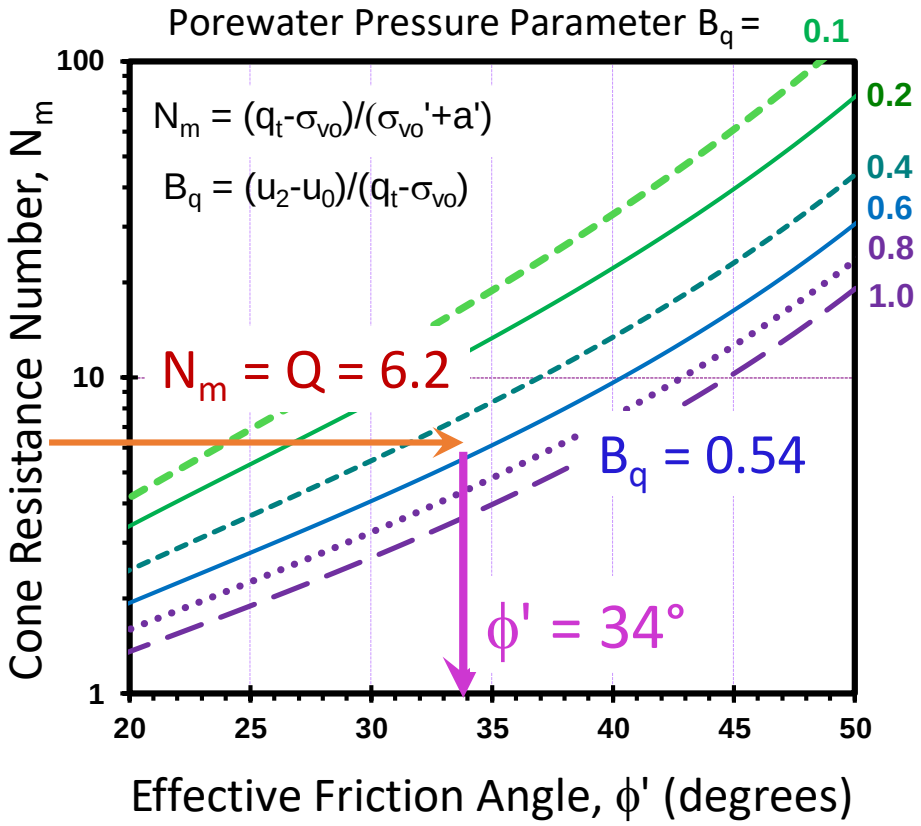

Figure 6.12. Evaluating ϕ' from DMT sounding at Bothkennar soft clay site

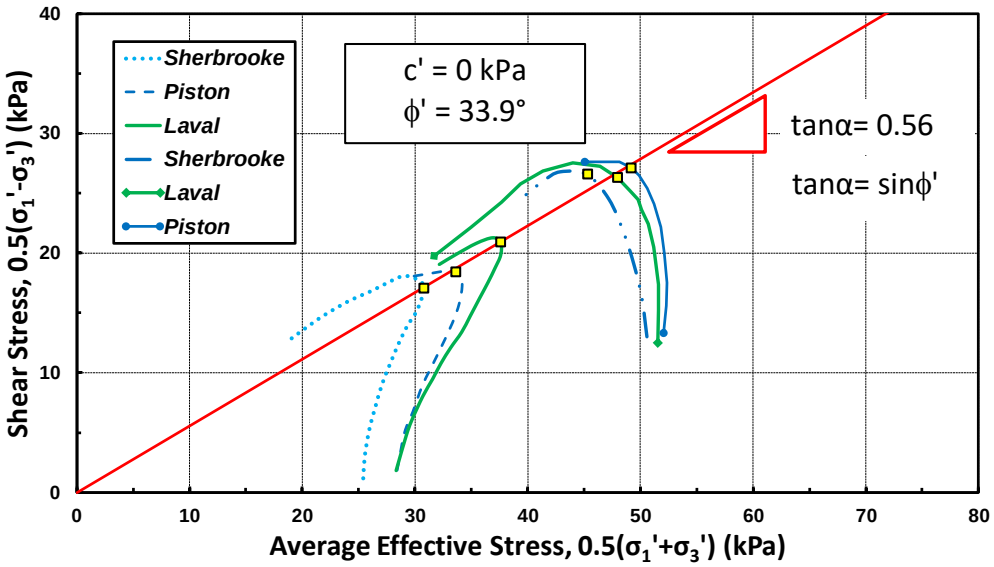

Figure 6.13. Laboratory triaxial stress paths showing the interpreted effective stress friction angle for Bothkennar soft clay (data from Hight et al., 2003)

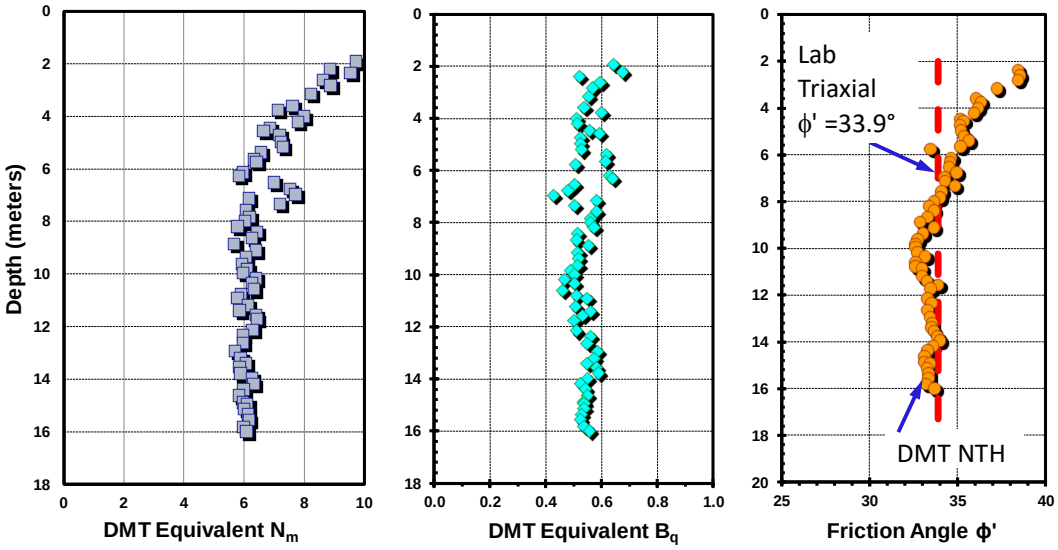

Figure 6.14. Profiles of DMT-equivalent resistance number ($N_{m\text{-}DMT}$), DMT-equivalent normalized porewater pressure ($B_{q\text{-}DMT}$) and effective stress friction angle in Bothkennar soft clay site

6.7 Conclusions

Application of spherical cavity expansion (SCE) theory (Vesić 1977) enables the development of direct closed-form interrelationships between the net cone resistance and excess porewater pressures from piezocone penetration tests (CPTu) and the pressure readings from flat dilatometer test (DMT) in soft to firm clays. Data from 27 soft to firm intact clays confirmed the trends and CPTu-DMT links that were established.

An effective stress limit plasticity NTH solution derived by Senneset et al. (1989) was then adopted for evaluating the effective friction angle (ϕ') of clays using the DMT contact pressure p_0 and expansion pressure p_1. Results from DMT data obtained at two sites are presented to illustrate the approach, including: (a) the national soft clay site Onsøy, Norway; and (b) the national geotechnical test site at Bothkennar, Scotland. Laboratory triaxial test results (CAUC) from these sites verified the reasonableness of the DMT equivalent NTH method in assessing ϕ'.

CHAPTER 7. SPHERICAL CAVITY EXPANSION NEXUS BETWEEN CPTU AND DMT IN SOFT-FIRM CLAYS

7.1 Introduction

Geotechnical site investigation is the initial and crucial first step for every geotechnical project in order to establish the stratigraphy and soil engineering properties. Among various practices for subsurface explorations, in-situ tests provide a quick, economical, and reliable assessment of geoparameters for analysis and design. Towards this purpose, cone penetration tests (CPTu) typically procure three measurements with depth, namely, the cone tip resistance (q_t), sleeve friction (f_s), and porewater pressure (u_2), taken at regular vertical intervals of between 1 and 5 cm. Flat dilatometer tests (DMT) provide two readings, the contact pressure (p_0) and the expansion pressure (p_1), at regular depth intervals of either 20 or 30 cm. Details concerning CPTu and DMT equipment, procedures, and interpretation method are found in Lunne et al. (1997) and Marchetti et al. (2006), respectively.

Using cavity expansion solutions for undrained penetration, a theoretical link is established between these two in-situ tests for soft to firm clays. This nexus permits an possible exchange of several theoretical, analytical, and empirical solutions between the two tests. Of specific interest, herein, is the extension of an existing solution for effective stress penetration that permits the effective stress friction angle (ϕ') of clays to be evaluated from DMT results.

7.1.1 Friction Angle From CPTu

For the CPTu, the evaluation of the effective stress friction angle ϕ' for a variety of soils ranging from sands to silts to clays is available via an effective stress limit plasticity solution, developed by the Norwegian Institute of Technology (NTH), as detailed by Senneset & Janbu (1985), Senneset et al. (1989), and Sandven (1990). Since the chapter focuses on CPTu in soft-to firm clay, the size of the failure region around the cone tip is established by the angle of plasticification (β) which herein takes on a value for the special case ($\beta = 0$) that is associated with undrained conditions at constant volume.

For the case of soft to firm clays ($c' = 0$), the closed-form theoretical expression for assessing the effective stress friction angle ϕ' is given as (Mayne 2016):

$$Q = \frac{\tan^2(45° + \phi'/2) \cdot \exp(\pi \cdot \tan\phi') - 1}{1 + 6 \cdot \tan\phi' \cdot (1 + \tan\phi) \cdot B_q} \qquad [7.1]$$

where $Q = (q_t - \sigma_{vo})/\sigma_{vo}'$ is the normalized cone tip resistance and $B_q = (u_2 - u_0)/(q_t - \sigma_{vo})$ is the normalized porewater pressure parameter.

An approximate equation for directly assessing the value of ϕ' from the above theoretical solution is expressed (Mayne 2007):

$$\phi' = 29.5 \cdot B_q^{0.121} \cdot [0.256 + 0.336 \cdot B_q + \log Q\,] \qquad [7.2]$$

where the following applicable limits apply: $18° < \phi' < 45°$ and $0.05 < B_q < 1.0$. The resulting relationships for ϕ' in terms of Q and select values of B_q are presented in graphic form in Figure 7.1.

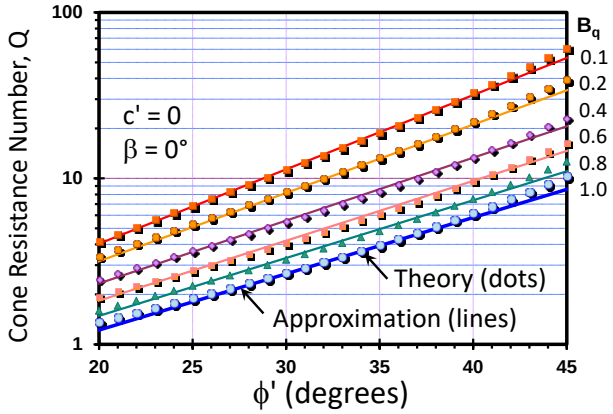

Figure 7.1. NTH graphical solution for ϕ' from CPTu data in soft-firm clays when c' = 0.

7.1.2 Case Study: CPTu at Sandpoint, Idaho

A case study from Sandpoint, Idaho is presented to show the process of interpreting effective friction angle using the NTH method. The Idaho Dept. of Transportation required soils information for design of approach embankments and a new bridge for State Route 95 highway. Figure 7.2 shows a representative CPTu at the site indicating over 80 m of soft silty clays, with occasional sand layers, lenses, and seams (Mayne 2014).

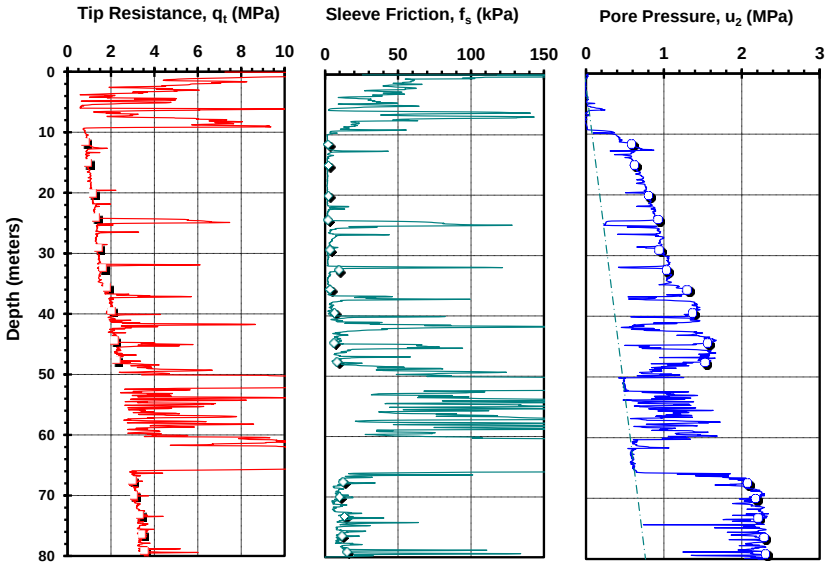

Figure 7.2. Deep CPTu profile at Sandpoint, Idaho with select data points for analysis

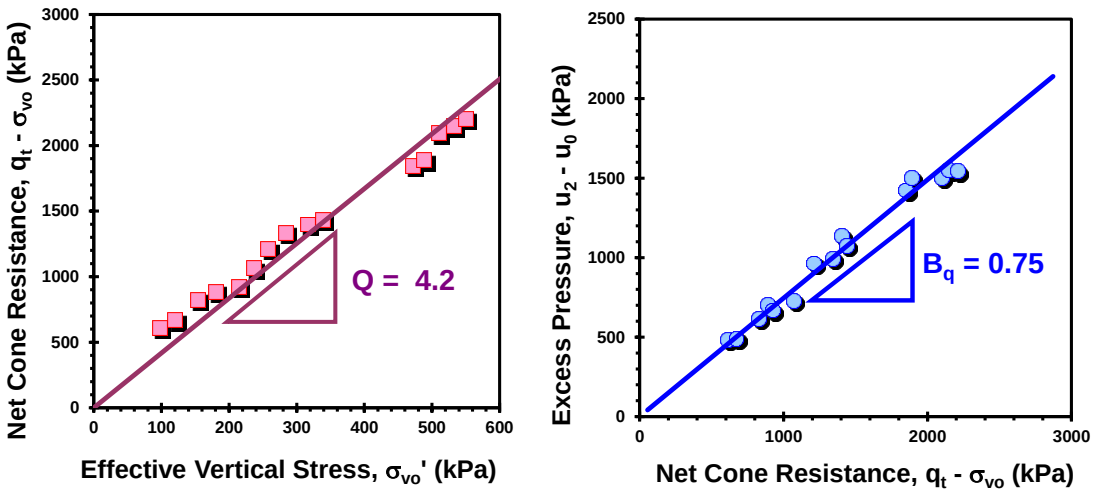

Figure 7.3. NTH post-processing of CPTu data for Q and B_q at Sandpoint

Figure 7.3 shows the procedure for determining Q and B_q. The parameter Q is found as the slope from plotting net cone resistance vs. the effective overburden stress. In this example, we force a best fit line through the origin (assuming c′=0) to obtain Q =4.2 by regression. By the same token, the porewater parameter B_q is determined as the slope of the Δu versus q_{net}, giving the value B_q = 0.75 for the Sandpoint site.

Results from 32 laboratory CIUC triaxial compression tests on undisturbed samples taken from 5 to 80 m depths are used as the reference benchmark values. Figure 7.4 shows the laboratory t-s' space of the triaxial tests that provided an effective friction angle of 33.1º. The NTH CPTu outputs an interpreted friction angle of 32.8º that is in excellent agreement.

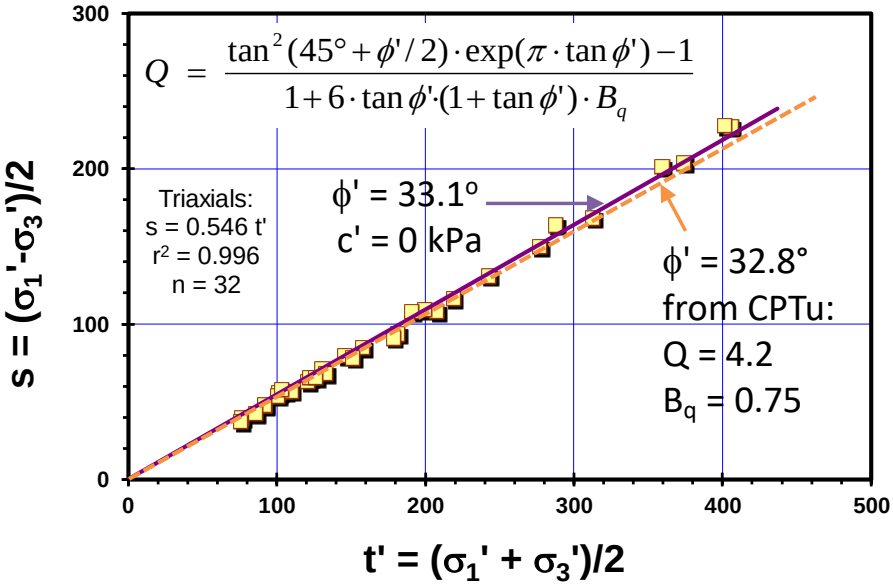

Figure 7.4. Laboratory triaxial effective stress friction angle ϕ′ versus interpreted ϕ′ from NTH using CPTu data at Sandpoint

7.2 Theoretical Nexus Between DMT and CPTu

7.2.1 Cavity Expansion solution for CPTu

For CPTu soundings in clays, spherical cavity expansion theory (SCE) expresses the net cone tip resistance ($q_{net} = q_t - \sigma_{vo}$) as a function of the undrained shear strength (s_u) from a triaxial compression mode and the rigidity index of the soil (I_R), which is defined as the G/s_u, where G=shear modulus, in the following form (Vesić 1977):

$$q_{net} = s_u \cdot \{ 4/3 \cdot [\ln(I_R) + 1] + \pi/2 + 1 \} \quad [7.3]$$

At the shoulder filter position, the measured excess porewater pressures (Δu_2) are due to: (a) increases in octahedral stress changes, and (b) shear-induced effects (Burns & Mayne 2002). In the case of normally-consolidated to lightly-overconsolidated clays, the portion of Δu due to octahedral stress changes dominate, and the shear-induced values are

rather small compared (< 20% of total) and thus can be neglected. Consequently, SCE can also be used to represent the magnitude of excess porewater pressures for the piezocone:

$$\Delta u = u_2 - u_0 = s_u \cdot 4/3 \cdot \ln (I_R) \quad [7.4]$$

7.2.2 Cavity Expansion solution for DMT

A study by Mayne & Bachus (1989) showed that the contact pressures (p_0) measured by the flat dilatometer tests (DMT) are quite similar in magnitude to that of the porewater pressures (u_2) measured at the cone shoulder position by piezocone tests, specifically: $p_0 \approx u_2$. Therefore, Equation [7.4] can also be used in the following manner to give an equivalent excess porewater pressure from the DMT:

$$\Delta u_{DMT} = p_0 - u_0 = s_u \cdot 4/3 \cdot \ln(I_R) \quad [7.5]$$

The Vesić (1972) SCE solution provides the magnitude of change in horizontal stress:

$$\Delta\sigma_h = s_u \cdot 4/3 \cdot [\ln (I_R) + 1] \quad [7.6]$$

This increase in horizontal stress can be related to the DMT expansion pressure (p_1), specifically the net expansion pressure ($p_1 - u_0$), as expressed:

$$\Delta\sigma_h = p_1 - u_0 \quad [7.7]$$

Substituting the spherical cavity expansion terms from Equations [7.5], [7.6] and [7.7] into [7.3] gives an equivalent net cone tip resistance (q_{net}) from the dilatometer results

$$q_{netDMT} = 2.93 \cdot p_1 - 1.93 \cdot p_0 - u_0 \quad [7.8]$$

Equation [7.8] gives a new approach that expresses an equivalent q_{net} resistance in terms of the DMT pressures. This nexus provides a link between the two tests for soils that

are characterized as normally-consolidated to lightly-overconsolidated clays. The above expressions and associated CPTu-DMT relationships for soft to firm clays are summarized in graphic form in Figure 7.5.

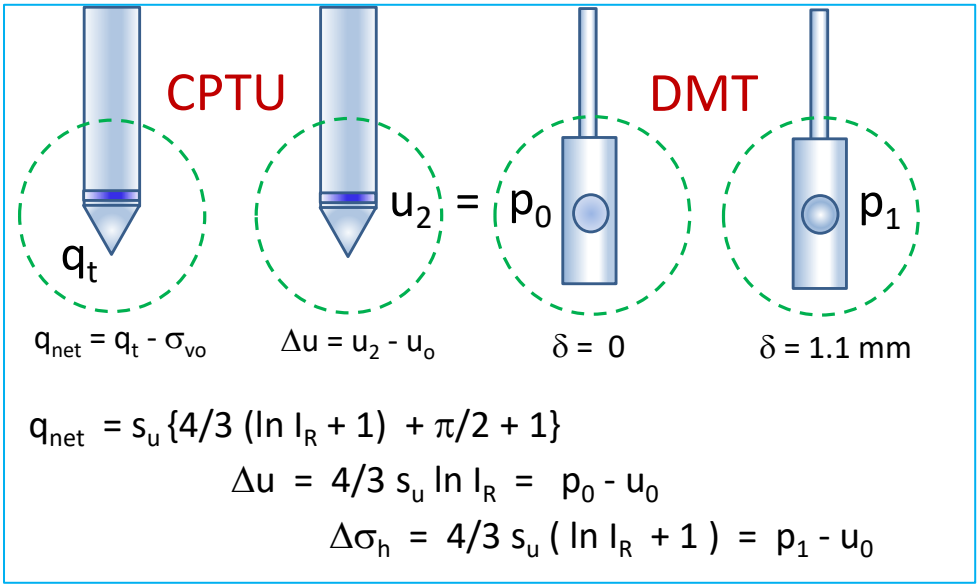

Figure 7.5. Summary of the nexus between CPTu and DMT readings in soft to firm clays using spherical cavity expansion solutions.

7.2.3 CPTu-DMT database in soft to firm clays

In order to verify the aforementioned relationships between CPTu and DMT readings, a special database was compiled. Paired sets of piezocone and flat dilatometer tests taken at 27 different clay sites were matched at respective elevations for the study (Ouyang & Mayne 2016). The individual symbols for each site are shown in the top half of Figure 7.6. In the lower portion of Figure 7.6, the measured excess porewater pressures from the CPTu soundings are shown to be comparable magnitude and in very good agreement with the calculated equivalent excess porewater pressures obtained from the DMT contact pressure, specifically $\Delta u \approx (p_0 - u_0)$ cited by Equation [7.5].

Similarly, a plot of the CPTu-measured net cone resistance is shown to be in rather good agreement with the DMT equivalent resistances given by Equation [7.8], as illustrated in Figure 7.7.

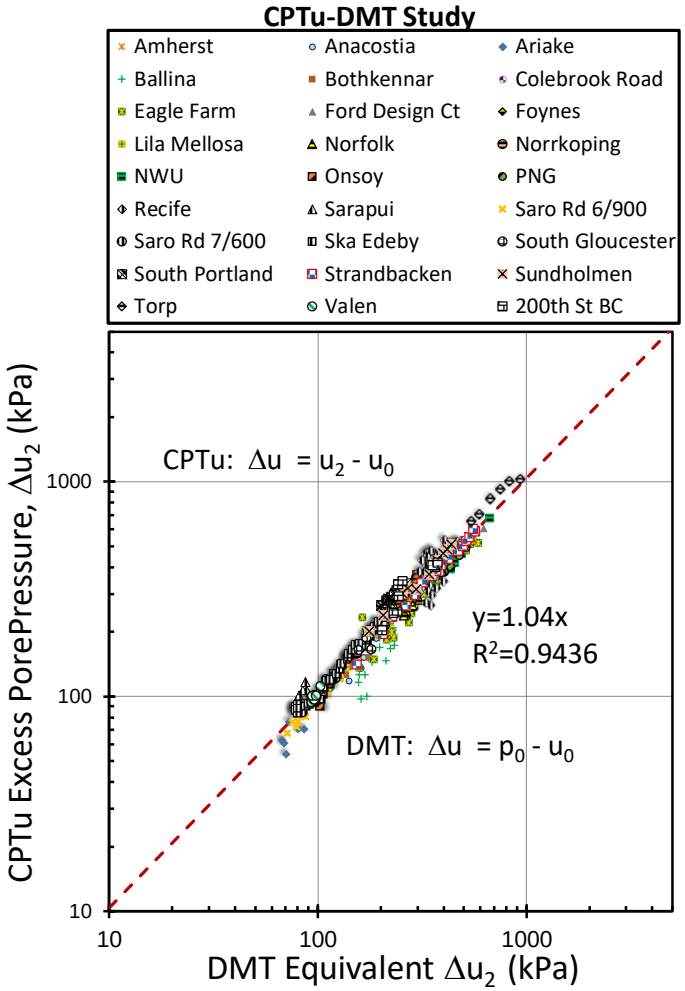

Figure 7.6. Excess porewater pressure from piezocone tests versus equivalent Δu from flat dilatometer tests for 27 soft-firm clays

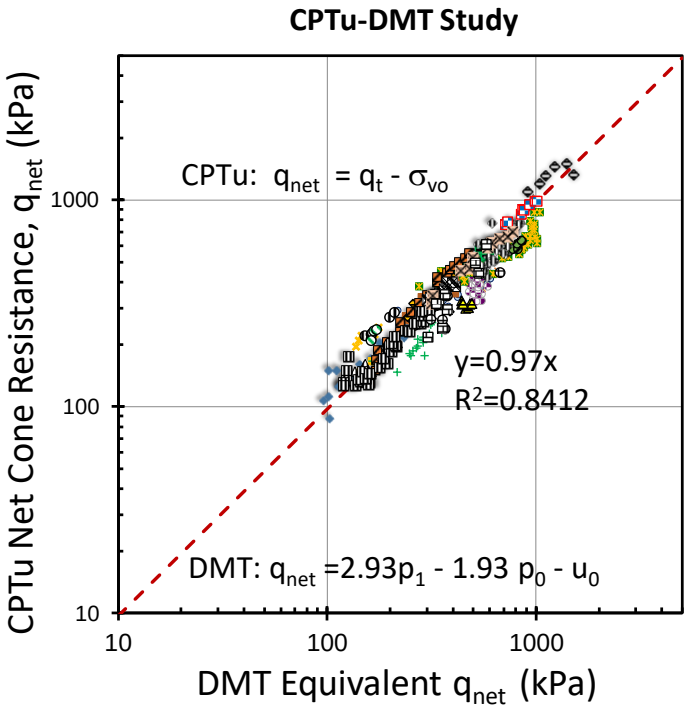

Figure 7.7. Net cone resistance q_{net} from piezocone tests versus DMT equivalent resistances for 27 soft-firm clays

7.3 Case Studies

7.3.1 Anacostia Naval Air Station, Washington, DC

Figure 7.8 shows a DMT sounding profile at the Anacostia NAS located at the confluence of the Potomac and Anacostia Rivers, Washington, DC. The site is underlain by soft alluvial clays that extend up to 30 m deep. Index parameters of the soft clay include: w_n = 68 %, LL = 83%; and PI = 37%.

The DMT-equivalent Q is found to be 4.5 and the DMT equivalent B_q = 0.92 for the Anacostia site, as indicated by Figure 7.9. These values are inputs to the solution chart in Figure 7.1, giving an NTH-interpreted effective friction angle of ϕ' =35.2° for the Anacostia clay. This is very comparable to the laboratory ϕ' from CIUC triaxial tests

(consolidated isotropic undrained triaxial compression tests) and shows an excellent match as indicated in Figure 7.10.

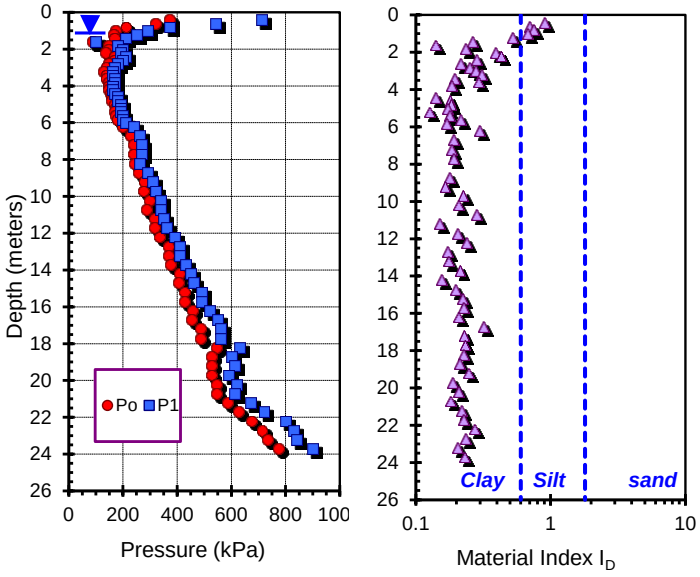

Figure 7.8. DMT profiles for Anacostia NAS clay site.

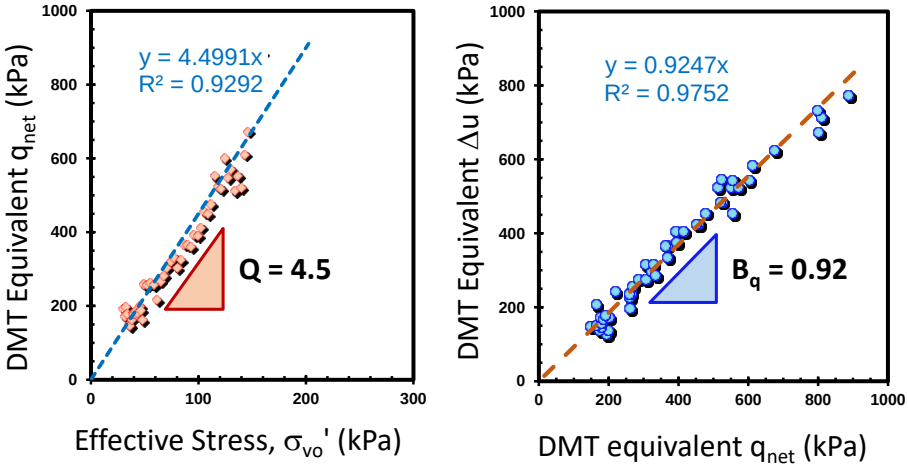

Figure 7.9. NTH post-processing of DMT data at Anacostia for DMT equivalent Q and DMT equivalent B_q

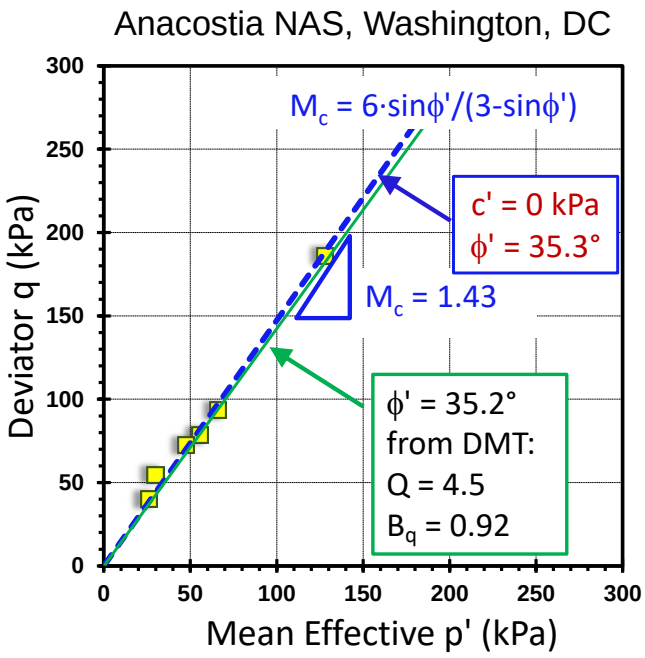

Figure 7.10. Laboratory triaxial test ϕ′ versus interpreted ϕ′ from NTH using DMT data at Anacostia

7.3.2 Northwestern University, Evanston, Illinois

One of six National Geotechnical Experimentation Site (NGES) for the USA is located at Northwestern University (NWU), north of Chicago. The upper layer of this site consists of about 9 to 10 m of sand underlain by a 10-m thick soft lacustrine clay deposited by Lake Michigan. Data from DMT soundings performed in the soft clay strata at this site will be used to verify the approximate NTH method given by Equation [7.2].

Results of laboratory CAUC tests (consolidated anisotropic undrained triaxial compression tests) are shown in Figure 7.11, which determined an effective friction angle of 28.3º (Chung & Finno 1992). In this study, the intermediate soft clay stratum from around 10 to 20 meters is adopted for analysis. The effective friction angle profile ϕ′

calculated using the approximate NTH solution and DMT data is shown in Figure 7.12, with good agreement evident.

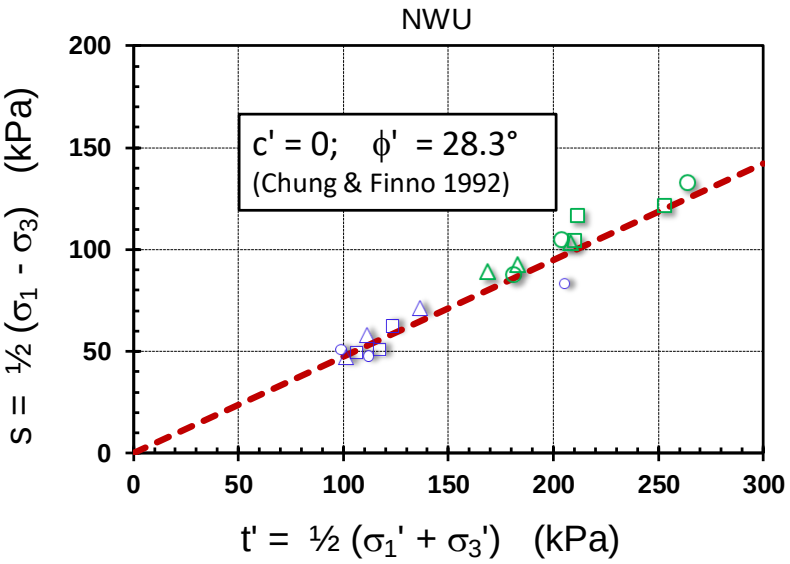

Figure 7.11. Laboratory CAUC test stress path at Northwestern University (data from Chung & Finno 1992).

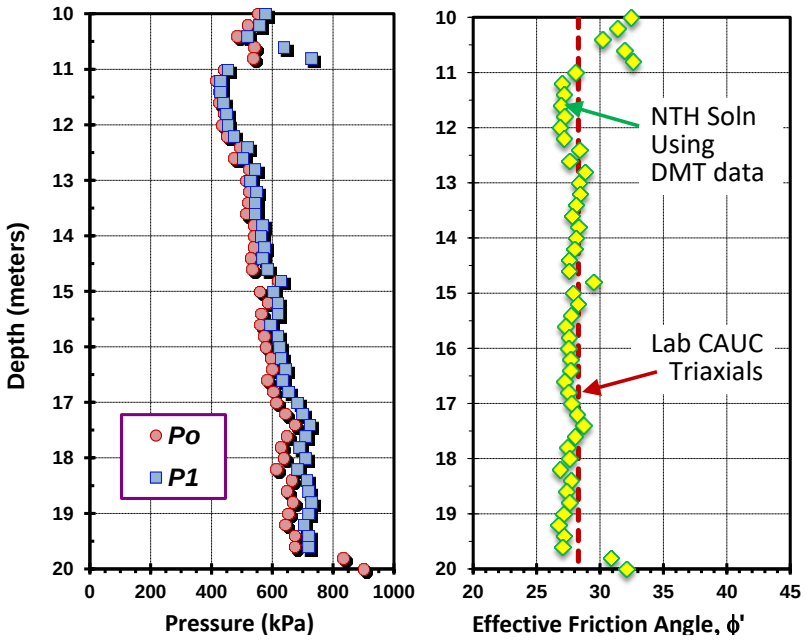

Figure 7.12. DMT data and comparison of NTH ϕ′ and lab ϕ′ at NWU

7.4 Conclusions

Links between CPTu and DMT measurements in soft to firm clays are generated through spherical cavity expansion theory. The effective stress friction angle for soft clays can be calculated from both of these in-situ tests using an effective stress limit plasticity solution established at NTH (Sandven 1990; Senneset et al. 1989). The friction angle ϕ' from laboratory triaxial testing was used as the reference benchmark value to compare effective friction angles from DMT data in soft clays located in Washington DC and near Chicago, Illinois.

CHAPTER 8. EFFECTIVE STRESS STRENGTH PARAMETERS OF CLAYS FROM DMT

8.1 Introduction

The flat plate dilatometer test (DMT) is a quick, reliable, and robust in-situ test that investigates subsurface stratigraphy and allows for the interpretation of geoparameters in an efficient, economic, and expedient manner along the soil profile. Details concerning the DMT equipment, field test procedures, and interpretations are given by Marchetti (1980). The reference guidelines are provided in ASTM D6635-15, *Standard Test Method for Performing the Flat Dilatometer Test (DMT).* Some recent updates to the test are discussed by Marchetti et al. (2006) and Marchetti (2015).

The flat dilatometer has a stainless-steel blade that is pushed into the ground at depth increments of either 20 or 30 cm using common field equipment, i.e., drill rigs or hydraulic pushing rigs. The blade has a 60-mm diameter flat circular steel membrane mounted flush on one side, which determines two separate pressure readings at each test depth by inflating the membrane with nitrogen gas. The two readings include: (1) A-pressure, which is required to simply begin to move the membrane against the soil, and (2) B-pressure, which is required to move the center of the membrane 1.1 mm against the soil. Per ASTM D6635-15, the A and B readings must be corrected by the values of ΔA and ΔB, which are determined by calibration, to account for membrane stiffness to obtain p_0 (contact pressure) and p_1 (expansion pressure), respectively, according to the following equations:

$$p_0 = 1.05(\text{A}+\Delta\text{A}) - 0.05(B - \Delta B) \quad [8.1]$$

$$p_1 = B - \Delta B \quad [8.2]$$

The DMT can evaluate a wide variety of geotechnical parameters, such as soil type, unit weight (γ_t), overconsolidation ratio (OCR), undrained shear strength (s_u) of clays, effective friction angle in sands (ϕ'), constrained modulus (D' or M'), lateral stress coefficient (K_0), and coefficient of consolidation (c_v), as well as provide an assessment of liquefaction potential (Marchetti 2015). Traditionally, the evaluation of clay strength by DMT focuses only on a total stress parameter, specifically the undrained shear strength (s_u). Yet, despite its relevance and importance, the effective stress friction angle (ϕ') of clays has not been conventionally determined using DMT readings, thus the purpose of this chapter.

The cone penetration test (CPTu) is another in-situ tool that provides quick and reliable subsurface exploration information by capturing three measurements with depth: cone tip resistance (q_t), sleeve friction (f_s), and porewater pressures at the shoulder of the cone (u_2). Details concerning CPTu equipment, procedures, and interpretation methods are found in Lunne et al. (1997) and Mayne (2007).

For DMT and CPTu soundings in soft to firm clays, a theoretical nexus has been established based on the spherical cavity expansion (SCE) theory (Ouyang and Mayne 2017b). This link provides a means for using an established theoretical solution for evaluating the effective friction angle of clays from the DMT, which is the focus of this study. A review of data from DMT soundings performed in 40 natural clays and 6 artificial clays affords the opportunity to verify the applicability of an effective stress solution for

evaluating ϕ' from penetration tests that was developed by the Norwegian Institute of Technology (NTH; now the Norwegian University for Science & Technology, NTNU). Results from the DMT assessments of ϕ' using the NTH solution are compared with benchmark values obtained from laboratory tests on these clays, specifically consolidated undrained triaxial compression tests with porewater pressure measurements.

8.2 Nexus between CPTu and DMT using spherical cavity expansion (SCE)

Results from CPTu and DMT are commonly used to determine the undrained shear strength of fine-grained soils. Interpretation methods include solutions based on limit plasticity, cavity expansion theory, strain path methods, analytical approaches, numerical simulations by finite elements, and correlation with either laboratory (e.g., triaxial, simple shear) or other field tests, such as vane shear or pressuremeter tests (e.g., Konrad and Law 1987; Lunne, Robertson, and Powell 1997; Yu and Mitchell 1998; Schnaid 2009; Agaiby 2018). In this chapter, the spherical cavity expansion (SCE) relationships developed by Vesic (1972, 1977) are adopted to illustrate a simple, yet elegant nexus between the CPTu and flat DMT.

For undrained loading, the net cone resistance from the CPTu ($q_{net} = q_t - \sigma_{vo}$) is expressed as a function of the undrained shear strength (s_u) and the rigidity index of the soil (I_R), defined as G/s_u, where G is the shear modulus of the soil:

$$q_{net}=s_u \cdot \{4/3 \cdot [\ln(I_R)+1]+\pi/2+1\} \quad [8.3]$$

During the advancement of the piezocone in soft to firm clays, the measured porewater pressures (u_2) will be higher than the hydrostatic porewater pressure (u_0) under undrained conditions, thus exhibiting excess porewater pressure ($\Delta u = u_2 - u_0 > 0$). These

measured excess porewater pressures (Δu) are due to two components: (a) increases in octahedral stress changes, and (b) shear-induced effects as the steel penetrometer rubs against the clay (Burns and Mayne 2002). In the case of normally consolidated (NC) to lightly overconsolidated (LOC) clays, the magnitude of the shear-induced components is rather small compared to the octahedral portion, usually less than 10 or 20 % (Baligh 1986; Mayne 1991). As a result, neglecting the latter component, SCE indicates that the excess porewater pressure from the piezocone can be approximately expressed by the following equation (Vesic 1972):

$$\Delta u_2 = u_2 - u_0 = s_u \cdot 4/3 \cdot \ln(I_R) \quad [8.4]$$

Previous studies have shown that the contact pressures (p_0) from the DMT are dominated by porewater pressure effects (Campanella et al. 1985). Thus the magnitude of DMT p_0 is quite similar to the porewater pressures (u_2) measured by the CPTu in intact clays and clayey silts (Mayne and Bachus 1989; Mayne 2006; Ouyang and Mayne 2017a). This relationship may be expressed as follows:

$$p_0 \approx u_2 \quad [8.5]$$

Thus, an equivalent excess porewater pressure from DMT can be written as such:

$$\Delta u_{-DMT} = p_0 - u_0 = s_u \cdot 4/3 \cdot \ln(I_R) \quad [8.6]$$

As for the change in total horizontal stress, SCE can be used to represent increase induced by the probe insertion is given by the following expression:

$$\Delta \sigma_h = s_u \cdot 4/3 \cdot [\ln(I_R)+1] \quad [8.7]$$

From a pragmatic viewpoint, the increase in horizontal stress can be related directly related to the DMT expansion pressure (p_1), specifically the net expansion pressure ($p_1 - u_0$) that is expressed by:

$$\Delta\sigma_h = p_1\text{-}u_0 \quad [8.8]$$

Substituting the SCE terms from Equations [8.3], [8.6] and [8.8] into Equation [8.7] gives an equivalent contact pressure p_1 from the piezocone readings:

$$p_1 = (q_t\text{+}1.93u_2\text{-}\sigma'_{v0})/2.93 \quad [8.9]$$

Therefore, SCE establishes simple links between the DMT pressures and CPTu readings. Specifically, the measured cone tip resistance (q_t) and porewater pressures (u_2) from the CPTu can be utilized to express equivalent readings for the DMT, namely contact pressure (p_0) and equivalent expansion pressure (p_1), and vice versa.

8.3 CPTu-DMT database

To verify the interrelationships between DMT and CPTu, data from 49 worldwide soft to firm clays and silts that are NC to LOC soils were collected. These soils exhibited 1 < OCRs < 2.5 and were subjected to side-by-side CPTu and DMT soundings (Ouyang and Mayne, 2017a, 2017b). Using equation [8.5] and equation [8.9], the measured DMT contact pressure (p_0) and expansion pressure (p_1) are plotted against their equivalent contact pressure ($p_{0–CPTu}$) and equivalent expansion pressure ($p_{1–CPTu}$) derived from the companion CPTu readings in Figure 8.1 and Figure 8.2, respectively. The good comparison and verification of the DMT-CPTu links are quite evident. The slight deviations can be partially explained in that q_t and u_2 are taken exactly during penetration (at time t = 0), whereas p_0 is obtained some 15 s after penetration and p_1 about 45 s after penetration. Thus,

some monotonic or dilatory dissipations may have occurred prior to obtaining the DMT readings, resulting is a slight offset in the timing of their data collection.

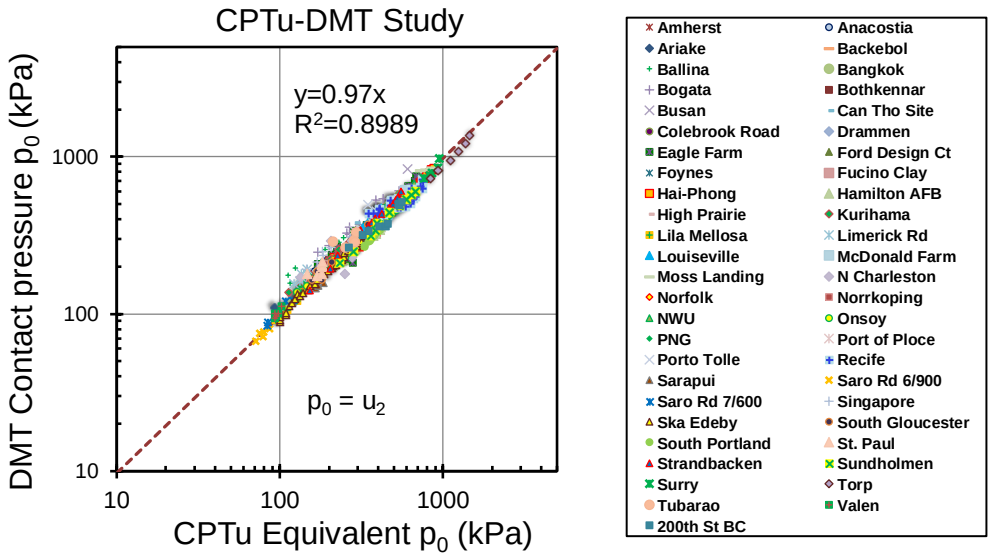

Figure 8.1. Comparison of measured DMT contact pressure p_0 and CPTu-estimated equivalent p_0 value for 49 clays.

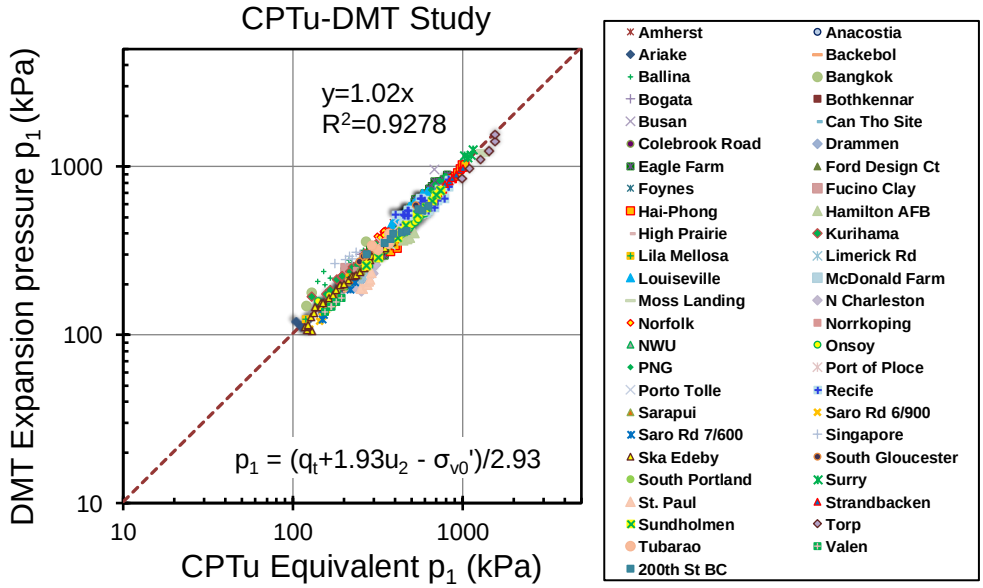

Figure 8.2. Comparison of measured DMT expansion pressure p_1 and CPTu-estimated equivalent p_1 for 49 clays.

8.4 DMT application of Effective Stress Limit Plasticity Solution

Senneset and Janbu (1985) developed an effective stress limit plasticity solution at the NTH for the CPTu toward the evaluation of effective stress parameters (c′ and ϕ′) for undrained penetration. In this approach, the cone resistance number (N_m) is defined as follows:

$$N_m = \frac{N_q - 1}{1 + N_u \cdot B_q} = \frac{q_t - \sigma_{vo}}{\sigma_{vo}' + a'} \quad [8.10]$$

where $B_q = \Delta u/q_{net}$ = normalized porewater pressure parameter, $a' = c' \cdot \cot\phi'$ = effective attraction, and c′ = effective cohesion intercept. The tip-bearing capacity factor (N_q) and the porewater pressure bearing factor N_u are given by the following equations (Senneset, Sandven, and Janbu 1989):

$$N_q = K_p exp[(\pi - 2\beta) tan\phi'] \quad [8.11]$$

$$N_u = 6 tan\phi'(1 + tan\phi') \quad [8.12]$$

$$K_p = (1 + sin\phi')/(1 - sin\phi') \quad [8.13]$$

where K_p is the passive lateral stress coefficient, and β is the angle of plastification ($-40° < \beta < +30°$) that defines the size of the failure zone around the tip (Senneset and Janbu 1985). The full solution allows for an interpretation of a paired set of effective stress Mohr-Coulomb strength parameters (c′ and ϕ′) for all soil types, including sands, silts, and clays, as well as mixed soils (Sandven1990). For the case where β = 0°, the N_q is identical to the classical solution for a deep foundation (i.e., Terzaghi equation). The parameter N_u is a porewater pressure bearing factor. When $a' = c' = 0$, the cone resistance N_m is identical to the normalized cone tip resistance $Q = q_{net}/\sigma_{vo}'$ that is used extensively in CPTu

interpretations (Lunne, Robertson, and Powell 1997; Mayne 2007; Robertson 2009). Thus, Figure 8.3 shows the relationship expressing ϕ′ in terms of normalized conetip resistance Q and normalized porewater pressure B_q, which is given in Equation [8.14]:

$$Q = \frac{\tan^2(45° + \phi'/2) \cdot \exp(\pi \cdot \tan\phi') - 1}{1 + 6 \cdot \tan\phi' \cdot (1 + \tan\phi) \cdot B_q} \qquad [8.14]$$

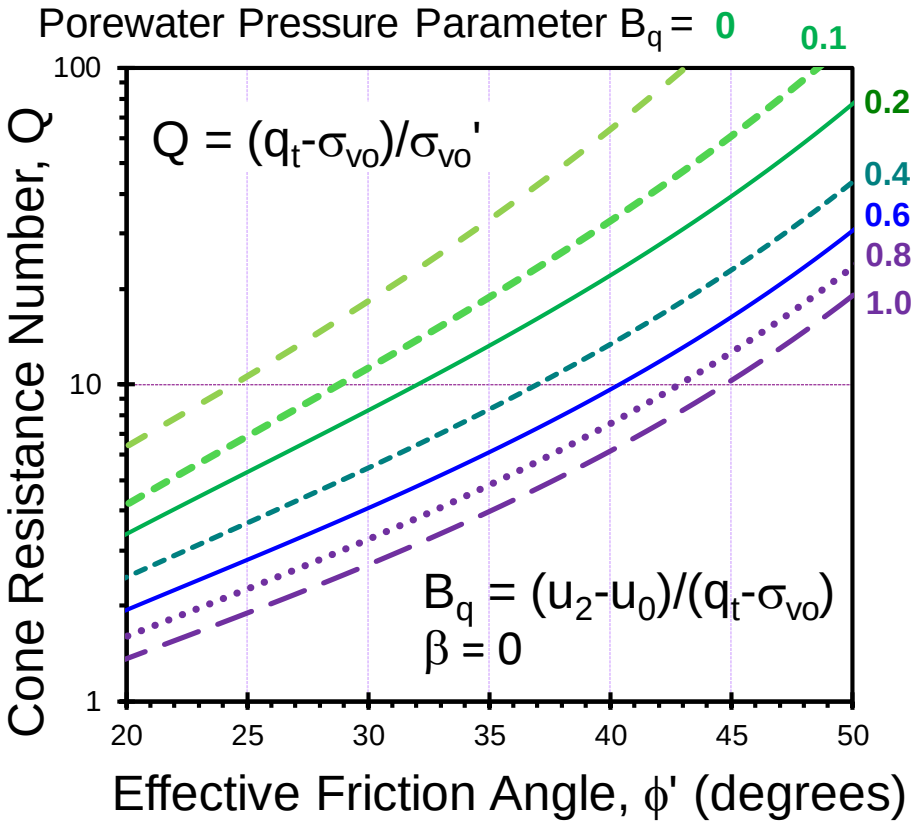

Figure 8.3. NTH solution for evaluating ϕ′ from CPTu in soft silts and clays where c' = 0

Based on the SCE relationships between DMT and CPTu readings, the established NTH effective stress limit plasticity solution for assessing ϕ' in soft clays can now be extended to the DMT. For this, an equivalent cone resistance number Q_{-DMT} and normalized porewater pressure parameter B_{q-DMT} are determined based on the previous derivations.

$$Q_{-DMT} = q_{netDMT}/\sigma'_{v0} = (2.93p_1\text{-}1.93p_0\text{-}u_0)/\sigma'_{v0} \qquad [8.15]$$

$$B_{q-DMT} = \Delta u_{-DMT}/q_{netDMT} = (p_0 - u_0)/(2.93p_1\text{-}1.93p_0\text{-}u_0) \quad [8.16]$$

The intent of parameters Q and B_q is to represent those data by a single representative normalized value for the in-situ results in that soft to firm clay deposit (Robertson 1990). The equivalent NTH-DMT can be also written into the following mathematical formula to evaluate the profile of operational effective friction angles with depth, provided that OCR< 2.5, $20° < \phi' < 45°$ and the values of the DMT-equivalent normalized porewater pressure parameter are within the range: $0.05 < B_{q\text{-}DMT} < 1.0$.

$$\phi' \approx 29.5 \cdot {B_{q-DMT}}^{0.121}[0.256 + 0.336\, B_{q-DMT} + logQ_{DMT}] \quad [8.17]$$

8.5 Case Studies

Four case studies are presented below to illustrate the methodology and show the reasonableness of interpreting effective friction angles ϕ' in two natural clays and two artificially prepared deposits using DMT readings in conjunction with the NTH solution. The selected examples were chosen to show a diversity of clay geomaterials that have low to high frictional characteristics, specifically: $21° \leq \phi' \leq 39°$. These fall within the range of expected effective friction angles for clays: $17° \leq \phi' \leq 45°$, as reported by Dìaz-Rodrìguez, et al. (1992) and Leroueil & Hight (2003).

8.5.1 Route 17 bridge, Chesapeake, Virginia

Results from field DMT and laboratory CIUC tests on a soft clay layer were available from a roadway improvement project that was constructed off Route 17 in Chesapeake, Virginia, between Interstate 64 and Military Highway where the Norfolk Western Railroad crosses the project site. The Chesapeake area is located within the

Atlantic Coastal Plain geologic province and underlain by approximately 800 m of marine and estuarine deposits. Standard soil test borings were performed to depths of up to 25 m at the site. Recovered undisturbed tube samples were subjected to one-dimensional consolidation testing for soil settlement characteristics. In addition, isotropically-consolidated undrained triaxial compression tests (CIUCs) were conducted to determine the total and effective stress strength parameters of the primary clay layer. In-situ flat DMTs were also carried out at the project site.

Soil test borings performed for this project encountered a subsurface stratigraphy consisting of three basic strata, where Upper Strata I and Bottom Strata III show interlayered, loose to dense, clean to clayey fine sands. The Strata II soils consist predominately of soft to firm, high- to low-plasticity clays about 10-m thick (Charles & Barnhill 1987). This layer created a major problem in regard to embankment stability and settlement and was characterized by an average unit weight of 15.6 kN/m^3. The natural moisture contents ranged from 53 to 92 %, and the plasticity index (PI) ranged from 31 to 68 %. The groundwater level was about 1 m below the surface.

Figure 8.4 shows a representative portion of a DMT sounding in the soft clay layer located from 6 to 16m depths with respective contact pressures (p_0) and expansion pressures (p_1). The equivalent DMT cone resistance number Q_{DMT} is found to be 9.73. and the equivalent DMT porewater parameter $B_{q\text{-}DMT}$ is calculated to be 0.52 for the clay layer at this site, as indicated by Figure 8.5. These values are input into the solution chart in Figure 8.6, determining an effective friction angle $\phi' = 38.6°$ for the soft Chesapeake clay. The DMT-NTH interpreted ϕ' is then compared with the laboratory value of the effective

stress friction angle from a series of CIUC triaxial tests on the soft clay. The results from the NTH method match reasonably well with the laboratory data, as shown by Figure 8.7.

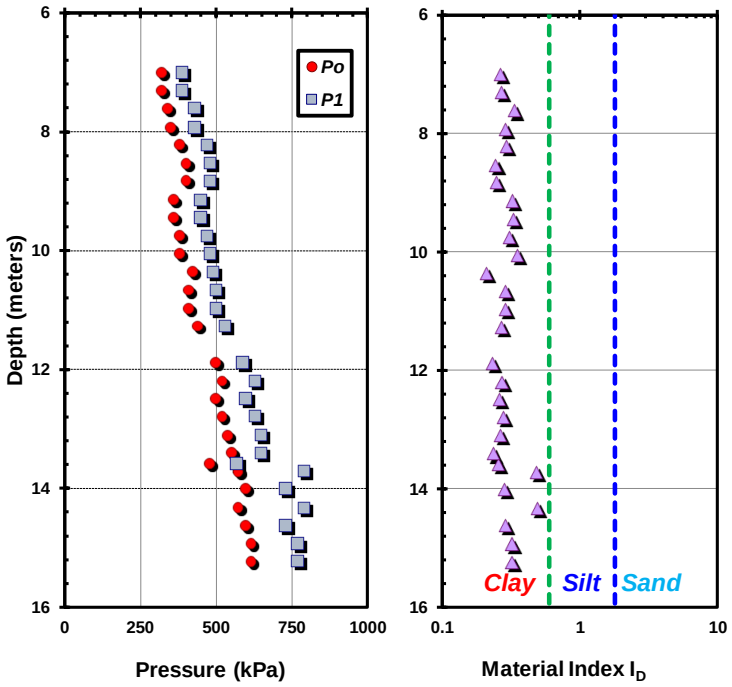

Figure 8.4. Representative DMT sounding at Route 17 bridge site, Chesapeake, VA (DMT data from Charles & Barnhill 1987).

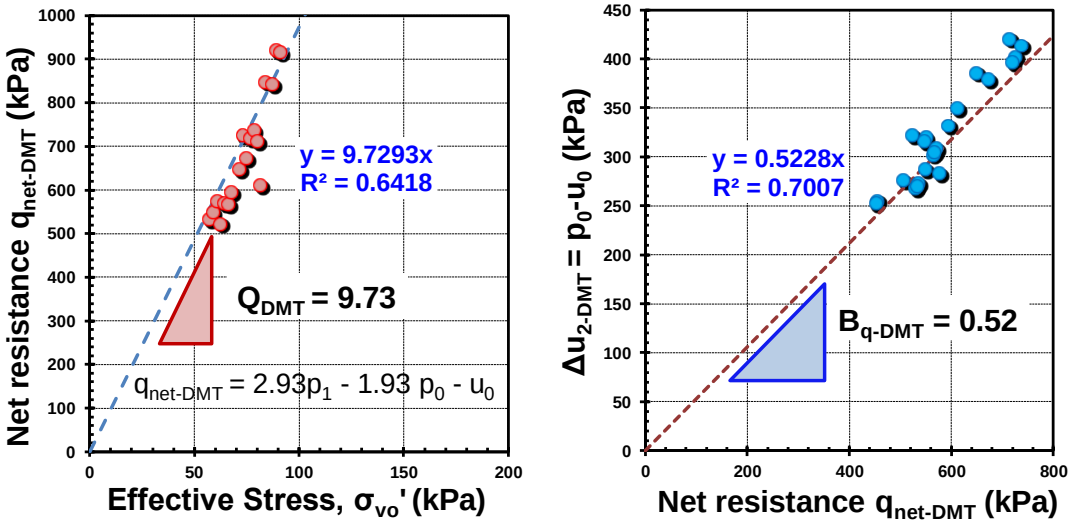

Figure 8.5. Postprocessing of the DMT data in soft clay layer at Chesapeake, Virginia: (a) DMT-equivalent Q_{DMT}; and (b) DMT-equivalent B_{q-DMT}.

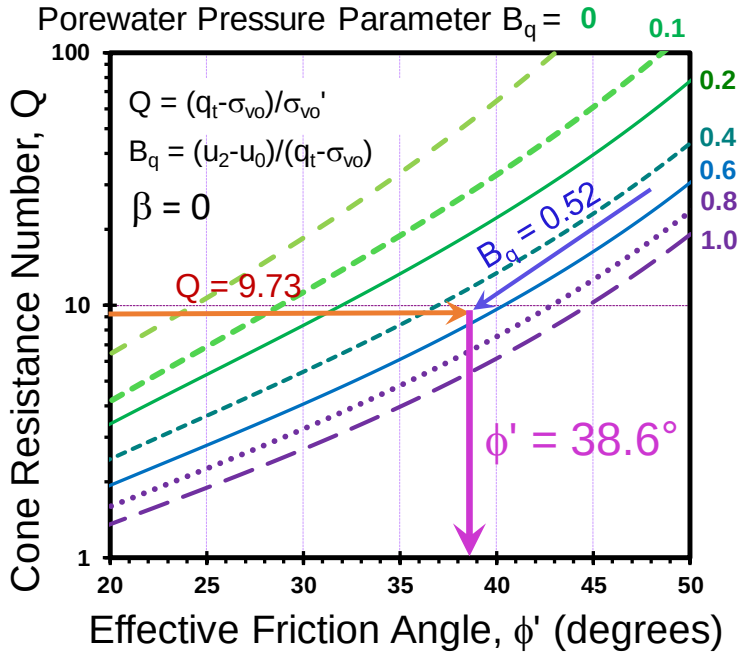

Figure 8.6. Evaluating ϕ′ from DMT results in soft clay layer at Chesapeake, Virginia using the NTH chart procedure.

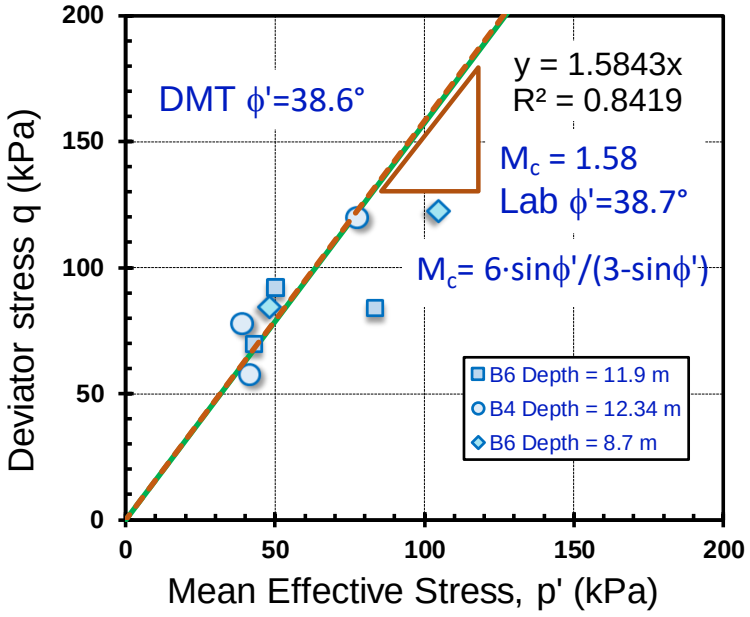

Figure 8.7. Comparison of effective friction angle measured by laboratory triaxial tests and NTH solution from DMT data in Chesapeake, Virginia (triaxial data from Charles & Barnhill 1987).

8.5.2 DMTs kaolin chamber tests, Oxford University

The use of laboratory testing on artificially-prepared soils helps mitigate the issues of inherent variability and scatter from natural soil deposits. Also, it is possible to minimize the uncertainty involved in the interpretation of in-situ test results by verifying, in a calibration chamber, any analytical, theoretical, numerical, or empirical relationship between a measured quantity and actual soil parameters. Kaolin is an interesting clay mineral as it has rather low frictional characteristics ($\phi' \approx 20°$) when compared with natural clays, yet when mixed with sand or silica, can develop friction angles that are similar to other clays: $\phi' \approx 30°$ (Rossato, Ninis, and Jardine 1992).

Smith (1993) designed and commissioned a large calibration chamber for clay at Oxford University and tested nine kaolin beds under different stress histories. The pressurized flexible wall chamber system as designed allows the manufacture and testing of a 1 m high by 1 m diameter clay deposit. Speswhite kaolin was selected for the test program because of its widely explored geotechnical properties and relatively easy and quick set-up time for calibration chamber testing. After preparation and consolidation, in each clay bed, DMTs were conducted every 100 mm to a depth of 800 mm to obtain the A and B pressure readings (Smith 1993). In this case study, four NC samples of the kaolin clay, namely, clay beds OA, OAB, OC, and OCD, were selected for study to validate the DMT-NTH method in assessment of the effective friction angle ϕ' of the kaolin. Table 8.1 shows the effective stress conditions, hydrostatic porewater pressures, induced preconsolidation stress state, and corresponding measured DMT p_0 and p_1 readings of the four NC clay beds.

Table 8.1. Summary of DMT readings and stress levels for NC kaolin beds in chamber tests (data from Smith 1993).

Clay Bed and Test No.	σ_V' (kPa)	σ_H' (kPa)	u_o (kPa)	σ_{Vmax}' (kPa)	σ_{Hmax}' (kPa)	p_0 (kPa)	p_1(kPa)	Q-$_{DMT}$	$B_{q\text{-}DMT}$	ϕ' (deg)
OA-1	268	158	4	268	219	364	405	1.79	0.75	21.69
OA-2	269	156	6	269	219	359	394	1.69	0.77	21.31
OA-3	270	156	7	270	219	373	418	1.84	0.74	21.85
OA-4	270	156	8	270	219	373	434	2.01	0.67	22.08
OA-5	271	156	9	271	219	387	463	2.22	0.63	22.68
OAB-1	609	379	6	609	451	920	1114	2.43	0.62	23.64
OAB-2	609	378	7	609	451	880	1094	2.46	0.58	23.29
OAB-3	609	378	8	609	451	896	1104	2.46	0.59	23.43
OAB-4	611	378	10	611	451	969	1149	2.43	0.65	24.03
OC-1	197	199	2	197	199	343	374	2.19	0.79	24.72
OC-2	198	199	3	198	199	332	359	2.06	0.81	24.17
OC-3	198	199	4	198	199	359	394	2.31	0.78	25.19
OC-4	199	199	5	199	199	340	380	2.27	0.74	24.51
OC-5	200	199	6	200	199	314	355	2.14	0.72	23.48
OCD-1	455	461	6	455	461	691	790	2.14	0.70	23.27
OCD-2	455	460	8	455	460	711	833	2.33	0.66	23.75
OCD-3	455	460	9	455	460	696	793	2.13	0.71	23.28
OCD-4	456	459	10	456	459	729	840	2.29	0.69	23.89
OCD-5	457	460	11	457	460	719	816	2.17	0.71	23.57

Figure 8.8 shows the determination of the equivalent normalized penetration parameters for all test chamber data, giving representative values $Q_{DMT} = 2.29$ and $B_{q\text{-}DMT} = 0.65$, respectively. Alternative, each of the four separate beds can be assessed individually yet found to be rather similar. As evidenced by Figure 8.9, an overall effective friction angle of 23° is computed based on the DMT-NTH approach. This is seen to reasonably capture the low frictional characteristics of the Speswhite kaolin measured by the laboratory triaxial series ($\phi' = 21.6°$) reported by Smith (1993). Similar low values of $\phi' \approx 20°$ to 22° are reported for Speswhite kaolin by Peric et al. (1998) and Rossato et al. (1992).

As an alternative to the rigorous solution given by equation [8.14], an approximate inversion solution is also available to provide the operational effective friction angle directly from Q and B_q, provided that: $20° < \phi' < 45°$ and $0.1 < B_{q\text{-}DMT} < 1.0$, as shown in Figure 8.10. It can be seen that the approximate solution is in reasonable agreement with the theoretical values over the specified ranges of ϕ' and B_q, as expressed by the following:

$$\phi' = 29.5\ B_q^{0.121}\ [0.256 + 0.336\ B_{q\text{-}DMT} + \log Q_{DMT}] \qquad [8.18]$$

The paired sets of Q_{DMT} and $B_{q\text{-}DMT}$ values are calculated for all chamber tests and the effective stress friction angle can be determined on a point-by-point basis in Table 8.1. It can be seen that each chamber test produces a value of ϕ' between of 21° to 25°, with a mean $\phi' = 23°$ which is comparable to the triaxial series.

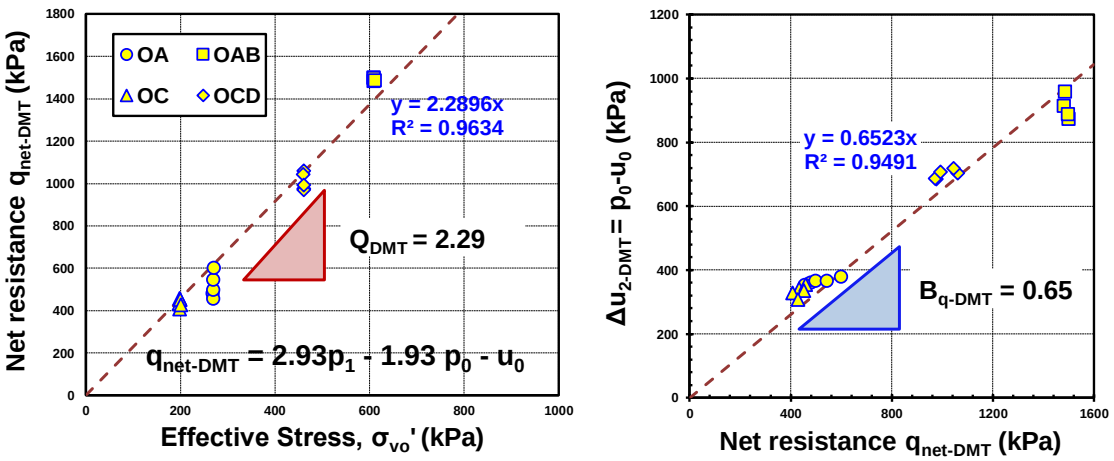

Figure 8.8. Postprocessing of DMT chamber data in kaolin clay for determining (a) DMT-equivalent resistance number, Q_{DMT}; and (b) DMT-equivalent porewater parameter, $B_{q\text{-}DMT}$ (data from Smith 1993).

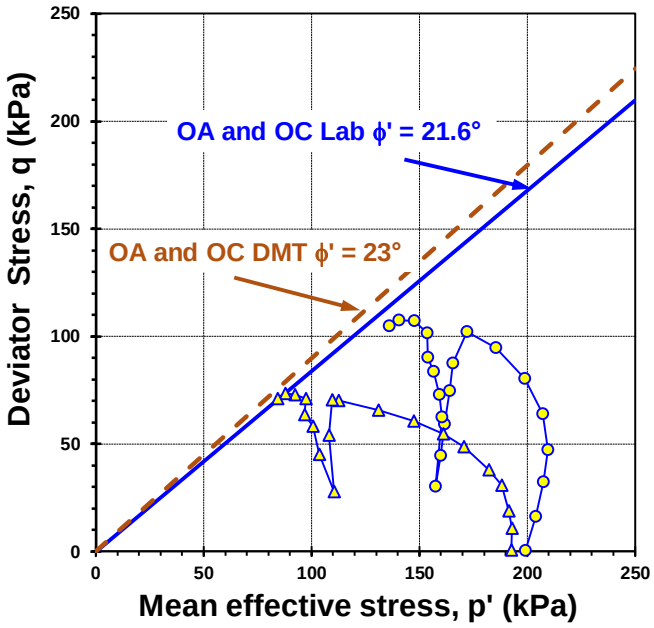

Figure 8.9. Comparison of effective friction angle measured by laboratory triaxial tests and the NTH solution from the DMT chamber series in kaolin (triaxial results from Smith 1993).

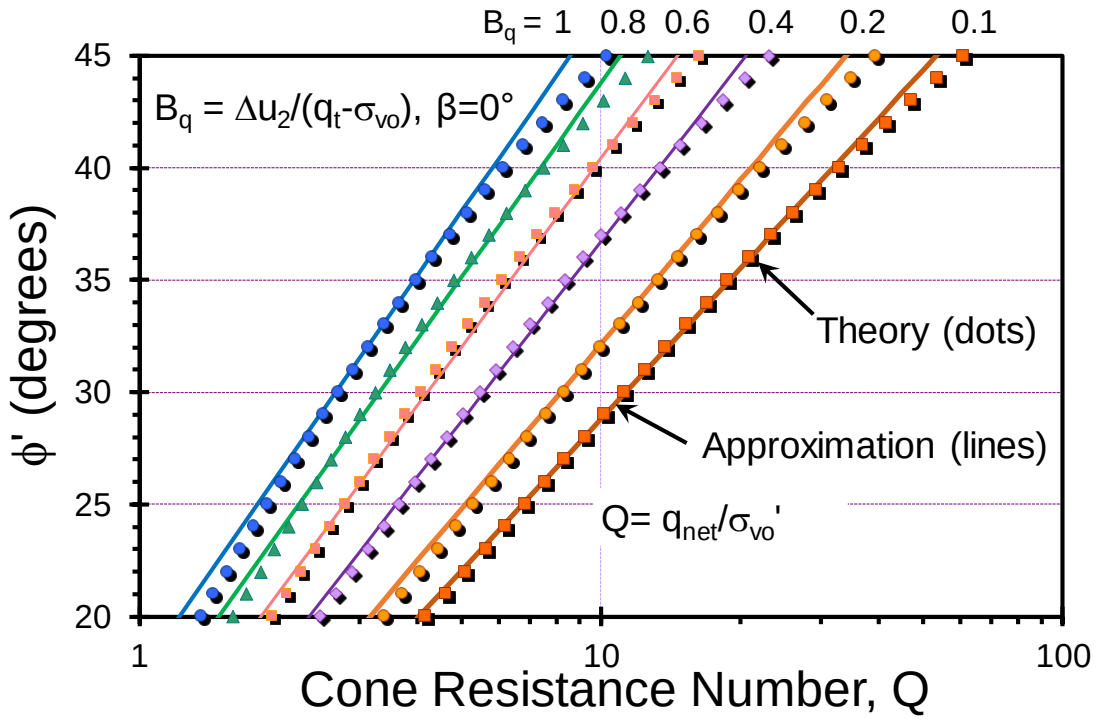

Figure 8.10. Exact and approximate NTH solutions for evaluating ϕ′ from CPTu and DMT readings in soft to firm clays.

8.5.3 DMTs in clay chamber tests, Cornell University

A special kaolin-silica mixture (50/50) developed by McManus and Kulhawy (1991) was used to create slurry deposits of clay in chambers for research testing. The chamber is an unpressurized rigid-wall type that measures 1.53 m in diameter and 2.13 m in height. The mixture is a 50/50 recipe of Peerless kaolin and a very fine silica (SuperSil), which has overall mean index properties: void ratio, e_0 = 0.91, mean grain size, D_{50} = 0.006 mm; G_s = 2.65; LL = 33; PI = 11 %, clay fraction (CF) = 33 %, and percent fines (PF) = 98 %. The samples were prepared as a slurry with an initial water content of 66 %, and after an applied preconsolidation of σ_p' = 50 kPa, were unloaded to atmospheric pressure. This resulted in corresponding to 5 < OCRs < 10 in the depth range of DMT readings. The

in-place water contents averaged at about 34 % after the consolidation and rebound stages (Mayne, Kulhawy, and Trautmann 1992).

Figure 8.11 demonstrates the results of a series of CIUC triaxial tests, which show an interpreted effective stress friction angle of 31.5°. Note that McManus & Kulhawy (1991) reported a similar interpretation at $\phi' \approx 31.3°$ at OCR = 4. The clay deposit was also subjected to minicone testing for q_t readings and minipiezoprobes with both u_1 and u_2 measurements, as shown in Figure 8.12 (Mayne, Kulhawy, and Trautmann 1992). Flat DMTs were also carried out (unpublished) to obtain p_0 and p_1 measurements, as indicated by Figure 8.12. Figure 8.13 demonstrates the approximate DMT-NTH method on the aforementioned large chamber test of Cornell clay (deposit ID number UU), and the evaluated effective friction angle is shown to match quite well with the triaxial laboratory effective friction angle ϕ'.

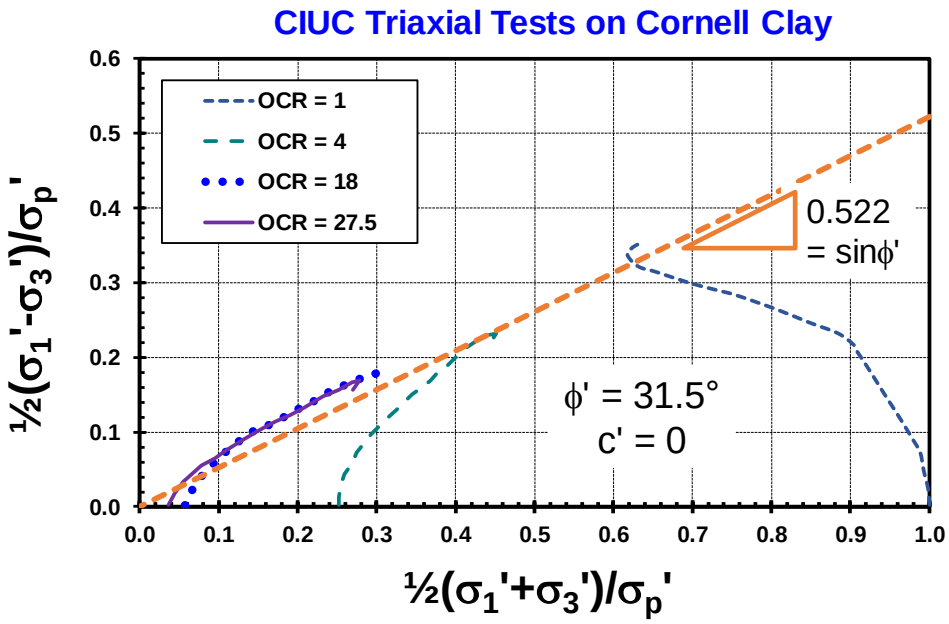

Figure 8.11. Laboratory CIUC triaxial stress paths showing effective strength envelope for Cornell clay (data from McManus and Kulhawy 1991).

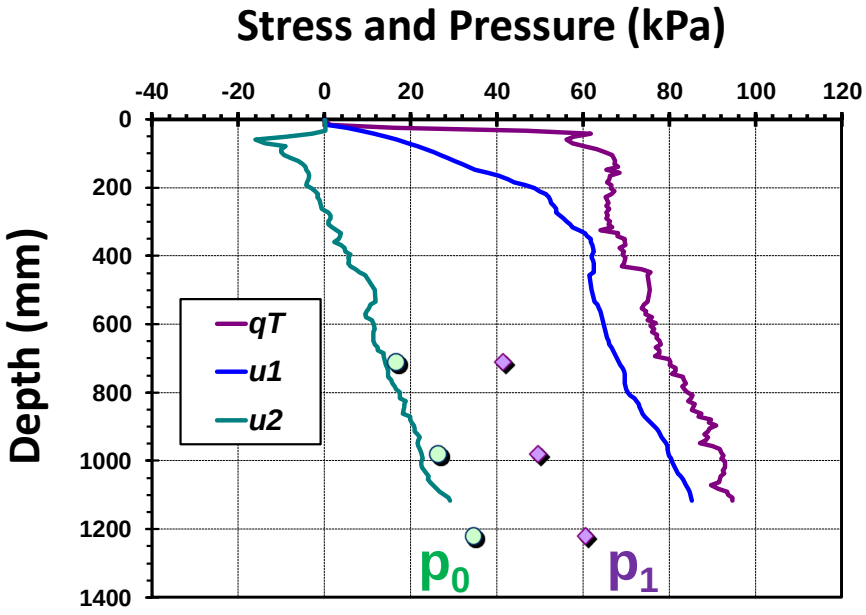

Figure 8.12. Profiles of mini-piezocone tests, mini-piezoprobes, and flat DMTs in a large chamber of Cornell clay.

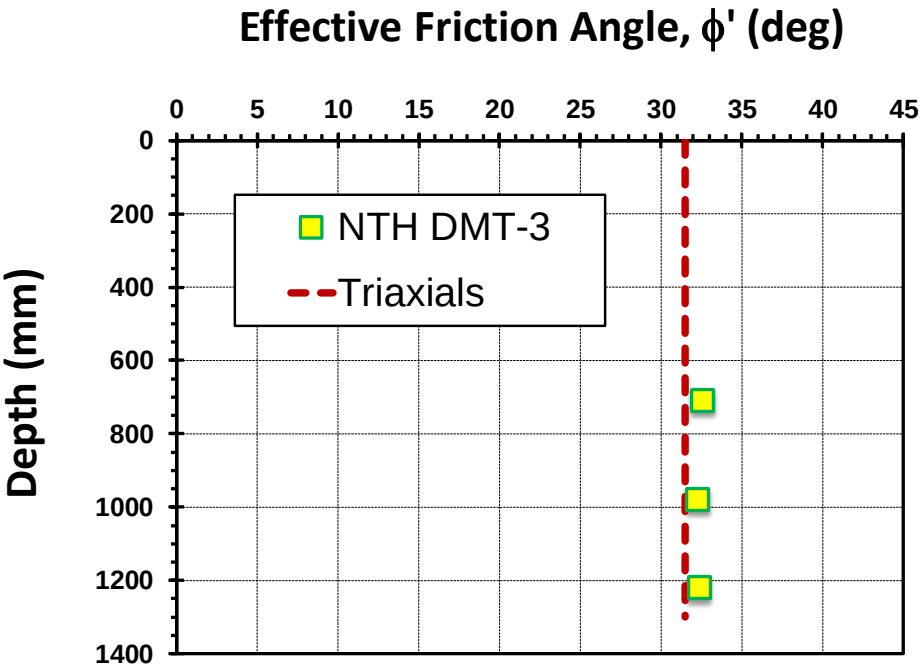

Figure 8.13. Profile of ϕ′ from flat dilatometer and laboratory triaxial tests in large chamber of Cornell clay.

8.5.4 DMT in Glava clay, Norway

The Glava clay deposit is located in Stjørdal, approximately 35 km east of Trondheim, Norway. The deposit consists of a homogeneous marine clay under a 0.5-m thick sand layer. The initial pore pressure distribution at the site is considered hydrostatic beneath the groundwater table at a depth of 1.5 m. The Glava clay can be classified as a medium stiff to stiff, LOC and sensitive clay with a mean unit weight of 19.4 kN/m3. The natural water content is about 30 %, and the plasticity is very low (PI = 5 %). The clay content (CF % < 2 μm) ranges from 35 to 48 % (Sandven 1990).

Field DMT soundings were performed in the Glava clay at Stjørdal, with measured pressure readings shown in Figure 8.14a (Roque, Janbu, and Senneset 1988). Series of CIUC triaxial tests on undisturbed samples taken at various elevations to investigate the total and effective stress strength parameters of the clay (Gylland, Jostad, and Nordal 2014). Results from four representative CIUC triaxial stress paths are shown in Figure 8.14b. The effective friction angle from the CIUC series averages about $\phi' = 34.1°$,

Figures 8.15a and 8.15b show the calculated profiles of the DMT-equivalent resistance number (Q_{DMT}) and porewater parameter ($B_{q\text{-}DMT}$), respectively. These are utilized as input into the approximate NTH solution and the corresponding profile of ϕ' is shown in Figure 8.15c. Also presented in this figure are the values of friction angle obtained from the four triaxial tests, illustrating good agreement with the NTH evaluation using DMT data.

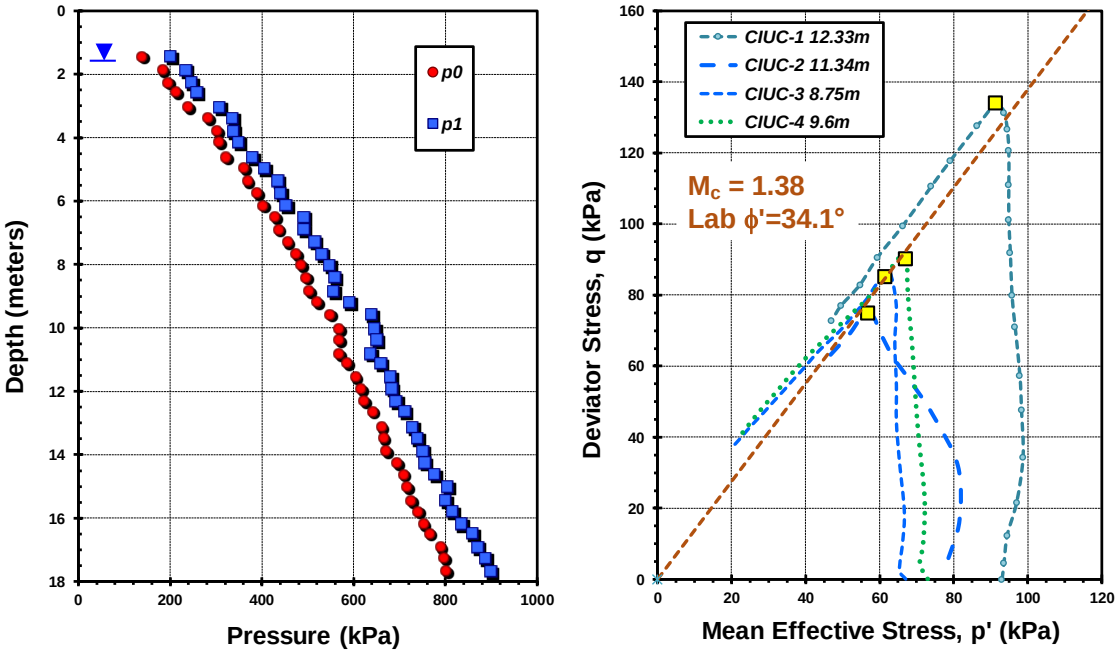

Figure 8.14. Data for Glava clay: (a) profiles from field DMT readings, (b) lab CIUC triaxial tests (note: DMTs from Roque et al. 1988; CIUCs from Gylland et al. 2014).

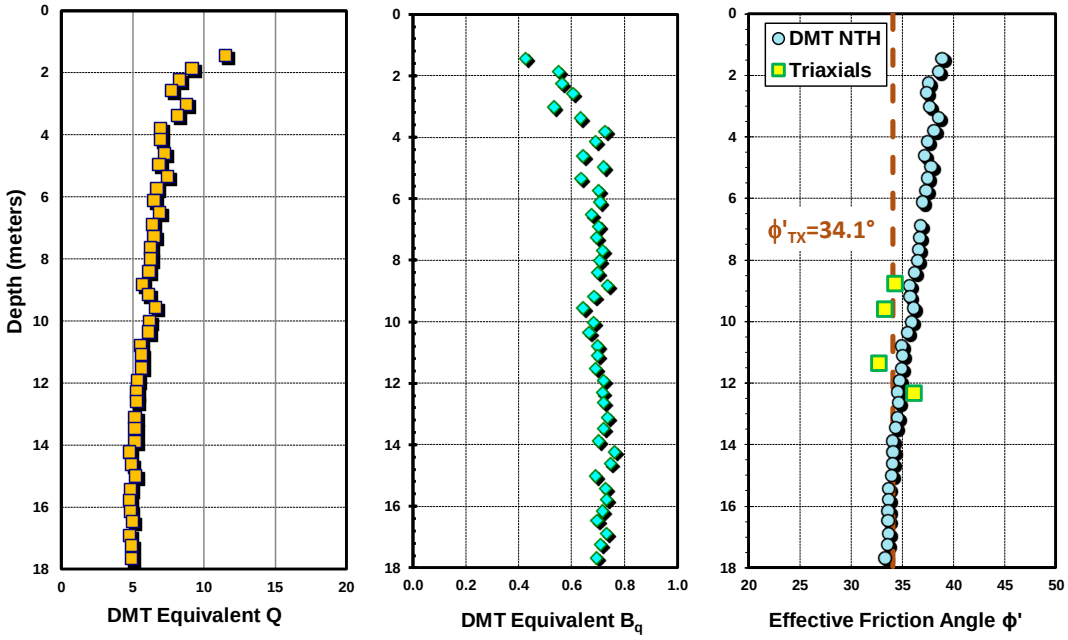

Figure 8.15. Profiles at Glava clay site, Norway: (a) DMT-equivalent resistance number (Q_{DMT}), (b) DMT-equivalent porewater parameter, ($B_{q\text{-}DMT}$), and (c) friction angle, ϕ'

8.6 DMT–Friction Angle ϕ′ Database

A special DMT-triaxial database was compiled from a variety of 46 clays and silty clay sites that were subjected to both flat DMTs and laboratory triaxial compression tests, as documented in Table 8.2. These sites generally consist of soft to firm intact clays and clayey silts that have various degrees and ranges of OCR. The majority of the sites were NC to LOC with 1 < OCRs < 2.5. Geologic origins of these soils vary from marine, alluvial, estuarine, glacial, and deltaic to lacustrine. In addition, data from three laboratory test programs involving artificial deposits conducted in 1-g chamber tests are included. The names of these clays, their locations, depth range of the soundings, mean water content (w), mean plasticity index (PI), unit weight, and their corresponding reference sources that reported the DMT data and laboratory results are noted in Table 8.2.

8.6.1 Index parameters

Overall, plasticity characteristics of these fine-grained soils ranged widely from very lean to highly plastic (4 % < PI < 92 %). The mean value of PI was 41.7 %, which had a standard deviation (SD) of 21.6. Water contents ranged from 20 to 135 % with a mean of 70 % and SD of 29 %. Effective stress friction angles from triaxial tests ranged from 21.6° to 45.0°, with a mean value $\phi' = 31.9°$ and SD of 6.2°, determining a coefficient of variation (COV) of 0.18. The NTH solution using DMT data gave a mean value $\phi' = 32.1°$ and SD of 5.9°, determining a COV of 0.185, which, overall indicates a very slight overprediction. Corresponding sensitivities generally were reported in the range of 2 to 8,

indicating low to medium sensitive soils for the vast majority of the clay sites, excepting a few sensitive clays located in eastern Canada and Scandinavia.

8.6.2 DMT parameters

All sites were subjected to flat DMTs at a standard pushing rate of 20 mm/s. For the database, the full range of measured contact pressure (p_0) from the DMT soundings at these sites ranged from 70 to 1,200 kPa. Correspondingly, the measured expansion pressure (p_1) generally varied from 100 to 2,000 kPa for the majority of the clay sites, with the exception of a few stiff clays. The DMT material index I_D ranges from 0.1 to 0.86 with an average I_D of 0.25, suggesting the database consist most of clays.

The normalized DMT parameters in Table 8.2 were given determined by averaging the Q_{DMT} and $B_{q\text{-}DMT}$ along the sounding profile in the clay formation or within a thick clay layer, or alternatively obtained from the regression plots. As noted previously, the intent of utilizing normalized parameters such as Q and B_q is to represent the overall in-situ test results with depth as a single parameter (Robertson 1990). The normalization also provided a single data point for each parameter of each clay so that no bias would be introduced into the statistics by any one particular clay.

8.6.3 Laboratory triaxial tests

Table 8.2 also provides the corresponding NTH–interpreted ϕ' and benchmark laboratory triaxial value of ϕ' for each clay. The triaxial ϕ' was obtained from either CIUC or anisotropically consolidated undrained triaxial compression tests (CAUC or CK_0UC). Note that a review of data from 48 NC clays that were tested with specimens both

isotropically and anisotropically showed that essentially the same friction angle is obtained over a full range of $18° \leq \phi' \leq 42°$ (Kulhawy & Mayne 1990). The values of ϕ' from CAUC and CK_0UC tests on these clays averaged only about 4% lower than ϕ' values obtained by CIUC tests on the same clay. More specifically, results of regression analyses on these clays indicated: n = 48; ϕ' (CAUC) = 0.96 ϕ' (CIUC), r^2 = 0.923, and S.E.Y. = 2.0°, as suggested by Figure 8.16.

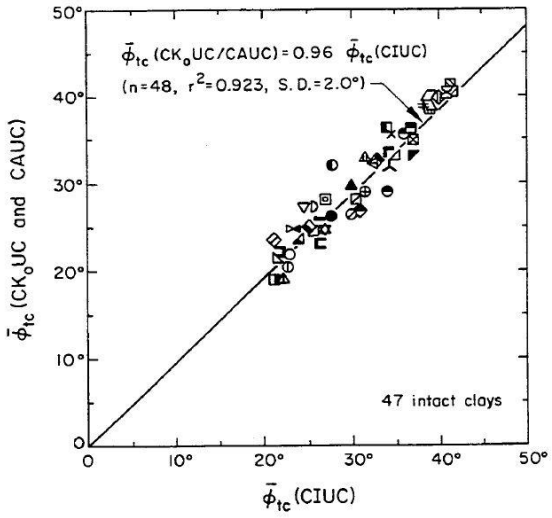

Figure 8.16. Effective stress friction angle ϕ' evaluated from CAUC versus CIUC of the same clays (adopted from Kulhawy & Mayne 1990)

8.7 Database Summary

Figure 8.17 presents a summary plot for the measured laboratory triaxial test ϕ' values versus the DMT-determined ϕ' values via the NTH solution. Each clay is represented by a unique symbol by both shape and color. Two sets of statistical measures were made on the dataset, including: (a) arithmetic statistics and (b) regression statistics, as indicated in the figure. The measured laboratory triaxial values of ϕ' cover the full range

from 21.6° to 45.0° and the DMT-evaluated ϕ' ranges from 21.7° to 48.2°. These agree with the observed ranges of effective friction angles reported for natural clays, as documented by Dìaz-Rodrìguez, Leroueil, and Alemàn (1992), whereby: $17.5° < \phi' < 43.0°$. From the arithmetic set of statistics, the ratio of measured/evaluated values ranges from 0.84 to 1.10 with an overall mean of 1.00 and SD of 0.05, giving a corresponding COV of 0.05. From the regression evaluations of lab versus field, the regression slope = 0.99 with a coefficient of determination of $r^2 = 0.920$ and standard error of the Y-estimator (SEY) = 1.76. The above statistics generally support the fact that the DMT-NTH method gives a reasonable evaluation of the effective friction angle of soft to firm clays when referenced to the laboratory triaxial test as the benchmark value.

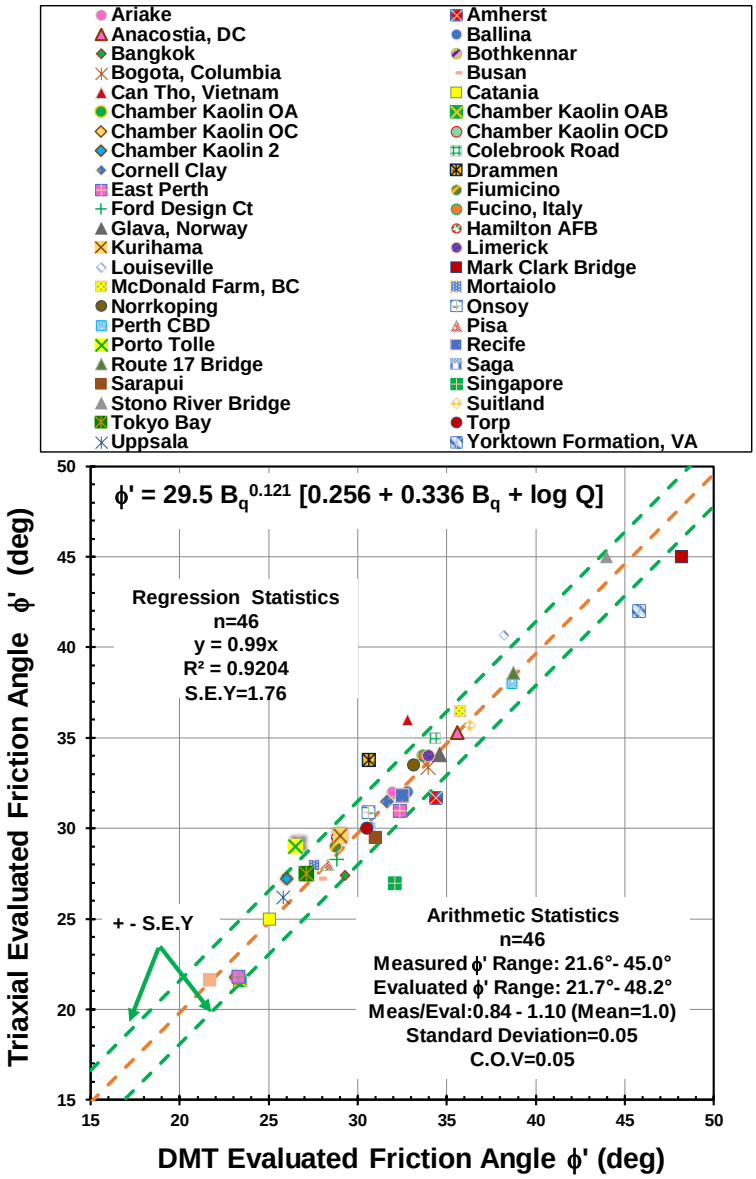

Figure 8.17. Summary plot of laboratory-measured triaxial friction angle ϕ′ versus effective friction angle ϕ′ from DMTs using the NTH solution.

8.8 Discussion and Applicability

8.8.1 Friction Angle Criteria

For the clays reviewed in this chapter, the effective stress friction angle ϕ′ was obtained from either isotropically consolidated (CIUC), K_0-consolidated (CK_0UC), or generally anisotropically-consolidated undrained triaxial compression tests (CAUC), or

various combinations of the these, on undisturbed samples to establish the benchmark value. In a handful of cases, drained tests (CIDC, CADC, or CK_0DC) were also performed. In general, recognized guidelines for the test procedures, such as ASTM standards (ASTM D4767-11, Standard Test Method for Consolidated Undrained Triaxial Compression Test for Cohesive Soils), Bishop and Henkel (1962), Germaine and Germaine (2009), and Lade (2016), were followed.

The effective friction angle obtained from triaxial tests can be evaluated on the basis of different criteria, including (a) value at maximum deviator stress (q_{max}), (b) value at maximum obliquity $(\sigma'_1/\sigma'_3)_{max}$, and (c) value taken at large strains, normally at 15 % axial strain, or, in some cases, at 20 % strain. The latter criterion is sometimes interpreted as the value corresponding to critical state (ϕ'_{cs}). For CIUC and CAUC tests on soft inorganic clays of low sensitivity and low OCRs, these criteria often occur at similar points on the effective stress path, so only minor differences are noted in their magnitudes (Lade 2016; Ouyang and Mayne 2017c). A study of 19 natural clays generally showed only minor differences in values of ϕ' defined at q_{max} and ϕ' at $(\sigma'_1/\sigma'_3)_{max}$ (Bjerrum and Simons 1960). For a large series of CK0UC tests on soft Chicago clays, Finno and Chung (1992) showed that $\phi' = 28.3°$ at $(\sigma'_1/\sigma'_3)_{max}$ and $\phi' = 27.6°$ at large strains, thus <1° difference. For sensitive and structured clays, however, the values can be several degrees different (Leroueil and Hight 2003). In most of the database, only a single reported value of ϕ' was provided by the sources of information, and the adopted criterion was often not identified. In some cases, an effective stress envelope was provided yet the criterion used was not noted. In a few cases, a complete effective stress path, a stress strain curve, or both, were provided and more than criteria could be used in determining ϕ'. It is believed that the

database primarily contains results from inorganic and insensitive clays where differences in ϕ' from the different criteria are relatively minor.

8.8.2 Effective Cohesion Intercept, c′

The general expression for the Mohr-Coulomb strength criterion of soils is given as follows:

$$\tau_{max} = c' + \sigma' \cdot \tan\phi' \qquad [8.19]$$

where τ_{max} = shear strength. Thus, a pair of the effective stress strength parameters include both c' and ϕ'. In fact, the NTH solution does permit an evaluation of c' from penetration tests, as denoted by Equation [8.10]. Details concerning this procedure are given elsewhere (Senneset et al. 1989; Sandven 1990; Mayne 2016).

For this study, the effective cohesion intercept (c') has been taken as zero ($c' = 0$) because the vast majority of the clays considered are NC to LOC with low OCRs < 2.5 (e.g., Finno and Chung 1992; Dìaz-Rodrìguez, Leroueil, and Alemàn 1992). Even for overconsolidated clays, only a small value of c' is appropriate (Lade 2016). If a value of c' is necessary, the ratio $c'/\sigma_p' \approx 0.03$ can be used, where σ_p' = effective preconsolidation stress (Larsson, Bergdahl, and Eriksson 1987; Mayne 2016).

A recent study by Amundsen and Thakur (2017) investigated the effects of sample disturbance on soft clay parameters. It was found that sample quality, storage time, and testing time between sampling and shearing appreciably affect the magnitude of preconsolidation stress, undrained shear strength, and constrained modulus. However, the magnitude of the effective stress friction angle was little affected by these same factors.

8.8.3 Partial Drainage Effect

The aforementioned approach is applicable to undrained conditions. For a standard penetration rate of 20 mm/s for both CPTu and DMT, it is generally accepted that clay soils with low permeability will experience an undrained penetration process. However, drainage conditions during DMTs in intermediate permeability soils, including sandy silts, coarse silts, and sandy clays, may be different. Schnaid et al. (2016) indicated that the DMT is essentially undrained in soft clay and dominated by penetration pore pressures, whereas the test exhibits drained behavior in clean sands and partially-drained response in intermediate permeability soils, such as cohesionless silts.

For the CPTu, a special series of tests at variable rates is termed "twitch" testing that allows the demarcation of undrained, partially drained, to fully-drained behaviour (Randolph 2004). DeJong et al. (2012) give an approximate range of c_v (coefficient of consolidation) that applies to clays, silts, and sands for field operation of CPTu during twitch testing. For clays, the expected range and upper limit for the coefficient of consolidation is approximately $c_v < 0.05$ cm^2/s. Thus, for soils with higher values, such as silts and sands, the SCE nexus in this study may no longer apply.

Also, as noted earlier, CPTu readings q_t and u_2 are taken during penetration at time $t = 0$, whereas the DMT readings p_0 and p_1 are obtained at approximately $t = 15$ s and $t = 45$ s after penetration, respectively. Thus, the method can become invalidated when dissipations occur in soils that do not maintain undrained conditions at constant volume.

Finally, special considerations should also be taken when conducting site investigations in more difficult soils, such as highly organic clays, peats, and muskegs, as

well as sensitive and structured geomaterials, because the aforementioned relationships may not apply. In highly stratified deposits where clay layers are sandwiched between more permeable silty and sandy layers, the effects of drainage and partial drainage may also influence the results, especially for thin clay strata. In these cases, caution is warranted.

8.9 Conclusions

A theoretical nexus between CPTu readings (q_t and u_2) and flat DMT pressures (p_0 and p_1) is built based on undrained cavity expansion theory for use in soft to firm clays with OCRs between 1 to 2.5. Field data from 49 paired CPTu-DMT soundings on natural clays are compiled to verify the link. An existing NTH limit plasticity solution that provides the evaluation of effective stress friction angle ϕ' in soft to firm clays from in-situ piezocone measurements is then extended to DMT measurements for the same purpose. Data from four case studies are presented to illustrate the DMT-NTH approach, including (a) soft clay from southeastern Virginia, (b) kaolin clay with low friction in a pressurized calibration chamber test, (c) a kaolin-silica mixture tested by DMT in unpressurized chamber tests, and (d) marine clay from Norway. Laboratory triaxial test results (CK_0UC, CAUC, or CIUC) with field DMT results from 40 natural clays and 3 DMT series in clay chamber test series were reviewed to corroborate the validity of the methodology. A full range of operational effective stress friction angles with $20° \leq \phi' \leq 45°$ are observed in both the triaxial data and NTH solution. The method is applicable to soft clays at low OCRs < 2.5, which are relatively insensitive and maintain undrained conditions with $c_v < 0.05$ cm^2/s. For fine-grained soils that are partially-saturated, highly organic, sensitive, structured, and/or heavily overconsolidated, the methodology may not be applicable and additional concerns and careful calibrations may be appropriate on a site-by-site basis.

Table 8.2. List of clays subjected to laboratory triaxial and flat DMTs for NTH study.

Site Name	Location	Description	Depth Range	Mean w_n	Mean PI	Mean γ_t[a]	Q_{DMT}	B_{qDMT}	DMT ϕ'	Triaxial ϕ'[b]	Reference Sources
			(m)	(%)	(%)	(kN/m^3)			(deg)	(deg)	
Amherst	Massachusetts	Lacustrine Varved Clay	5-11	48	15	17.1	6.50	0.55	34.8	31.7*	DeGroot & Lutenegger (2003); Sambhandharaska (1977) Hegazy (1998)
Anacostia NAS	Washington, DC	Soft Alluvial Clay	5-18	65	32	15.9	4.50	0.92	36.0	35.1	Mayne (1987)
Ariake	Japan	Soft Marine Clay	4-17	106	68	13.5	4.21	0.73	31.7	32.0	Watabe et al (2003)
Ballina	Australia	Soft Estuarine Clay	3-11	107	66	14.1	4.73	0.69	29.3	32.0	Pineda et al (2014)
Bangkok	Thailand	Soft Marine Clay	4-9	74	61	15.4	4.46	0.51	29.6	27.4	Tanaka et al (2001)
Bogota	Colombia	Soft Plastic Clay	5-24	108	96	13.6	5.00	0.72	34.4	35.0	Diaz-Rodriguez et al (1992); Rodriguez (2016)
Bothkennar	Scotland	Soft Estuarine Clay	3-11	61	40	16.5	6.20	0.54	34.4	34.0	Hight et al. (2003) Nash et al (1992)

Table 8.2. List of clays subjected to laboratory triaxial and flat DMTs for NTH study. (continued)

Site Name	Location	Description	Depth Range	Mean w_n	Mean PI	Mean γ_t[a]	Q_{DMT}	B_{qDMT}	DMT ϕ'	Triaxial ϕ'[b]	Reference Sources
			(m)	(%)	(%)	(kN/m^3)			(deg)	(deg)	
Can Tho	Vietnam	Soft Alluvial Clay	2-25	58	38	16.3	5.30	0.60	30.9	36.0	Takemura et al (2006)
Chamber Kaolin OA	Oxford, England	Speswhite Kaolin (100%)	NA	44	31	17.4	1.79	0.75	21.7	21.6	Smith (1993)
Chamber Kaolin OAB	Oxford, England	Speswhite Kaolin (100%)	NA	37	31	16.6	2.43	0.6	23.4	21.6	Smith (1993)
Chamber Kaolin OC	Oxford, England	Speswhite Kaolin (100%)	NA	45	31	17.6	2.25	0.65	23.0	21.8	Smith (1993)
Chamber Kaolin OCD	Oxford, England	Speswhite Kaolin (100%)	NA	40	31	16.9	2.13	0.71	23.3	21.8	Smith (1993)
Chamber Kaolin 2	Potsdam, New York	50-50 Kaolin-Edgar Sand Mix	NA	100	24	15.7	2.48	0.77	26.0	27.2	Huang et al (1990)
Chamber Cornell Clay	Ithaca, New York	50-50 Kaolin-Fine Silica Mix	NA	34	11	18.5	8.30	0.26	31.6	31.5	Mayne et al (1992)
Drammen	Norway	Sensitive Marine Clay	5-25	52	28	16.6	4.60	0.57	34.0	34.2	Lunne & Lacasse (1997); Lunne et al (1997)

Table 8.2. List of clays subjected to laboratory triaxial and flat DMTs for NTH study. (continued)

Site Name	Location	Description	Depth Range	Mean w_n	Mean PI	Mean γ_t[a]	Q_{DMT}	B_{qDMT}	DMT ϕ'	Triaxial ϕ'[b]	Reference Sources
			(m)	(%)	(%)	(kN/m^3)			(deg)	(deg)	
Fucino	Italy	Soft Carbonate Clay	5-30	78	60	15.1	4.80	0.74	35.1	34.0	Soccodato (2002)
Glava	Norway	Sensitive Clay	2-20	32	5	19.4	5.40	0.70	34.6	34.7	Sandven (1990) Roque et al (1988) Gylland et al (2014)
Hamilton AFB	California	Soft Bay Mud	2-14	95	45	13.7	3.50	0.67	29.7	29.5	Bonaparte et al (1979); Masood et al (1988)
Kurihama	Japan	Soft Marine Clay	5-30	98	61	15.2	4.25	0.53	28.0	29.6	Tanaka (1995)
Louiseville	Quebec	Soft Sensitive Leda Clay	2-13	72	42	15.6	9.50	0.51	39.5	40.7	Leroueil et al (2003)
Mark Clark Bridge	South Carolina	Calcareous Cooper Marl	2-30	36	28	18.5	19.10	0.60	46.7	45.0	Camp et al (2002a&b, 2004), personal communication
McDonald Farm	British Columbia	Soft Clayey Silt	2-25	55	66	16.7	16.50	0.15	35.6	36.5	Robertson et al (1992)
Norrköping	Sweden	Soft Inorganic Clay	2-12	66	42	15.7	5.05	0.66	33.1	33.5*	Larsson & Mulabdić (1991)

Table 8.2. List of clays subjected to laboratory triaxial and flat DMTs for NTH study. (continued)

Site Name	Location	Description	Depth Range	Mean w_n	Mean PI	Mean γ_t[a]	Q_{DMT}	B_{qDMT}	DMT ϕ'	Triaxial ϕ'[b]	Reference Sources
			(m)	(%)	(%)	(kN/m^3)			(deg)	(deg)	
Ford Design Center	Evanston, Illinois	Soft Lacustrine Chicago Clay	11-20	20	12	21.0	3.05	0.79	28.8	28.3*	Mayne (2006); Chung & Finno (1992)
Onsøy	Norway	Soft Marine Clay	4-19	64	41	15.9	4.10	0.66	30.8	34.0	Lunne et al. (2003)
Porto Tolle	Italy	Firm NC Silty Clay	6-28	35	26	18.2	3.73	0.47	28.7	29.0	Hansbo et al (1981)
Route 17 Bridge	Chesapeake, Virginia	Soft Slightly Organic Clay	6-16	76.5	55	15.6	9.80	0.52	38.7	38.6	Charles and Barnhill (1987)
Recife	Brazil	Soft Organic Clay	8-25	123	69	15.6	4.69	0.68	32.5	31.8	Danziger (2007)
Sarapuí	Brazil	Soft organic Clay	5-11	135	65	13.2	4.03	0.70	31.0	29.5	Almeida et al. (2003); Danziger (2007)
Singapore	Singapore	Soft Marine Clay	2-28	55	50	16.0	5.00	0.60	29.6	27.0	Cao (2003)
Stono River Bridge	South Carolina	Calcareous Cooper Marl	2-39	36	28	18.5	14.75	0.54	44.0	45.0	Camp (2004)

Table 8.2. List of clays subjected to laboratory triaxial and flat DMTs for NTH study. (continued)

Site Name	Location	Description	Depth Range	Mean w_n	Mean PI	Mean γ_t[a]	Q_{DMT}	B_{qDMT}	DMT ϕ'	Triaxial ϕ'[b]	Reference Sources
			(m)	(%)	(%)	(kN/m^3)			(deg)	(deg)	
Tokyo Bay	Japan	Soft Marine Clay	5-35	46	25	17.0	3.44	0.57	28.1	27.5	Takesue (2001)
Torp	Sweden	Soft Sensitive Clay	10-40	48	29	17.5	5.24	0.47	30.8	30.0	Larsson and Åhnberg (2003)
Yorktown Formation	Newport News, Virginia	Stiff OC Carbonate Sandy Clay	2-16	31	4	19.0	24.00	0.36	40.9	38.0	Mayne (1989)

Note:

[a] γ_t= unit weight

[b] Effective stress friction angle from CAUC or CIUC triaxial test defined at maximum shear stress; otherwise, an asterisk (*) notes another criterion: either maximum obliquity orlarge strains.

CHAPTER 9. EVALUATING EFFECTIVE FRICION ANGLE, RIGIDITY INDEX, OCR, AND S_u FROM DILATOMETER DATA IN SOFT TO FIRM CLAYS

9.1 Introduction

Using a hybrid of spherical cavity expansion (SCE) theory with critical state soil mechanics (CSSM) and an effective stress limit plasticity solution from NTH, it is feasible to analytically determine four important geoparameters from the results of flat plate dilatometer tests in soft-firm clays: (a) effective stress friction angle, ϕ', (b) undrained rigidity index, I_R, (c) overconsolidation ratio, OCR, and (d) undrained shear strength. s_u.

The effective stress friction angle (ϕ') represents the drained strength of all soils and is fundamental as a soil property within the context of effective stress paths obtained in triaxial tests (Bishop & Henkel 1960; Lambe & Whitman 1979; Lade 2016). The friction angle is a major component in CSSM and constitutive modeling of soils, particularly useful in predicting pore pressure behavior in the ground during simulations of embankment construction, excavations, and soil liquefaction. An existing method developed at NTH for undrained penetration can be utilized for evaluating ϕ' from DMTs in soft-firm clays via an established nexus based on SCE (Ouyang & Mayne 2017).

The rigidity index of soil is defined as the ratio of shear modulus (G) to shear strength ($\tau_{max)}$, thus: $I_R = G/\tau_{max}$. Its value is often difficult to assess because the value of G varies over one order of magnitude, ranging from small-strains (G_{max}) to intermediate (G), to that corresponding to peak strength (G_f). The rigidity index is an important input

parameter for geotechnical calculations on bearing capacity, pile driving, and porewater pressure generation. It is also needed in evaluating the coefficient of consolidation (c_{vh}) from piezocone dissipation tests using solutions based on cavity expansion, strain path method, and FEM. Agaiby & Mayne (2018) utilized data from piezocone penetration tests (CPTu) to evaluate the undrained rigidity index of clays, which in turn was successfully used in assessing c_{vh} from piezocone dissipation tests at several field sites.

In the usual interpretative approach, the DMT evaluation of overconsolidation ratio (OCR) and undrained shear strength (s_u) of clays is done via empirical correlations. However, a nexus between CPTu and DMT measurements in soft-firm clays with low OCRs < 2.5 was established using spherical cavity expansion (SCE) in Chapter 8. This link between the DMT and CPTu in clays is further exploited in this chapter to develop an approach to obtain undrained rigidity index (I_R) from DMT readings under a hybrid formulation of spherical cavity expansion and critical state soil mechanics (SCE-CSSM) for assessing both OCR and s_u in analytical form. The value of I_R obtained can be used to ascertain the undrained shear strength from SCE. Furthermore, a hybrid SCE-CSSM formulation provides a means for determining the profile of OCR in the clay.

9.2 SCE-CSSM solution for undrained rigidity index for soft to firm clays

9.2.1 Original SCE-CSSM solution

A hybrid formulation of spherical cavity expansion theory and critical state soil mechanics (SCE-CSSM) expresses readings from CPTu, namely the cone tip resistance (q_t) and penetration porewater pressure (u_2) using closed-form equations (Mayne 1991, 2007):

$$q_t = \sigma_{v0} + [(4/3) \cdot (\ln I_R + 1) + \pi/2 + 1] \cdot (M/2) \cdot (OCR/2)^{\Lambda} \cdot \sigma'_{v0} \quad [9.1]$$

$$u_2 = u_0 + [(2/3) \cdot (\ln I_R + 1) \cdot M \cdot (OCR/2)^{\Lambda} \cdot \sigma'_{v0}] + [1 - (OCR/2)^{\Lambda}] \cdot \sigma'_{v0}) \quad [9.2]$$

where q_t is the total cone resistance, σ_{vo} = total overburden stress, u_2 = measured porewater pressure at the shoulder position of the piezocone, u_0 = hydrostatic porewater pressure, $M = (q/p')_f = (6 \cdot \sin\phi')/(3 - \sin\phi')$ = slope of the frictional envelope for triaxial compression in q-p' space, $OCR = (\sigma'_p/\sigma'_{vo})$ is the overconsolidation ratio, σ'_p = preconsolidation stress and σ'_{vo}= effective overburden stress. The parameter $\Lambda = (1 - C_s / C_c)$ = plastic volumetric strain potential, where C_s =swelling index, C_c = virgin compression index, and typically, $\Lambda \approx 0.8 - 1.0$ for most clays.

The hybrid SCE-CSSM model can be rearranged to express overconsolidation ratio (OCR) of the clay in terms of three separate formulations using: (a) net cone resistance ($q_{net} = q_t - \sigma_{vo}$), (b) excess pore pressure ($\Delta u = u_2 - u_0$), and (c) effective cone resistance ($q_E = q_t - u_2$), as follows:

$$OCR = 2 \cdot \left[\frac{(2/M) \cdot (q_{net}/\sigma'_{v0})}{4/3 \cdot (\ln I_R + 1) + \pi/2 + 1}\right]^{1/\Lambda} \quad [9.3]$$

$$OCR = 2 \cdot \left[\frac{(\Delta u/\sigma'_{v0}) - 1}{2/3 \cdot M \cdot \ln I_R - 1}\right]^{1/\Lambda} \quad [9.4]$$

$$OCR = 2 \cdot \left[\frac{1}{1.95 \cdot M + 1} \left(\frac{q_t - u_2}{\sigma'_{v0}}\right)\right]^{1/\Lambda} \quad [9.5]$$

Combining equation [9.3] and [9.4], the value of the rigidity index can be obtained in terms of normalized CPTu measurements and friction parameter M:

$$I_R = \exp \cdot \left[\frac{1.5 + 2.925M \cdot (U^* - 1)/Q}{M - M(U-1)/Q}\right] \quad [9.6]$$

where Q = normalized tip resistance = q_{net}/σ'_{vo} and U = normalized porewater pressure parameter = $\Delta u_2/\sigma'_{vo}$. Note that the alternate and more common porewater pressure parameter, $B_q = \Delta u/q_{net}$ is determined simply as $B_q = U/Q$.

In addition, a stable representation for [9.6] can be obtained in the following format:

$$I_R = \exp\cdot\left[\frac{1.5 + 2.925M \cdot a_q}{M - M\cdot a_q}\right] \quad [9.7]$$

alternate: $I_R = \exp\cdot\left[\frac{1.5/M + 2.925 \cdot a_q}{1 - a_q}\right]$

where $a_q = (U^* - 1)/Q = (u_2 - \sigma_{vo})/(q_t - \sigma_{vo})$. Hence, a_q can be determined as a single value for any clay deposit or clay layer by taking the slope of a plot of the parameter (U*-1) versus Q, or alternatively taken as the slope of $(u_2 - \sigma_{vo})$ versus $(q_t - \sigma_{vo})$. Of course, the method only applies where groundwater depths are shallow, as is common in soft-firm clay deposits, since a requirement for performance is that $u_2 > \sigma_{vo}$.

9.2.2 Nexus between CPTu and DMT to determine I_R

Ouyang & Mayne (2017, 2018) derived two SCE links between measurements taken by CPTu and DMT in soft to firm clays using spherical cavity expansion theory (SCE). As such, an equivalent net cone resistance (q_{netDMT}) and excess porewater pressure (Δu) from DMTs soundings can be expressed:

$$q_{net\text{-}DMT} = 2.93p_1 - 1.93p_0 - u_0 \quad [9.8]$$

$$\Delta u_{\text{-}DMT} = p_0 - u_0 \quad [9.9]$$

where p_0 and p_1 are the contact and expansion pressures from the DMT, respectively.

This nexus provides two links between the two tests for soils that are characterized as normally-consolidated to lightly-overconsolidated clays with OCR between 1 to 2.5. The above expressions and associated CPTu-DMT relationships for soft to firm clays are summarized in graphic form in Figure 9.1.

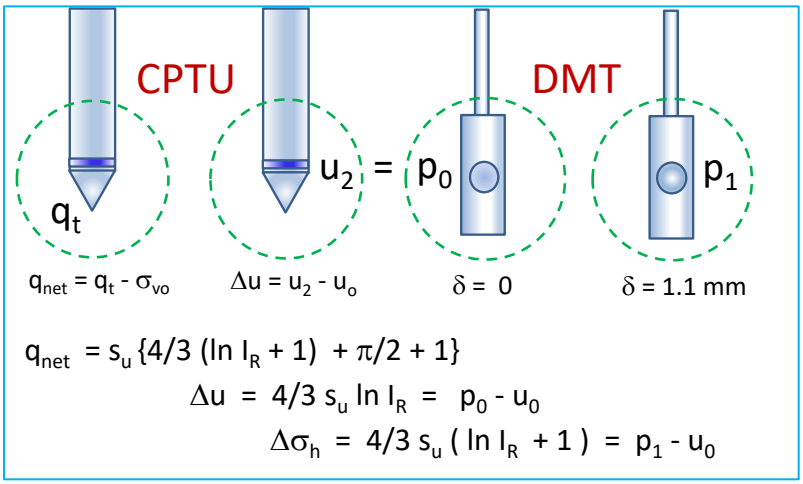

Figure 9.1. Summary of the nexus between CPTu and DMT readings in soft to firm clays using spherical cavity expansion solutions.

From the linkages, the undrained rigidity index I_R derived from equation [9.7] can be re-expressed using DMT based readings p_0 and p_1:

$$I_R = \exp\cdot\left[\frac{1.5 + 2.925M \cdot a_{q\text{-}DMT}}{M - M\cdot a_{q\text{-}DMT}}\right] \qquad [9.10]$$

where $a_{q\text{-}DMT} = (U^*_{DMT} - 1)/Q_{DMT}$. The equivalent normalized porewater pressure parameter (U^*) and equivalent normalized resistance (Q) from the DMT are found as:

$$U^*_{DMT} = (p_0 - u_o)/\sigma'_{vo} \qquad [9.11]$$

$$Q_{DMT} = (2.93p_1 - 1.93p_0 - u_0)/\ \sigma'_{vo} \qquad [9.12]$$

As noted earlier, $a_{q\text{-}DMT}$ can be determined as a single value for any clay deposit by taking the slope of a plot of the parameter (U^*_{DMT}-1) versus Q_{DMT}. Alternatively, the value

of $a_{q\text{-}DMT}$ is found as the slope of a plot of the DMT equivalent for excess porewater pressure difference, $\Delta u_{DMT} = (p_0 - \sigma_{vo})$ versus DMT equivalent for net cone resistance, $q_{net\text{-}DMT} = (2.93p_1 - 1.93p_0 - u_0)$.

In the event that laboratory-measured ϕ' values from triaxial tests are not available, the effective friction angle of soft-firm clays can be evaluated using the DMT-NTH solution, as detailed in previous chapters. Because of the SCE link, the effective stress friction angle ϕ' can now be evaluated using the following closed-form solution from DMT measurements, given in chapter 8:

$$Q_{DMT} = \frac{\tan^2(45° + \phi'/2) \cdot \exp(\pi \cdot \tan\phi') - 1}{1 + 6 \cdot \tan\phi' \cdot (1 + \tan\phi') \cdot (U^*_{DMT}/Q_{DMT})} \quad [9.13]$$

For the inversion solution, an approximate expression for directly assessing ϕ' is given by the following:

$$\phi' \approx 29.5 \cdot (U^*_{DMT}/Q_{DMT})^{0.121} [0.256 + 0.336 \cdot (U^*_{DMT}/Q_{DMT}) + \log Q_{DMT} \quad [9.14]$$

which is valid for the following ranges: $20° \leq \phi' \leq 45°$ and $0 \leq U^*_{DMT} \leq 4$.

9.2.3 Undrained Shear Strength Evaluation

The undrained shear strength of clays (s_u) can be evaluated from the equivalent $q_{net\text{-}DMT}$ and a bearing capacity factor (N_{kt}) that depends upon the operational rigidity index IR. The undrained shear strength is obtained from:

$$s_u = q_{net\text{-}DMT} / N_{kt} \quad [9.15]$$

Spherical cavity expansion (SCE) provides N_{kt} in terms of rigidity index I_R (Vesic 1977, Ouyang & Mayne 2017):

$$N_{kt} = (4/3)\cdot(\ln I_R + 1) + \pi/2 + 1 \qquad [9.16]$$

Combining equations [9.8], [9.15] and [9.16], the undrained shear strength s_u of soft to firm clays can be evaluated from DMT readings as:

$$s_u = (2.93p_1 - 1.93p_0 - u_0) / [(4/3)\cdot(\ln I_R + 1) + \pi/2 + 1] \qquad [9.17]$$

9.3 Case Studies validating the I_R evaluation

Two case studies are presented to illustrate the application of the DMT methodology for assessing ϕ', I_R, OCR, and s_u in clays.

9.3.1 Bothkennar, UK

Bothkennar clay is a lightly- to normally-consolidated estuarine soft clay deposit in Scotland that serves as a national test site for geotechnical experimentation in the UK (Hight et al. 1992; 2003). Within the upper 16 m, the clay has OCR values decreasing with depth that range from 3 to 1.5 below a 2-meter crustal layer. The water table at the site is relatively shallow, typically on the order of 1 m depth. Representative DMT readings and the derived DMT material index parameter (I_D) with depth at the site are shown in Figure 9.2.

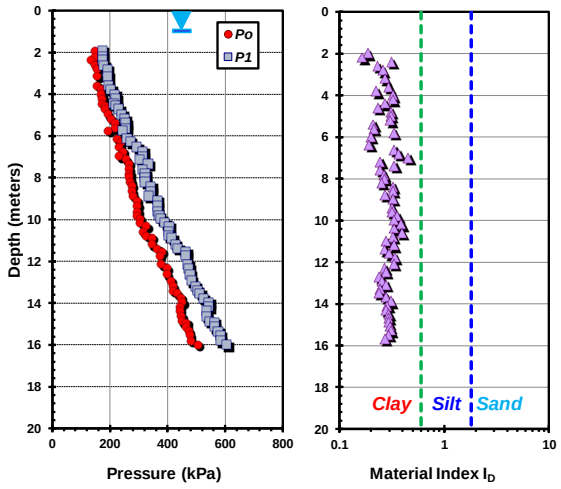

Figure 9.2. DMT profiles for soft Bothkennar clay, UK (data from Hight et al. 2003).

Based on the DMT data, the NTH solution outputs a value of effective friction angle of $\phi'=34°$ for this soft clay, giving a corresponding value of M=1.37. Series of triaxial tests (CK_0UC, CK_0DC, CK_0UE, and CK_0DE) also confirmed that $\phi'=34°$ for Bothkennar clay (Allman & Atkinson 1992).

Figure 9.3 shows the evaluation of the slope parameter a_q at Bothkennar where (p_0-σ_{vo}) is plotted versus $q_{net\text{-}DMT}$ =(2.93p_1-1.93p_0-u_0), giving a parametric value a_q = 0.38. This slope value is used with the effective friction angle to give an operational rigidity index I_R = 34.

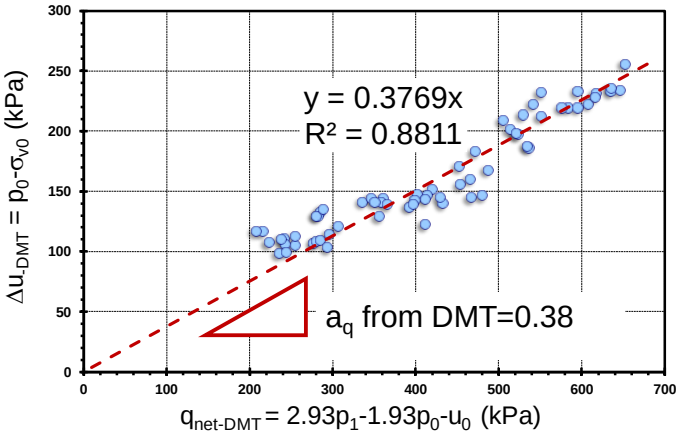

Figure 9.3. Evaluation of slope parameter a_q to determine I_R for Bothkennar, UK

Applying equations [9.3], [9.4] and [9.5] of the hybrid SCE-CSSM solution to the DMT data with input parameters (I_R = 39, ϕ' = 34°, Λ = 1), three assessment of stress history show consistent results, as seen in Figure 9.4. Overall, good agreement is observed when compared with laboratory-measured σ'_p and OCR profiles obtained from consolidation testing reported by Hight et al. (1992, 2003). Also, the evaluated I_R value of 34 gives the magnitude of N_{kt} = 8.9 that provides a DMT profile of s_u in general agreement yet higher than laboratory CAUC triaxial compression tests and field vane shear tests (VST) at the site. Technically speaking, the SCE-CSSM solution actually applies to s_u for a CIUC mode. It is recognized in fact that CIUC tests give s_u values slightly higher than s_u from CAUC and CK_0UC tests, with a dependency that tracks with the ϕ' of the clay (Kulhawy & Mayne 1990).

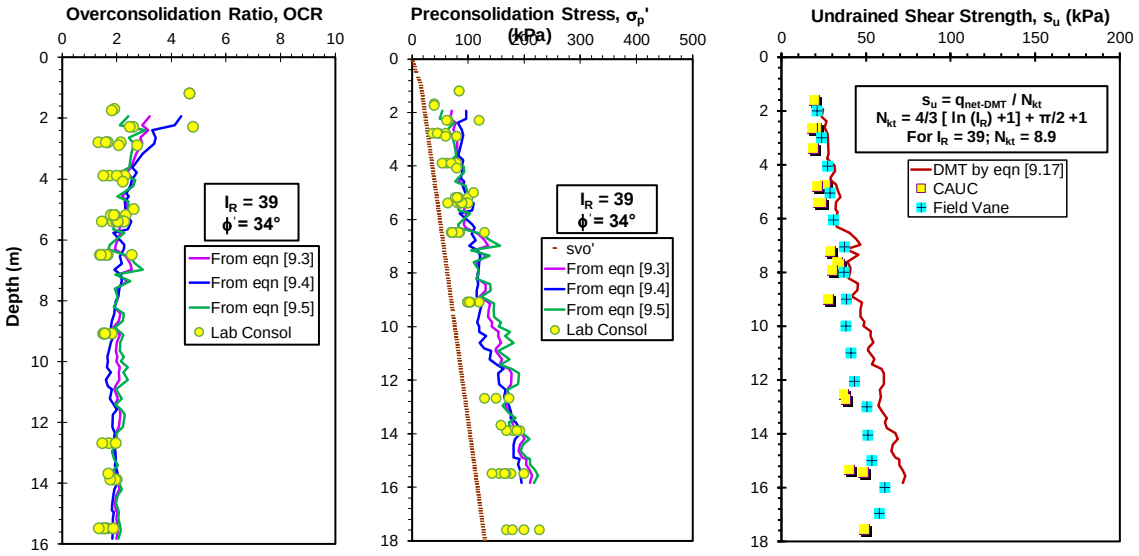

Figure 9.4. OCR and preconsolidation stress profiles using the SCE-CSSM framework for Bothkennar, UK

9.3.2 Northwestern University

The National Geotechnical Experimentation Site (NGES) located at Northwestern University (NWU) in Evanston, Illinois serves as a testing grounds for research (Finno 2000). The site is layered with approximately 6+ m of clean sand over a 10+ m thick layer of soft clay and underlain by silt layers and deeper strata. The lacustrine deposits of interest here occur as a soft clay stratum from around 11 to 20 meters depths and have been a focus of laboratory testing by NWU (Chung & Finno 1992).

For the soft Chicago clays at Northwestern University, the measured pressures from a representative DMT conducted by Georgia Tech personnel in 2004 are presented in Figure 9.5a. The profile of interpreted effective stress friction angle using the approximate DMT-NTH equation is compared with the effective strength envelope determined by a series of laboratory CK_0UC triaxial compression tests reported by Chung & Finno (1992), as shown in Figure 9.5b. It can be seen that the field DMT ϕ' is in good agreement with the laboratory value, both giving a friction angle of around $\phi' = 28.8°$ (M=1.15).

Follow the aforementioned procedures, Figure 9.6 illustrates the plot of $(U^*_{DMT}-1)$ versus $Q_{DMT,}$ giving a slope value $a_q = 0.43$. Together with the characteristic friction parameter M = 1.15, an operational rigidity index I_R =103 is determined for the soft lacustrine clay layer under investigation.

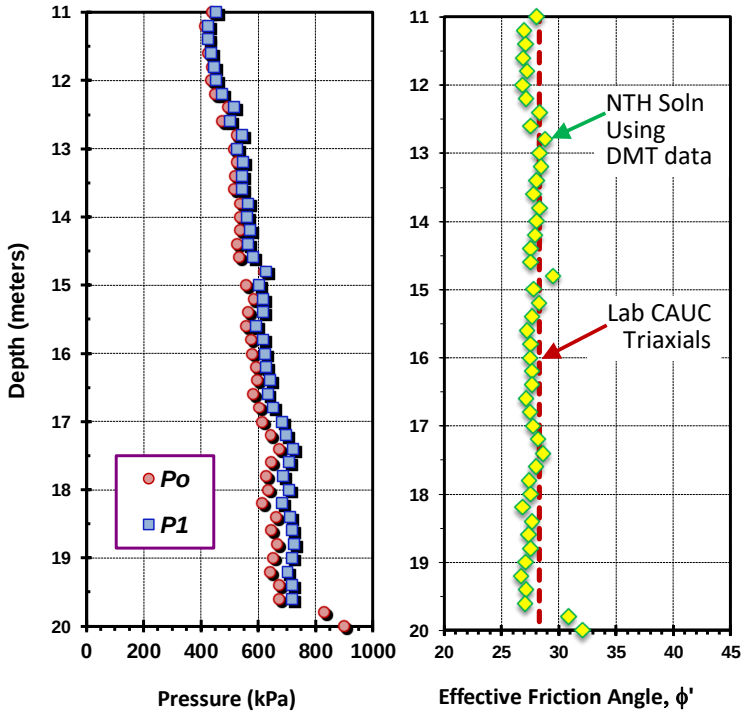

Figure 9.5. Profiles of DMT pressures and effective stress friction angle ϕ′ in soft Chicago clay at Northwestern University

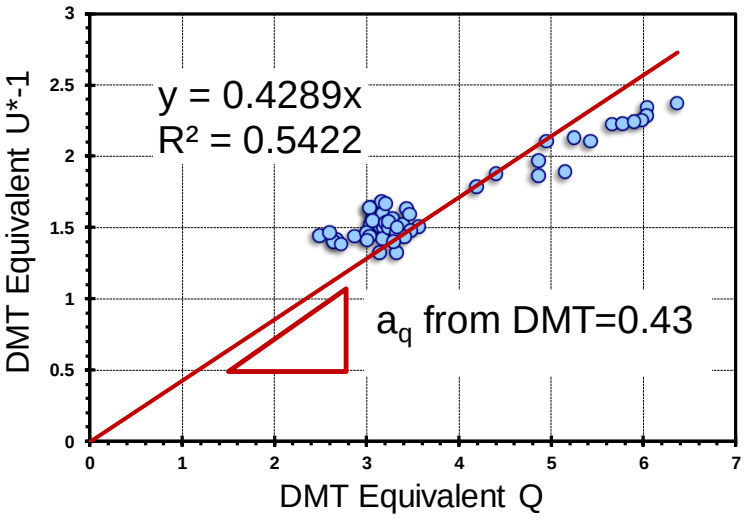

Figure 9.6. Evaluation of slope parameter a_q to determine I_R in soft Chicago clay at Northwestern University

Applying the SCE-CSSM equations with $I_R = 103$ and $\phi' = 28.8°$ (adopting $\Lambda = 1$), the three OCR profiles determined by Equations [9.3], [9.4] and [9.5] give good agreement

with each other at depths between 11m to 20m, as presented in Figure 9.7. Very good agreement is also observed in comparison with laboratory-measured σ'_p and corresponding OCR profiles obtained from consolidation tests. The value I_R = 103 also provides the corresponding N_{kt} = 10.2 which shows excellent agreement with the CAUC undrained shear strength data reported by Chung & Finno (1992).

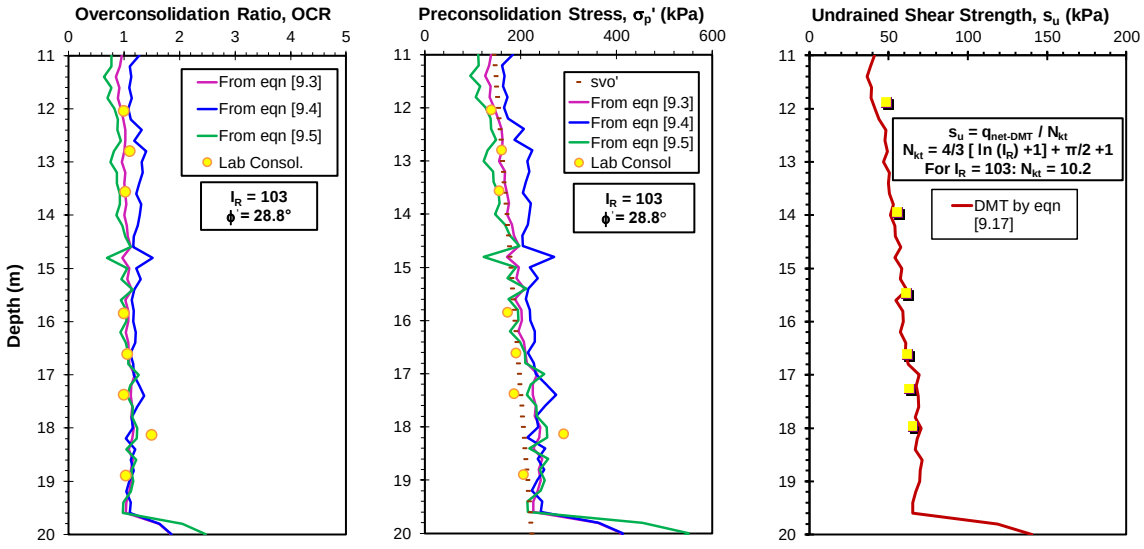

Figure 9.7. Interpreted profiles of OCR, preconsolidation stress, and undrained shear strength in the soft Chicago clay layer at NWU

9.4 Conclusions

Analytical closed-form solutions are presented for interpreting ϕ', I_R, s_u, and OCR in soft-firm clays from DMT soundings. The effective stress friction angle of the clay (ϕ') is obtained from a limit plasticity solution developed by NTH for the piezocone test (CPTu) and an established link from SCE permits its extension to the DMT. Using a hybrid framework derived from spherical cavity expansion and critical state soil mechanics (SCE-CSSM), it is shown that an operational value of rigidity index (I_R) of soft to firm clays can be obtained from the NTH ϕ' coupled with readings from flat plate dilatometer test (DMT),

namely, the contact pressure p_0 and the expansion pressure p_1. This value of I_R is used to provide the bearing factor (N_{kt}) which profiles the undrained shear strength (s_u) with depth. The two parameters together (I_R and ϕ') are further used in the SCE-CSSM algorithms to assess the profiles of OCR and s_u in soft-firm clays in closed-form analytical solutions, where OCRs < 2.5. Two case studies covering natural clays with different geologies are used to demonstrate the effectiveness of the methodology and the results compare well with values of ϕ' and s_u obtained in independent lab testing by triaxial compression modes and profiles of σ_p' and OCRs determined from conventional one-dimensional consolidation tests.

CHAPTER 10. MODIFIED NTH METHOD FOR ASSESSING THE EFFECTIVE FRICTION ANGLE OF NC-OC CLAYS FROM PIEZOCONE TESTS

10.1 Introduction

During site investigation, the standard CPTu obtains three separate readings with depth, including: total cone tip resistance (q_t), sleeve friction (f_s), and porewater pressure at the shoulder (u_2). When CPTu soundings are advanced into clays and fine-grained soils at the standard push rate, the interpretation by geotechnical engineers traditionally centers around a total stress analysis, and consequently, the evaluation is focused on the undrained shear strength (s_u). However, it is well recognized that the fundamental behavior of soils belongs to an effective stress framework, as established by several avenues: (a) laboratory stress path response from triaxial tests (e.g., Lambe & Whitman 1979; Mayne et al. 2009), (b) critical state soil mechanics (e.g., Schofield & Wroth 1968; Holtz et al. 2010), and (c) numerical modeling of soil behavior in triaxial compression, extension, and simple shear modes (Whittle et al. 1994). Therefore, the fundamental strength of clays is represented by effective stress strength parameters, including: ϕ' = effective friction angle and c' = effective cohesion intercept. However, the parameter c' indicates existence of tensile strength which requires cementation that most soils do not truly exhibit, unless they are structured and bonded. Often, an observed value of c' may in fact be a manifestation of that portion of the yield surface that extends above the frictional envelope (Leroueil & Hight 2003). In this viewpoint, often $c' \approx 0$ is a more probable scenario in many geologic formations.

For the CPTu, an effective stress limit plasticity solution was in fact developed by the Norwegian Institute of Technology (NTH; now NTNU = Norwegian University of Science & Technology) for the evaluation of effective stress parameters in all soil types (Janbu & Senneset 1974; Senneset & Janbu 1985; Senneset et al. 1989). While the method received attention in projects involving Norwegian clays (Sandven 1990; Sandven & Watn 1995), it appears little recognition has been given outside of Scandinavia. Consequently, a calibration study using the NTH method for evaluating the effective stress friction angle (c' = 0) from piezocone results obtained in approximately 100 soft to firm fine-grained clays where OCRs < 2.5 was carried out to demonstrate its applicability, using data from worldwide sources (Ouyang & Mayne 2018a). Modified versions of the NTH method are now presented for analyzing the frictional characteristics of overconsolidated (OC) intact clays, as well as fissured OC fine-grained geomaterials.

In this study, laboratory CIUC/CAUC triaxial shear tests and CPTu data from laboratory chamber deposits, centrifuge tests, and field sites involving clay soils were obtained from the published literature, authors' files, and private geotechnical reports. The data can be separated into six categories: (a) 10 series of 1-g laboratory chamber tests in NC clays; (b) 13 series of centrifuge CPTu in NC clays; (c) 2 series of centrifuge CPTu in OC clays; (3) 98 field CPTu in natural NC-LOC clays, (e) 9 field CPTu in OC intact clays with OCR > 2.5, and (f) 8 field CPTu in OC fissured clays.

Sources of data reviewed in this paper utilized either electric (analog) or electronic (digital) cone penetrometers with measurements of q_t and u_2, and in most cases, f_s readings, with depth. Field test procedures followed either ASTM standards (D 5778) at 20 mm/s, or an equivalent test method (Lunne et al. 1997). Comparative field CPTu results obtained

at four clay sites showed essentially no differences in q_t and u_2 measurements taken by 10-cm^2 and 15-cm^2 penetrometers (Powell & Lunne 2005). Similar findings that compared 5-cm^2 and 10-cm^2 size penetrometers in soft Swiss clay suggest scale effects are generally not significant for CPTu soundings in clays (Hird & Springman 2006). For lab test series, general testing procedures were followed for mini-penetrometers advanced into artificial clays in chamber tests or centrifuge deposits, however, rates were adjusted accordingly for size effects and strain rate behavior, specifically to obtain an undrained response (DeJong et al. 2012).

From prior reviews, the full range of effective friction angles from triaxial compression tests on intact natural clays is observed to be: $17° \leq \phi' \leq 45°$, as discussed by Diaz-Rodriguez et al. (1992), Leroueil & Hight (2003), and Ouyang & Mayne (2018a). Certainly, lower values are found for pure clay minerals such as montmorillonite, smectite, and bentonite, particularly when these are prepared as slurry mixtures from powders, sedimentation, and/or remolding procedures. However, for laboratory strength data on 453 natural fine-grained geomaterials, the aforementioned ranges of ϕ' values prevail (Mayne 2012, 2013).

10.2 Effective Stress Limit Plasticity Solution

The original NTH effective stress limit plasticity solution for the CPTu was derived for evaluating ϕ' during drained penetration of sands and undrained penetration involving silts and clays (Senneset et al. 1989). The relationship between ϕ' and two normalized cone parameters (N_m and B_q) applies to CPTu in soft-firm clays that can be expressed as a single equation:

$$N_m = \frac{\tan^2(45°+\phi'/2)\cdot \exp(\pi\cdot\tan\phi')-1}{1+6\cdot\tan\phi'\cdot(1+\tan\phi')\cdot B_q} \quad [10.1]$$

where the cone resistance number (N_m) is defined as $N_m = \frac{q_{net}}{\sigma_{vo}'+a'}$, $q_{net} = (q_t - \sigma_{v0})$ is the net cone resistance, $B_q = \Delta u/q_{net}$ is a porewater pressure parameter, $\Delta u = u_2 - u_0$ = excess porewater pressure, σ_{v0} = total overburden stress, σ_{v0}' = effective overburden stress, $a' = c'\cdot\cot\phi'$ = effective attraction, and c' = effective cohesion intercept. In the current study, an angle of plastification (Sandven 1990) is set $\beta = 0$ as it represents the constant volume case, corresponding to undrained penetration (Ouyang & Mayne 2018a).

The full solution allows for an interpretation of a paired set of effective stress Mohr-Coulomb strength parameters (c' and ϕ') for all soil types, including: sands, silts and clays, as well as mixed soils (Sandven 1990). For soft to firm clays that are not cemented or highly structured or sensitive, it is common to assign c' = 0 (Mesri & Abdel-Ghaffar 1993; Lade 2016; Mayne 2016). When $a' = c' = 0$, the cone resistance number N_m is identical to the normalized cone resistance, $N_m = Q = (q_t - \sigma_{vo})/\sigma_{vo}$' that is used extensively in CPTu interpretations regarding soil type, stress history of clays, and other geoparameters (Mayne 2007; Robertson 2009, 2016).

An approximate expression for directly assessing ϕ' from CPTu readings is given by (Mayne 2007):

$$\phi' \approx 29.5 \cdot B_q^{0.121} [0.256 + 0.336 \cdot B_q + \log N_m] \quad [10.2]$$

which is restricted to the following applicable ranges: $18^o \le \phi' \le 45^o$ and $0.05 \le B_q \le 1.0$. This expression is considered valid for intact clays and clayey silts that are soft to firm with

OCRs < 2.5. Both the closed-form solution and its corresponding approximate equation are shown in Figure 10.1.

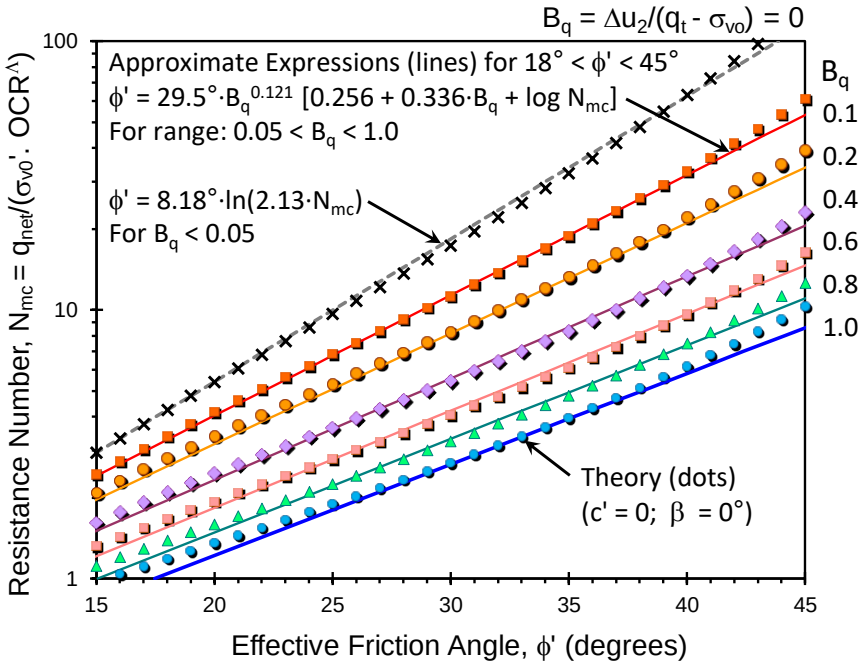

Figure 10.1. NTH solution for evaluating ϕ' from CPTu results using the exact analytical and approximate expression

For uncemented soft to firm clays and silts, especially those that are normally-consolidated (NC) to lightly overconsolidated (LOC) with OCRs < 2, the effective cohesion intercept can be taken as c' = 0 (Mayne & Stewart 1988, Mesri & Abdel-Ghaffar 1993). As for the interpretation of the effective stress parameters (ϕ' and c') for overconsolidated (OC) clays, a small value of c' may be appropriate (Lade 2016). In truth, c' commonly represents that portion of the yield surface that extends above the frictional envelope, such that c' = 0 also applies to many if not most OC clays (Leroueil & Hight 2003; Mayne 2016).

10.3 Case Study: CPTu in San Francisco Bay Mud, California

To illustrate the aforementioned NTH solution, representative piezocone data in soft Bay Mud from Islais Creek in San Francisco, California are presented in Figure 10.2 (Pestana et al. 2002). Bay Mud is a young aged marine clay deposited within the last 11,000 years and found throughout San Francisco Bay area. Results of laboratory index tests showed a mean total unit weight γ_t = 15 kN/m^3, natural water contents ≈ 65%, liquid limits in the range of 60 to 70%, and plasticity index (PI) between 35% to 45%. Figure 10.2 indicates the site has an old upper fill layer extending to approximately 5 m, underlain by two layers of soft Bay Mud (upper and lower) which are separated by a stiffer sandy layer at depths of between 15.5 m to 17 m. Both layers of soft Bay Mud are considered to be normally-consolidated to lightly overconsoldiated with an overall mean of OCR=1.2 (Hunt 2000). Groundwater lies at a depth of approximately 3 m.

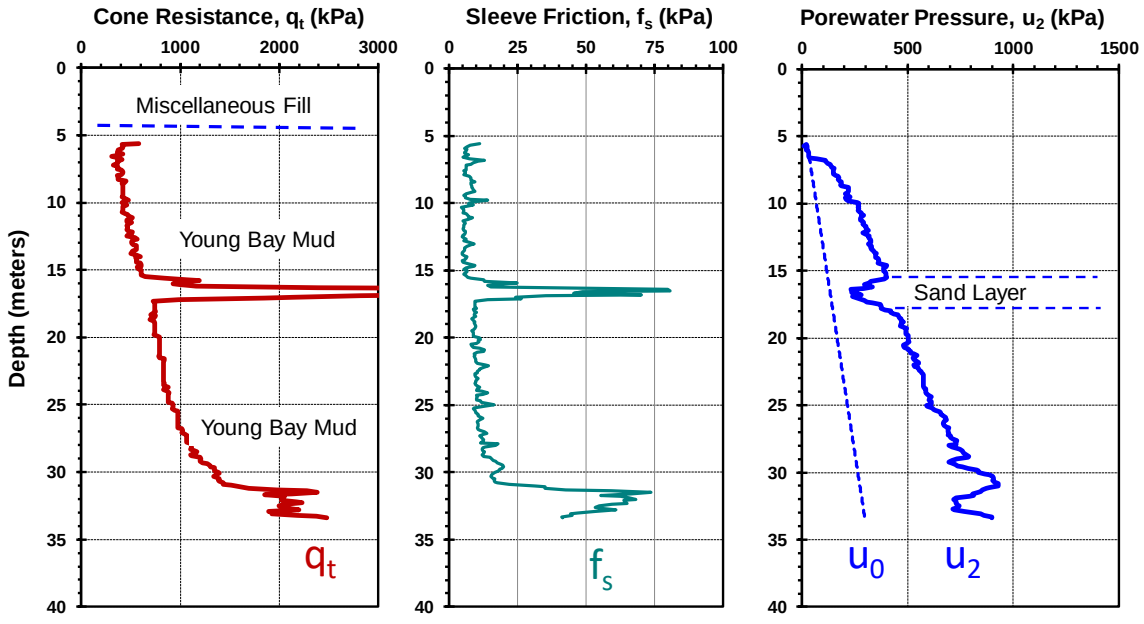

Figure 10.2. Representative CPTu sounding at Islais Creek, San Francisco: (a) total cone resistance, (b) sleeve resistance, and (c) penetration porewater pressure (data from Pestana et al. 2002)

In the standard NTH procedure, by plotting net cone resistance q_{net} vs. effective overburden stress σ_{v0}', as illustrated in Figure 10.3a, the slope determines the value of cone resistance number N_m. In this case, the best fit line is forced through the origin to obtain N_m = 3.71 (upper layer from 8m to 15m) and N_m = 3.64 (lower layer from 17m to 29m). The corresponding porewater pressure parameters B_q of the upper and lower Bay Mud layers are evaluated in Figure 10.3b. This parameter is found as the slope of measured $\Delta u = (u_2-u_0)$ versus the net cone resistance q_{net}, giving B_q = 0.69 (upper layer) and B_q = 0.73 (lower layer) for the Islais Creek site. The paired set of N_m and B_q values provide the input to the solution chart in Figure 10.1, indicating an effective friction angle ϕ'=29.9° for the upper Bay Mud and corresponding ϕ'=30.2° for lower Bay Mud, respectively.

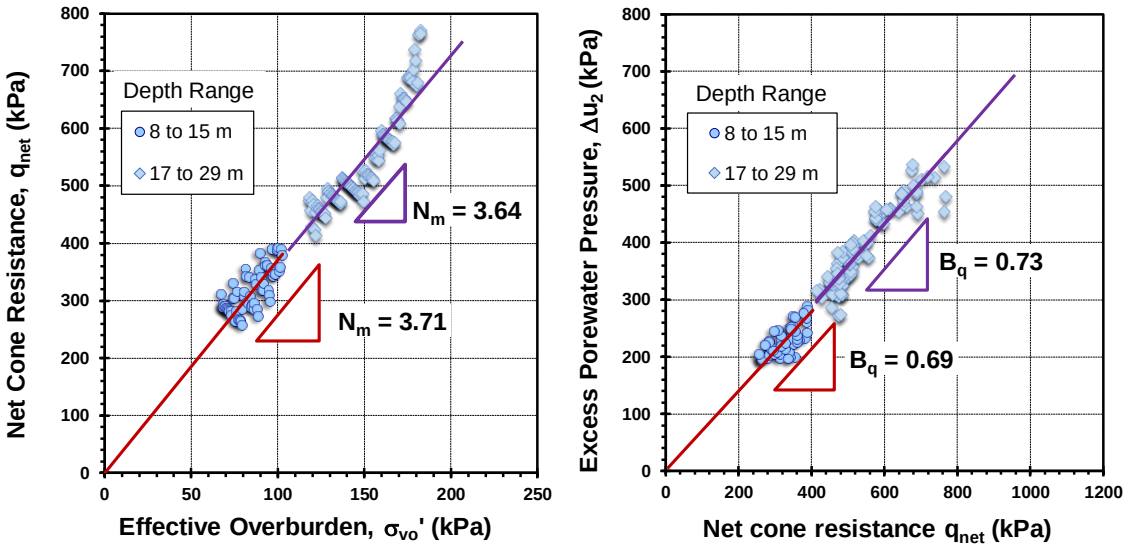

Figure 10.3. Post-processing of NTH parameters from CPTu in soft Bay Mud at Islais Creek: (a) cone resistance number, N_m and (b) porewater pressure parameter, B_q

Effective stress paths from a series of CAUC triaxial tests conducted on undisturbed samples of these soft clays are shown in Figure 10.4 (Hunt et al. 2002). The mean envelope for effective stress friction angle from the triaxial tests interpreted at the criterion for

maximum deviatoric stress (q_{max}) is found to be: $\phi' = 30.0^{o}$ with an effective cohesion intercept $c' = 0$. This is in good agreement with the aforementioned values for the Bay Mud using the original NTH solution and CPTu data. If the criterion for interpreting the ϕ' is taken at the maximum obliquity and or large strain, the laboratory measured ϕ' is slightly higher (ϕ'=32.0°) and the effective cohesion intercept $c' = 0$.

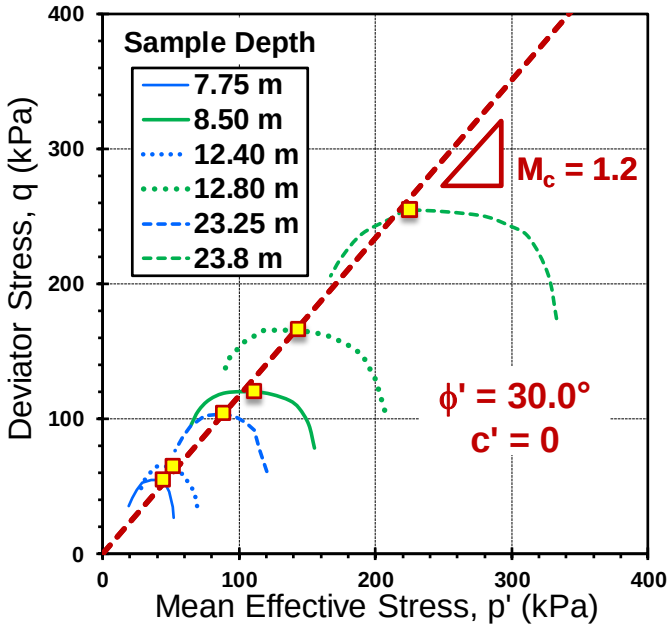

Figure 10.4. CK_0UC triaxial stress path for soft Bay Mud at Islais Creek (data from Hunt et al. 2002)

Using the approximate NTH solution from Equation [10.2], the profiles of the CPTu parameters N_m and B_q with depth at Islais Creek are shown in Figure 10.5a. The corresponding profile of the evaluated effective friction angle ϕ' using the approximate NTH equation, together with the triaxial values at their respective sampling depths, is shown in Figure 10.5b, indicating that the NTH solution successfully captures the frictional characteristics of soft Bay Mud.

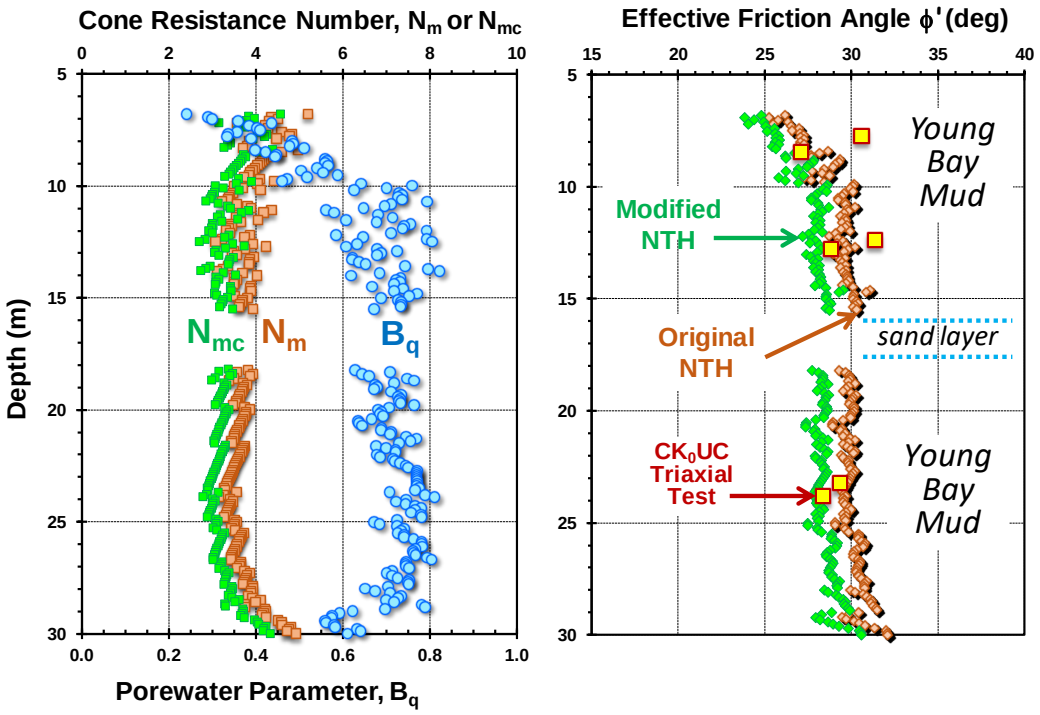

Figure 10.5. Profiles in soft Bay Mud at Islais Creek: (a) normalized CPTu parameters; (b) evaluations of ϕ′ from lab triaxials and NTH solution

10.4 Modified NTH Solution for OC clays

For overconsolidated clays, a modification to the original NTH solution is necessary in order to account for stress history effects on the measured CPTu data (Sandven et al. 2015, 2016). A revised definition of Equation [10.1] gives the modified cone resistance number (N_{mc}):

$$N_{mc} = \frac{q_t - \sigma_{vo}}{\sigma_e' + a'} \qquad [10.3]$$

in which σ_e' is called the equivalent stress and determined from:

$$\sigma_e' = \sigma_{vo}' \cdot OCR^{\Lambda} = \sigma_p'^{\,\Lambda} \cdot \sigma_{vo}'^{\,(1-\Lambda)} \qquad [10.4]$$

where $OCR = \sigma_p'/\sigma_{vo}'$ = overconsolidation ratio, σ_p' = effective preconsolidation stress, $\Lambda = 1 - C_s/C_c$ = plastic volumetric strain potential, C_s = swelling index, and C_c = virgin

compression index. The concept of equivalent stress is detailed by Hvorslev (1960) and found within the framework of critical state soil mechanics (e.g., Schofield & Wroth 1968; Mayne et al. 2009). The modified cone resistance number requires knowledge of the overconsolidation ratio (OCR) which should be determined from a series of laboratory consolidation tests, although can alternatively be found from the interpretation of triaxial data (Mayne 1988) or CPTu results (Lunne et al. 1997; Mayne 2007; Robertson 2009).

In lieu of B_q, a modified normalized porewater pressure parameter U* can be defined as:

$$U^* = \frac{u_2 - u_0}{\sigma_e'} \quad [10.5]$$

The parameter U* reflects the variation of the excess porewater pressure with the equivalent stress σ_e'. It is similar to the parameter $U = (\Delta u/\sigma_{vo}')$ adopted by Schneider et al. (2008, 2012) and identical to their parameter when the soils are normally consolidated, since $\sigma_e' = \sigma_{v0}'$ when OCR = 1. As a result, B_q can be determined simply from:

$$B_q = U^*/N_{mc} \quad [10.6]$$

As such, Equation [10.1] and [10.2] can be used directly to determine ϕ' by substituting $N_m = N_{mc}$ and $B_q = U^*/N_{mc}$ from CPTu soundings advanced into NC and OC intact clays.

The relationship between the original cone resistance number N_m and the revised cone resistance N_{mc} when the attraction $a' = 0$ is simply:

$$N_{mc} = N_m / OCR^{\Lambda} \quad [10.7]$$

Thus, the modified NTH method is identical to the original NTH when the soils are normally consolidated (OCR=1).

10.5 Exponent Parameter Λ

From critical state soil mechanics (CSSM), the stress exponent Λ is theoretically defined as $\Lambda = 1 - \kappa/\lambda$, where κ and λ are the swelling and compression indices from isotropic consolidation tests (Schofield & Wroth 1968). A simplified approach takes $\Lambda \approx 1 - C_s/C_c$, where C_c = virgin compression index and C_s = swelling index that is assumed more or less equal to the recompression index (C_r), and this requires information from one-dimensional consolidation tests. However, this is more of a physical rendering of Λ within CSSM than a pragmatic approach to its assessment. More practically, an operational exponent Λ is found as the slope of the normalized undrained shear strength ratio (s_u/σ_{v0}') versus overconsolidation ratio (OCR) on a log-log plot (Ramalho-Ortigao 1982; Ladd 1991; Ladd & DeGroot 2003). If the OCR is not known, the slope Λ is obtained from $\log(s_u/\sigma_{v0}')$ vs. $\log(1/\sigma_{v0}')$, provided that values of $(s_u/\sigma_{v0}') > S$, where $S = (s_u/\sigma_{v0}')_{NC}$ is the normally consolidated strength ratio (Mayne 1980).

The stress exponent Λ is also found in the empirical SHANSEP procedure by Ladd & Foott (1974) where it is termed "m". For natural clays, a representative value for $m = \Lambda \approx 0.80$ is often cited that corresponds to direct simple shear (DSS) testing (Ladd 1991). Mitchell & Soga (2005) note that the range of the exponent is between 0.7 to 0.9 for clays of low to medium sensitivity. For structured soils and sensitive clays, a higher value of about 1.0 applies (Ladd & DeGroot 2003). For remolded, compacted, and artificially-

prepared clays, the observed value of Λ is lower and in the range of 0.5 to 0.7 (Mayne 1988). Sandven et al. (2016) suggest a value Λ on the order of 0.7 to 0.8 for Norwegian clays subjected to triaxial compression tests. In reality, the value of Λ is mode-dependent, and values of 0.72, 0.78, and 0.85 may be assigned to triaxial compression, simple shear, and triaxial extension, respectively (Kulhawy & Mayne 1990).

For the case study on the field CPTu in San Francisco Bay Mud described above, the modified NTH method is also applied to investigate the influence of stress history on the interpretation of the effective friction angle using OCR = 1.2 and Λ= 0.7 for triaxial compression mode. The profiles of modified resistance number N_{mc} and re-interpreted ϕ' are presented by Figure 10.5. It is evident that the modified NTH solution produces a similar friction angle profile to the original NTH method in soft to firm clays with low OCRs, in this case only about 0.5° to 1.5° lower.

10.6 Case Study: Miniature CPTu in centrifuge model tests of OC kaolin

Results from mini-CPTu tests in centrifuge models of OC Speswhite kaolin are reviewed and analyzed using the modified NTH solution to obtain ϕ' in these characteristically low-frictional geomaterials. The centrifuge employed in this test series is located at the University of Colorado at Boulder with details regarding the sample dimensions, clay preparation, penetrometer, payload capacity, and working mechanisms given by Cinicioglu (2005). The Speswhite kaolin prepared for these centrifuge model tests has the following index properties: liquid limit = 53 %, plasticity index = 21 %, and specific gravity = 2.66. Test water contents and void ratios varied with the specific test OCR that was induced.

Figure 10.6 shows the CIUC effective stress paths of Speswhite kaolin at different OCRs (Perić et al. 1988). Specimens were tested at four OCRs and the effective stress friction angle is interpreted as $\phi' = 20°$ (defined at maximum shear stress) with a cohesion intercept $c' = 0$. Additional CIUC results on Speswhite kaolin reported by Smith (1993) are also shown. The operational value of Λ is determined as the slope of normalized undrained shear strength ratio (s_u/σ_{vc}') versus OCR in log-log scale and found be to 0.72. Laboratory consolidation data from Perić et al. (1988) indicate $C_c = 0.35$ and $C_s = 0.10$, with a corresponding theoretical value $\Lambda = 1 - C_s/C_c = 0.71$ that agrees well with the triaxial value.

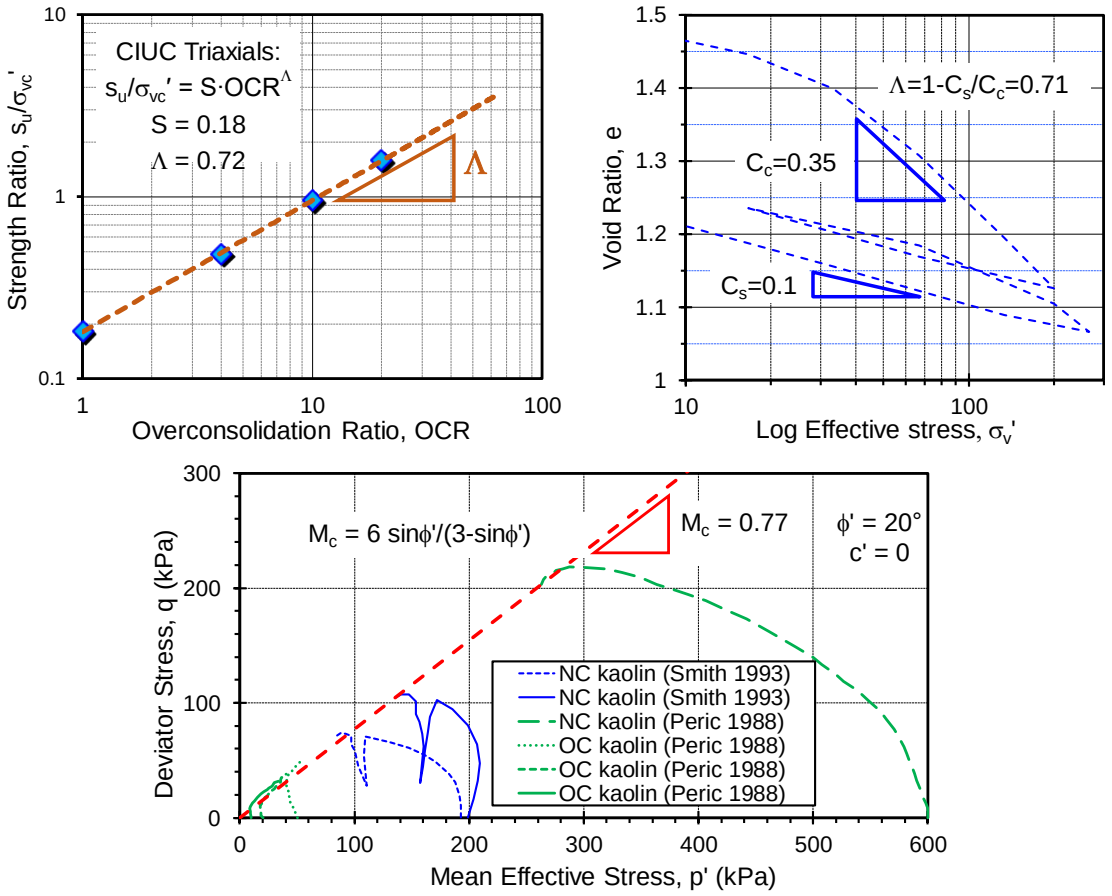

Figure 10.6. Parameters for Speswhite kaolin: (a) evaluation of Λ from triaxial tests; (b) Λ from consolidation test; (c) triaxial stress paths and effective stress envelope (data from Peric 1998, Smith 1993)

A 1-cm^2 Fugro mini-penetrometer was used for piezocone testing in the centrifuge deposits and obtained readings of q_t, f_s, and u_2 with depth. The kaolinitic clay deposits were prepared with an initial thickness of 157mm. The clay was first consolidated outside the centrifuge to impart a preconsolidation stress of 70kPa and then loaded under an acceleration of 150g. Due to the nature of centrifuge tests, the vertical stresses within the soils becomes a function of depth and the applied *g* level, therefore the bottom half of the soil reached normal consolidation during this loading stage and remained constant at OCR = 1. Then the sample was step-unloaded by decreasing the acceleration of the centrifuge from 150g to 50g, 30g, 15g and 1g, with the corresponding OCRs of the bottom half of the sample established as a function of the corresponding *g* level. These OCRs for the soils are 1, 3, 5, 10 and 150, respectively. Such centrifuge testing method causes unloading, resulting in mechanical overconsolidation and therefore termed a "descending gravity test" (Cinicioglu et al. 2006). At the end of each unloading stage when the soils have fully rebounded and reached a stable OCR, the miniature piezocone was pushed in-flight at a steadily downward rate of 10 mm/s, which was deemed sufficient for undrained penetration.

The general post-processing of the piezocone readings to obtain the modified cone resistance number N_{mc} and porewater pressure parameter U* is shown in Figure 10.7a. By plotting net cone resistance q_{net} vs. equivalent stress σ_e', the slope determines the value of modified cone resistance number N_{mc}. In this case, the best fit line is forced through the origin using a value of $\Lambda = 0.7$ for determining σ_e'. By the same token, the porewater pressure parameter U* is found as the slope of measured $\Delta u = (u_2-u_0)$ versus equivalent stress σ_e'. The evaluations of both parameters for five different accelerations are presented

in Figure 10.7b through Figure 10.7f for 1 ≤ OCRs ≤ 150. The deduced parameters from the centrifuge testing are utilized to interpret the effective stress friction angle ϕ′. for each of the five test OCRs, with results summarized in Table 1.

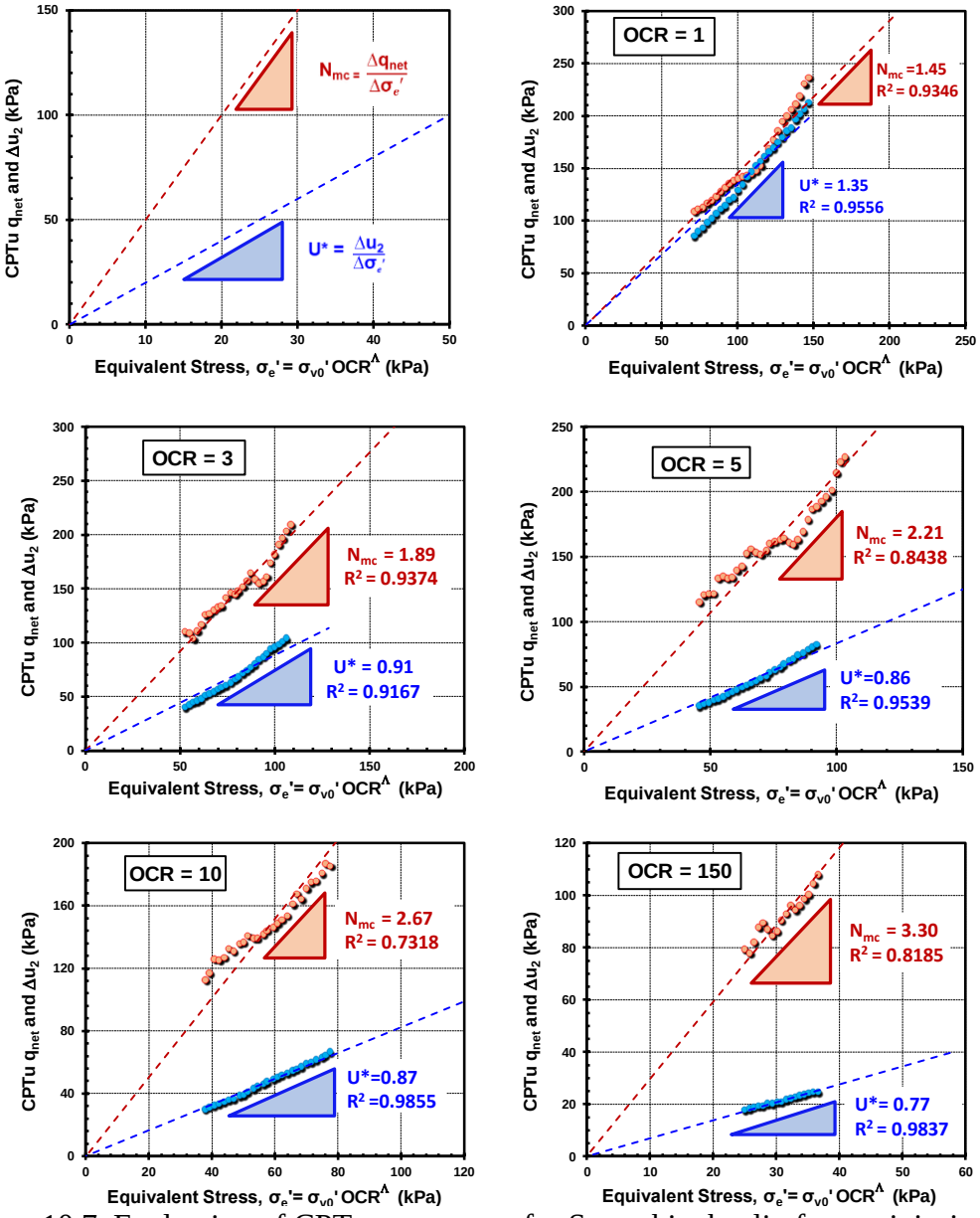

Figure 10.7. Evaluation of CPTu parameters for Speswhite kaolin from mini-piezocone tests in centrifuge series (Λ=0.7), including: (a) definitions of N_{mc} and U*, (b) OCR = 1, (c) OCR =3, (d) OCR = 5, (e) OCR = 10, and (f) OCR = 150 (data from Cinicioglu 2005)

Figure 10.8 shows that the modified cone resistance number N_{mc} increases with OCR, while in contrast, the corresponding porewater parameter B_q (and U*) decreases with OCR. Nevertheless, each paired set of N_{mc} and B_q data follow the NTH established contour for $\phi' = 20°$. The mean interpreted $\phi' = 19.5°$ from the modified NTH solution matches well with the laboratory triaxial results reported in Figure 6. Note that the original NTH method without considering the stress history effects on cone resistance would give a much higher interpreted ϕ', as indicated in Table 10.1.

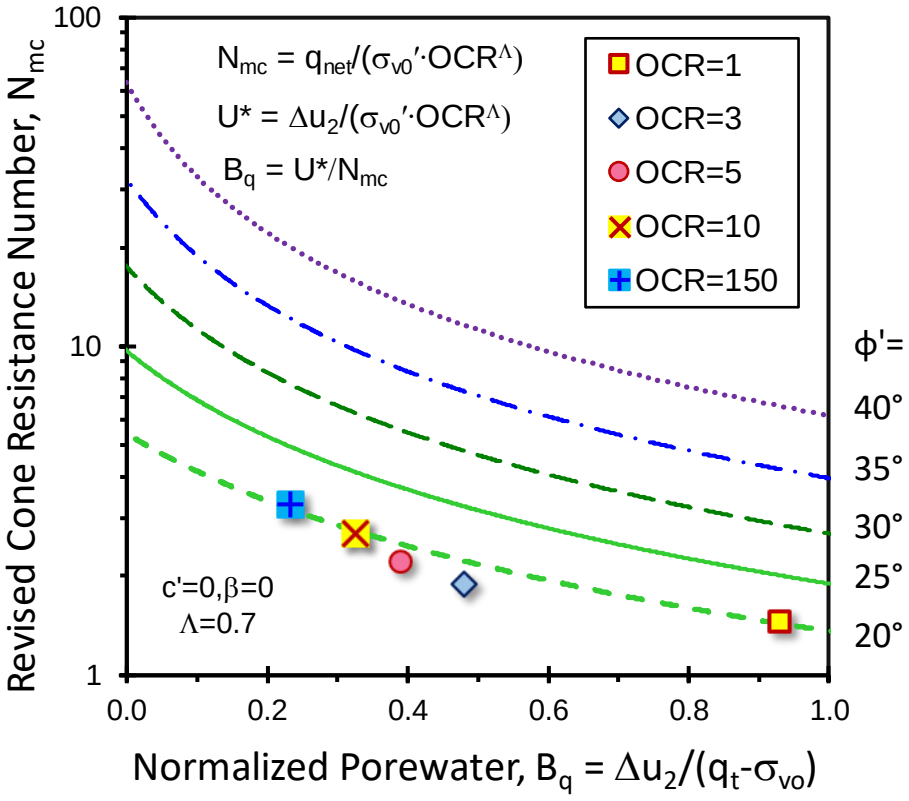

Figure 10.8. Results of modified NTH solution for interpretation of ϕ' from mini-CPTu in centrifuge deposits of OC Speswhite kaolin

Table 10.1. Results using modified NTH solution for mini-CPTu series in centrifuge tests of overconsolidated Speswhite kaolin (data from Cinicioglu 2005)

Centrifuge acceleration	OCR	N_m	N_{mc}	U*	B_q = U*/N_{mc}	Original NTH ϕ' (°)	Modified NTH ϕ' (°)
150g	1	1.45	1.45	1.35	0.93	20.2	20.2
50g	3	4.10	1.89	0.91	0.48	27.7	18.2
30g	5	6.83	2.21	0.86	0.39	32.1	18.7
15g	10	13.36	2.67	0.87	0.33	38.4	19.8
1g	150	110.10	3.30	0.77	0.23	58.6	20.4
Notes: N_{mc} calculated using c' = 0 and Λ = 0.7					Mean ϕ' =	35.7	19.5

Note:

OCR = overconsolidation ratio

$N_m = (q_t - \sigma_{v0})/\sigma_{v0}'$

$N_{mc} = (q_t - \sigma_{v0})/(\sigma_{v0}' \cdot OCR^{\Lambda})$

$U^* = (u_2 - u_0)/(\sigma_{v0}' \cdot OCR^{\Lambda})$

10.7 Case Study: CPTu in overconsolidated Presumpscot clay, ME

A field case study with CPTu soundings in natural overconsolidated intact clays is presented using data from Martin's Point Bridge, near Portland, Maine (Hardison & Landon 2015). The general stratification of the site consists of an organic silt layer underlain by firm to stiff OC Presumpscot clay that overlies lower strata comprised of glacial outwash sand and bedrock. Shelby tube samples of Presumpscot clay were collected at the site from different elevations and tested for index properties, consolidation parameters, and strength characteristics. The results of laboratory testing on the OC clay layer gave an average total

unit weight γ_t = 16.5 kN/m^3, natural water contents ≈ 30 to 40%, liquid limits in the range of 20 to 45%, and a plasticity index (PI) between 10% to 20%.

Figure 10.9a shows a representative CPTu sounding at the site with profiles of q_t and u_2 with depth. Depths of 2 to 14 m represent the extent of the OC Presumpscot clay of interest at this location with the groundwater table located at about 2 m. The corresponding profile of overconsolidation ratio (OCR = σ_p'/σ_{vo}') determined by constant-rate-of-strain (CRS) consolidation tests is shown in Figure 10.9b (Hardison & Landon 2015).

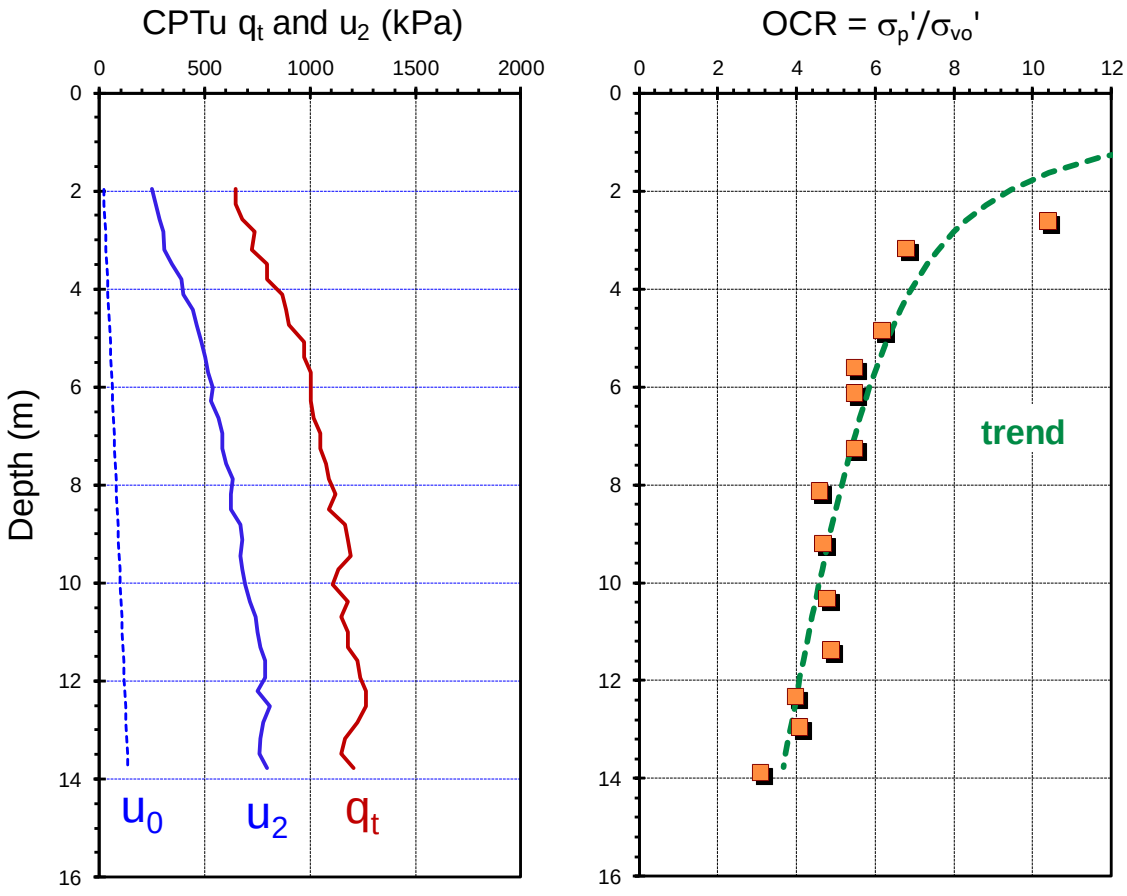

Figure 10.9. Profiles at Martin's Point Bridge, Maine: (a) piezocone readings; (b) OCR from CRS consolidation tests (data from Hardison & Landon 2015)

Following the modified NTH approach, Figure 10.10 shows the modified cone resistance number is N_{mc} = 7.3 and corresponding porewater pressure parameter U* = 3.38 using Λ = 0.7. A comparison of the NTH-evaluated value of ϕ' = 34.1° from CPTu data shows good agreement with the average CAUC-determined ϕ' = 33.4°, as indicated by Figure 10.11.

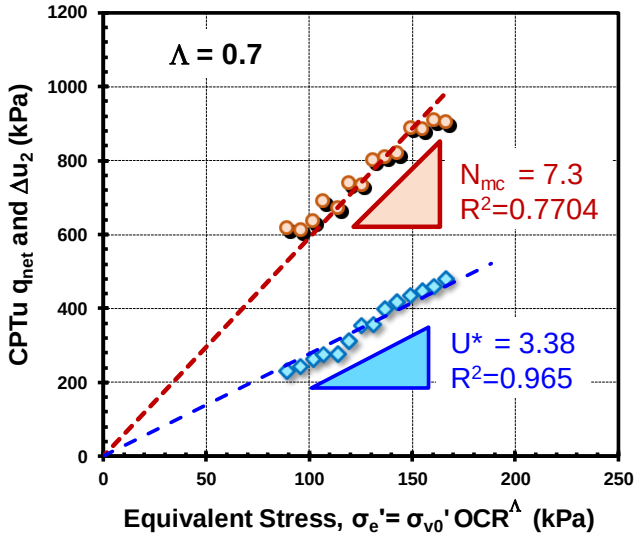

Figure 10.10. Evaluation of CPTu parameters Nmc and U* at Martin's Point Bridge site for modified NTH analysis

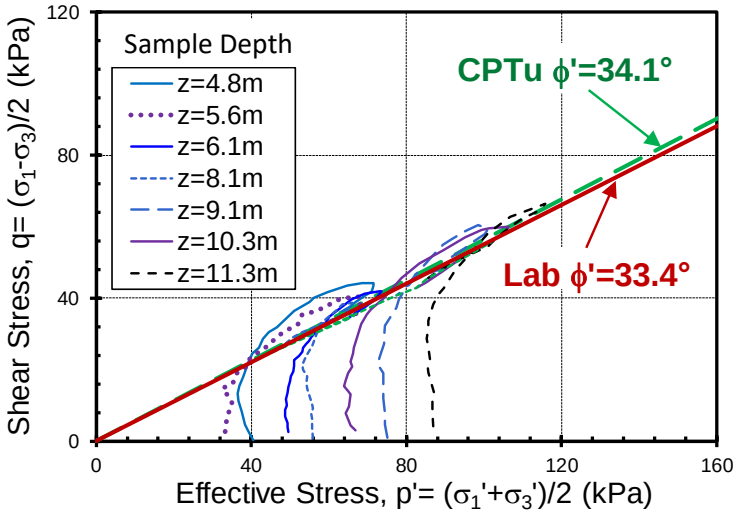

Figure 10.11. Comparison between NTH CPTu evaluated ϕ' and ϕ' from CIUC triaxial tests at Martin's Point Bridge site (data from Hardison & Landon 2015)

The profiles of the cone resistance numbers (N_m and N_{mc}) with normalized porewater parameter B_q are shown in Figure 10.12a. These are utilized to produce depth profiles of ϕ' in direct comparison with the CIUC triaxial data that are shown at their respective sampling depths in Figure 10.12b. Overall, the values from CIUC results are in good agreement with those from CPTu using the modified NTH solution.

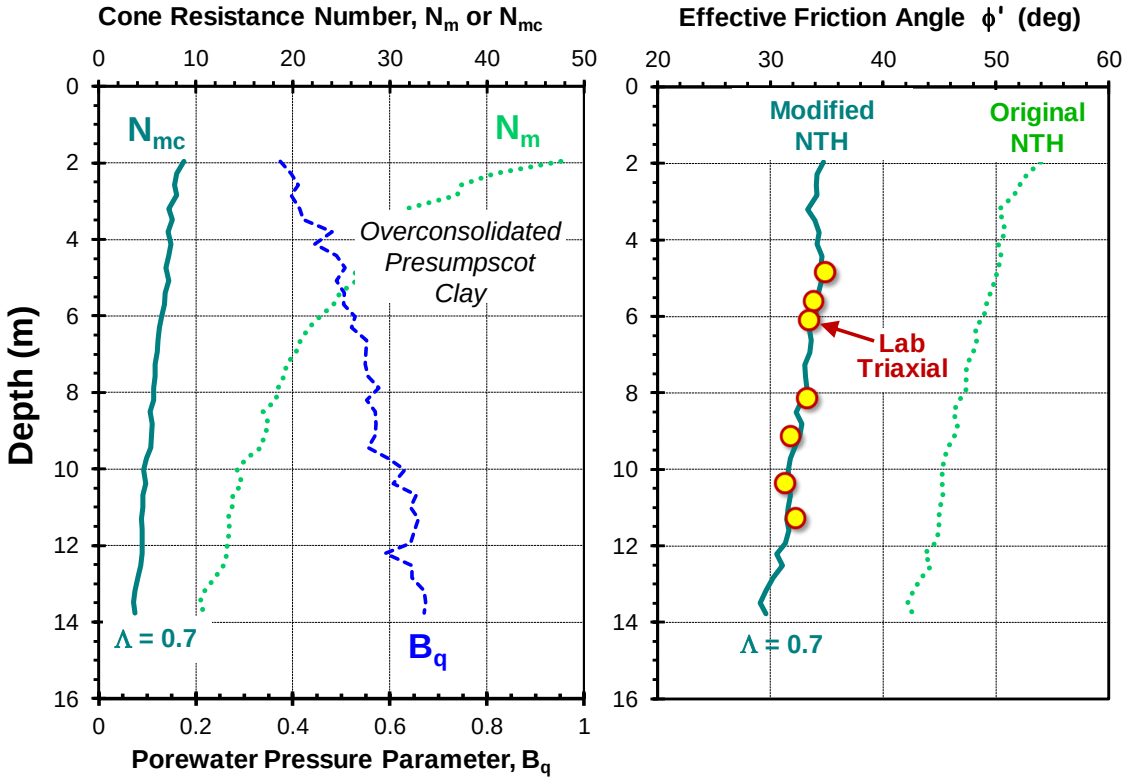

Figure 10.12. Profiles for Presumpscot clay at Martin's Point Bridge: (a) N_m, N_{mc} and B_q using Λ=0.7; (b) original NTH ϕ', modified NTH ϕ' and CIUC triaxial ϕ'

10.8 Re-evaluation of soft-firm clay CPTU database using the modified NTH approach

In a recent study of 105 natural clay sites tested by CPTu, data for a variety of fine-grained soils ranging from natural lean to plastic clays and clayey silts from marine, alluvial, lacustrine, deltaic and glacio-fluvial origins were examined using the original

NTH approach (Ouyang & Mayne 2018a). The data set excluded results taken in organic clays and highly sensitive or structured soils. In comparison with laboratory benchmark values obtained from CAUC and/or CIUC triaxial tests on undisturbed samples, statistical analyses showed reasonable and reliable results from CPTu interpretations with corresponding effective stress friction angles in the range: $20° \leq \phi' \leq 45°$.

The impact of using the modified NTH solution on that dataset needs to be explored. Fortunately, the majority of the soils investigated consisted of soft to firm clays that were normally-consolidated (NC) to lightly overconsolidated (LOC). More specifically, for 98 of the clay sites, the mean OCR = 1.53 with a standard deviation ± 1.23. In the dataset, seven sites were overconsolidated (OC): Baytown, Baton Rouge, Madingley, Brent Cross, St. Jean Vianney, Yorktown, and Taranto. Removing those OC sites, the modified NTH approach was applied to the 98 clay sites of low OCR using a representative stress exponent Λ=0.7 and corresponding OCR from each site. In a re-evaluation, the measured benchmark friction angle from triaxial tests is compared with the re-interpreted ϕ' from CPTu data using the modified NTH solution in Figure 10.13. From the arithmetic measures shown on Figure 10.13, the ratio of measured to evaluated values ranges from 0.9 to 1.26 with an overall mean of 1.06 and standard deviation = 0.07, giving a corresponding COV (coefficient of variation) = 0.07. From the regression evaluations of laboratory vs. field values, the regression slope = 1.06 with a coefficient of determination of r^2 = 0.747 and standard error of the Y-estimate of SEY = 2.16. The above statistics of the modified NTH approach indicates that there is a slightly conservative estimation of the effective friction angle compared with results from the original NTH approach. Overall, for soft to firm NC-OC clays, the modified NTH solution gives ϕ' values approximately 1

to 7% lower than the original NTH approach reported by Ouyang & Mayne (2018a), corresponding to a reduction of 0.5° to 2.0° in the assessed ϕ' values.

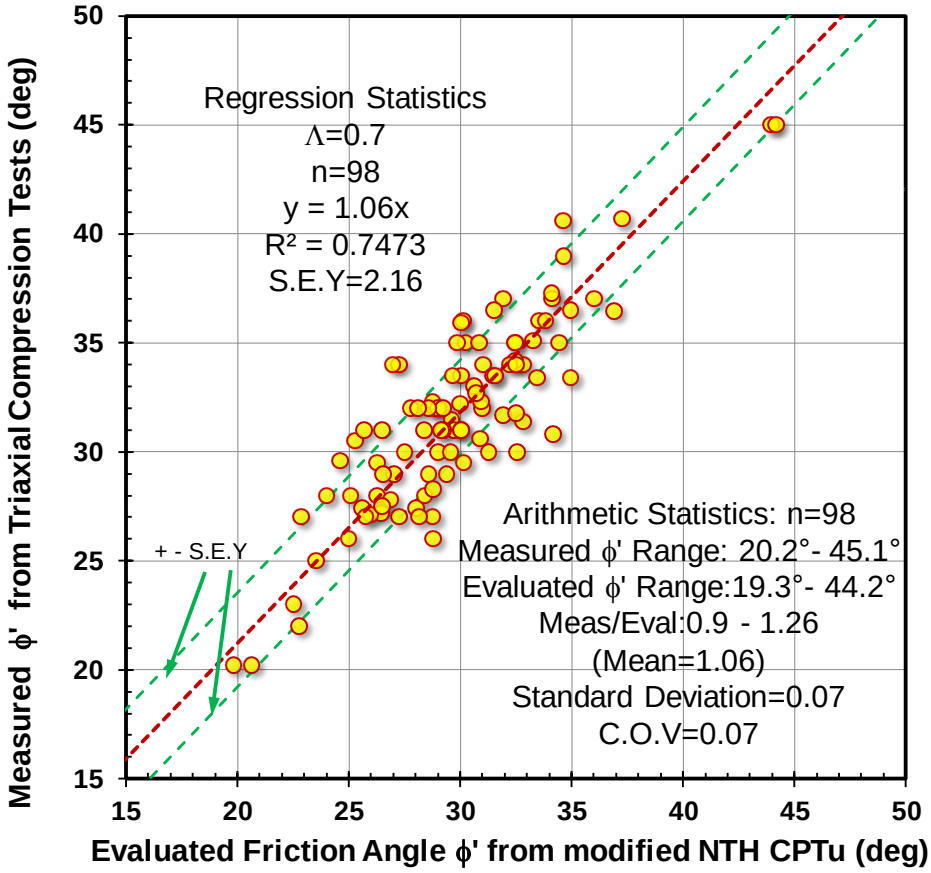

Figure 10.13. plot of laboratory triaxial measured ϕ′ versus CPTu ϕ′ (Re-evaluation of 98 soft-firm clay CPTu database using the modified NTH approach)

10.9 Fissured Clays

Results of piezocone tests in fissured overconsolidated fine-grained soils typically show a characteristic porewater pressure with $u_2 \approx 0$ (Lunne, et al. 1986; Mayne et al. 1990; O'Neill & Yoon, 1995; Lunne et al. 1997). In some cases, the u_2 reading is slightly positive or slightly negative, depending upon the specific width of the filter element, saturating fluid (water, glycerine, silicone), ambient temperature, and other factors (Campanella & Robertson, 1988). While the NTH solution cannot handle negative u_2 readings directly

(Sandven 1990), a practical solution is to take $u_2 = 0$ for fissured clays, as recommended by Powell & Quarterman (1988). When $B_q = 0$, the approximation to the NTH solution is given by the following equation:

$$\phi' \approx 8.18 \ln \cdot (2.13 \cdot N_{mc}) \qquad [10.8]$$

Both the exact and approximate solutions are shown in Figure 10.1.

10.10 Case Study: fissured London clay at Brent Cross, UK

Brent Cross serves as an experimental test site involving London clay (Powell & Quarterman 1988). London Clay is an overconsolidated Eocene marine formation that is notable for the presence of discontinuities in the form of fissures and cracks (Lunne et al. 1986). Uplift and erosion have removed overburden soils, with the overconsolidation difference (OCD = $\sigma_p' - \sigma_{v0}'$) on the order of 1500 kPa or more (Skempton 1961). The characteristic effective strength of the fissured clay can be represented by a lower bound envelope given by: $c' = 0$ and $\phi' = 19.5°$ (Hight & Jardine 1993).

Laboratory testing on the London clay at Brent Cross has shown a representative total unit weight $\gamma_t = 20$ kN/m^3, natural water contents ≈ 28 to 32%, liquid limits in the range of 65 to 85%, and plasticity index (PI) between 55% to 65%. Representative triaxial stress paths and effective strength envelope are shown in Figure 10.14, indicating an effective friction angle of $\phi' = 19.5°$ can be assigned to these fissured clays between depths of 2m to 12m (Gasparre et al. 2007; Hight et al. 2003). Compression and swelling indices from oedometer tests show a theoretical value of Λ=0.63, while the undrained shear strength ratio (s_u/σ_{v0}') versus OCR plot from triaxial compression tests indicate $\Lambda = 0.57$.

As such, a representative exponent Λ=0.6 has been assigned to the fissured London clay at Brent Cross.

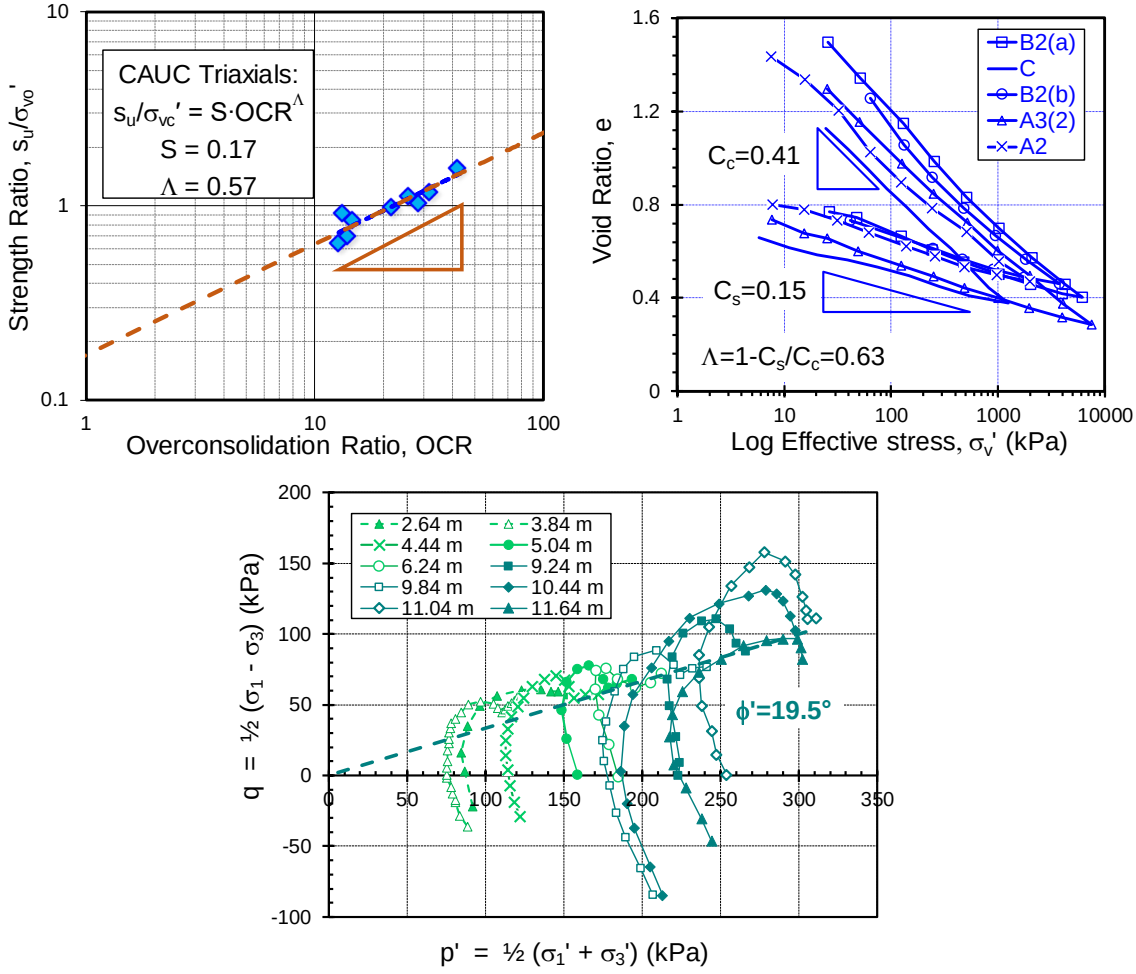

Figure 10.14. Parameters for fissured London clay at Brent Cross: (a) evaluation of Λ from triaxial tests; (b) Λ from consolidation tests; (c) triaxial stress paths and strength envelope (data from Hight et al. 2003, Gasparre et al. 2007)

Representative data from piezocone tests at Brent Cross are shown in Figure 10.15a with the profiles of q_t and u_2 with depth (Lunne et al. 1986). In Figure 10.15b, the cone resistance number N_m and modified cone resistance number N_{mc} (using Λ=0.6 and OCD = 1600 kPa) are presented along with the porewater pressure parameter B_q. It is observed that the value of B_q is essentially zero throughout the entire profile, which again is

indicative of a fissured clay. The modified NTH solution using the approximate expression for $B_q = 0$ appears in good agreement with the laboratory triaxial interpretation of the effective friction angle, specifically $\phi' \approx 19.5°$.

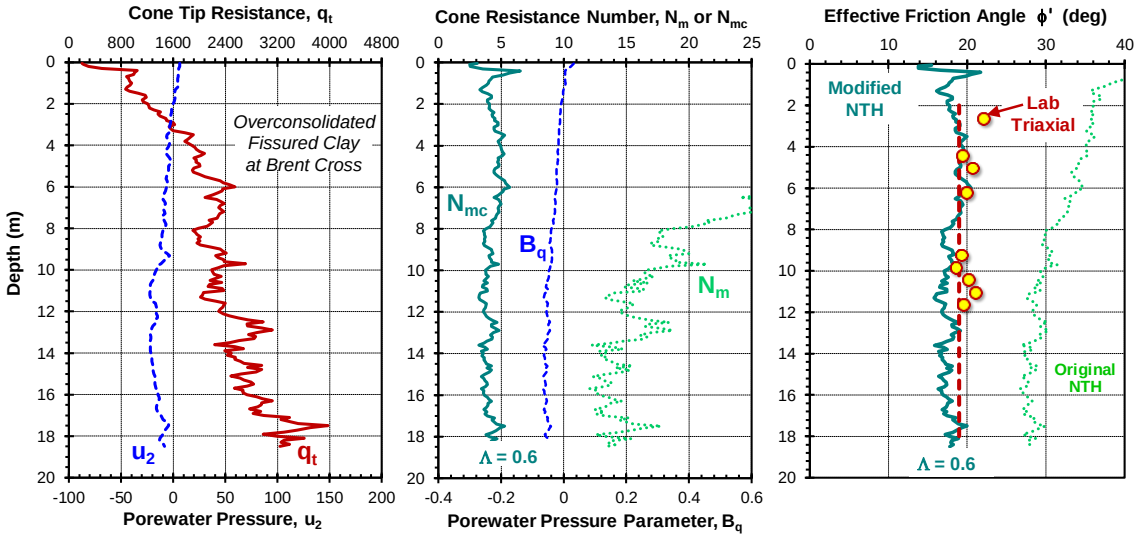

Figure 10.15. Profiles for fissured London clay at Brent Cross: (a) Piezocone penetration data; (b) N_m, N_{mc} and B_q using Λ=0.6; (c) original NTH ϕ', modified NTH ϕ' and CAUC triaxial ϕ' (data from Lunne et al. 1986, Hight et al. 2003)

10.11 Triaxial -CPTu Database on NC-OC Clays

For the examination of the modified NTH solution for normally consolidated and overconsolidated clays, six separate databases were assembled for study. These categories include: (a) 10 series of 1-g laboratory chamber tests in NC clays (data reported by Ouyang et al. 2016); (b) 13 series of centrifuge CPTu in NC clays (reported data in Ouyang & Mayne 2018); (c) 2 series of centrifuge CPTu in OC clays (this study); (d) 98 soft to firm clays with OCRs < 2.5 subjected to standard field CPTu (data reported in Ouyang & Mayne 2018), (e) 9 field CPTu in OC intact clays with OCR > 2.5 (this study); and (f) 8 field CPTu in OC fissured clays (this study).

In each grouping, high-quality triaxial data (CIUC, CAUC, or CK_0UC) and piezocone results were available on the clay materials. Table 10.2 and Table 10.3 contain a listing of OC intact clays and OC fissured clays, respectively, where the application of the modified NTH method on the interpretation of effective friction angle ϕ' has been applied. Note also that seven OC clays (three intact clays: St. Jean Vianney, Yorktown, and Taranto; and four fissured clays: Baytown, Baton Rouge, Madingley, and Brent Cross) that were originally reported in Ouyang & Mayne (2018a) have now been re-examined and placed into their proper category.

All the geomaterials from the above six datasets were subjected to laboratory triaxial compression tests with porewater pressure measurements, where the value of ϕ' is taken as the reference benchmark test in this paper. The definition of ϕ' was normally taken at peak strength (q_{max}), although in a few cases, the value at maximum obliquity $(\sigma_1'/\sigma_3')_{max}$ was reported by the source, and in some cases, the definition adopted was not cited. These included isotropically- (CIUC) or anisotropically-consolidated (CAUC or CK_0UC) type tests. A master summary plot for the triaxial-measured ϕ' versus the CPTu-determined values via the modified NTH solution is shown in Figure 10.16.

Overall, the triaxial results show a mean value of $\phi' = 29.8°$ with a standard deviation (S.D) of $\pm$ 5.2° for the dataset of clays considered. In the calibration of the modified NTH solution for CPTu, two sets of statistical measures were made on the compiled data set (n = 140), including: (a) arithmetic statistics, and (b) regression statistics, as shown in Figure 10.16. The measured laboratory values of ϕ' covers the full expected range from 20.2° to 45.1° and the CPTu-evaluated ϕ' range extends similarly, from 18.5°

to 44°. From the arithmetic measures, the ratio of measured-to-evaluated values ranges from 0.9 to 1.4 with an overall mean of 1.06 and standard deviation = 0.08, giving a corresponding COV (coefficient of variation) = 0.08. From the statistical regression evaluations of laboratory vs. field values, the regression slope = 1.043 with a coefficient of determination of r^2 = 0.8071 and standard error of the y-estimator gives SEY = 2.2, as shown by the dark red dashed line representing the best fit line to the revised NTH solution. The above statistics generally support that the revised NTH method gives a reasonable evaluation, albeit about 4% to 5% conservative, on the effective friction angle when referenced to the benchmark triaxial value.

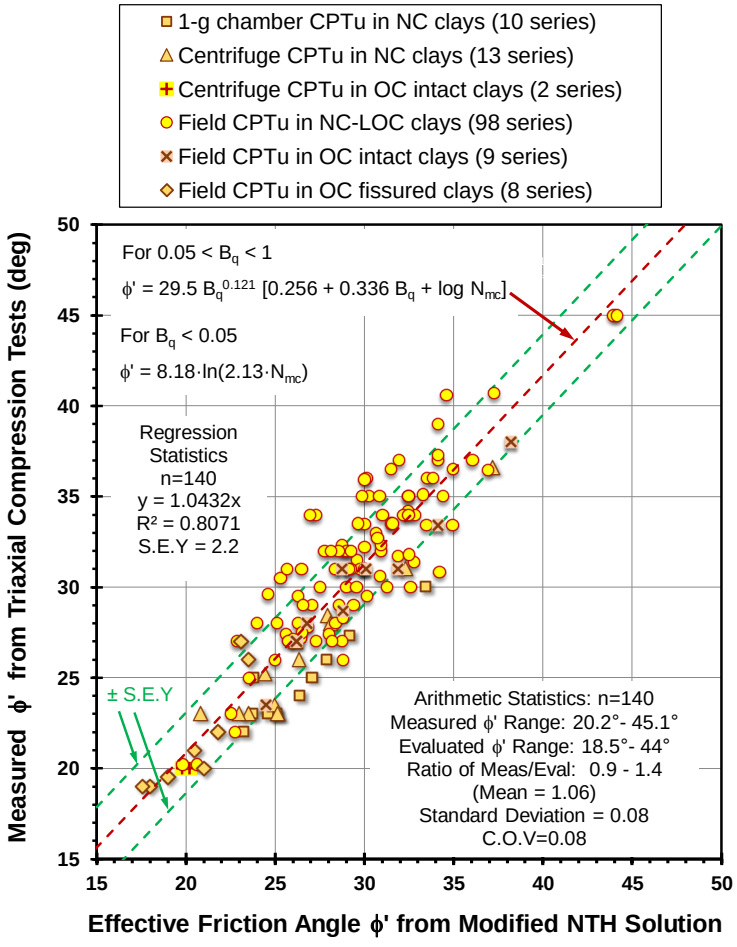

Figure 10.16. Summary plot of laboratory triaxial measured ϕ' versus CPTu ϕ' from different test series using modified NTH method

In early presentations of the NTH solution (e.g., Senneset & Janbu 1985), it was suggested that β values were associated with soil types, including clays, silts, and sands. For clays, the range indicated was approximately: $0° \leq \beta \leq +15°$while other ranges were assigned to silts and sands. Later, Sandven re-evaluated data in soft-firm clays and suggested the range: $-10° \leq \beta \leq +10°$. However, both studies were based on limited data, mainly obtained from the North Sea and Norway, the latter also known for having lean clays, as well as being sensitive to quick deposits. For the artificially-prepared soils such as kaolinite-based clays and sand-clay mixtures investigated in many of the 1-g laboratory chamber tests and centrifuge model tests, the NTH solution with $\beta = 0°$ did capture their characteristic low friction angles of $\phi' \approx 20°$ to 22°. Also, Ouyang et al. (2016) suggested that a value of $\beta = -5°$ degrees would give a slightly better fit for the kaolin clays. Parametric studies by the authors reveal that for every 10° increase of β, the interpreted ϕ' would decrease by about 1.5°, and vice versa. Perhaps, additional future studies including clay mineralogy, origin, clay fraction, and other parameters will better define an improved accuracy of the NTH solution by inclusion of the beta angle. Herein, the value of $\beta = 0$ has been adopted for the time being.

10.12 Special considerations for organic soils, sensitive clays, and structured geomaterials

For the data that were considered in these studies, CPTu and triaxial data were obtained from clays and clayey silts that were primarily inorganic soils of low-medium sensitivity. The characteristic porewater pressure response for this group exhibits: $0.5 < B_q < 0.6$ (Mayne & Peuchen 2018). However, it is recognized that natural organic clays

tend to generate lower normalized porewater pressure (B_q < 0.5) while sensitive and structured clays generally exhibit higher values (B_q > 0.8) when compared to "normal" or "well-behaved" clays. Therefore, special caution should be taken when evaluating CPTu in organic clays, sensitive or structured soils, or clays of special mineralogy, as the application of the NTH solution should only be undertaken after careful calibration with triaxial tests on high-quality laboratory samples to confirm the appropriate effective stress friction angles are valid in the specific geologic setting of study.

10.13 Conclusions

A modified NTH effective stress limit plasticity solution for evaluating the effective stress friction angle (ϕ') in NC to OC clays from piezocone penetration tests (CPTu) is presented where the cone resistance number is adjusted to reflect stress history effects, i.e. OCR. The calibration was accomplished by collection of six databases, including triaxial data and CPTu soundings obtained from: (a) laboratory chamber tests in NC clays; (b) centrifuge testing in NC clays; (c) centrifuge tests in OC clays; (d) field CPTu in natural NC-LOC clays, (e) field CPTu in OC intact clays with OCR > 2.5, and (f) field CPTu in OC fissured clays. The magnitudes of effective stress friction angle ϕ' interpreted by both CPTu and triaxial tests cover a wide range of values: 19° < ϕ' < 45°. A mean value ϕ' = 30°± 4° was determined from all triaxial compression tests (CIUC, CK_0UC, and/or CAUC) and the modified NTH solution using CPTu data gave comparable values, albeit averaging about 1.5° lower. Several case studies involving NC and OC clays are presented to detail the NTH post-processing procedure. In lieu of the exact solution, two approximate NTH

expressions are given, one applicable for intact NC to OC clays and a second applicable to fissured OC clays that exhibit $B_q \approx 0$.

Table 10.2. Database of CPTu soundings in intact overconsolidated clays subjected to laboratory triaxial testing.

Site name and location	Depth Range (m)	In-Situ or Test OCR (Note a)	Mean w_n (%)	Mean LL (%)	Mean PI (%)	Total unit weight (kN/m^3)	Parameter Λ (Note b)	N_{mc} (Note c)	U* (Note d)	B_q (Note e)	Mod NTH ϕ'(deg) (Note f)	Triaxial ϕ' (deg) (Note g)	Reference Source
Anchorage, AK	5-30	2-8	25	45	24	17.1	0.75	3.6	2.3	0.64	28.8°	28.7°	Mayne & Pearce (2005)
East Hartford, CT	12-26	2.5 - 4	55	42	20	17.2	0.9	2.7	1.6	0.6	24.5°	23.5°	Authors' Private Files (2010)
Lower clay McArthur Dyke, MB	4-11	5-10	51	108	88	16.9	0.8	4.18	2.51	0.6	30.1°	31.0°	Van Helden (2013)
Marquette Interchange, WI	2-25	2-12	20	25	15	20.2	0.8	7.1	2.5	0.36	31.9°	31.0°	Schneider & Hotstream (2011)
Martin's Point Bridge, ME	2-14	2.5-10	55	43	18	16.5	0.7	7.3	3.4	0.46	34.1°	33.4°	Hardison & Landon (2015)
OC Speswhite Kaolin-1	NA	3-150	60	53	21	17	0.7	1.4 - 3.3	0.8-1.3	0.2-0.9	20.2°	20.0°	Cinicioglu (2005)
OC Speswhite Kaolin-2	NA	4-12	60	53	21	17	0.7	2 - 2.60	0.7-0.8	0.3-0.4	19.8°	20.0°	Esquivel (1995)
Saint Jean Vianney, Quebec*	1-6	24-28	40	28	8	16.5	0.9	4.2	2.7	0.52	29.0°	31°	Demers (2001)
Taranto, Italy*	7-20	10-30	25	NA	20	22	0.7	4.2	1.7	0.4	26.8°	28°	Jamiolkowski et al. (1985); Bruzzi & Battaglio (1987)
Upper clay McArthur Dyke, MB	1-4	7-15	63	53	33	16.1	0.8	4.87	1.36	0.28	26.2°	27.0°	Van Helden (2013)

10.2. Database of CPTu soundings in intact overconsolidated clays subjected to laboratory triaxial testing, continued

Site name and location	Depth Range (m)	In-Situ or Test OCR (Note a)	Mean w_n (%)	Mean LL (%)	Mean PI (%)	Total unit weight (kN/m^3)	Parameter Λ (Note b)	N_{mc} (Note c)	U* (Note d)	B_q (Note e)	Mod NTH ϕ'(deg) (Note f)	Triaxial ϕ' (deg) (Note g)	Reference Source
Yorktown Formation, VA*	2-16	3-9	31	NA	4	19	0.7	11.4	4.6	0.4	38.2°	38°	Mayne (1988)

Notes:

*****Site in database reported by Ouyang & Mayne (2018a); data re-evaluated here using Modified NTH solution.

a. OCR is determined by lab consolidation tests, excepting: (a) Speswhite kaolin where OCRs were induced and (b) McArthur Dyke, where OCRs estimated from triaxial and CPTu data

b. Value of Λ from (s_u/σ_{vo}') vs. OCR and/or consolidation data; excepting: (a) Marquette Interchange, and (b) McArthur Dyke, where assumed value taken as $\Lambda = 0.8$

c. Modified cone resistance number: $N_{mc} = q_{net}/(\sigma_{v0}' \cdot OCR^{\Lambda})$

d. Normalized porewater parameter: $U^* = \Delta u_2/(\sigma_{v0}' \cdot OCR^{\Lambda})$

e. Porewater pressure parameter, $B_q = \Delta u_2/q_{net} = U^*/N_{mc}$

f. Modified NTH solution for intact OC clay with $B_q > 0.05$; using Equations [10.1] or [10.2]

g. Effective stress friction angle from CAUC and/or CIUC triaxial tests

Table 10.3. Database of CPTu soundings in fissured overconsolidated clays subjected to laboratory triaxial testing.

Site name and location	Depth Range (m)	Test OCR (Note a)	Mean w_n (%)	Mean LL (%)	Mean PI (%)	Total unit weight (kN/m^3)	Parameter Λ (Note b)	N_{mc} (Note c)	Mod NTH ϕ'(deg) (Note d)	Triaxial ϕ' (deg) (Note e)	Reference Source
Baton Rouge, LA*	16-30	2-6	30	60	33	18.2	0.7	7.9	23.1°	28°	Chen & Mayne (1994)
Baytown, TX*	2-16	4-20	22	70	31	19.8	0.6	6.6	21.6°	22°	Stuedlein et al. (2012)
Brent Cross, UK*	2-19	20-60	30	75	50	20	0.6	4.3	18.3°	19.5°	Gasparre et al. (2007); Hight et al. (2003) Lunne et al. (1986)
Canon's Park, UK	3-17	10-60	26	66	46	19.4	0.6	4.2	18°	19°	Gasparre et al. (2007) Hight et al. (2003) Lunne et al. (1986)
Heathrow T5, UK	5-20	10-60	26	62	42	20.5	0.6	4.0	17.6°	19°	Gasparre et al. (2007) Hight et al. (2003) Lunne et al. (1986)
Lower Bangkok, Thailand	15-20	2.5-3	35	46	12	16.8	0.75	5.6	20.5°	21.0°	Shibuya et al. (2003)
Madingley, UK*	1-22	5-45	31	40	15	19.3	0.6	8.5	23.7°	26°	Lunne et al. (1986)
Paddington, UK	3-32	10-60	23	68	40	19.7	0.6	6.5	21.2°	20°	Gasparre et al. (2007); Hight et al. (2003); Lunne et al. (1986)

Table 10.3 continued

Notes:

*****Site in database reported by Ouyang & Mayne (2018a); data re-evaluated here using Modified NTH solution.

a. OCR is determined by lab consolidation tests

b. Value of Λ from (s_u/σ_{vo}') vs. OCR and/or consolidation data

c. Modified cone resistance number: $N_{mc} = q_{net}/(\sigma_{v0}' \cdot OCR^{\Lambda})$

d. Fissured OC clay uses either exact Equation [10.1], for $B_q = 0$ or approximate NTH Equation [10.8].

e. Effective stress friction angle from CAUC and/or CIUC triaxial tests

CHAPTER 11. LIMITATIONS AND DISCUSSIONS OF THE MODIFIED NTH SOLUTION

11.1 Synopsis

While the aforementioned chapters showed the general applicability of the NTH and modified NTH solutions for evaluating ϕ' in soft-firm NC-LOC and overconsolidated clays from CPTu and DMT results, some limitations of the approach need to be noted. This chapter contains additional discussions on these topics and related aspects, including statistical analysis of the modified NTH solution on evaluating the effective stress friction angle ϕ′ of clays and comparison of the results from the modified NTH solution. Limitations of both laboratory testing and field testing on the interpreted value of ϕ′ are also illustrated. Effect of different size piezocones on affecting interpretation results is elaborated. Special considerations for organic soils, sensitive clays, soils with differing mineralogy and plasticity, and structured geomaterials are also given.

11.2 Statistics of modified NTH solution and reference friction angle from laboratory triaxial tests

Figure 11.1a shows a histogram of the laboratory triaxial measured effective friction angle ϕ′ in percentage with a friction angle interval of 4 degrees. A Gaussian distribution curve is constructed to fit the laboratory measured effective friction angle ϕ′ data. It is shown that the mean effective friction angle ϕ′ of the compiled clay databases is 29.8° and the standard deviation (S.D) is 5.2°. Statistically 71.1% of the reported ϕ′ from the laboratory triaxial are clustered between 24° to 36° (approximately one S.D higher and

lower than the mean value). Figure 11.1b demonstrates the histogram of the evaluated effective friction angle ϕ′ using the modified NTH solution applied to CPTu data. Similar statistics are shown for the histogram, e.g. the mean effective friction angle ϕ′ from modified NTH solution of the compiled clay databases is 28.6° and the standard deviation (S.D) is 4.6°. Statistically 77% of the evaluated ϕ′ values from the modified NTH solution are clustered between 24° to 36°. It can be concluded that the modified NTH solution generates comparable effective stress friction angles and similar variants (COV ≈ 0.17) to the benchmark reference value determined from triaxial compression tests.

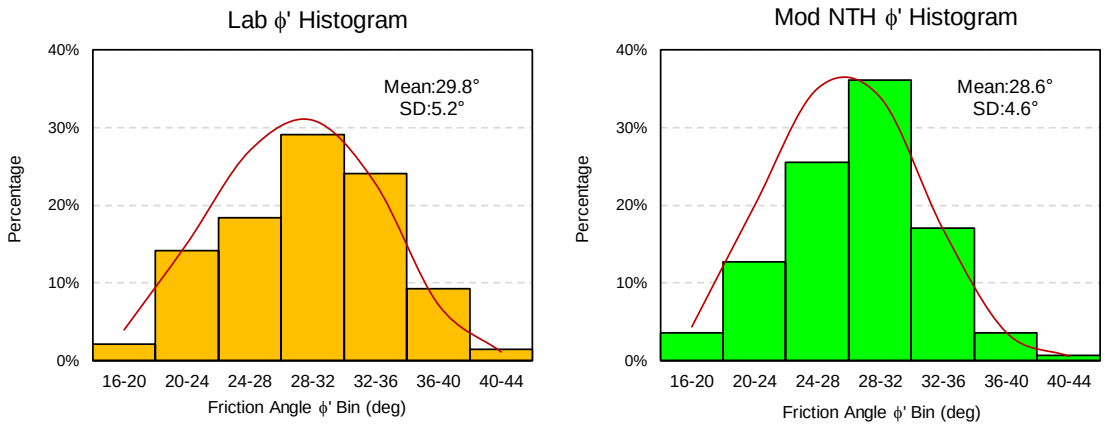

Figure 11.1. (a) Lab triaxial ϕ′ histogram; (b) Mod NTH ϕ′ histogram from CPTu data

11.3 Correlation between plasticity index and friction angle

Some 6 decades ago, Bjerrum and Simons (1960) proposed a correlation between the effective friction angle ϕ′ and the plasticity index (PI) of clays. This general notion has found to be popular with geoengineers, resulting in additional developed correlations of these two parameters (e.g., Wood 1990, Mesri & Abdel-Ghaffar 1993; Terzaghi et al. 1996, Knappett and Craig 2012). For example, Figure 11.2 shows the trend of friction angle

versus plasticity index (PI) of soft clays, soft to stiff clays, shales, and clay minerals for PI < 100 (data from Mesri & Abdel-Ghaffar and Terzaghi, et al. 1996).

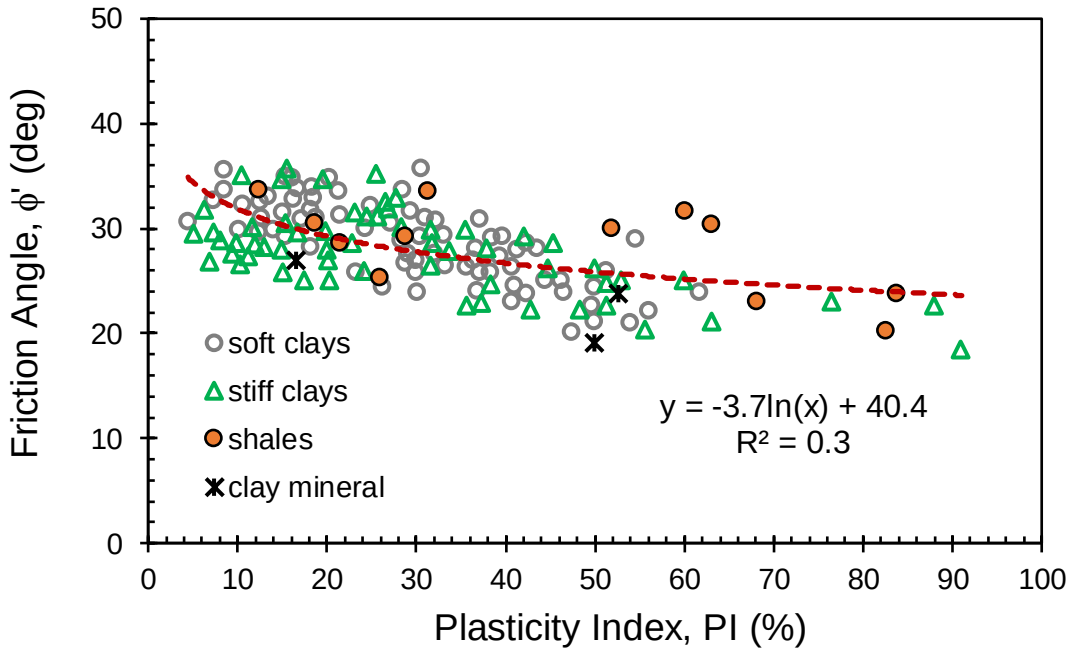

Figure 11.2. Values of friction angle ϕ′ for clays of various compositions versus plasticity index (data from Terzaghi et al. 1996)

The lab measured friction angle is plotted against the evaluated friction angle using this empirical correlation and shown by Figure 11.3. Although a general trend between the friction angle and plasticity index can be seen, the significant scatter of the data around the empirical relationship shown by the figure suggests such correlation should only be used as a first approximation, as pointed out also by Santamarina & Diaz-Rodriguez (2003), Locat, et al. (2003), Mayne (2013), and others.

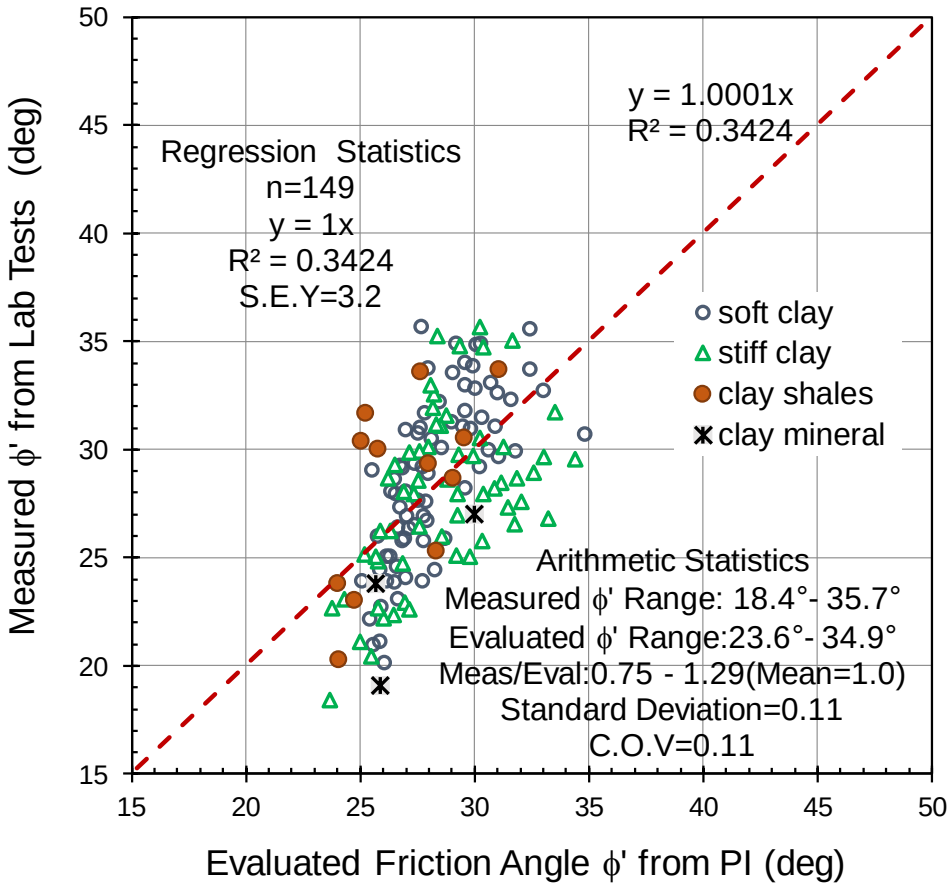

Figure 11.3. Measured friction angle ϕ′ for clays of various compositions versus evaluated value of ϕ′ from PI correlation

Sorensen and Okkels (2013) compiled a number of triaxial compression tests on undisturbed overconsolidated Danish clays, ranging from clay till of low plasticity to extremely high plasticity marine Tertiary clays. They made an attempt to correlate the effective stress friction angle ϕ′ to the plasticity index and also observed a large scatter, as suggested by Figure 11.4.

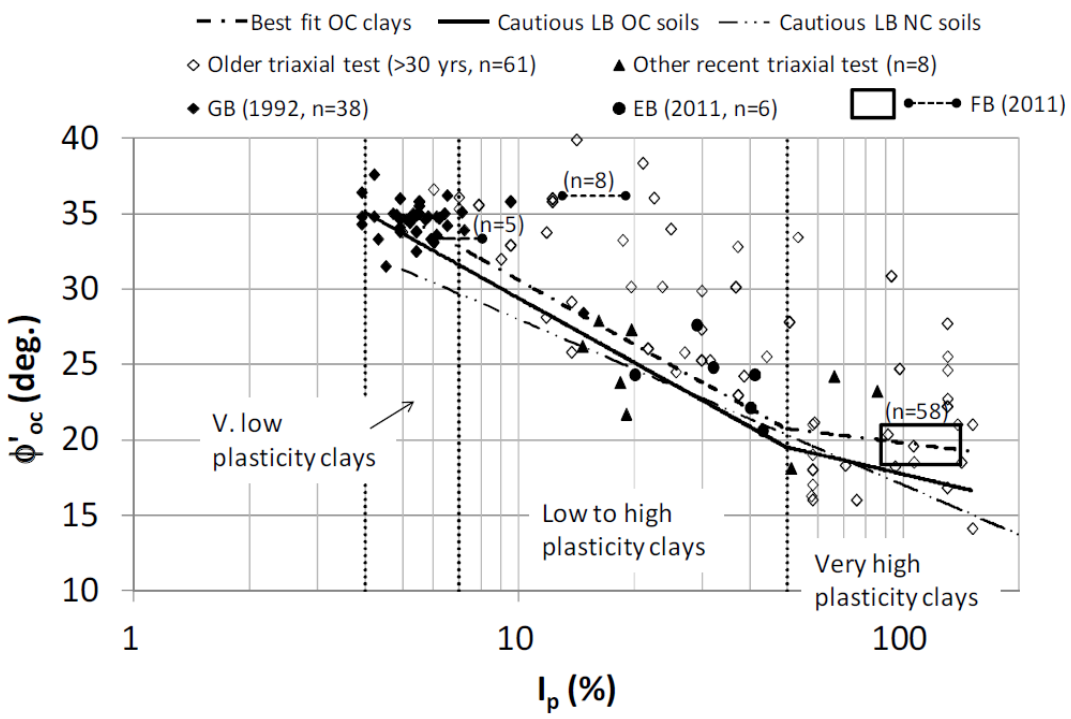

Figure 11.4. Relationship between peak angle of shearing resistance ϕ'_{oc} and plasticity index PI for overconsolidated undisturbed Danish clays (after Sorensen and Okkels 2013)

Figure 11.5 shows master summary plot for the triaxial-measured ϕ' versus the CPTu-determined values via the modified NTH solution. It is clearly evident that better reliability and improved statistics are obtained using the piezocone to evaluate ϕ' in clays than use of the plasticity index.

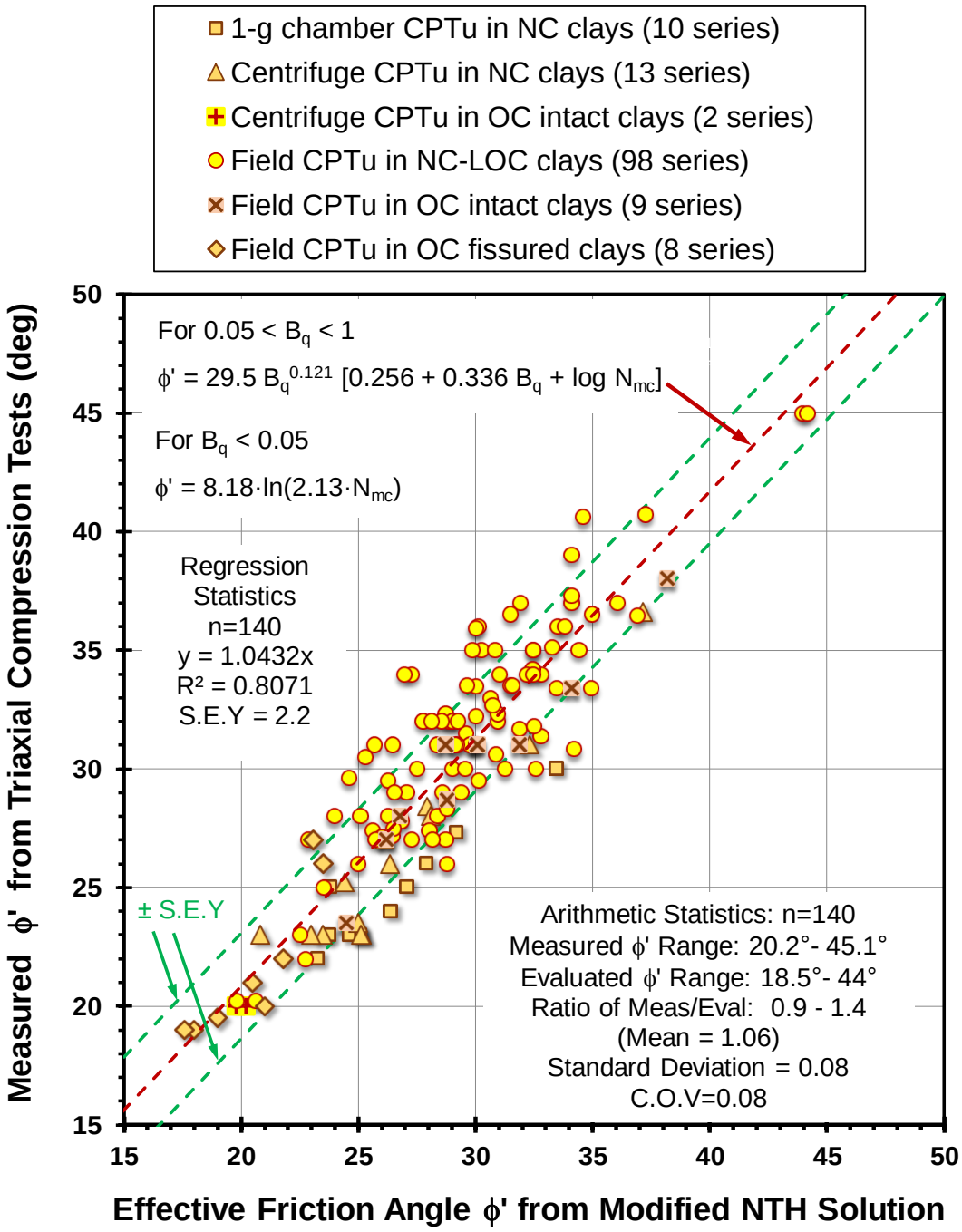

Figure 11.5. Summary plot of laboratory triaxial measured ϕ' versus CPTu ϕ' from different test series using modified NTH method

11.4 Limitations on interpreting ϕ' from laboratory triaxial tests and modified NTH solution using CPTu

While established as a versatile approach to CPT interpretation in soils, several limitations and qualifications should be made regarding the evaluation of ϕ' in clays and fine-grained soils. These discussions are separated into the two main categories of testing for this project; namely, laboratory triaxial tests and field piezocone results.

11.4.1 Triaxial test interpretations and strength criteria

Results from triaxial compression tests with porewater pressure measurements can be interpreted in light of different criteria, as detailed by Lade (2016). The three most common criteria are (i) ϕ' at peak shear stress, or $(\sigma_1 - \sigma_3)_{max}$, where σ_1 and σ_3 are the major and minor principal stresses, respectively; (ii) ϕ' at maximum obliquity where the maximum principal stress ratio $(\sigma'_1/\sigma'_3)_{max}$ is reached; and (iii) ϕ' defined at large strains (sometimes referred to as critical state).

The triaxial compression test stress path and stress strain curve of Tiller clay are illustrated in Figure 11.6 and the effective stress friction angle defined at different criteria are presented. The value of friction angle using the three criteria above show: (i) $\phi' = 33.5°$ at peak shear stress (at axial strain of 1.6%); (ii) maximum obliquity gave $\phi' = 34.3°$ (at axial strain of 7.6%), and (iii) $\phi' = 34°$ at large strains (10% axial strain). For this clay, all three criteria output very comparable value of effective stress friction angle.

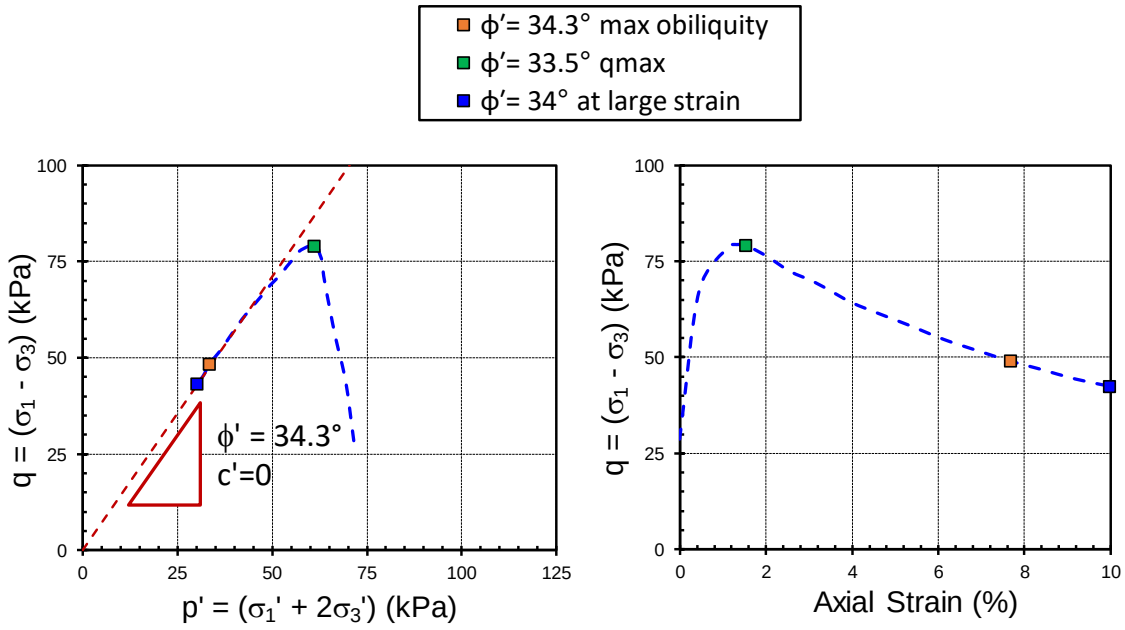

Figure 11.6. Comparison of three criteria for defining magnitude of ϕ′ for Tiller clay from triaxial test results (data from Amundsen and Thakur 2017)

The database of 98 normally consolidated to lightly overconsolidated clay sites in this study exhibit a mean OCR = 1.53 with S.D. = 1.23. Soft to firm LOC clays, such as Anacostia (Mayne 1987), Swiss clay (Springman et al. 1999), Sarapui (Almeida and Marques 2003), Nykirke (Powell and Lunne 2005), Luva (Lunne et al. 2012), Tiller (Amundsen and Thakur 2017), Chicago (Finno and Chung 1992), and other clays all show essentially the same ϕ′ for both the q_{max} and $(\sigma'_1/\sigma'_3)_{max}$ criteria.

For the overconsolidated intact clays, such as Anchorage (Mayne and Pearce 2005), Martin's Point Bridge (Hardison and Landon 2015), and other OC clays generally show comparable ϕ′ for both the q_{max} and $(\sigma'_1/\sigma'_3)_{max}$ criteria. For the overconsolidated fissured clays, such as fissured London clays at Brent Cross, Madingley, Paddington, and Canon's Park, a representative ϕ′ of 20 degrees are given which matched well with the modified

NTH solution. For the rest of the overconsolidated fissured clays in the database, both the q_{max} and $(\sigma'_1/\sigma'_3)_{max}$ criteria gave comparable ϕ'.

For the Bothkennar soft clay, Hight et al. (2003) reported a value of $\phi' = 34°$ at q_{max} on natural samples that correspond well to drained and undrained triaxial tests on reconstituted samples; whereas, at large strains and maximum obliquity, higher values with $\phi' \approx 41°$ are observed. In other cases, the value of ϕ' at q_{max} represents a lower bound, such as the Ballina clay site where Kelly et al. (2017) showed that the NTH method more closely aligns with ϕ' at constant volume ($\phi' \approx 29.5°$) whereas the peak values are much higher, averaging around 35.7°. Similar results are observed for the soft clay at Burswood (Low et al. 2011).

In a few cases, a stress history and normalized soil engineering properties (SHANSEP) procedure was used and this may have resulted in differences in reported ϕ' values (Jardine et al. 2003; Bay et al. 2005). Tanaka et al. (2003) applied SHANSEP procedure for six different natural clays of OCRs between 1.9 to 5.0 and found that the stress-strain relations as well as stress paths are somewhat different between the SHANSEP and the recompression methods and showed larger strain and smaller interpreted ϕ' at failure for the SHANSEP approach.

As noted previously, in many cases, the cited source of data did not report the criterion used to define ϕ', nor was the effective stress path or set of stress–strain curves and pore-water pressure data provided, so a re-interpretation and (or) comparison of ϕ' by various criteria could not be performed. In any event, it is believed that the values of ϕ'

contained herein are lower bound values and consequently the modified NTH method provides a conservative evaluation.

11.4.2 Piezocone results

Sources of piezocone data reviewed in this dissertation utilized either electric (analog) or electronic (digital) cone penetrometers with measurements of q_t and u_2, and in most cases, f_s readings, with depth. Field test procedures followed either ASTM standards (D 5778) at 20 mm/s, or an equivalent test method such as CEN (European) or ISO (international standards), as detailed by Lunne et al. (1997).

A brief discussion of penetrometer size effects may be warranted, since both regular field CPTs and mini-CPTs from lab tests have been compiled in the datasets. Comparative field CPTu results obtained at four clay sites showed essentially no differences in q_t and u_2 measurements taken by 10-cm^2 and 15-cm^2 penetrometers (Powell & Lunne 2005). Similar findings that compared 5-cm^2 and 10-cm^2 size penetrometers in soft Swiss clay suggest scale effects are generally not significant for CPTu soundings in clays (Hird & Springman 2006). Hird et al. (2003) studied two piezocones with cross-sectional areas of 1 cm^2 and 5 cm^2 and a variety of pore pressure filters under standard rate of 20mm/s, and the experiment results showed comparable capability of these miniature piezocones in detecting thin permeable layers in normally and lightly overconsolidated clay deposits. Furthermore, Tumay & Kurup (2001) developed, calibrated and implemented a continuous intrusion miniature piezocone penetration test system in shallow depth site characterization using 2 cm^2 miniature piezocone penetrometer and found consistent results with those obtained

from the standard 10 cm^2 piezocone penetrometer (only about 11% higher tip resistance are recorded by the miniature cone).

For lab test series, general testing procedures were followed for mini-penetrometers advanced into artificial clays in chamber tests or centrifuge deposits, however, rates were adjusted accordingly for size effects and strain rate behavior, specifically to obtain an undrained response (DeJong et al. 2012). The representative strain level corresponding to piezocone penetration tests is generally determined as around 20% shear strain illustrated by Figure 11.7. For a typical undrained penetration process with a Poisson's ratio $\upsilon = 0.5$, a corresponding axial strain level is calculated as $\varepsilon_a = \gamma/(1+\upsilon) = 13\%$. The benchmark reference triaxial compression interpreted ϕ' taken at both large strain (around 10%) and maximum obliquity (around 6% to 8%) for the example shown by Figure 11.7 gave compatible level of strain compared to the piezocone penetrometer results.

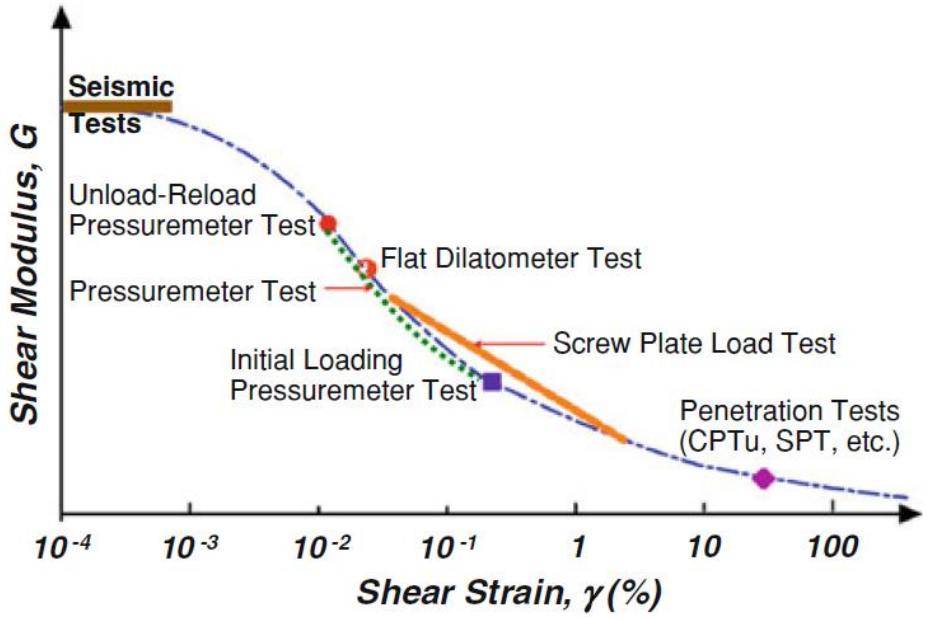

Figure 11.7. Schematic order of strains corresponding to various field test measurements (modified after Mayne and Schneider 2001)

For the modified NTH to produce reliable ϕ' profiles in clays, quality measurements of q_t and u_2 are required. Therefore, results depend upon proper procedures for saturation of the porous filter element and cone cavities during preparation in the field (Campanella and Robertson 1988; Lunne et al. 1997). In certain geologic settings, an upper crustal layer of desiccated soils and (or) vadose zone comprising unsaturated soils may cause desaturation of the filter element, thus rendering the u_2 readings inaccurate. Insufficiently high vacuum applied during filter preparation and (or) use of various saturating fluids (water, glycerine, silicone oils) may also adversely affect the pore-water pressure readings. The magnitude of total (or corrected) q_t also depends upon the u_2 reading. Thus, care should be implemented in properly obtaining and maintaining saturation throughout the CPTu measurements.

11.5 Influence of soil minerology on effective friction angle of clays and special considerations for organic soils, sensitive clays, and structured geomaterials

11.5.1 Mineralogy

Mineralogy affects the frictional characteristics of soils. Olson (1974) compiled a range of shear strength data from multiple tests on specimens of relatively pure kaolinite, illite, and montmorillonite, in which he observed that kaolin has the highest friction angle (20° to 28°), followed by illite (15° to 23°), with montmorillonite coming in with very low friction angles (around 6° to 12°), as illustrated by Figure 11.8.

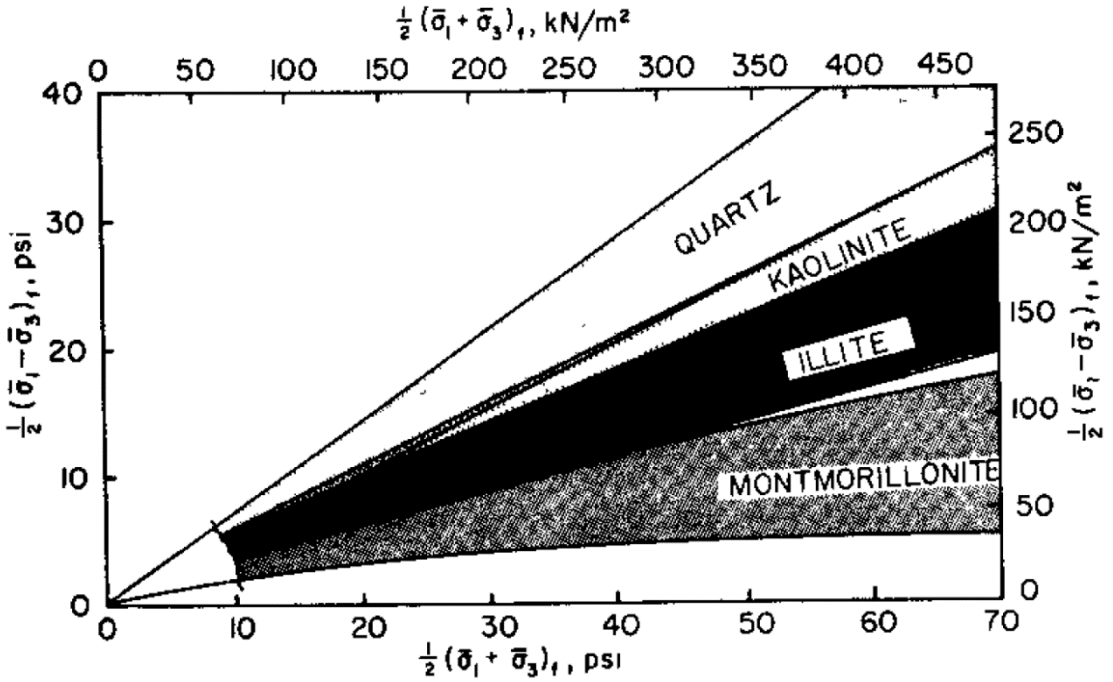

Figure 11.8. Range of failure envelope for soils composed of pure clay minerals or quartz (after Olson 1974)

Hattab et al. (2015) presented an extensive study of a variable model clayey material, made of mixtures of montmorillonite characterized by a high plasticity, and kaolin P300, which is a more stable clay with low plasticity. A marked decrease in the internal friction angle for the soil mixtures is observed by increasing the concentration of the montmorillonite, evidenced by Figure 11.9.

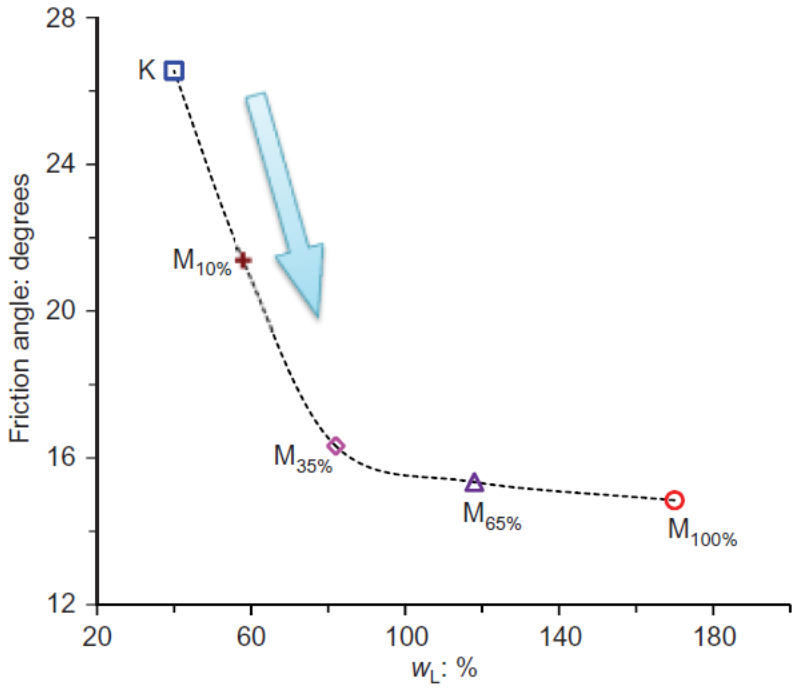

Figure 11.9. Change of friction angle value with respect to concentration of the montmorillonite in the soil mixture (after Hattab et al. 2015, percentage representing concentration of added montmorillonite)

Some clays exhibit very high frictional characteristics. Mesri et al. (1975) demonstrated the unique behaviour of Mexico City clay, i.e. a friction angle ≈ 40° with a plasticity index of about 300% to 500%. This high frictional characteristic was due to the presence of large quantities of diatoms (microfossils) in the soil, which can alter the strength parameters, specifically the friction angle.

In controlled experiments, Shiwakoti et al. (2002) report test results obtained on two clays (kaolin and Singapore clay) both mixed with increasing amounts of diatomite and observed drastic increases in the friction angle for both soil mixtures with 25% of diatomite to 50% and eventually up to 75% of diatomite. Concurrently, the plasticity index did not change significantly up to a concentration in diatomite of 75%. With the addition of diatoms, the kaolin friction angle increased from 24° to 39° while Singapore clay went

from 22° to nearly 38°, as illustrated by Figure 11.10. Even with only 25% of diatomite added, both soils exhibit a sudden increase of friction angle value. These results show that if a non-fossiliferous clay is mixed with diatom, its friction angle move well above the expected trend. These experiments show that the well-known simple ϕ'-PI trends are very limited to pure clay minerals, remoulded soils, and artificially-prepared clays. Therefore, these should be used with caution and consideration.

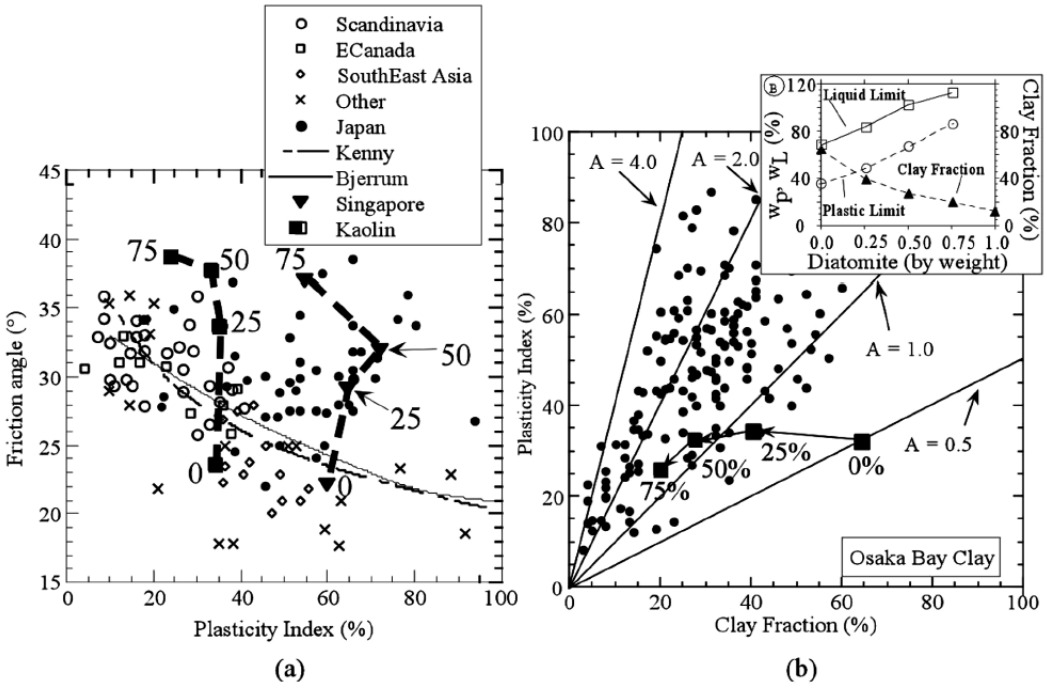

Figure 11.10. (a) Effect of diatom concentration on the plasticity index and friction angle relationship, and (b) effect of diatom microfossils on Atterberg's limits and Activity (adopted after Locat et al. 2003).

Further evidence on mineralogical effects on ϕ' are found in the recent offshore soils in western Africa. Colliat et al. (2011) studied the geotechnical properties of deepwater sediments encountered on the continental slopes of the Gulf of Guinea, in water depth ranging from about 400m to 2000 m. The deep-water West Africa clays are generally

normally consolidated and exhibit high plasticity index around 100%, however, the laboratory triaxial compression tests suggest a high effective stress friction angle ϕ' around 41° to 43°.

Of additional note, Takai et al (2016) also conducted experimental study in soil-bentonite mixture and found decrease in friction angle value for the clay mixture due to increasing concentration of bentonite.

11.5.2 Organic soils

Organic soils such as peat will exhibit different mechanical properties than the behaviour of inorganic clays because of their organic solids and high water content. Edil and Wang (2000) conducted an extensive laboratory testing program on peats and organic soils regarding lateral earth pressure, effective stress friction angle, and undrained shear strength. Laboratory undrained triaxial compression tests show the effective friction angle for normally consolidated peats (more than 25% organic content) varying between 40° to 60° with an average effective friction angle of 53° and 41° for organic soils (less than approximately 25% organic content), as illustrated by Figure 11.11. The cohesion intercept is in general small for peats.

Zwanenburg & Jardine (2015) describe full-scale field tests conducted on peats in the Netherlands under different pre-loading conditions to investigate the peat layers' consolidation behaviour and mechanical properties of peats. Furthermore, they also observed very high friction angles ($\phi' > 60°$) for Dutch peat tested under laboratory triaxial compression tests.

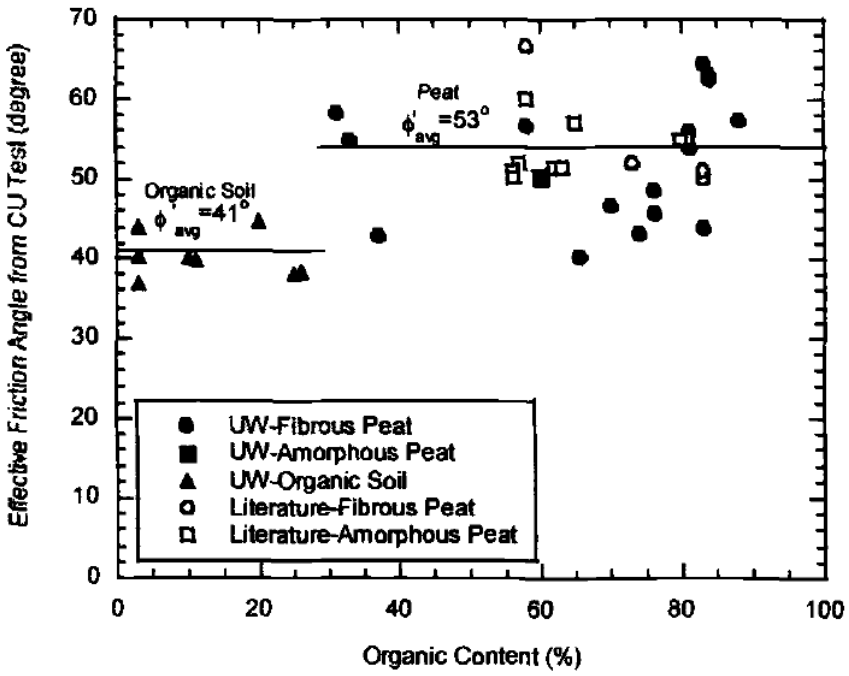

Figure 11.11. Effective friction angle versus organic content (after Edil and Wang 2000)

11.5.3 Sensitive/Structured clays

For triaxial testing of sensitive clays, peak strength is reached early followed by strain softening in the stress-strain response, whereas porewater pressures exhibit a maximum value at higher strains. Figure 11.12 shows results of CIUC and CAUC tests on sensitive Haney clay and the effective friction angle corresponding to the peak shear strength (q_{max} criterion) demonstrates lower value ($\phi' = 22.5°$) than effective friction angle associated with maximum obliquity ($\phi' = 32.3°$).

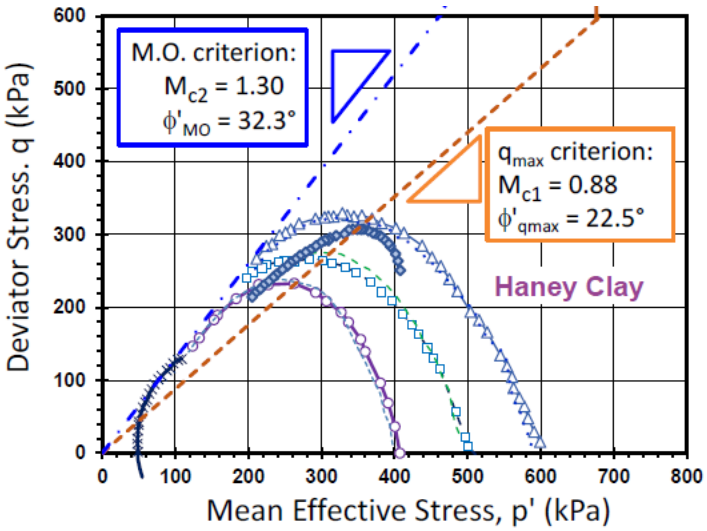

Figure 11.12. Triaxial results on Haney clay reported by UBC (after Mayne et al. 2018)

Mayne et al. (2018, 2019) studied CPTu in sensitive clays and reported that sensitive clays generally show strain incompatibility for peak shear strength and porewater pressures development from triaxial compression test, resulting in different interpreted effective friction angle value by different criteria. Further study is warranted to calibrate NTH results in such clays to interpret the effective friction angle in sensitive clays.

11.5.4 Screening of Normal vs Organic vs Sensitive/Structured clay

For the data that were considered in the dissertation, CPTu and triaxial data were obtained from clays and clayey silts that were primarily inorganic soils of low-medium sensitivity. The characteristic normalized porewater pressure response for this group exhibits values: $0.5 < B_q < 0.6$ (Mayne & Peuchen 2018). However, it is recognized that natural organic clays tend to generate lower normalized porewater pressure ($B_q < 0.5$). while sensitive and structured clays generally exhibit higher values ($B_q > 0.8$) when compared to "normal" or "well-behaved" clays.

Agaiby (2018) introduced a CPTu based screening method for identification of sensitive/structured clays, organic clay and normal or well-behaved clay. For these clays, different hierarchies are observed for using CPTu reading (net cone resistance $q_{net}=q_t-\sigma_{v0}$, excess porewater pressure $\Delta u_2 =u_2-u_0$ and effective cone resistance $q_E=q_t-u_2$) to express the preconsolidation stress σ_p' where:

- Normal or well-behaved clays (generally OCR < 3):

$\sigma_p' \approx 0.33\ q_{net} \approx 0.53\ \Delta u_2 \approx 0.60\ q_E$

- Organic clays (generally OCR < 3):

$\sigma_p' \approx 0.53\ \Delta u_2 < 0.33\ q_{net} < 0.60\ q_E$

- Sensitive or structure clays (generally OCR < 3):

$\sigma_p' \approx 0.60\ q_E < 0.33\ q_{net} < 0.53\ \Delta u_2$

Thus, special caution should be taken when evaluating CPTu in organic clays, sensitive or structured soils, or clays of special mineralogy, as the application of the modified NTH solution should only be undertaken after careful calibration with triaxial tests on high-quality laboratory samples to confirm the appropriate effective stress friction angles are valid in the specific geologic setting of study.

11.6 Final word

It is always prudent practice to collect undisturbed samples of the given clay during the site investigation and then conduct a series of laboratory CIUC-CAUC triaxial tests to verify the benchmark values of Phi'. Then, site-specific calibration of the modified NTH solution with CPTu can be used reassuringly and with confidence.

CHAPTER 12. CONCLUSIONS AND FUTURE WORK

12.1 Conclusions

- This research effort was focused on the evaluation of the effective stress strength envelope of clays from piezocone penetration test results, specifically the determination of ϕ' with $c' = 0$. An existing effective stress limit plasticity solution developed by Janbu & Senneset (1974) at NTH was implemented, calibrated, and modified to permit its application in soft to firm to stiff clays and fissured fine-grained soils that cover a full range of OCRs. Four main databases were created from information found in the open literature, geotechnical reports, and unpublished documents, including: (a) 1-g chamber tests series, (b) centrifuge testing programs, (c) field site investigations, and (d) variable rate CPT soundings known as twitch testing. Reference values of ϕ' of clays were available from companion laboratory triaxial compression (TC) tests to validate the findings. Traditionally, CPT results taken in clays are utilized to assess the undrained shear strength (s_u) from a total stress analysis point of view. Yet, the effective stress regime is a more fundamental framework that includes total stress analysis, therefore the evaluation of ϕ' from CPTu in clays is considered an important contribution towards geotechnical practice. An understanding of effective stress response is important in the soil behavior of clays, critical state soil mechanics, predicting pore pressure behavior during construction of embankments, and FEM numerical simulations of levees, dams, and offshore structures.

- The research program conducted a review of mini-piezocone test data from 11 separate series of pressurized and unpressurized calibration chamber tests on prepared clay deposits. These clay beds were constructed mainly from kaolin and/or kaolin-sand mixed geomaterials of normally consolidated to lightly over-consolidated nature.
- Data from 13 series of in-flight mini-piezocone penetrometer tests in centrifuge deposits were reviewed for verifying the NTH limit plasticity solution in assessing the effective friction angle of normally consolidated to lightly over-consolidated clays and clayey silts. The majority of artificially-prepared deposits of clays included kaolinites or kaolin-sand mixtures.
- Paired data from 105 natural clay deposits, which included both laboratory triaxial tests (CK_0UC, CAUC or CIUC) and field CPTu soundings, were compiled to validate the NTH solution. The findings show that the methodology provides statistically sound results for CPTu testing conducted in insensitive and inorganic clays with corresponding ϕ' values in the range $20° \leqslant \phi' \leqslant 45°$. The NTH theoretical solution and a corresponding approximate equation were used towards the evaluation of the effective stress friction angle ϕ' in soft to firm clays from CPTu readings.
- The NTH solution was also applied to data obtained in variable rate CPTu testing, i.e. twitch tests. This permits an evaluation of ϕ' under undrained to partially-drained to fully-drained conditions. Where available, benchmark ϕ' results from CIUC and CAUC triaxial compression tests were used to verify the CPTu ϕ' values from the NTH solution, obtaining good statistical results. Results show that the

NTH solution for ϕ' is insensitive to penetration rate and provides a consistent output result, regardless of drainage conditions.

- A theoretical nexus between CPTu readings (q_t and u_2) and flat DMT pressures (p_0 and p_1) was established based on spherical cavity expansion (SCE) theory (Vesić 1977) for use in soft to firm clays with OCRs between 1 to 2.5. These links were verified by compilation of data from 49 paired CPTu-DMT soundings on natural clays. The NTH limit plasticity for evaluating ϕ' from CPTu in soft to firm clays is then extended to DMT measurements for the same purpose. Laboratory triaxial test results (CK_0UC, CAUC, or CIUC) with field DMT results from across the planet and DMT series in clay chamber test series were reviewed to corroborate the validity of the methodology. A full range of operational effective stress friction angles with $20° \leq \phi' \leq 45°$ are observed in both the triaxial data and NTH solution, as verified by a number of case studies. The method is applicable to soft clays at low OCRs < 2.5, which are inorganic, insensitive, and tested under undrained conditions with $c_v < 0.05$ cm^2/s.
- Analytical closed-form solutions are presented for interpreting ϕ', I_R, s_u, and OCR in soft-firm clays from DMT soundings. Using a hybrid framework derived from spherical cavity expansion and critical state soil mechanics (SCE-CSSM), it is shown that an operational value of rigidity index (I_R) of soft to firm clays can be obtained from the NTH ϕ' coupled with readings from flat plate dilatometer test (DMT), namely, the contact pressure p_0 and the expansion pressure p_1. This value of I_R is used to provide the bearing factor (N_{kt}) which profiles the undrained shear strength (s_u) with depth. The two parameters together (I_R and ϕ') are further used in

the SCE-CSSM algorithms to assess the profiles of OCR and s_u in soft-firm clays in closed-form analytical solutions, where OCRs < 2.5.

- A modified NTH effective stress limit plasticity solution for evaluating ϕ' in overconsolidated (OC) clays from CPTu is presented where the cone resistance number is adjusted to reflect stress history effects, i.e. OCR by introducing concepts from critical state soil mechanics. Specifically, the normalized cone tip resistance is adjusted using the equivalent stress concept (Hvorslev 1960; Schofield & Wroth 1968; Mayne et al. 2009). This permits a unified approach that is applicable to soft to firm NC and LOC clays to OC intact and fissured OC clays. The calibration was accomplished by collection of six databases, including triaxial data and CPTu soundings obtained from: (a) laboratory chamber tests in NC clays; (b) centrifuge testing in NC clays; (c) centrifuge tests in OC clays; (d) field CPTu in natural NC-LOC clays, (e) field CPTu in OC intact clays with OCR > 2.5, and (f) field CPTu in OC fissured clays. The magnitudes of effective stress friction angle ϕ' interpreted by both CPTu and triaxial tests cover a wide range of values: $19° < \phi' < 45°$. Case studies involving NC and OC clays are presented to detail the modified NTH post-processing procedure. In lieu of the exact solution, two approximate NTH expressions are given, one applicable for intact NC to OC clays and a second applicable to fissured OC clays that exhibit $B_q \approx 0$.

12.2 Recommendations for future work

For future research on these topics, the following tasks should be considered:

- For the data that were considered in these studies, CPTu and triaxial data were obtained from clays and clayey silts that were primarily inorganic soils of low-medium sensitivity. The characteristic porewater pressure response for this group exhibits: $0.5 < B_q < 0.6$. However, it is recognized that natural organic clays tend to generate lower normalized porewater pressure ($B_q < 0.5$) while sensitive and structured clays generally exhibit higher values ($B_q > 0.8$) when compared to "normal" or "well-behaved" clays. Further investigation is warranted for potential modification of the NTH limit plasticity solution in assessment of the effective friction angle ϕ' of clays with high organic content and clays that are sensitive and structured.
- Conduct series of CIUC/CAUC triaxials and mini-CPTu in lab chamber tests or centrifuge series with similarly prepared deposits of kaolin, illite, and montmorillonite, as well as sand-clay mixtures, and special clays such as halloysite and attapulgite.
- Investigate evaluation of effective stress strength parameter of intermediate grain size geomaterials from clayed silts to silty sands from CPTu/DMT, possible solutions including implementation of various β' angle value (angle of plastification) from the NTH limit plasticity solution. Eventually develop an integrated methodology of evaluation of effective stress strength parameter of soils with different grain size ranging from clays to silts to sands. Possible solutions include modification of the input parameters of the NTH method (cone resistance

numbers Q and N_m and the normalized porewater pressure B_q) to account for the effect of the different soil types, extending the normalized cone resistance Q from CPTu readings to Q_{tn}, which reflects the soil behavior. The subscript n corresponds to different soil types, where n=1 designates soft clays, and decreases as the grain size increases till eventually reaches n=0.5 for sands (Robertson 2009). Also, stress history effects can be also considered by introducing the "equivalent stress" concept as described in chapter 10 and potentially modify N_{mc} with Q_{tn} in different soil type. The Q-B_q and Q_{tn}-B_q and/or N_{mc}-B_q paired set parameters could be utilized to reflect both soil behavior type and the effective stress strength characteristics of the soil.

- Calibration and/or modification of the NTH limit plasticity solution would be of interest in the assessment of the effective friction angle ϕ' of clays with high organic content and clays that are sensitive and structured using DMT data.
- Needs for application and extension of the modified NTH solution towards flat plate dilatometer test results in stiff clays with high overconsoldiation ratio (OCR) may be possible with the aid of the nexus built between piezocone penetration test and flat plate dilatometer in this research program.
- Further calibration of the spherical cavity expansion-critical state soil mechanics (SCE-CSSM) solution that provides the direct CPTu and DMT evaluation of undrained rigidity index could possibly be used towards assessing the coefficient of consolidation (c_v) and hydraulic conductivity (k) from CPTu porewater pressure dissipation test and/or from DMT A-dissipation testing.

APPENDIX A. FIELD TESTING AT GEORGIA TECH W-21 EXPERIMENTATION SITE

A.1 Introduction

A variety of in-situ tests were conducted at the W-21 test site on the Georgia Institute of Technology campus during 2013 to 2018. This appendix presents a summary of these field testing conducted at W-21 geotechnical testing site which is adjacent to a parking lot located northwest of the CEE Mason Building in Atlanta. Figure A. 1 shows the general vicinity of the area and the testing location that is primarily wooded. The terrain is mainly flat with some slight slopes from the wooded area down to the pavements.

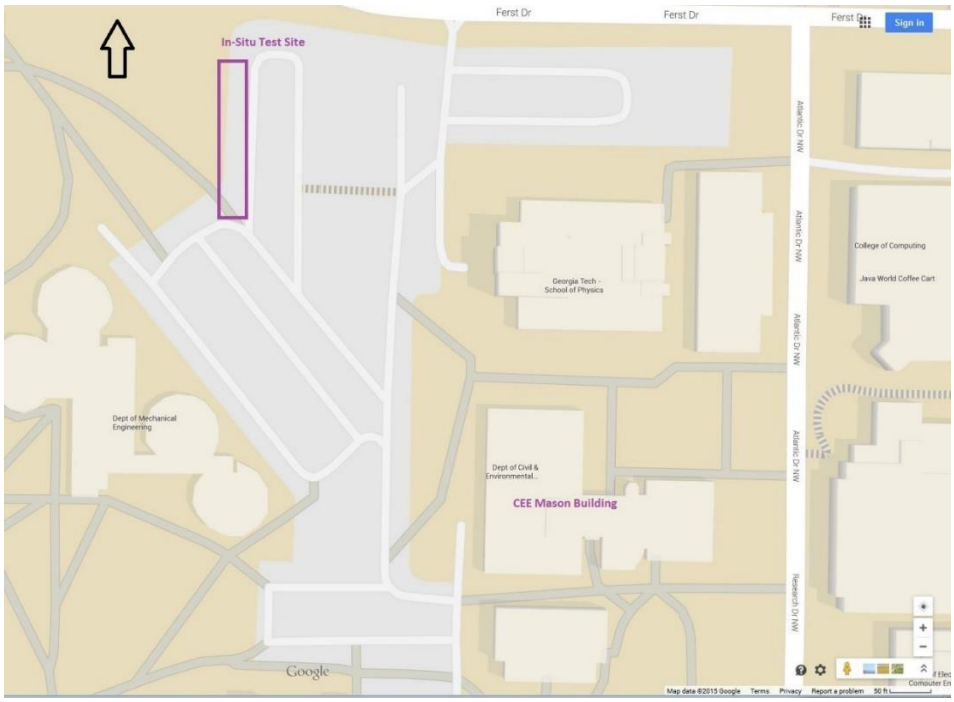

Figure A. 1. Geotechnical test site at W-21 parking are, Georgia Tech

The site is underlain by native residual soils of the Appalachian Piedmont geologic province. These are mainly silty soils, ranging from micaceous fine sandy silts to silty fine sands that grade with depth to saprolites and partially-weathered rocks (PWR), eventually reaching bedrock refusal. At this site, refusal is encountered at about 12.8 m (42 feet) with groundwater variable but often found at depths of about 12 m (40 feet). The performed field geotechnical site investigations included: seismic cone penetration tests (SCPTu), flat plate dilatometer tests (DMT) and helical probe tests (HPT).

A.2 Geology of the state of Georgia

The state of Georgia is composed of four separate geologic areas, as illustrated by Figure A. 2: Piedmont; Blue Ridge, Coastal Plain, and Valley & Ridge Plateau. As such, the natural soils and rocks, as well as compacted fills made from native geomaterials in these regions, can behave somewhat differently from each other. We can group the Appalachian Piedmont and Blue Ridge together due to their similarity. At one time, a range of mountains over 12 km in height dominated the region but have since essentially vanished due to extensive erosion, weathering, decomposition, and exposure to the elements over many millennia (Chew 1993). Parent bedrock is comprised primarily of gneiss and schist of Pre-Cambrian Z-age, with lesser amounts of igneous intrusives (granites) that appeared in Paleozoic times. The ground is underlain by residuum derived by the in-place weathering of metamorphic and igneous bedrock. The residual soils are often found to be silty, ranging from micaceous fine sandy silts to silty fine sands, that transition with depth to saprolites, partially-weathered rocks, and bedrock refusal. Locally, the layman's term for the upper few centimeters of native soils are called "Georgia red clay" due to the red-orange-tan colors due to iron oxides (Mayne 2013).

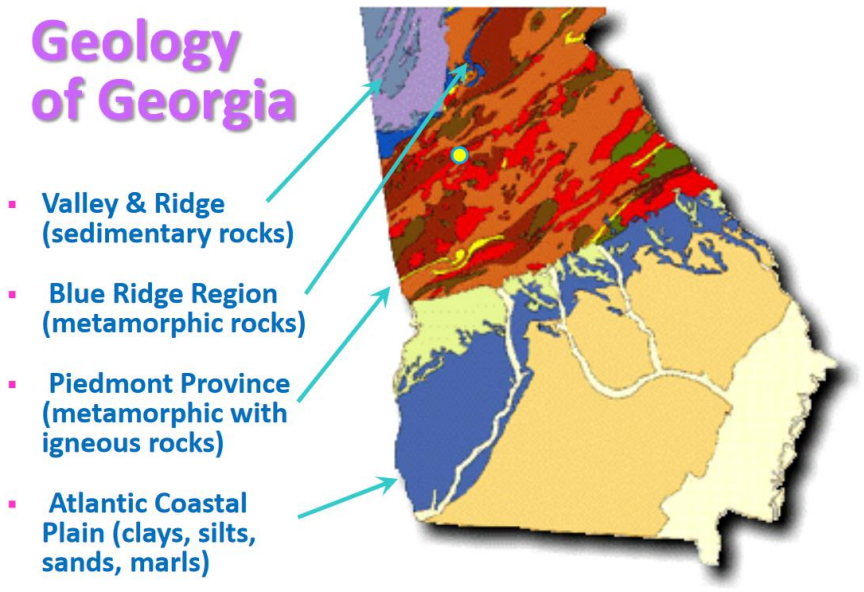

Figure A. 2. Geology of the state of Georgia (Mayne 2013)

Figure A. 3 illustrates a representative subsurface profile of the Appalachian Piedmont. In contrast, the Coastal Plain consists of various marine sediments that were deposited in various times ranging from very old Cretaceous to Miocene to recent Holocene ages, including complex interbedding of clays, silts, sands, and gravels. Finally, the Valley & Ridge Plateau include sedimentary type bedrocks (shales, limestones, sandstones) that have also produced a clayey to sandy type residuum cover, as well as karstic terrain, sinkholes, and caves (Weary, 2005).

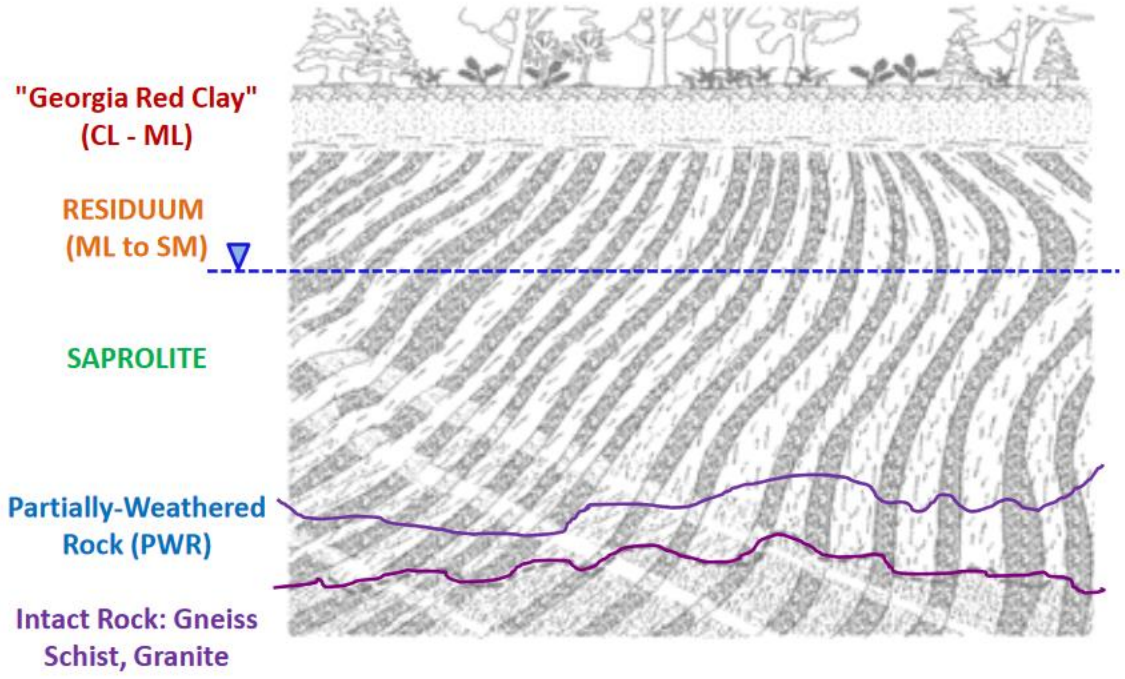

Figure A. 3. Generalized subsurface profile in the Appalachian Piedmont Province (Mayne 2013)

A.3 Seismic Cone Penetration Testing (SCPTu)

The cone penetration test (CPT) involves the hydraulic pushing of a highly-instrumented electronic steel probe into the ground at a constant rate to obtain continuous vertical profiles of stress, friction, and pressure with depth. Cone penetration testing can be conducted for the measurement of tip and sleeve resistances (i.e., CPT) as well as the additional readings of penetration porewater pressures using a piezocone (i.e., CPTu). Some equipment includes the ability to measure shear wave velocities, called a seismic piezocone test and designated SCPTu. The data presentation from a SCPTu sounding includes: cone resistance (q_t), sleeve friction (f_s), porewater pressures (u_2), and downhole shear wave velocity (V_{sVH}) plotted with depth in side-by-side graphs.

A standard cone penetrometer is a 35.7-mm diameter cylindrical probe with a 60° apex at the tip, 10-cm^2 cross-sectional area, and a 150-cm^2 sleeve surface area. More robust penetrometers are available with a 44-mm diameter body, a 15-cm^2 projected tip area, and 200- to 225-cm^2 sleeve surface area. For a piezocone penetration test (CPTu), the penetration porewater pressures are monitored using a transducer and porous filter element. Porewater readings can be taken at the apex or mid-face (designated u_1), shoulder (just above the cone tip, or u_2), or behind the sleeve (u_3). The standard required position per ASTM D 5778 is the shoulder position (type 2) because the u_2 value is required for the correction of tip resistance. Filter elements consist of high-density polypropylene, ceramic, or sintered metal. Fluids for saturation include: water, glycerin, or silicone oil.

For the seismic piezocone test, a geophone is located approximately 500 mm above the cone tip. The geophone detects the arrival of shear waves at depth after they are generated at the ground surface using a seismic source. The V_s data are acquired at depth intervals of approximately 1-meter, corresponding to successive rod additions (Agaiby & Mayne, 2016).

Over the past few years, the testing site at W-21 has been used for academic class demonstrations and the collection of in-situ data in a program of geotechnical field characterization. A large 25-tonne cone truck was used by ConeTec for performing invasive downhole tests (DHT) via ASTM D 7400 using seismic piezocone testing (SCPTu). Four standard seismic piezocone soundings (SCPTu) conducted in 2014, 2015, and 2016. The SCPTu were performed with pseudo-interval arrays at 1-m depth intervals where paired sets of left and right strikes were accomplished using a sledge hammer and horizontal beam arrangement.

Figure A. 4 summarizes the results of the four seismic piezocone soundings conducted at W-21 test site over 3 years with soundings A and B conducted in 2014, sounding C in 2015 and sounding D in 2016. Relatively consistent and comparable data were obtained for all four readings. The material

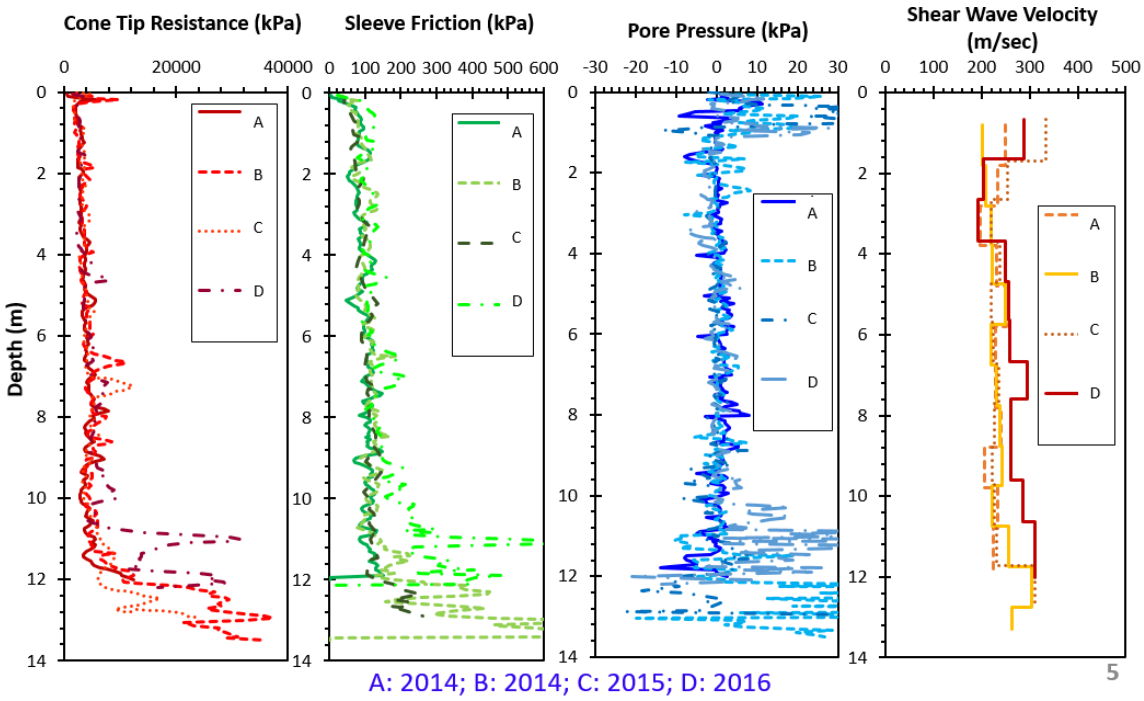

Figure A. 4. Seismic piezocone soundings conducted at W-21 site on Georgia Tech campus by ConeTec showing: (a) cone tip resistance, q_t, (b) sleeve friction, f_s, (c) penetration porewater pressure, u_2, and (d) shear wave velocity, V_{sVH}

Figure A. 5 presents the profile for the CPT material index, I_c with depth for the four conducted CPTu indicating that the studied soil at W-21 site can be mainly classified as sand mix and/ or silty mix except for the crust layer within the top 0.5m that can be identified as sand.

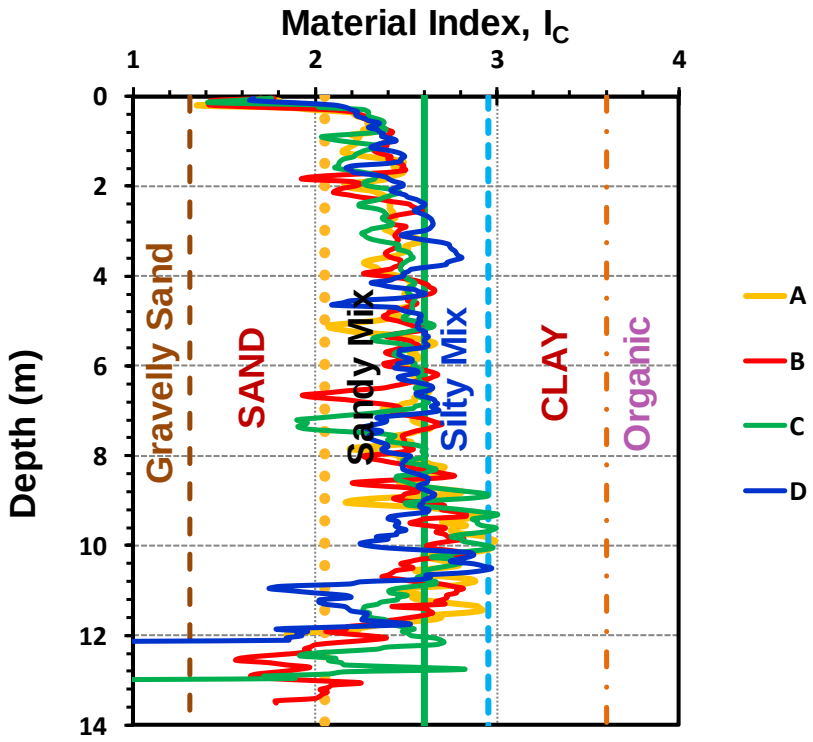

Figure A. 5. Profile of CPT material indices (I_c) at W-21 site

For evaluating the friction angle for the geomaterials at W-21 site, two different approaches are demonstrated below. Based on the above CPT I_c, the soils are characterized as sand mix and/ or silty mix. Mayne (2006) compiled an elite database from special expensive undisturbed samples of clean sands. Primarily, these sands were initially frozen in-place using one-dimensional thermal techniques and, after careful mounting of specimens in triaxial apparatuses with membranes and confinement, they were allowed to thaw, then sheared to failure in triaxial compression. The results from undisturbed sands was shown to match well with the expression derived by Kulhawy & Mayne (1990):

$$\phi' \quad (\text{in degrees}) = 17.6° + 11.0 \cdot \log \frac{(q_t/\sigma_{atm})}{\sqrt{(\sigma'_{v0}/\sigma_{atm})}} \qquad [1]$$

The NTH approach is also adopted to evaluate the effective stress friction angle at W-21 site. Since the excess porewater pressure $\Delta u=u_2-u_0$ at the site is practically zero, the NTH approximate equation for zero excess porewater pressure is applied:

$$\phi' \approx 8.24 \ln\cdot(2.13\cdot N_m) \qquad [2]$$

Both interpretations of effective stress friction angle ϕ' for the representative CPTu sounding A are presented in Figure A. 6.

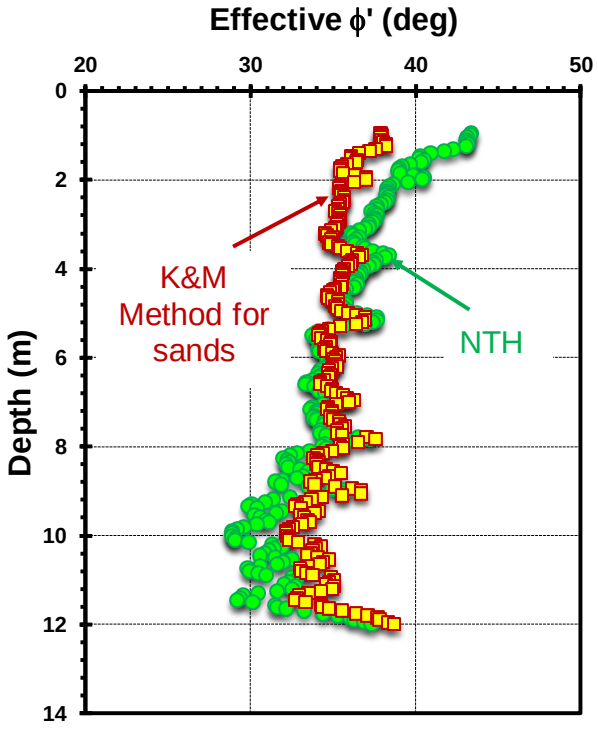

Figure A. 6. Interpreted effective stress friction angle profile at W-21 site for CPTu sounding A

EGSci Consulting Inc also conducted SCPTu demonstration at the W-21 site to the students of Georgia Tech for graduate class CEE 6423 and CEE 6443 which the author

served as the teaching assistant (TA). Figure A. 7 shows a photo of SCPTu demo for fall 2018

Figure A. 7. CPTu demo by EGSci Consulting Inc

A.4 Flat Plate Dilatometre Tests (DMT)

The flat plate dilatometer test (DMT) is an in-situ method that involves vertically pushing an instrumented flat steel blade into soils and recording two horizontal pressures to inflate a circular membrane at each test depth. The specific pressure measurements are utilized to obtain stratigraphy and estimates of geoparameters, including: unit weight, at-rest lateral stresses, elastic modulus, stress history, and shear strength.

The flat dilatometer test is simple, robust, repeatable, quick, economic, and operator-independent. The field of applications of the DMT is diverse, ranging from extremely soft soils to dense sands. However, the DMT is difficult to push in very dense

and hard materials and not applicable to gravels. The DMT analyses primarily relies on correlative relationships and requires calculations for local geologies.

Procedures for the test are given by ASTM D 6635 and Schmertmann (1986). Figure A. 8 provides an overview of the DMT test and its setup. Two calibration readings are taken for membrane stiffness: ΔA = pressure required in air to move the flexible membrane inward a distance 0.05 mm; ΔB = pressure required in air to move membrane outward a distance 1.1 mm. Each of the pressure readings A and B are then converted into p_0 (contact pressure) and p_1 (expansion pressure), respectively per Figure A. 8.

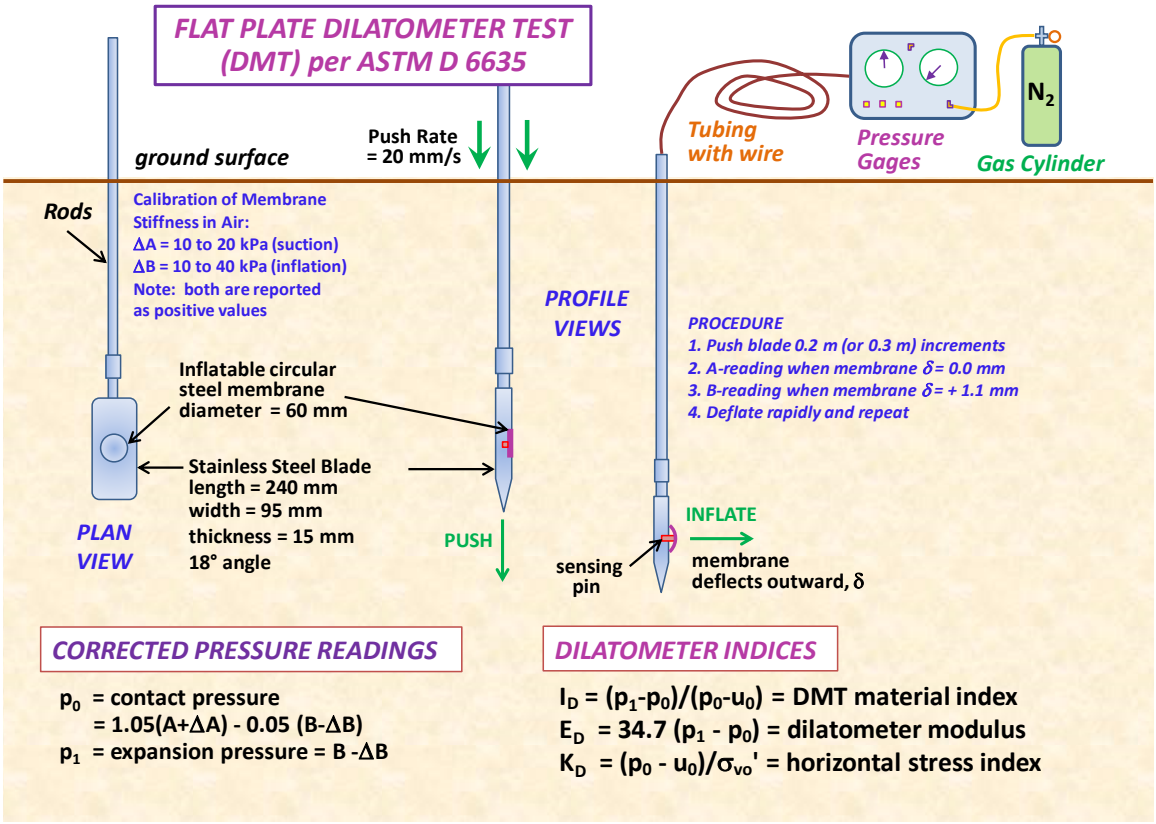

Figure A. 8. Illustration of Setup and Procedure for the Flat Dilatometer Test (DMT)

The two dilatometer pressures, p_0 and p_1, are combined with the hydrostatic water pressure, u_o, to provide three index parameters: (a) material index I_D, (b) horizontal stress index K_D, and (c) dilatometer modulus E_D. These were developed by Marchetti (1980) to provide information on the stratigraphy, soil types, and the evaluation of soil parameters. Hydrostatic water pressure (u_0) can be evaluated based on available groundwater table information, e.g. $u_0 = (z - z_w) \cdot \gamma_w$., where z_w is the depth of the ground water table and γ_w is the water unit weight.

The DMT material index, I_D, is related to the soil classification and is presented as:

$$I_D = (p_1 - p_0) / (p_0 - u_0) \quad [3]$$

The above definition of I_D was introduced having observed that the p_0 and p_1 profiles are systematically "close" to each other in clay and "distant" in sand. According to Marchetti (1980), the soil type can be identified: clay: $0.1 < I_D < 0.6$, silt: $0.6 < I_D < 1.8$, and sand: $1.8 < I_D < 10$. In general, I_D provides an expressive profile of soil type, and for normal soils, a reasonable soil description.

The horizontal stress index, K_D, is related to the in-situ horizontal stress-state of the soil. The index K_D will always be greater than K_0 due to disturbance caused during insertion of the blade. This parameter is presented as:

$$K_D = (p_0 - u_0)/\sigma_{v0}^{'} \quad [4]$$

K_D provides the basis for several soil parameter correlations and is a key result of the dilatometer test. The horizontal stress index K_D can be regarded as K_0 amplified by the penetration (Marchetti et al., 2001). In NC clays; with no aging, structure, cementation; the value of $K_D \approx 2$. The K_D profile is similar in shape to the OCR profile with depth, hence

can be used to better understand the soil deposit and its stress history (Marchetti 1980, Jamiolkowski et al. 1988).

For the 60 mm membrane diameter and required 1.1 mm displacement, it is found (Marchetti 1980):

$$E_D = 34.7(p_1 - p_0) \quad [5]$$

Figure A. 9 shows photos of the Georgia Tech cone truck that was used to conduct the DMT at W-21 site, and Figure A. 10 presents the results of three flat plate dilatometer soundings conducted at the W-21 test site using the GT cone truck showing the corrected p_0 and p_1. Figure A. 11 shows the DMT-1 sounding with the corrected p_0 and p_1 readings along with the interpreted material index (I_D), horizontal stress index (K_D), and dilatometer modulus (E_D) profiles with depth. As illustrated from the material index profile, the soils at the W-21 site are mostly silt to sandy silt, with some silty sands, as anticipated from the Piedmont geology.

Figure A. 9. Georgia Tech Cone Truck

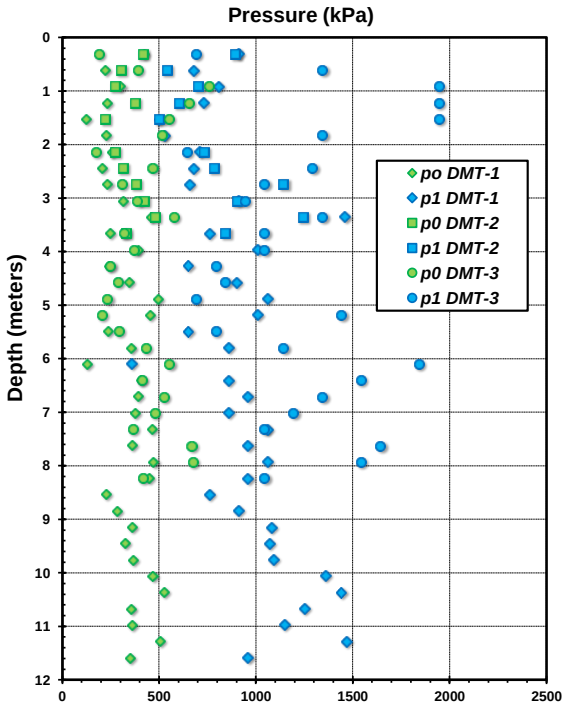

Figure A. 10. DMT soundings conducted at W-21 site on Georgia Tech campus by the GT cone truck

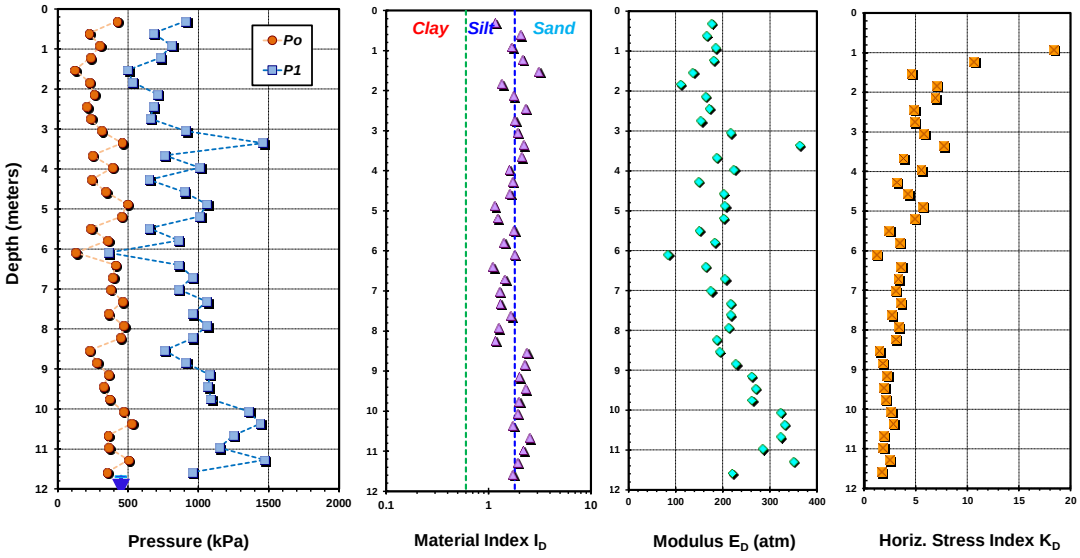

Figure A. 11. DMT-1sounding at the W-21 test site: (a) p_0 and p_1 readings, (b) material index (I_D), (c) dilatometer modulus (E_D); (d) horizontal stress index (K_D)

As mentioned above, the ground water table is estimated to locate at around 40 feet below the ground surface. Based on the DMT sounding, the contact pressure p_0 ranges from 122kPa to 527kPa and the expansion pressure p_1 ranges from 360kPa to 1470kPa, the DMT material index I_D suggest that the subsoil consist of sandy silt to silty sand, which are typical geomaterial in the local geology.

A.5 Helical Probe Testing (HPT)

Helical probe tests (HPT) are a quick and economical means for manual field testing of soils to depths of 1.5 m with readings taken at 0.15-m intervals in only 10 minutes. HPT is a simple and inexpensive device which can provide quick and dependable means for evaluating geostratigraphic profiles and soil properties at relatively shallow depths. It is advantageous on small geotechnical projects because it is lightweight, portable, and can be performed by one person very quickly. Small cuttings are also available from the auger to confirm soil type. The idea of applying a measured torque to the top of a steel rod to advance a small auger was first used by Robinson and Taylor (1969). The torque required to turn the probe is used as an index measure of the natural soil's in-place strength or stiffness, or in the case of controlled fills, a measure of the degree of compaction. Preliminary ASTM reporting (Yokel and Mayne 1988) has determined that the HPT method correlates well to standard penetration testing (SPT: ASTM D 1586), cone penetration testing (CPT: ASTM D 5778), and flat plate dilatometer tests (DMT: ASTM D 6635).

Typical HPT soil probes are about 1.5 m (60 inches) long and manufactured using precision machined helical bits with a 19 mm (0.75 in) auger diameter welded at the rod

bottom. A hex coupler fits at the top of alloy steel shaft head to permit contact with the torquemeter. The entire system weighs approximately 2.2 kg (4.8 lb) so that the device is easily carried to the field for deployment by a single individual. Components of the HPT are shown in Figure A. 12.

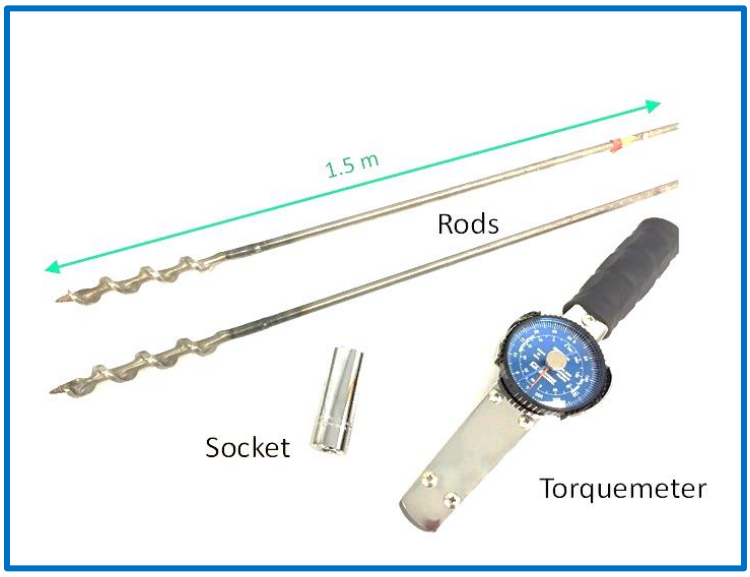

Figure A. 12. Helical probe testing (HPT) equipment including steel rod with augers, rods, socket, and torquemeter

The HPT can be used for exploration of natural soils and/or compacted fills (Yokel and Mayne 1986, 1988). A moment is applied at the top of the rod and the torque is measured at 150 mm (6 in) intervals during the auger penetration. For the operation of the helical probe, a beam style torque wrench is fitted to the hex coupler using a socket. The rods are then rotated by hand using the wrench at about 90°/s while the peak torque is noted. The value of torque is used as a measure, usually in either unit of inch-pounds (in-lb) or Newton-meters (N-m).

A.6 HPT at W-21 site

Agaiby et al. (2018) compiled HPT readings from 58 tests from 18 project sites within the Washington, DC - Virginia - Maryland area where the data are grouped from two main geologic regions: (a) Appalachian Piedmont Region and (b) Atlantic Coastal Plain. For the Piedmont region, the ground is underlain by residuum derived by the in-place weathering of metamorphic and igneous bedrock. The residual soils are often found to be silty, ranging from micaceous fine sandy silts to silty fine sands, that transition with depth to saprolites, partially-weathered rocks, and bedrock refusal. In contrast, the Atlantic Coastal Plain consists of various marine sediments that were deposited in various times ranging from very old Cretaceous to Miocene to recent Holocene ages, including complex interbedding of clays, silts, sands, and gravels. The results were used to develop correlations with the torque readings within the shallow depths where HPTs were performed. These relationships can be used for estimating corrected cone tip resistance (q_t) or uncorrected cone tip resistance (q_c) from CPTu, or the dilatometer modulus (E_D).

A number of helical probe tests were recently performed at the site that has been used for class demonstrations on campus over the past several years. The results of 4 helical probe tests advanced to depths of 1.1 meters are presented in Figure A. 13. The mean torque (t_{HPT}) from these series is also shown.

The measured cone tip readings from aforementioned CPTu sounding conducted at the same site are present in Figure A. 14 over a shallow depth range of 1.2 meters. According to Agaiby et al. (2018), the correlation between the measured uncorrected cone tip resistance q_c in sand and the torque readings (t_{HPT}) can be expressed as:

q_{cSANDS} (bar) $\approx$ 0.8 t_{HPT} (in-lb) [6]

the estimated cone tip resistance obtained from the mean helical probe torque readings using Equation [6]. A rather good agreement is observed indicating the general applicability of using the HPT to estimate the cone tip resistances at shallow depths. For other geologic settings, a localized calibration between CPT and HPT would be warranted in order to verify the trends and confirm the relationships for general use in geotechnical engineering practice.

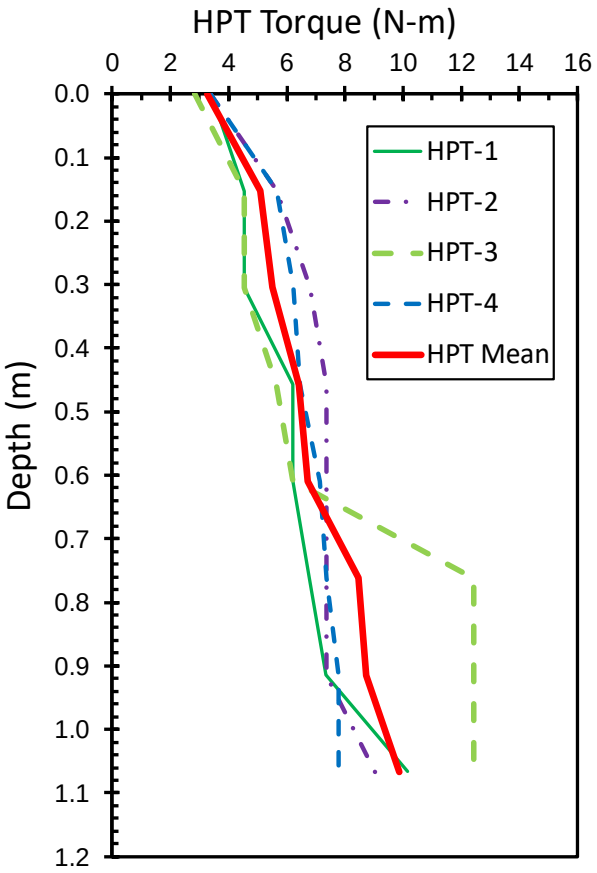

Figure A. 13. Results from four helical probe soundings at the Georgia Tech W21 test site with mean trend

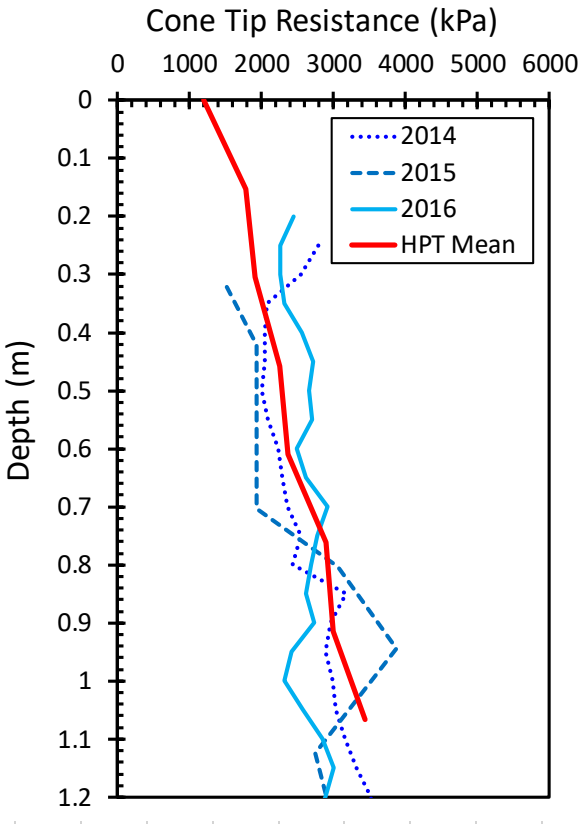

Figure A. 14. Estimated cone tip resistance (q_c) from mean helical probe readings compared to in-situ measured values at Georgia Tech W21 test site

The dilatometer modulus (E_D) evaluated by the DMT data at the same site is also compared with the estimated moduli by HPT reading using the following equation proposed by Agaiby et al. (2018):

$$E_D \text{ (MPa)} \approx 0.2\ t_{HPT} \text{ (in-lb)} \qquad [7]$$

From the presented results shown by Figure A. 15, a fair to good agreement is evident, indicating the possibility of using HPT in estimating dilatometer moduli at shallow depths.

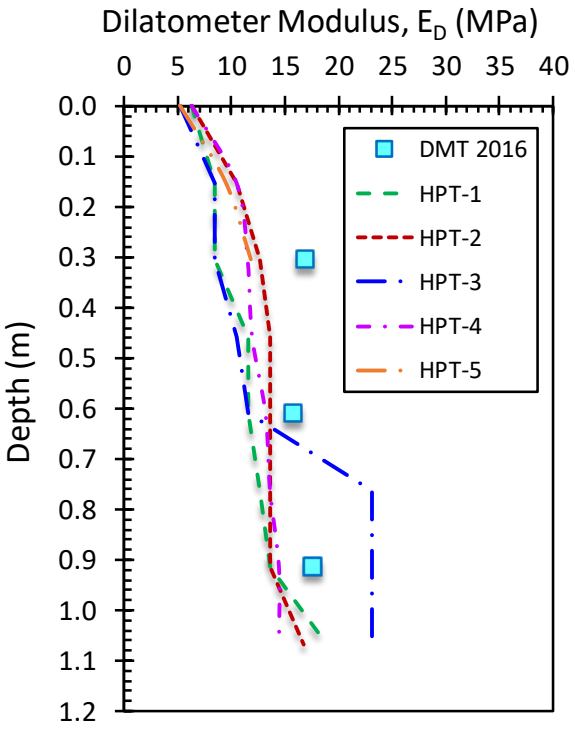

Figure A. 15. Measured dilatometer modulus (E_D) and estimated profiles from individual helical probe readings at Georgia Tech W21

APPENDIX B. LABORATORY TRIAXIAL TESTING AT GEOTECHNICAL LAB, GOLDER ASSOCIATES INC. ATLANTA, GA

B.1 Introduction

Even though the focus of the author's research is on the application of piezocone penetration test (CPTu) and flat plate dilatometer (DMT), it is critical for the author to gain sufficient knowledge on laboratory testing, especially on the triaxial test as it is adopted as the benchmark reference test to calibrate the results interpreted from CPTu and DMT. This appendix illustrates the findings of the triaxial tests conducted by the author during his visit to the geotechnical lab of Golder Associate Inc, located in Atlanta, GA in November 2017.

B.2 Purpose of triaxial tests

The triaxial test is one of the most versatile and widely performed geotechnical laboratory tests, allowing the shear strength and stiffness of soil and rock to be determined for use in geotechnical design. The purpose of performing triaxial tests is to determine the mechanical properties of the geomaterials. Advantages over simpler procedures, such as the direct shear test, include the ability to control specimen drainage and take measurements of pore water pressures. Primary parameters obtained from the test may include the angle of shearing resistance ϕ', cohesion intercept c', and undrained shear strength s_u, although other parameters such as the shear stiffness G and permeability k may be also determined. It is assumed that the soil specimens to be tested are homogeneous and representative of the material in the field, and that the desired soil properties can in fact be obtained from the triaxial testes, either directly or by interpretation through some theory.

The capability to seek stress-strain relations, volume change or pore pressure behavior, and shear strength of the soil makes triaxial testing ideal when it comes to evaluation of the mechanical properties of the geomaterial. However, it the crucial that the natural soil deposit or the fill from which soil samples have been taken in the field are sufficiently uniform that the soil samples possess the properties which are appropriate and representative of the soil mass in the field.

B.3 Common types of triaxial test

There are three primary triaxial tests conducted in the laboratory, each allowing the soil response for different engineering applications to be observed. There are

- Unconsolidated Undrained test (UU)
- Consolidated Drained test (CD)
- Consolidated Undrained test (CU)

Work by Keaveny & Mitchell (1986) and Baligh (1984) show that triaxial compression mode dominates at the cone tip. Thus, this research program adopts the consolidated undrained test of compression mode as the benchmark reference test to calibrate the effective friction angle ϕ' evaluated by the CPTu and DMT data in fine grained soils as it allows strength to be determined based on the effective stresses (i.e. ϕ' and c') when permitting a faster rate of shearing compared with the drained test. This is achieved by recording the excess pore pressure change within the specimen as shearing takes place. These included isotropically consolidated (undrained triaxial compression (CIUC)), K_0-consolidated (CK_0UC), as well as general anisotropic (undrained consolidated anisotropic (CAUC)) types.

Triaxial test procedures generally follow ASTM standards (ASTM (2011) D4767) or other recognized equivalent guidelines (e.g., Bishop and Henkel 1962; Germaine and Germaine 2009; Lade 2016). The consolidated undrained compression test typically consists of four main stages: specimen preparation, saturation, consolidation, and shearing. Figure B 1 shows typical components of triaxial apparatus.

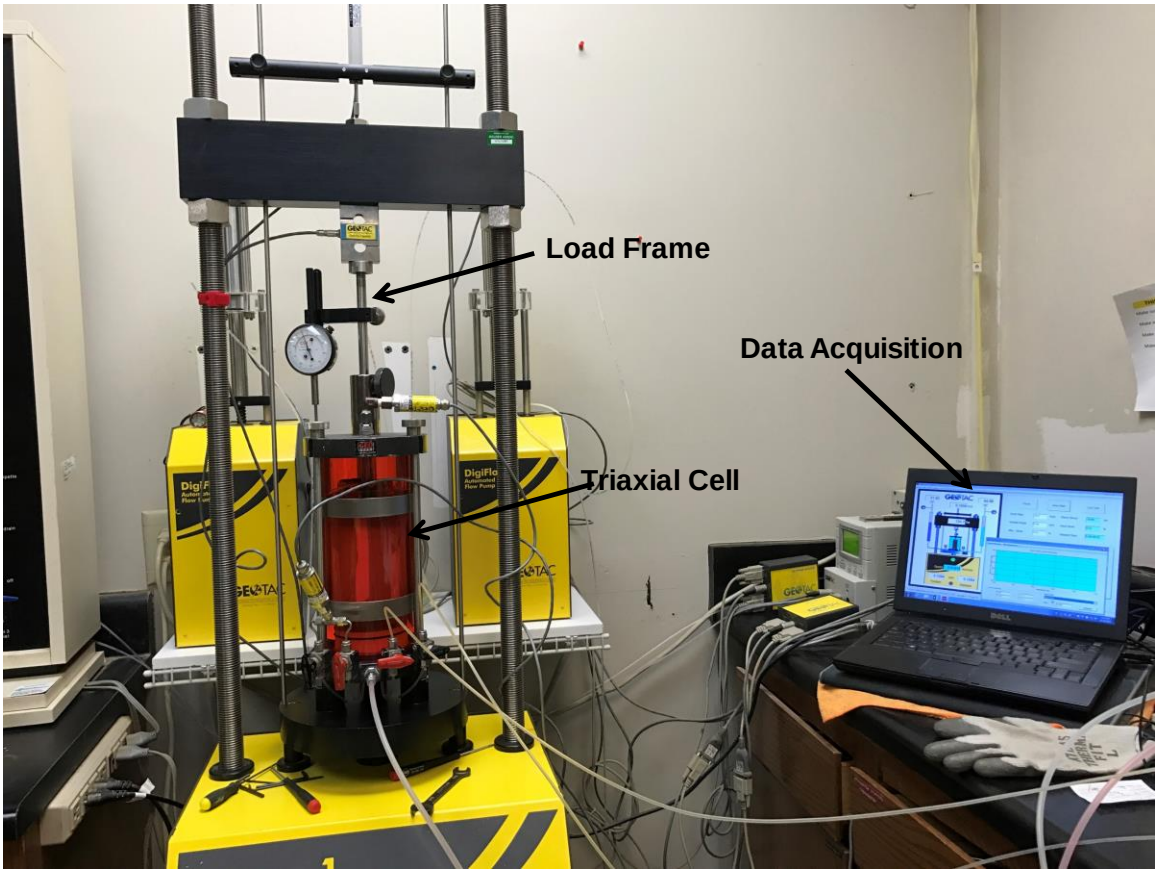

Figure B 1. Typical Triaxial Test Components

B.4 Triaxial Testing at the Geotechnical Lab, Golder Associates Inc

The author visited the geotechnical lab of Golder Associates Inc at Atlanta, GA in November 2017 and conducted a series of consolidated undrained (CU) triaxial

compression test with the help of the lab technician. Figure B 2 shows some photos regarding specimen trimming, preparing apparatus for the test, specimen before and after the triaxial testing.

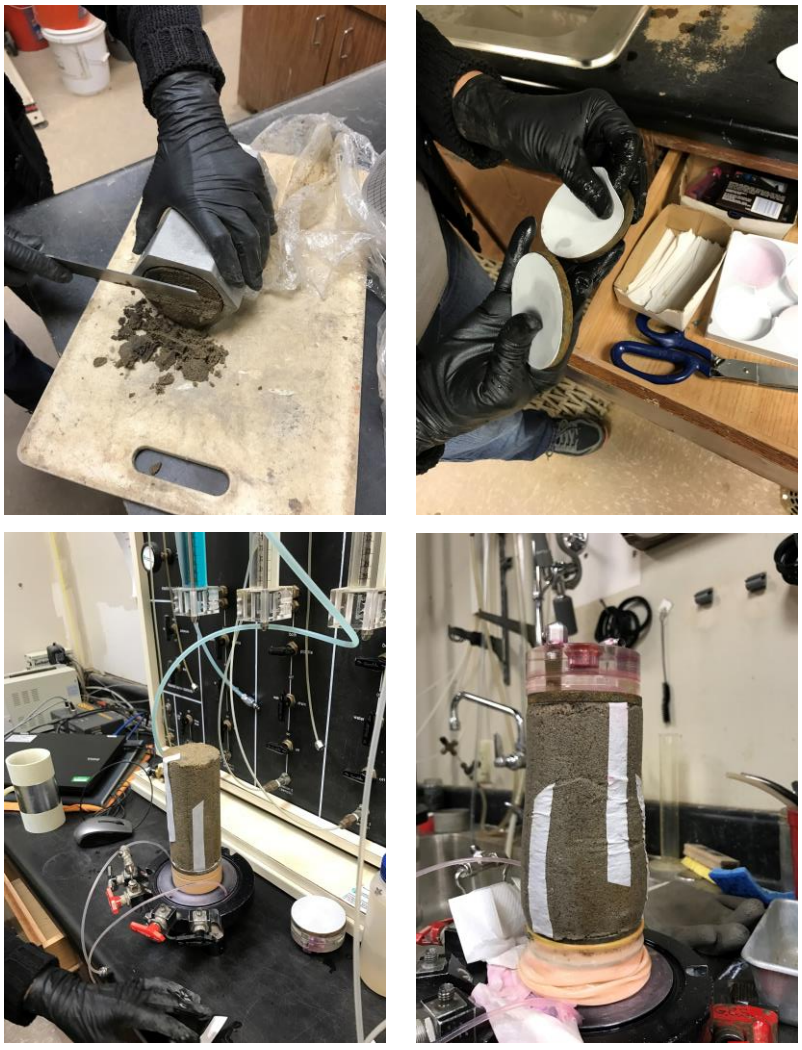

Figure B 2. Photos showing triaxial testing procedure: (a) trimming specimen, (b) preparing the top and bottom porous stones, (c) specimen before testing, and (d) specimen after testing

Figure B 3 shows the shear stress versus axial strain, and the excess porewater pressure versus of a representative triaxial compression test. It can be seen that the porewater pressure increases at the beginning of the shearing as the axial strain increases

and the shear stress reaches peak (42kPa) at about 1% strain, the decreases monotonically till the end of the strain and reaches a negative porewater pressure of -305kPa. The shear stress recorded increases with the axial strain and reaches the maximum shear stress at 15% strain of 566kPa.

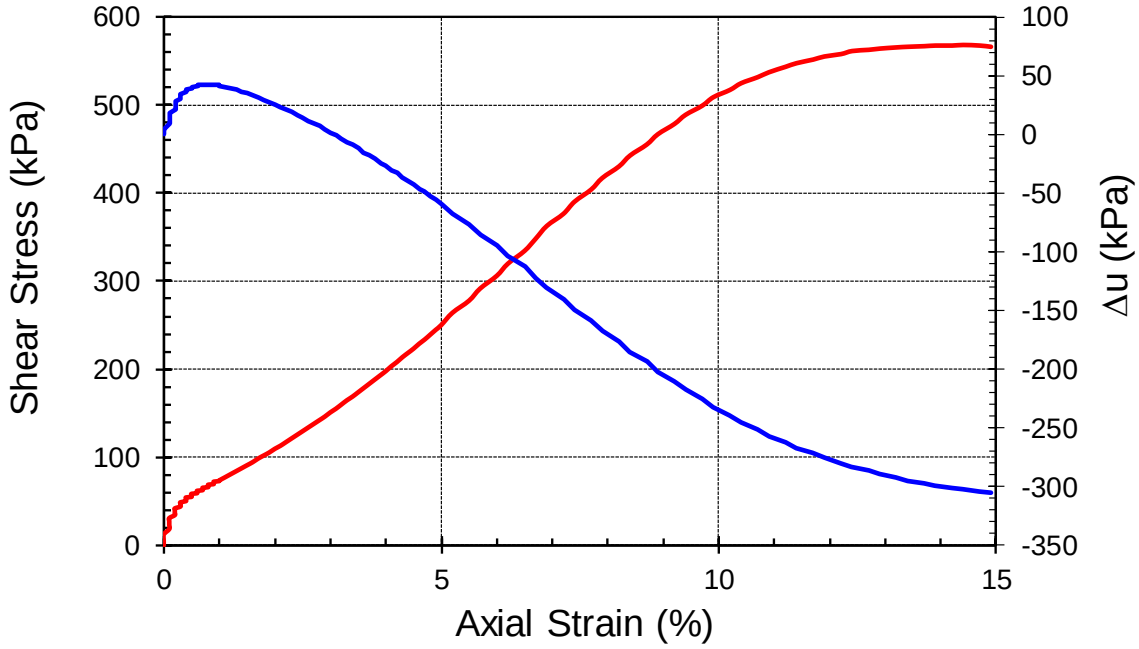

Figure B 3. Shear stress (red) and excess porewater pressure (blue) versus axial strain

The shear stress $s = \frac{1}{2}(\sigma_1 - \sigma_3)$ is plotted against the average stress $t' = \frac{1}{2}(\sigma_1' + \sigma_3')$ and the effective stress friction angle ϕ' is interpreted as 35.7°, as shown by Figure B 4.

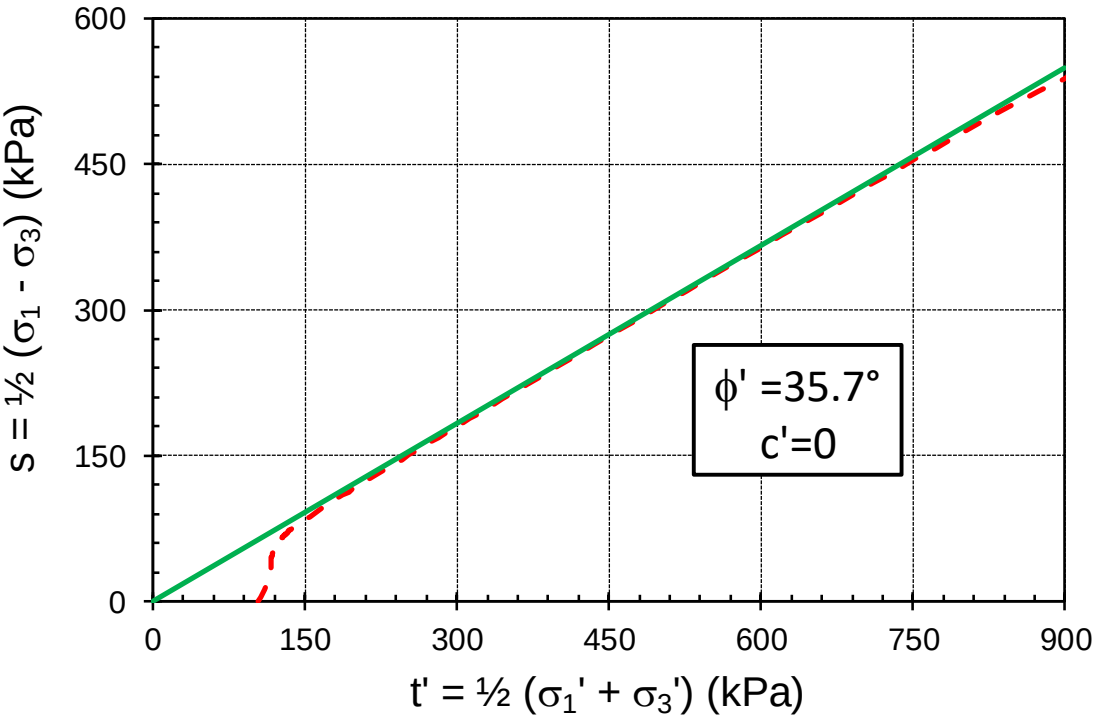

Figure B 4. Effective stress path in MIT t′-s diagram

APPENDIX C. RAW DATA FROM INVESTIGATED PIEZOCONE PENETRATION TESTS

This appendix contains the raw data from CPTu used in this research program.

17th St Canal, New Orleans, LA.

Data after Seed et al. (2006) (2008)

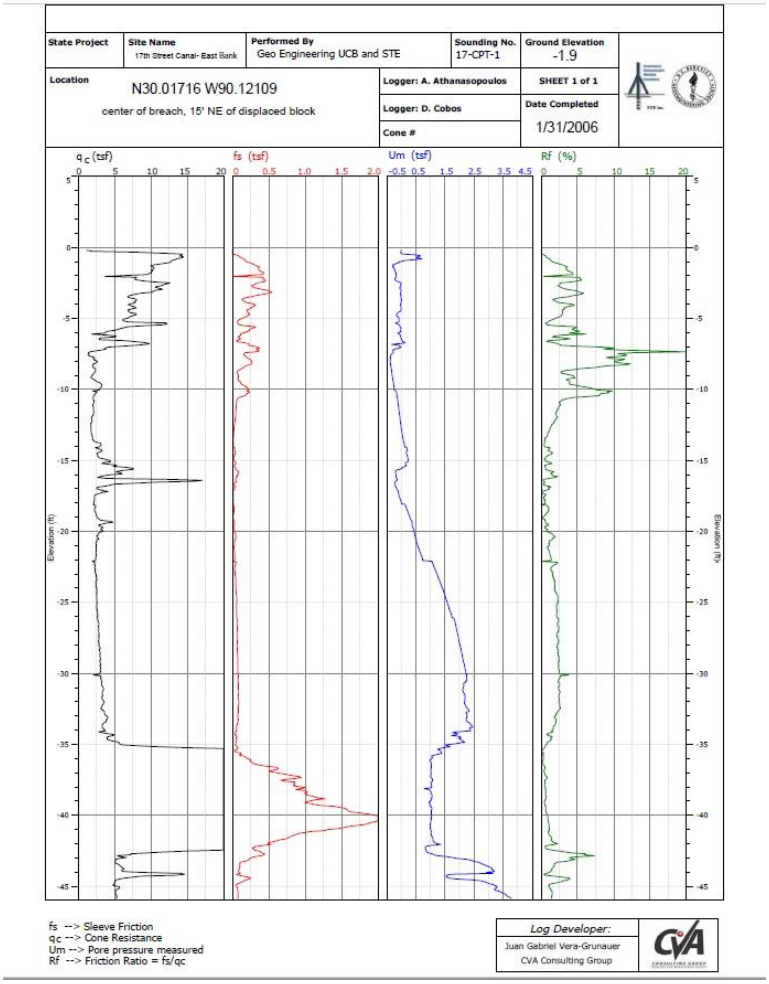

Adriatic shelf, Italy

Data after Sultan et al. (2008)

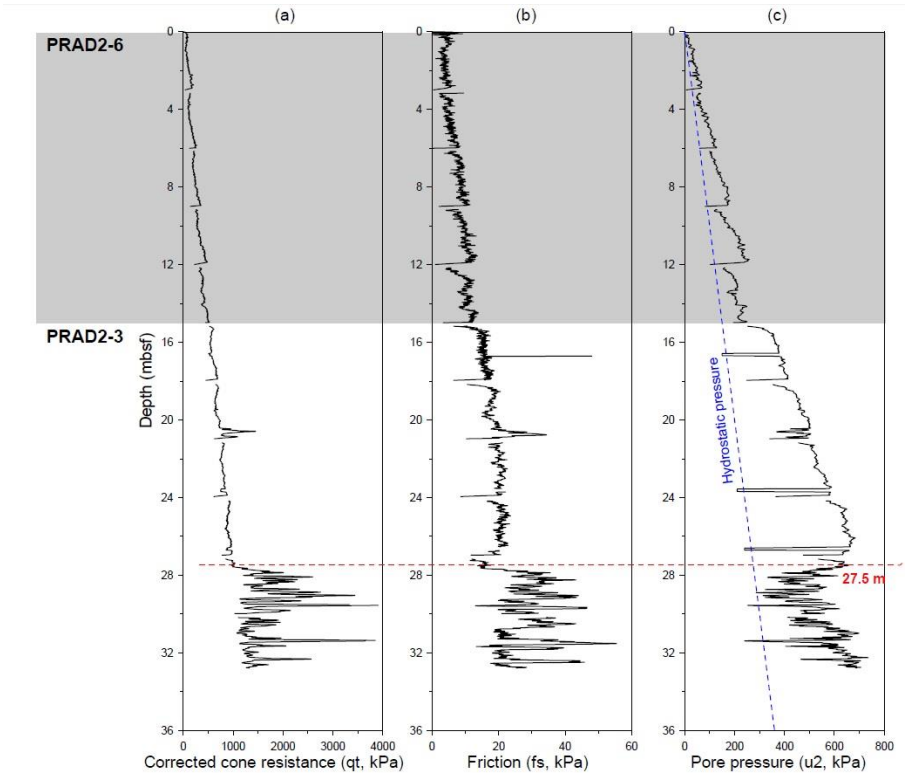

Agnesburg, Norway

Data after Åhnberg (1995)

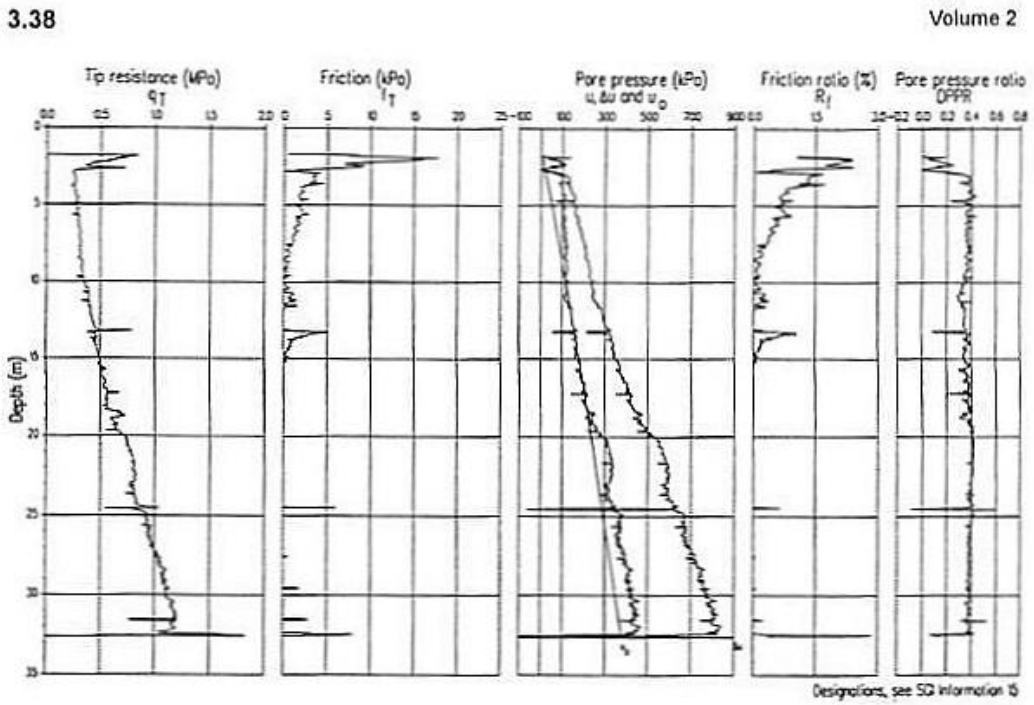

Figure 4. Results from CPT tests at borehole SGI 1.

Amazon River, Brazil

Sandroni et al. (2015)

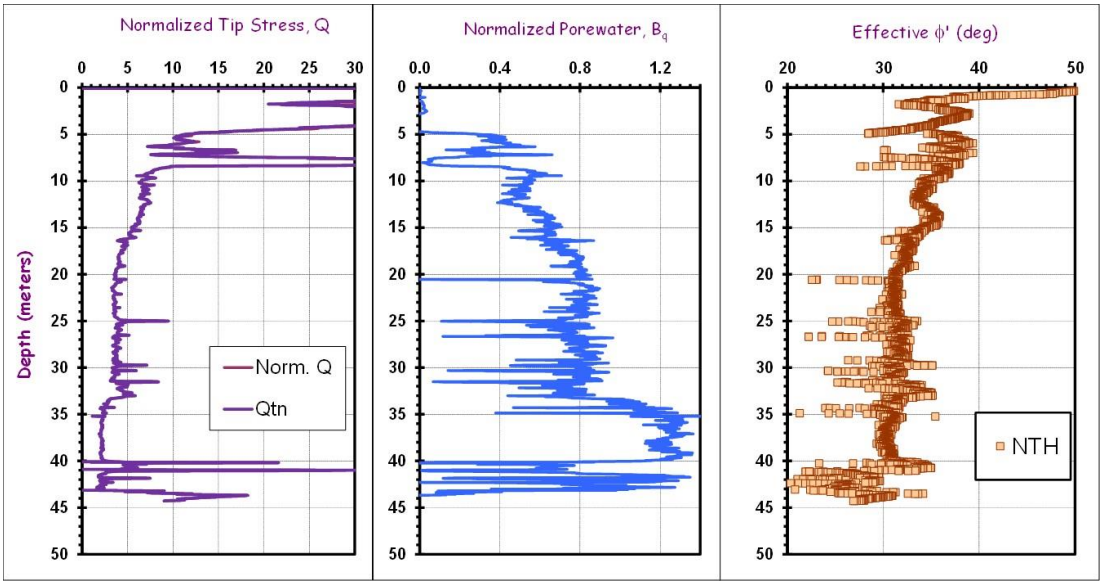

Amherst, MA

Data from GT in-situ testing group

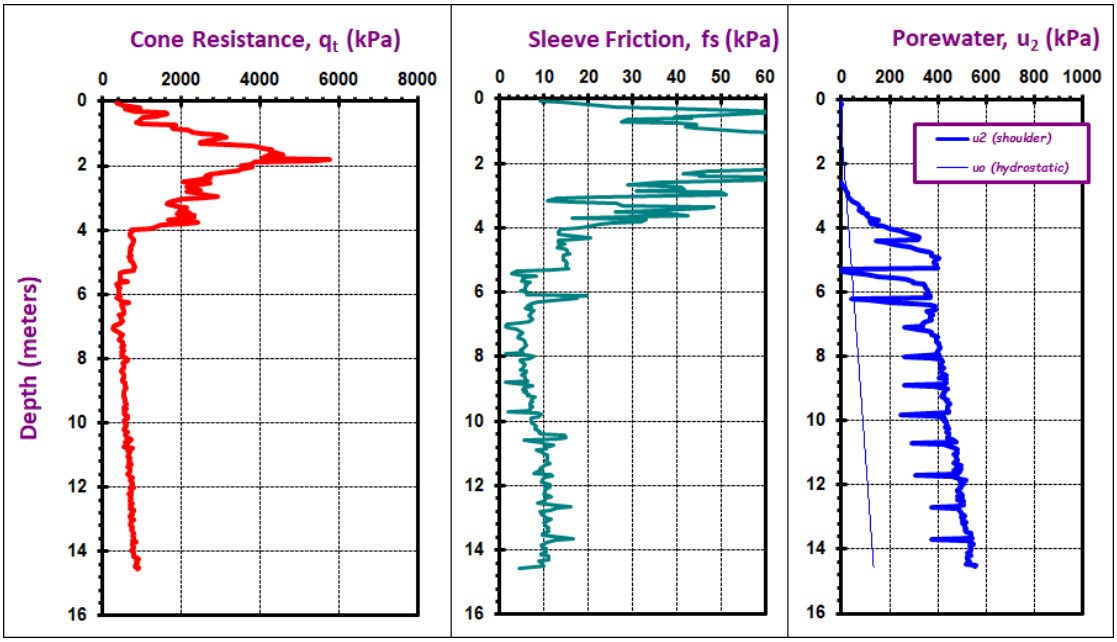

Anacostia NAS, Washington, DC

Data from Mayne (1987)

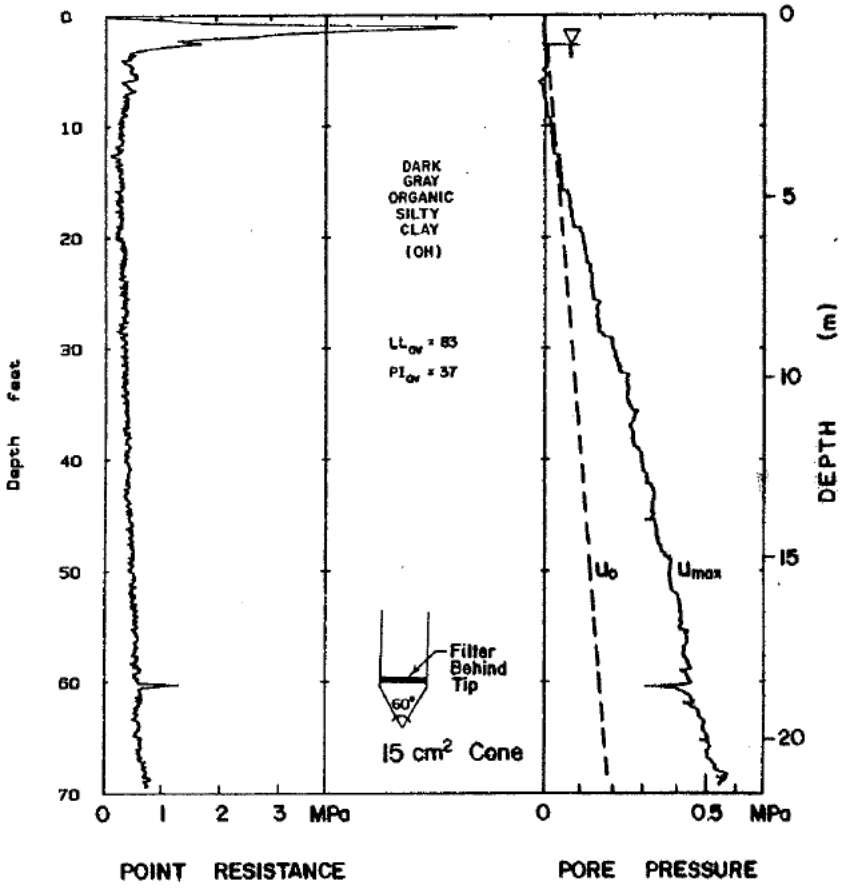

FIG. 2—*Typical piezocone sounding in Potomac River alluvial clay.*

Anchorage, AK

Data from Mayne & Pearce (2005)

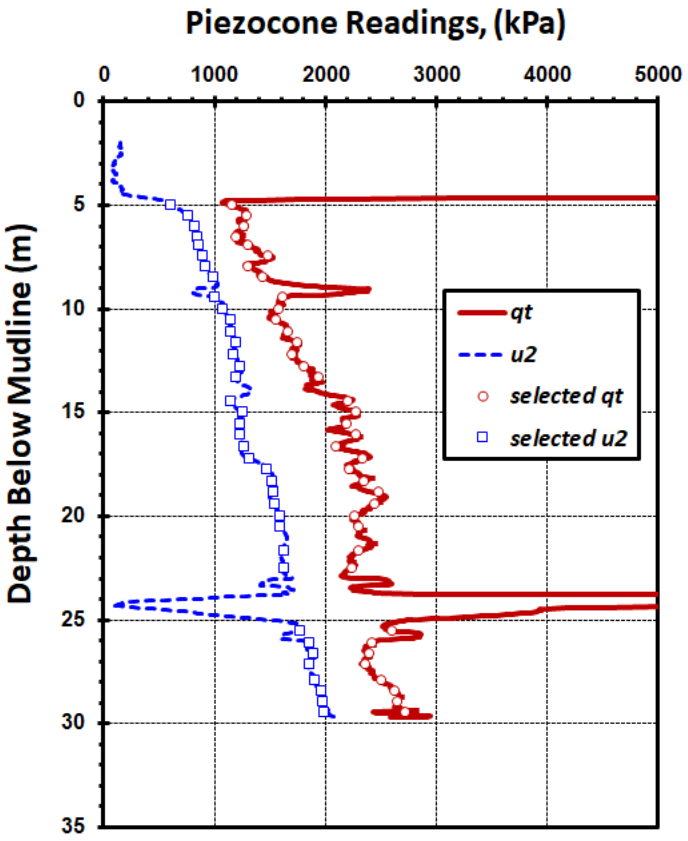

Ariake, Japan

Data from Watabe et al. (2004)

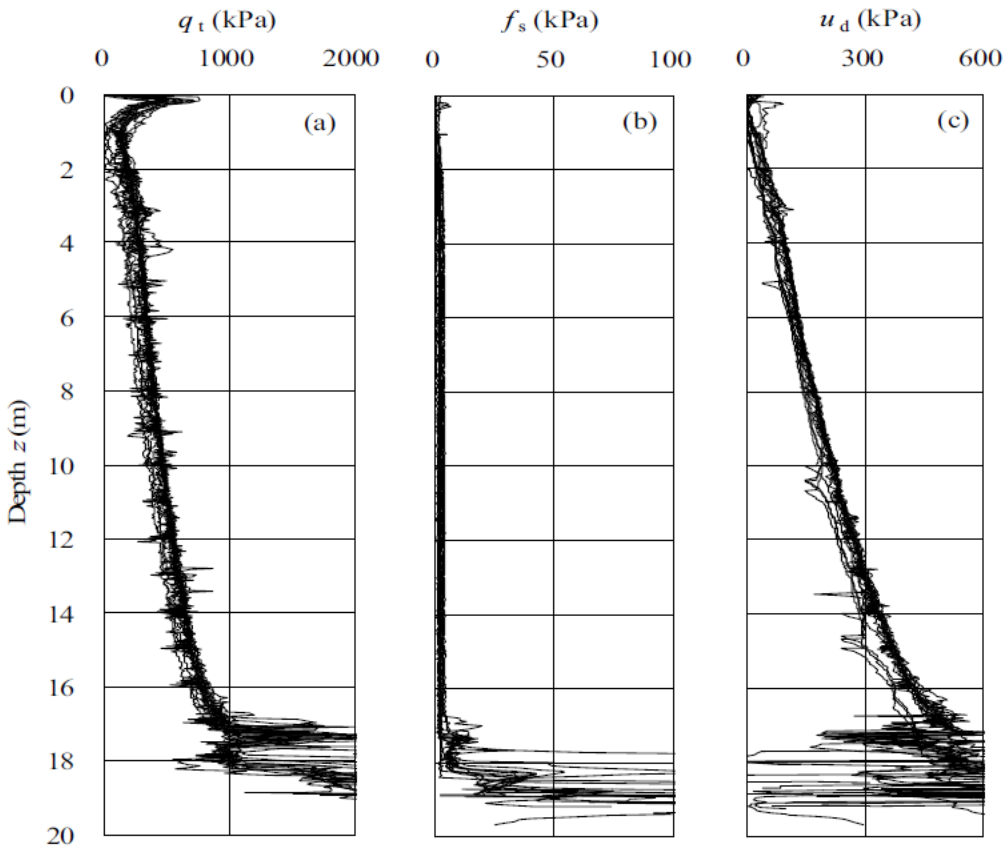

Athlone, Ireland

Data from Long and O'Riordan (2001)

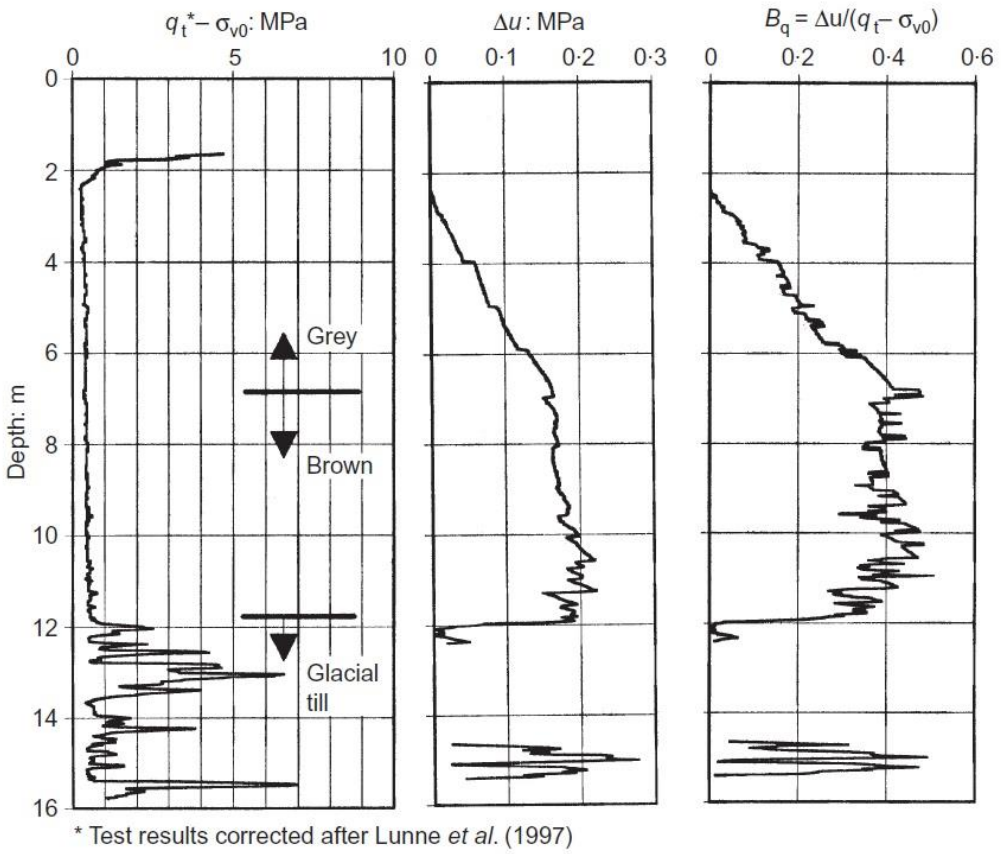

Bäckebol, Sweden

Data from Larsson & Mulabdić (1991)

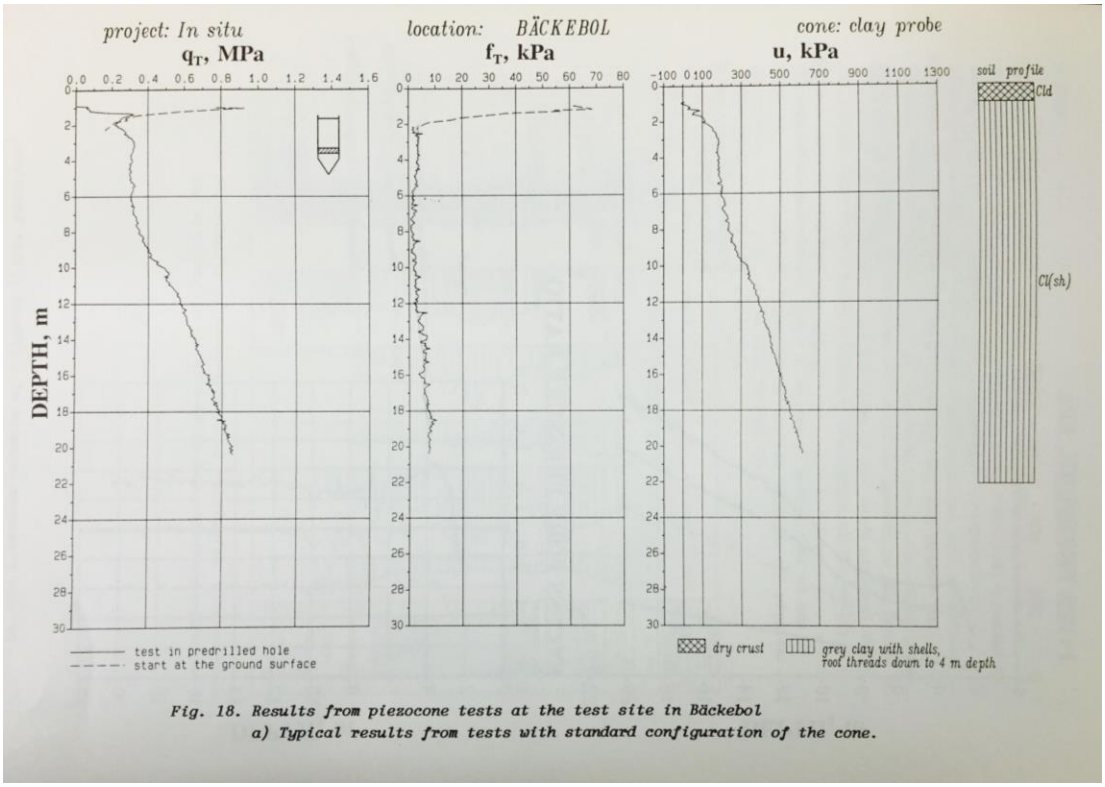

Fig. 18. Results from piezocone tests at the test site in Bäckebol
a) Typical results from tests with standard configuration of the cone.

Ballina, Australia

Data from Pineda et al. (2014); Kelly et al. (2017)

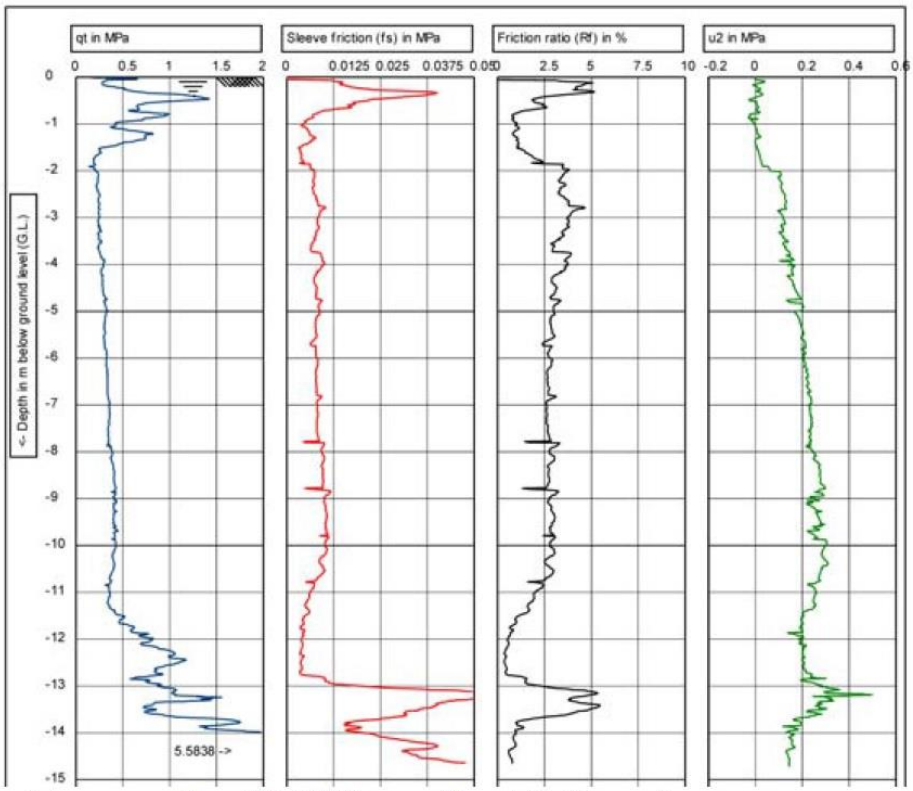

.e piston sampler. (b) CPTu profile at Ballina site

Bangkok, Thailand

Data from Watabe et al (2004)

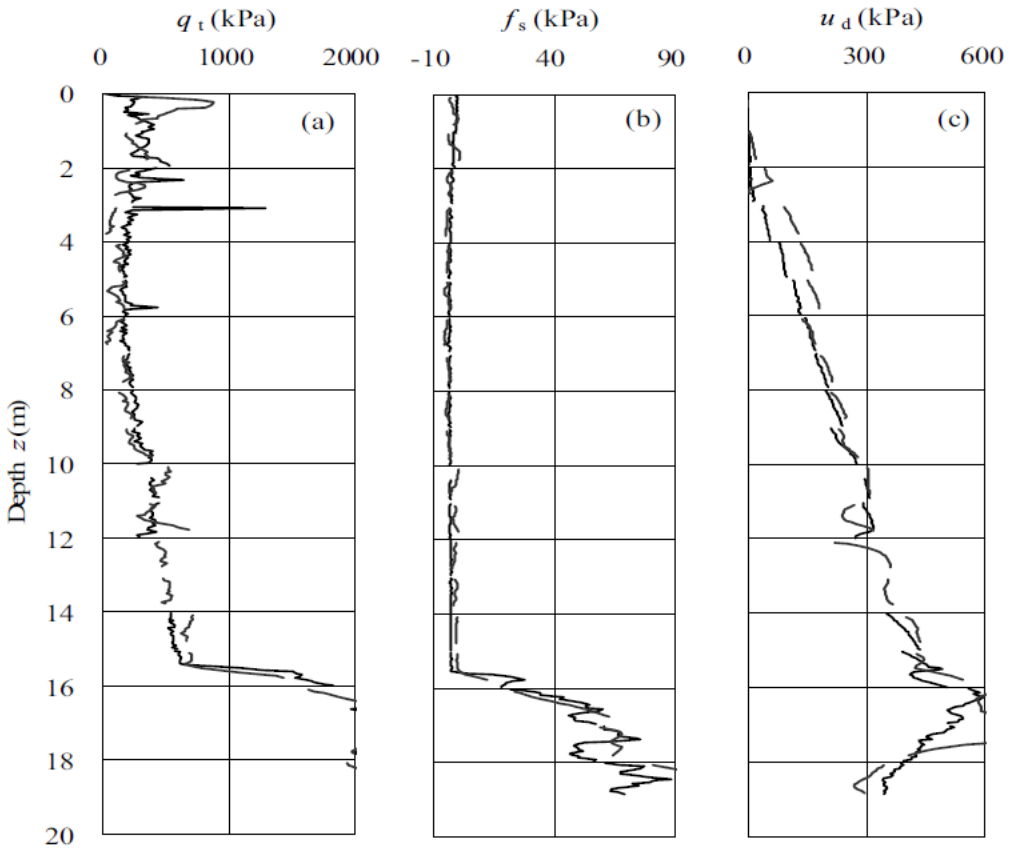

Figure 11. CPT and DMT results at Bangkok.

Barra da Tijuca, Brazil

Data from Almeida (2015)

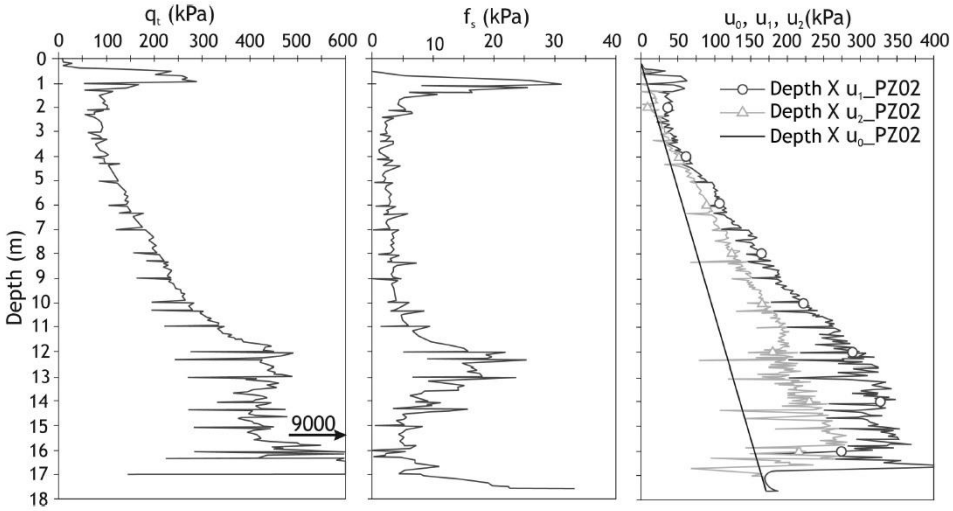

Figure 2.11 Typical results of a vertical piezocone test conducted in Barra da Tijuca (RJ). (A) q_t profile; (B) lateral friction strength profile, f_s; (C) pore pressure profile (Baroni, 2010).

Bassendean, Australia

Data from Suzuki (2015)

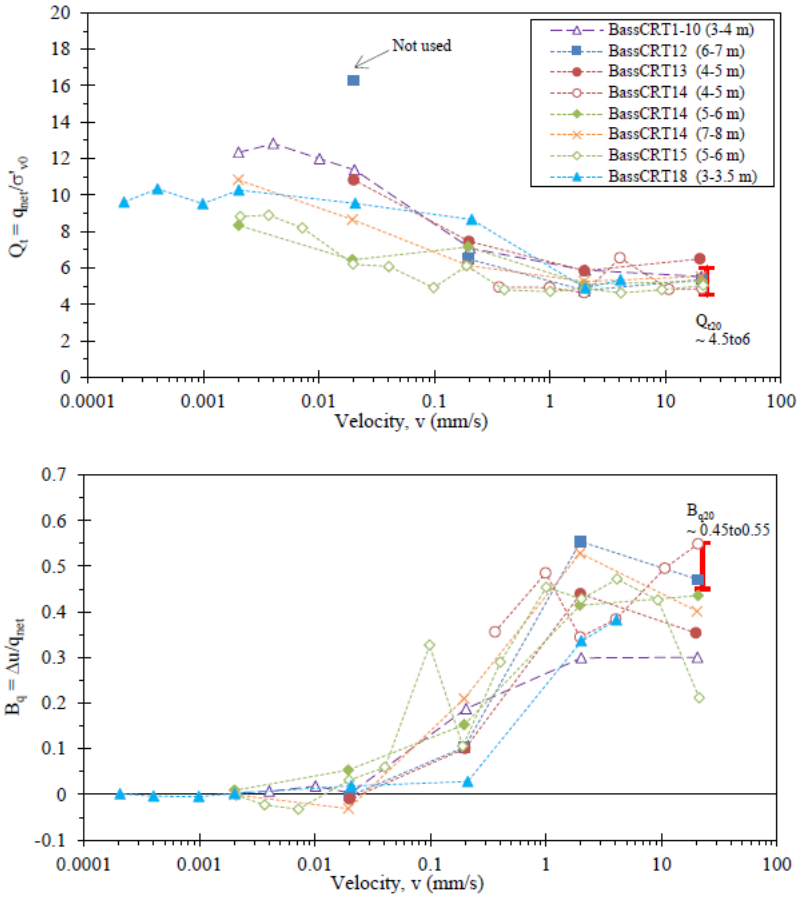

Baton Rouge, LA

Data from Chen & Mayne (1994)

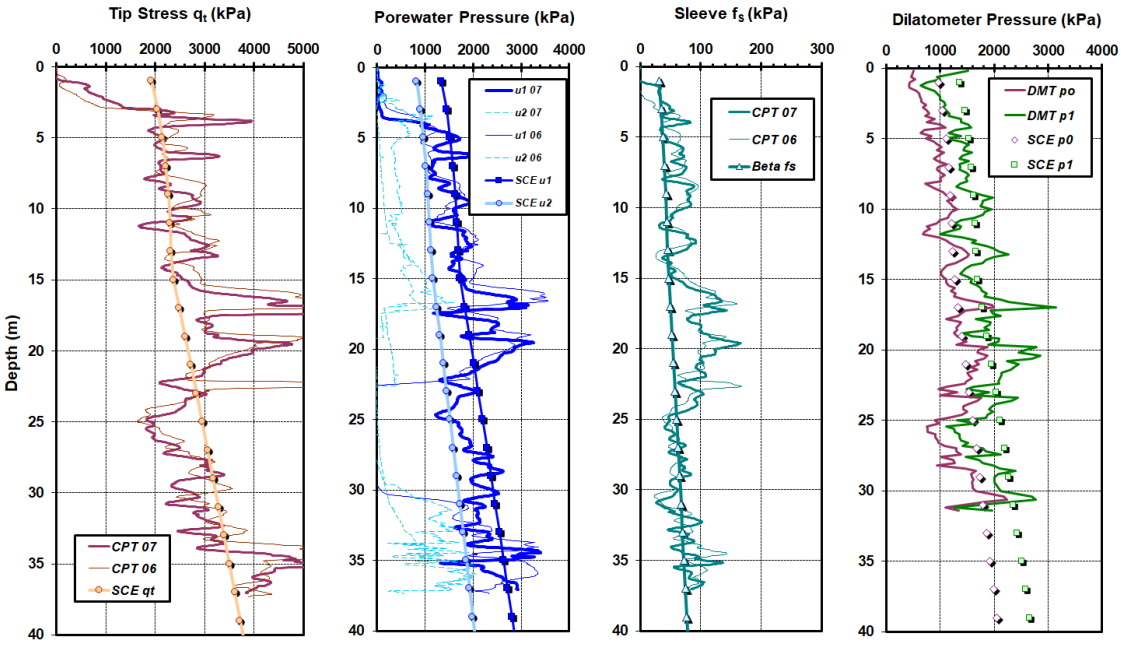

Baytown, TX

Data from Stuedlein et al. (2012)

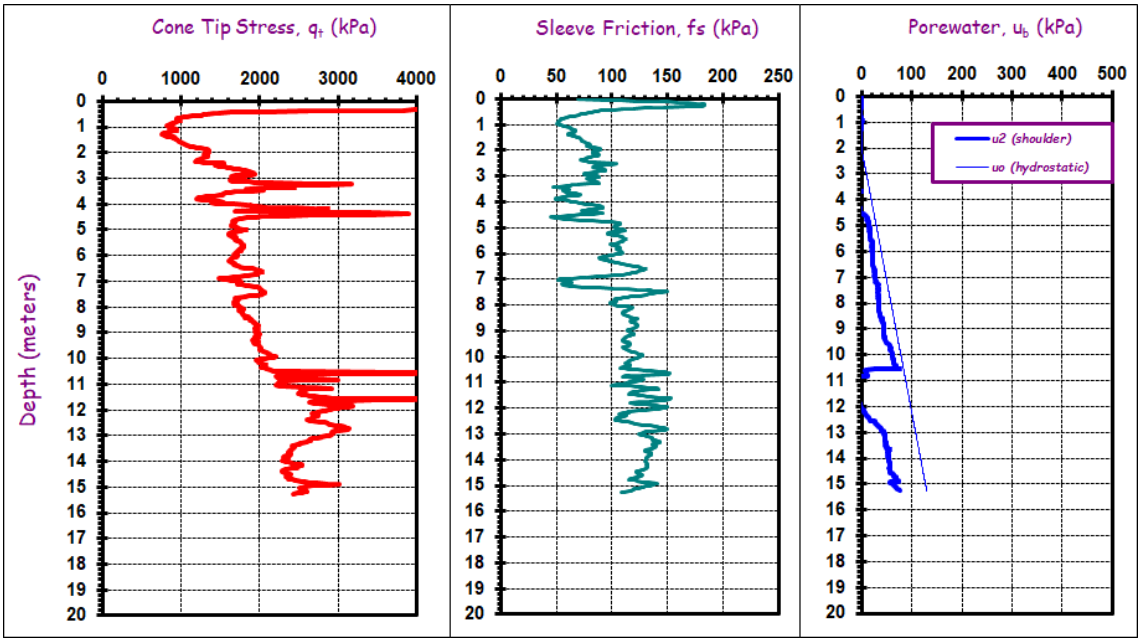

Boston Blue Clay, MA

Data from Whittle et al. (2001)

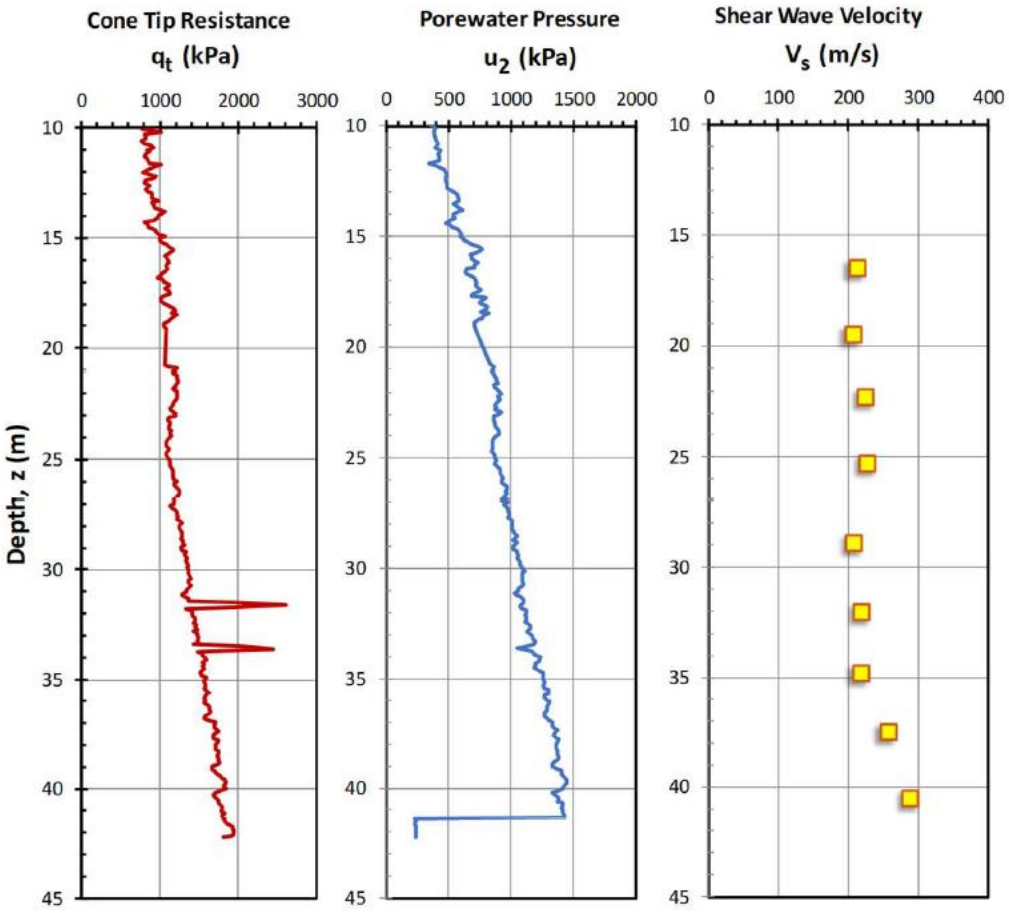

Belfast, Ireland

Data from CIUC Lehane (2003)

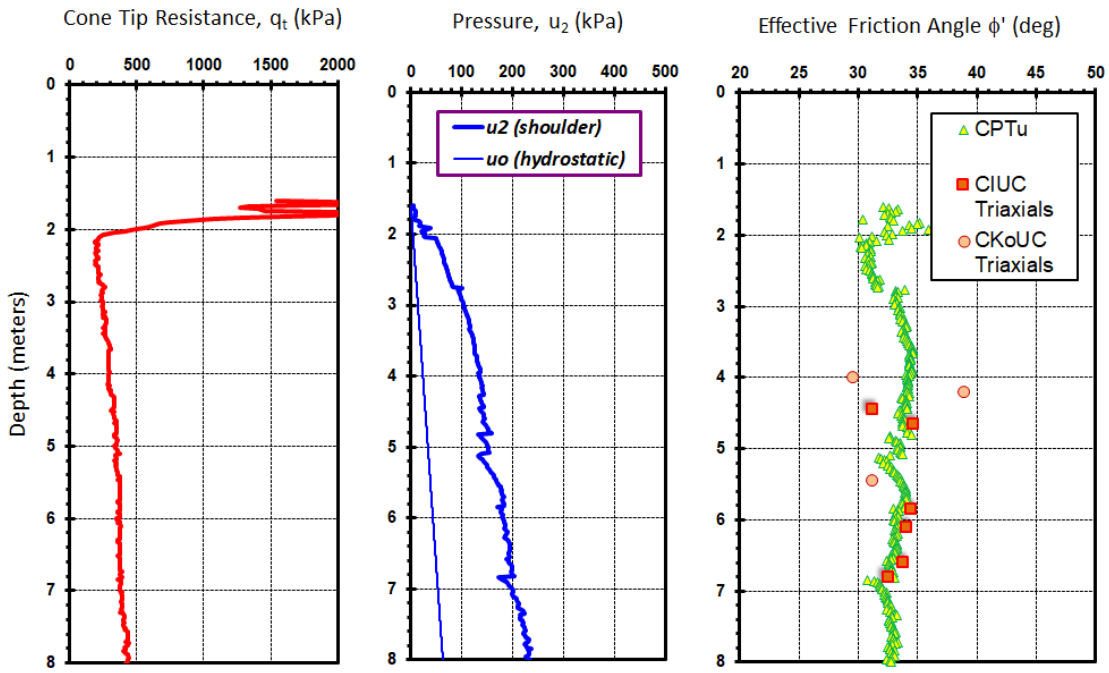

Berthierville, Canada

Data from Demers (2001) units in kPa

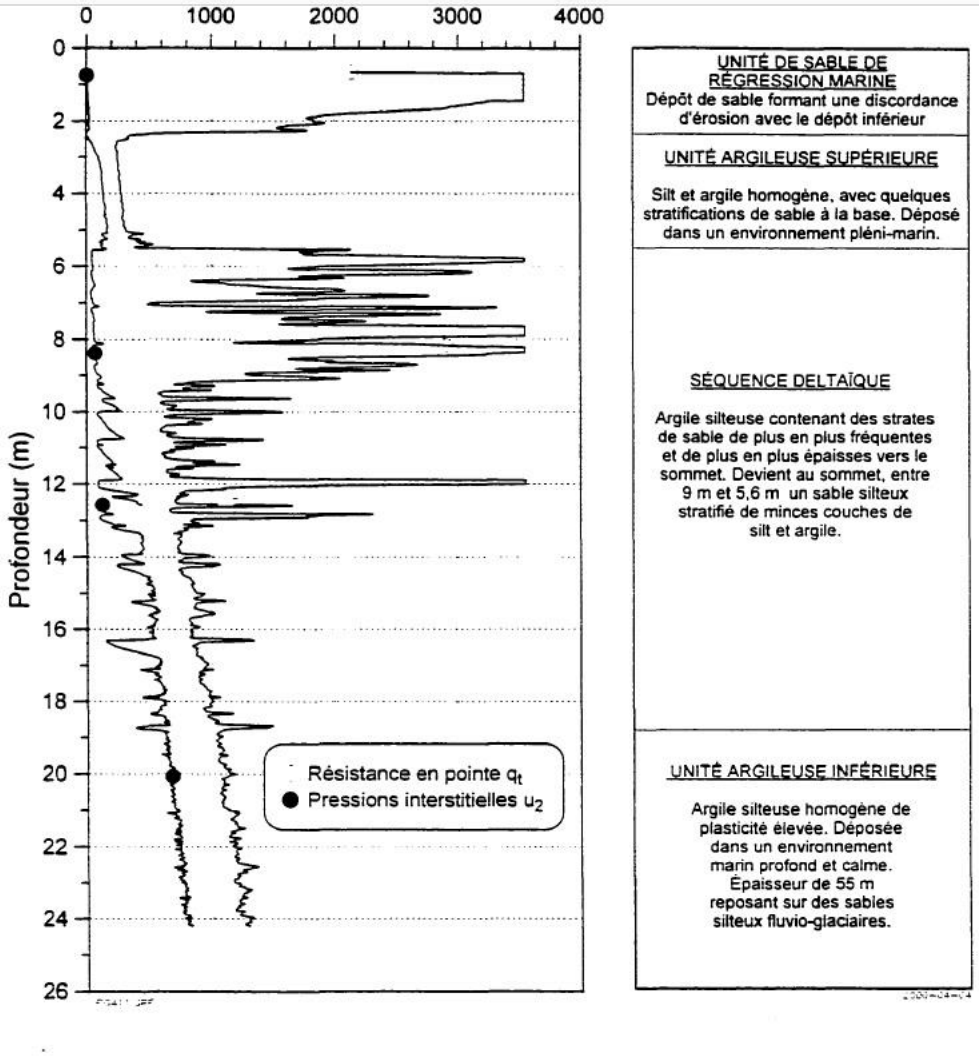

Figure 4.11: Profil au piézocône CPTU50, illustrant la stratigraphie locale. Berthierville.

Bogota, Columbia

Data shared by Mr. Edgar E. Rodíguez G

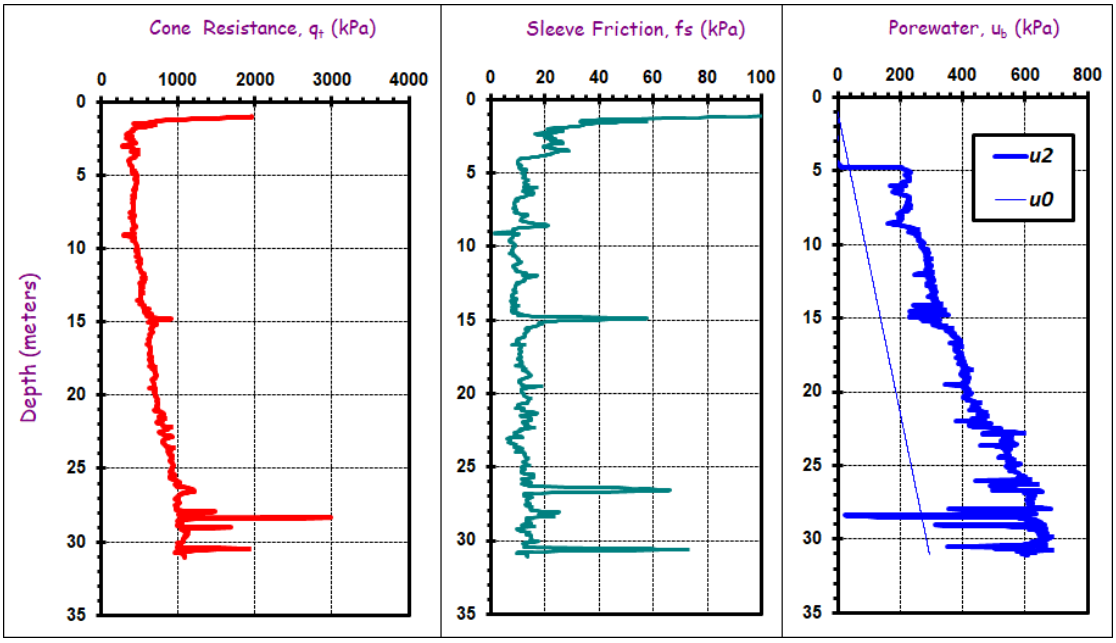

Bonneville, Utah

Data from Garner (2007)

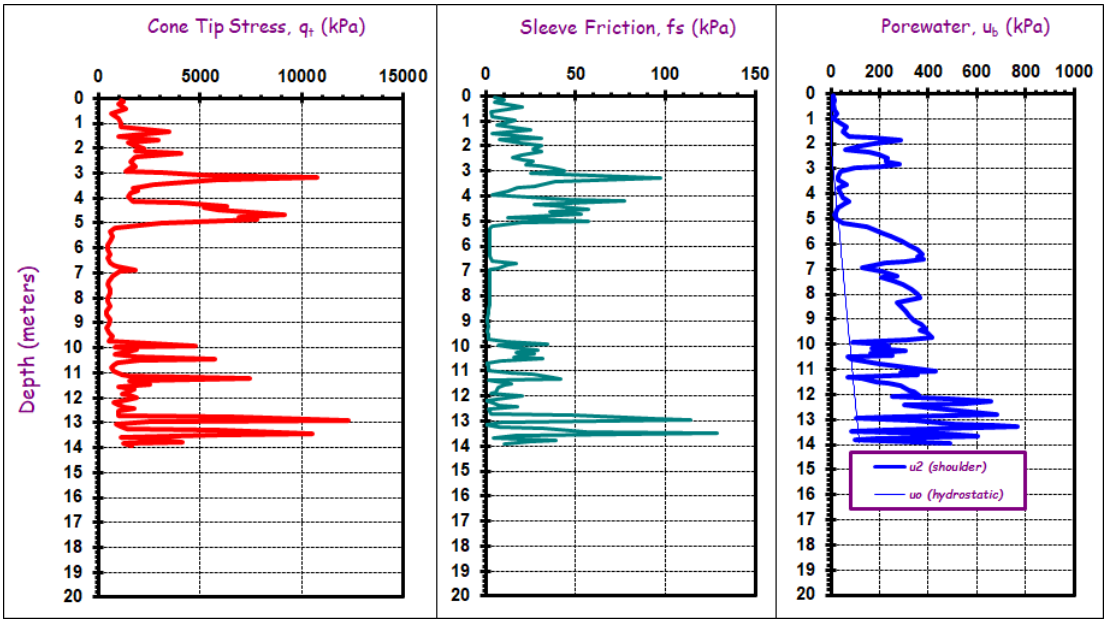

Bothkennar, Scotland

Data from Hight et al. (2003); Nash et al. (1992)

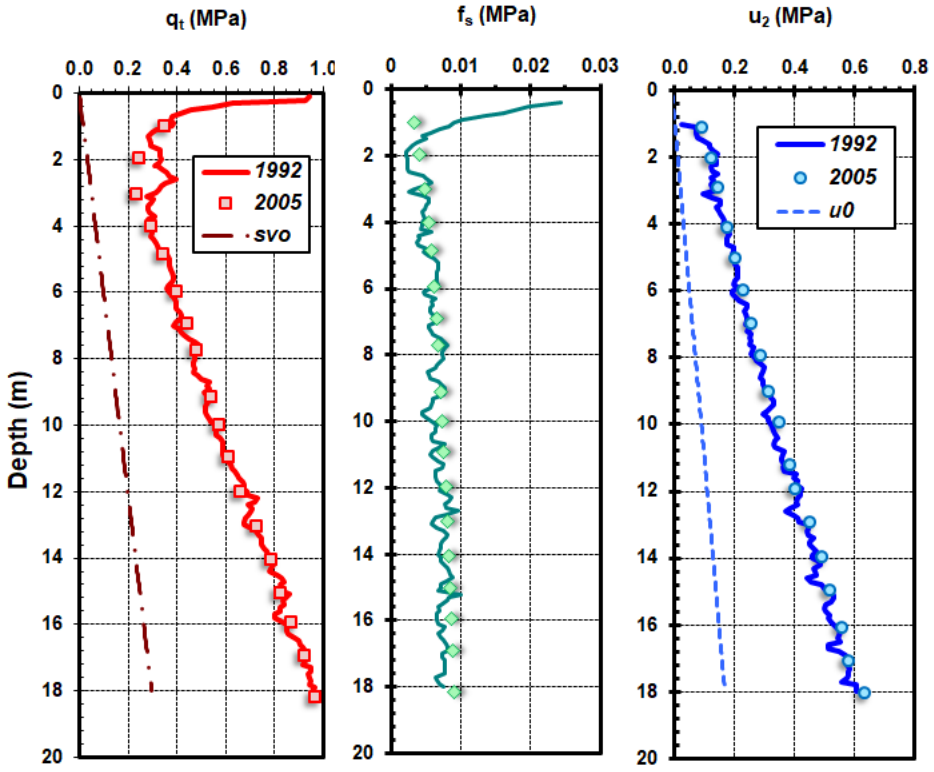

Brent Cross, UK

Data from Hight et al. (2003)

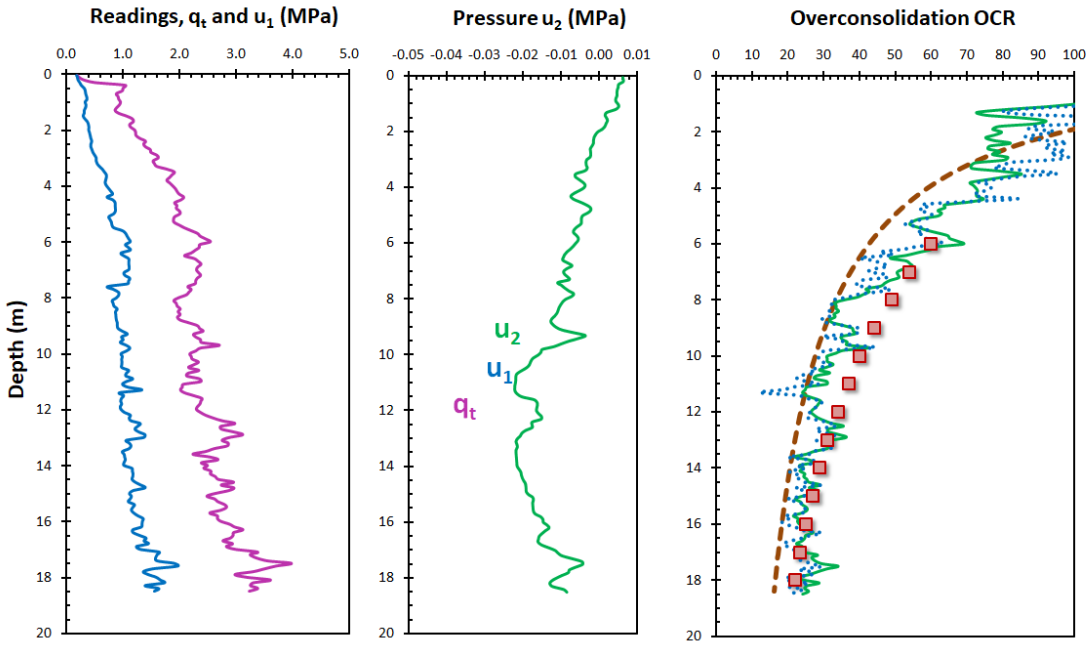

Broadback B6, Canada

Data from Demers (2001)

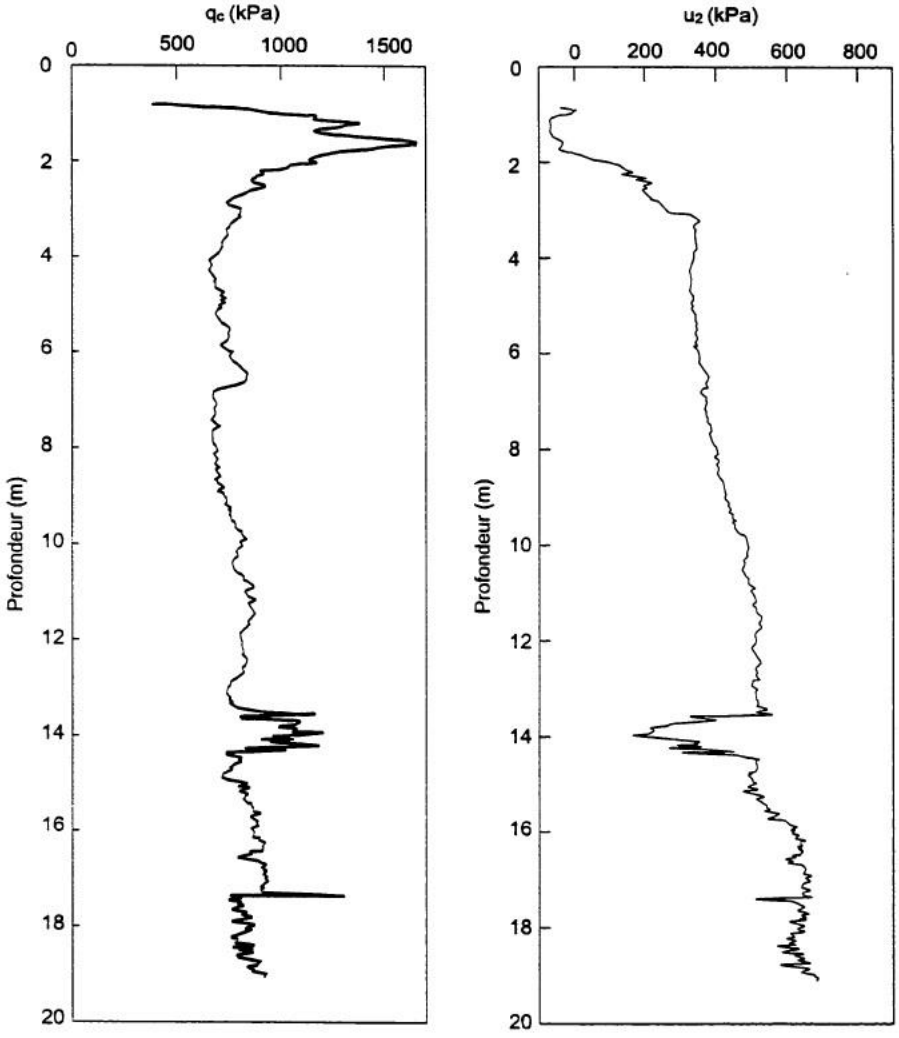

Figure 2.76 - Essais au piézocône au site B6, rivière Broadback (tiré de Tavenas et Tremblay, 1981).

Burswood, Australia

Data from Low et al. (2011)

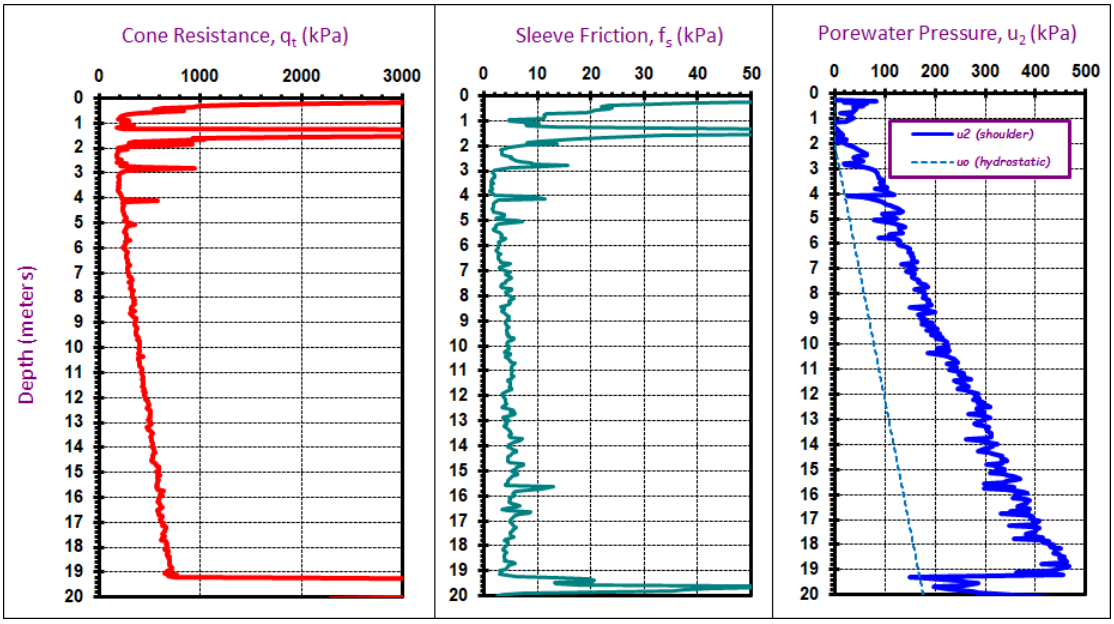

Busan, South Korea

Data from Chung et al (2012)

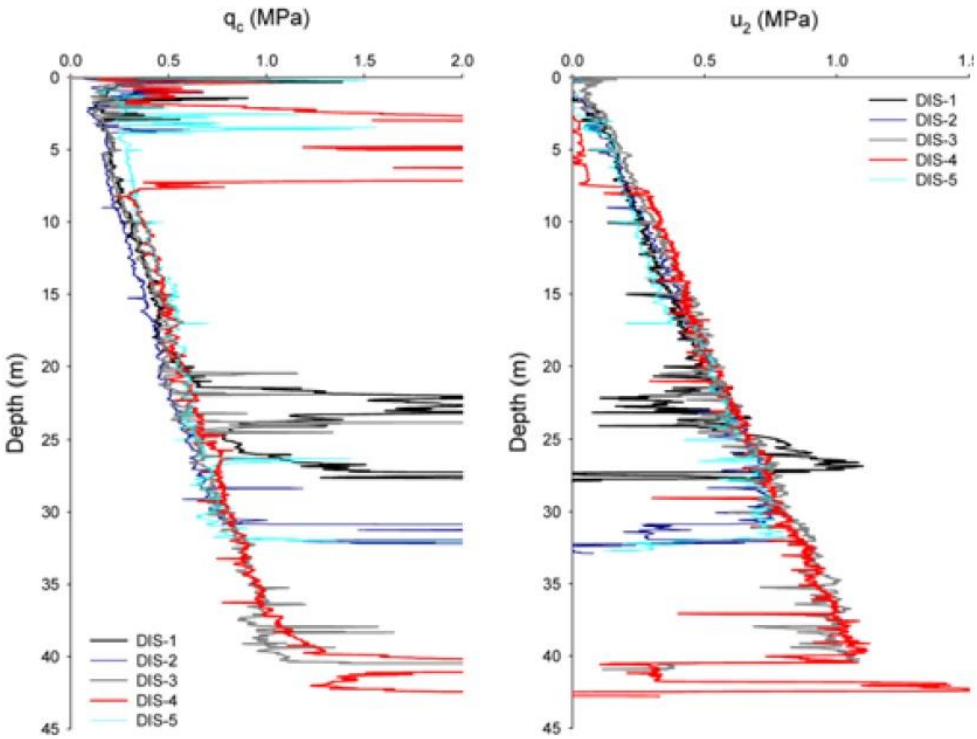

Fig. 3. The Combined CPT Profiles

Can Tho, Vietnam

Data from Takemura & Watabe (2006)

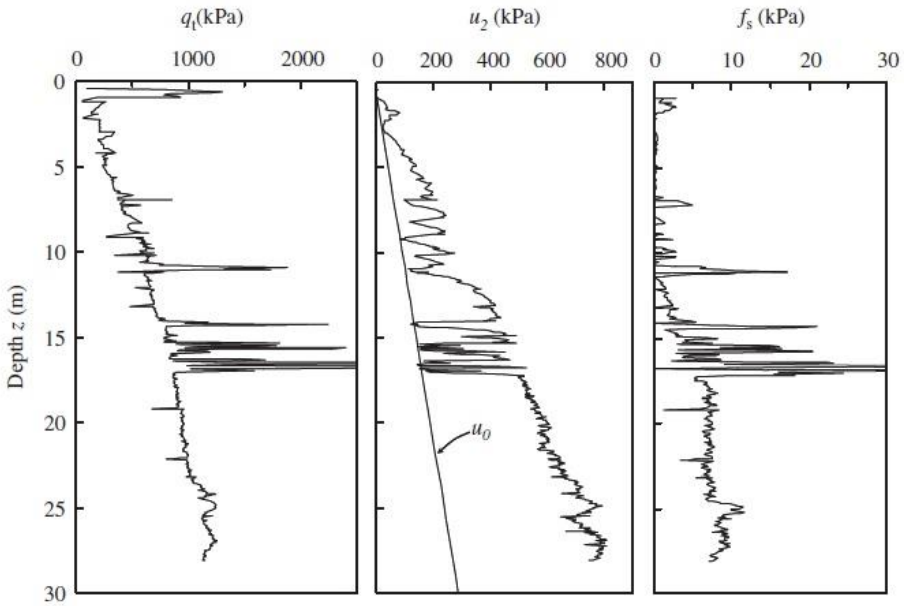

Figure 9. Results of CPTU at Can Tho site.

Canons Park, UK

Data from Hight et al. (2003)

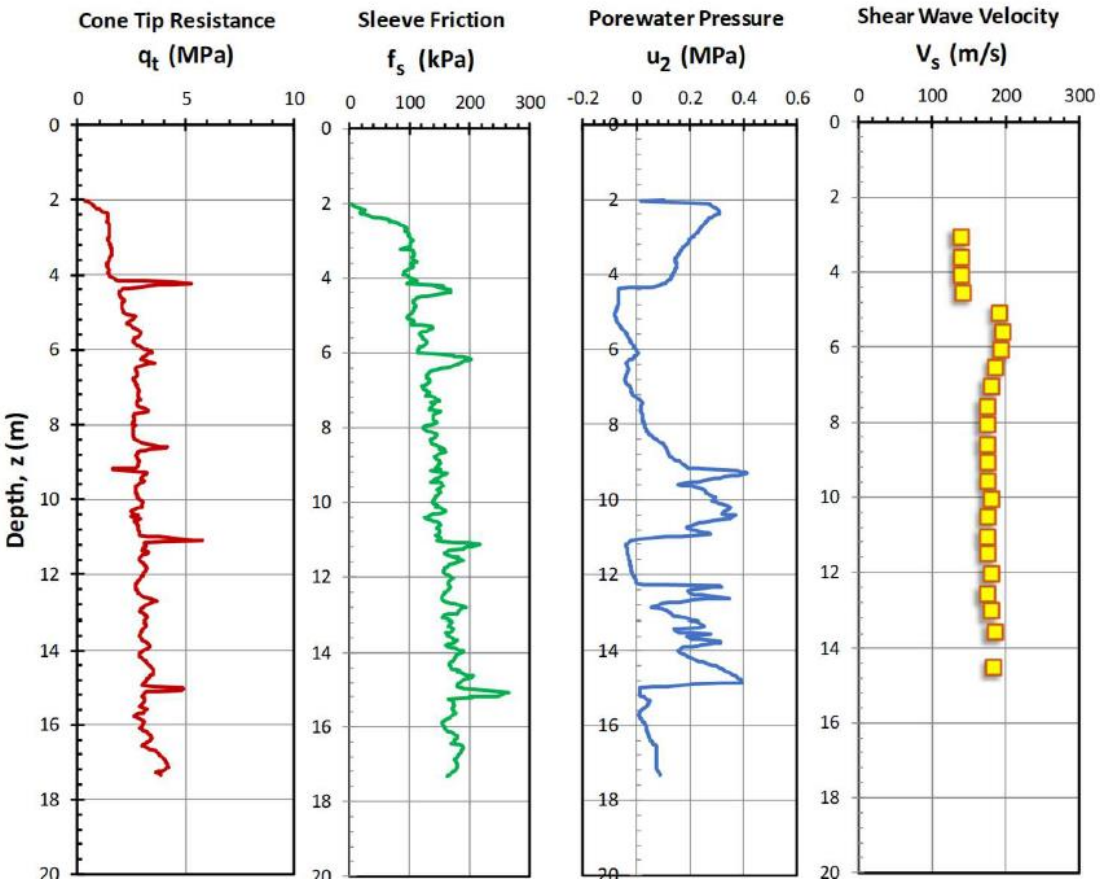

CF Mining -Hardee, Florida

Data from Wissa et al. (1983) (1991)

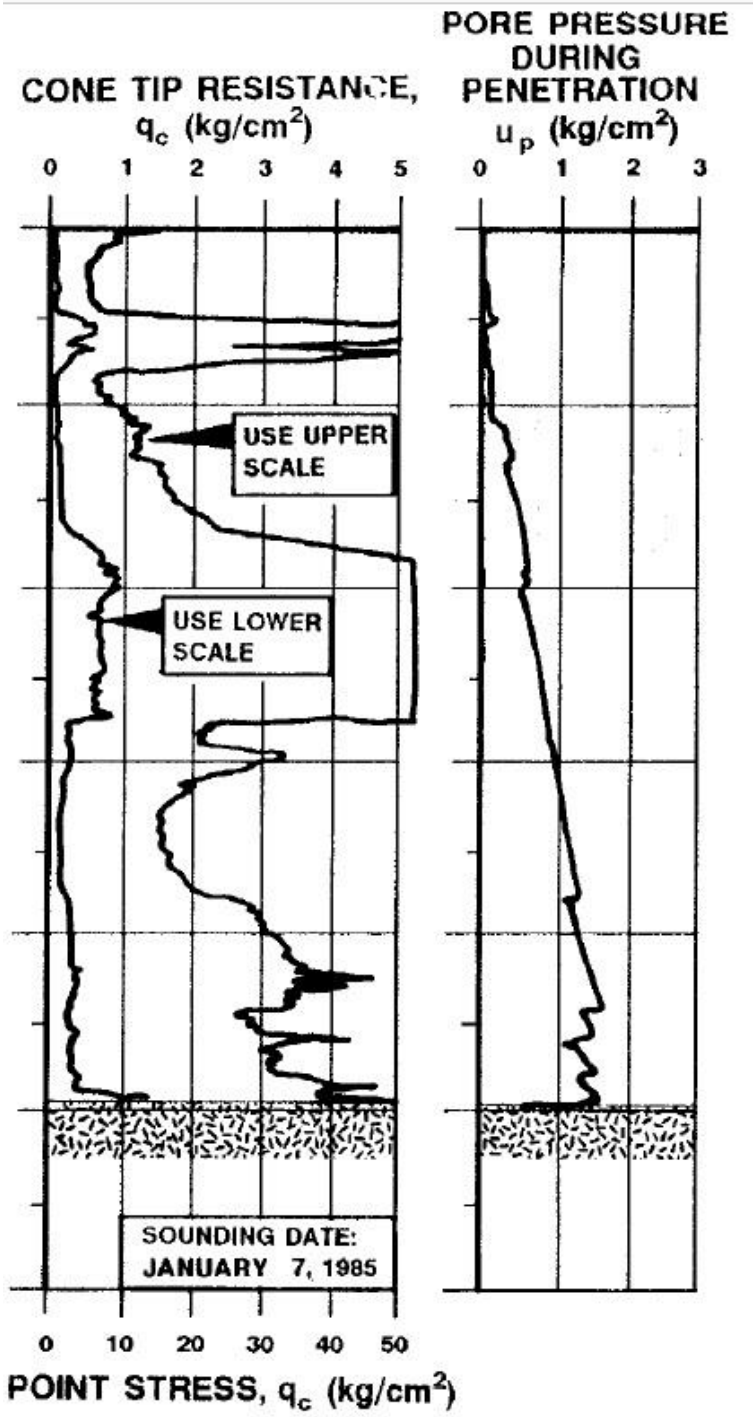

Clayey Sand under 30g centrifuge CPTu

Data from Zhou et al (2014)

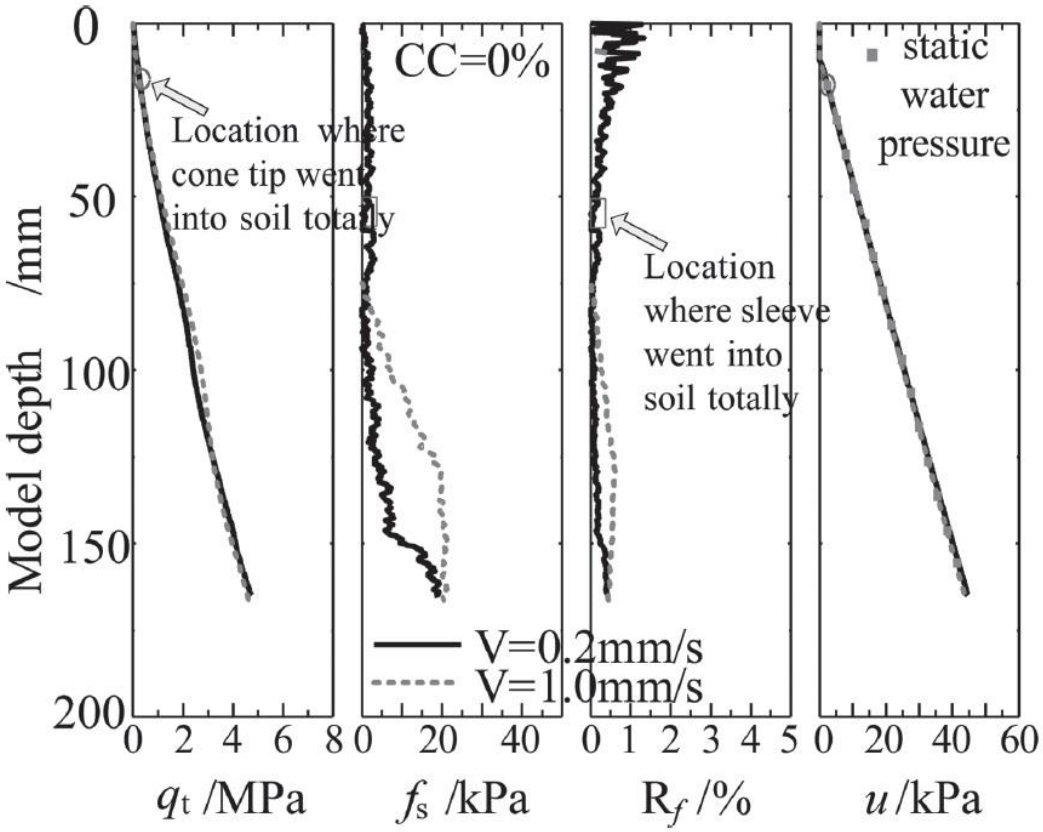

Figure 8. CTPu data in clean sand model.

Colebrook Overpass, BC, Canada

Data after Crawford and Campanella (1991); Weech (2002)

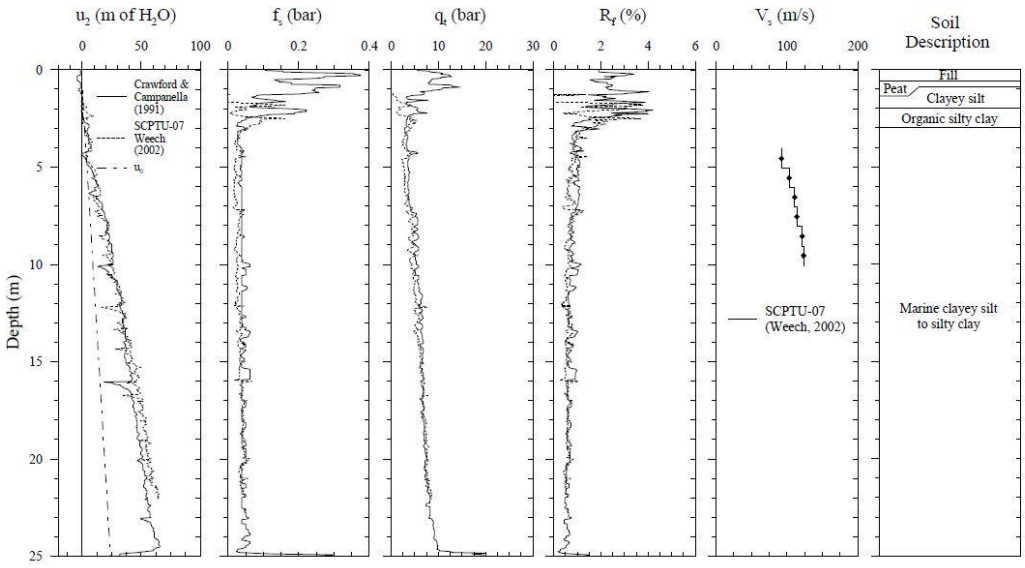

Figure 3.8 CPTU and SCPTU profiles at Colebrook Overpass site (data from Crawford & Campanella, 1991; and Weech 2002).

Cooper River, South Carolina

Data from Singha (1998); Camp (2004); and Mayne (2005)

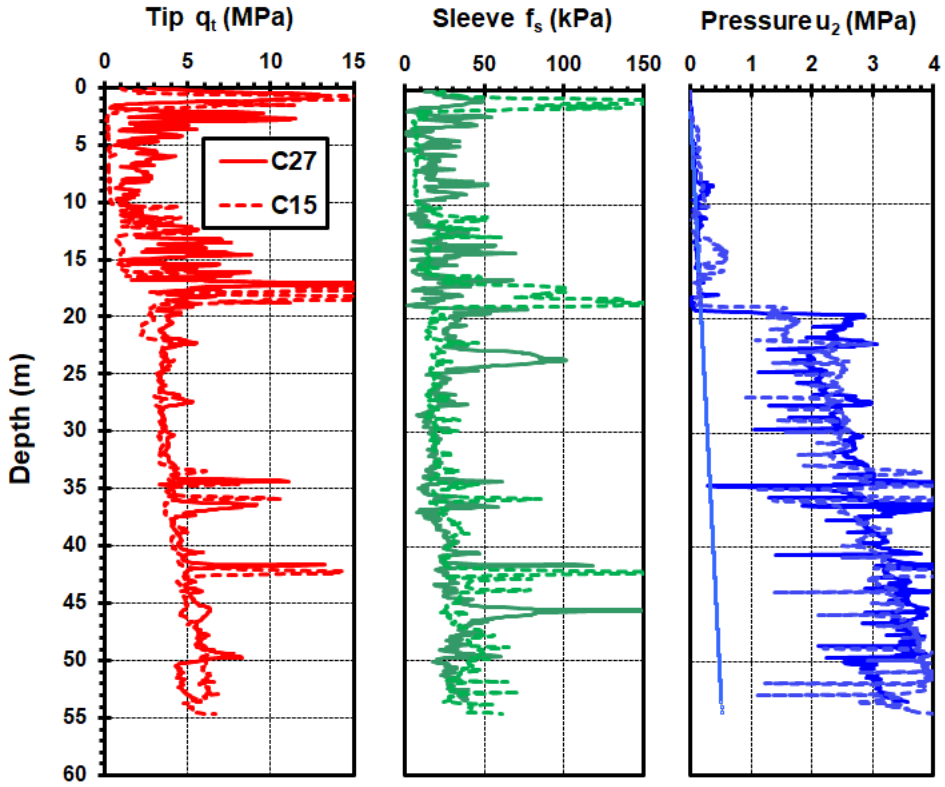

East Hartford, Connecticut

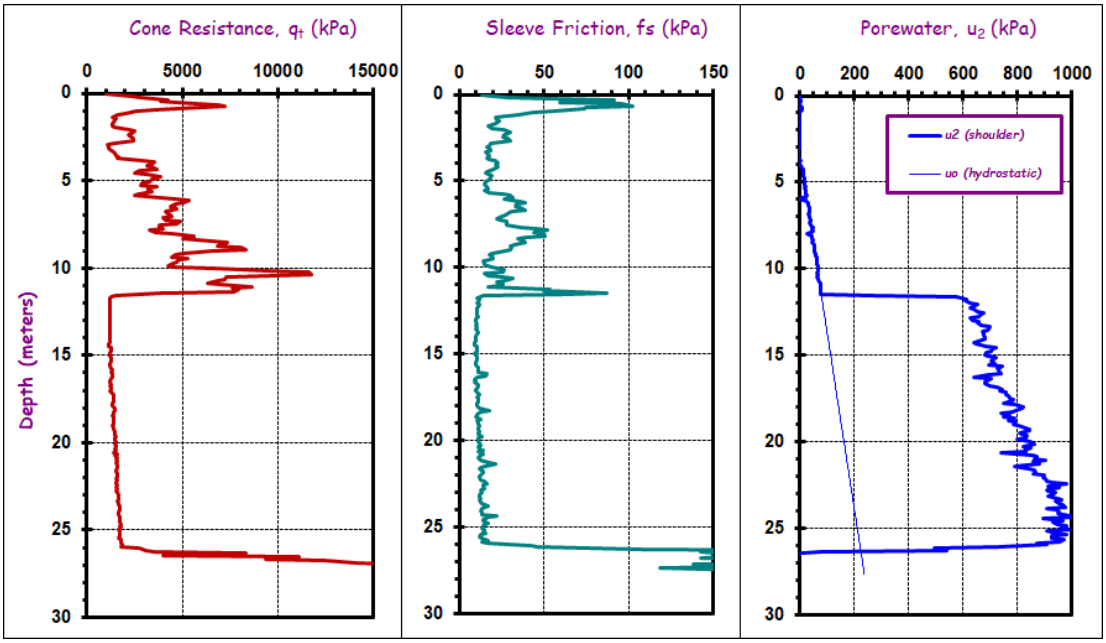

Eidsvoll Norway

Data from Karlsrud et al. (1996)

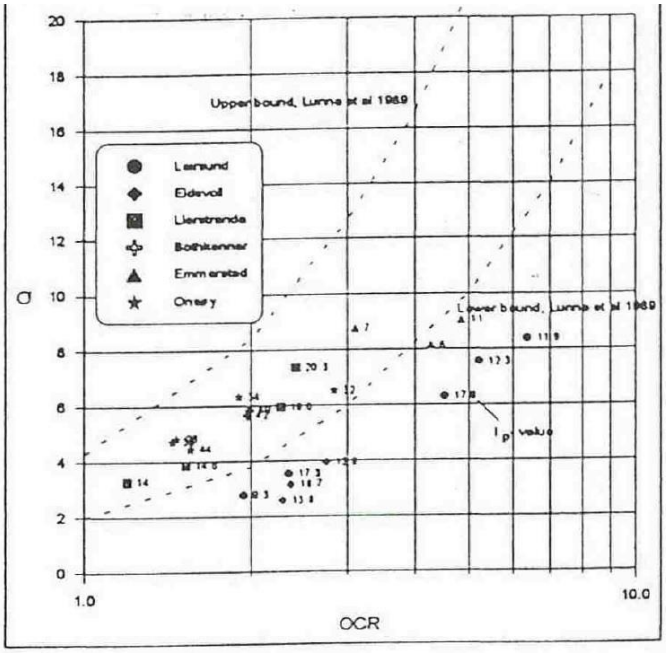

Fig. 3. Correlation between Q and OCR

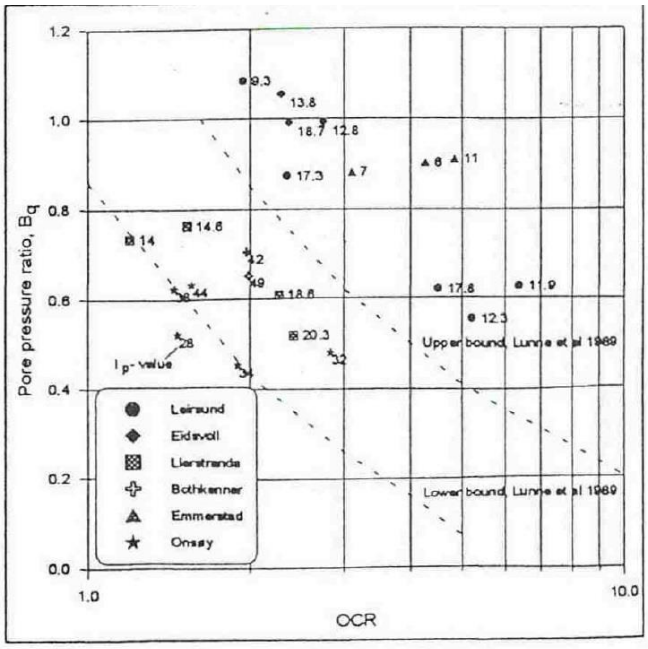

Fig. 4. Correlation between B_q and OCR

Frazenda Brasileiro, Brazil

Data from Dienstmann et al. (2018)

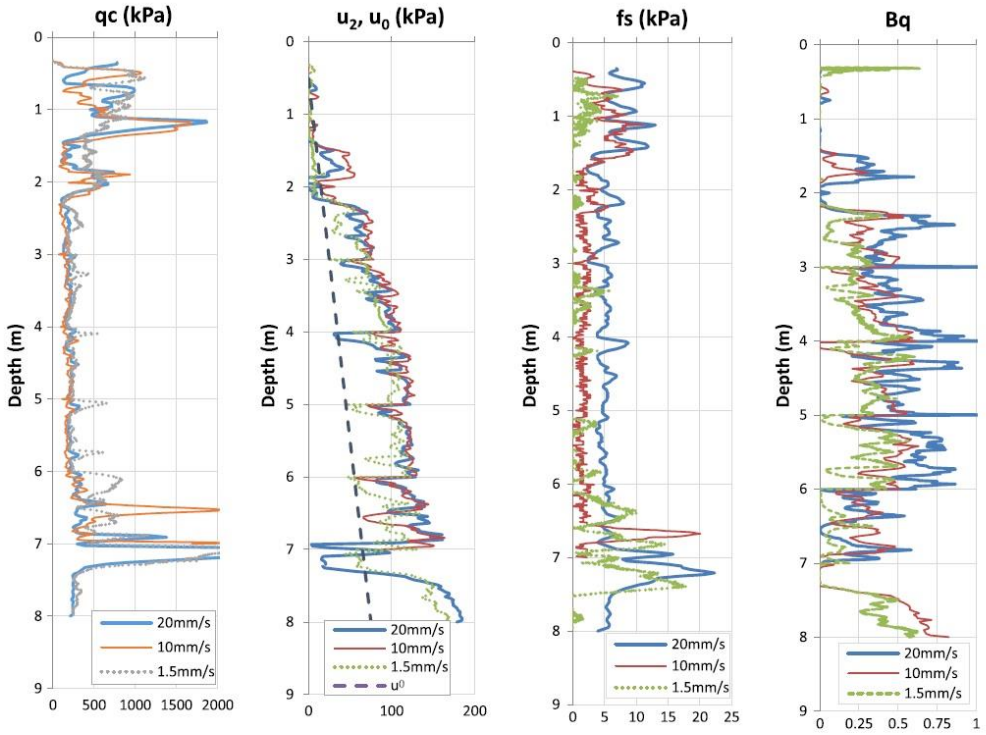

Fig. 4. Piezocone profiles characteristic of silty tailings at variable penetration rates

Fucino, Italy

Data from Soccodato (2002)

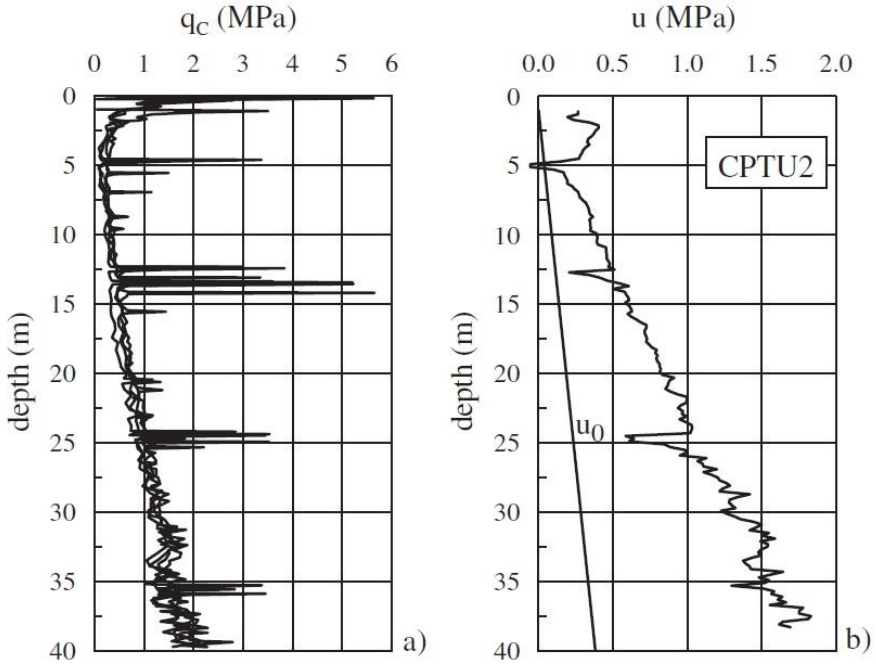

a) Cone tip resistance from CPT tests; b) pore pressure from CPTU tests.

Gault clay CPTu chamber test

Data from Almeida and Parry (1985)

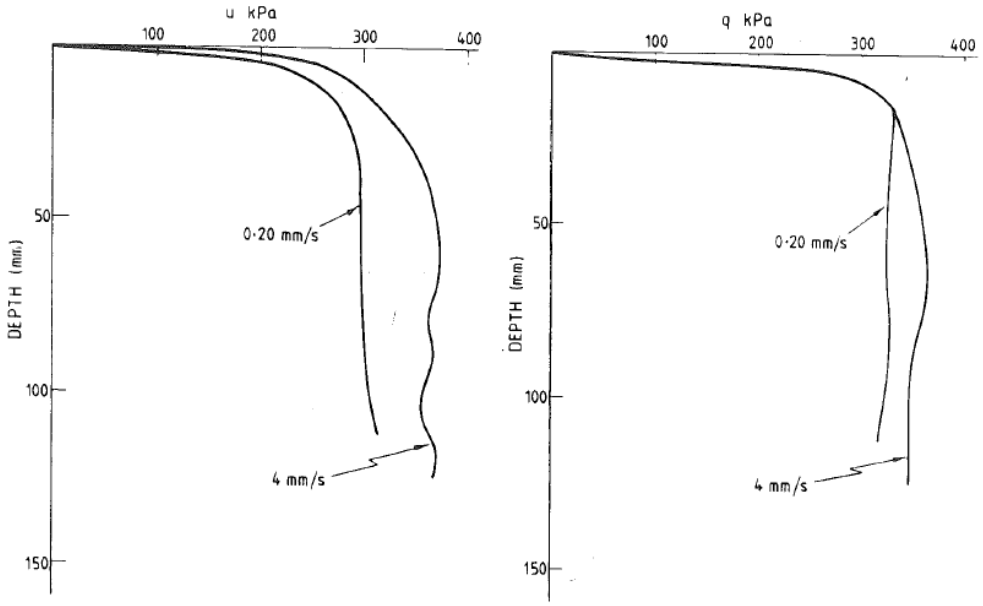

FIG. 11—*Influence of the rate of penetration in Gault clay, OCR = 1.*

Gingin, Australia

Data from Suzuki (2015)

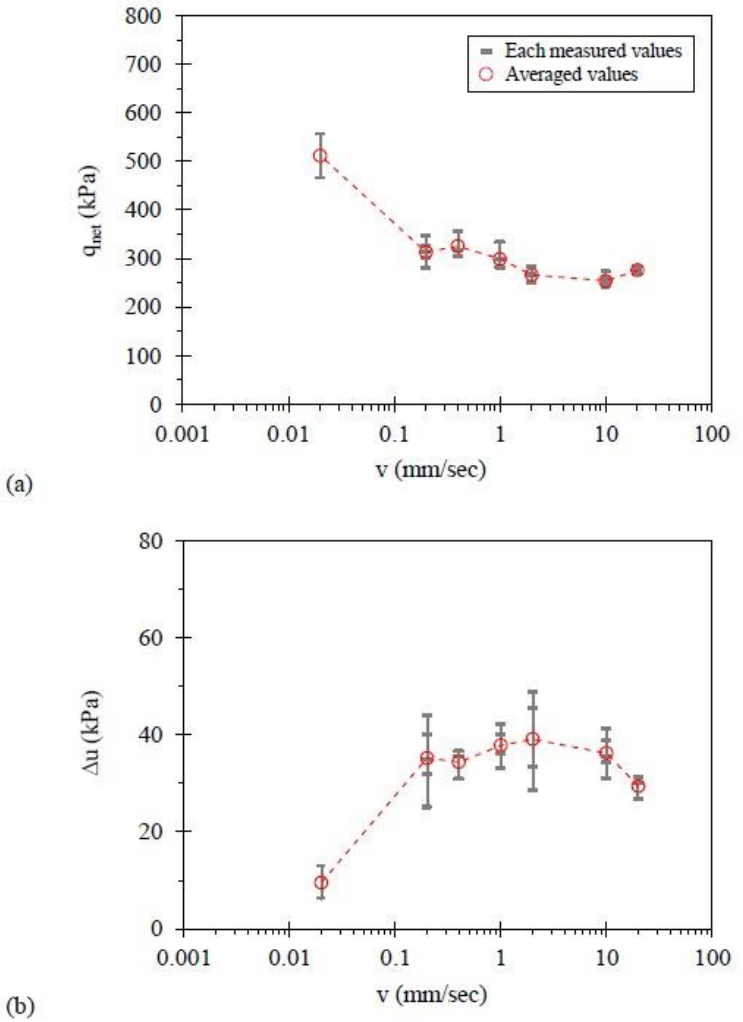

Figure 4.3 Penetration rate effects at the Gingin site: (a) q_{net} and (b) Δu

Gloucester, Canada

Data from McQueen et al. (2016); Landon (2007); McRostie & Crawford (2001); Styler & Mayne (2013)

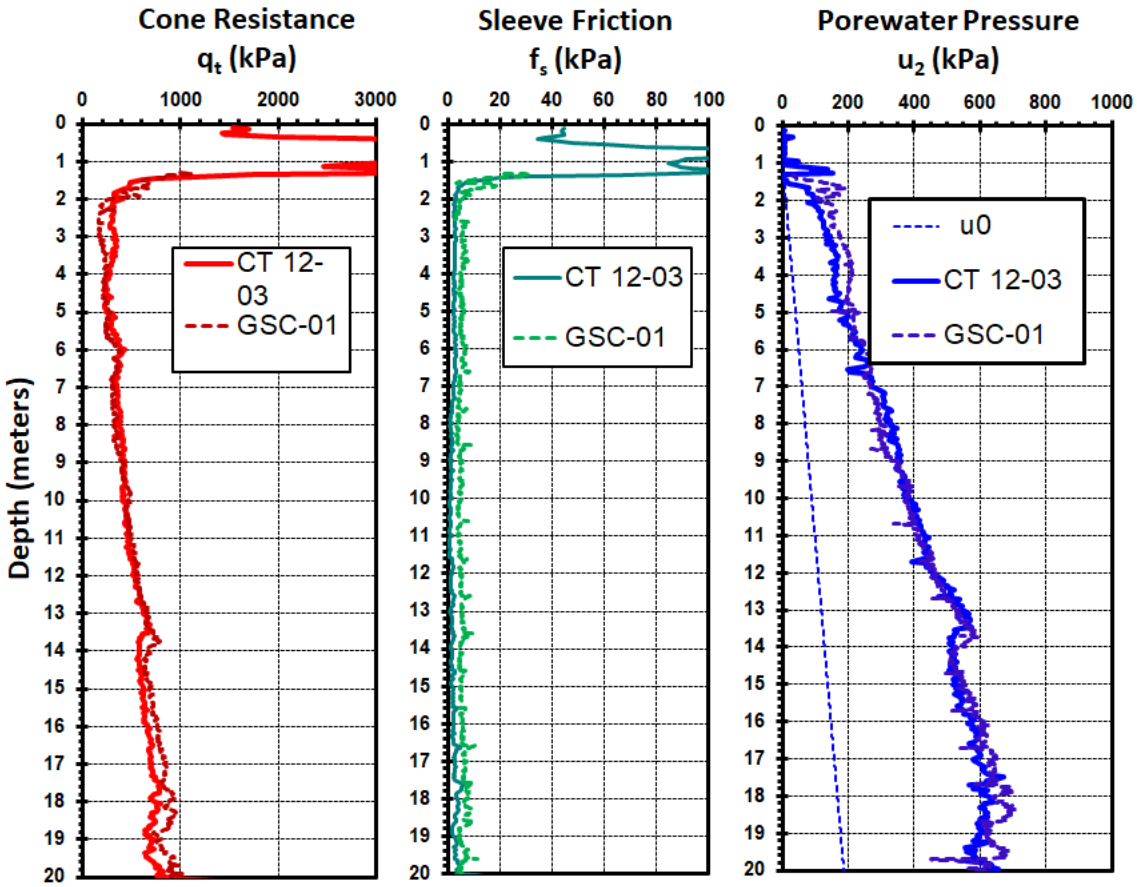

GOG 1, Gulf of Guinea, West Africa

Data after Lunne at al. (2006)

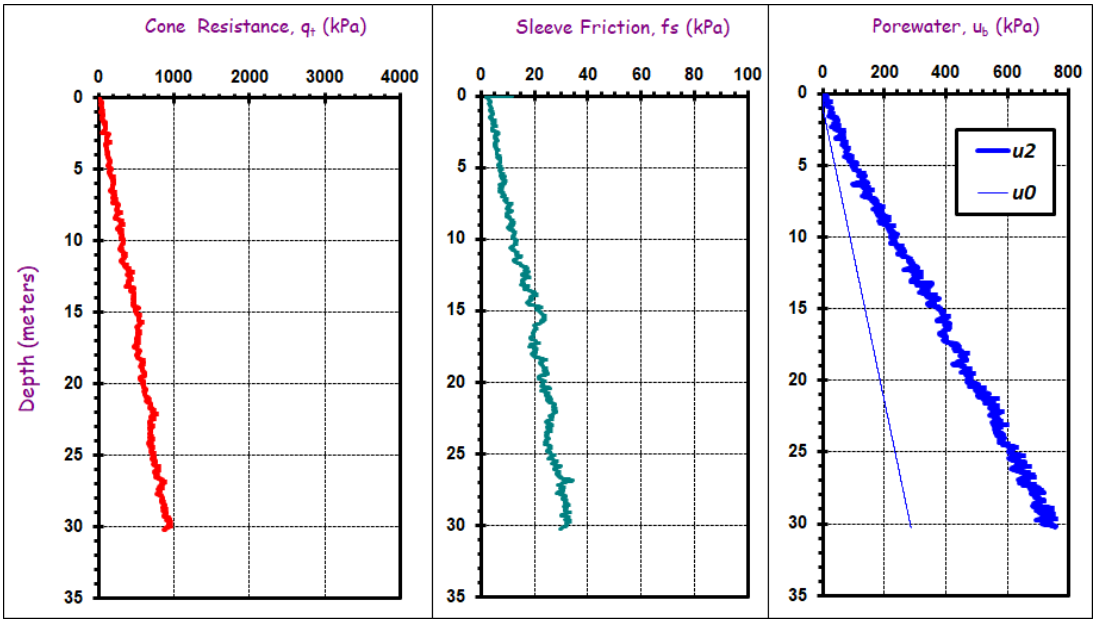

GOG2b, Gulf of Guinea, West Africa

Data from Mayne et al. (2015)

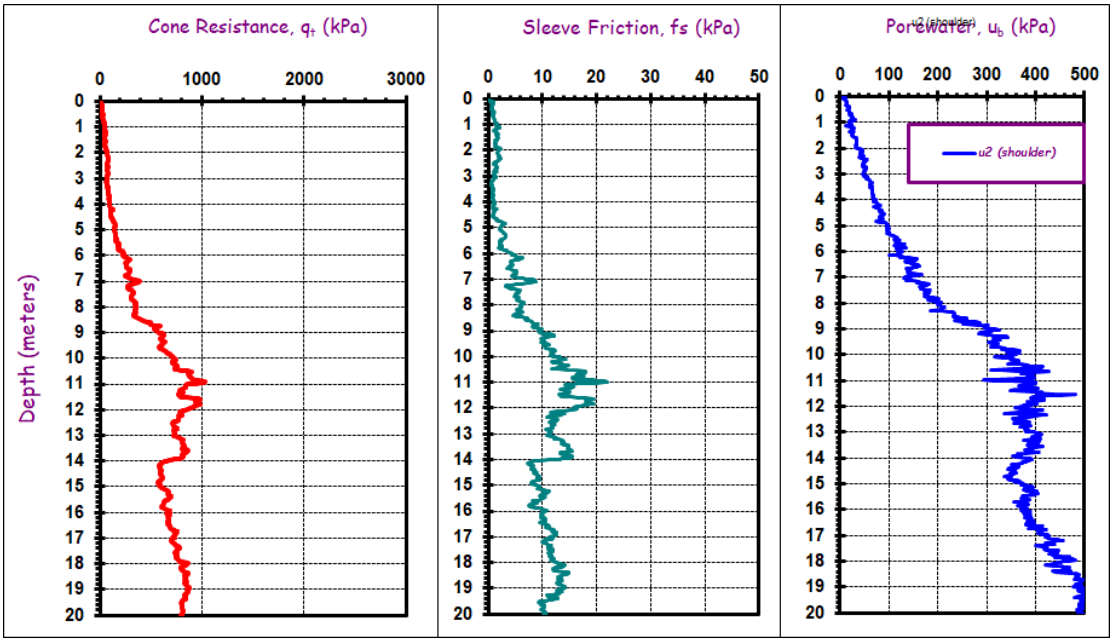

Gotaleden, Sweden

Data from Persson (2004)

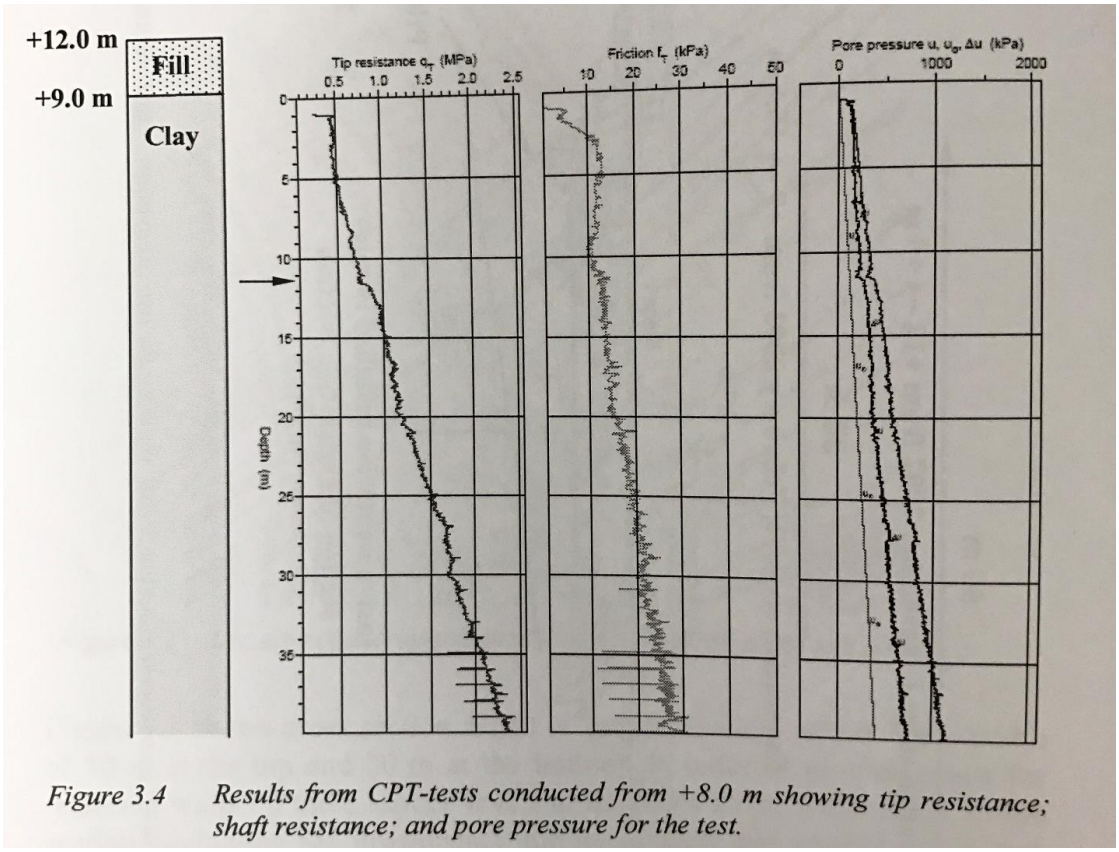

Figure 3.4 *Results from CPT-tests conducted from +8.0 m showing tip resistance; shaft resistance; and pore pressure for the test.*

Grande-Baleine, Canada

Data from Demers (2001)

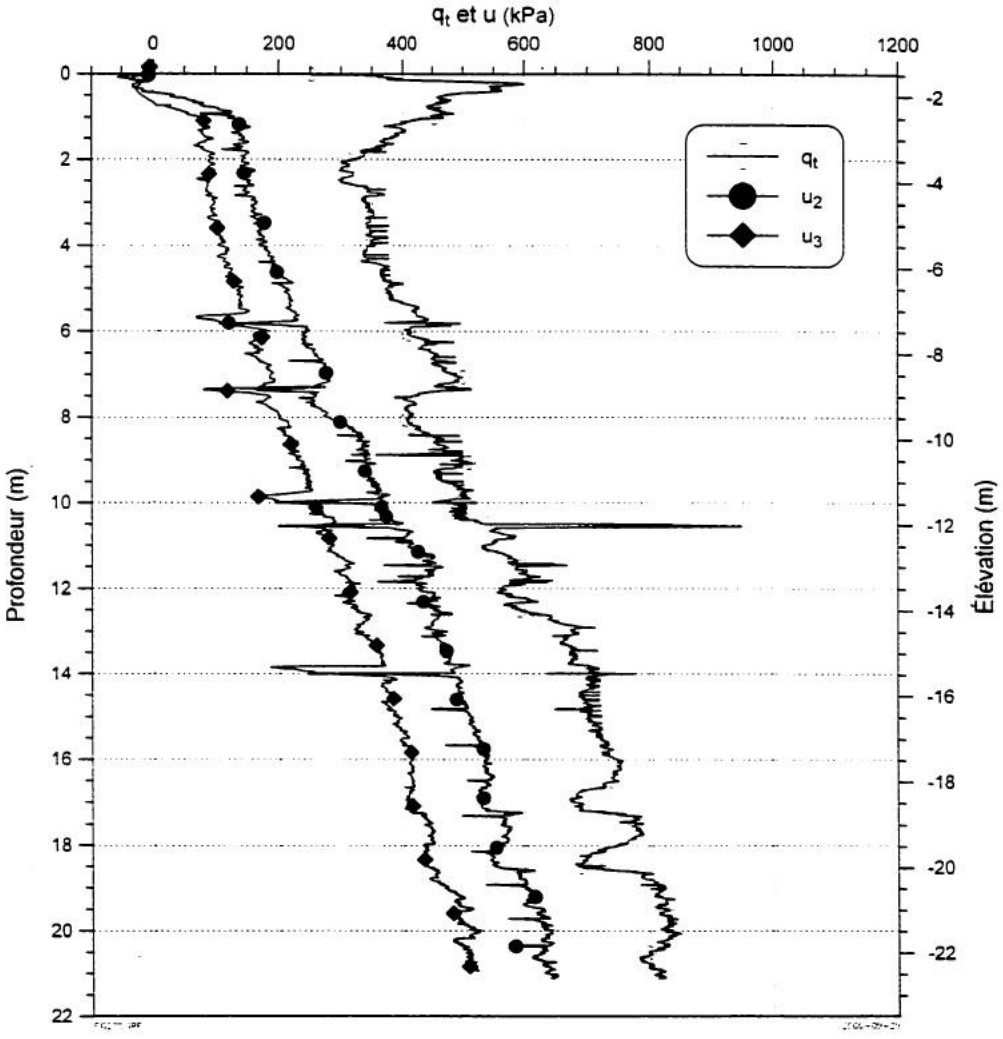

Figure 2.70: Essai au piézocône CPTU4, au site de Grande Baleine.

Grandes-Bergeronnes, Canada

Data from Demers (2001)

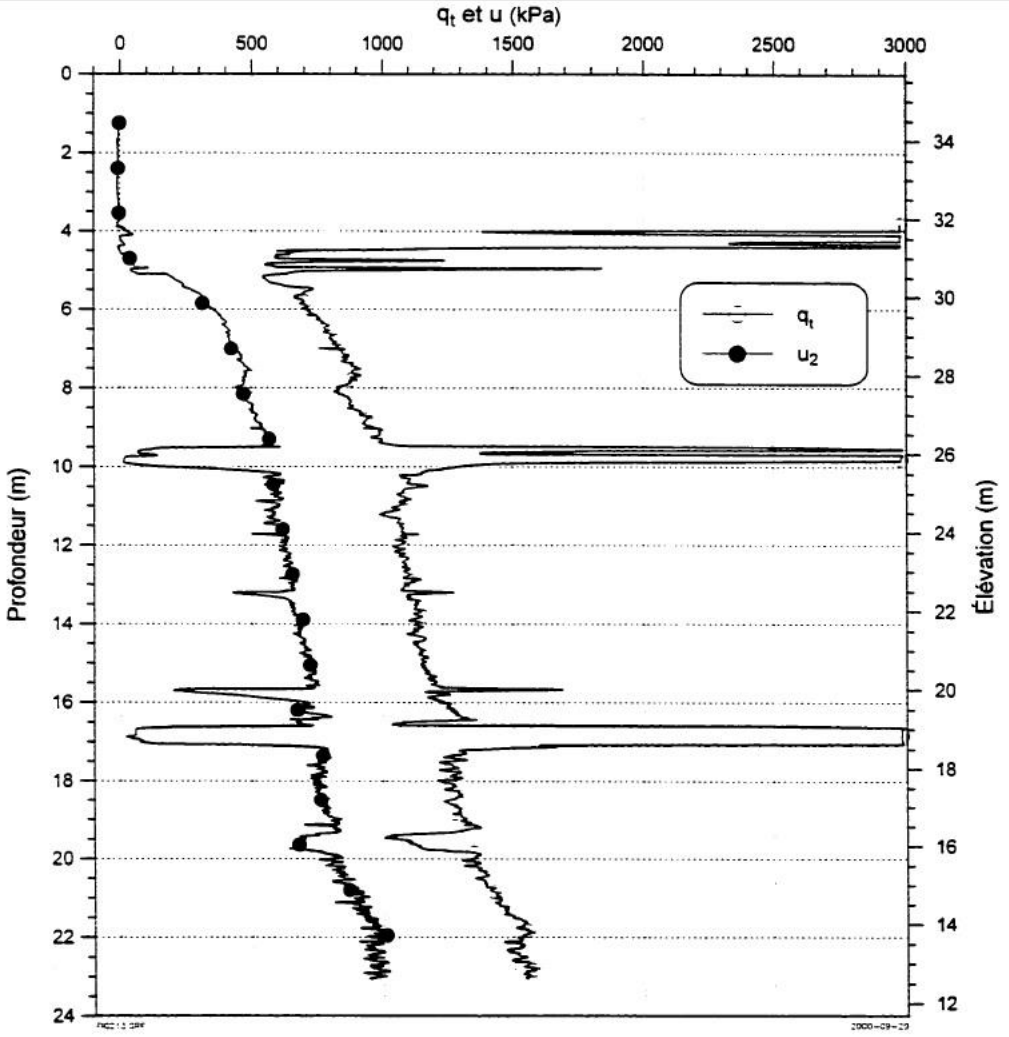

Figure 2.13: Essai au piézocône CPTU1, à Grandes-Bergeronnes (rivière des Petites Bergeronnes).

Granite, California

Data from Krage & DeJong (2014)

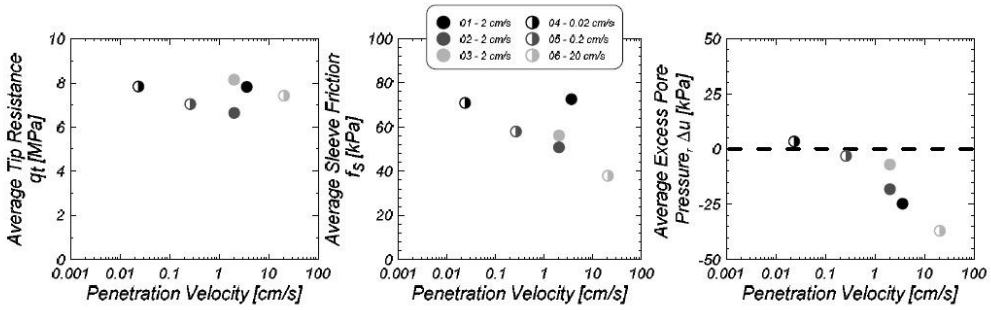

FIG. 6 - Granite 123 Interval Summary 6.6 to 8 m

Hachirogata, Japan

Data from Tanaka (2006)

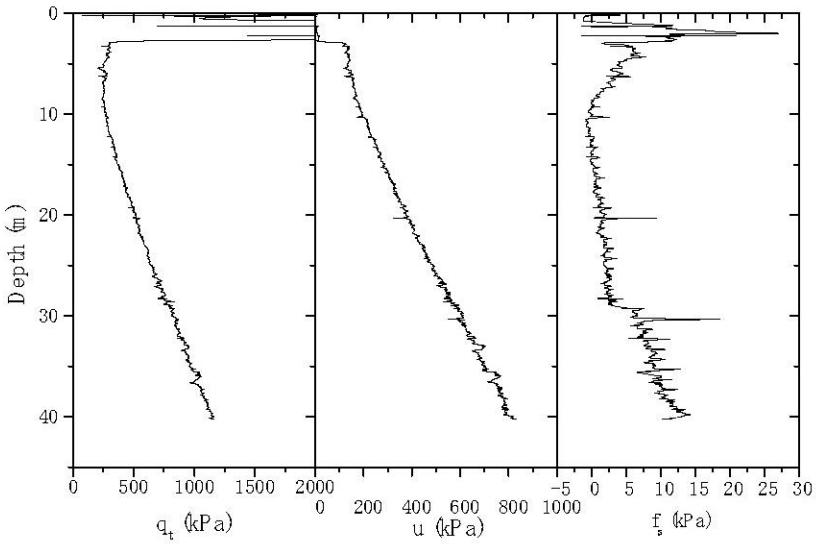

Haga, Norway

Data form Lunne et al (1986) ASCE GSP 6

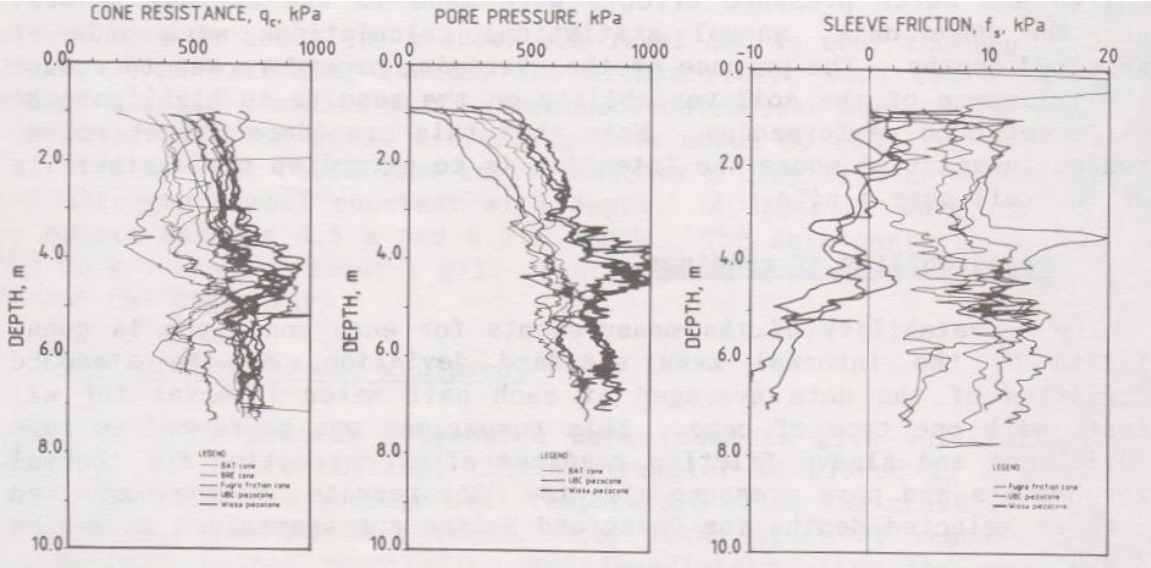

Fig. 5 Typical uncorrected piezocone test results from Haga test site

Hai-Phong, Vietnam

Data from Watabe et al (2004)

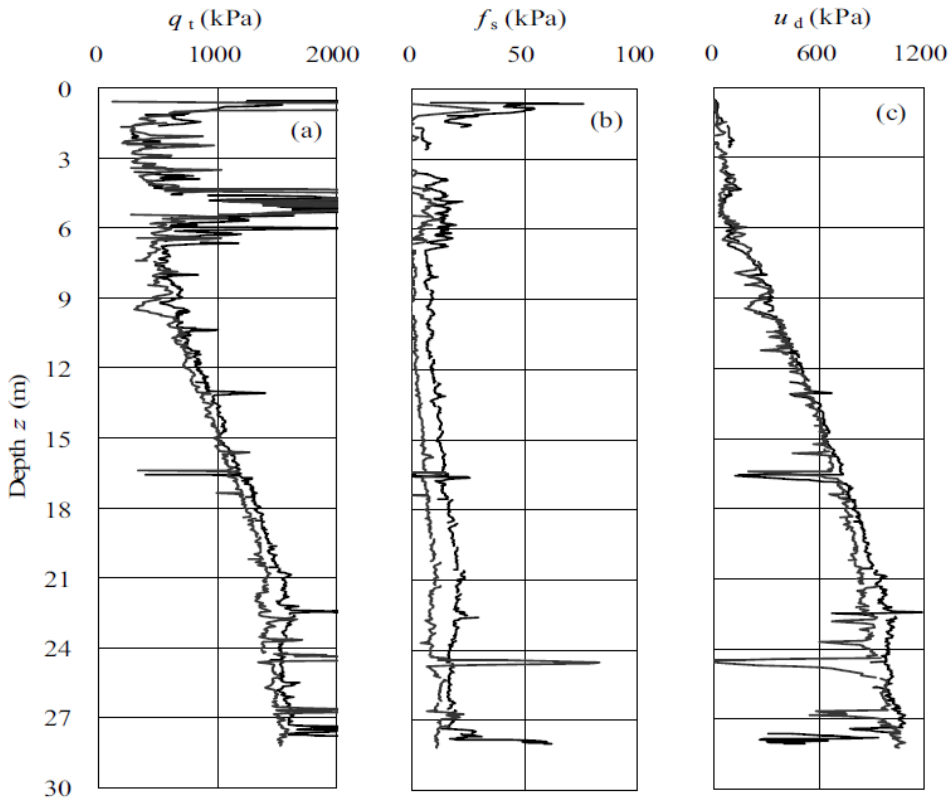

Figure 14. CPT and DMT results at Hai-Phong.

Halden Silt, Norway

Data from Blaker et al (2016)

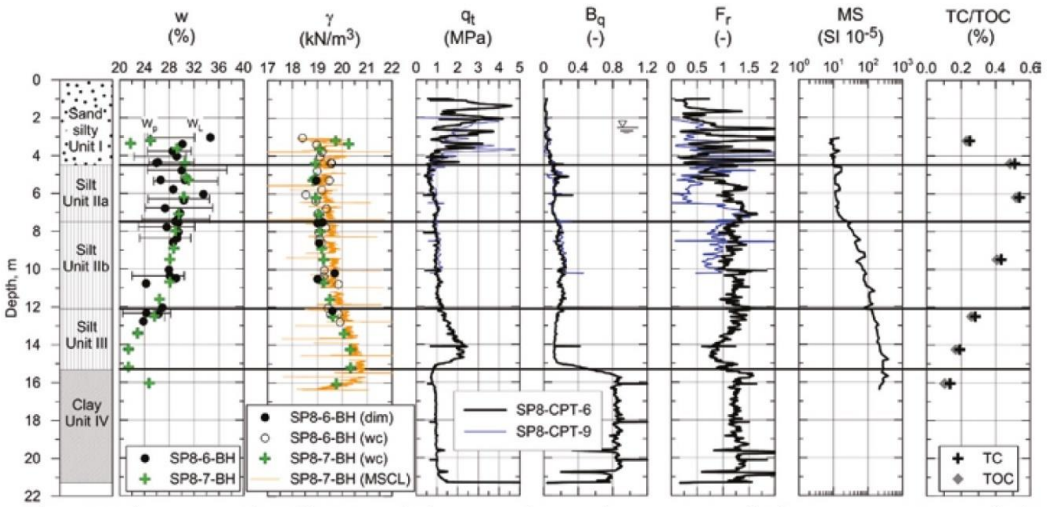

Figure 2. Basic parameters for Halden Research Site, corrected cone resistance, qt, normalised pore pressure, Bq, normalised friction, Fr, versus depth from CPTU, magnetic susceptibility from MSCL, and TC/TOC. Whole core Gamma density (i.e. wet bulk density) is shown in yellow on the total unit weight log.

Hamilton AFB, CA

Data from Masood et al. (1988)

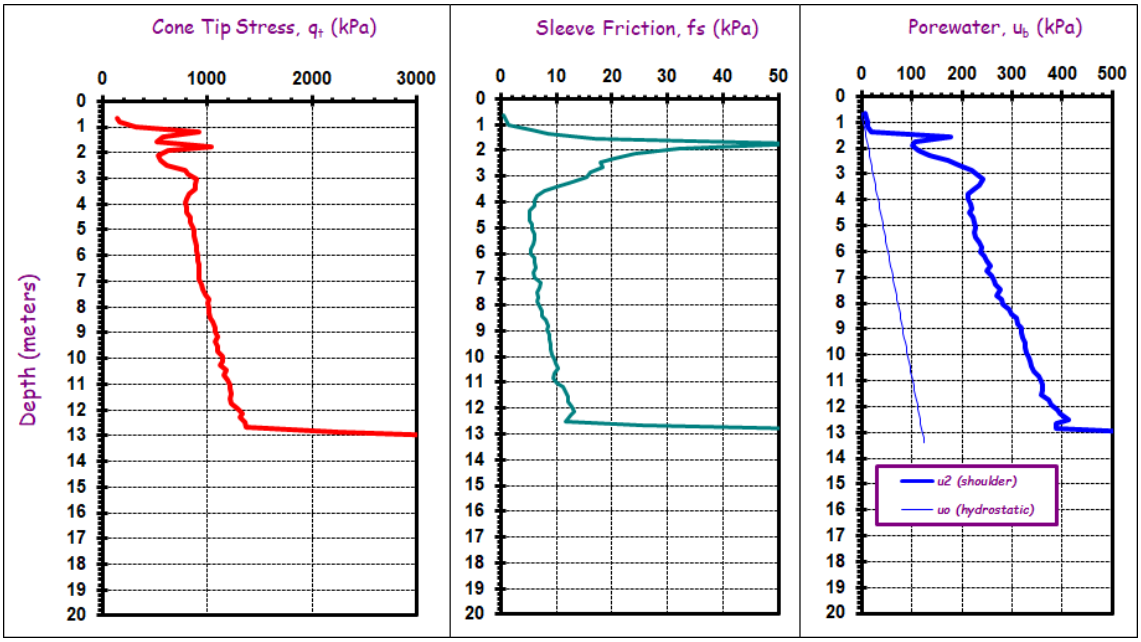

Heathrow T5, UK

Data from Hight et al. (2003)

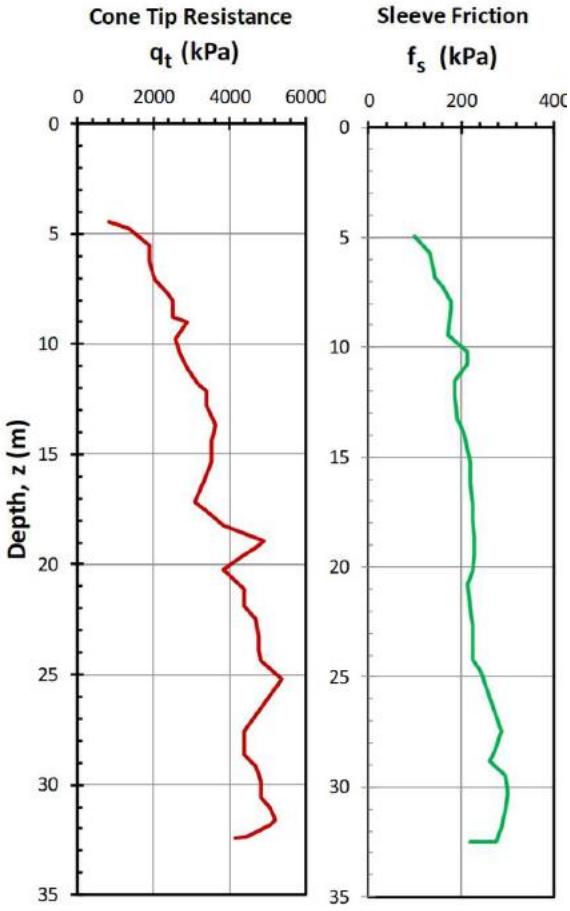

Hilleren, Norway

Data from Long et al. (2009)

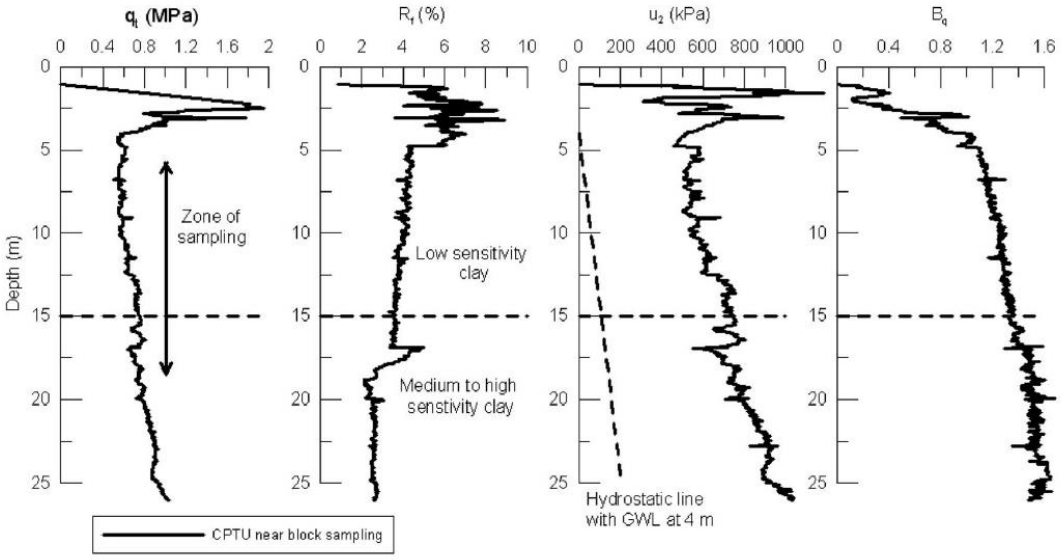

Fig. 1. CPTU test results

Hongkong, China

Data from So (2009)

Fig. 12. Typical CPTU results of the nearshore marine deposits.

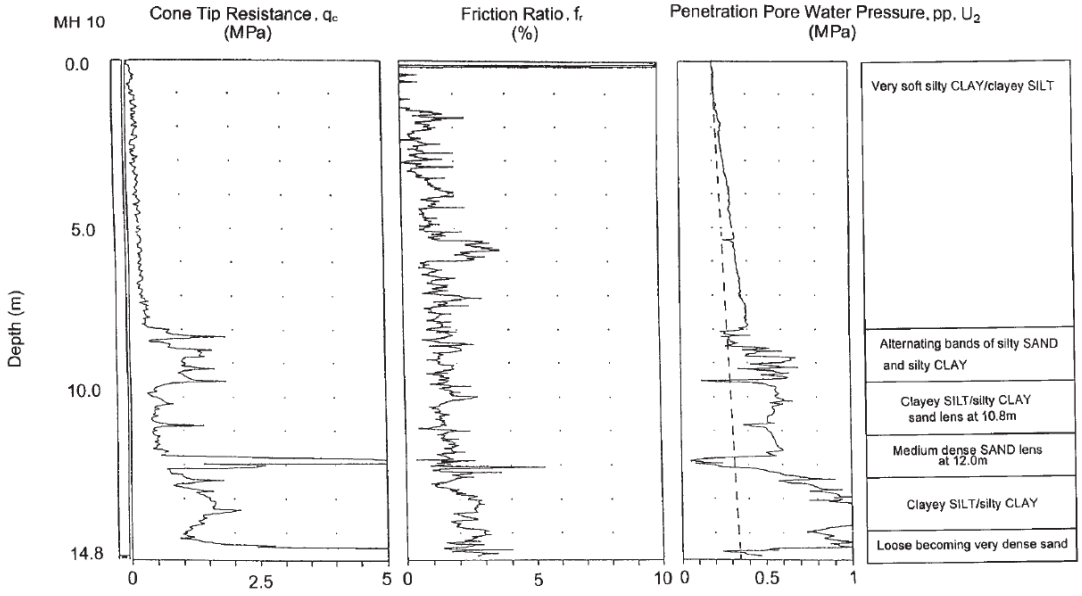

Houma, LA

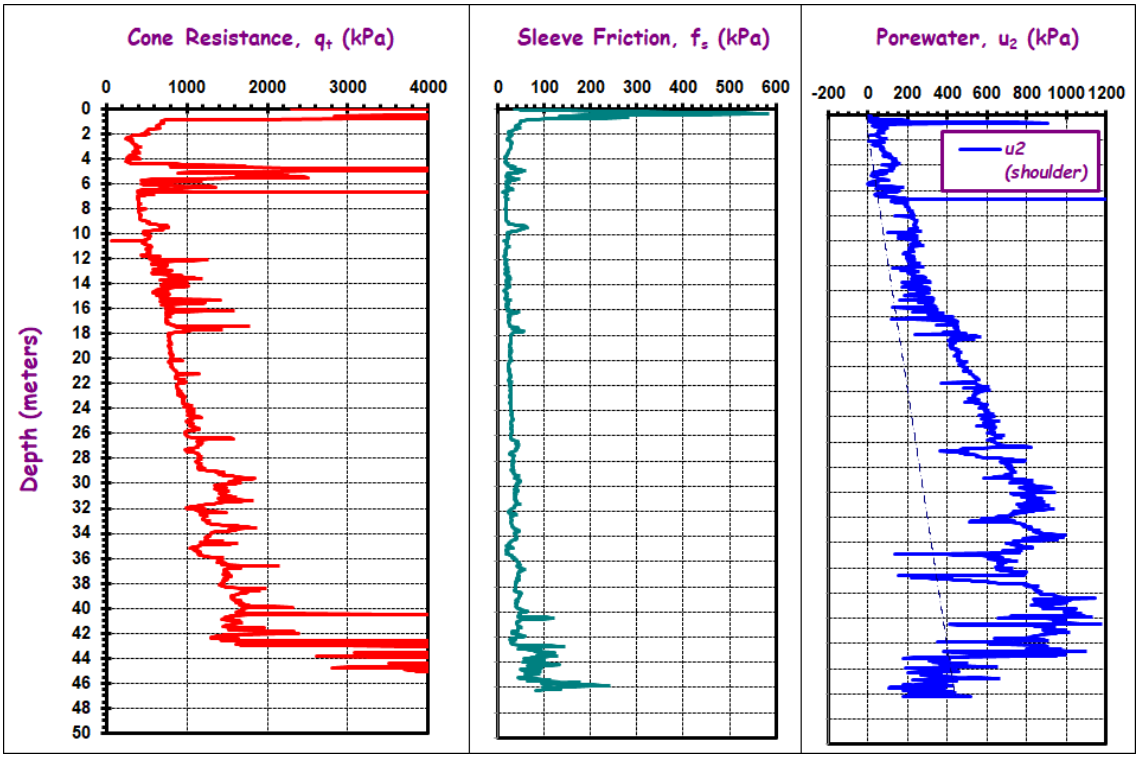
Cone Resistance, q_t (kPa)
Sleeve Friction, f_s (kPa)
Porewater, u_2 (kPa)
Depth (meters)
0 1000 2000 3000 4000
0 100 200 300 400 500 600
-200 0 200 400 600 800 1000 1200
u2
(shoulder)
0 2 4 6 8 10 12 14 16 18 20 22 24 26 28 30 32 34 36 38 40 42 44 46 48 50

Islais Creek, CA

Data from Hunt et al. (2002); Pestana et al. (2002)

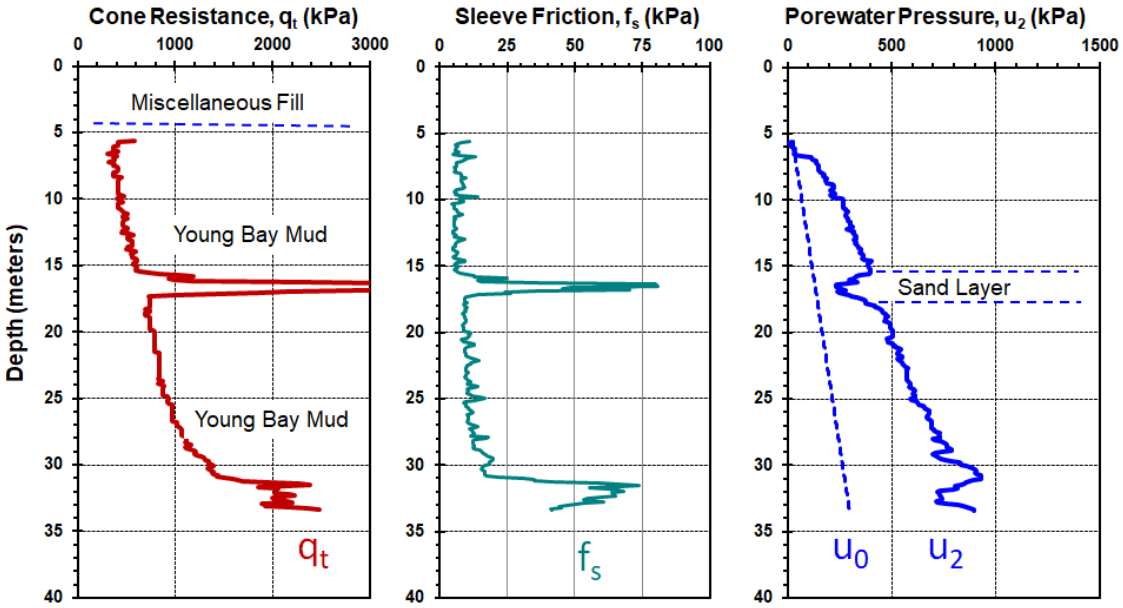

Jutland, Denmark

Data from Poulsen et al (2013)

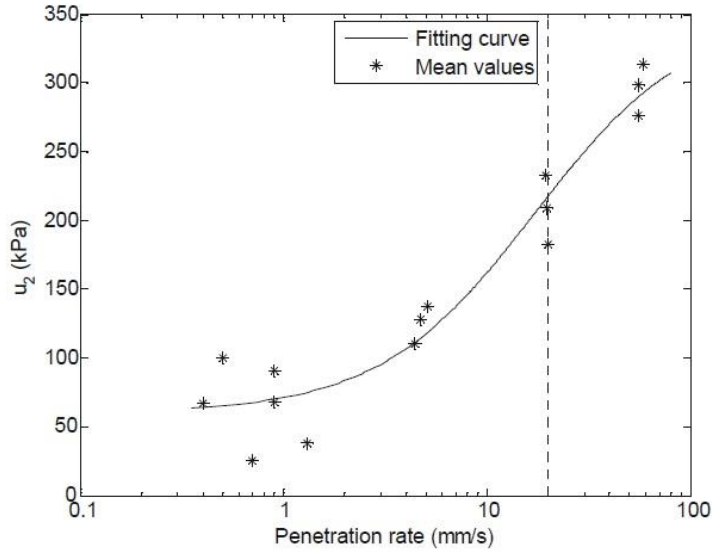

Figure 6. Correlation between the mean pore pressure and the mean penetration rate from 4.5 to 11.4 m below ground level. The standard rate of penetration of 20 mm/s has been marked with a dotted line.

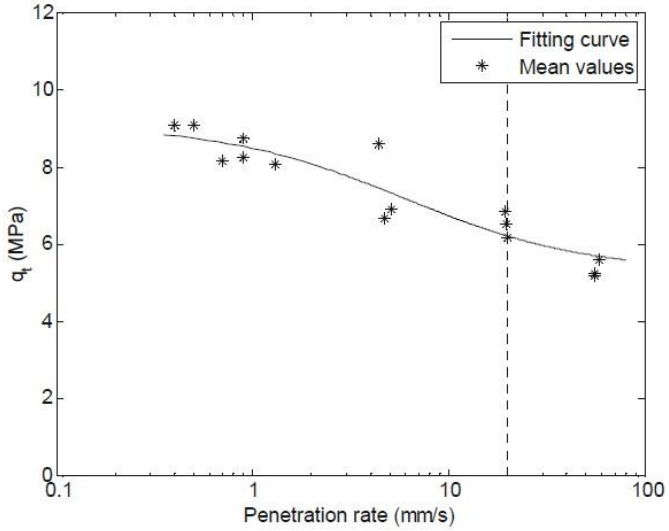

Figure 7. Correlation between the mean cone resistance and the mean penetration rate from 4.5 to 11.4 m below ground level. The standard rate of penetration of 20 mm/s has been marked with a dotted line.

K25 and K100 CPTu chamber

Data from Suzuki (2015)

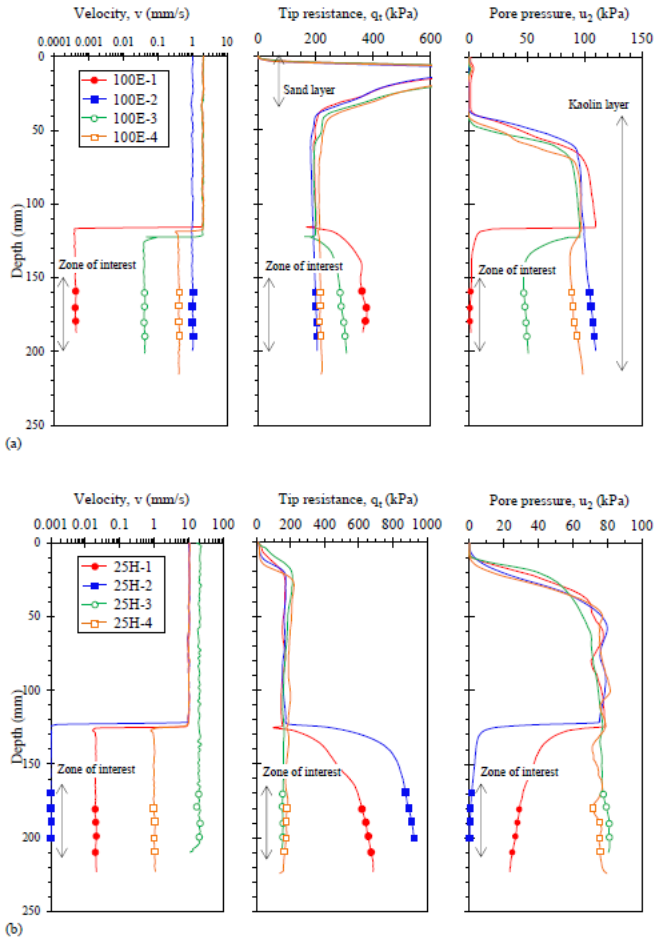

Figure 6.6 Typical CPTU penetration profiles in: (a) 100% kaolin sample and (b) 25% kaolin sample

K25 centrifuge test CPTu

Data from Suzuki (2015)

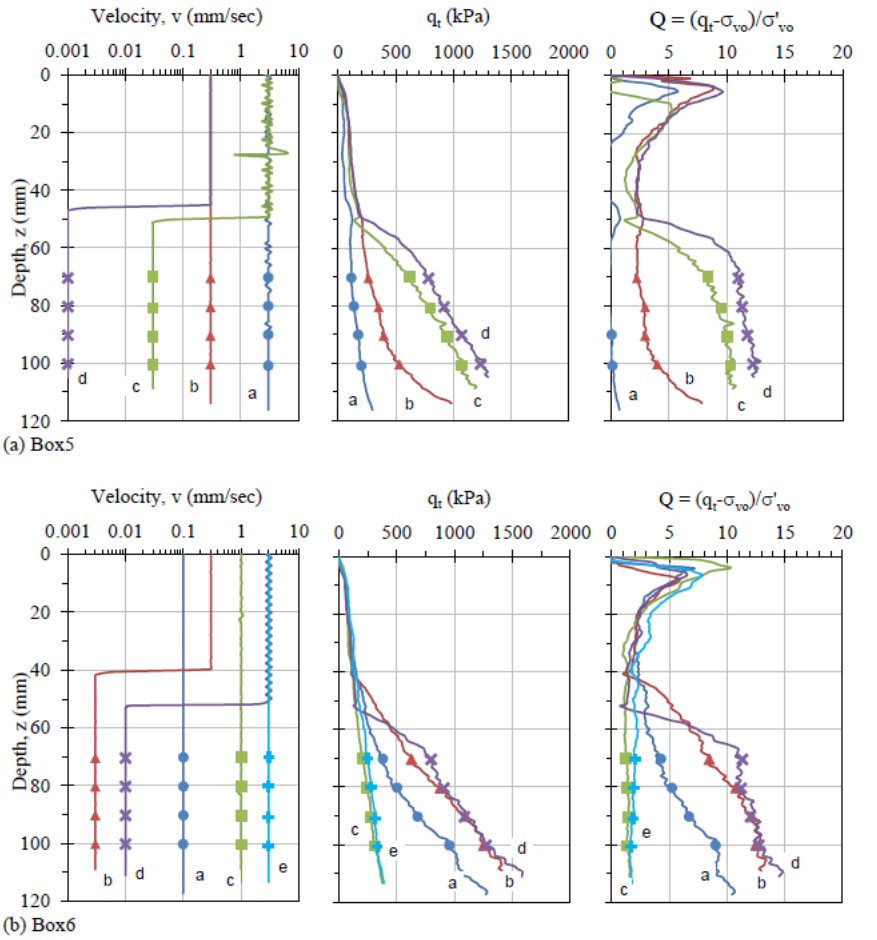

Figure 5.9 CPT penetration profiles for the 25% kaolin mixtures: (a) Box5 and (b) Box6

K50 CPTu chamber test

Data from Tumay (1994)

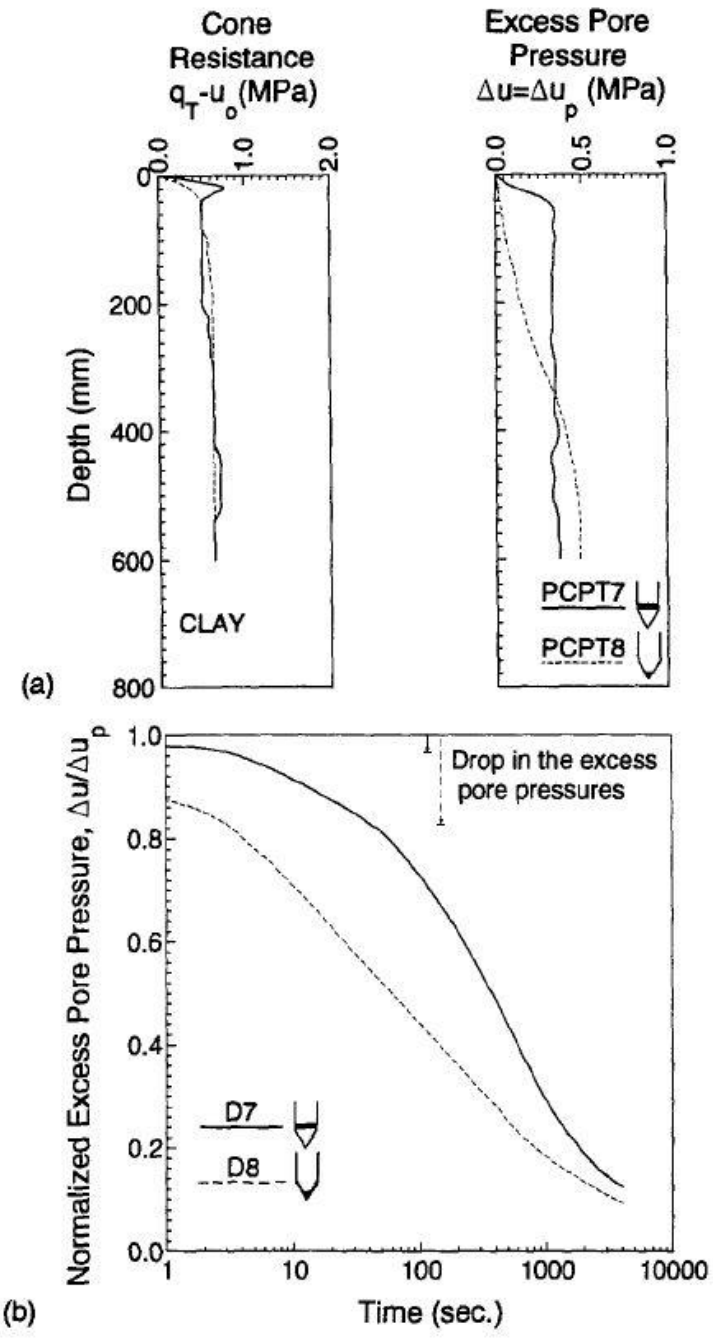

FIG. 8. Specimen 4: (*a*) PCPT Profiles; (*b*) Dissipation Results

K75-S25 CPTu

Data from Fitzgerald (2009)

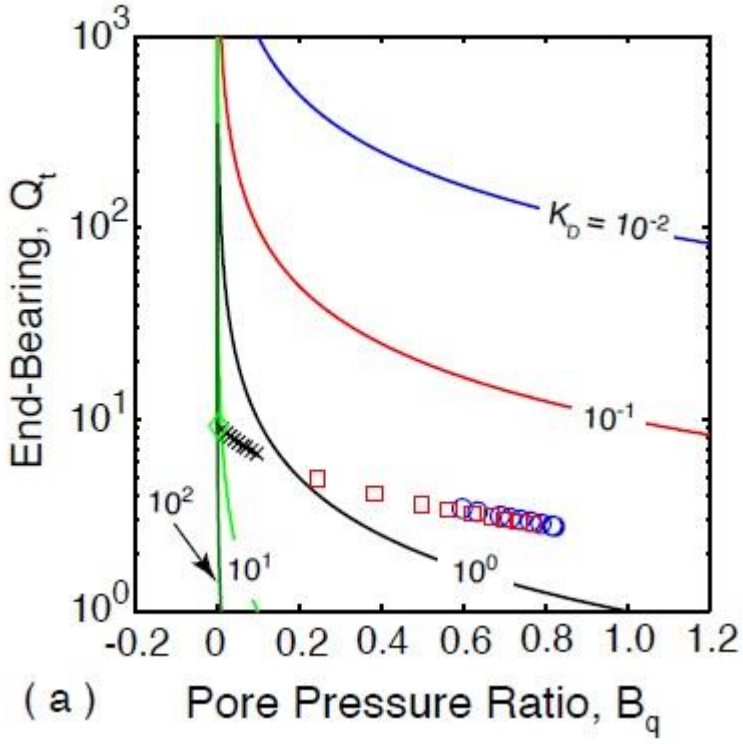

Kaolin 100g Centrifuge CPTu

Data from Teh et al 2007

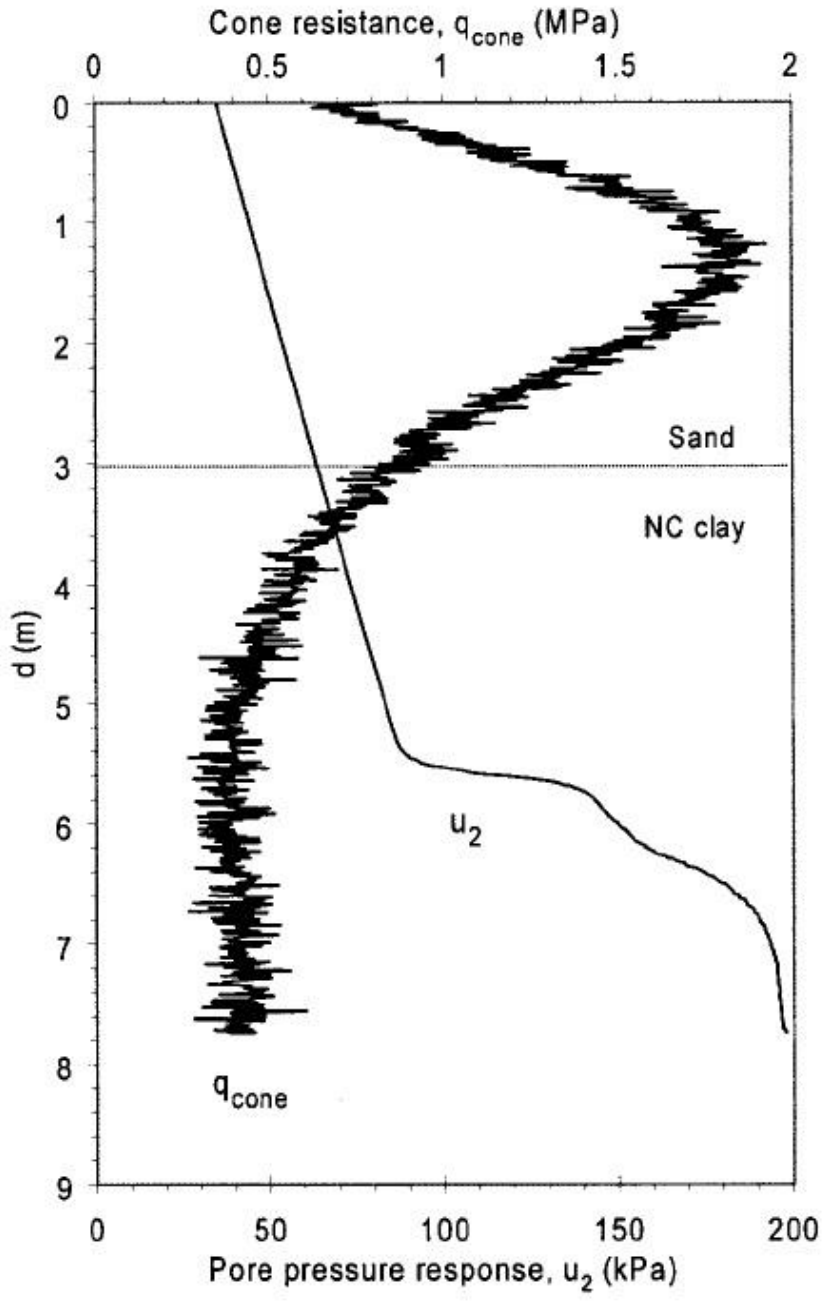

Fig. 3 Miniature piezocone penetration test (PCPT) results

Kaolin 110 CPTu Centrifuge

Data from Mahmoodzadeh & Randolph (2014)

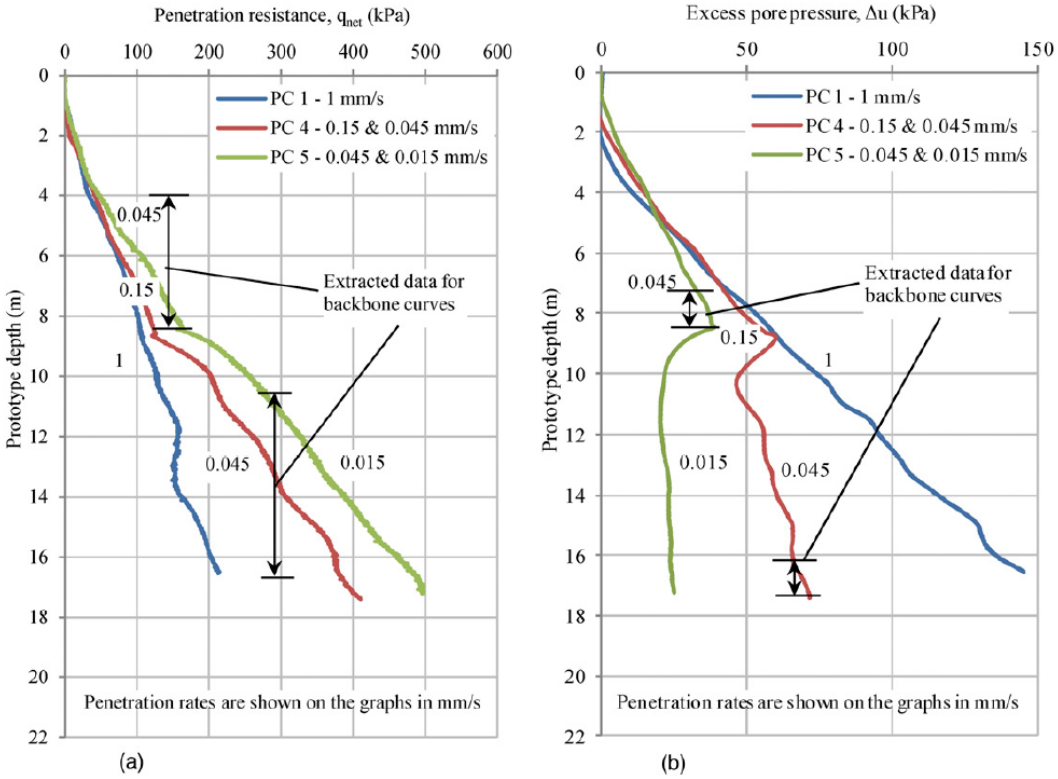

Fig. 4. Example penetration responses for piezocone: (a) penetration resistance; (b) excess pore pressure

Kaolin 160 CPTu centrifuge

Data from Schneider (2008)

Table 2. Summary of kaolin data points used in analysis of piezocone behaviour (see Appendix A12 for detailed profiles)

Soil	g	Depth (mm)	v (mm/s)	d (mm)	q_{inet} (kPa)	Δu_2 (kPa)	B_q	σ_{v0} (kPa)	u_0 (kPa)	σ'_{v0} (kPa)	$c_{v,NC}$ (m^2/yr)	Q	$\Delta u_2/\sigma'_{v0}$	σ'_{vy} (kPa)	OCR	q_{inet}/σ'_{vy}
NC kaolin	160	75	3	10	266	136	0.51	194	117	77	1.9	3.4	1.76	77	1	3.4
NC kaolin	160	85	3	10	320	162	0.51	222	133	88	2.1	3.6	1.84	88	1	3.6
NC kaolin	160	95	3	10	378	189	0.5	249	150	99	2.3	3.8	1.90	99	1	3.8
NC kaolin	160	75	3	10	242	138	0.57	195	117	78	1.9	3.1	1.78	78	1	3.1
NC kaolin	160	85	3	10	288	173	0.6	223	134	89	2.1	3.2	1.95	89	1	3.2
NC kaolin	160	95	3	10	333	199	0.6	251	151	100	2.4	3.3	1.99	100	1	3.3
NC kaolin	160	75	1	10	262	137	0.53	195	118	78	1.9	3.4	1.77	78	1	3.4
NC kaolin	160	85	1	10	292	160	0.55	223	134	89	2.1	3.3	1.80	89	1	3.3
NC kaolin	160	95	1	10	350	184	0.53	252	151	100	2.4	3.5	1.84	100	1	3.5
NC kaolin	160	75	0.3	10	295	120	0.41	193	116	78	1.9	3.8	1.55	78	1	3.8
NC kaolin	160	85	0.3	10	356	138	0.39	221	133	89	2.1	4	1.56	89	1	4
NC kaolin	160	95	0.3	10	425	164	0.39	249	149	100	2.4	4.3	1.64	100	1	4.3
NC kaolin	160	75	0.03	10	320	78	0.24	203	126	78	1.9	4.1	1.00	78	1	4.1
NC kaolin	160	85	0.03	10	426	91	0.21	231	142	89	2.1	4.8	1.03	89	1	4.8
NC kaolin	160	95	0.03	10	544	92	0.17	259	159	100	2.4	5.4	0.92	100	1	5.4
NC kaolin	160	75	0.003	10	471	5	0.01	198	120	78	1.9	6.1	0.06	78	1	6.1
NC kaolin	160	85	0.003	10	562	5	0.01	225	136	89	2.1	6.3	0.05	89	1	6.3
NC kaolin	160	95	0.003	10	678	4	0.01	253	153	100	2.4	6.8	0.04	100	1	6.8
NC kaolin	160	75	0.0004	10	536	0	0	192	115	77	1.9	6.9	0.00	77	1	6.9
NC kaolin	160	85	0.0004	10	642	1	0	224	135	89	2.1	7.2	0.01	89	1	7.2
NC kaolin	160	95	0.0004	10	734	1	0	250	151	100	2.4	7.4	0.01	100	1	7.4
OC kaolin	40	84	0.004	10	687	4	0.01	56	33	23	0.5	29.8	0.18	150	6.5	4.6
OC kaolin	40	84	0.03	10	499	26	0.05	56	33	23	0.5	21.6	1.13	150	6.5	3.3
OC kaolin	40	84	0.299	10	219	69	0.32	56	33	23	0.5	9.5	3.00	150	6.5	1.5
OC kaolin	40	86	3.54	10	497	90	0.18	57	34	24	0.6	21.1	3.80	150	6.4	3.3
OC kaolin	40	100	0.004	10	789	6	0.01	66	39	27	0.6	28.9	0.23	150	5.5	5.3
OC kaolin	40	100	0.03	10	531	38	0.07	66	39	27	0.6	19.5	1.40	150	5.5	3.5
OC kaolin	40	100	0.298	10	335	83	0.25	66	39	27	0.6	12.3	3.04	150	5.5	2.2
OC kaolin	40	100	3.12	10	511	102	0.2	66	39	27	0.6	18.7	3.72	150	5.5	3.4
OC kaolin	40	109	0.004	10	820	8	0.01	73	43	30	0.7	27.4	0.27	150	5	5.5
OC kaolin	40	109	0.03	10	530	45	0.08	73	43	30	0.7	17.7	1.50	150	5	3.5
OC kaolin	40	109	0.3	10	377	90	0.24	73	43	30	0.7	12.6	3.02	150	5	2.5
OC kaolin	40	112	3.63	10	526	115	0.22	75	44	31	0.7	17.1	3.75	150	4.9	3.5

Kaolin Centrifuge CPTu

Data from Cinicioglo (2005)

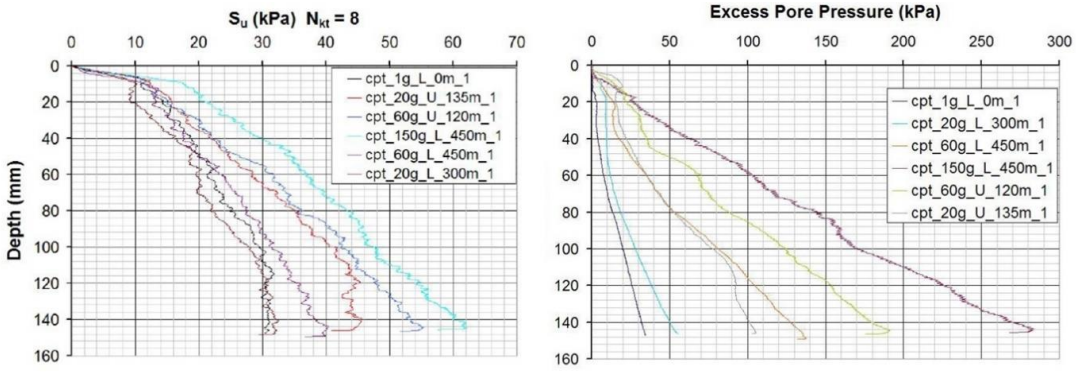

Figure 5.32. Excess pore pressures generated by cone penetration at the end of consolidation at each g-level of Test 1.

Kaolin CPTu chamber test

Data from Hird & Sangtian (2004)

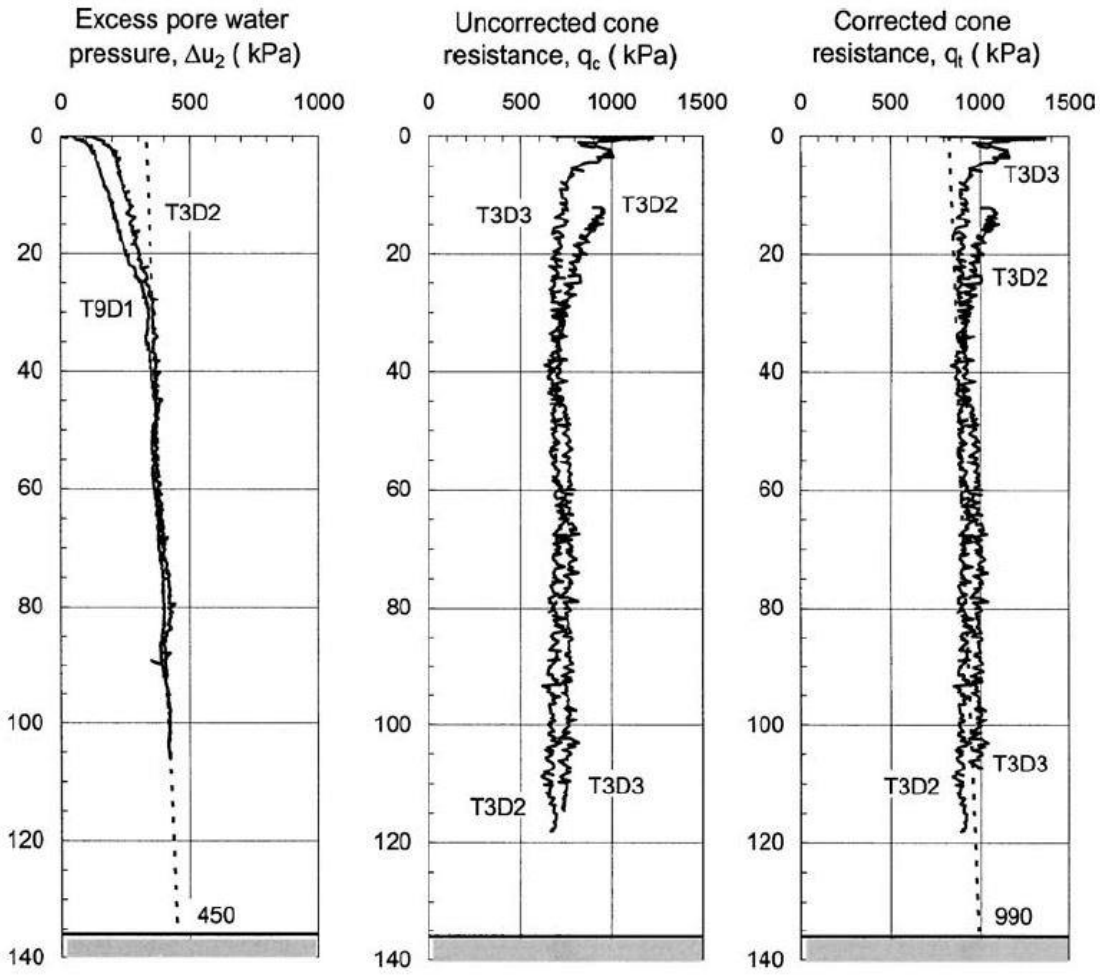

Kaolin CPTu chamber test

Data from May 1987

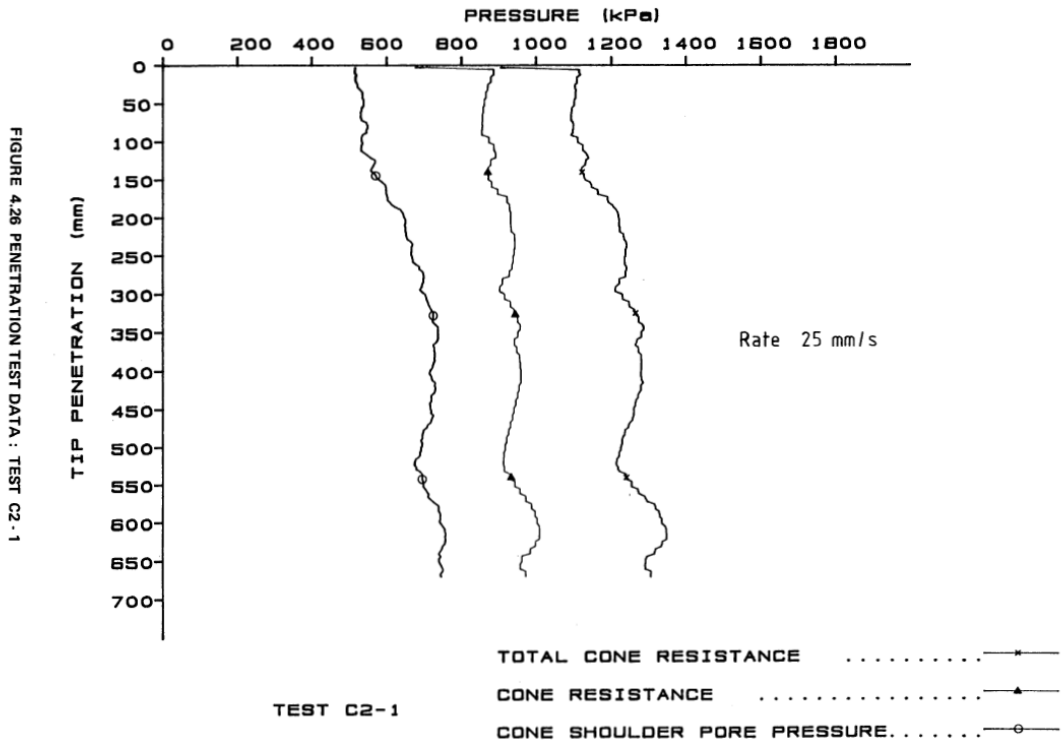

FIGURE 4.26 PENETRATION TEST DATA : TEST C2-1

Kaolin CPTu chamber test

Data from Nyirenda (1989)

Table 6.2A Results of penetration tests

Test Series No.	q_t kPa	Skin Friction kPa	U_1 kPa	U_{Shld} kPa	U_3 kPa	U_4 kPa
Z14C	2370			1157		
Z13C	2462			1289		
Z21B	1824			948		
Z22B	1420			790		
Z33A	1450			634		
Z34A	1500			680		
Z41C	943		631	422	291	251
Z42C	912		604	355	266	186
Z43C	888		588	367	233	170
Z53B	824			317		
Z54B	832			304		
Z61A	951			369		
Z62A	829			356		
Z63A	832			352		

Table 6.2B Results of penetration tests (continued)

Test Series No.	q_t kPa	Skin Friction kPa	U_{Face} kPa	U_{Shld} kPa	$U_{M.sleeve}$ kPa	$U_{T.sleeve}$ kPa
Z71C	1190	24	716	558	256	154
Z72C	1255	18	646	511	265	178
Z73C	1213	39	832	524	250	177
Z74C	1279	14	870	487	278	182
Z81B	2086			1185		
Z82B	1899			1170		
Z84B	2123			1062		
Z91C	1973	13.5	1638	1236	930	712
Z92C	2077	11	1724	1264	911	699
Z93C	1967	8.5	1632	1186	898	640
Z94C	1943	11	1605	1205	870	661
Z101A	1453			563		
Z102A	1530			529		
Z103A	958			522		
Z104A	1165			459		
Z111B	787			308		
Z112B	764			268		
Z113B	738			280		
Z114B	747			221		
Z121C	1112	9.3	874	635	409	281
Z122C	1054	8.6	657	545	376	260
Z123C	1019	5.6	812	567	390	267
Z124C	1035	6.1	837	610	353	261

Cornell clay CPTu chamber test UU

Data from Mayne (1993)

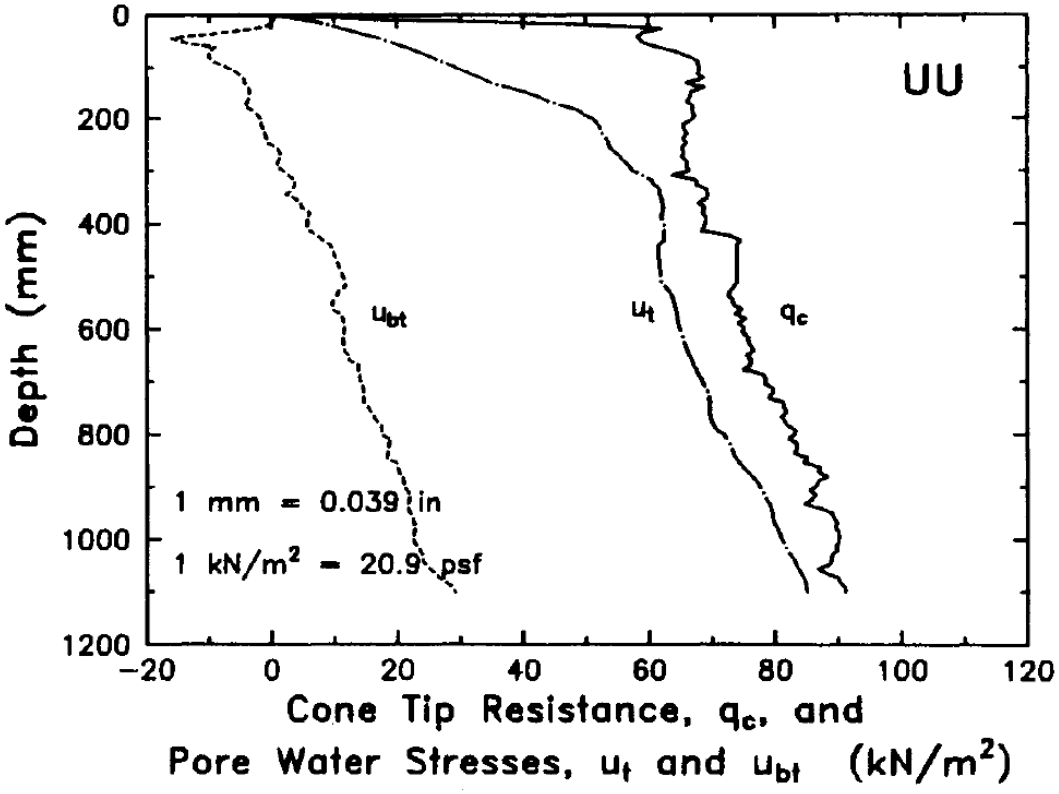

Kaolin centrifuge CPTu

Data from Esquivel (1995)

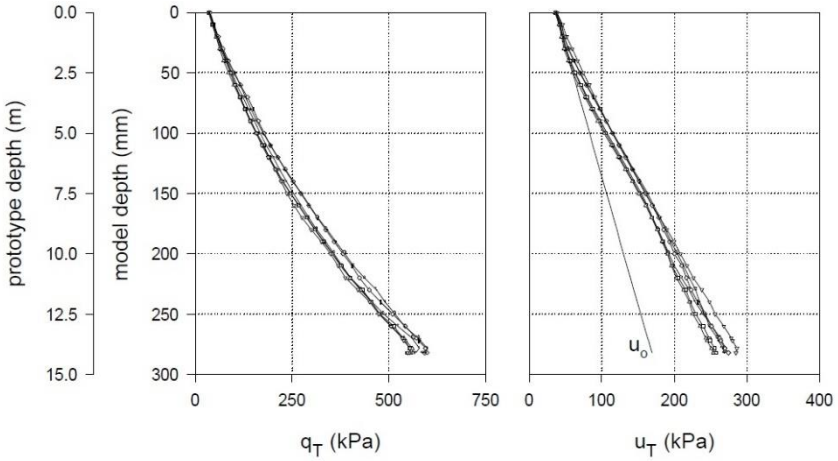

Fig. 6. CPTU Performed in Normally Consolidated Clay (g-level=50)

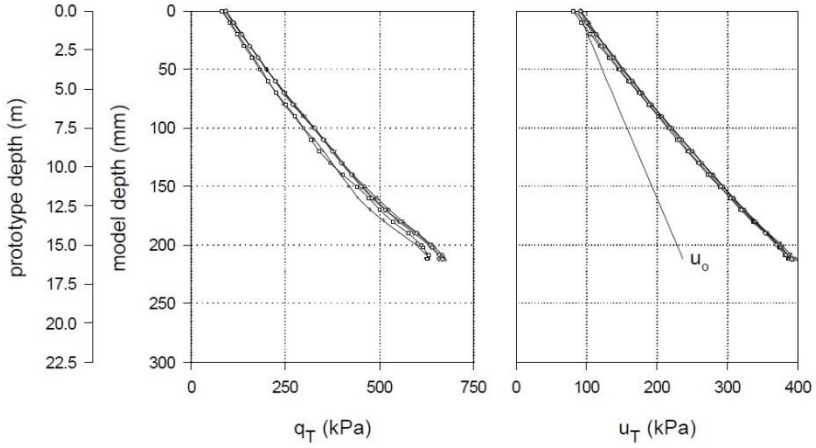

Fig. 5. CPTU Performed in Normally Consolidated Clay (g-level=75)

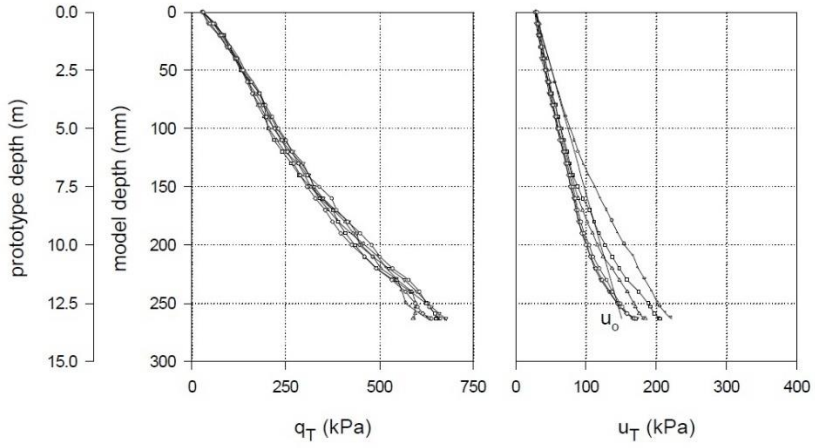

Fig. 4. CPTU Performed in Overconsolidated Clay (4<OCR<10, g-level=50)

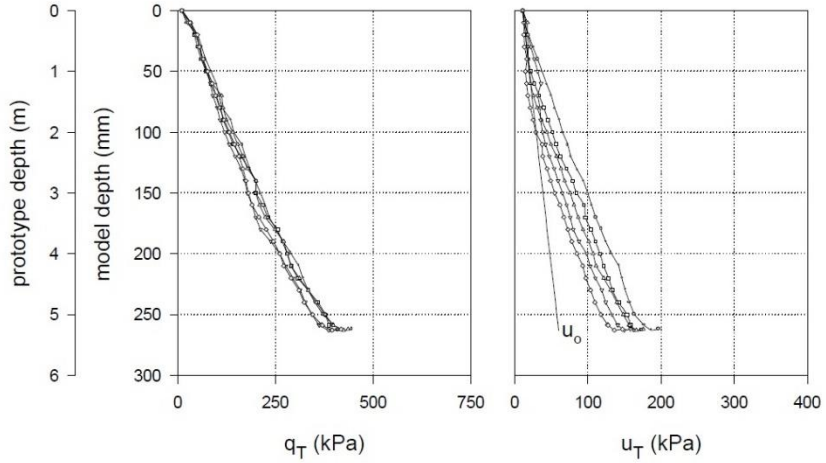

Fig. 3. CPTU Performed in Overconsolidated Clay (6<OCR<14, g-level=20)

Kaolin mix CPTu chamber test

Data from Kim & Tumay (2007)

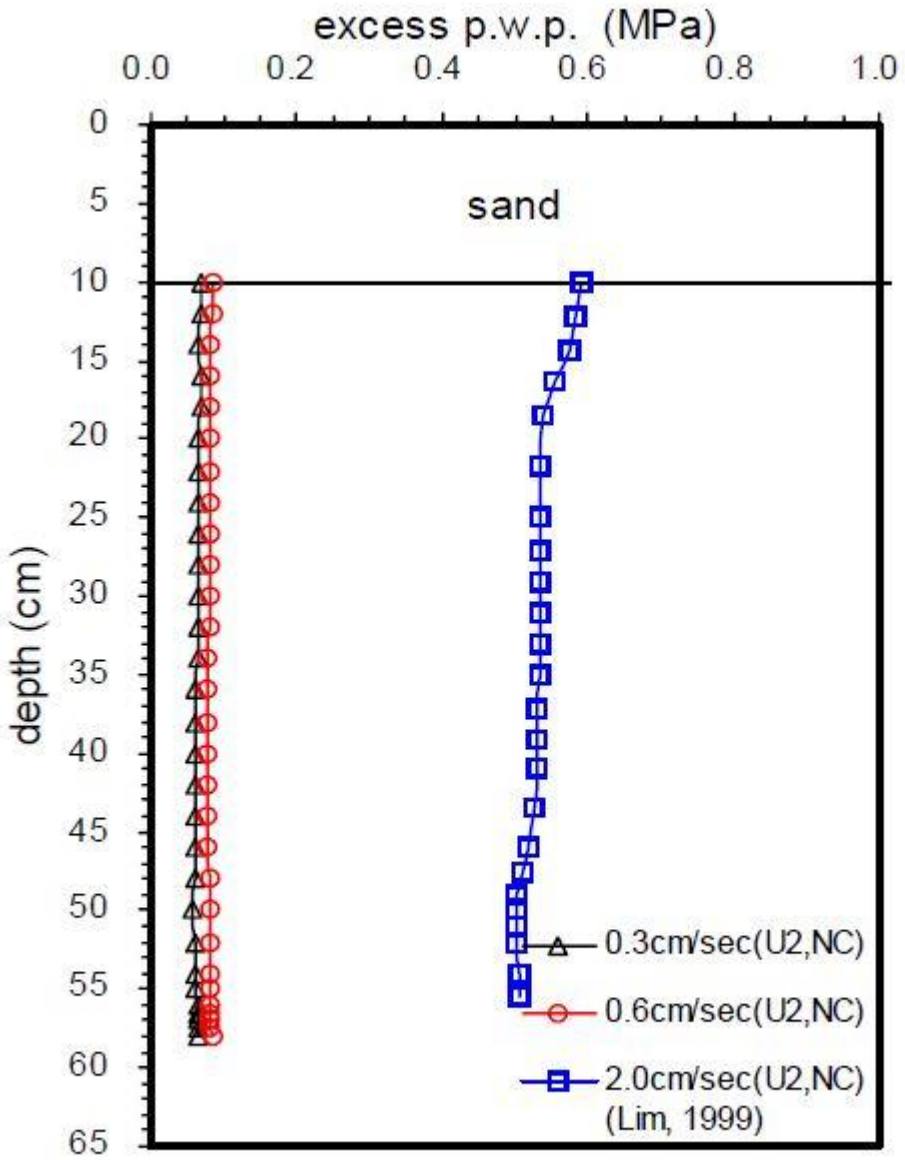

Fig. 14: Excess p.w.p. Profiles for U2 and NC Specimens.

Kaolin mix P1 and P2

Data from Kim (2005)

Table 5.1 Values of q_t, pore pressure, and f_s of minicone penetration tests for various rates performed in calibration chamber sample P1.

Penetration rate (mm/sec)	20	8	2	0.25	0.1	0.05	0.035	0.02	0.01
q_t (MPa)	0.71	0.69	0.83	0.91	1.37	2.26	2.48	3.14	3.13
Pore pressure (kPa)	295	270	233.2	222.6	184.9	82.4	63.4	8	13
Local friction f_s (kPa)	-	14.2	12.9	11.0	12.2	13.1	11.8	12.5	12.1

Table 5.3 q_t, u, and f_s for various penetration rates in P2.

Penetration rate (mm/sec)	20	10	2	1	0.5	0.2	0.1	0.05
q_t (MPa)	1.28	1.34	1.65	2.28	2.78	3.49	3.99	3.9
Pore pressure (kPa)	246	219.1	145.8	103.3	48.2	23.9	6.26	6.26
Sleeve friction f_s (kPa)	6.9	10.2	7.0	11.6	10.8	13.3	15.8	16.7

Kreuzlingen, Switzerland

Data from Heil et al 1997

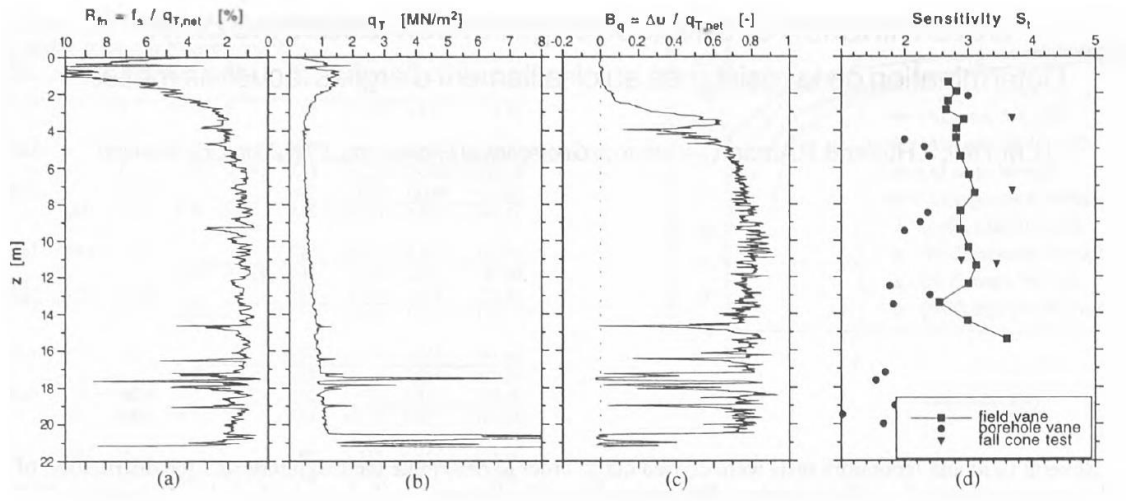

Fig. 1: Typical CPT results and sensitivity for Kreuzlingen clay

Kurihama Japan

Data from Tanaka (1995)

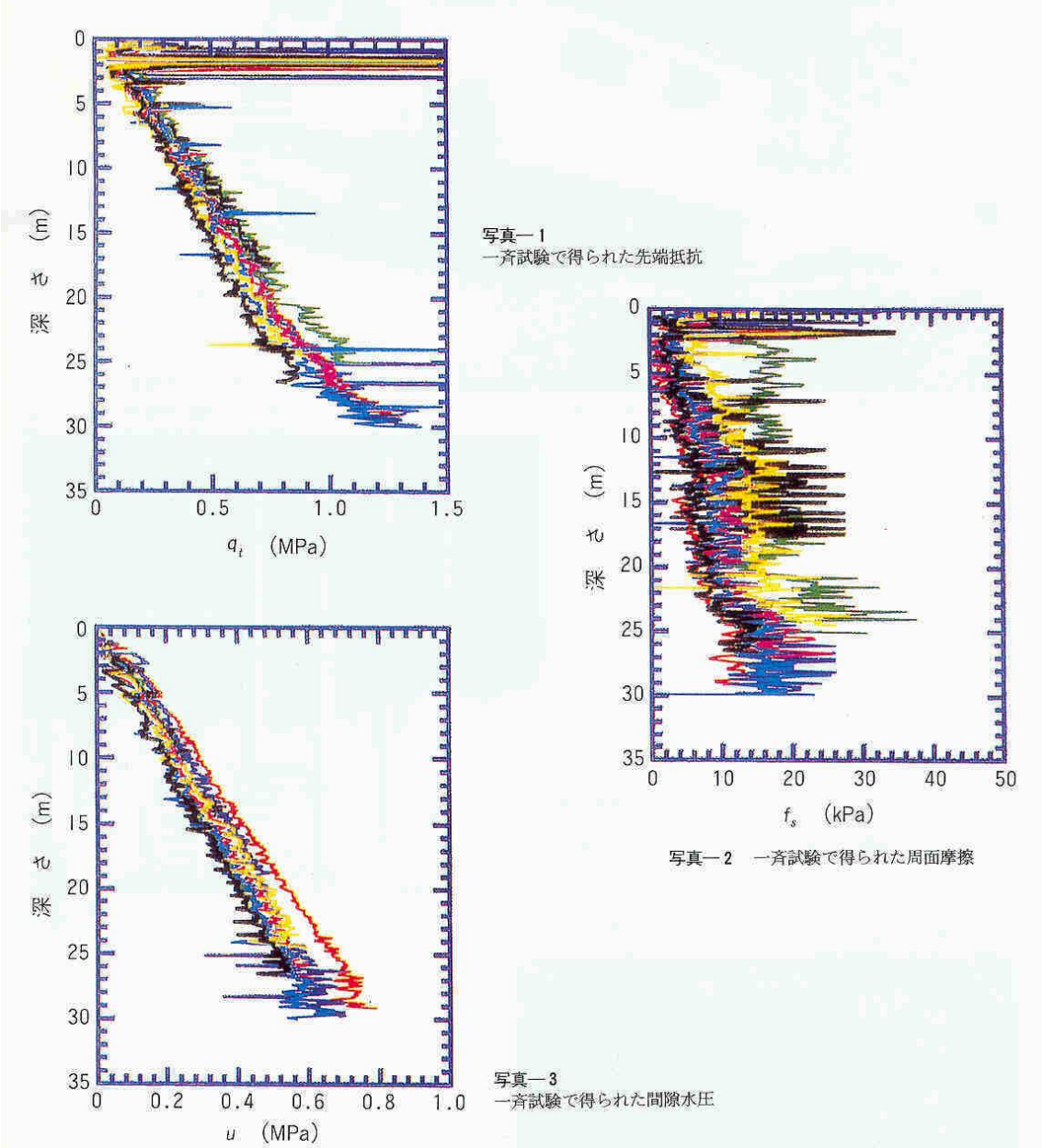

写真―1
一斉試験で得られた先端抵抗

写真―2　一斉試験で得られた周面摩擦

写真―3
一斉試験で得られた間隙水圧

La Baie, Canada

Data from Demers (2001)

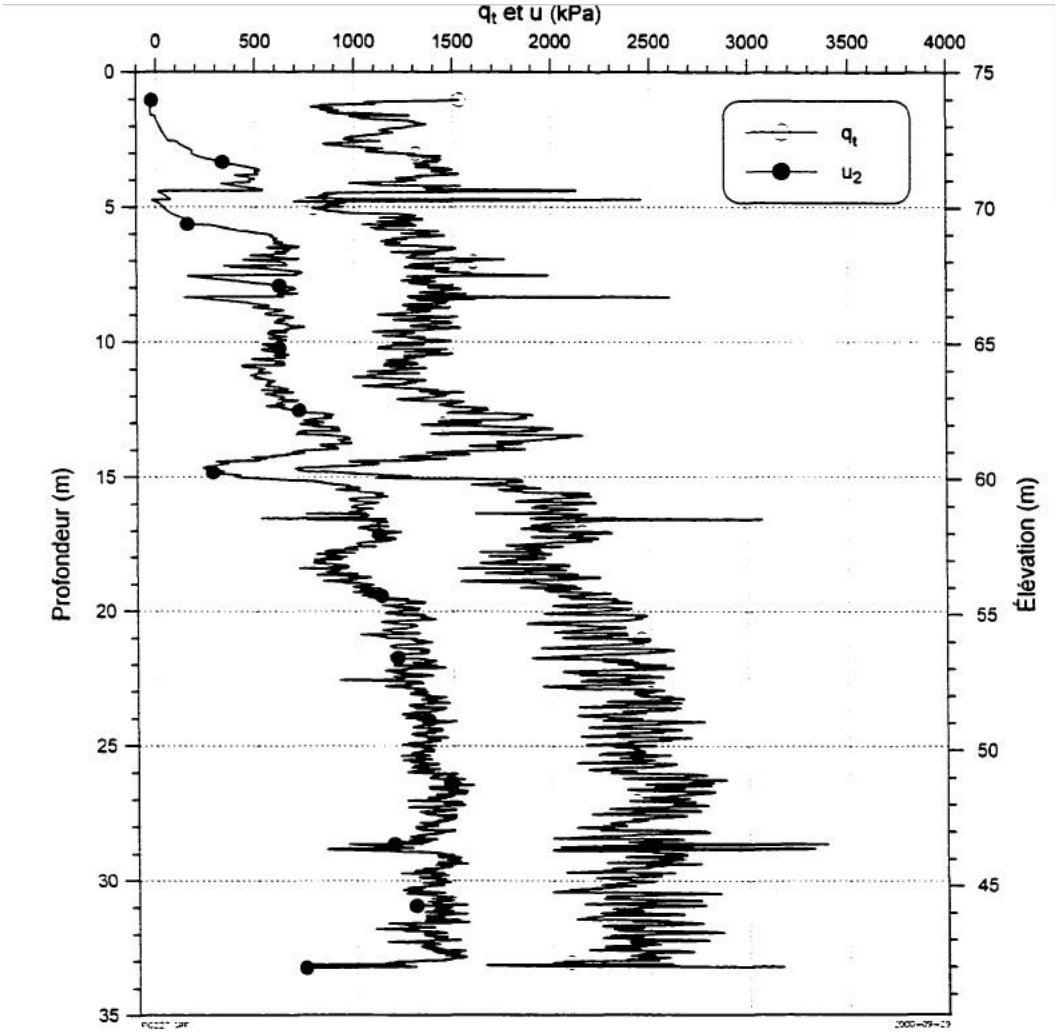

Figure 2.27: Essai au piézocône PCPT1, à La Baie.

Lenordini 51, California

Data from Krage & DeJong (2014)

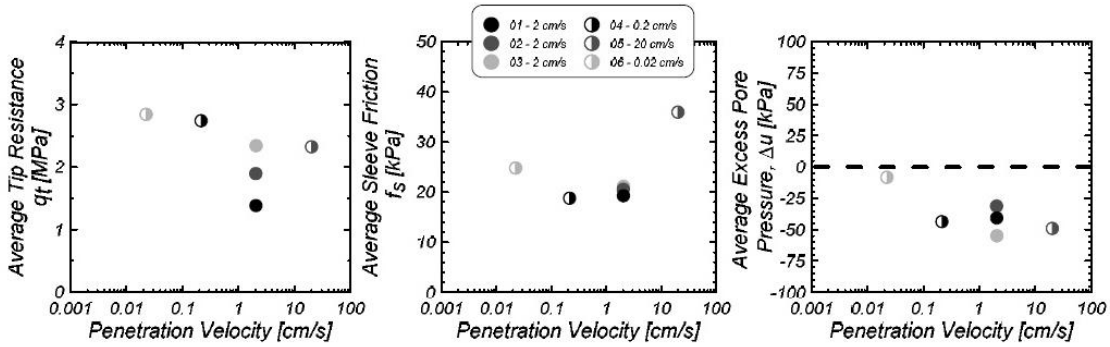

FIG. 8 - Lenordini 51 Interval Summary 3.5 to 4.3 m

Les-Cedres, Canada

Data from Demers (2001)

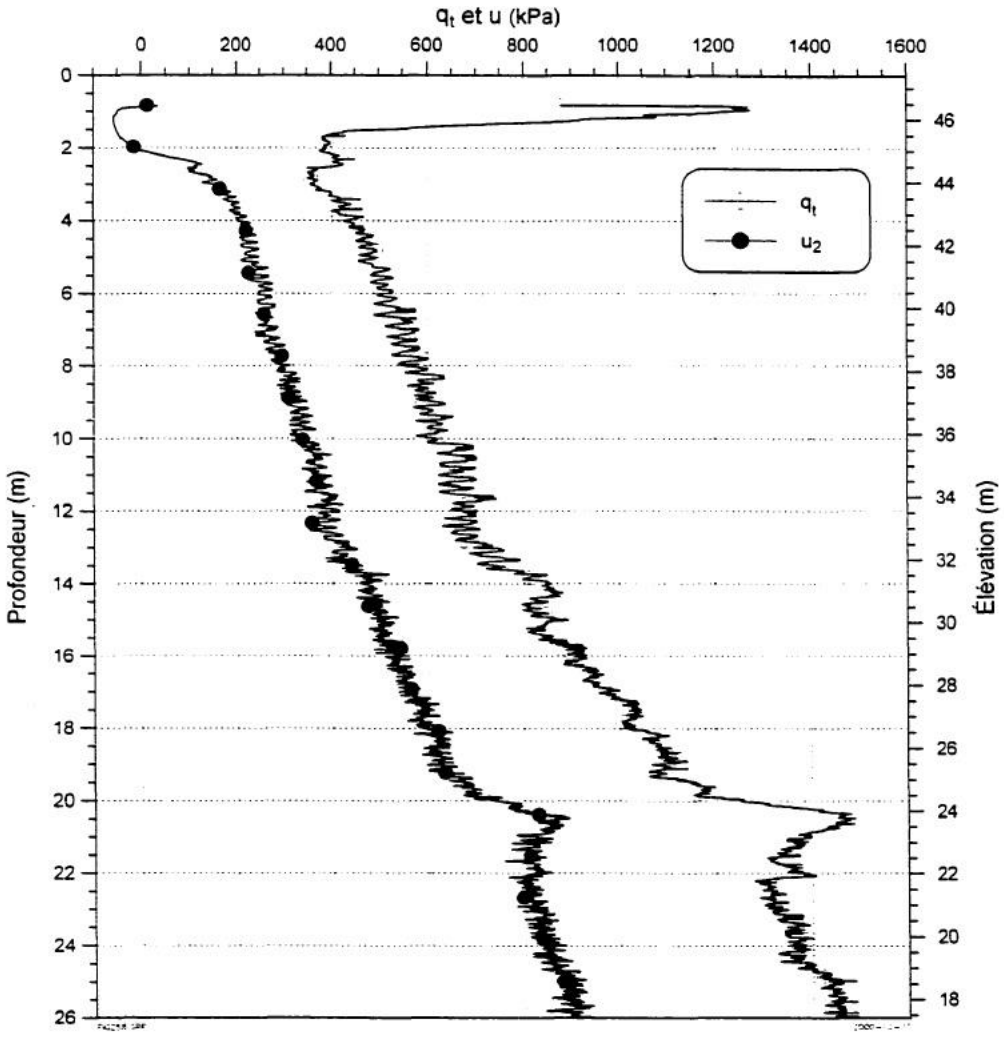

Figure 2.58: Essai au piézocône CPTU2, au site de Les Cèdres.

Lianyungang, China

Data from Liu et al. (2011)

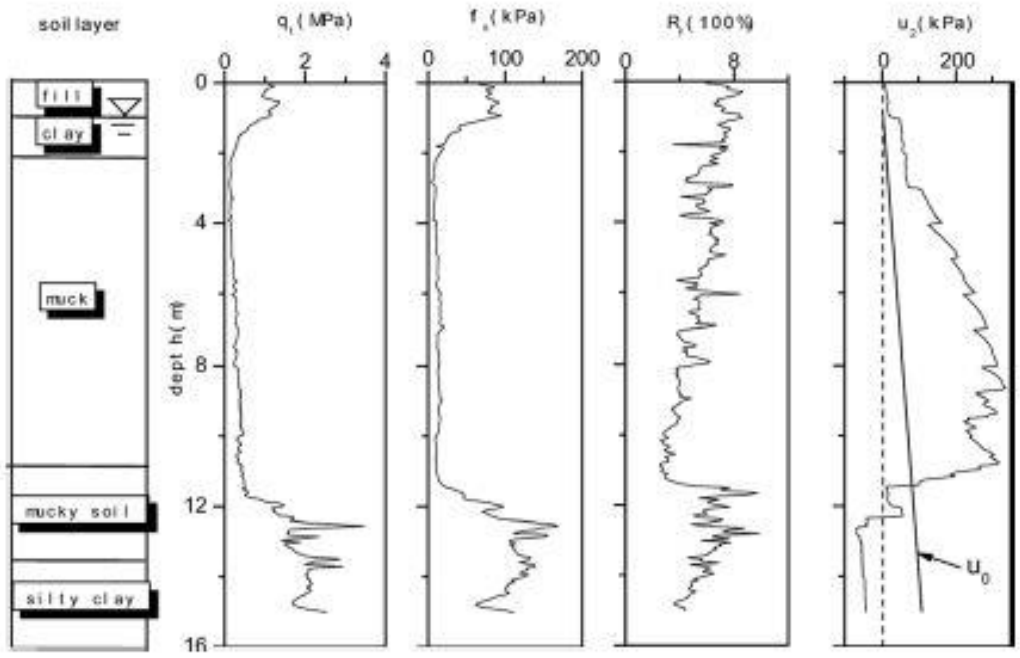

Figure 2. Typical result from piezocone tests.

Louiseville, USA

Data from Demers (2001)

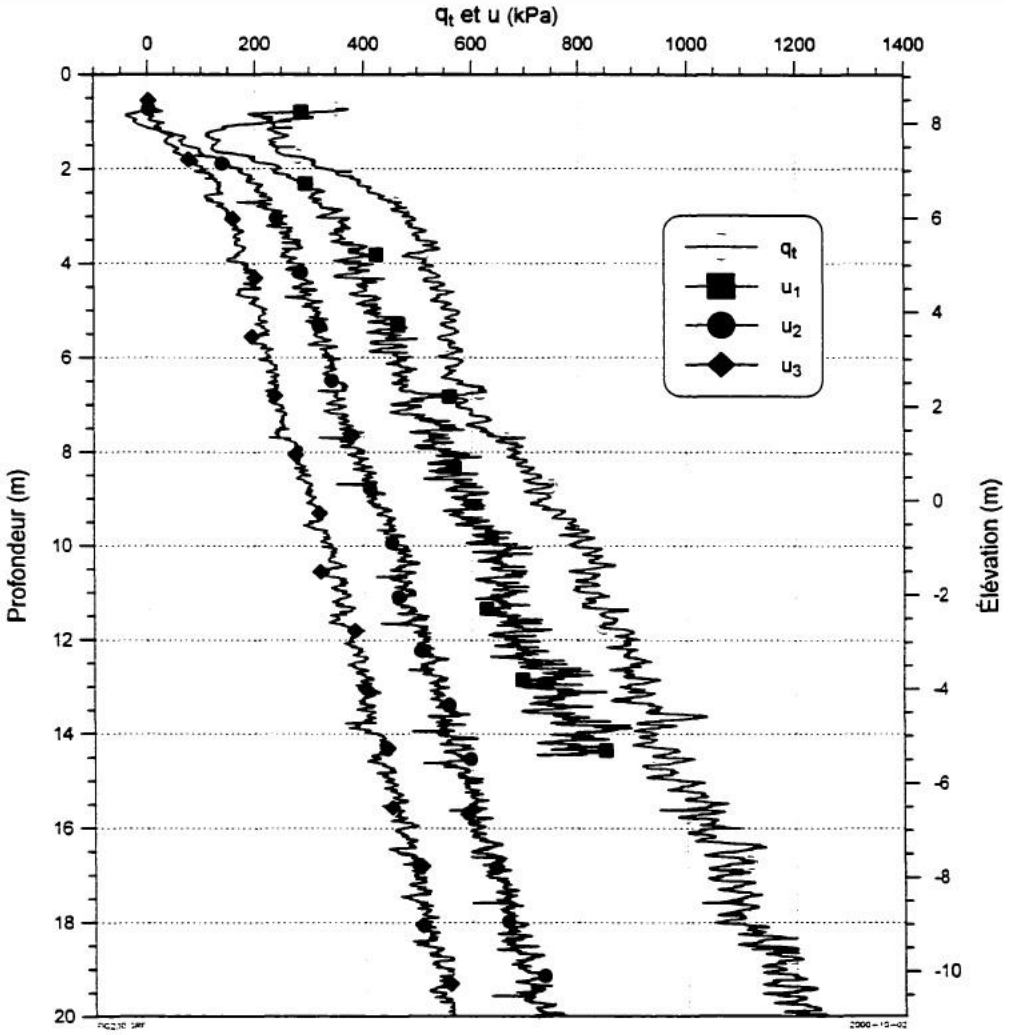

Figure 2.44: Essasi au piézocône CPTU12 et 20, à Louiseville.

Luva, Norway

Data from Lunne 2013

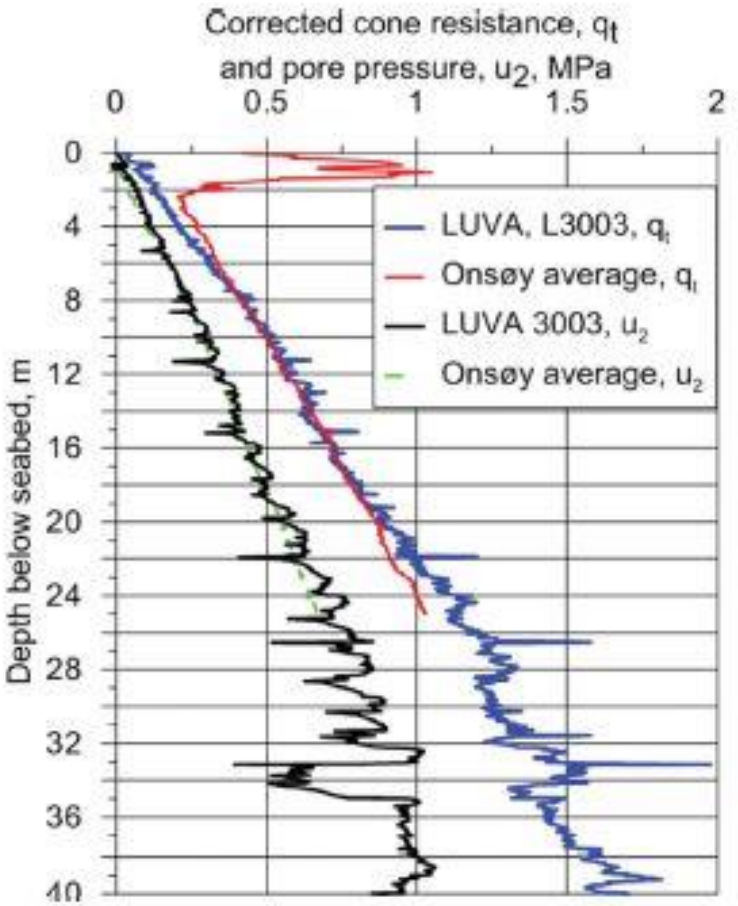

Figure 7. Corrected cone resistance and pore pressure at LUVA and Onsøy areas.

Madingley, UK

Data from Lunne and Powell (1986)

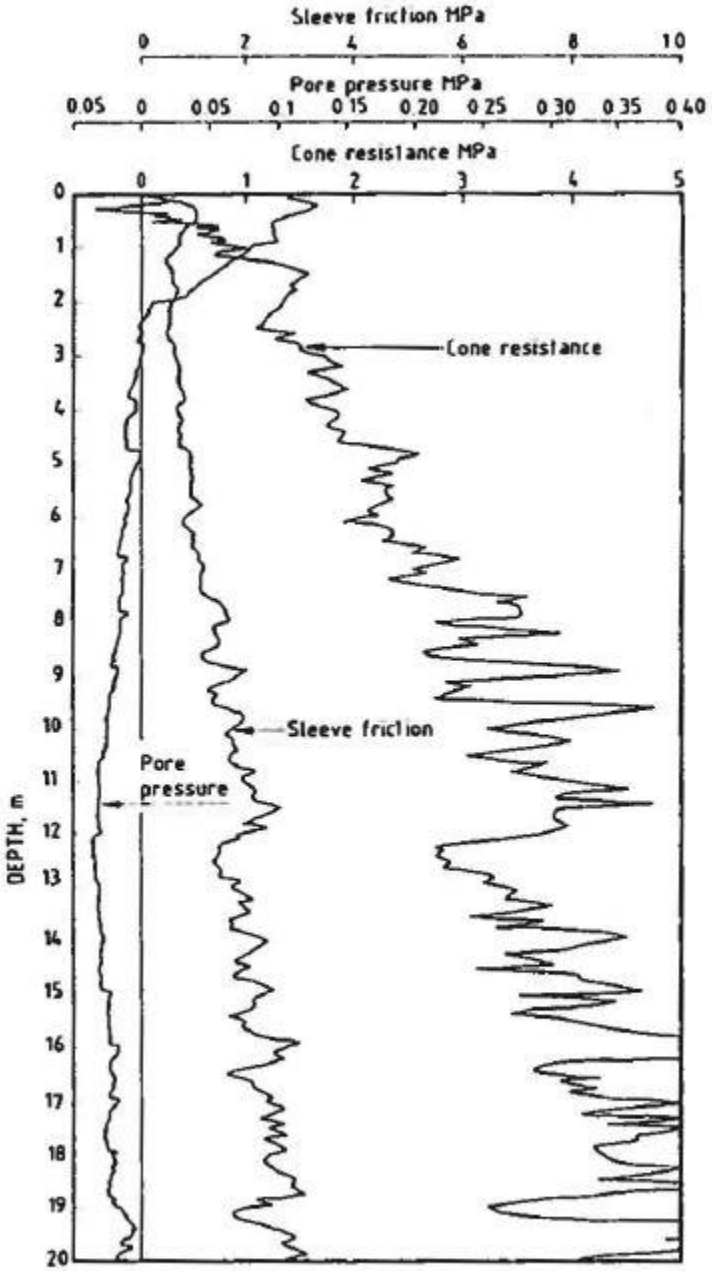

ig. 11. Typical DSML piezocone test results, Madingley

Madison, Indiana

Data from El Howayek et al 2015

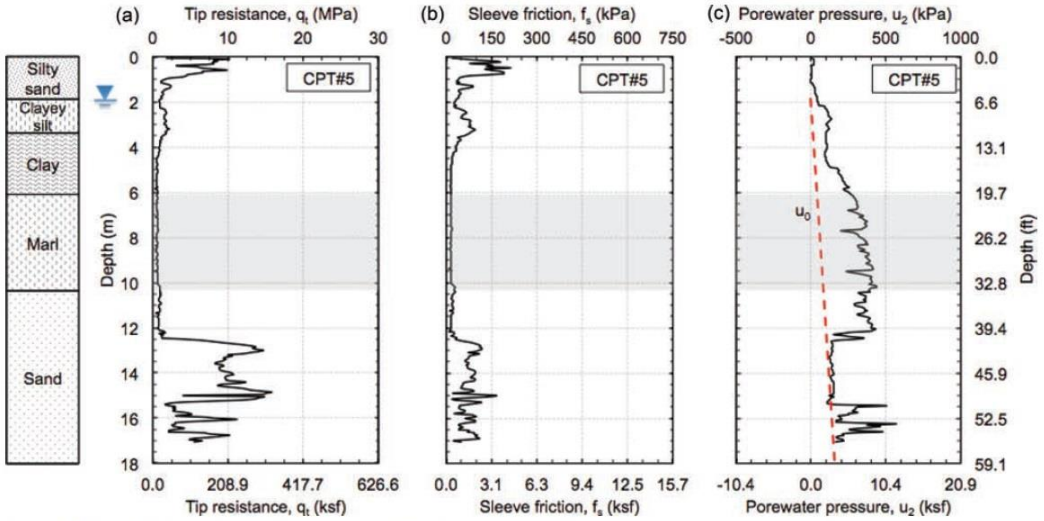

Figure A.7.5 CPT#5 results: (a) tip resistance, (b) skin friction, and (c) porewater pressure versus depth.

Marquette Interchange, Wisconsin

Data from Schneider & Hotstream 2011

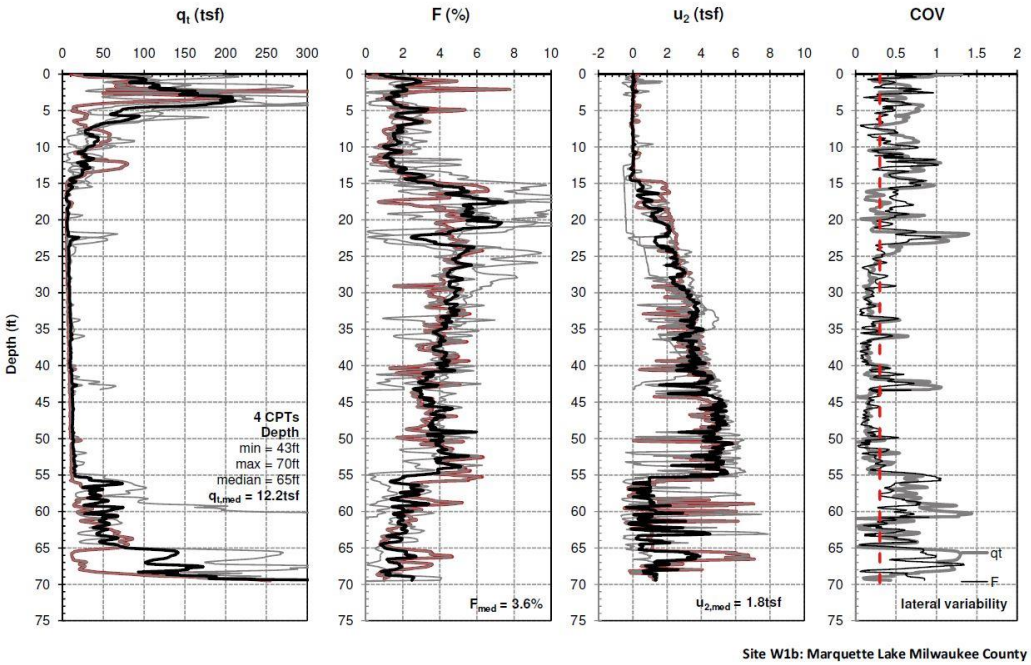

Martin’s Point Bridge, Maine

Data from Hardison (2015)

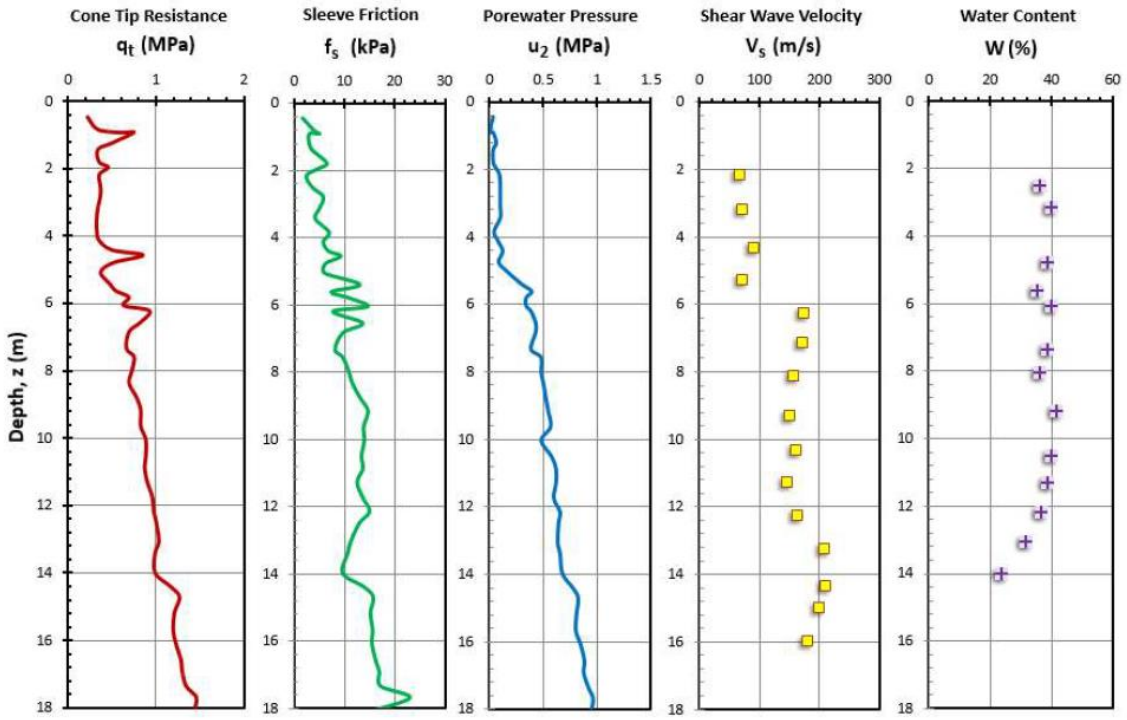

Maskinonge, Canada

Data from Demers (2001)

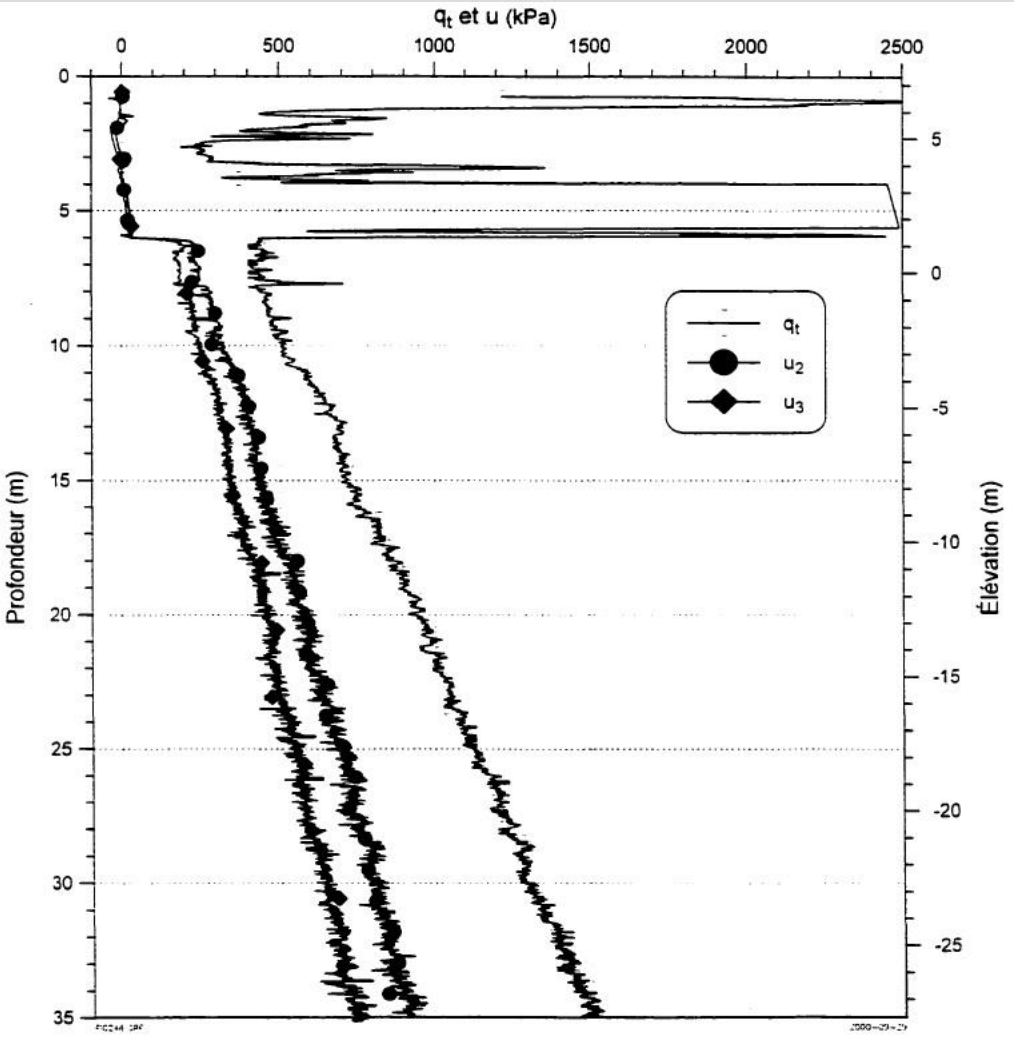

Figure 2.46: Essai au piézocône CPTU5, à Maskinongé (autoroute 40).

Massueville, Cananda

Data from Demers (2001)

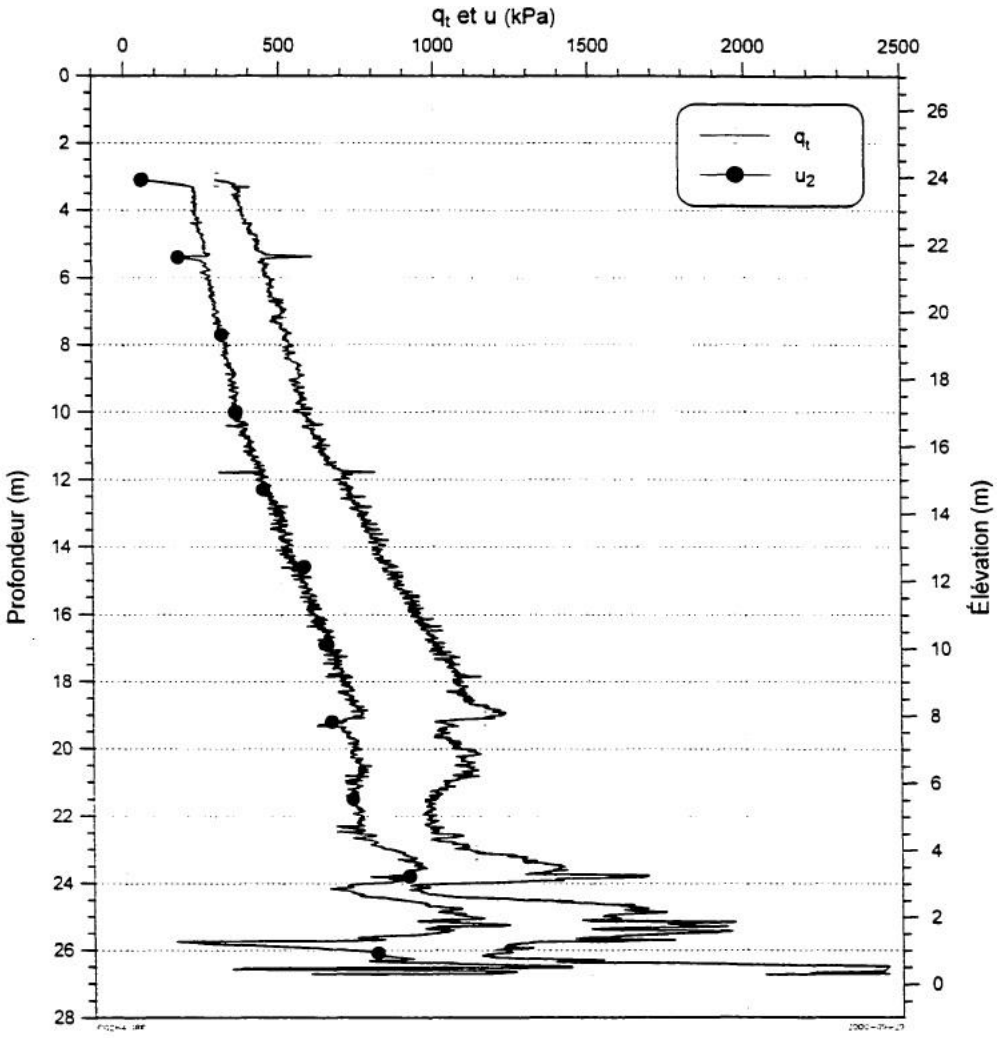

Figure 2.64: Essai au piézocône CPTU1, au site de Massueville.

Matagami, Canada

Data from Demers (2001)

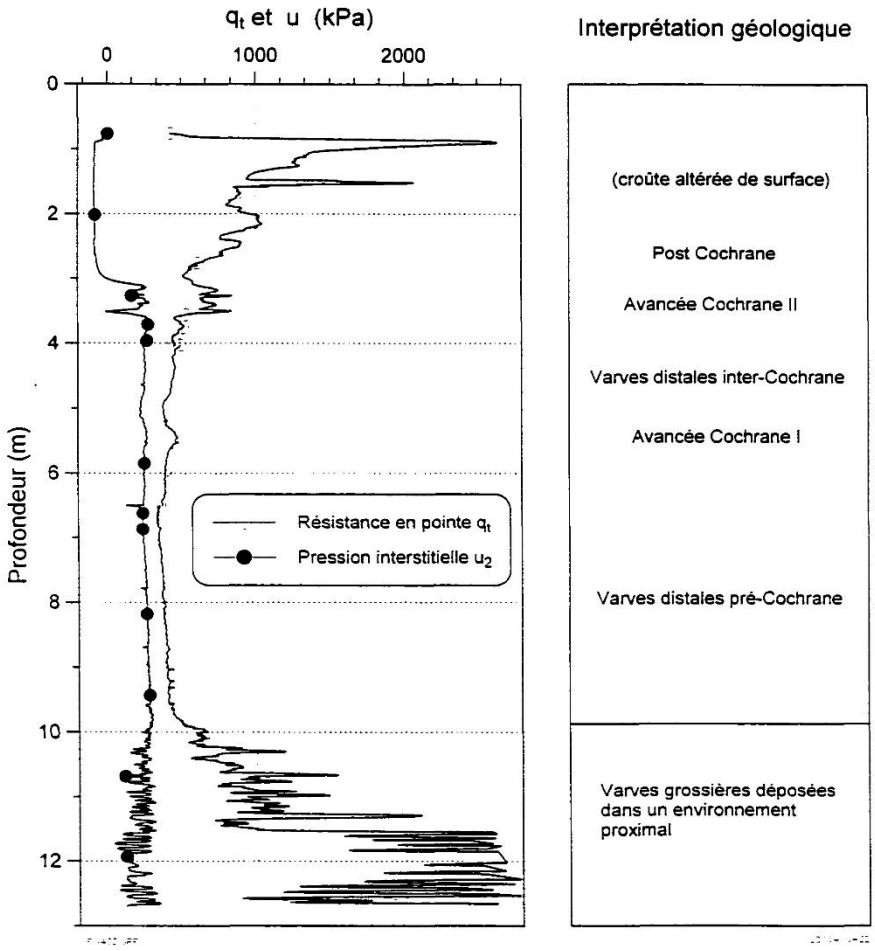

Figure 4.33: Profil au piézocône CPTU17, illustrant la stratigraphie locale.

352

McDonald Farm, BC

Data from Robertson et al. (1992)

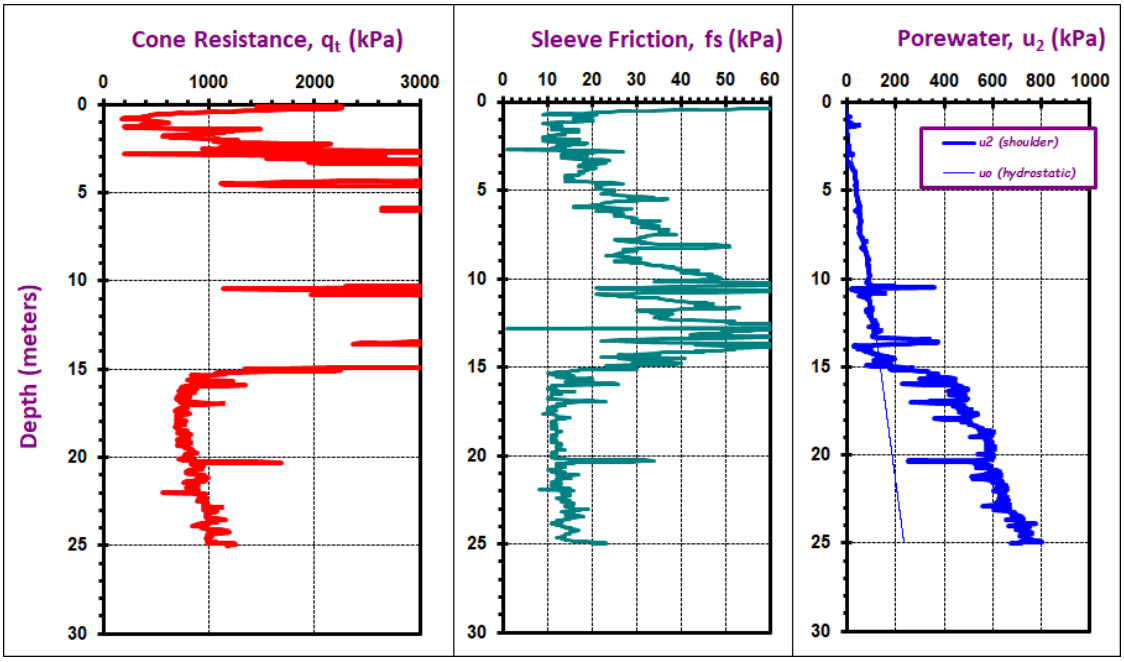

Mexico City

Data from Cruz &Mayne (2006)

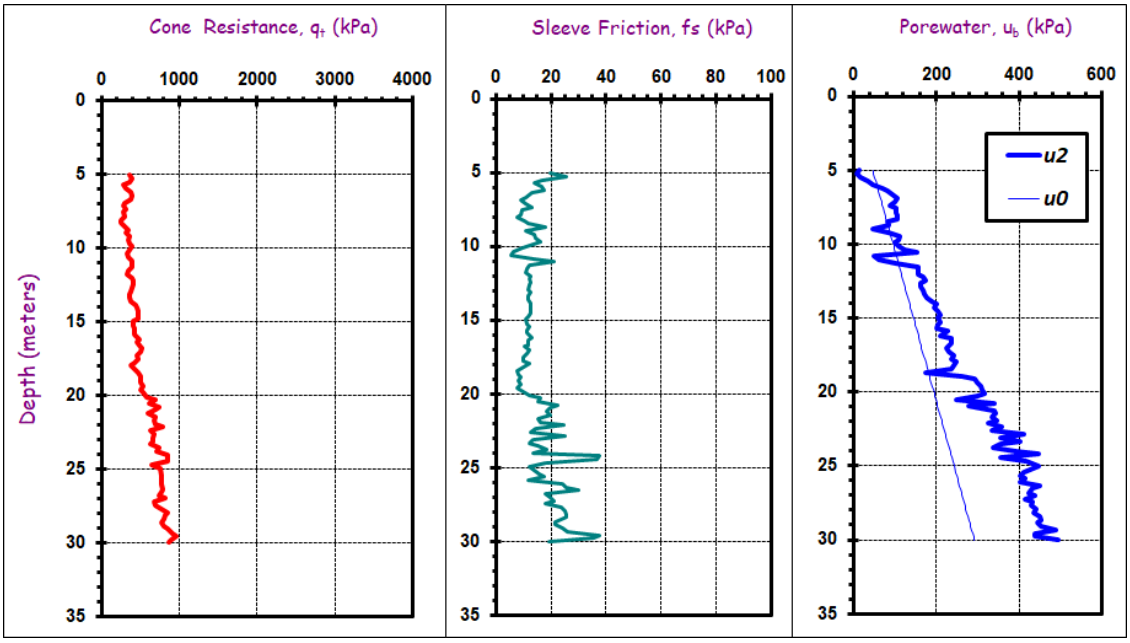

Mirabello, Italy

Data from Garcia Martinea PhD 2014

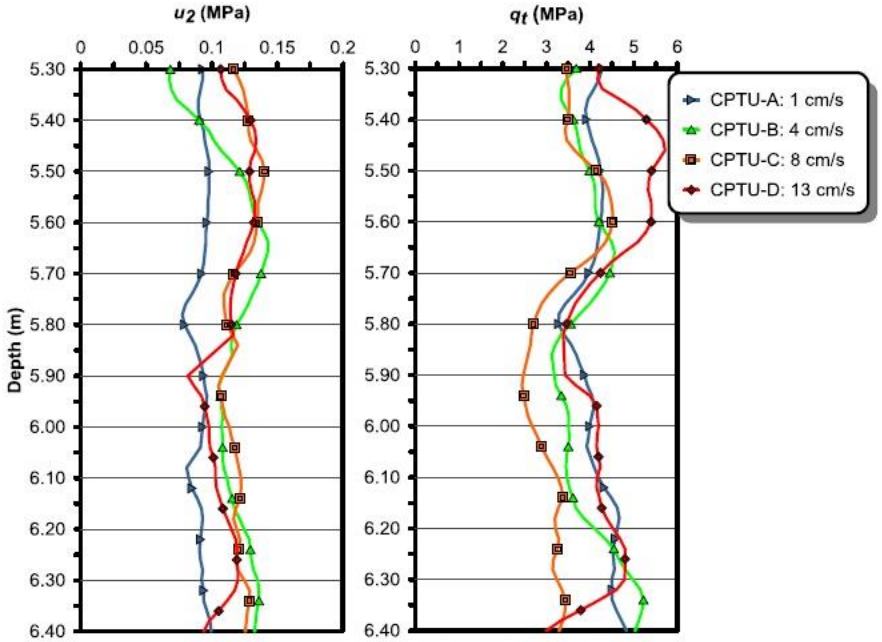

Figure 3.19: Comparison for the rate tests from 5.3 to 6.4 m

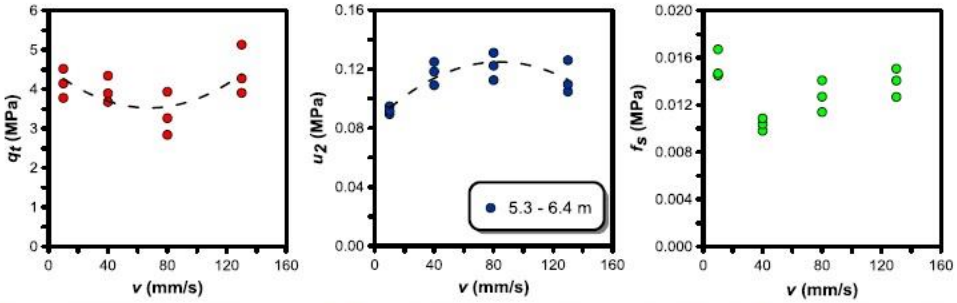

Figure 3.20: Effect of penetration rate on the cone resistance, q_t, pore pressure u_2 and sleeve friction f_s measurements

Newbury, Massachusetts

Data from Landon (2007)

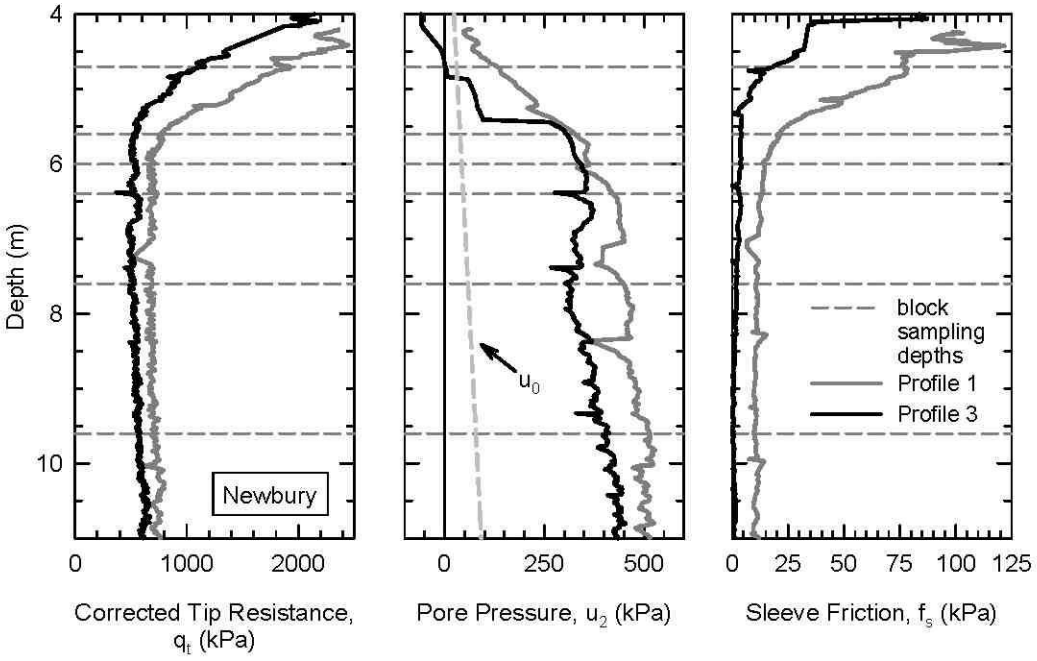

Nice airport, France

Data from Sultan et al 2007

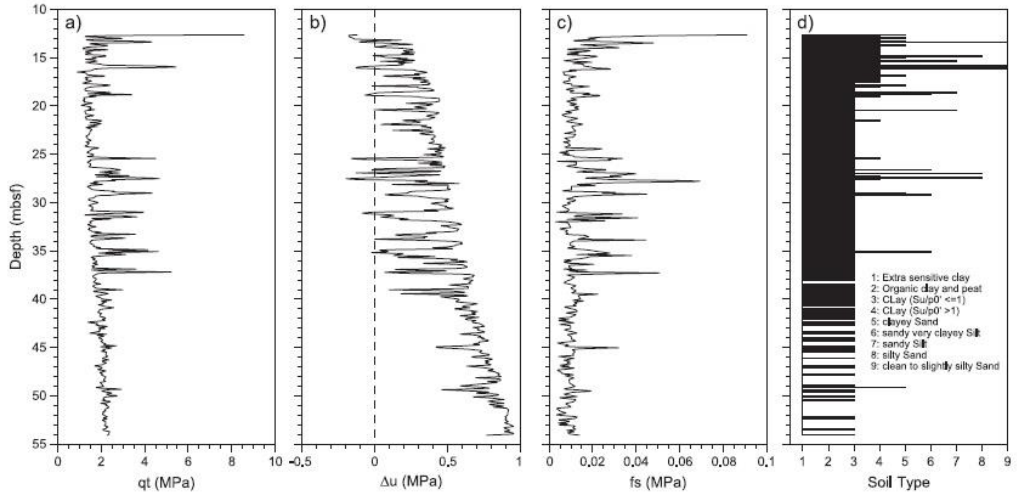

Fig. 15. Results of pz11 piezocone test (for location refer to Fig. 13a) including measurements of (a) corrected cone tip resistance (qt), (b) differential porewater pressure (Δu), (c) sleeve friction (fs), and (d) lithology profiles (see text for discussion).

Niger Delta

Sultan et al 2007

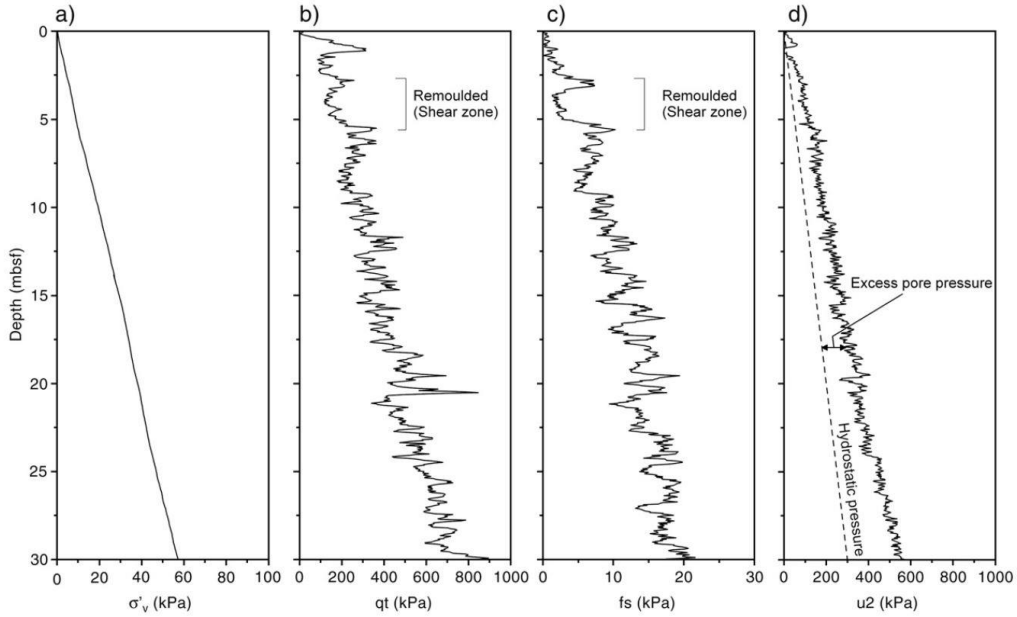

Fig. 6. Site N2-PM35-b: a) vertical effective stress vs depth below seafloor, b) corrected cone resistance qt versus depth, b) unit sleeve friction resistance fs vs depth and c) pore pressure u_2 vs depth.

North Charleston, SC

Data from Camp (2002)

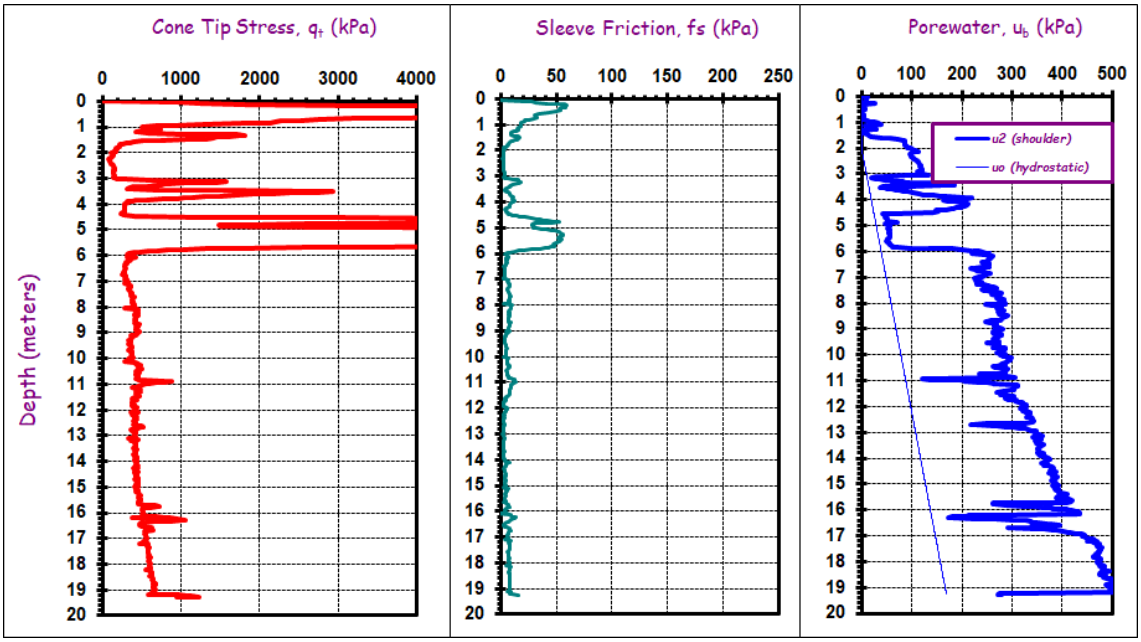

Ford Design Center, Evanston, IL

Data after Mayne (2007 b)

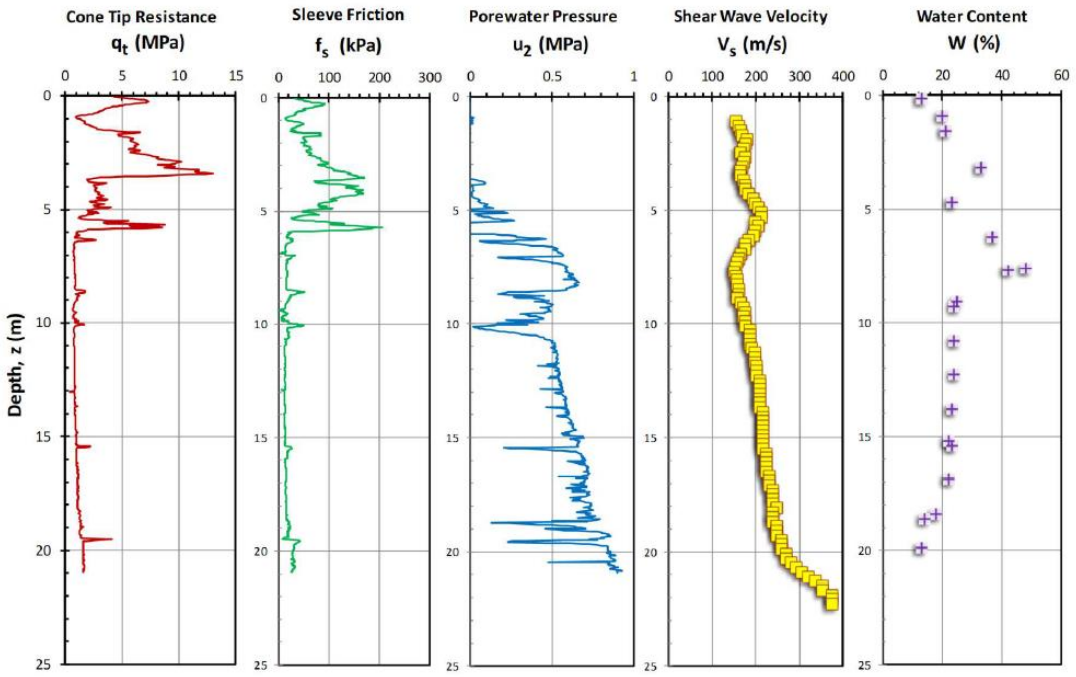

Nykirke CPTu in Norway

Data from Powell & Lunne (2006)

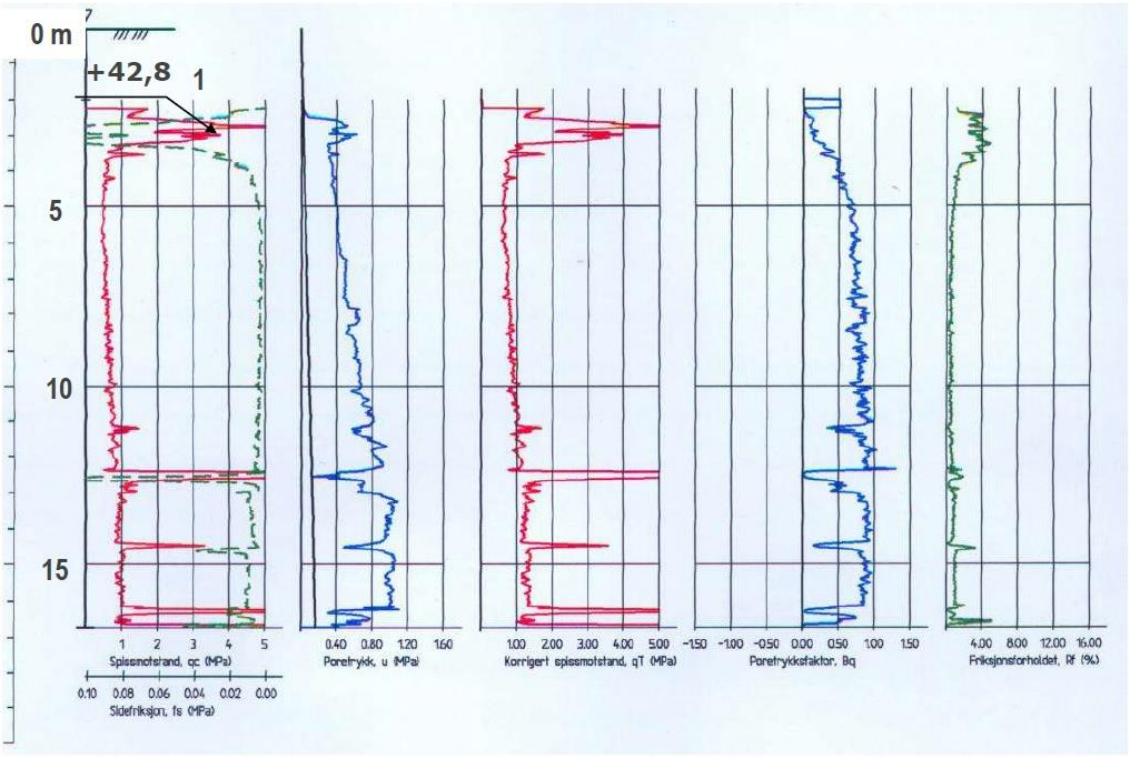

Onsoy CPTu from Lunne 2010

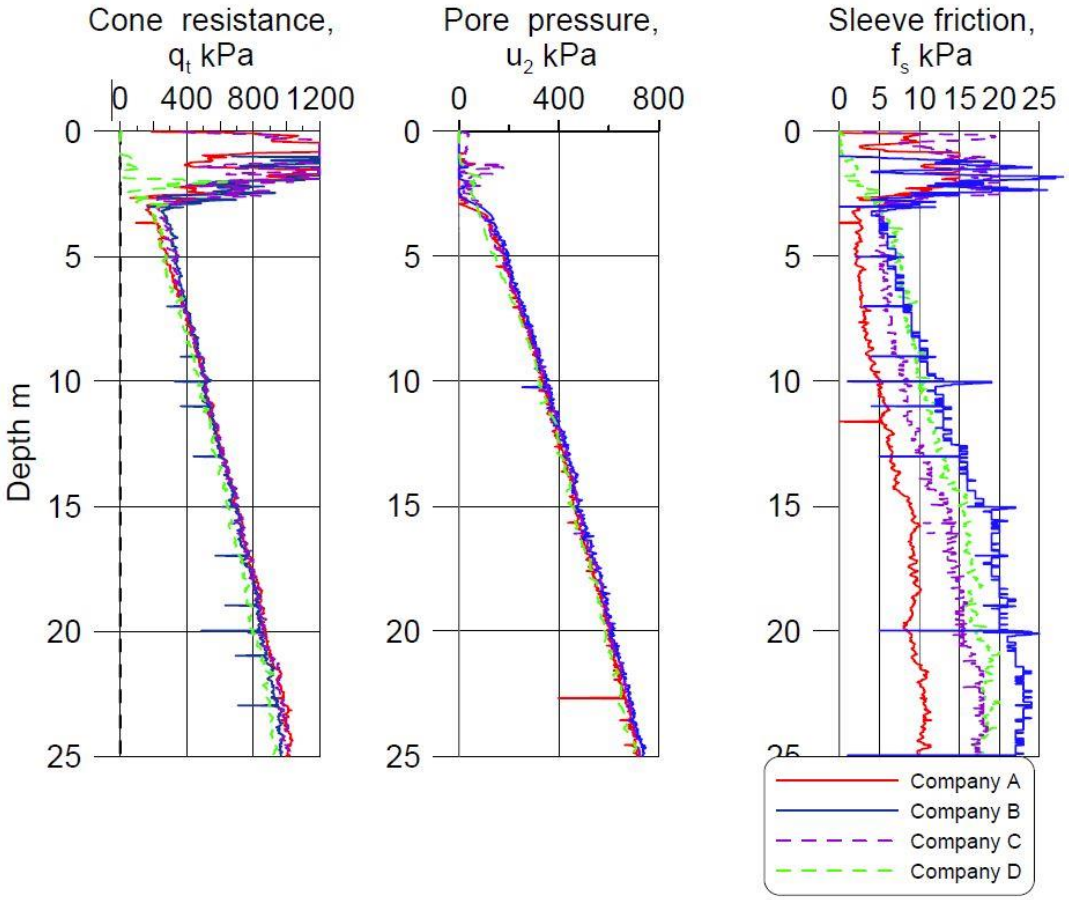

Os, Norway

Data after Long et al. (2010)

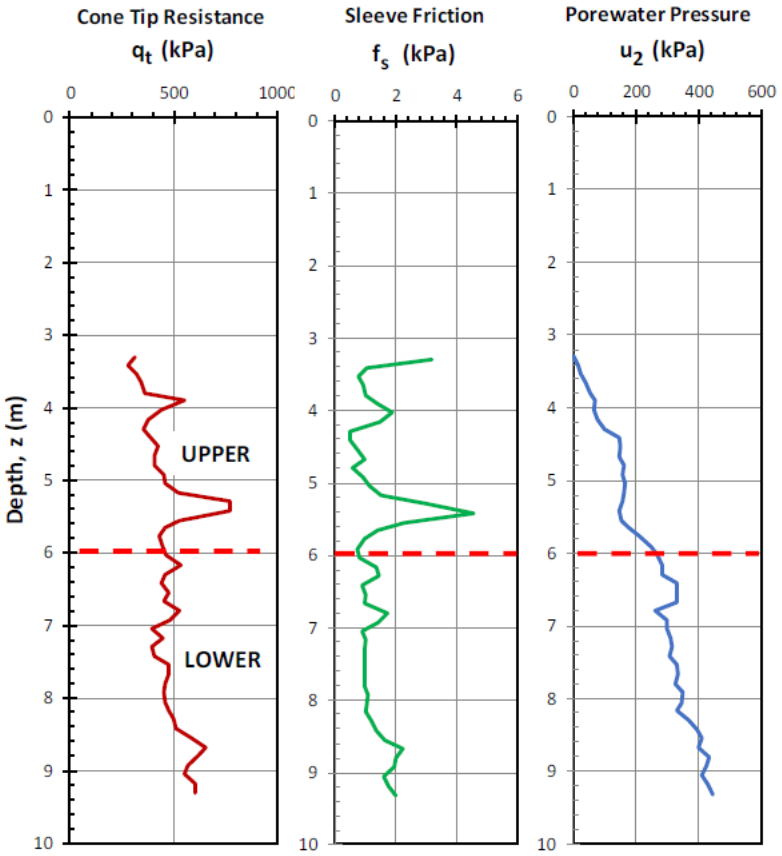

Osaka Bay, Japan

Data from Tanaka et al. (2003)

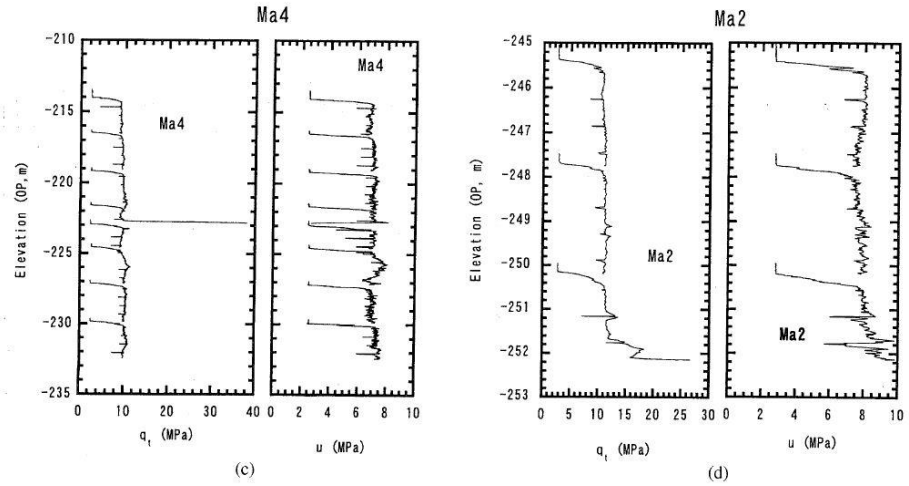

Fig. 4. Measured point resistance and pore water pressure: (a) Doc5, (b) Ma7, (c) Ma4 and (d) Ma2

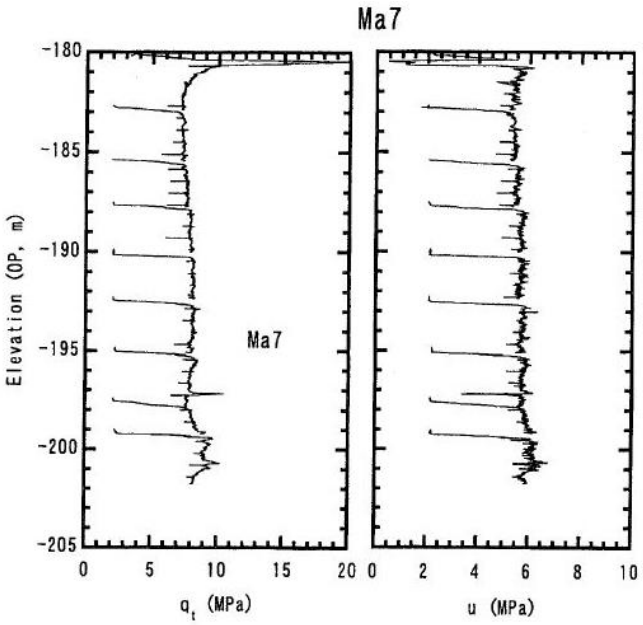

Paddington UK CPTu Hight 2003

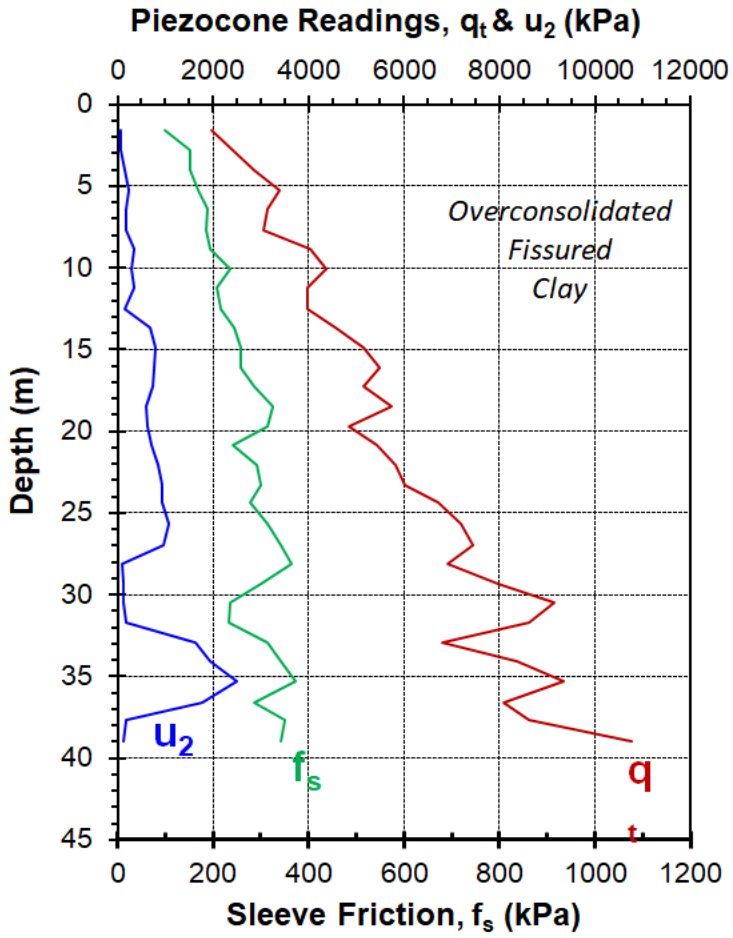

Partille clay CPTu chamber

Data from Lofroth (2008)

Resultat: Korrigerat spetstryck: $q_T = q_c - Oc + u(1-a)$.
Efter utförd kalibrering 02-09-17: Oc = 0; a = 0,421

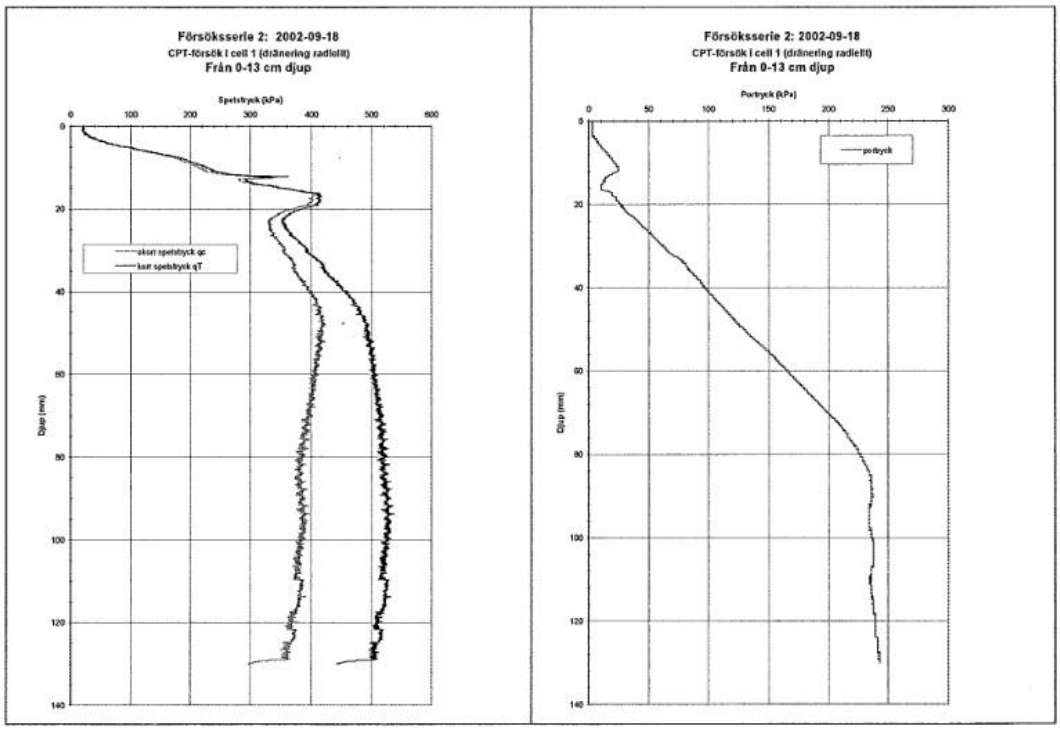

Patterson CPTu SESI (2006)

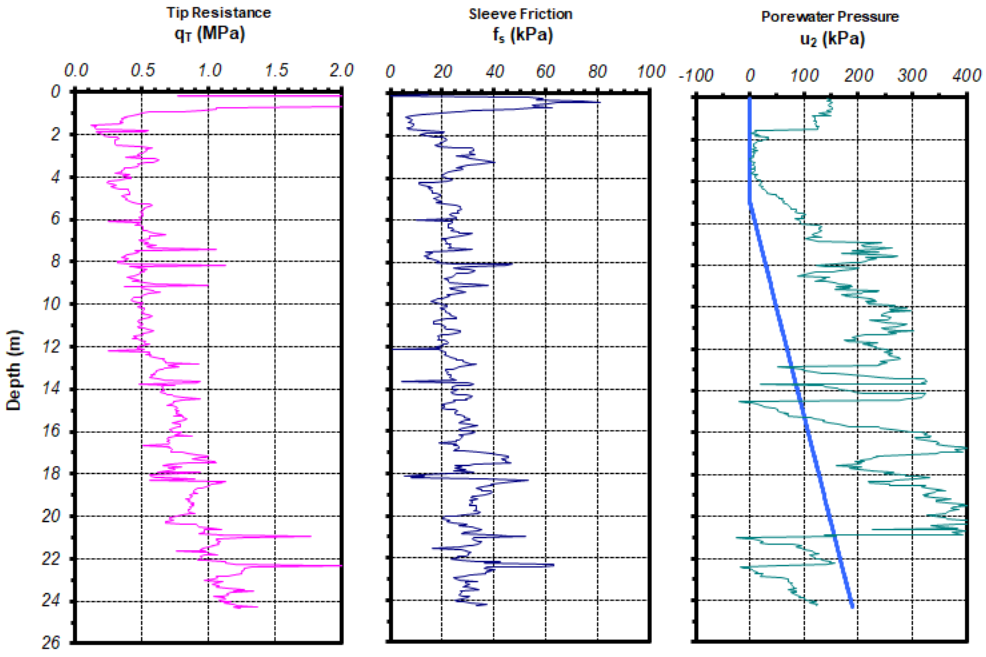

Pentre, UK

Data from Powell & Lunne (2005)

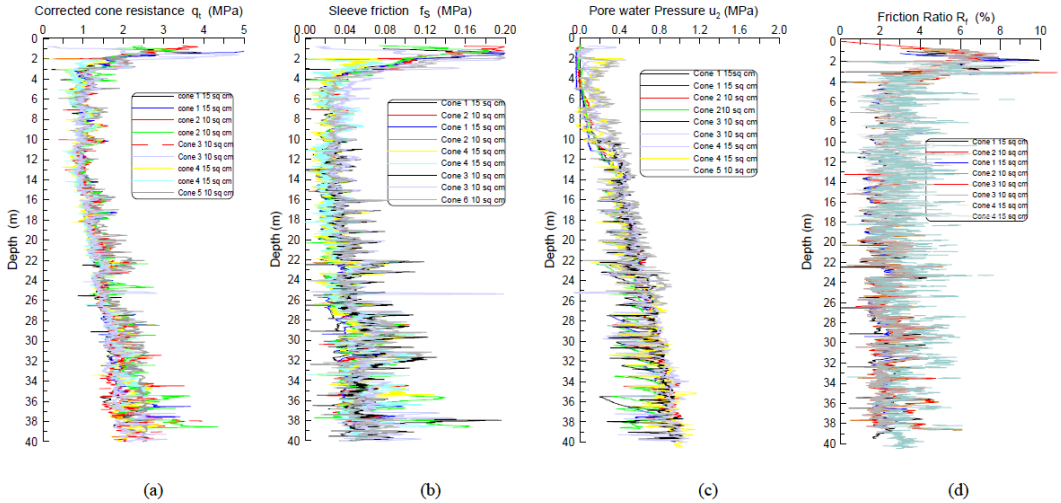

Figure 5. Pentre, (a) q_t (b) Sleeve friction (c) Pore water pressure (d) Friction ration

Pernio, Finland

Lehtonen (2015)

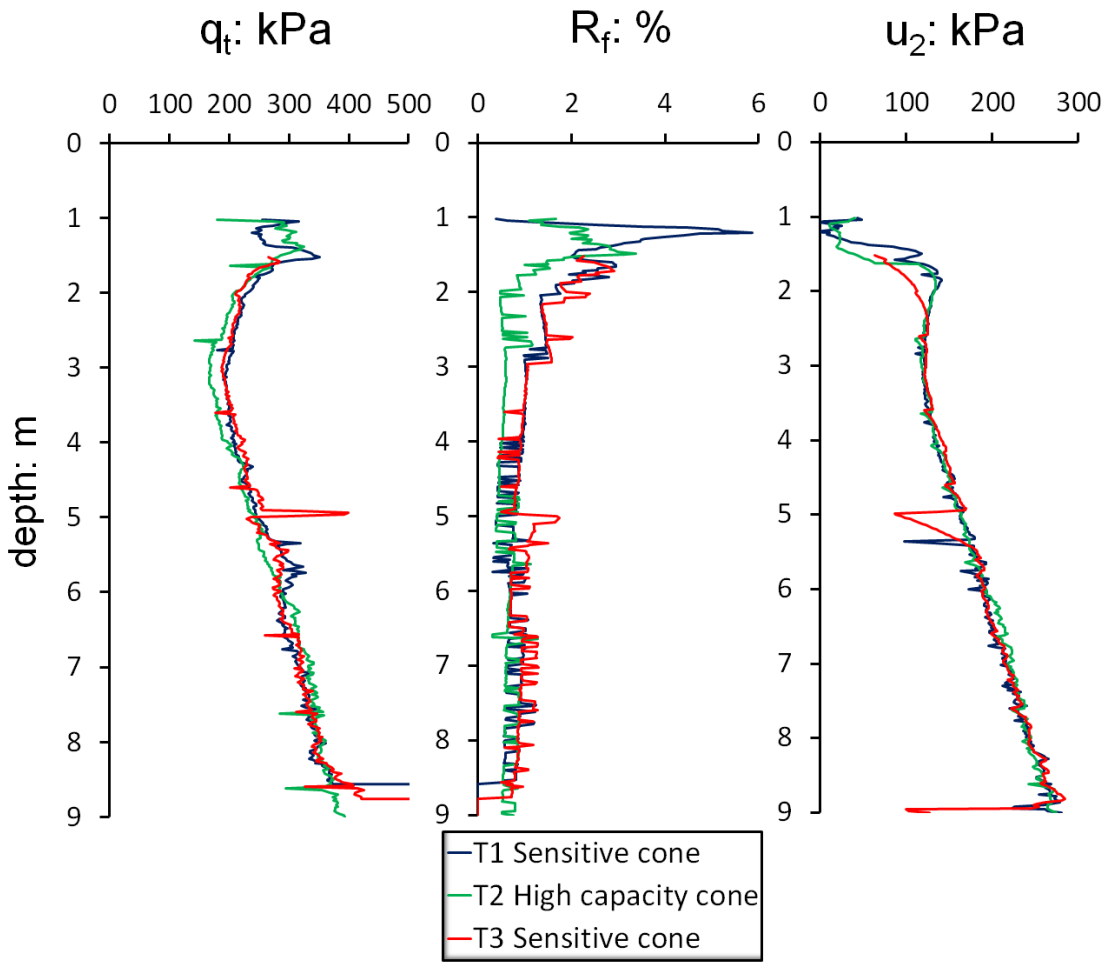

Pisa Clay 100g centrifuge

Data from Burland et al (2003)

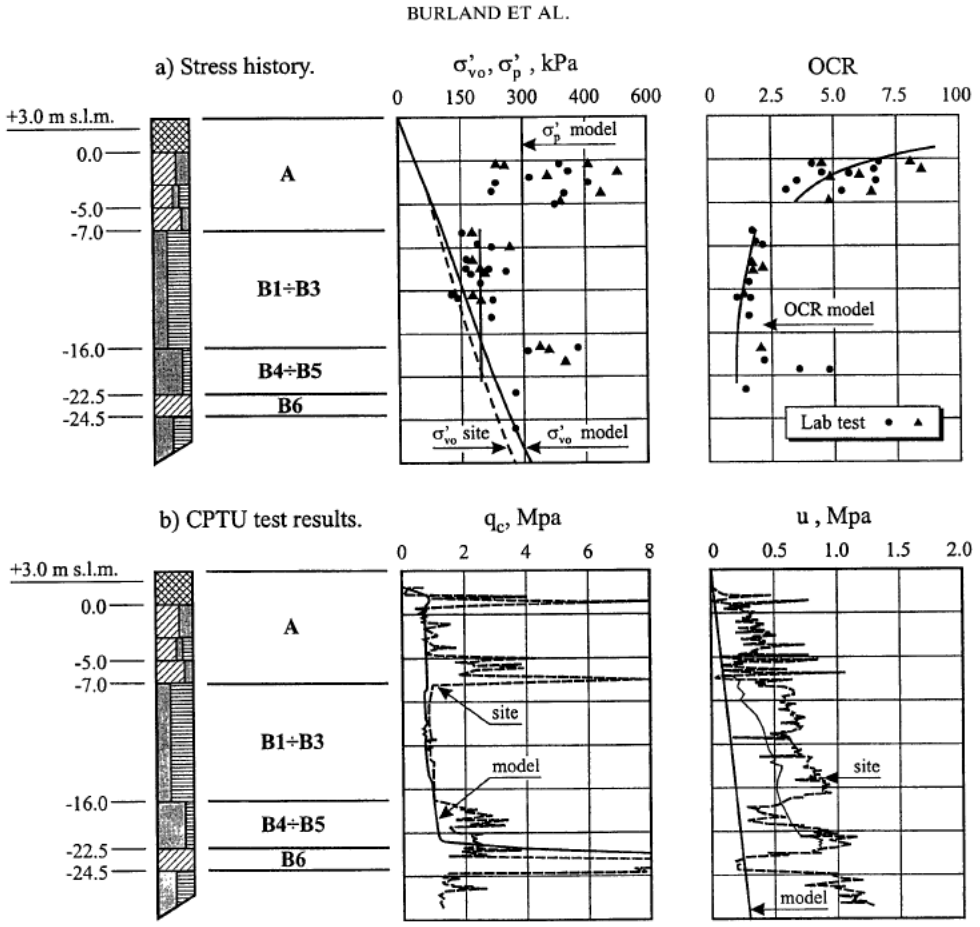

Fig. 14. Subsoil model used in centrifuge tests

Pisa clay, Italu

Data from LoPresti et al. (2003)

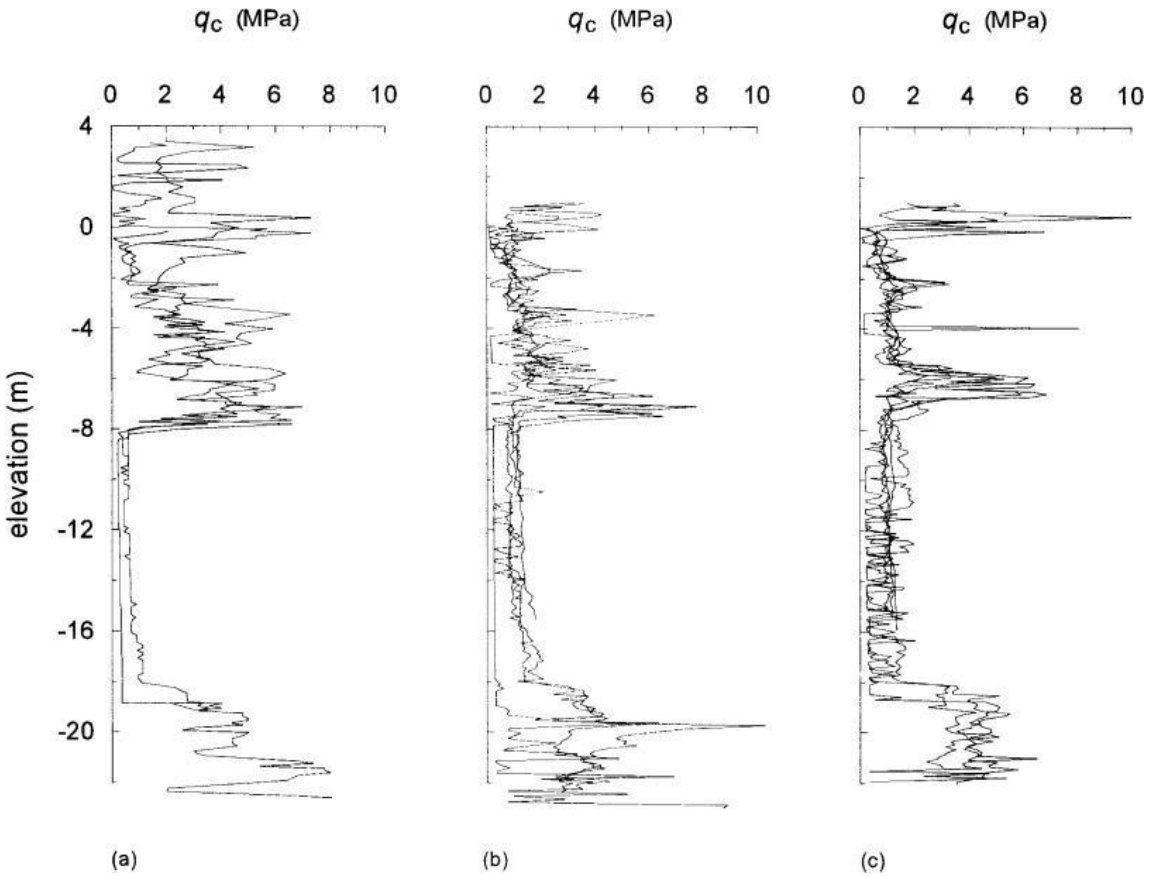

Port Huron Chen and Mayne (1994)

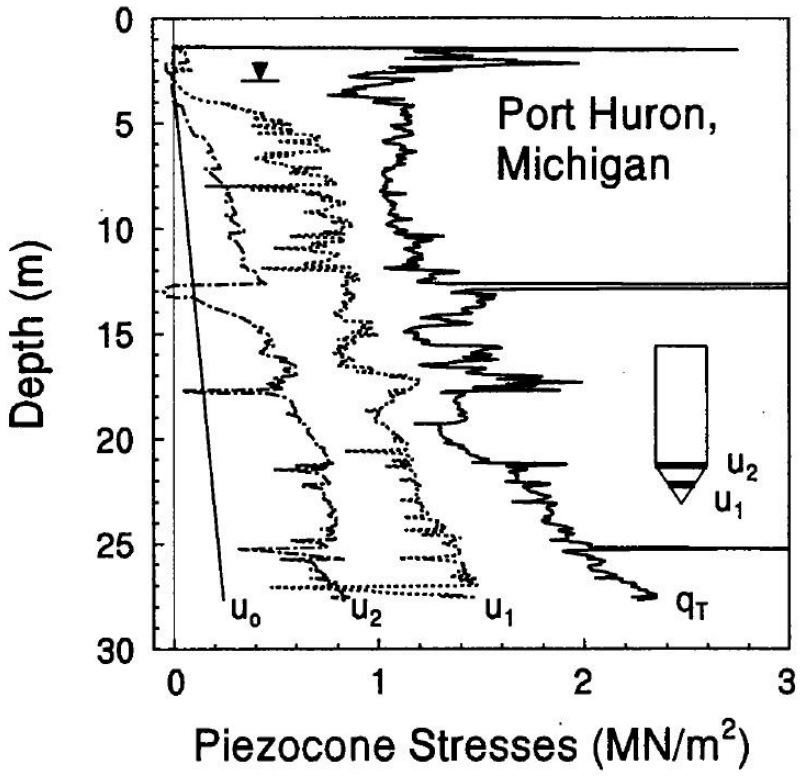

Figure 4.3. Results from a Paired Set of Piezocone Soundings at Port Huron Site.

Port-Cartier, Canada

Data from Demers (2001)

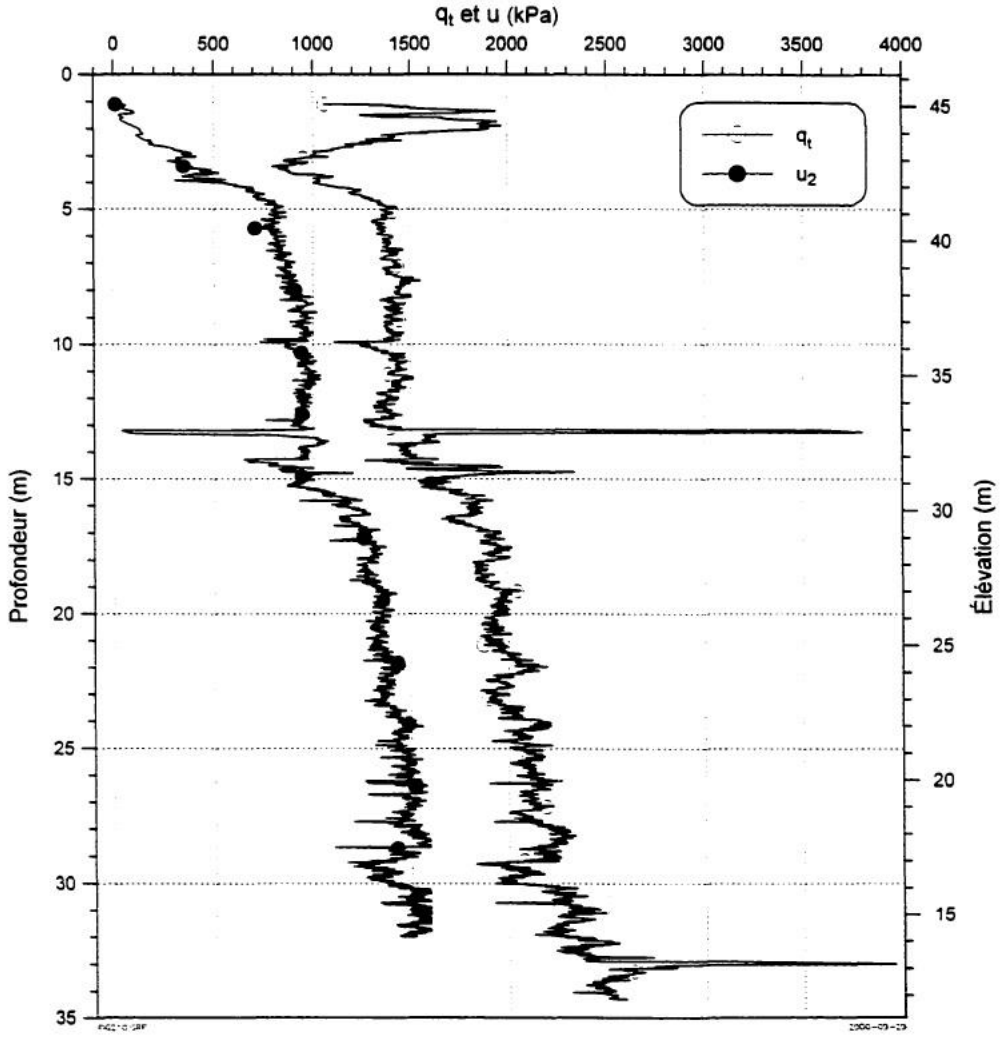

Figure 2.10: Essai au piézocône CPTU3, à Port-Cartier (rivière Vachon).

Porto Tolle, Italy

Data from Cortellazzo & Simonini 2001

Fig. 4. Typical CPTU profile. q_c, piezocone tip resistance; u, pore pressure.

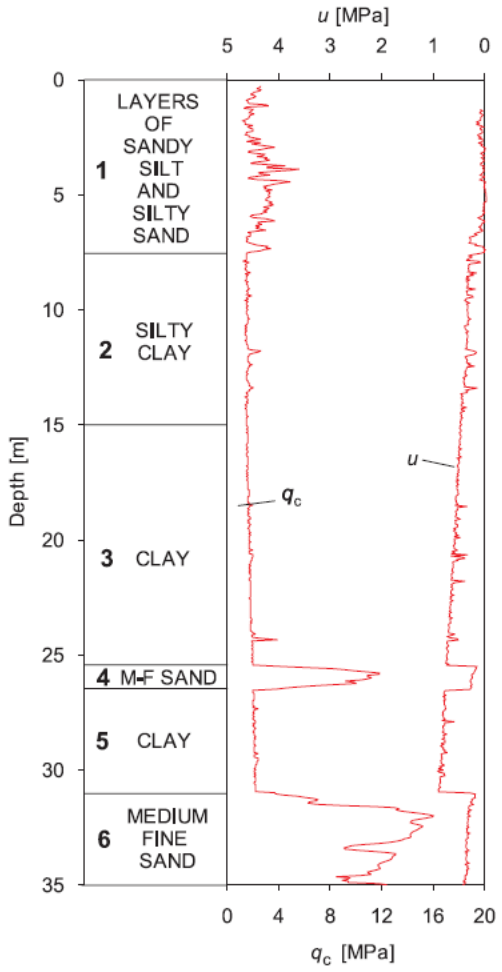

Queensborough Clay, UK

Data from Jardine 2003

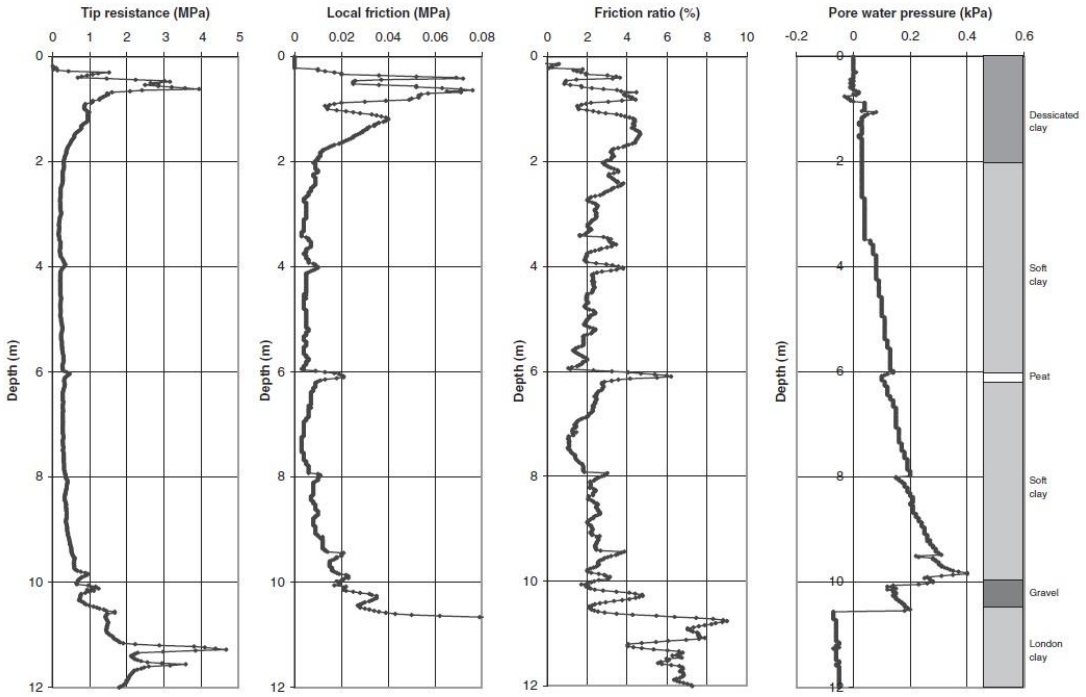

Figure 17. Queenborough CPTU data provided in tests by Lankelma Ltd (June 2002).

Recife RRS1, Brazil

Data after Coutinho (2007)

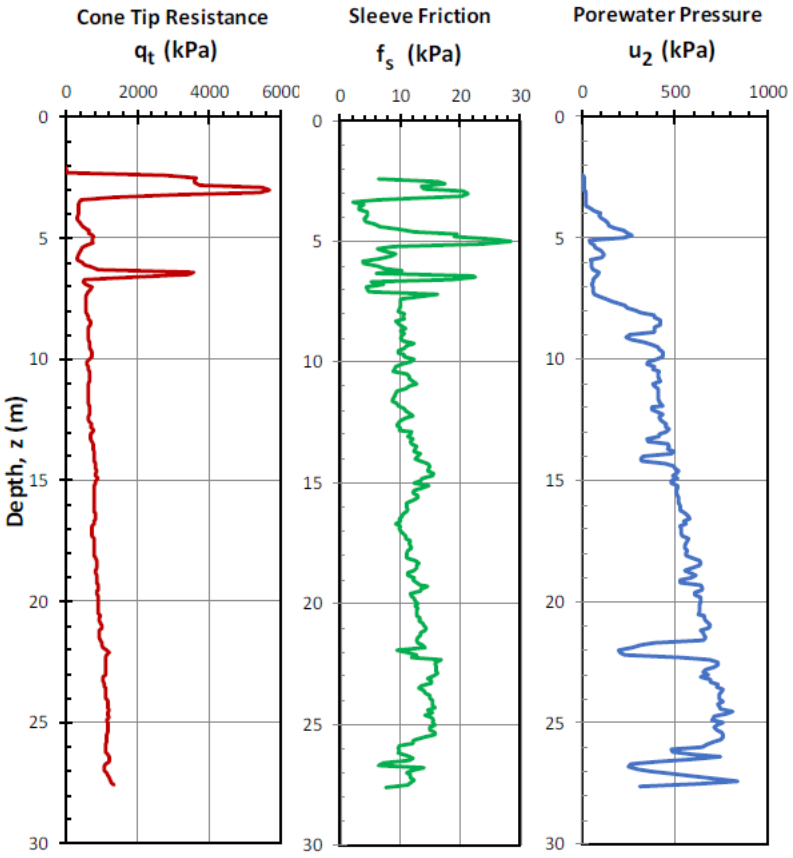

Saint Alban, Québec, Canada[1]

Data after LaRochelle et al. (1974); Lefebvre et al. (1994); Leroueil et al. (1995)

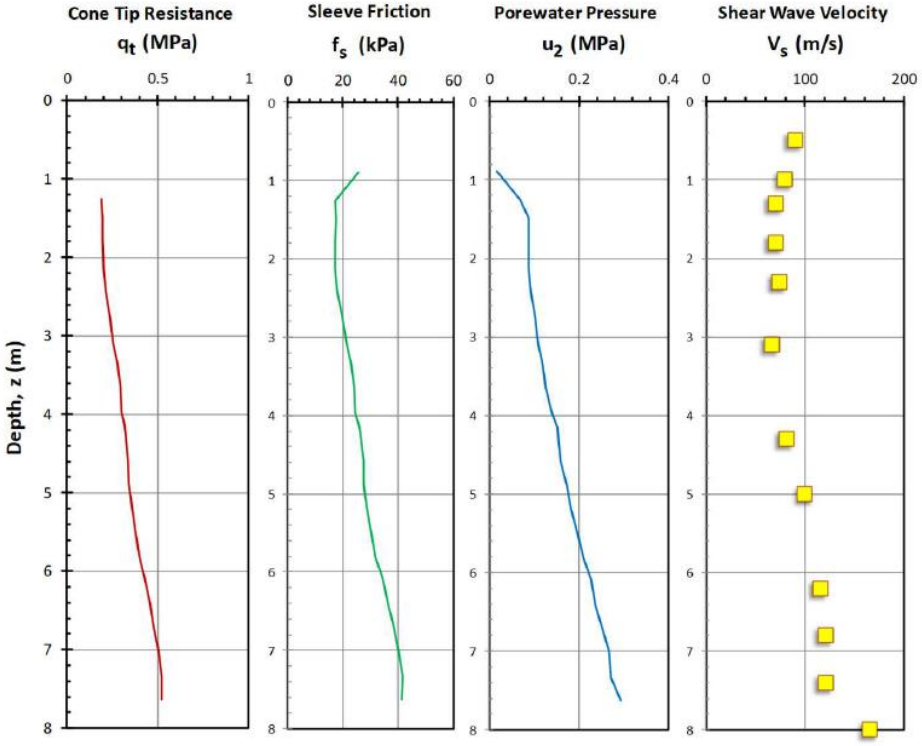

Saint Jude Quebec

Data from Locat et al. (2011)

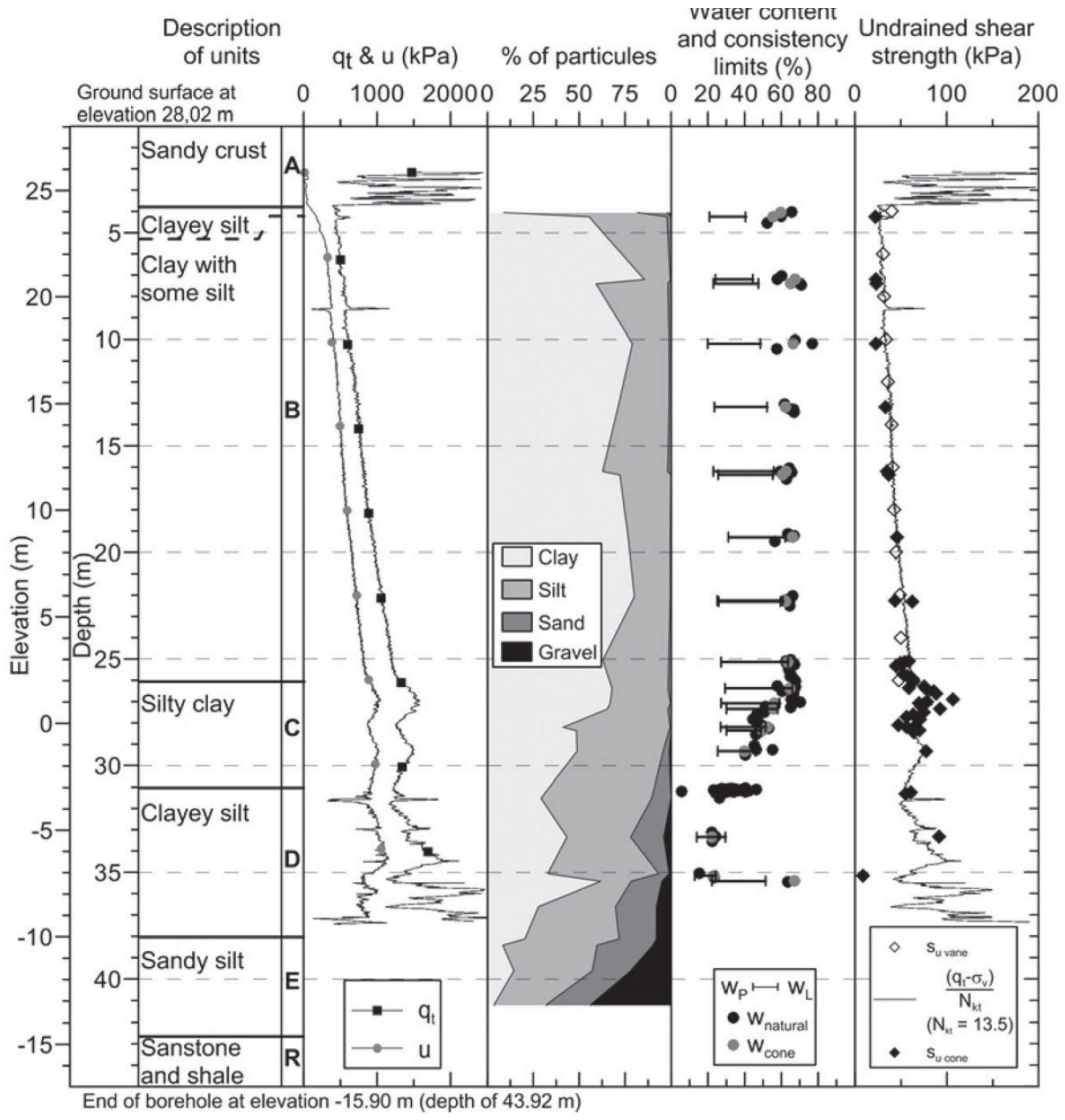

Saint Monique de Nicole, Canada

Data after Locat (2012) – No sleeve friction data available

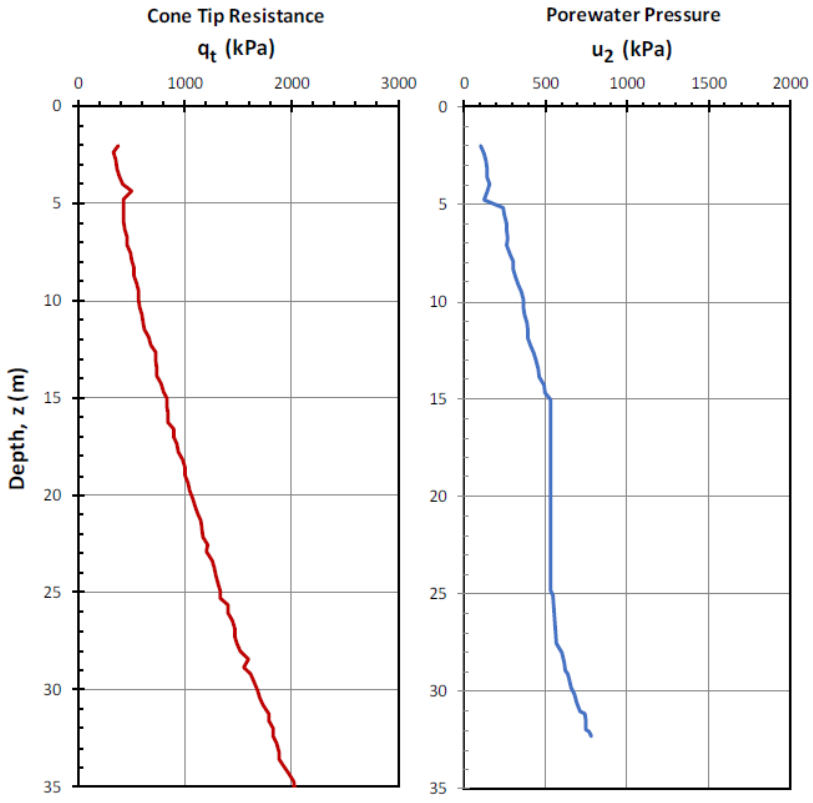

San Carlo Site, Italy

Data from Garcia Martinea PhD 2014

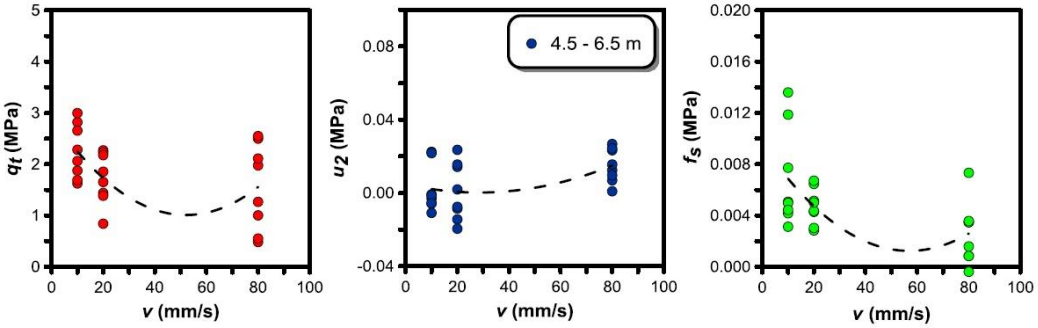

Figure 3.28: Effect of penetration rate on the cone resistance q_t, pore pressure u_2 and sleeve friction f_s measurements

Sandpoint, Idaho

Data after Altaee & Fellenius (2002); Mayne (2005)

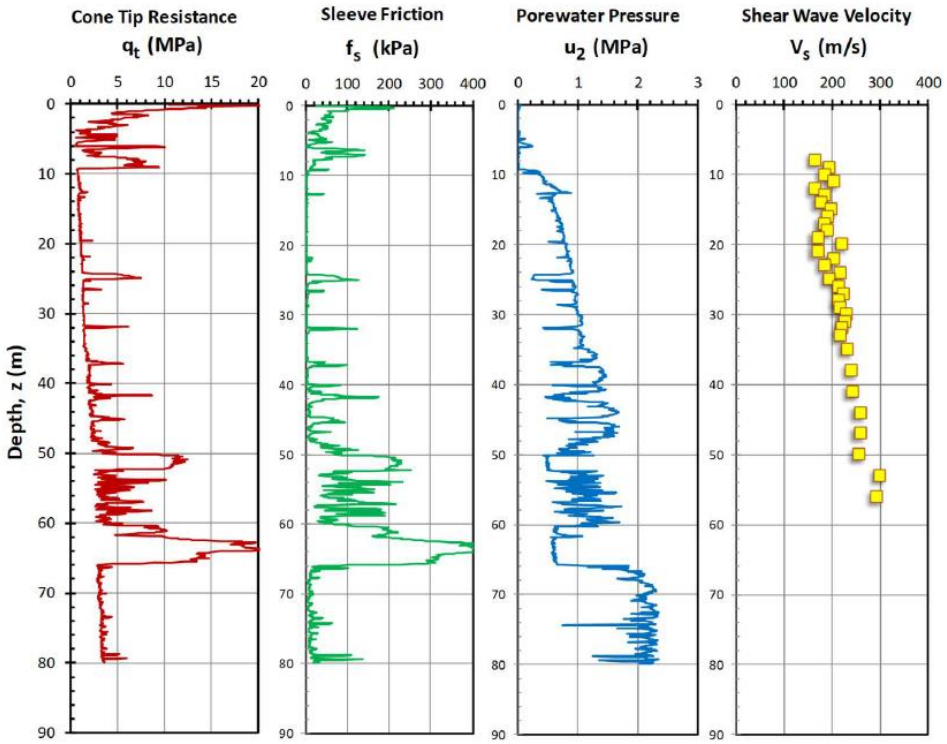

Sandy Kaolin 100g centrifuge CPTu

Data from Teh et al 2006

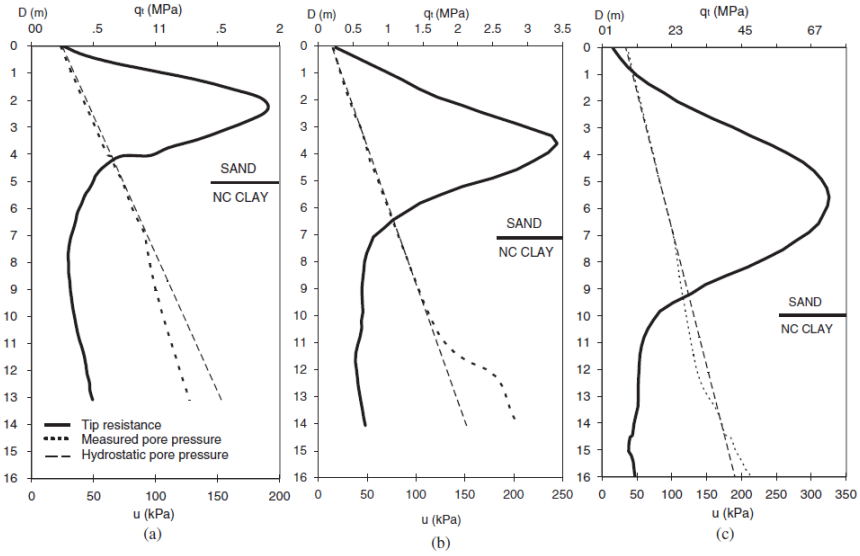

Figure 4. CPTu results for (a) $H = 5$ m. (b) $H = 7$ m. (c) $H = 10$ m.

Sarapuí II, Brazil

Data after Jannuzzi et al. (2015)

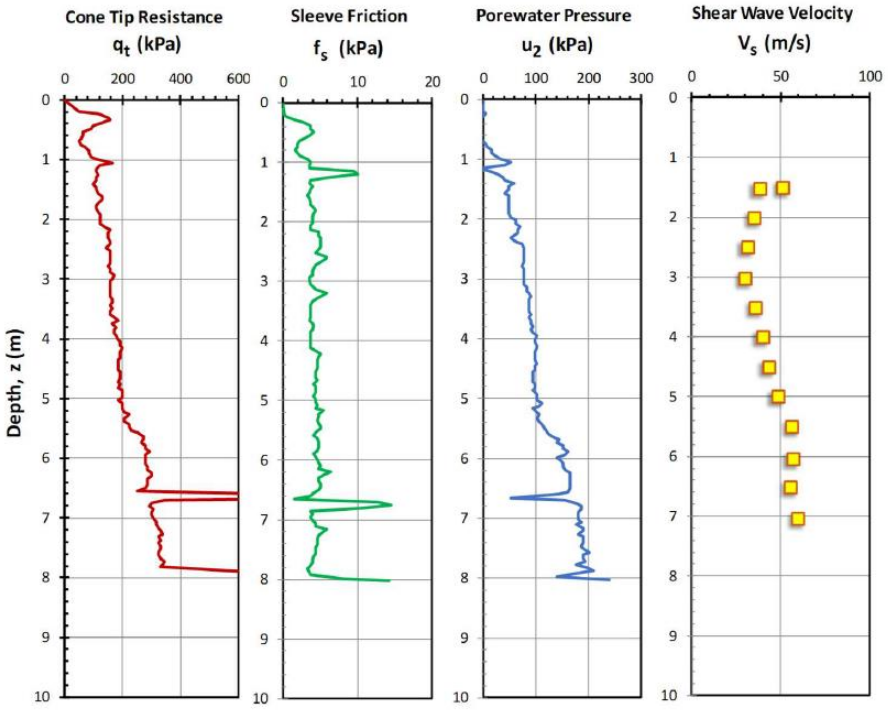

Silica flour centrifuge CPTu

Data from Silva and Bolton 2005

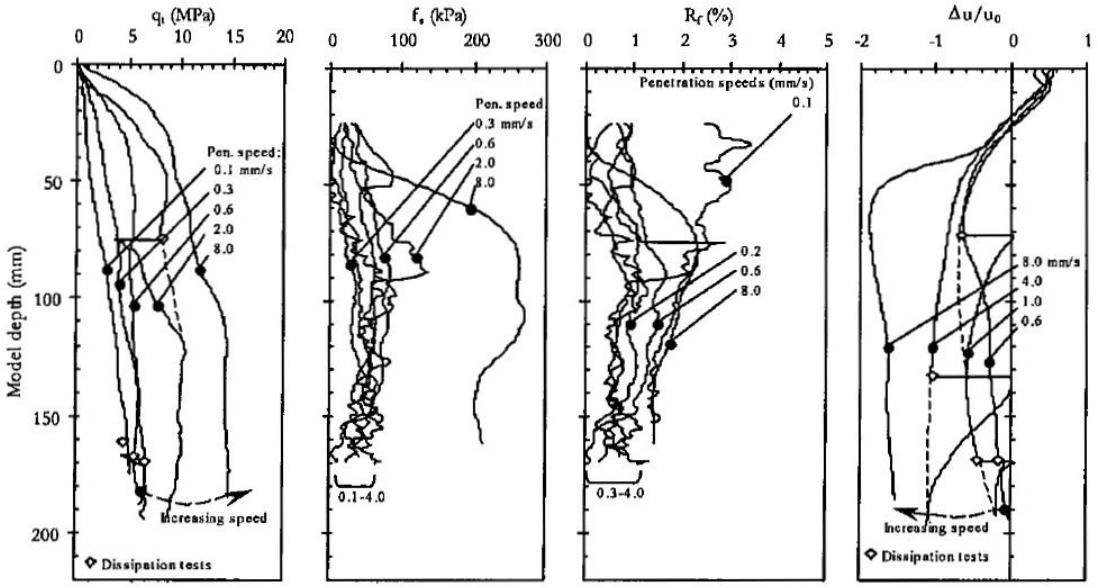

Figure 4. Penetration-graph results

Singapore CPTu at FT-2

Data from Cao (2003)

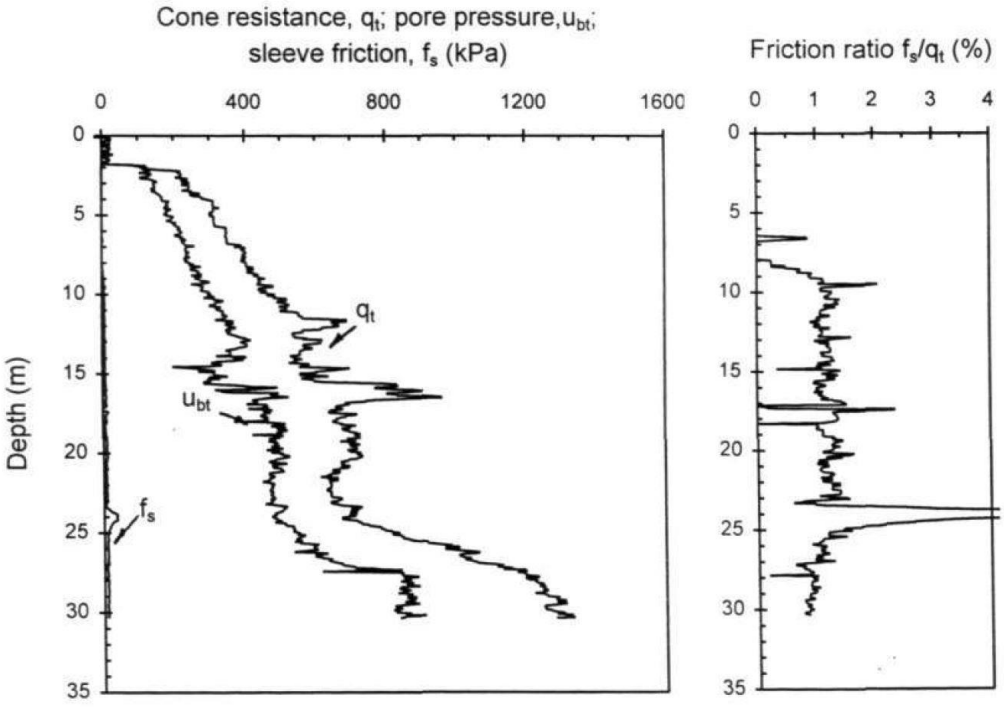

Fig. 8.12 Piezocone test results at FT-2

SR18 and SR 49 Indiana

Data from Kim et al 2008

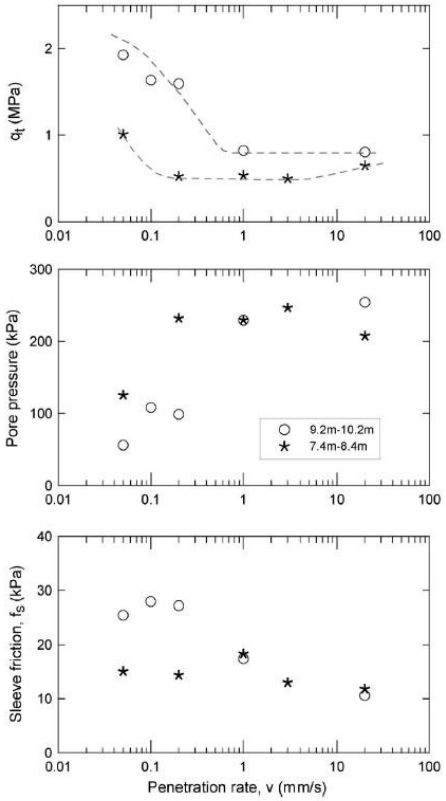

Fig. 3. Effect of penetration rate on average q_t, pore pressure, and f_s (SR 18)

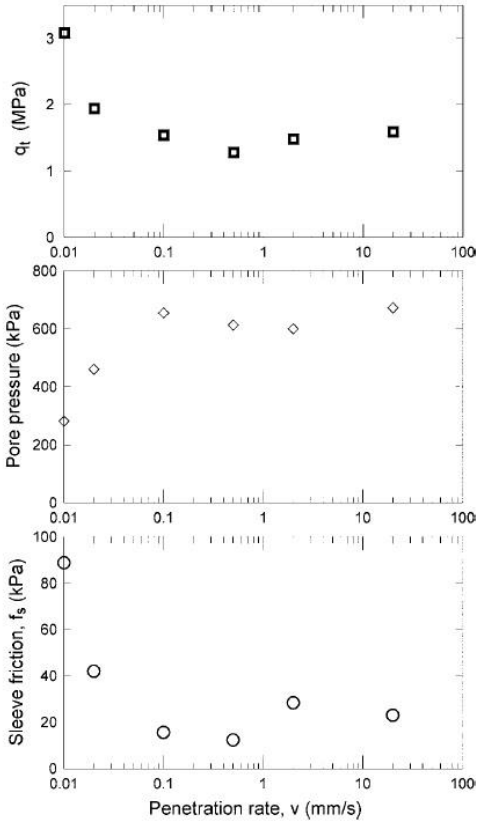

Fig. 4. Effect of penetration rate on average q_t, pore pressure, and f_s (13–14 m depth, SR 49)

St. Hilaire, Québec

Data from LaFleur et al (1988)

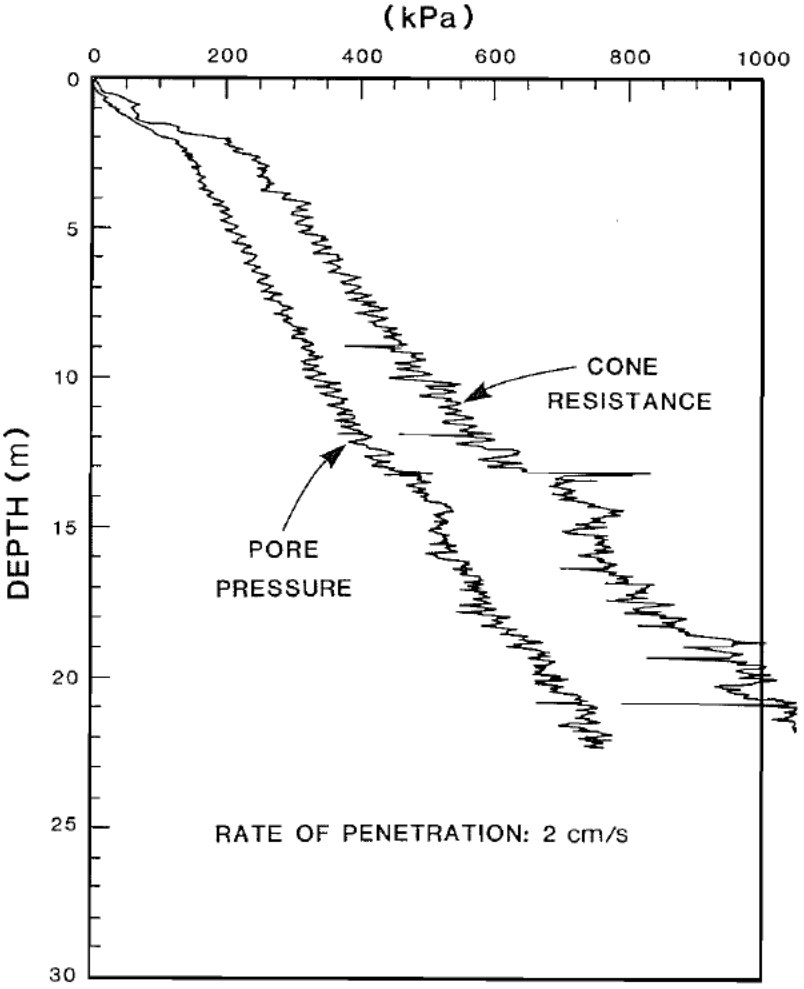

FIG. 4. Piezocone profile.

St. Jean Vianney, Canada

Data from Demers (2001)

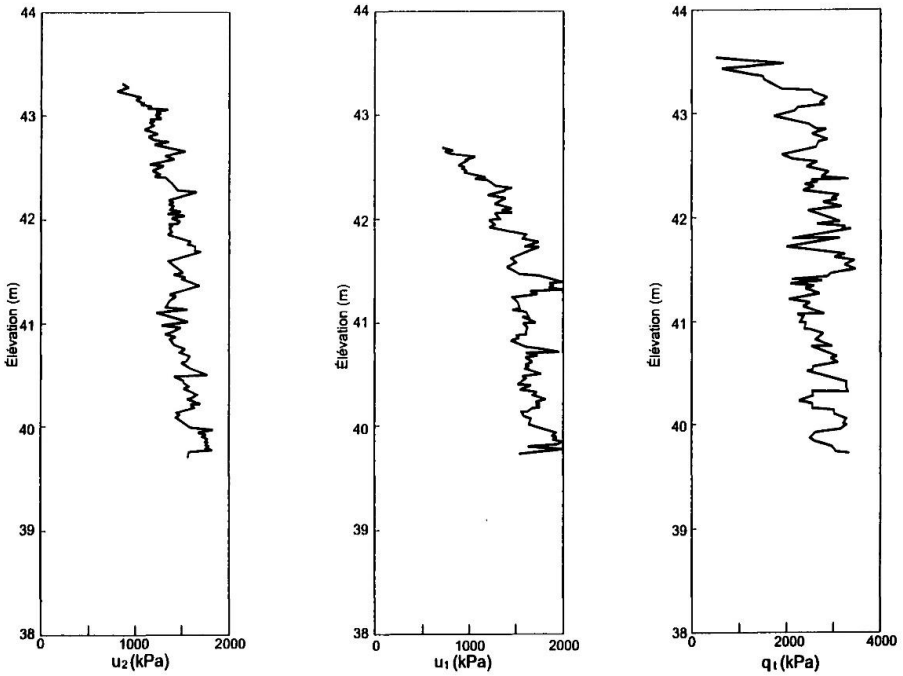

Figure 2.22 - Essais au piézocône (moyenne de trois profils) à Saint-Jean-Vianney (modifié de Zebdi, 1987).

St. Thuribe, Canada

Data from Demers (2001)

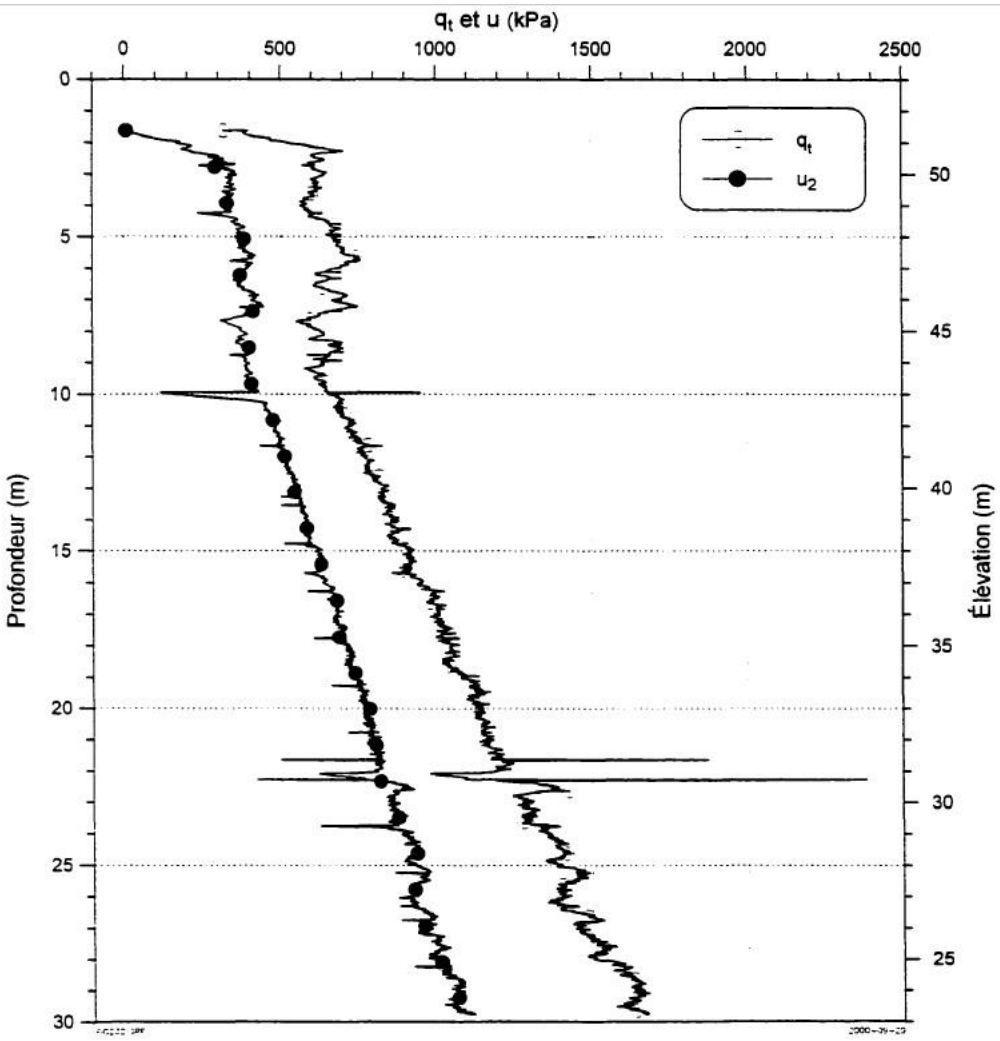

Figure 2.32: Essai au piézocône CPTU1, à Saint-Thuribe.

St. Polycarpe, Canada

Data from Demers (2001)

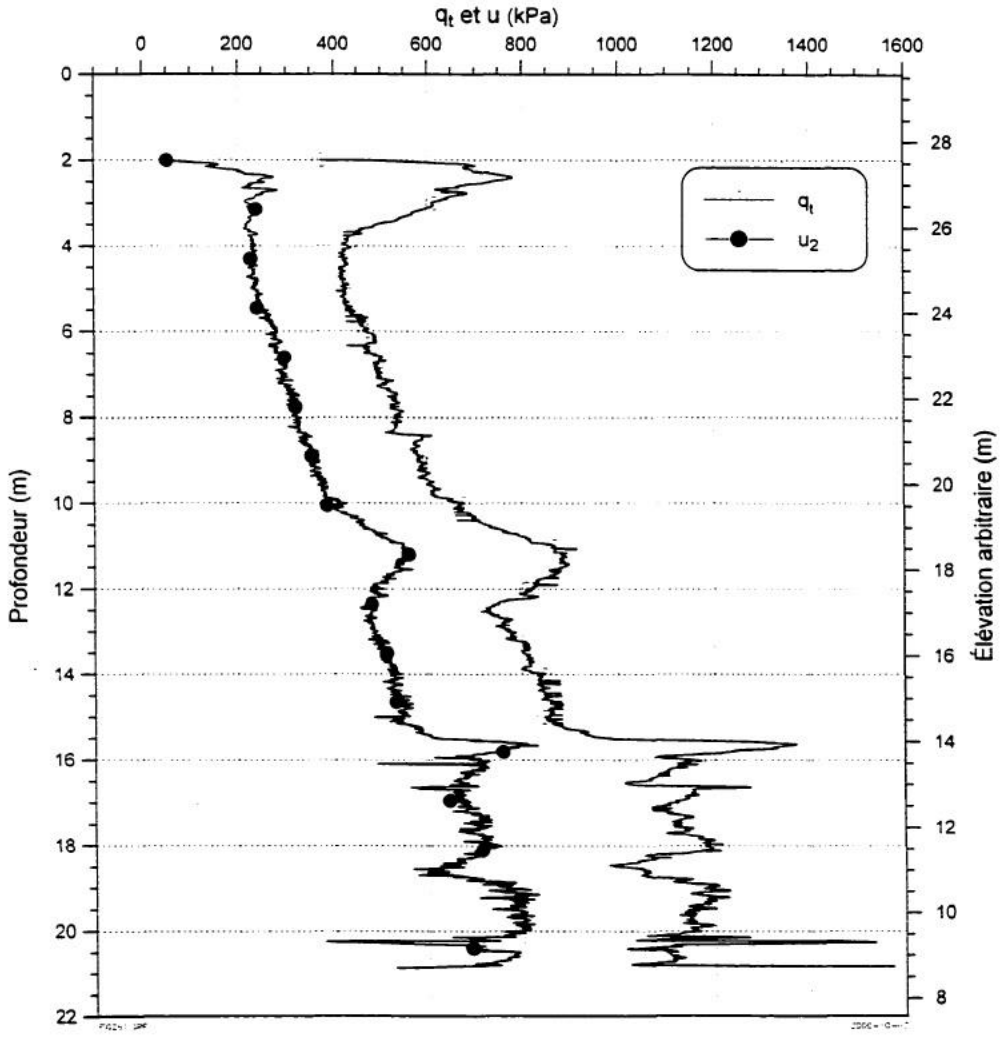

Figure 2.61: Essai au piézocône CPTU1, à Saint-Polycarpe.

Taranto, Italy

Data from Battaglio & Bruzzi 1987

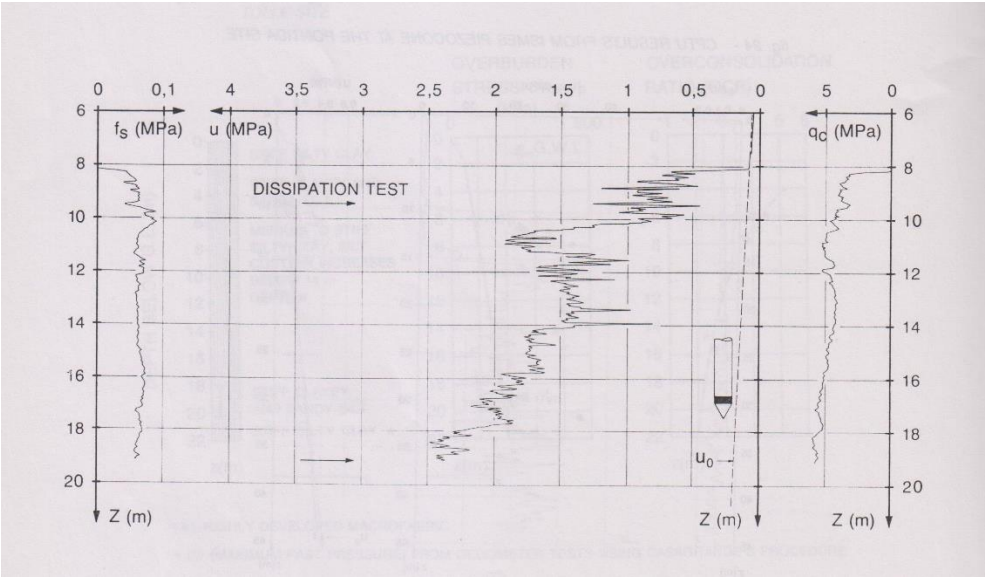

Teg, Sweden

Data from Larsson et al (2007)

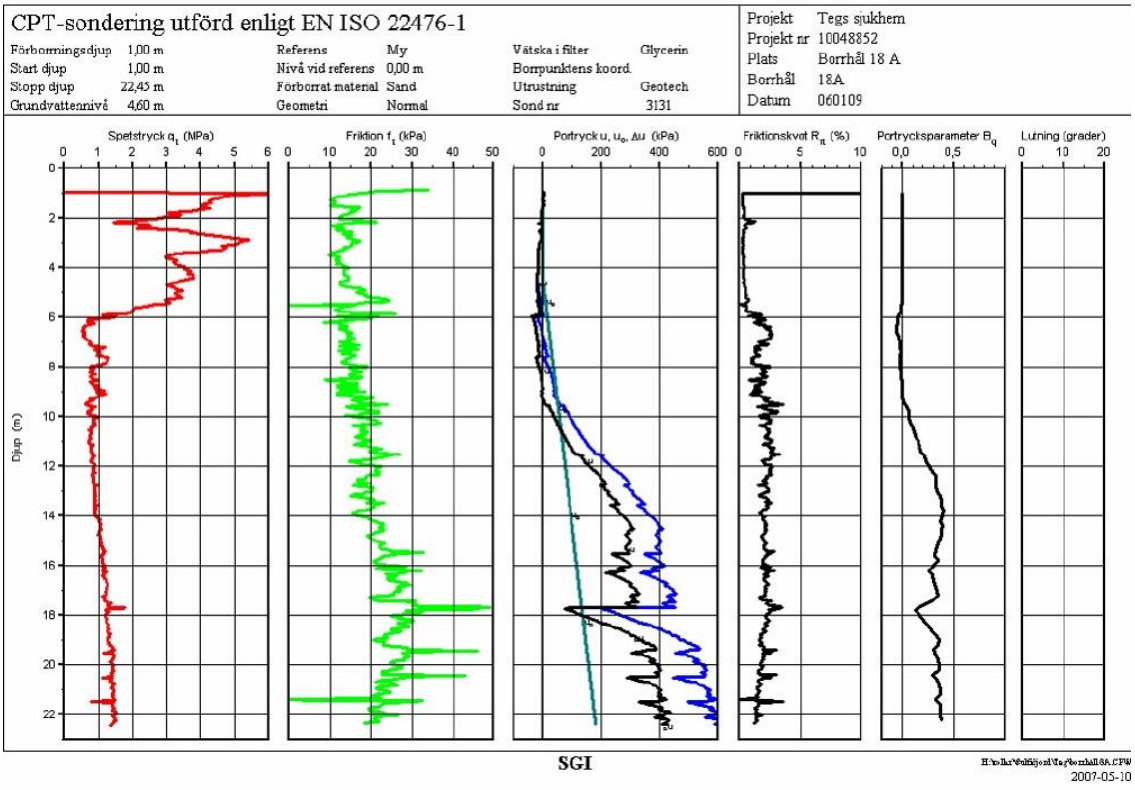

Fig. 54. Resultat från CPT-sondering i Teg.

Tiller, Norway

Data after Gylland et al. (2013; 2014); L'Heureux & Long (2016)

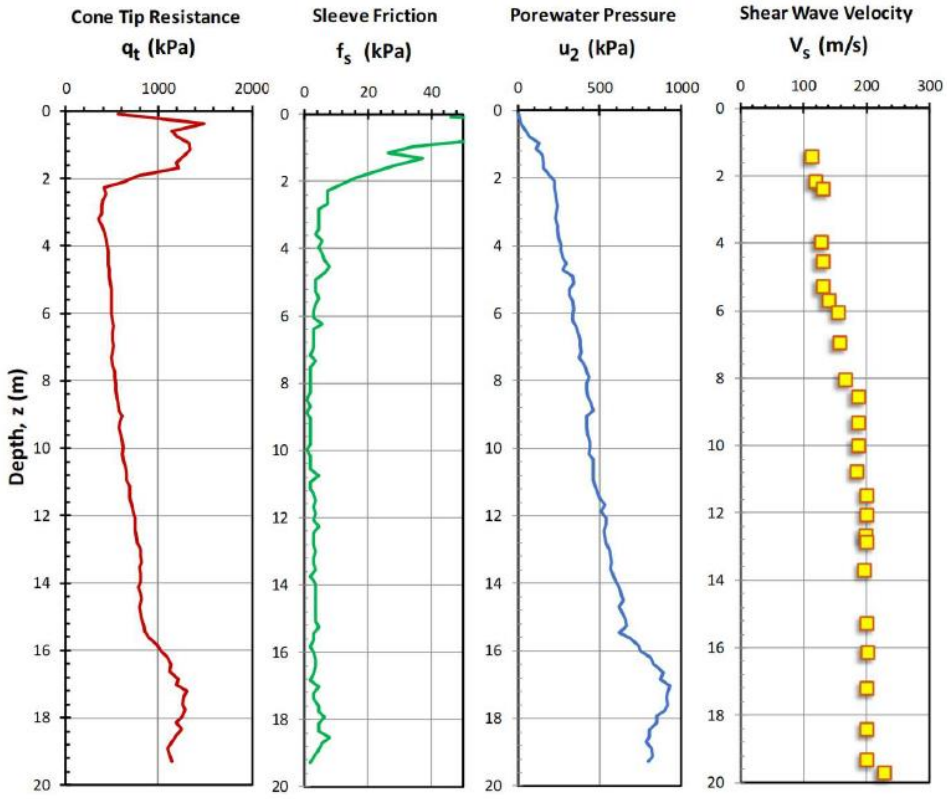

Tokyo Bay CPTu, Japan

Data from Takesue and Isano (2001)

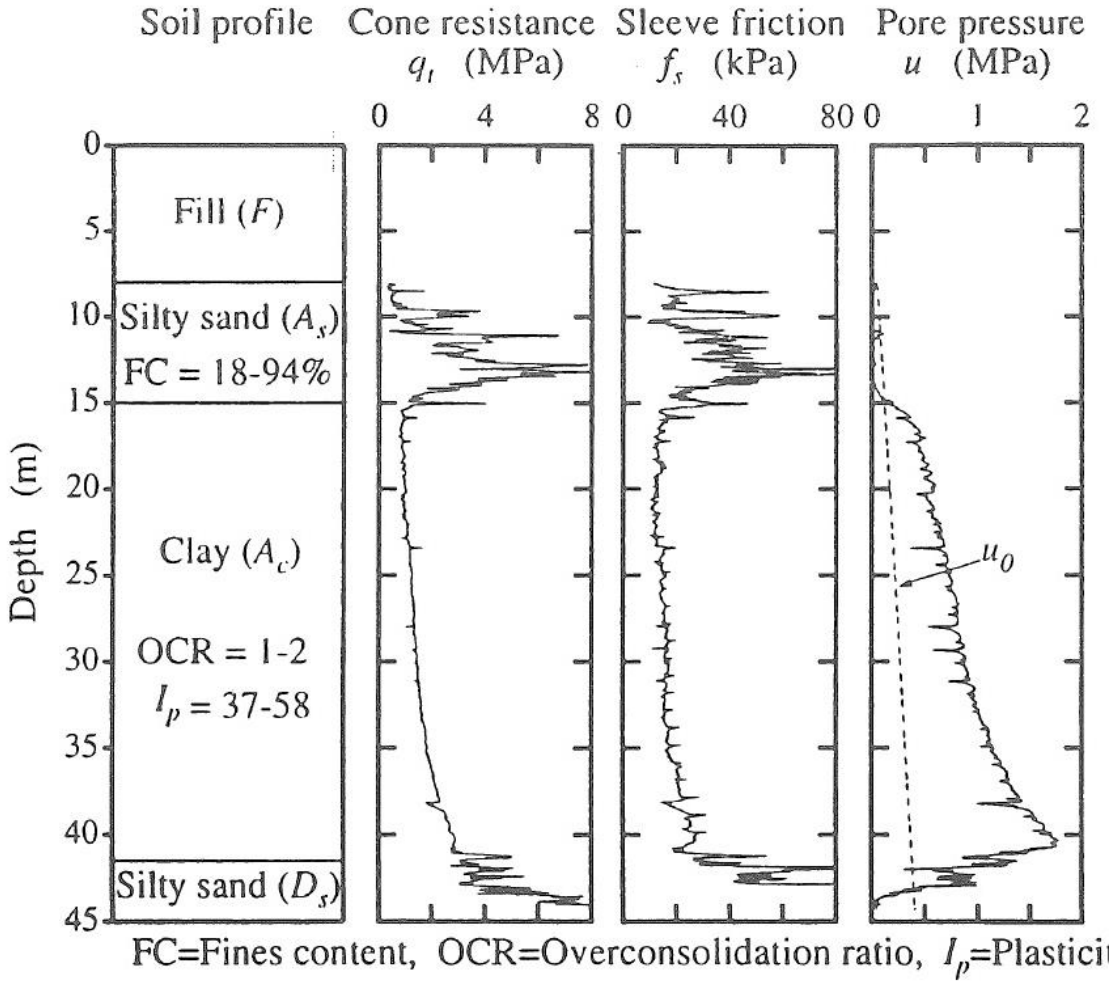

Figure 2. Soil profile and CPT and LPT results at tests site.

Torp, Sweden

Data from Larsson and Åhnberg (2003)

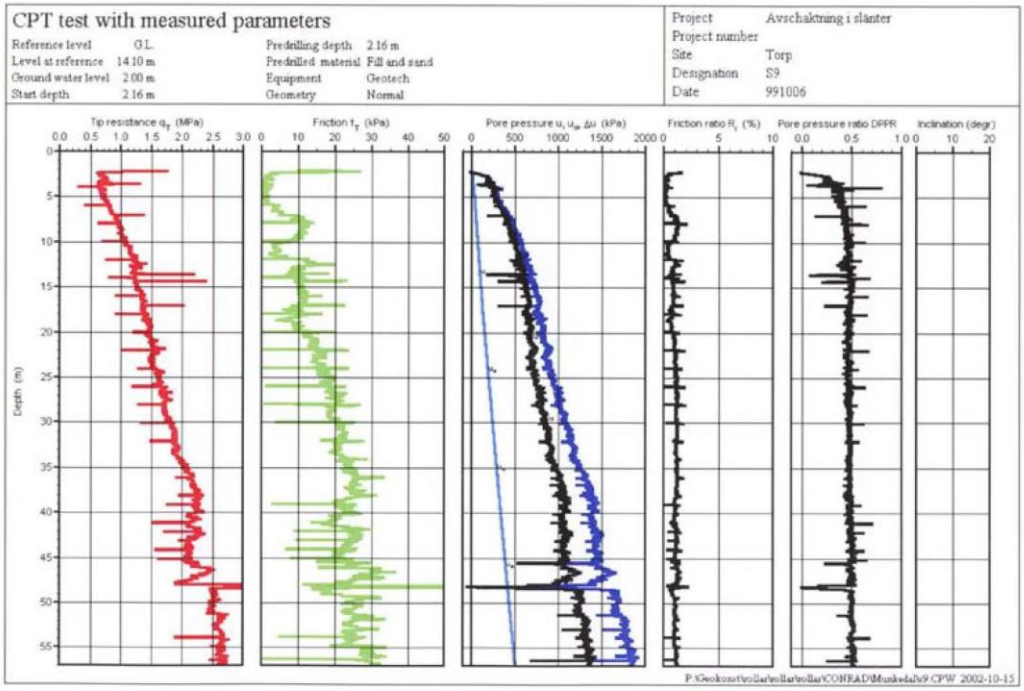

Fig. 14. Results from the CPT tests in Section C presented using the program CONRAD. c) Point S9

Torpa, Sweden

Data from Lofroth (2012)

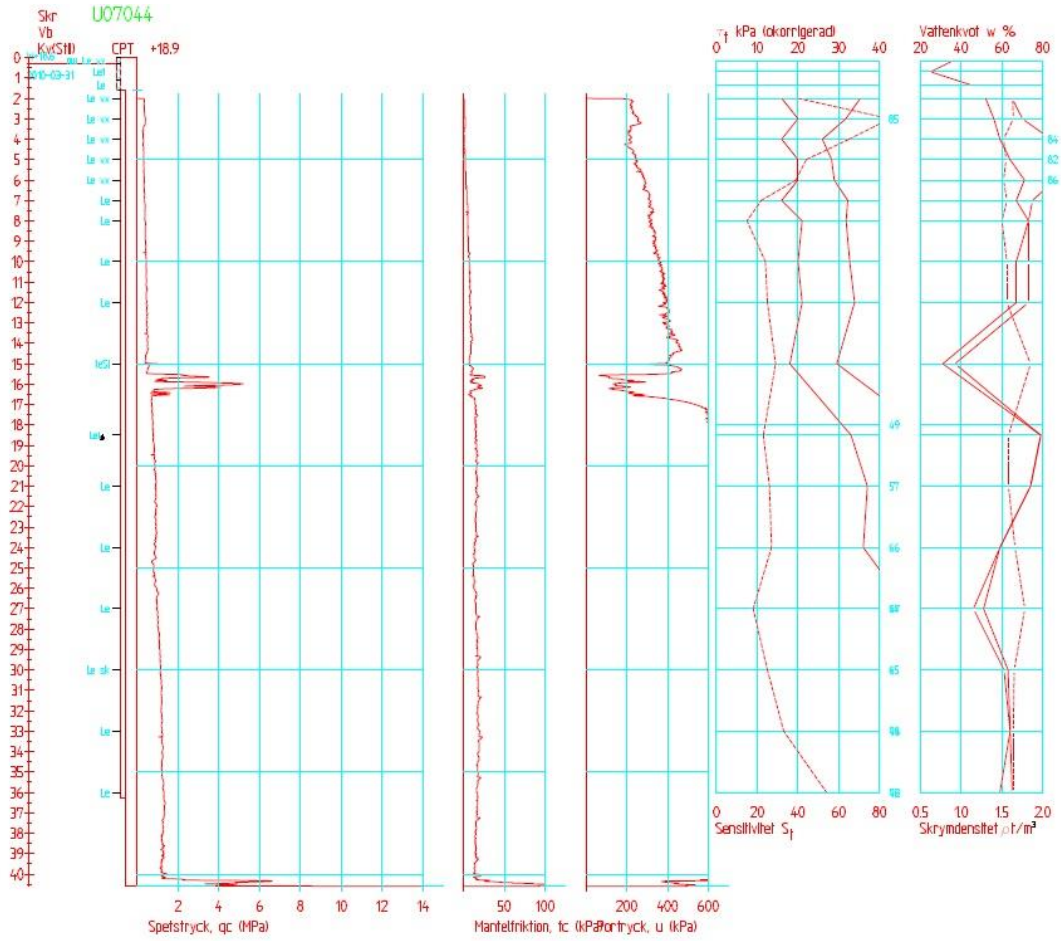

Troll, North Sea

Data from Amundsen et al. (1985); Lunne et al. (2007)

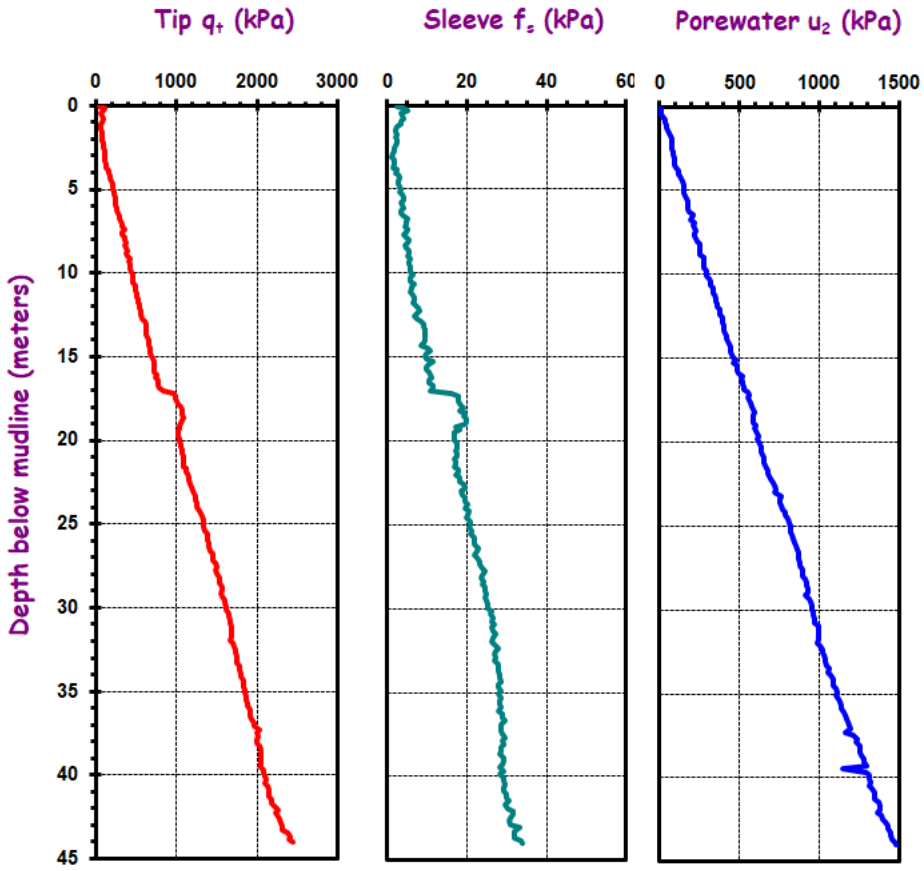

Vagverket, Sweden

Data from Larsson (1997)

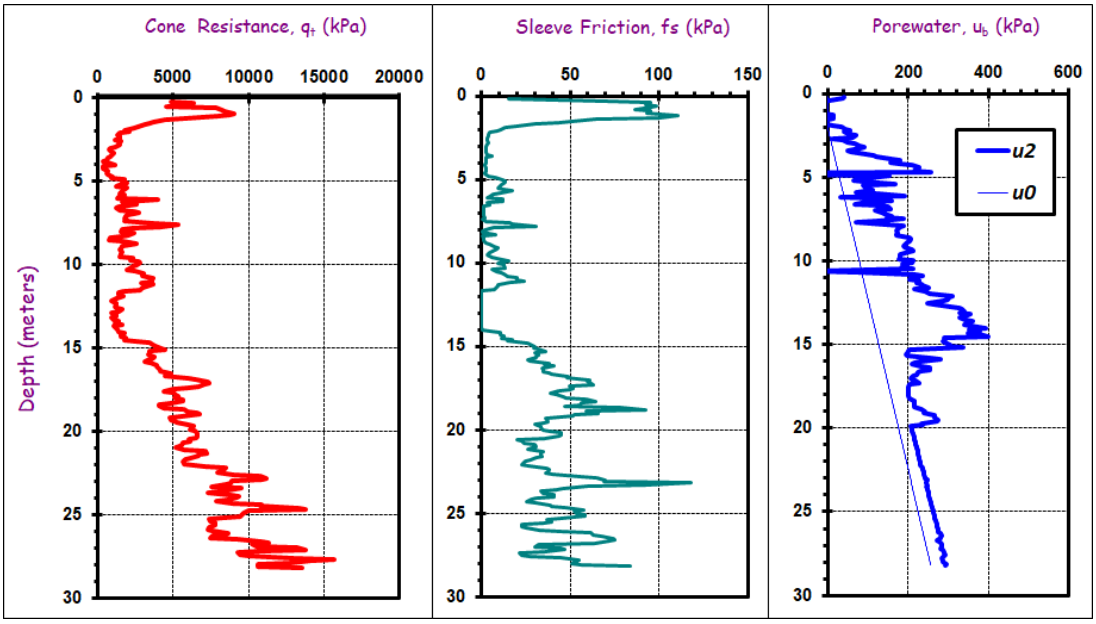

Wauwill Switzerland

Data from Springman et al. (1999)

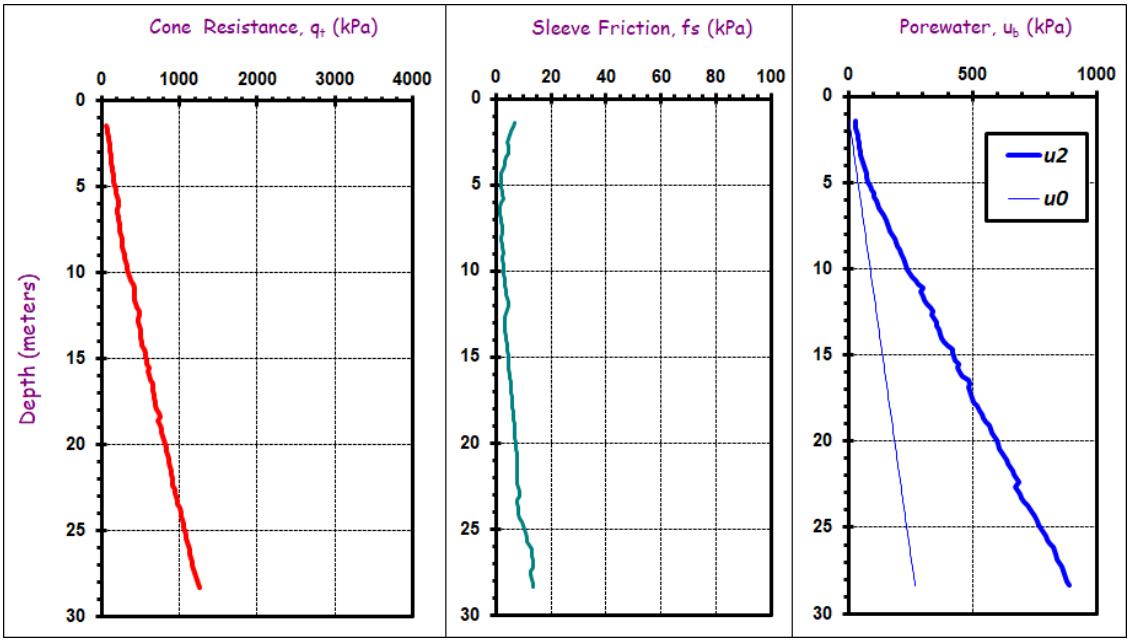

Yorktown Formation, VA

Data from Mayne (1998)

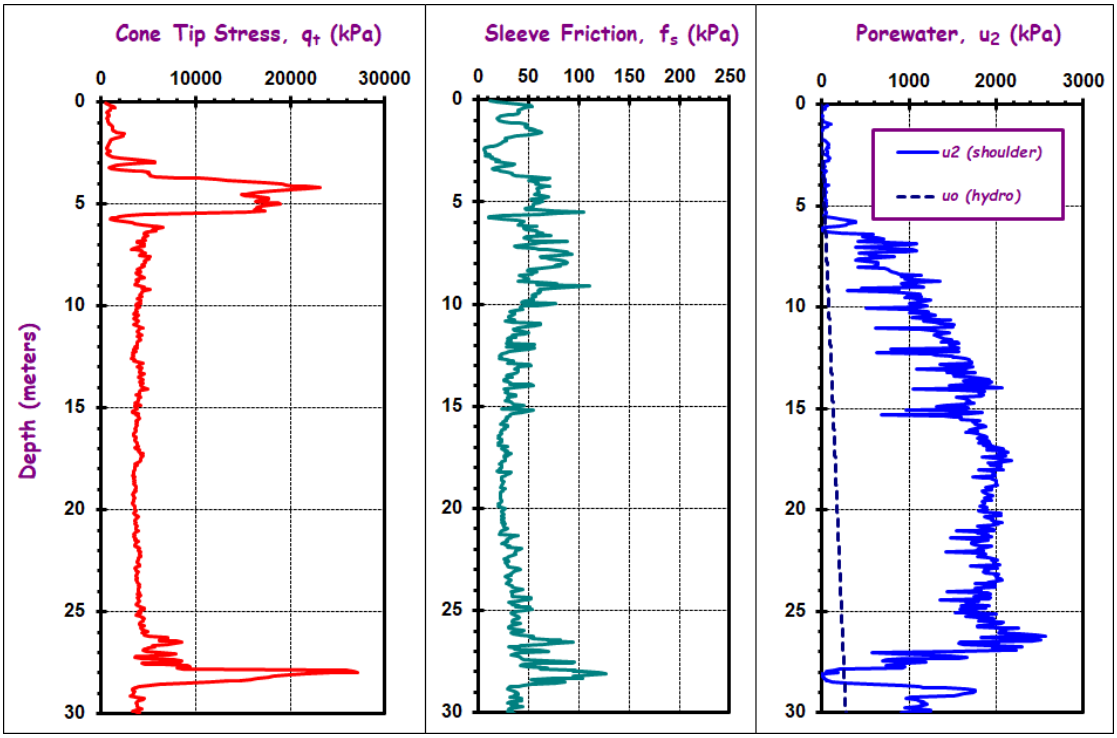

APPENDIX D. RAW DATA FROM INVESTIGATED FLAT PLATE DILATOMETER TESTS

This appendix contains the raw data from DMT used in this research program.

200th ST overpass,BC

Data from Cruz (2009).

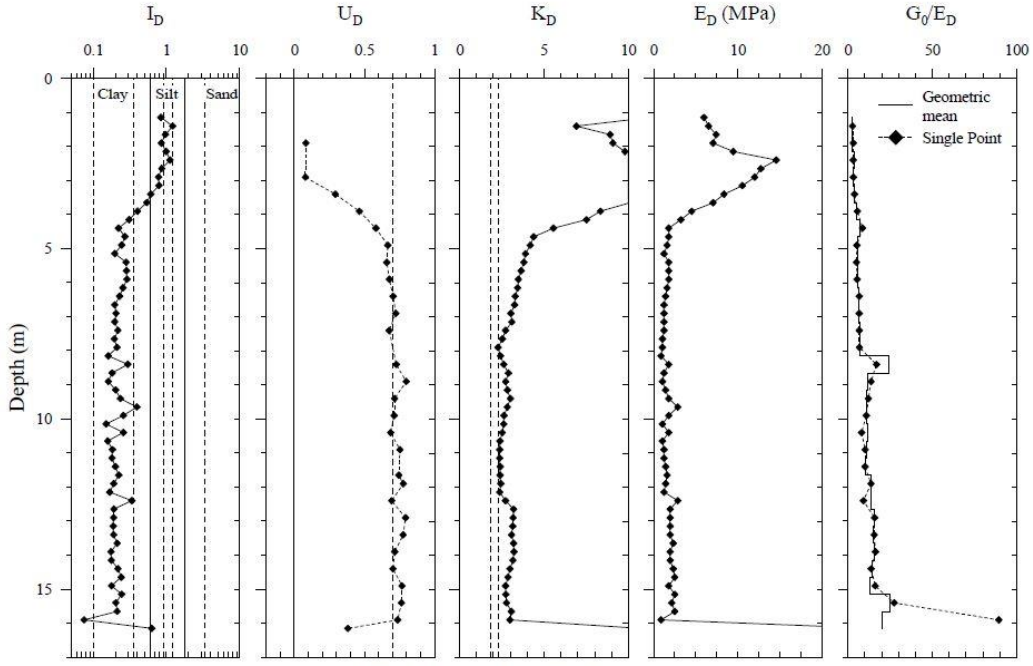

Figure 4.12 SDMT profile, 200th Street Overpass.

Amherts, MA

DMT by GT in-situ testing group

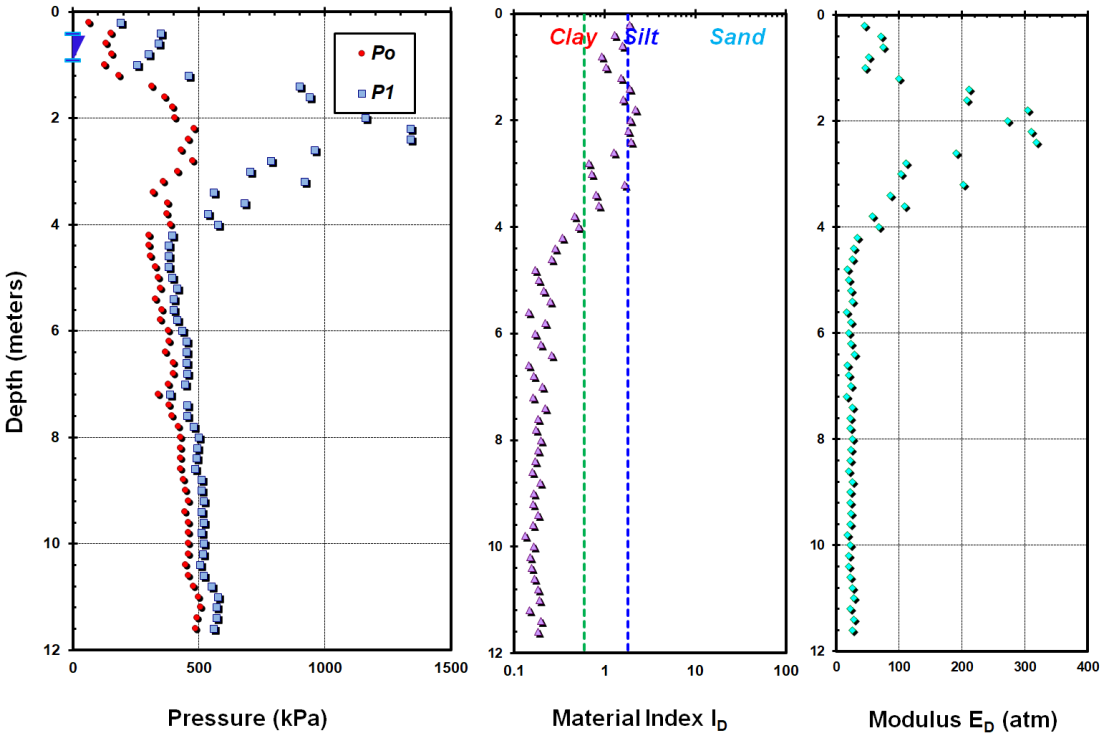

Anacostia, Washington DC

DMT by Mayne (1987)

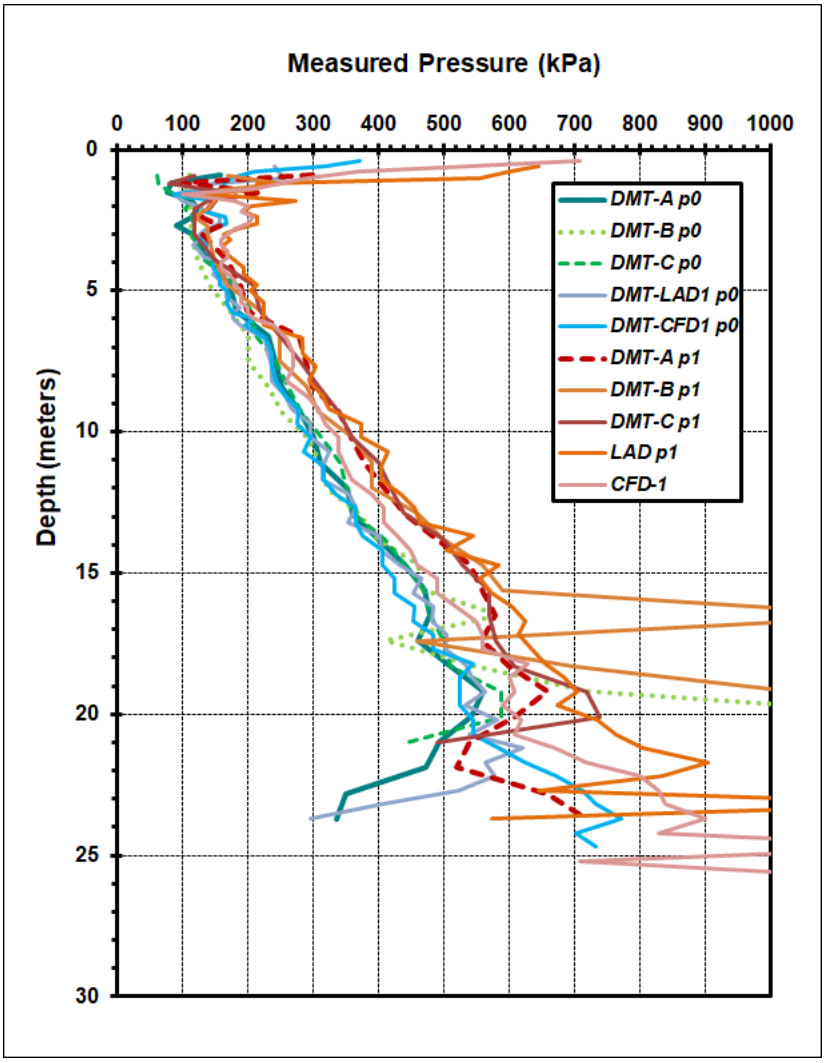

Ariake DMT, Japan

Data from Watabe et al 2004

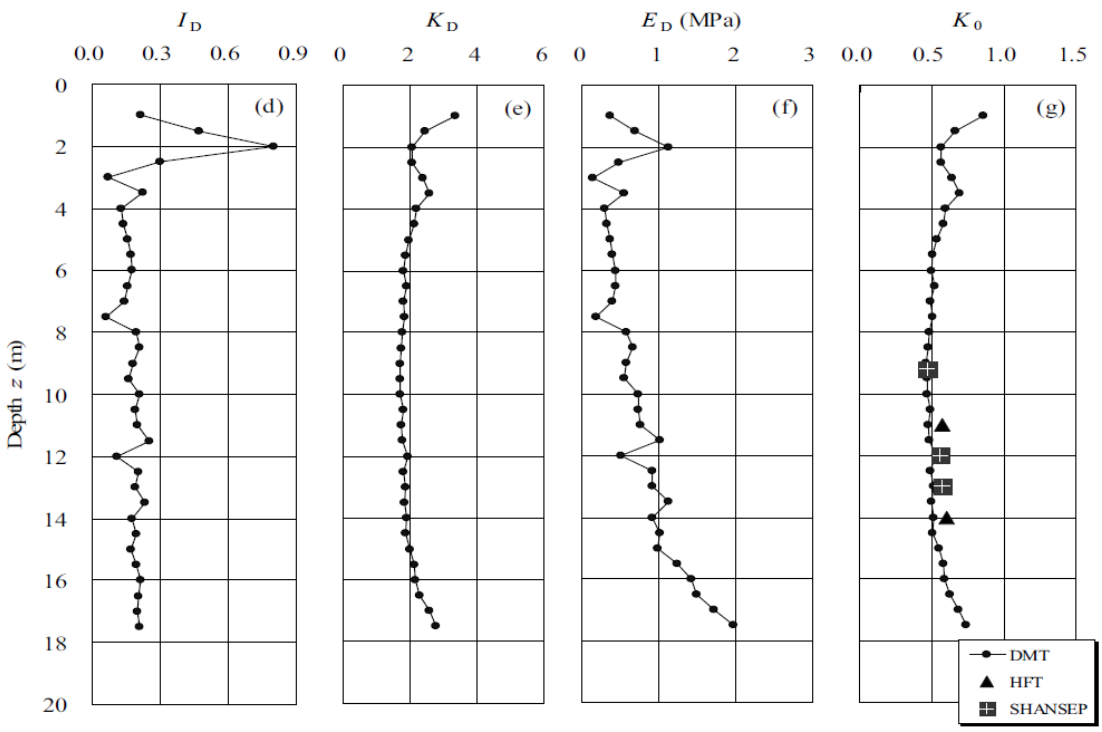

Balina, Australia

DMT data from Pineda et al (2014)

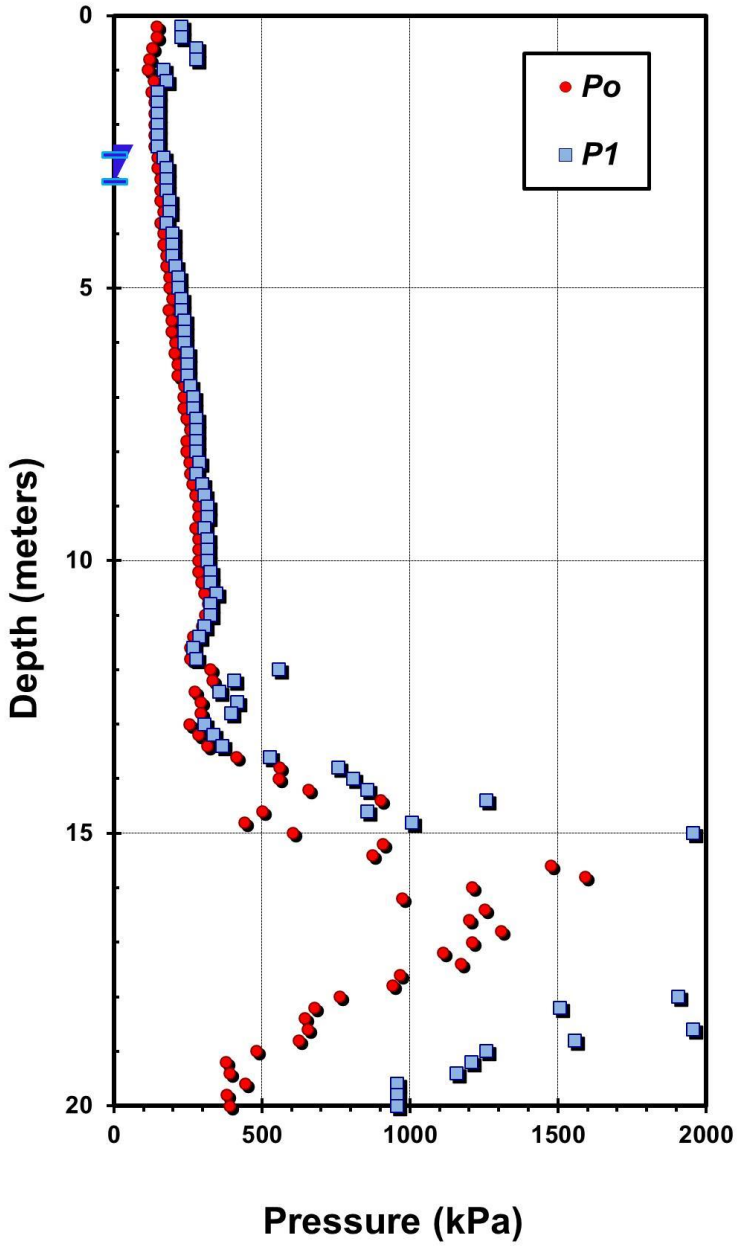

Bangkok, Thailand

DMT from Watabe et al 2004

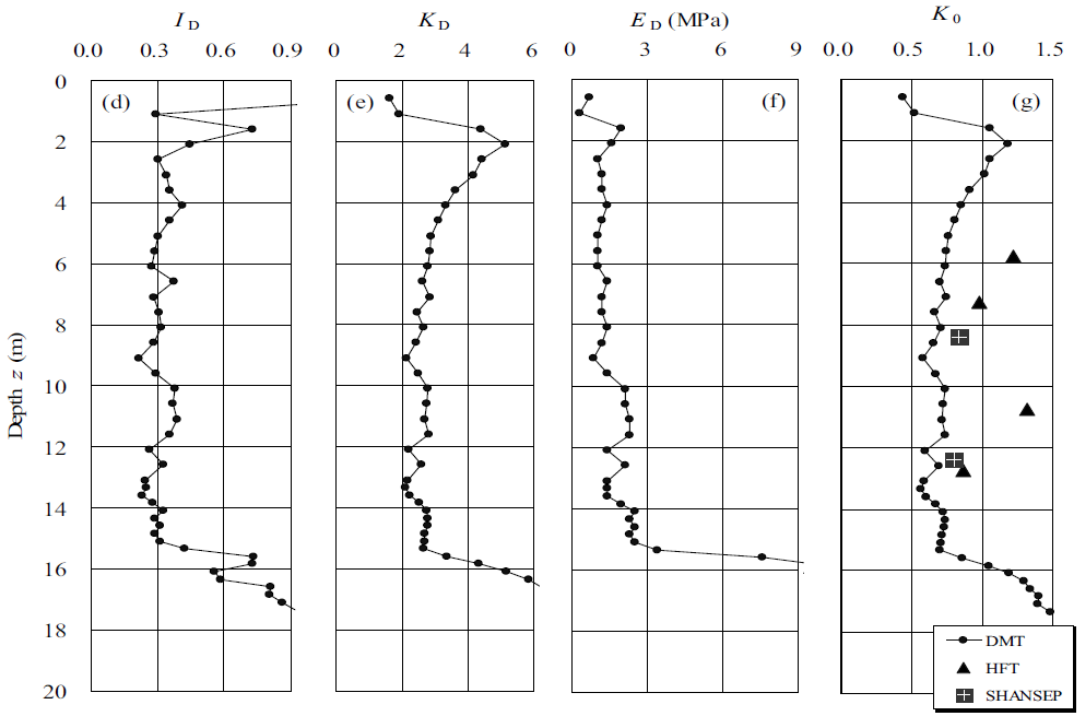

Bogota, Columbia

Data shared by Mr. Edgar E. Rodíguez G

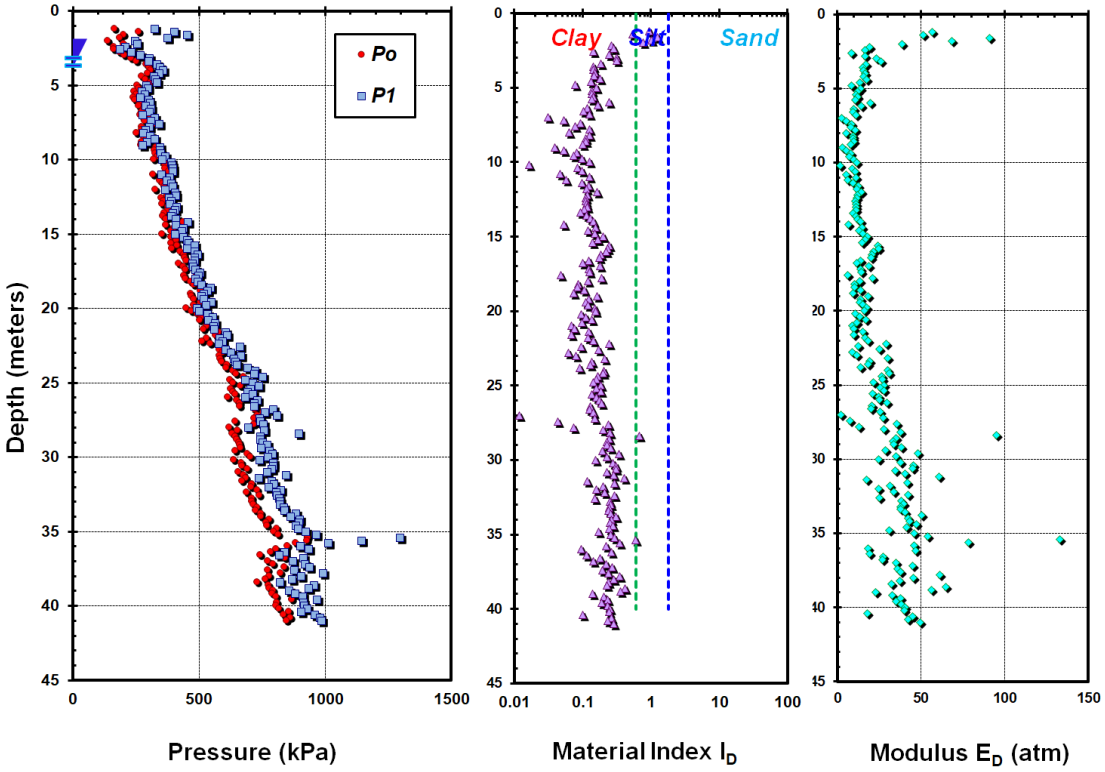

Can Tho

Data from Takemura&Watabe 2006

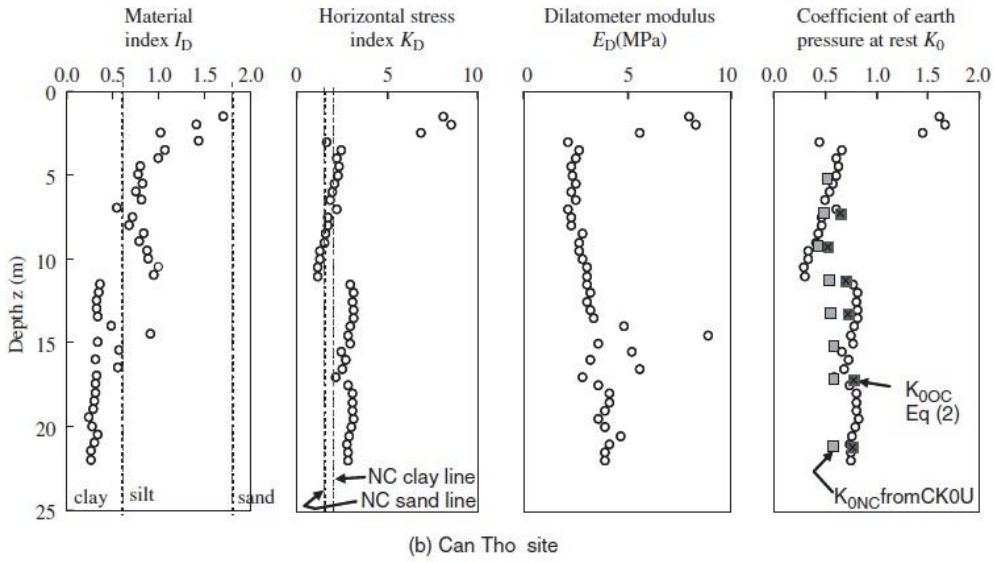

Figure 36. Results of dilatometer tests at Tan An and Can Tho sites.

Colebrook Overpass, BC, Canada

Data after Crawford and Campanella (1991)

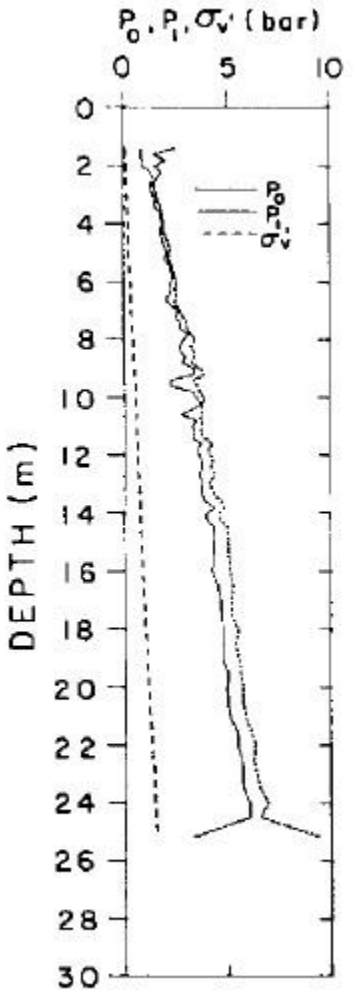

FIG. 9. Flat

Cooper River, South Carolina

Data from Camp (2004); and Mayne (2005)

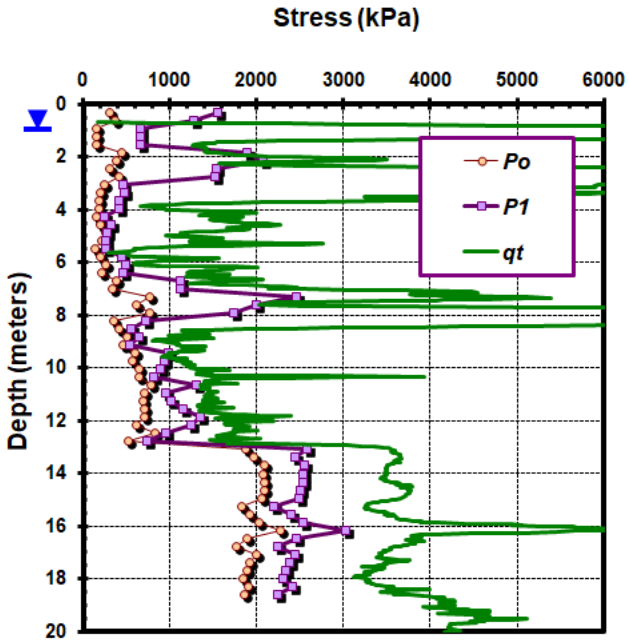

Drammen, Norway

DMT from Lunne & Lacasse (1997)

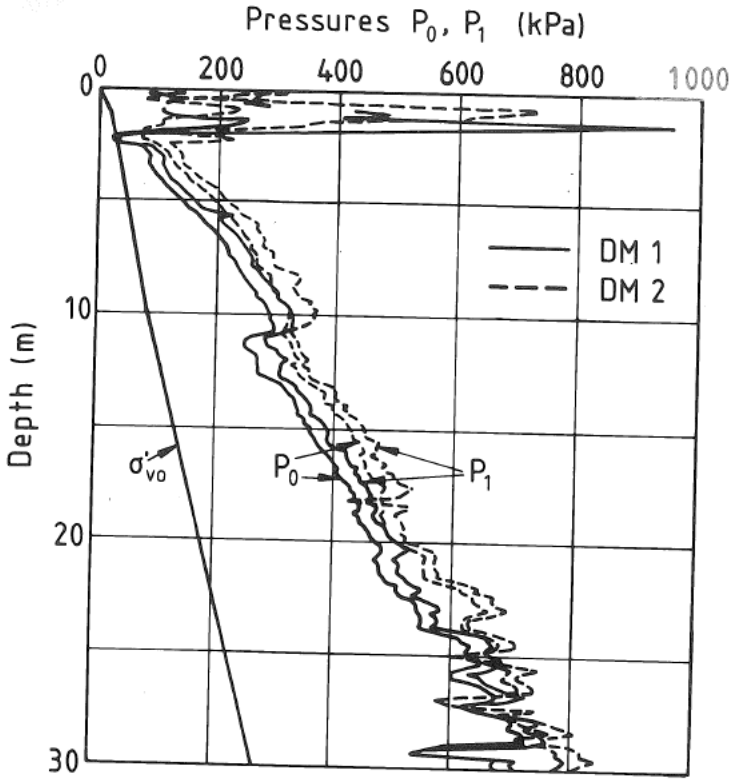

Fig. 8. Contact and expansion pressures in Drammen.

Eagle Farm, Australia DMT

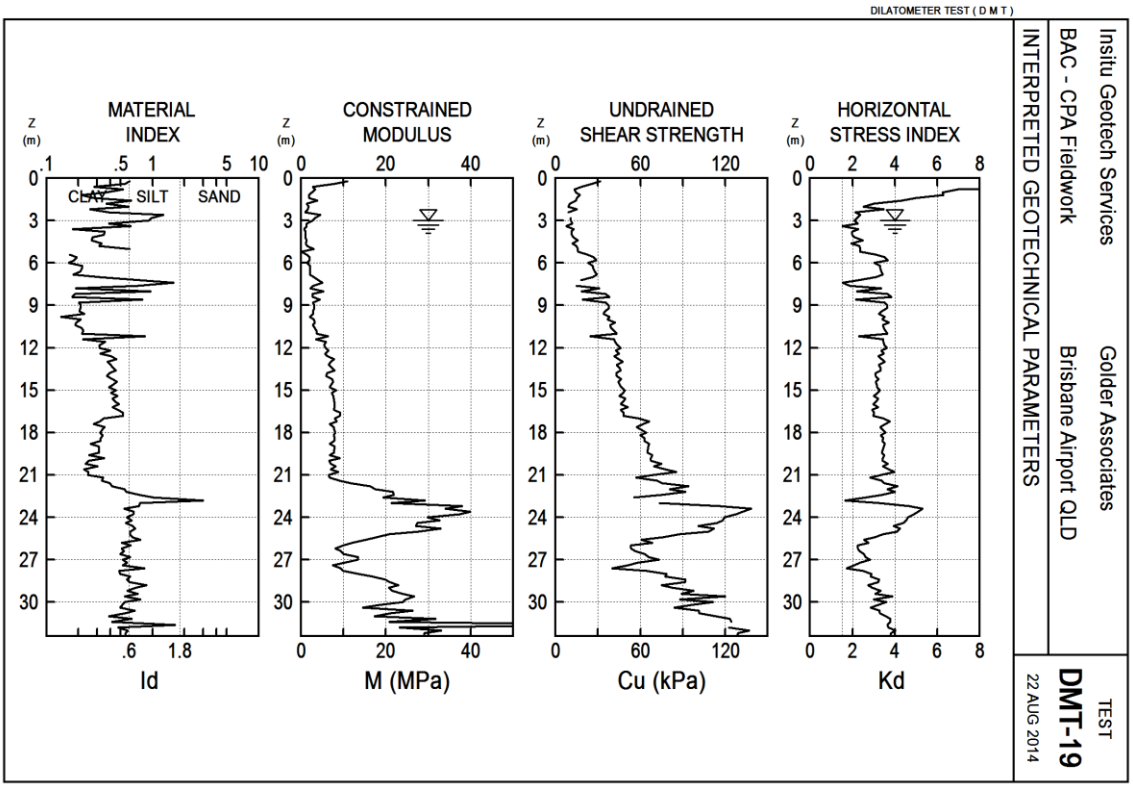

Ford Design Center at NWU, Illinois

DMT by GT

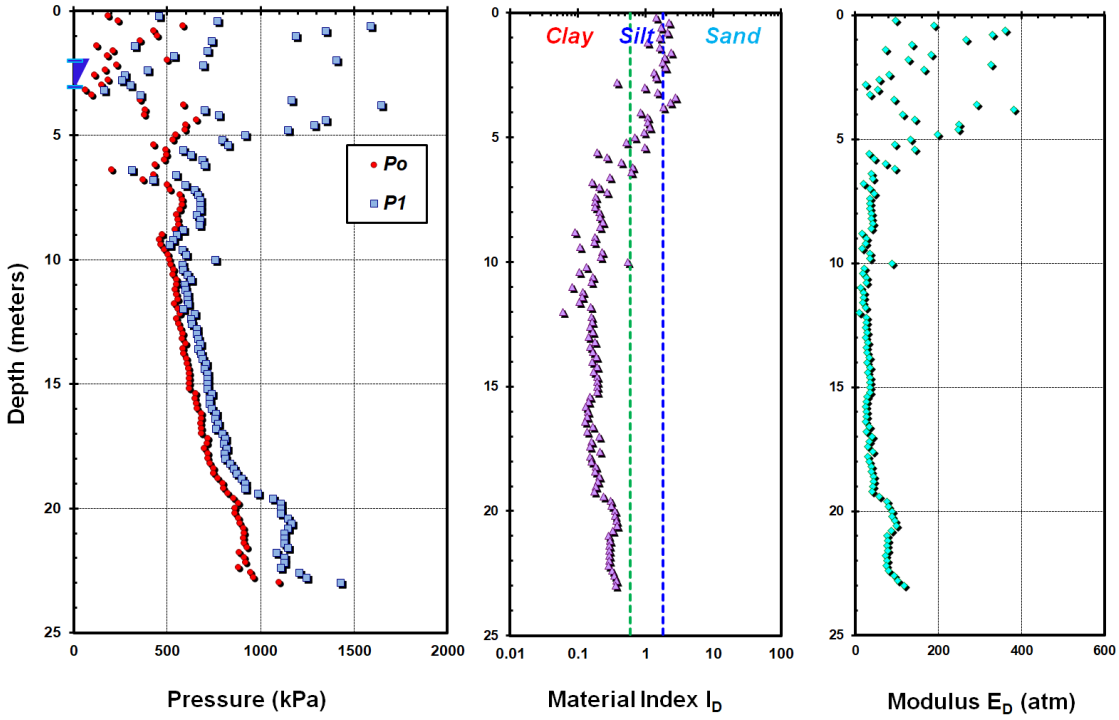

Foynes Irish Silty Clay SDMT

Carroll and Long (2012)

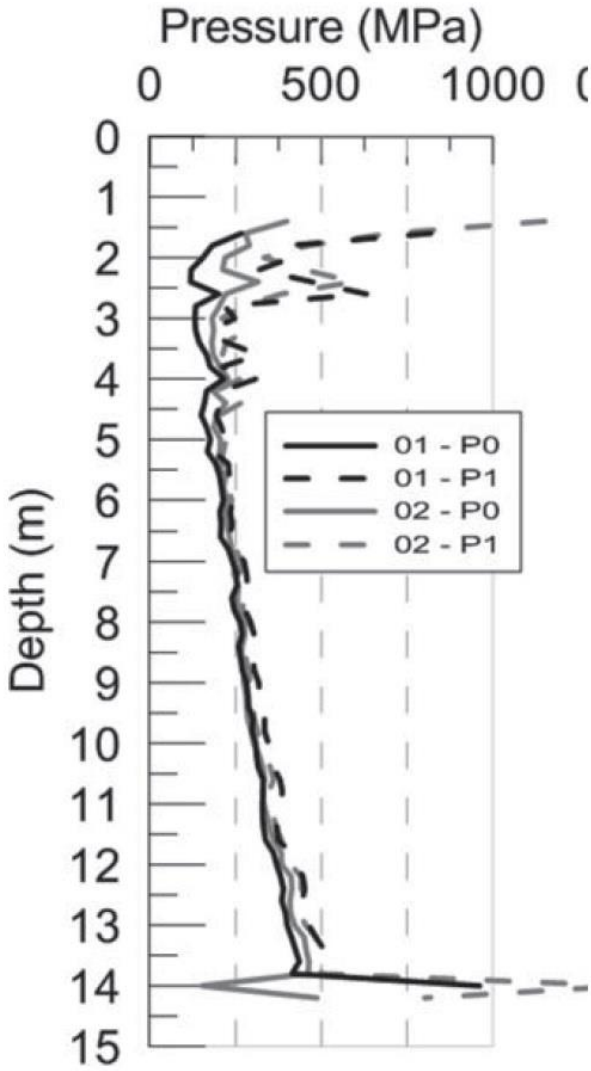

Fucino, Italy

DMT from Soccodato (2002)

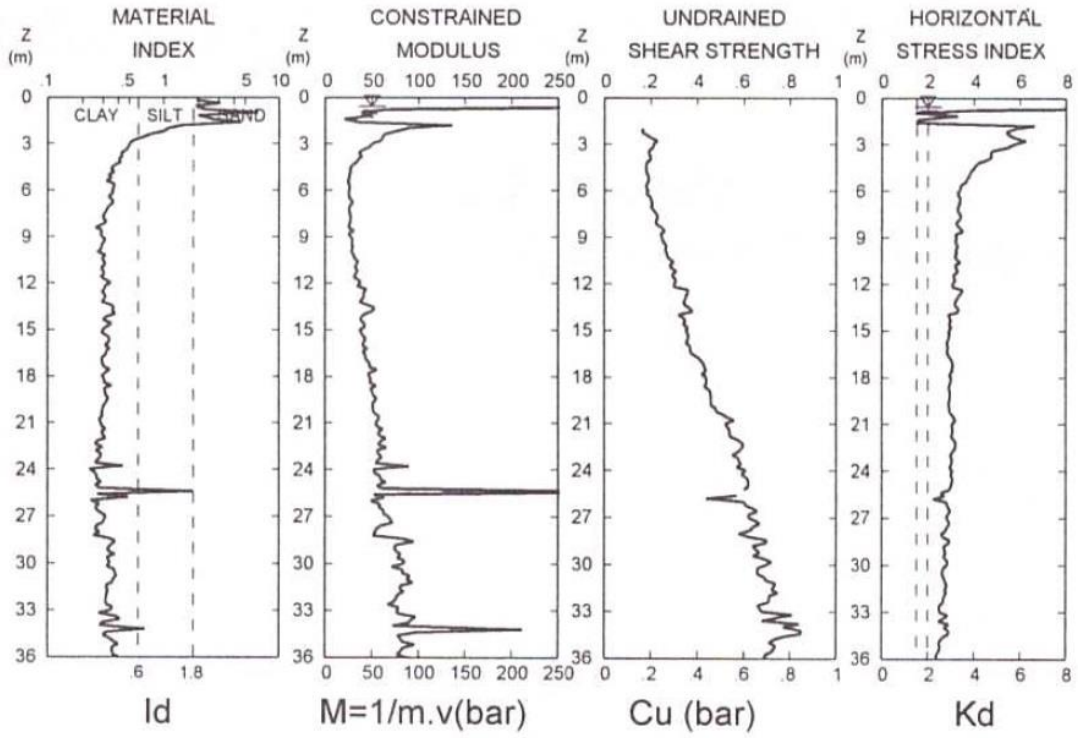

Figure 1. Fucino - Typical DMT profiles

Glava Clay Norway

DMT from Roque et al. 1988

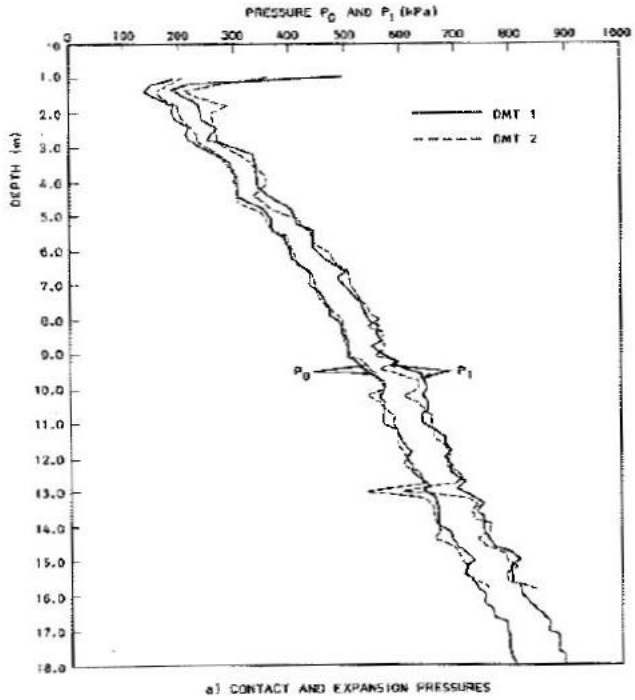

Fig.2. Test results, Glava clay

Hai-Phong, Vietnam

DMT from Watabe et al 2004

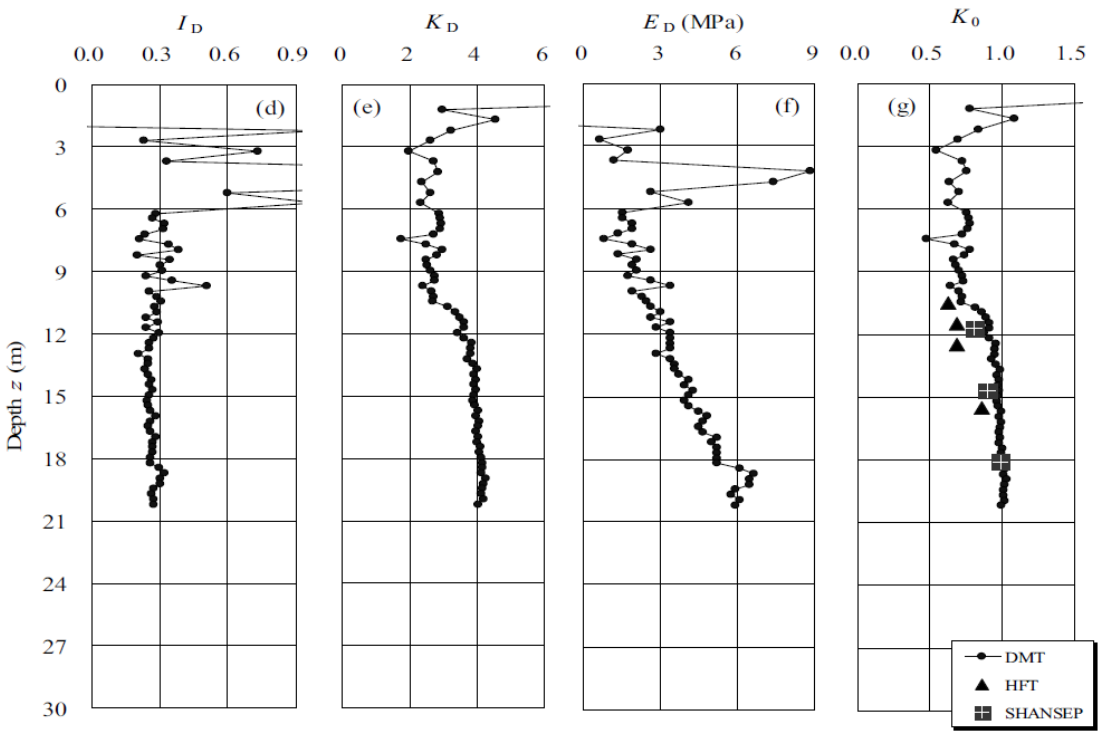

Hamilton AFB, CA

Data from Benoit et al. 1990

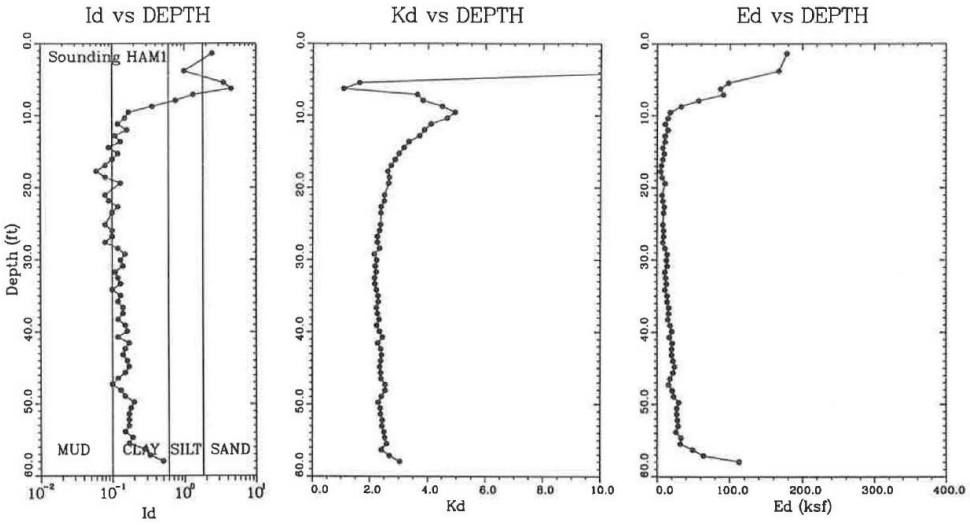

FIGURE 2 Typical profile of dilatometer indices at Hamilton Air Force Base, California.

Kurihama, Japan

Kamei and Iwasaki1995

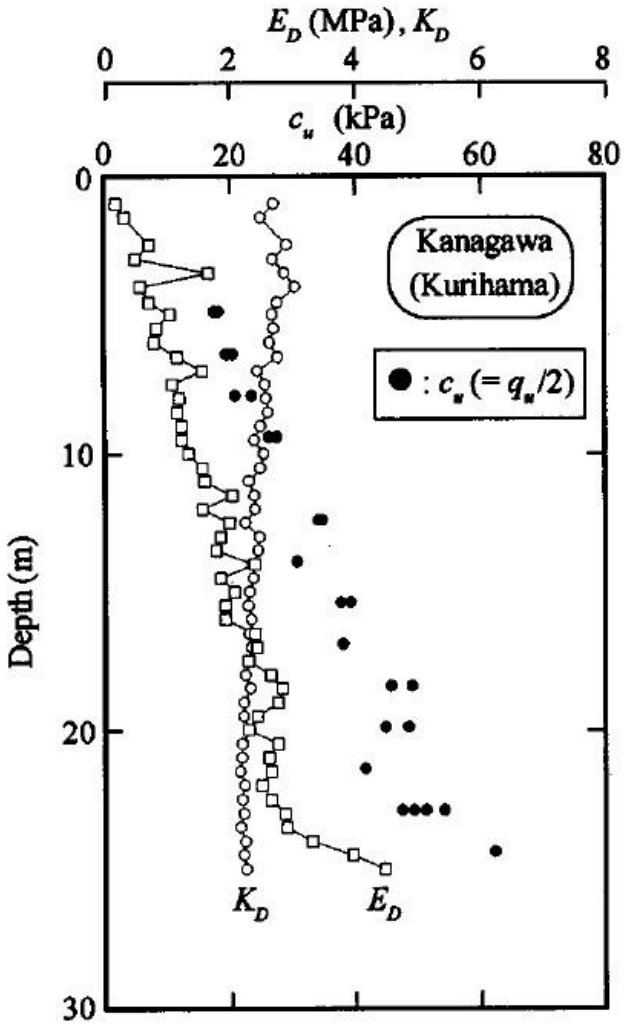

Fig. 4. Profiles of DMT horizontal stress index K_D, dilatometer modulus E_D and undrained shear strength c_u obtained from unconfined compression tests at Kanagawa (Kurihama) site.

Lilla Mellosa, Sweden

Data from Larsson & Mulabdic (1991)

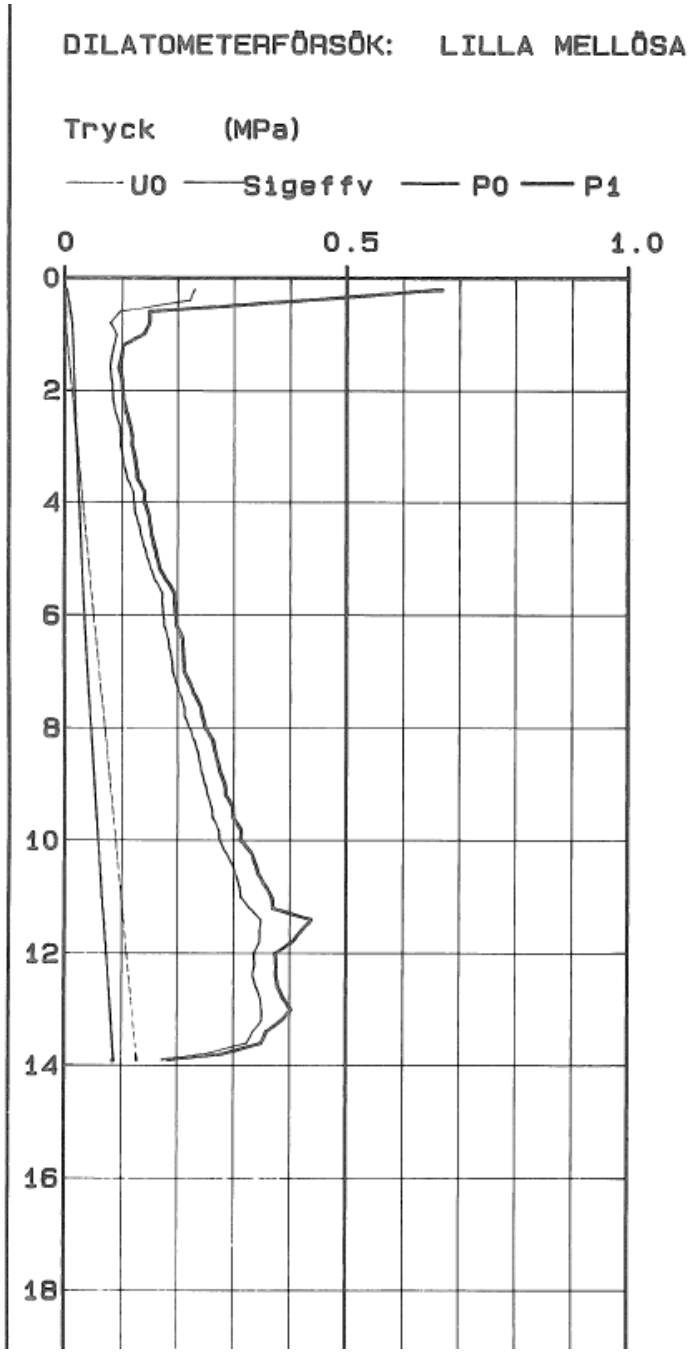

Louiseville, USA

Data from Tanaka et al 2001

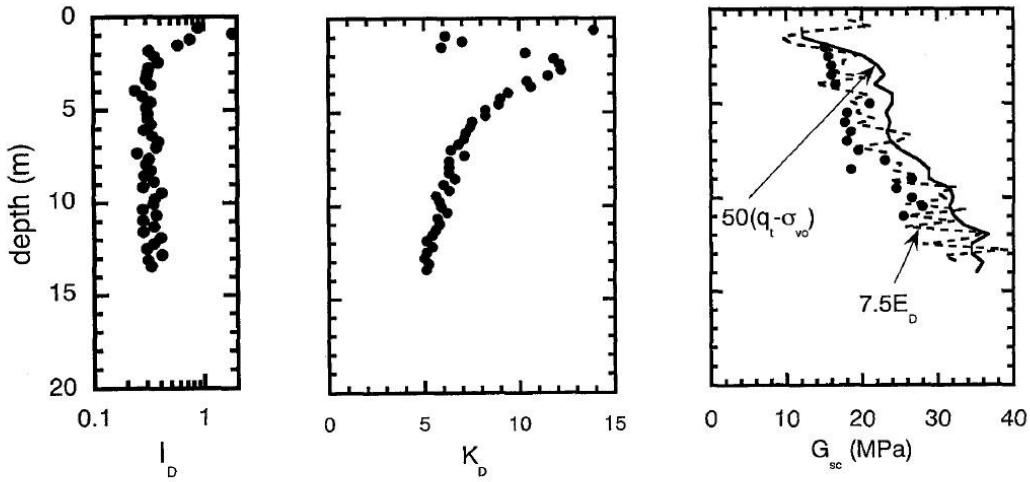

Fig. 2. Soil properties of Louiseville site

Mark Clark Bridge, SC

Data from Camp et al (2002a&b)

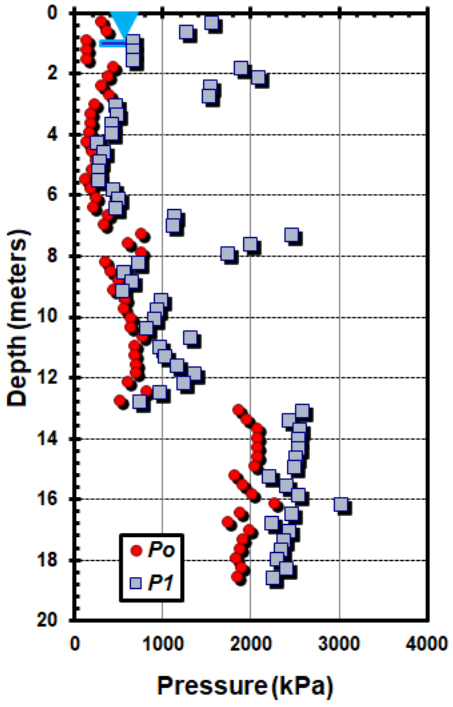

Mcdonald Farm, BC

DMT from Robertson et al. (1992)

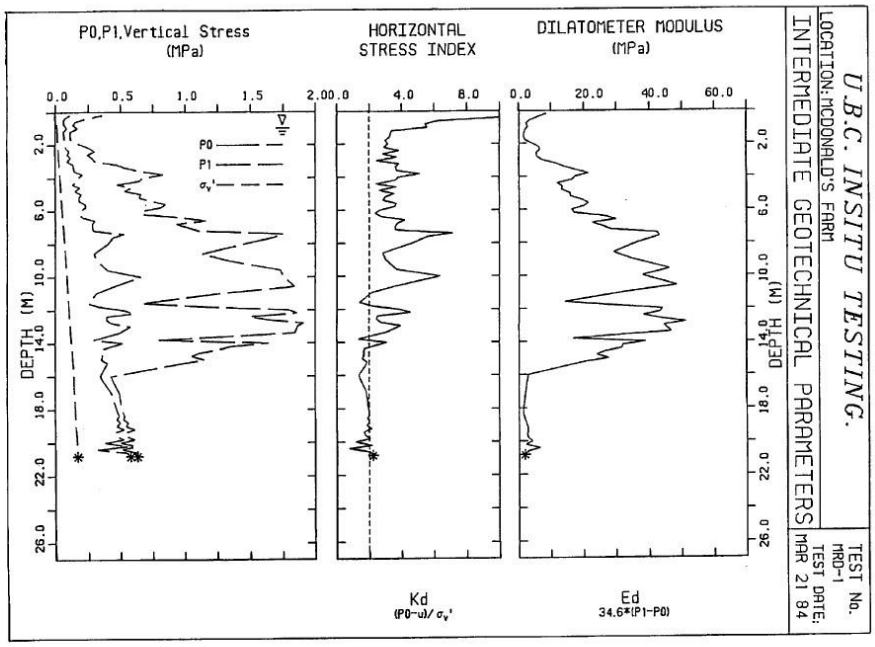

Figure 4.4 DMT Profile at McDonald's Farm - Intermediate Geotechnical Parameters (Sounding MRD-1, DIL.RED)

Norfolk, VA

DMT by E.Cargill

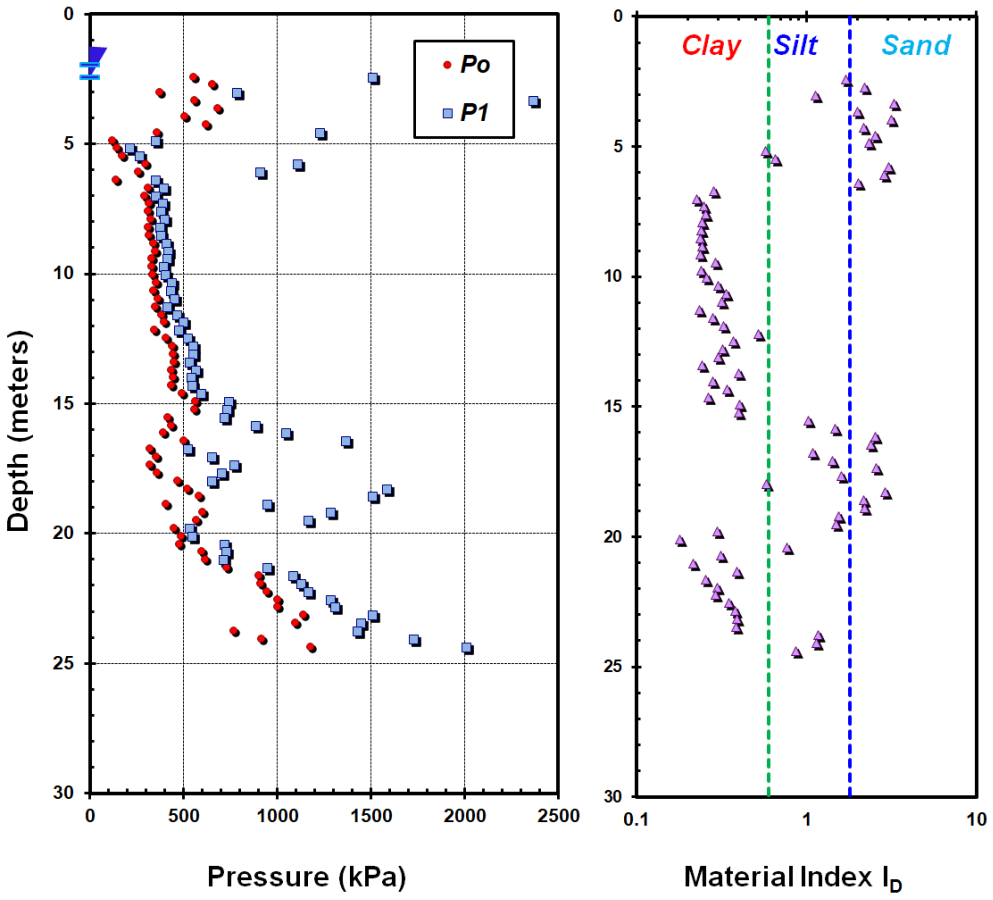

Norrkoping, Sweden

DMT from Larsson & Mulabdić (1991)

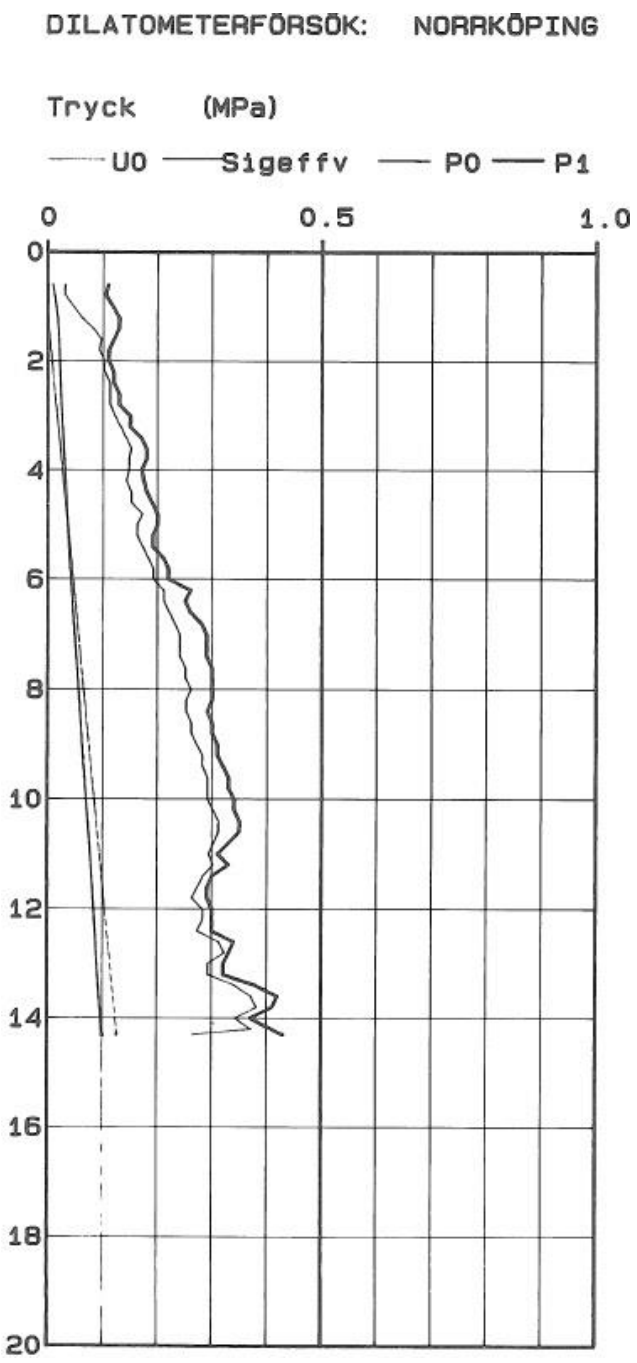

Onsøy clay, Norway

DMT data from Lunne et al. 2003

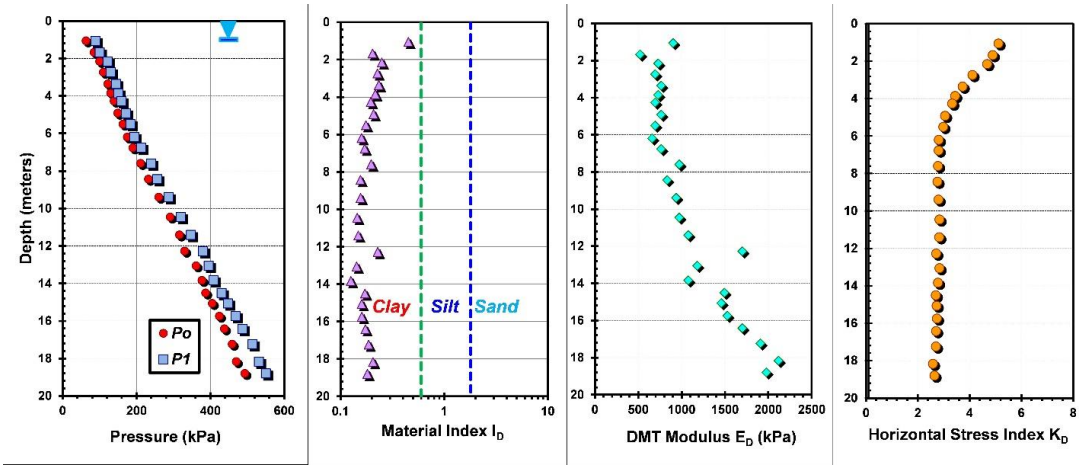

Pisa, Italy

DMT by Marchetti et al. (2001)

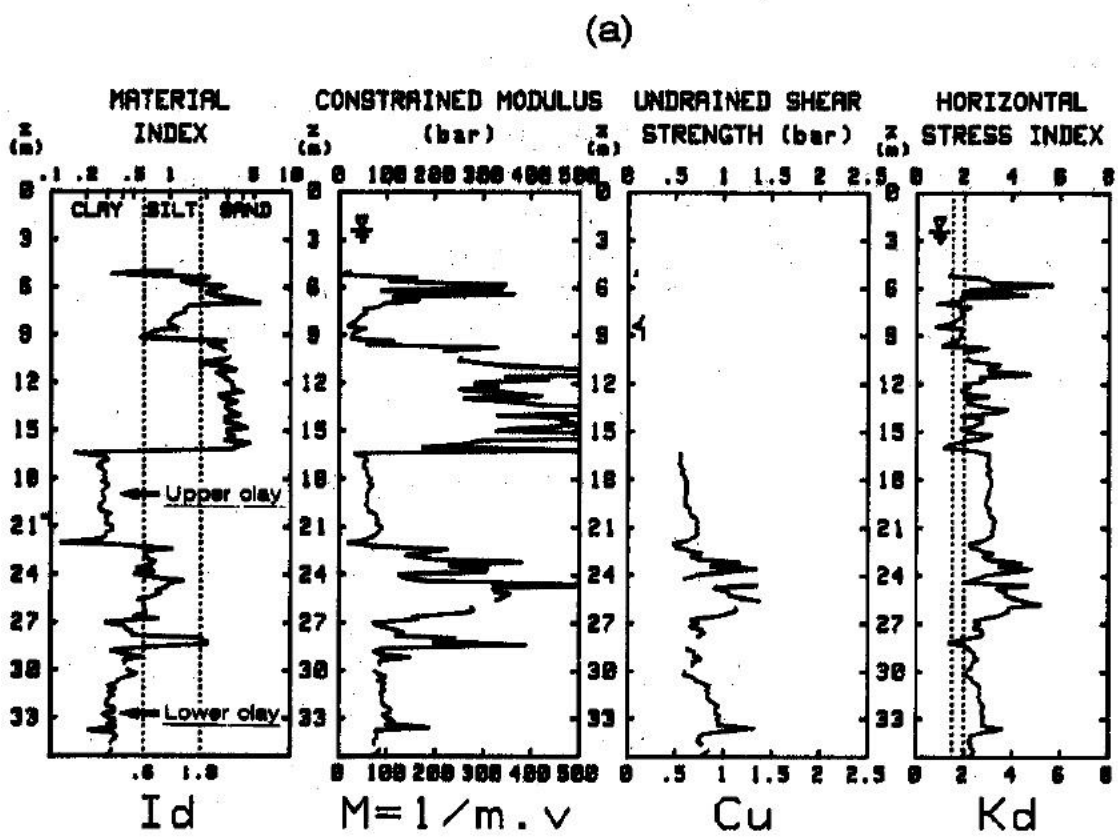

PNG, Australia

Data from Golder Associates Inc

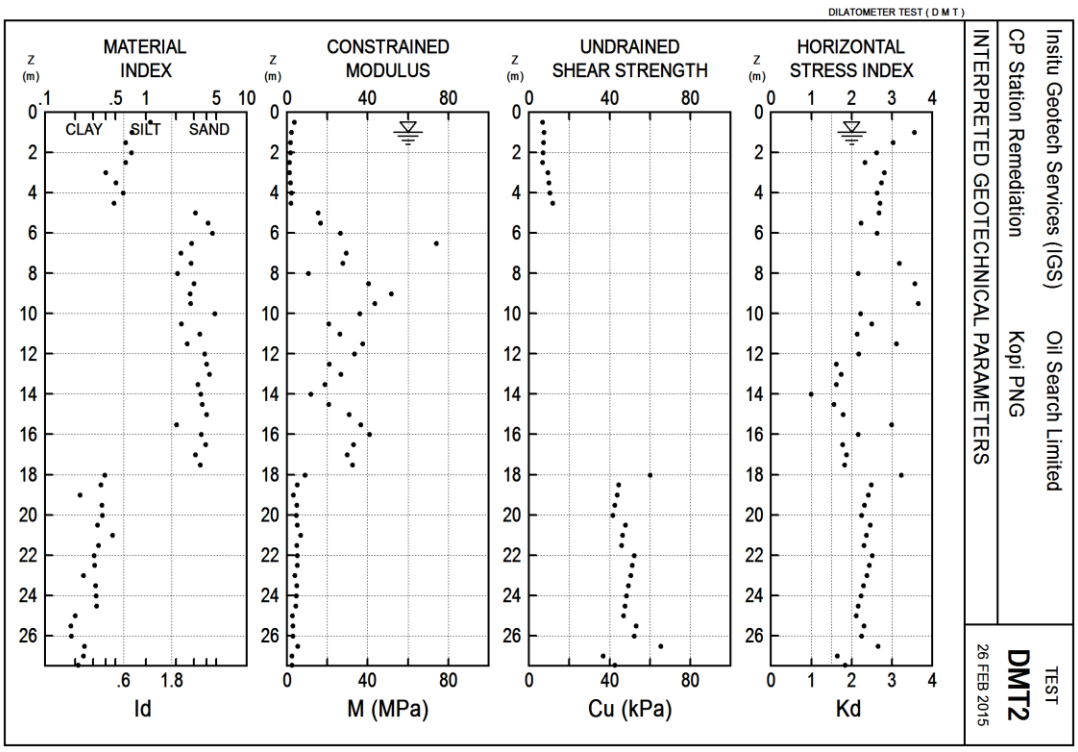

Port Huron, MI

Data from Chen and Mayne (1994)

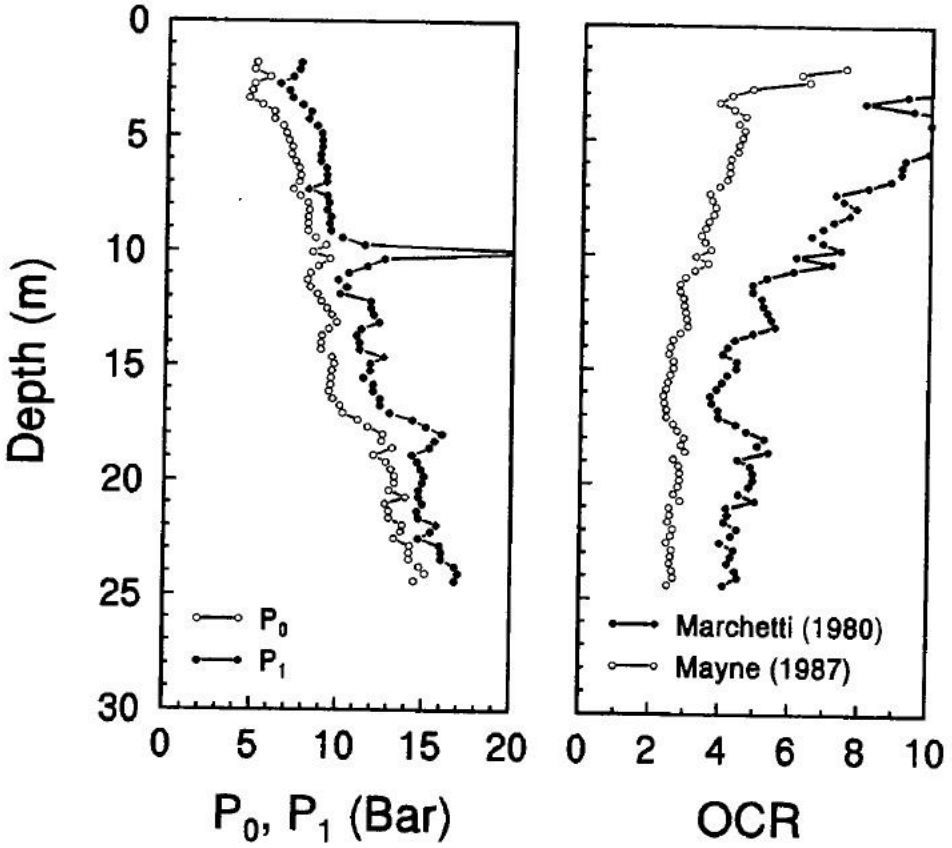

Figure 4.4. Results from a Dilatometer Sounding at Port Huron Site.

Porto Tolle, Italy

DMT Hansbo et al (1981)

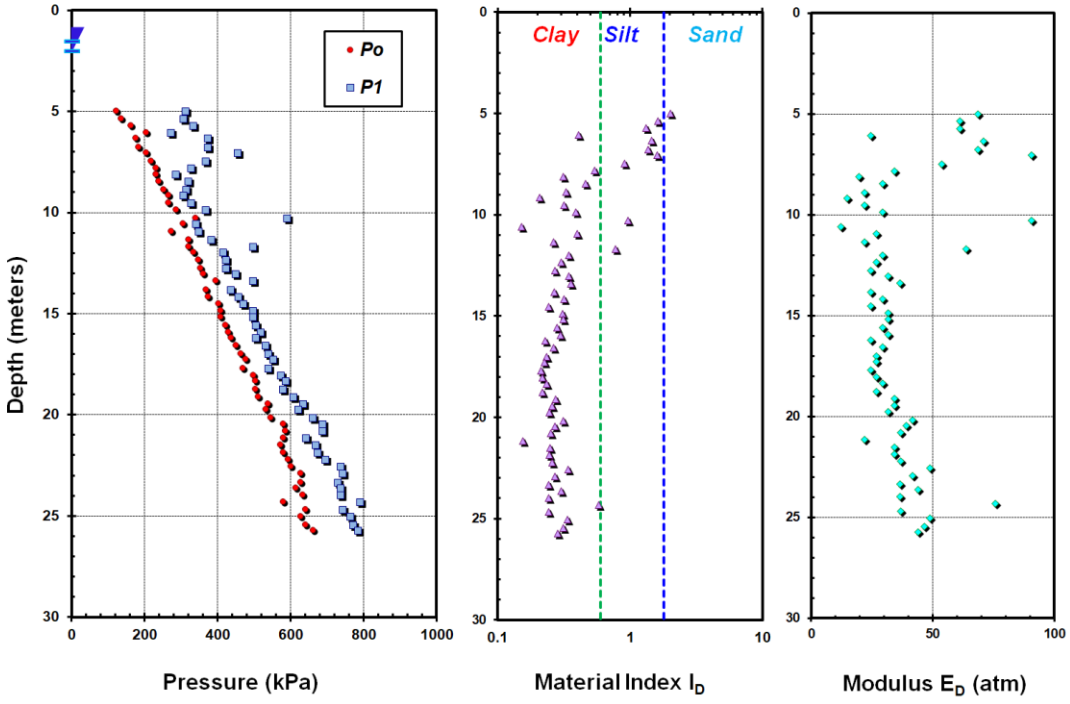

Recife, Brazil DMT data Danziger (2007)

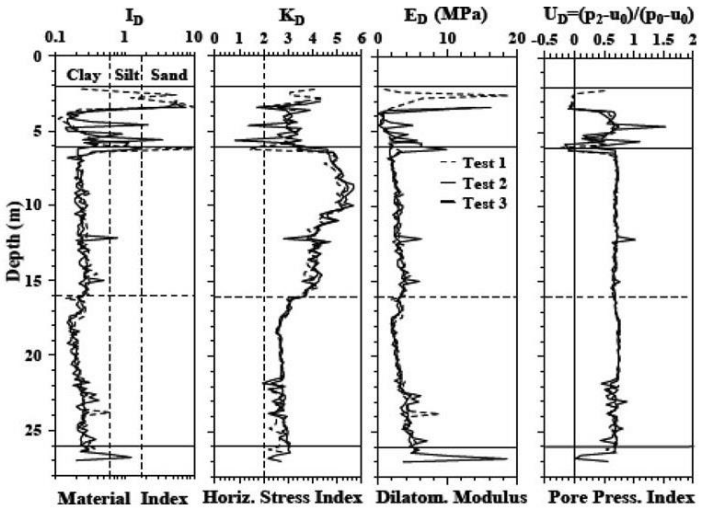

Figure 19. Dilatometer tests results – I_D, K_D, E_D, U_D vs Depth – RRS1 (Coutinho & Oliveira 1997).

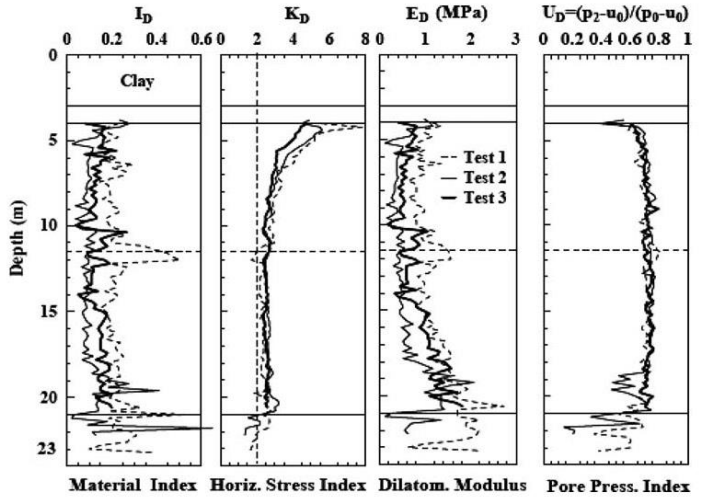

Figure 20. Dilatometer tests results – I_D, K_D, E_D, $U_D = (p_2-u_0)/(p_0-u_0)$ vs Depth – RRS2 (Coutinho et al. 1999).

Route 17 bridge site, Chesapeake, VA. DMT data from Charles and Barnhill 1987

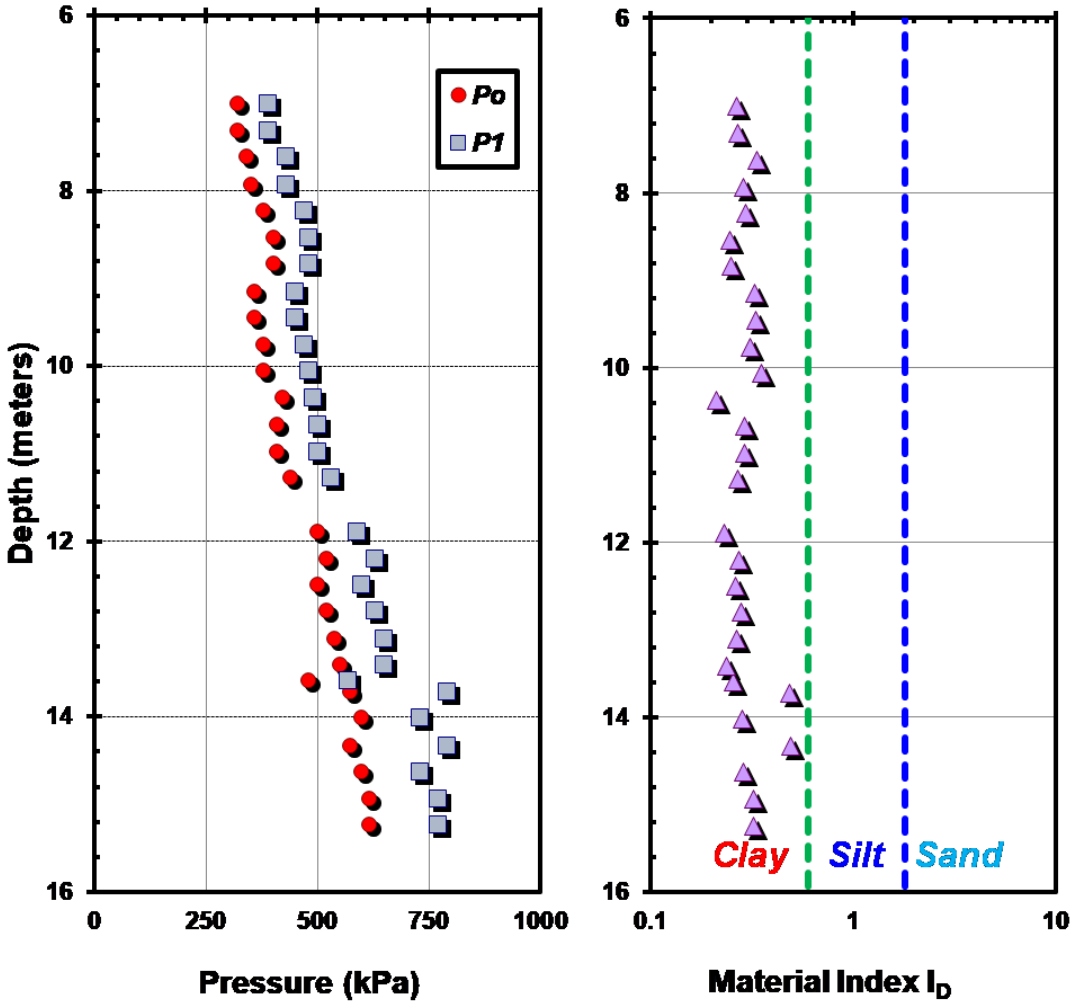

Sarapui, Brazil

DMT Danziger (2007)

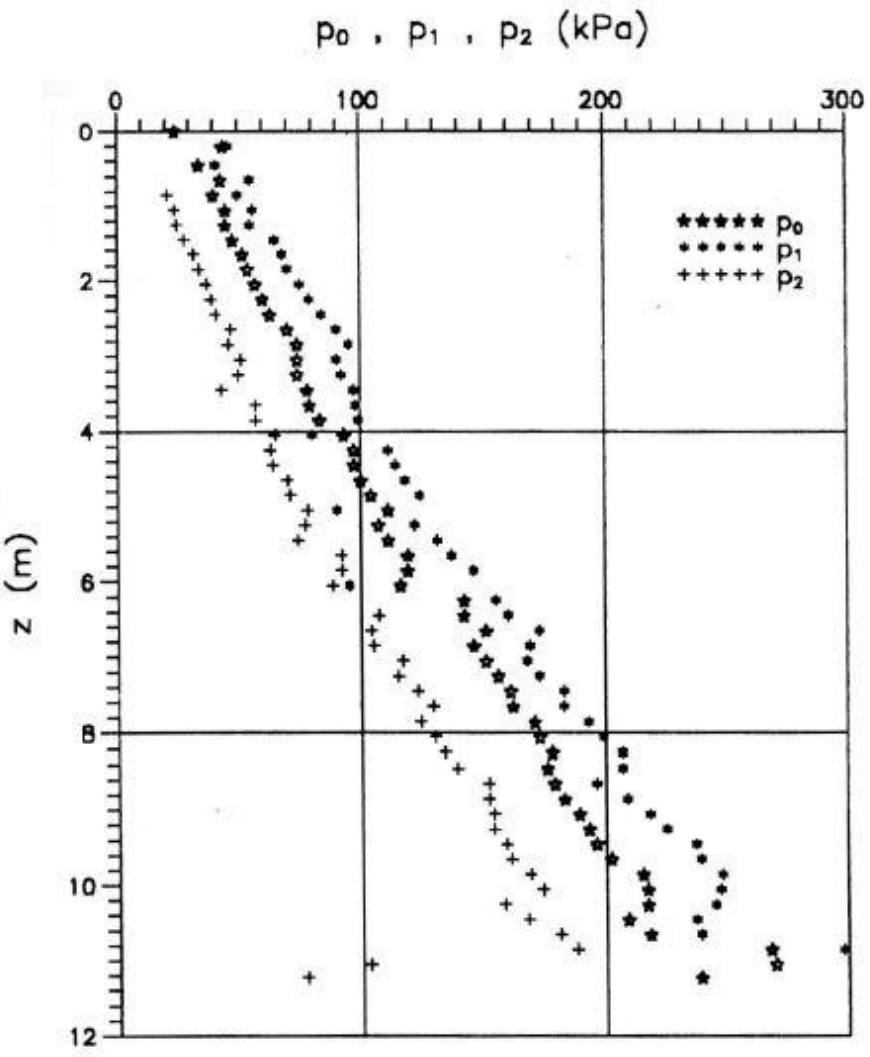

Fig. 4. Dilatometer test. Values of p_0, p_1 and p_2 versus depth (VIEIRA [66]). p_0 – corrected A reading, p_1 – corrected B reading, p_2 – corrected C reading

Saro Rd 6-900 and 7-600, Sweden

Larsson & Mulabdic (1991)

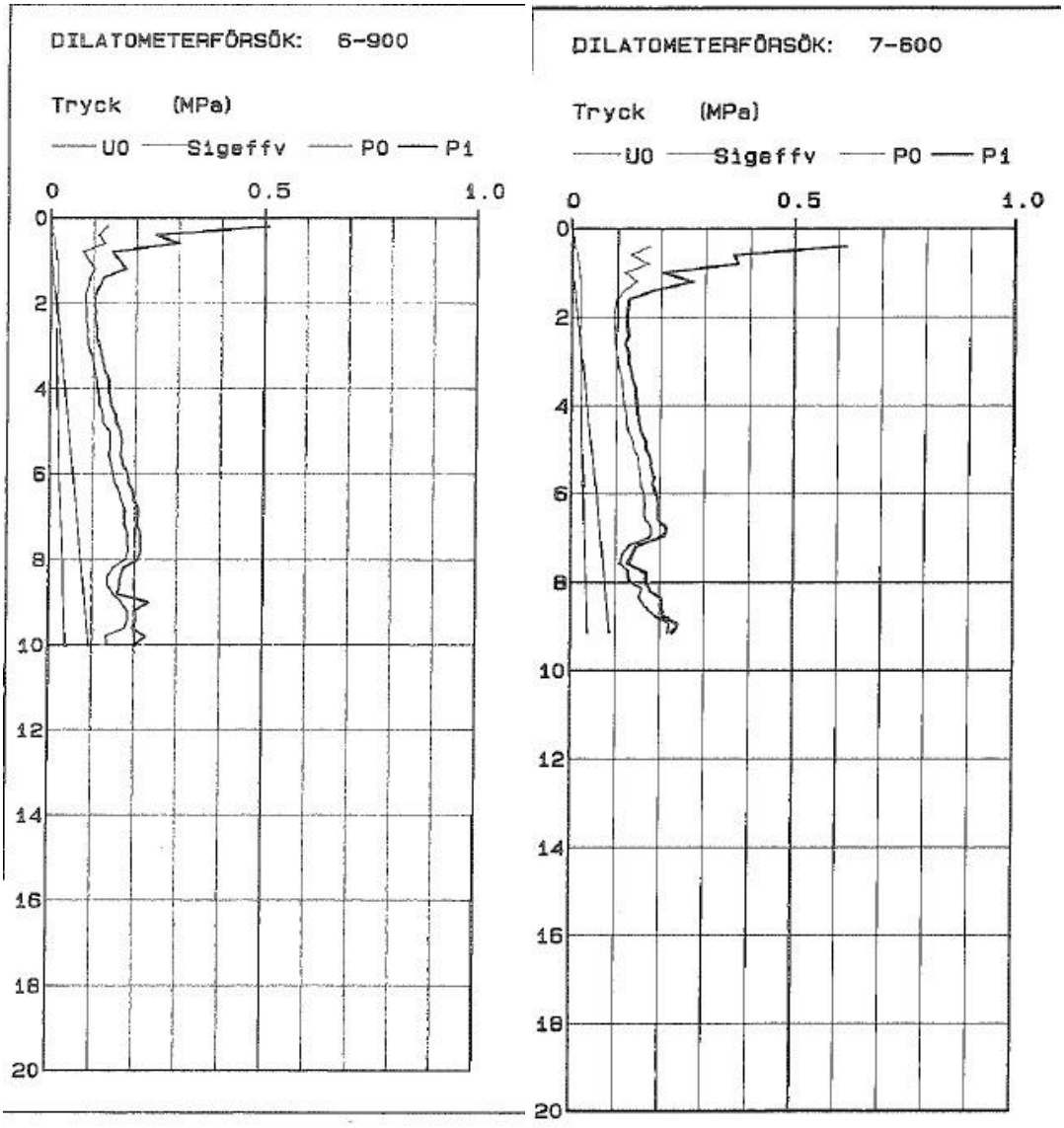

Singapore DMT at FT-2 Cao (2003)

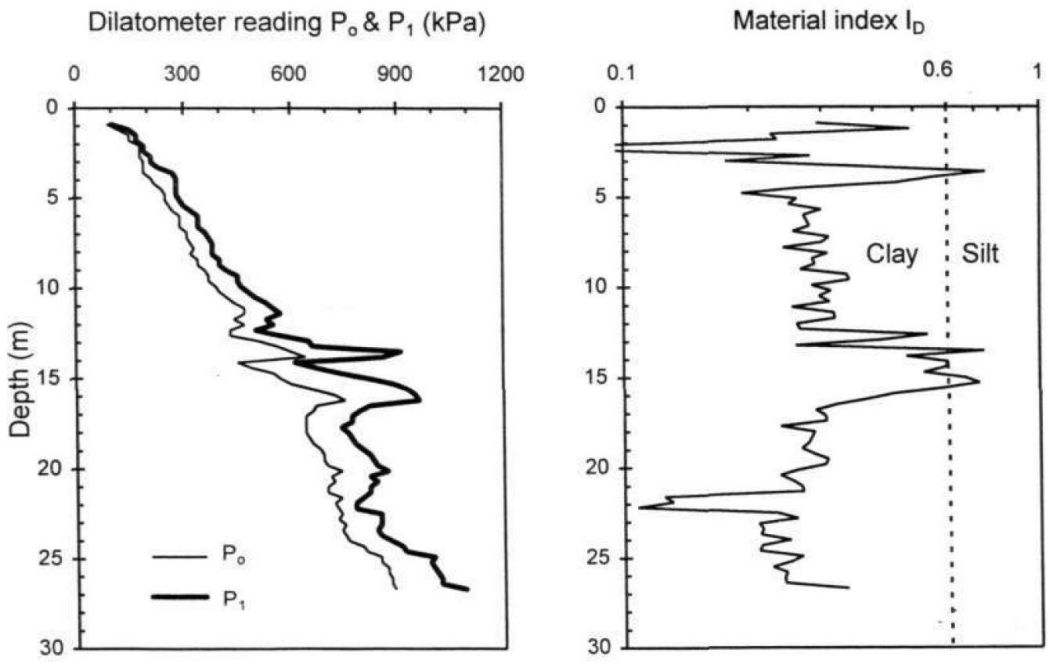

Fig. 8.17 Dilatometer test results at FT-2

Ska-Edeby, Sweden. DMT by Larsson & Mulabdic (1991)

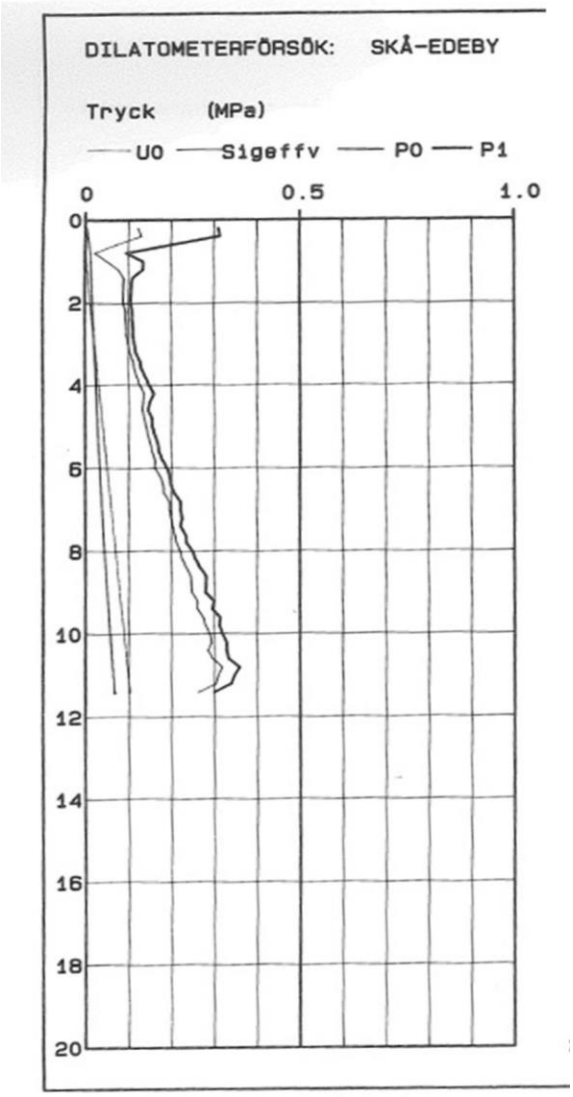

South Gloucester, Ontario DMT from Professor Lutenegger

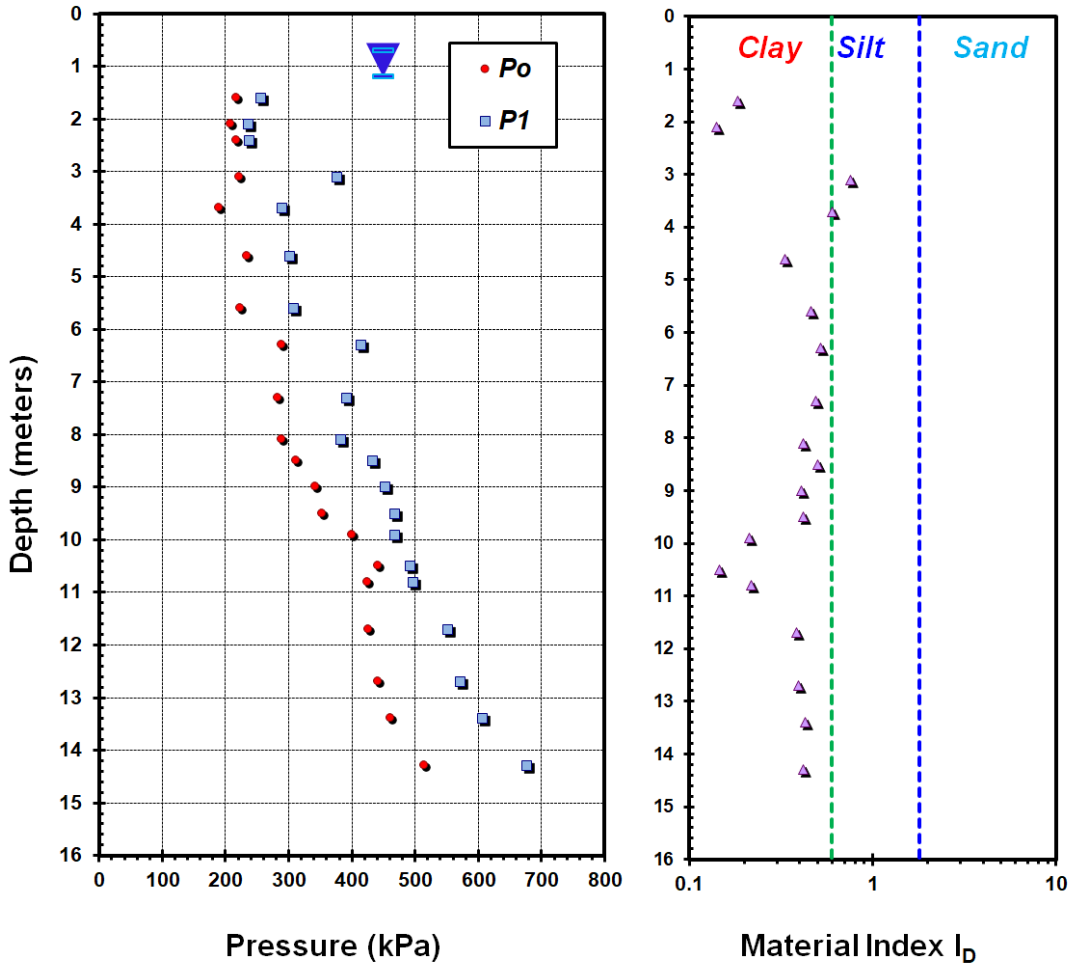

South Portland, Maine DMT by Roche 2006

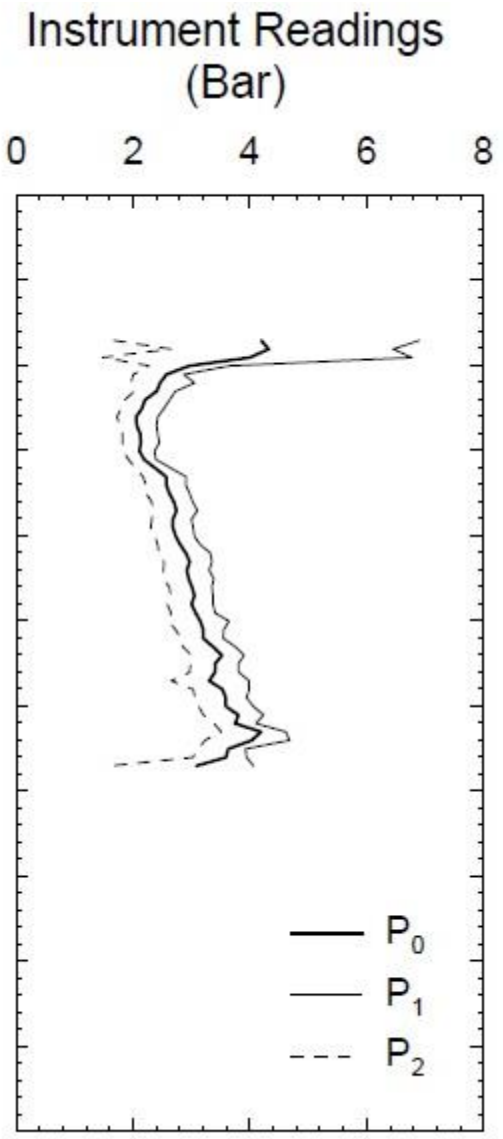

Stono River Bridge, SC. DMT by Camp (2004)

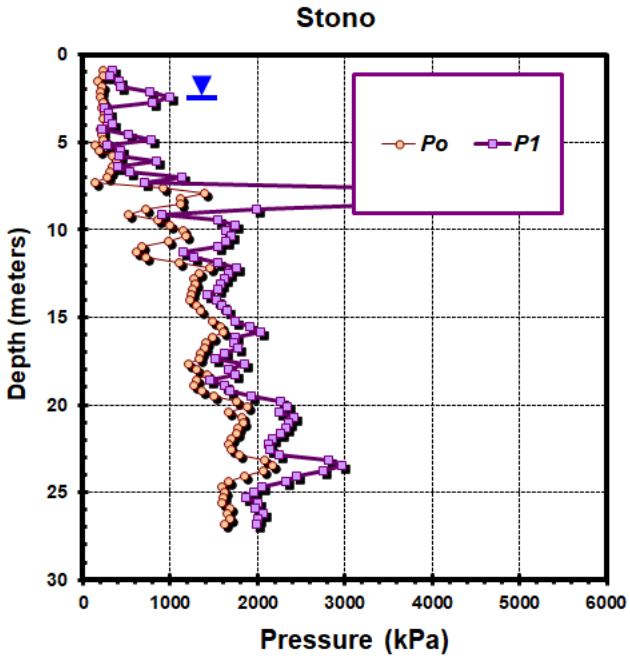

Strandbacken, Sweden. DMT Larsson and Ahnberg (2003)

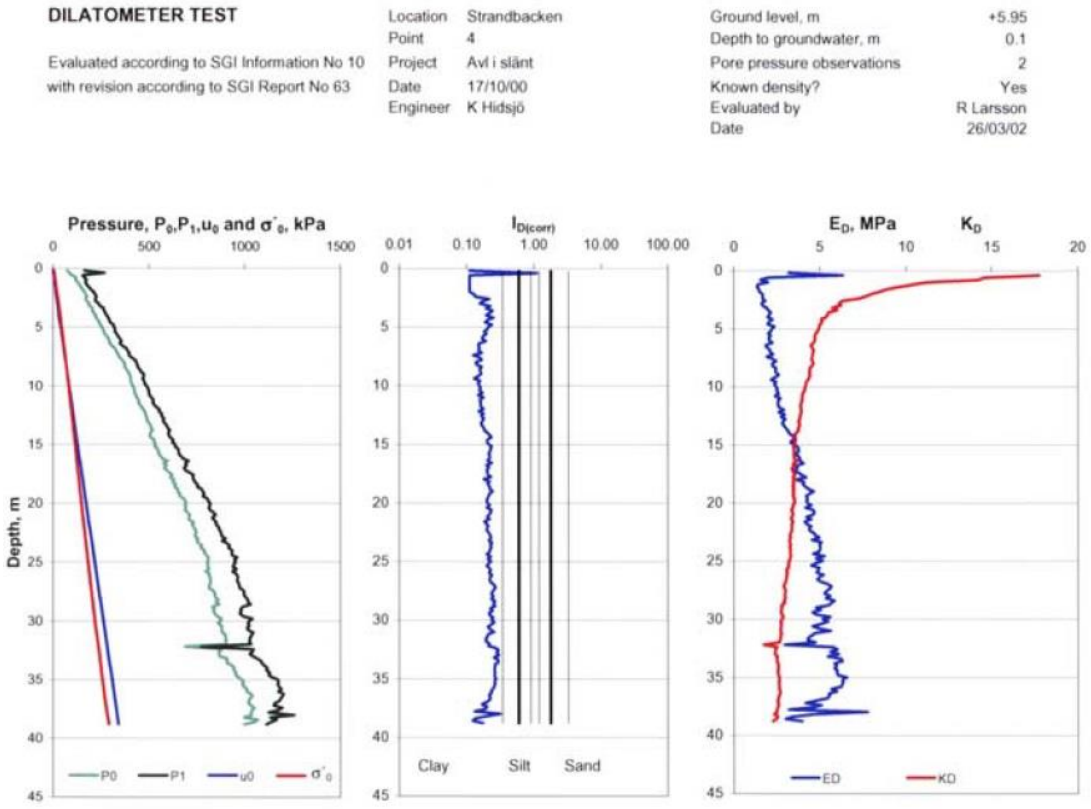

Sundholmen river, Sweden. DMT by Larsson and Ahnberg (2003)

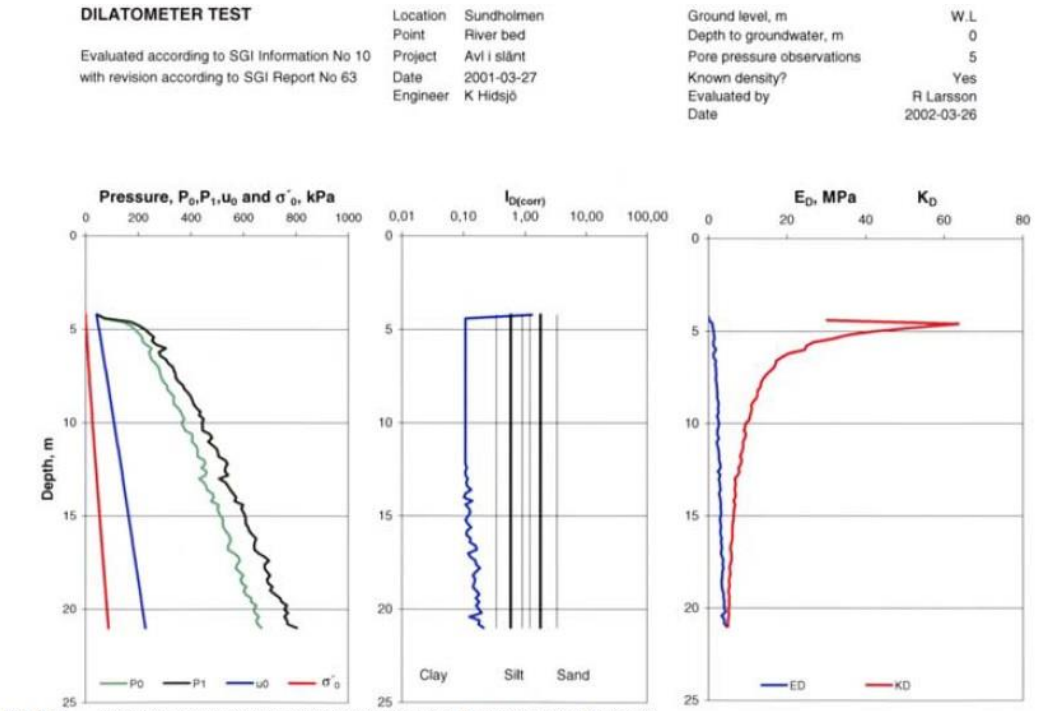

Fig. 141. Results of dilatometer tests below the river bottom in Sundholmen. a) base data

Tokyo Bay DMT Takesue and Isano (2001)

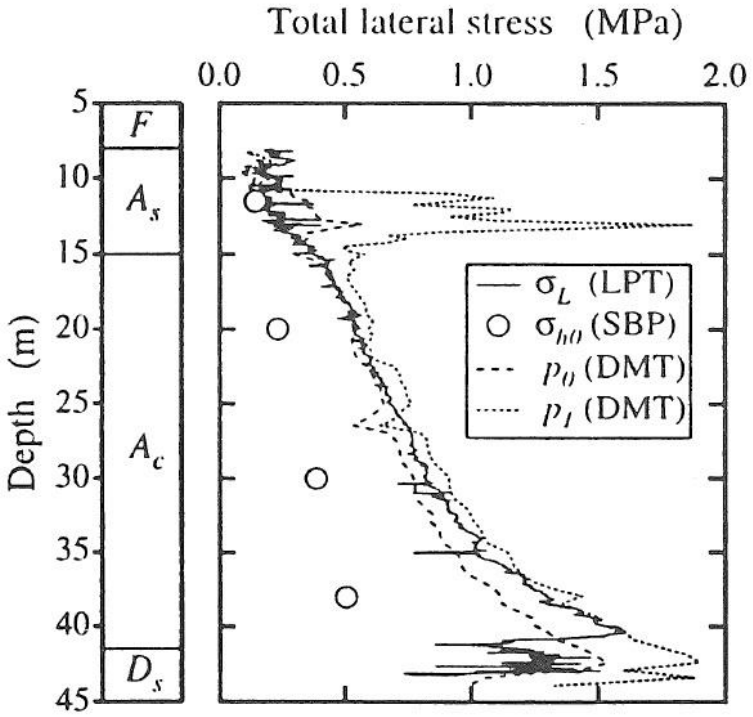

Figure 4. Comparison between LPT total lateral stress cry and measurements of DMT and SBP tests.

Torp, Sweden. DMT by Larsson and Åhnberg (2003)

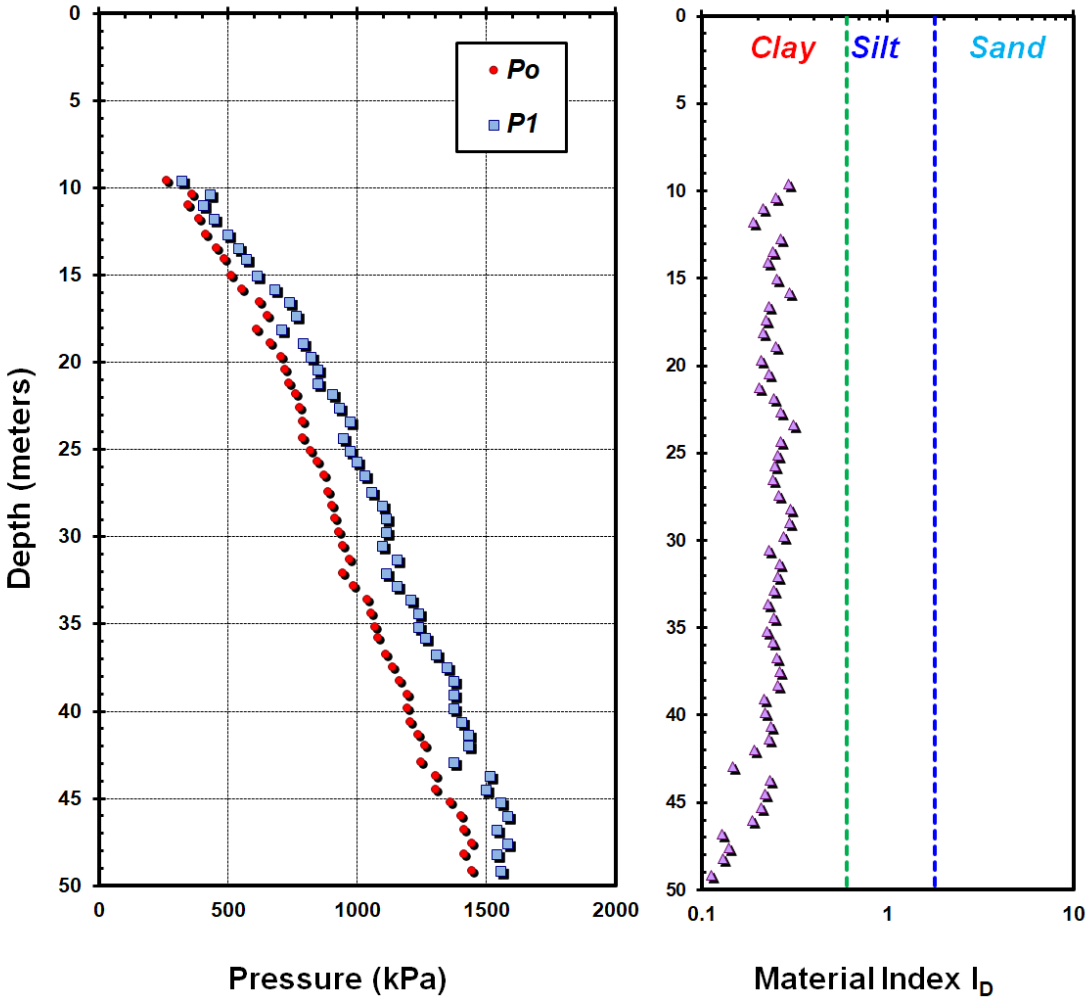

Valen, Sweden. DMT by Larsson & Mulabdic (1991)

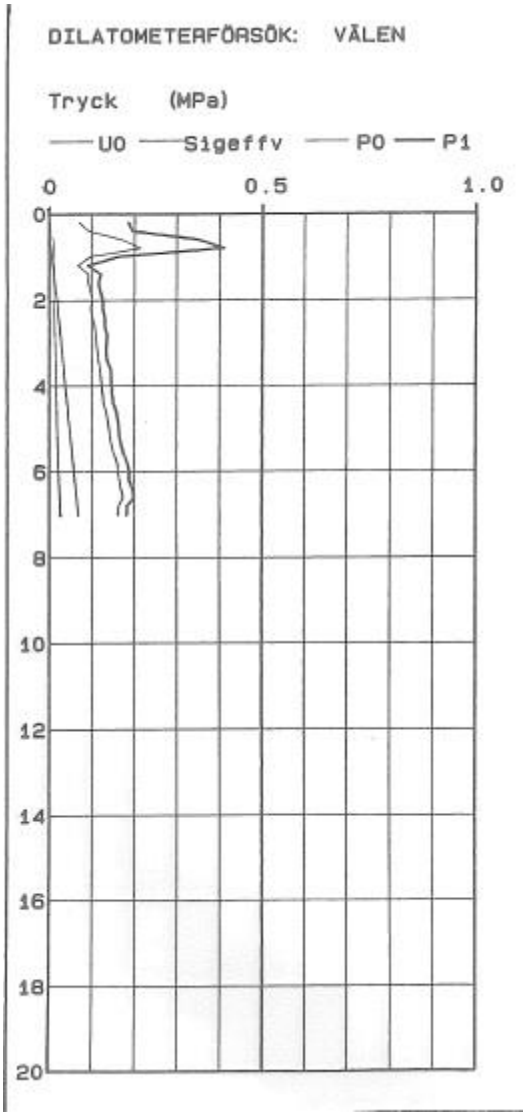

Yorktown Formation, VA. DMT by Dr. Paul Mayne

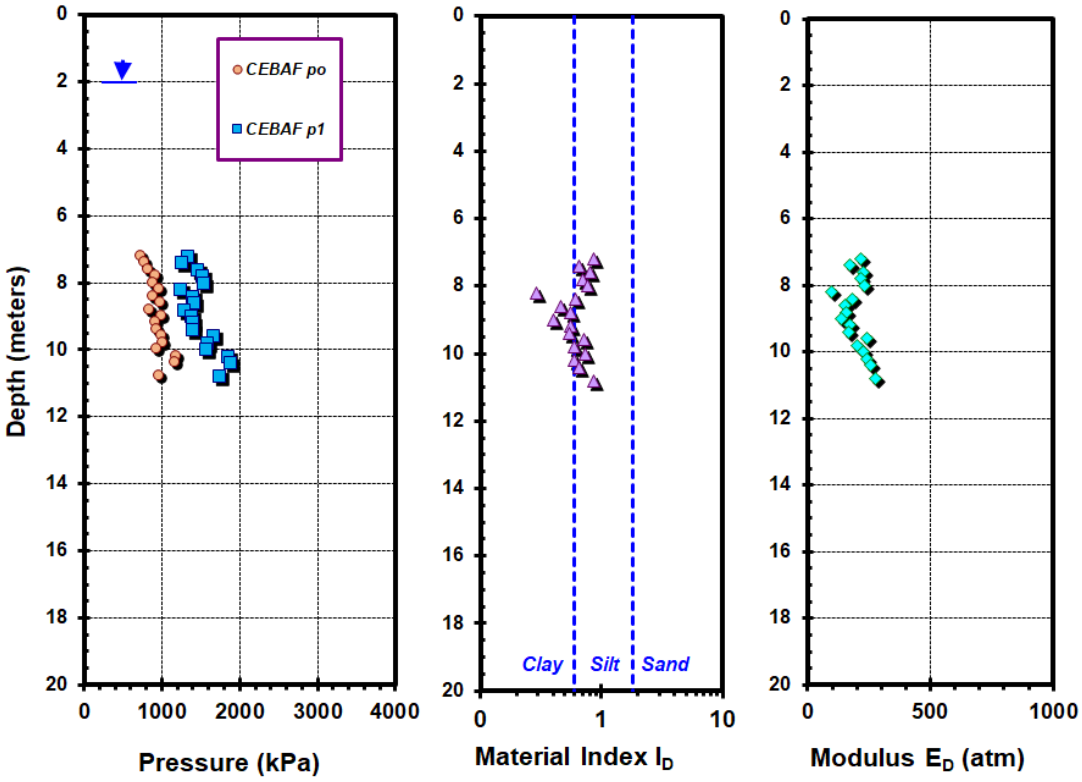

APPENDIX E. RAW DATA FROM LABORATORY CIUC/CAUC/CK$_0$UC TRIAXIAL TESTS

This appendix contains the raw data from laboratory CIUC/CAUC/CK$_0$UC triaxial tests used in this research program.

Amazon river site

Data from Sandroni et al. (2015)

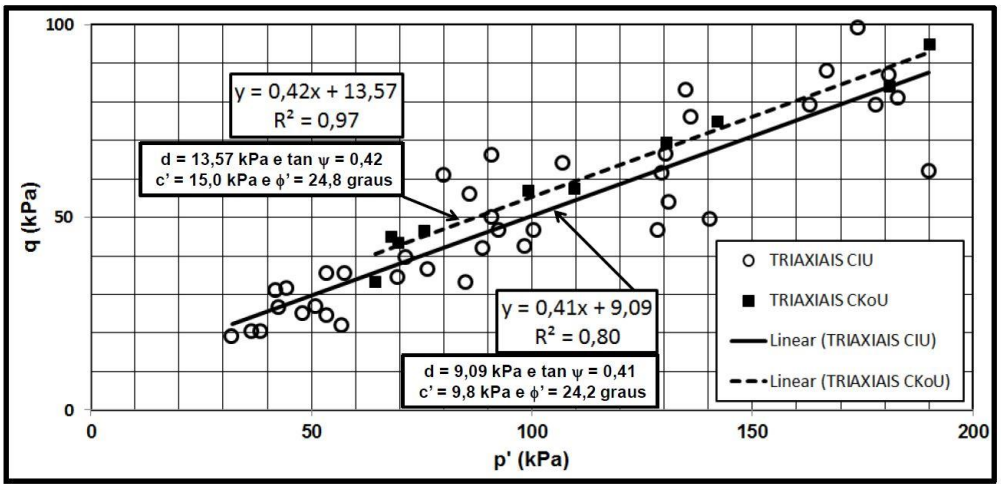

Figura 25 Envoltória efetiva dos triaxiais CIU e CKoU com p' até 200 kPa

Ballina CK_oUC test

Data from Pineda et al. (2014)

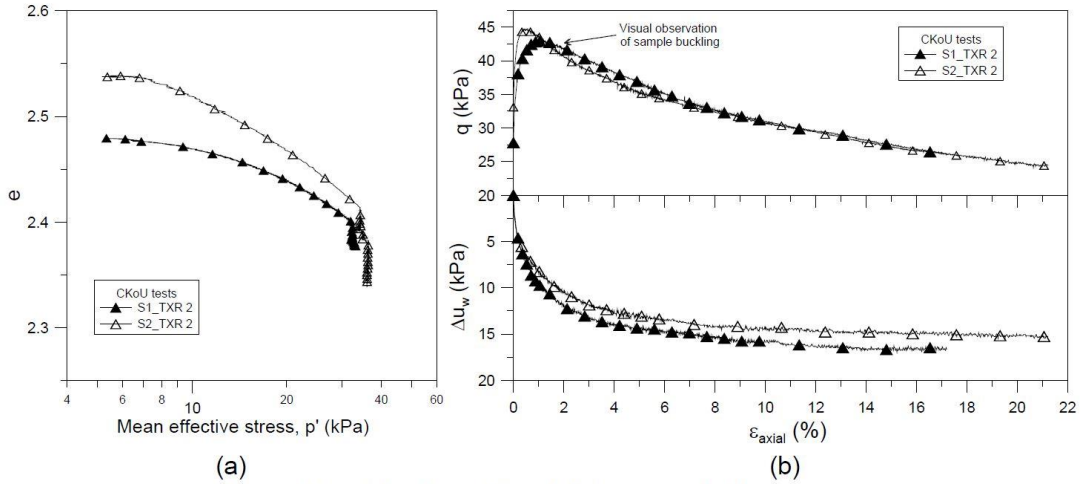

Figure 4.Triaxial tests. (a) Consolidation stage. (b) Shearing stage.

Bassendean, Australia

Data from Suzuki (2015)

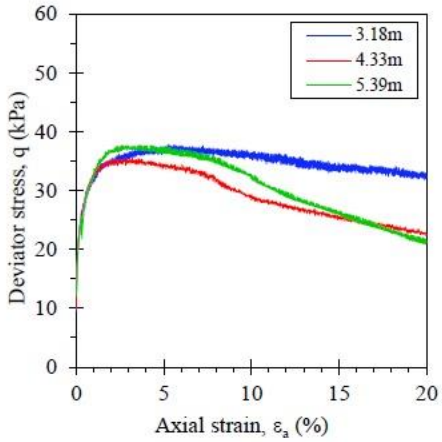

(c) deviator stress - axial strain

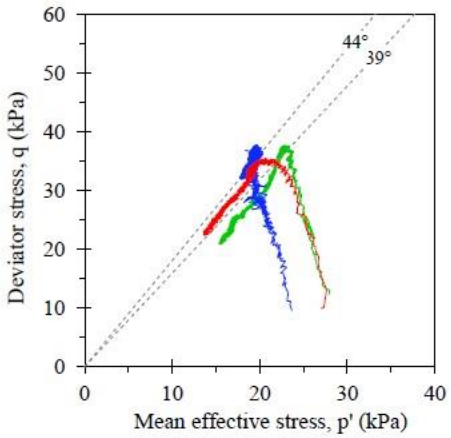

(d) deviator stress - mean effective stress

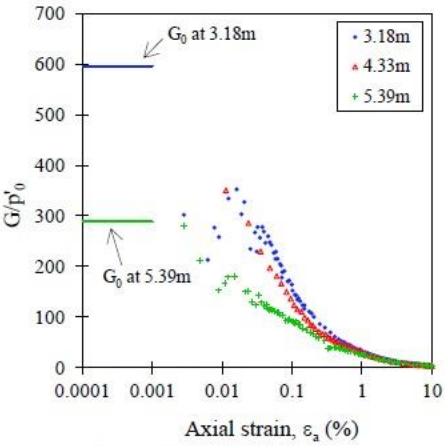

(e) shear modulus ratio - axial strain

Figure 3.16 CAU triaxial test results for the Bassendean soil: (a) photograph of 5.39m specimen, (b) photograph of 3.18m specimen, (c) q-ε_a, (d) q-p' and (e) G/p'_0-ε_a

Baton Rouge, LA

CIUC from Chen and Mayne 1994

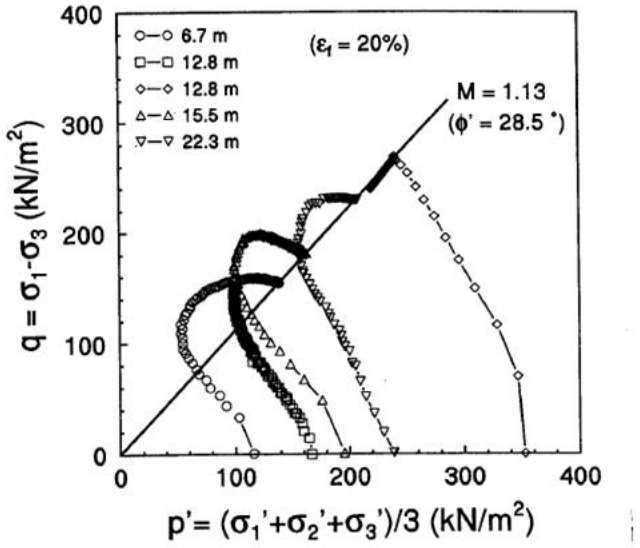

Figure 4.24. Summary Cambridge q-p' Stress Paths for Baton Rouge Site.

Baytown, TX

Triaxial test from Stuedlein et al. (2012)

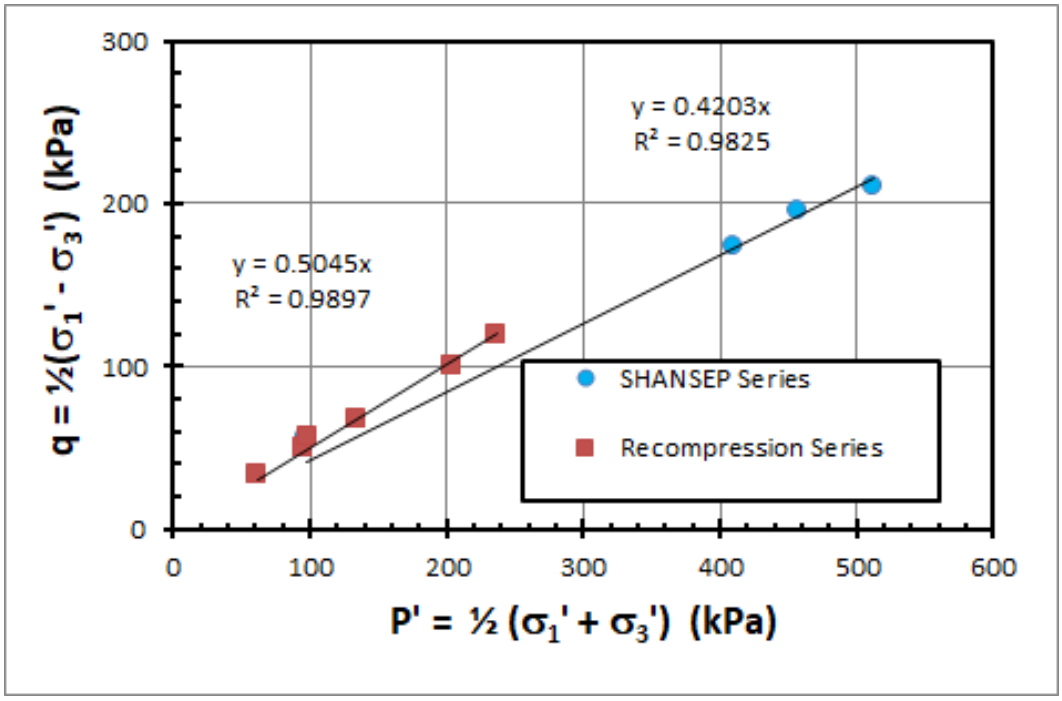

Bogota, Columbia

Data from Caicedo et al 2018

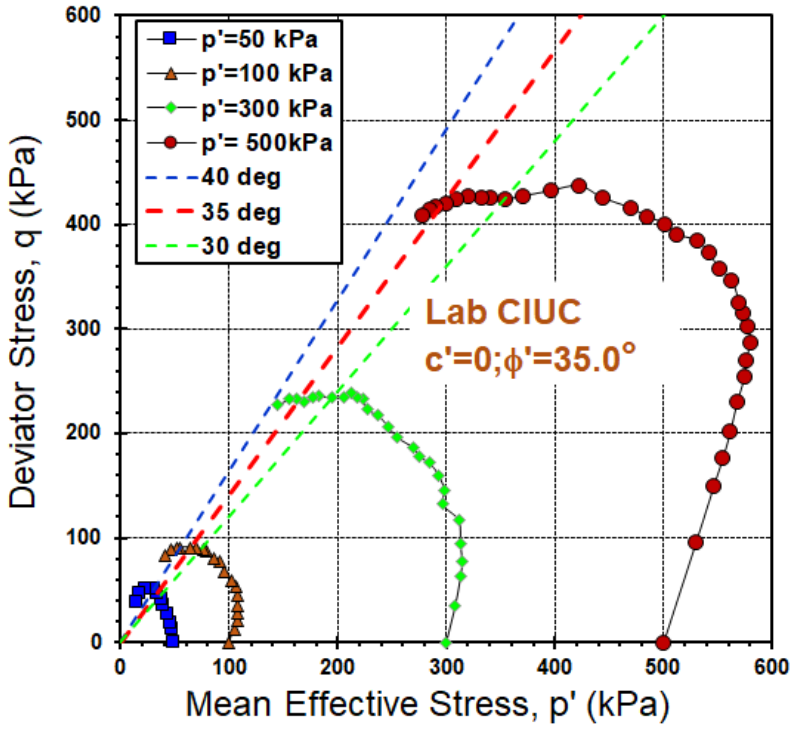

Bothkennar, Scotland

Data from Allman and Atkinson (1992)

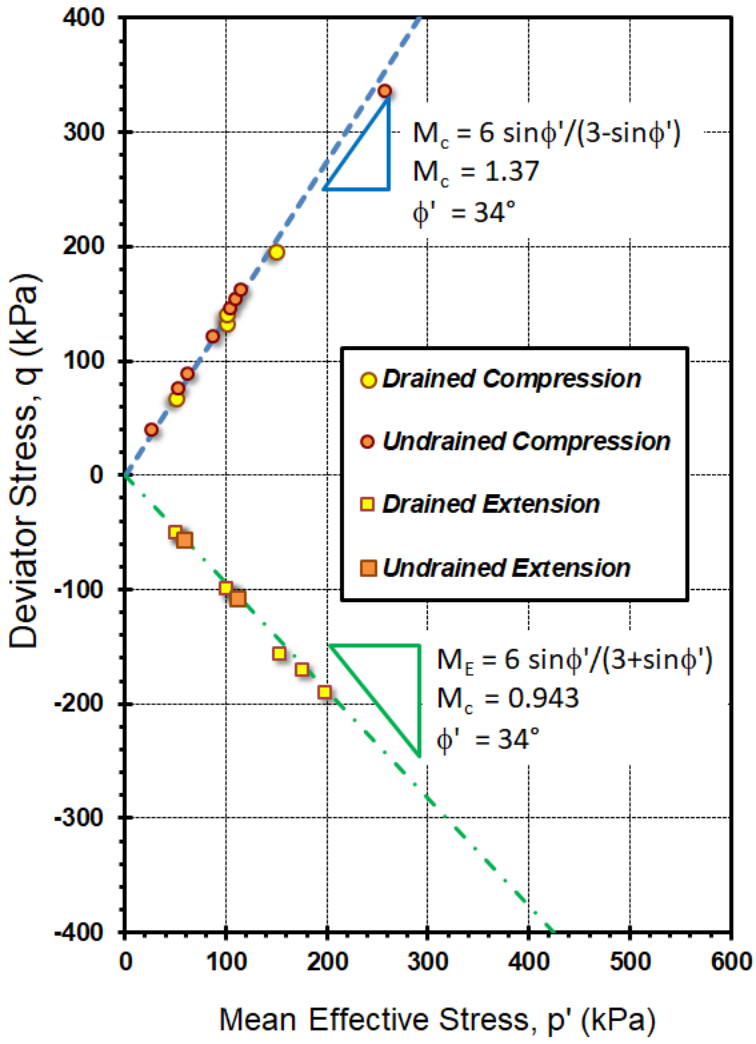

Brent Cross CAUC

Data from Hight et al 2003

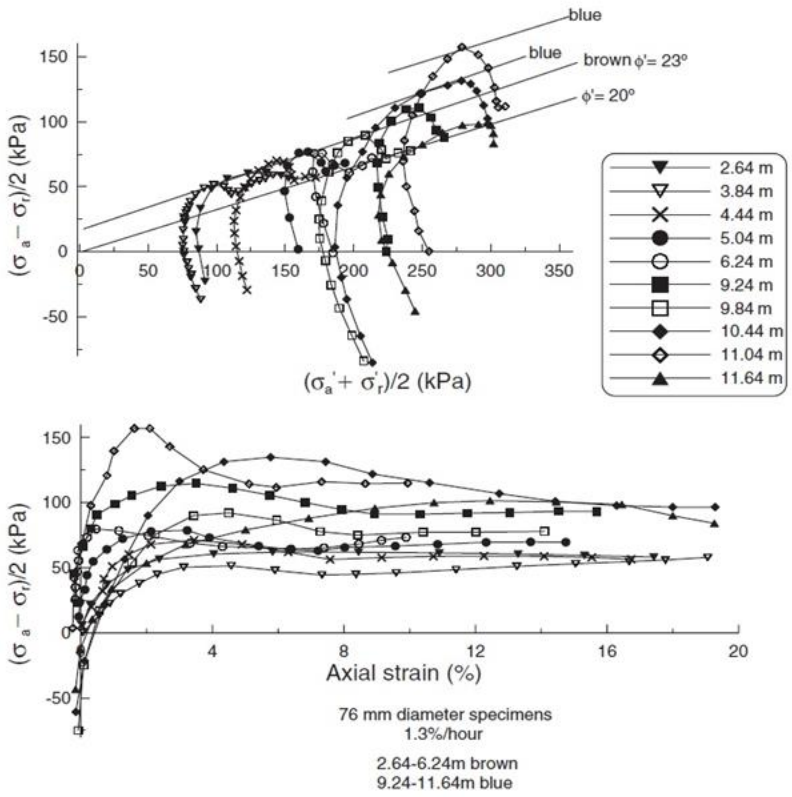

Figure 37. Results of CAU tests on tube samples from Brent Cross.

Busan, South Korea

Data from Chung et al 2012

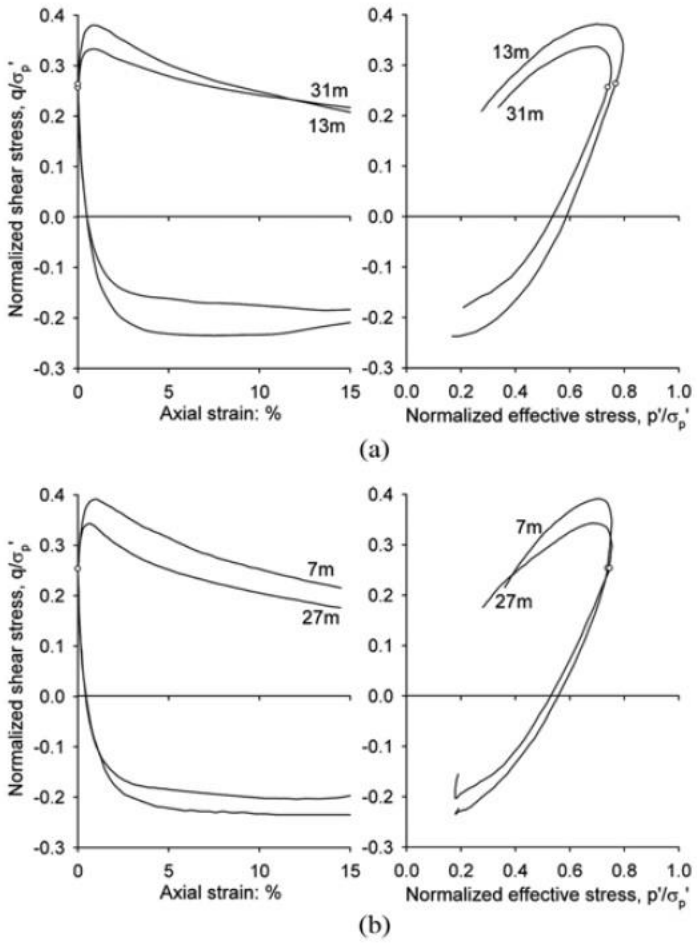

Fig. 7. Typical Normalized Shear Stress-strain Relationships an effective stress paths from CK_0CU and CK_0EU Tests: (a DIS-4, (b) DIS-5

Can Tho, Vietnam

Data from Takemura & Watabe 2006

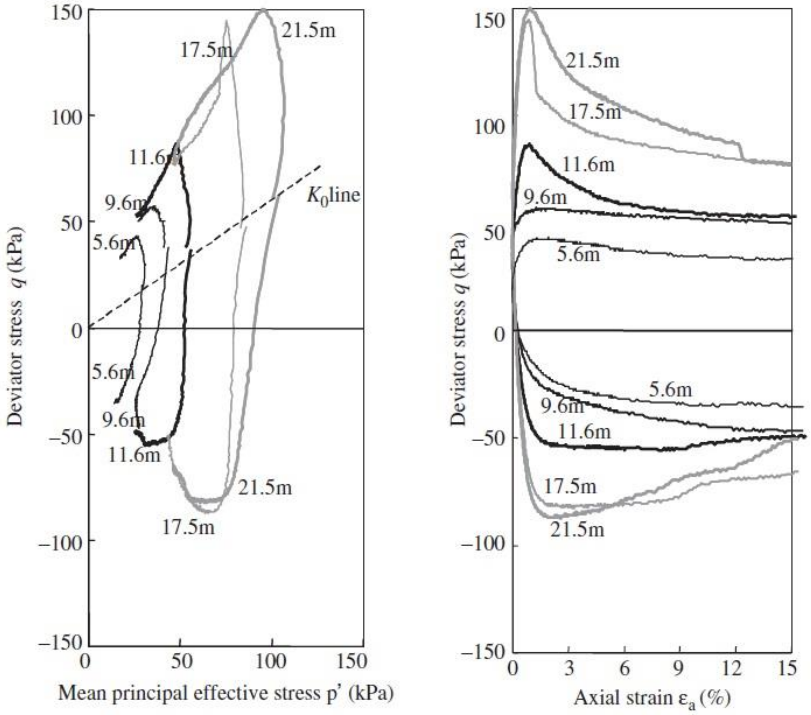

Figure 32. Results of triaxial CK_0U test for Can Tho clay: JFP samples.

CF Mining -Hardee, Florida

Data from Wissa et al. (1983) (1991)

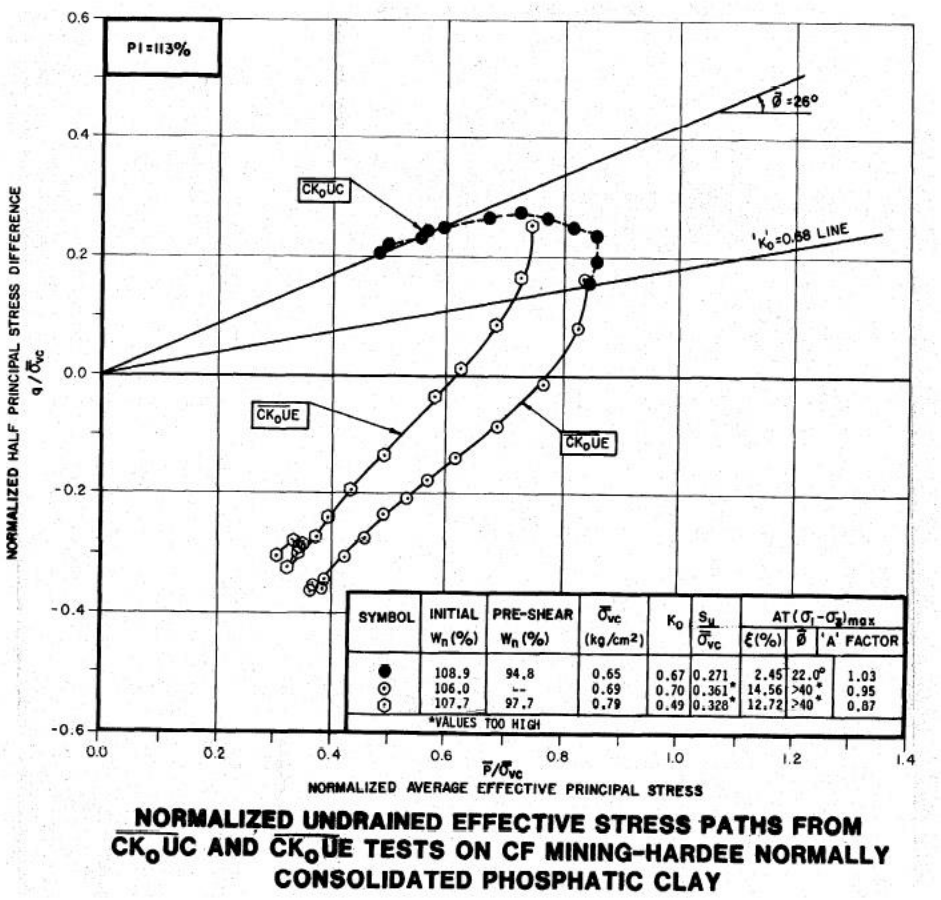

SYMBOL	INITIAL W_n(%)	PRE-SHEAR W_n(%)	$\bar{\sigma}_{vc}$ (kg/cm²)	K_o	$S_u/\bar{\sigma}_{vc}$	AT $(\sigma_1-\sigma_3)_{max}$ ε(%)	$\bar{\phi}$	'A' FACTOR
●	108.9	94.8	0.65	0.67	0.271	2.45	22.0°	1.03
⊙	106.0	--	0.69	0.70	0.361*	14.56	>40°	0.95
⊙	107.7	97.7	0.79	0.49	0.328*	12.72	>40°	0.87

*VALUES TOO HIGH

FIGURE 2-22

NORMALIZED UNDRAINED EFFECTIVE STRESS PATHS FROM $\overline{CK_oUC}$ AND $\overline{CK_oUE}$ TESTS ON CF MINING-HARDEE NORMALLY CONSOLIDATED PHOSPHATIC CLAY

Cooper River, South Carolina

Data from Mayne (2005)

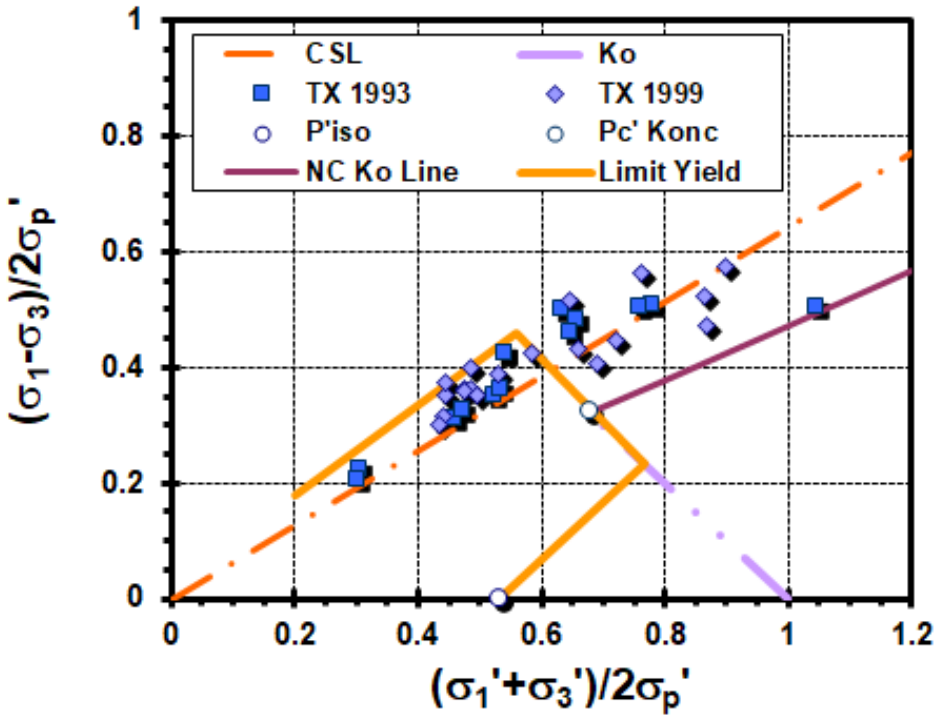

Eidsvoll, Norway

Data from Karlsru et al. (1996)

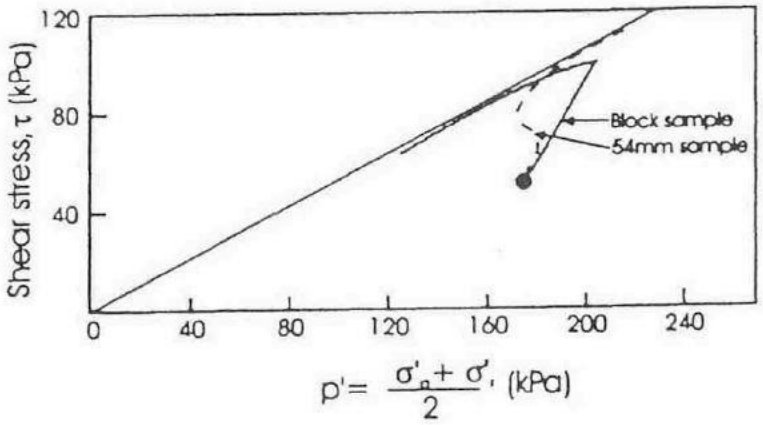

Fig. 1. Results of triaxial tests

Empire clay triaxial testing

Data from Azzouz and Baligh 1984

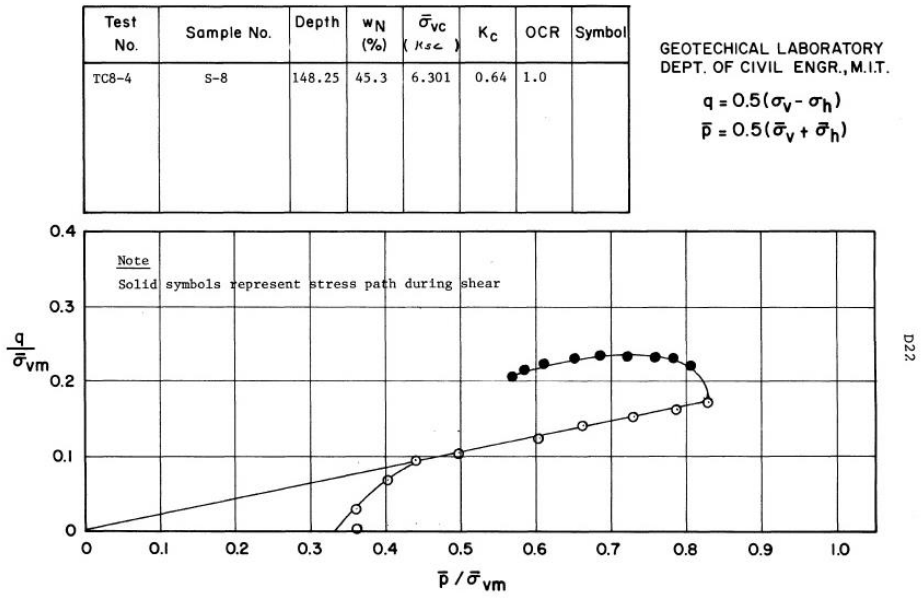

Silica flour,

Data from Silva and Bolton 2005

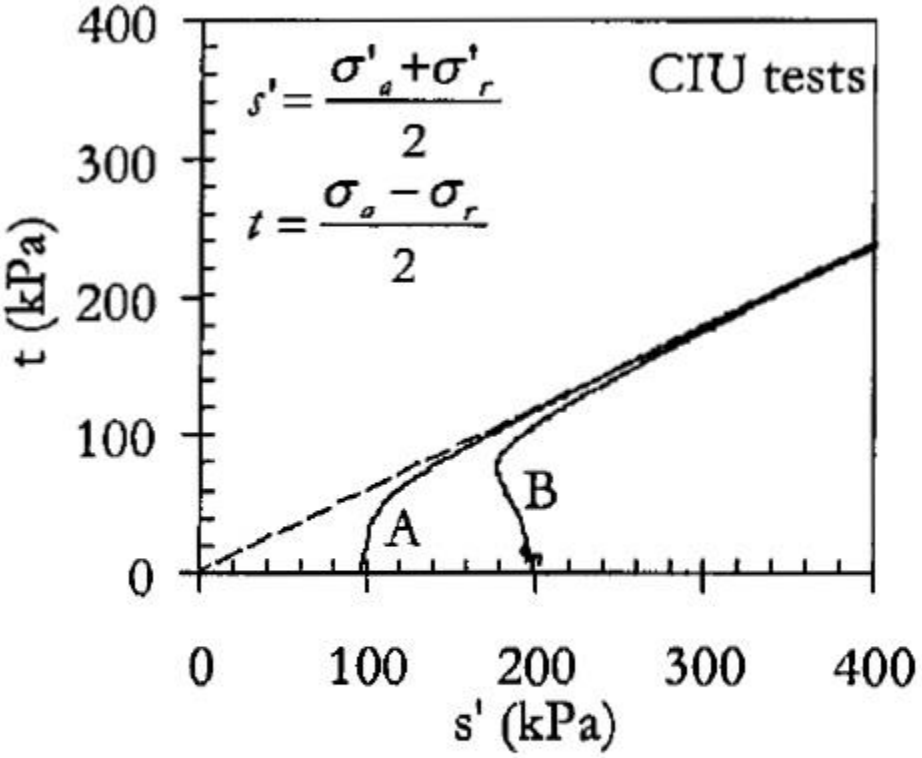

(a) Effective stress paths

Figure 2. Results of undrained compres

Gotaleden, Sweden

Data from Persson (2004)

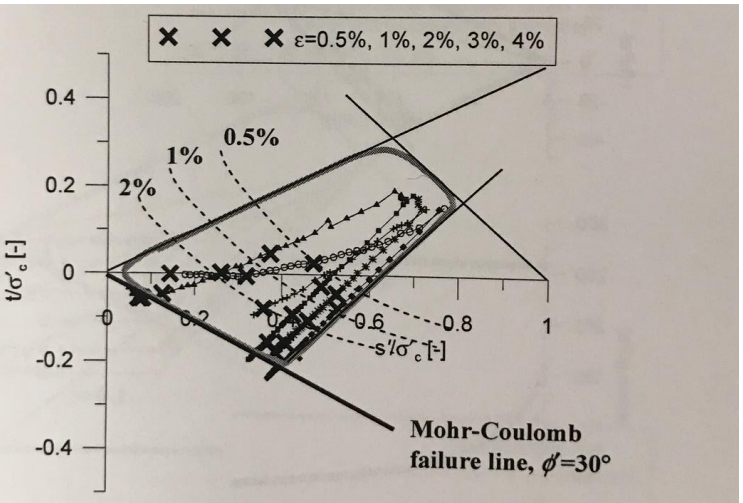

Figure 5.34 *Normalised stress paths with respect to σ'_c, for standard triaxial unloading and K_0-unloading, showing the axial strain that developed during the tests.*

Hamilton AFB, CA

Data from Bonaparte 1979

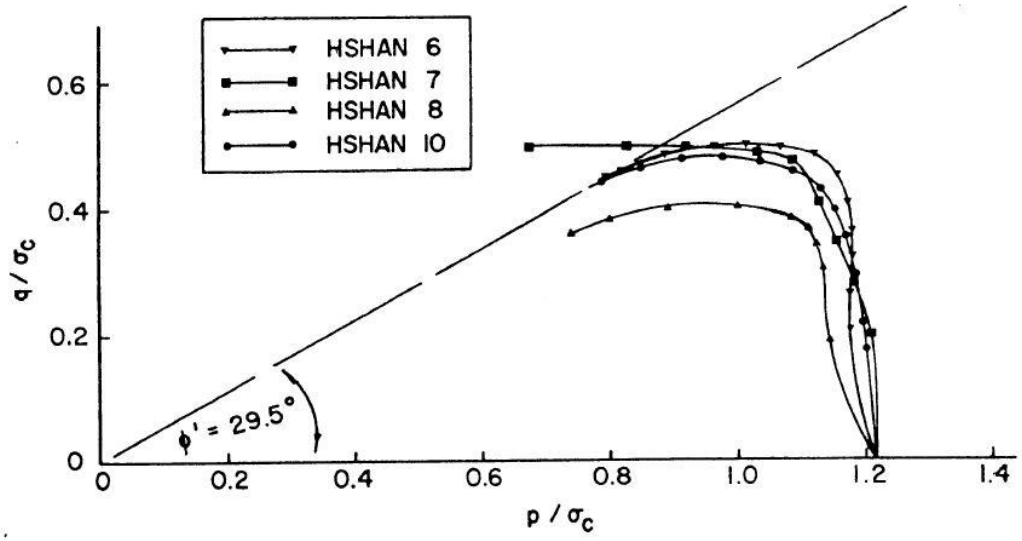

FIGURE 73 NORMALIZED EFFECTIVE STRESS PATHS FOR $\overline{AC-U}$ TESTS ON BAY MUD. TESTS PERFORMED BY DENBY (1978)

Hilleren, Norway

Data from Long et al. (2009)

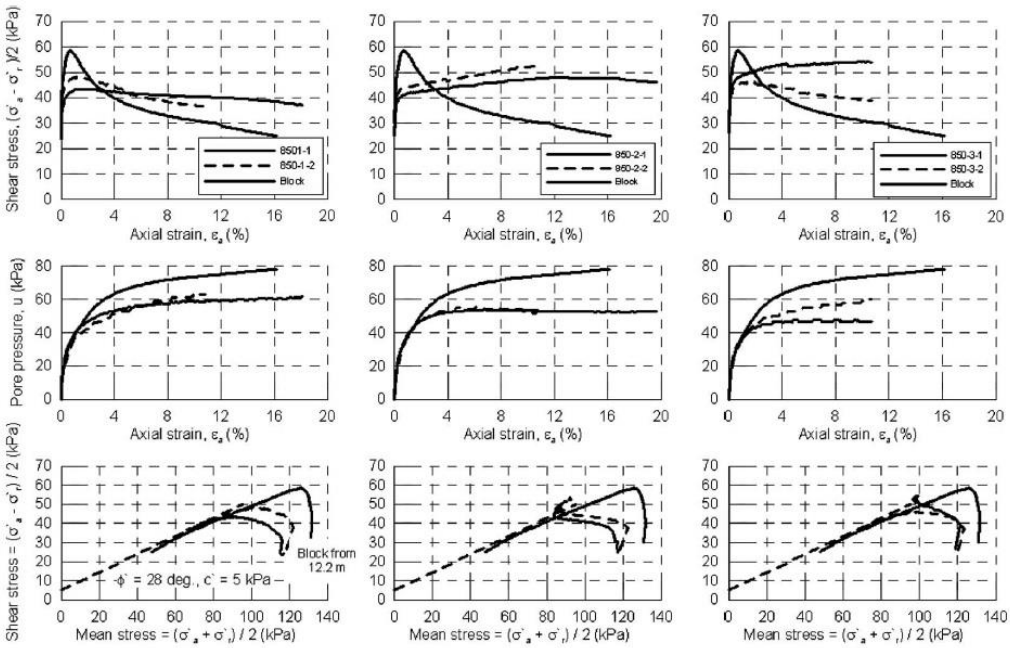

Fig. 9. CAUC triaxial tests at about 11.3 m

Islais Creek, CA

Data from Hunt et al. (2002); Pestana et al. (2002)

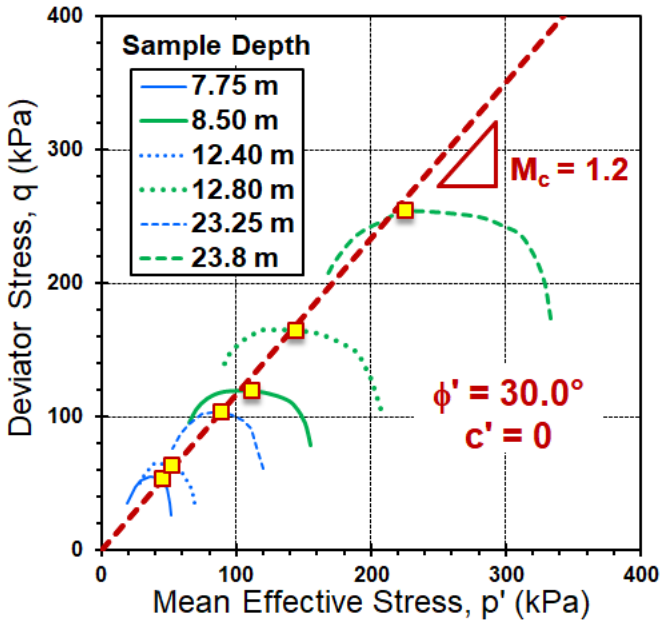

Troll, North Sea

Data from UGI (2006)

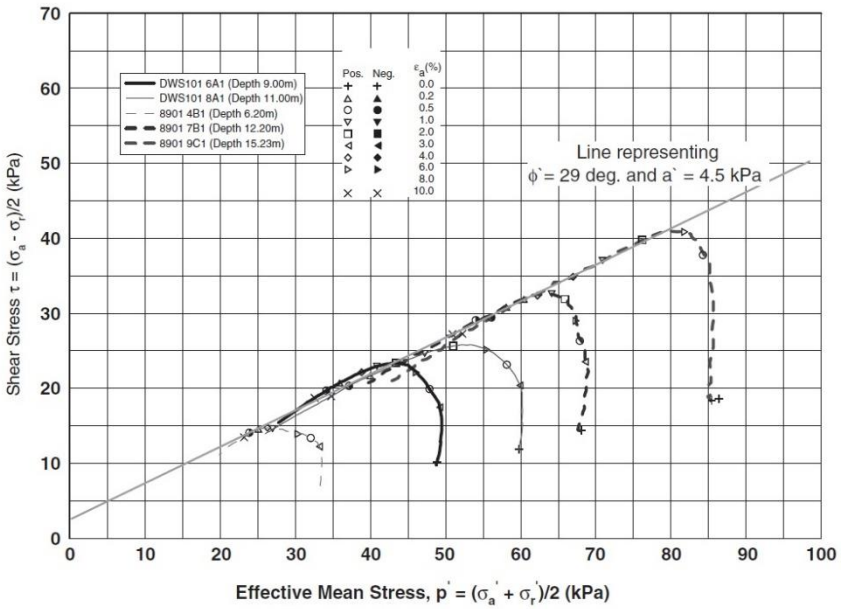

Figure 6.15. CAUC triaxial stress paths for Unit I (NGI 2006).

Luva, Norway

Data from Yang Lunne et al 2013

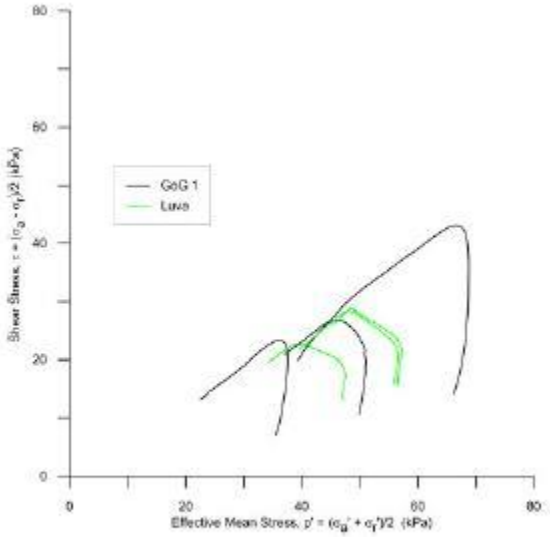

Figure 3. Typical stress path for GoG 1 clay compared with Luva clays.

Newbury, MA

Data from Landon (2007)

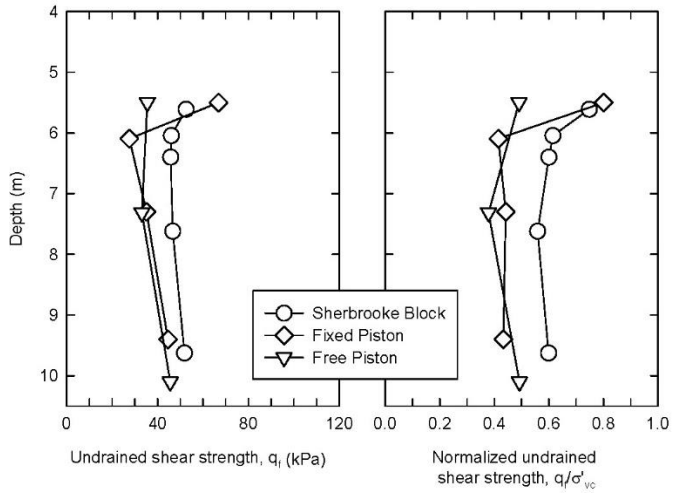

Figure 4.30: Strength profiles determined from triaxial CAUC Recompression tests on Sherbrooke block and tube samples of Newbury BBC (after Poirier 2005).

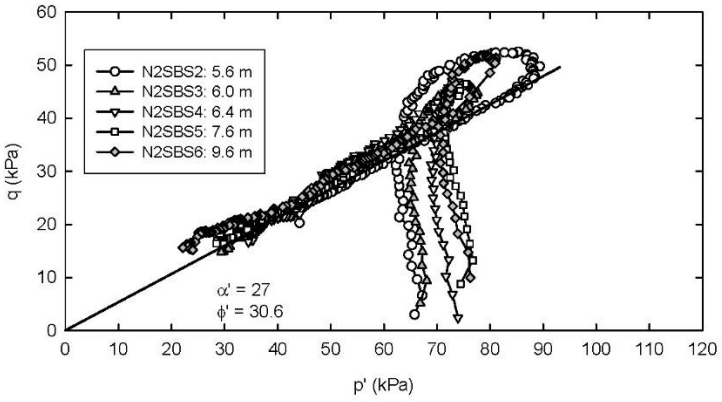

Figure 4.31: Combined Newbury BBC Sherbrooke block sample triaxial CAUC Recompression stress paths.

Norrköping, Sweden

Data from Larsson & Mulabdić (1991)

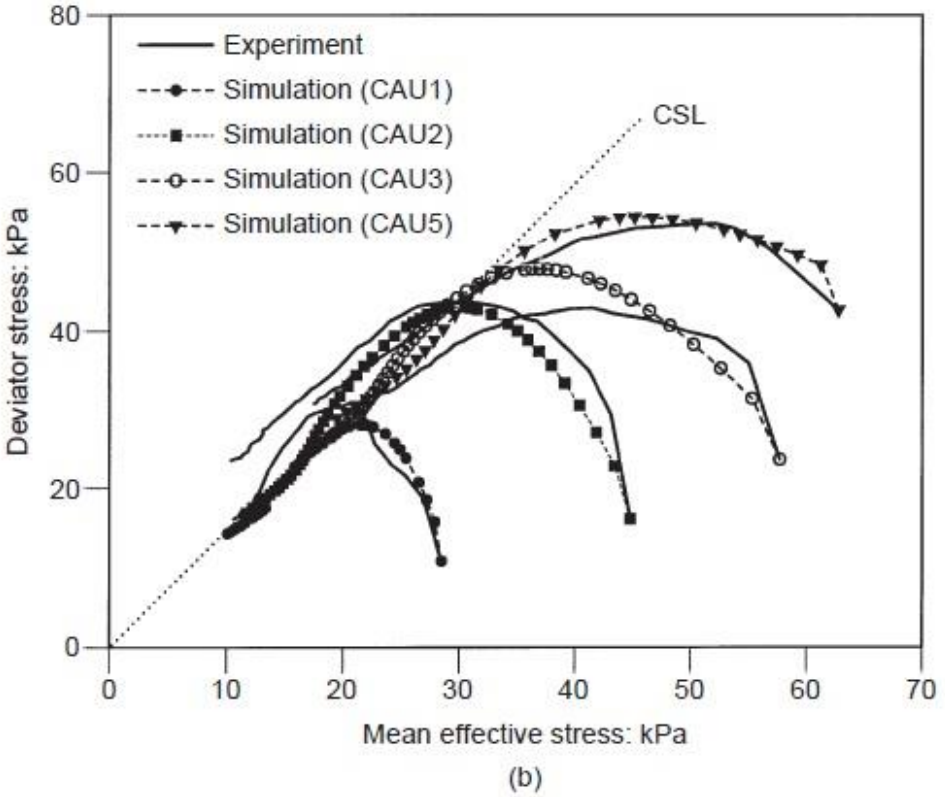

Fig. 8. Comparison of model predictions and experimental results for undrained triaxial compression tests on anisotropically consolidated clay: (a) stress–strain response; (b) effective stress paths. CSL: critical state line

North Charleston, SC

Data from S&ME

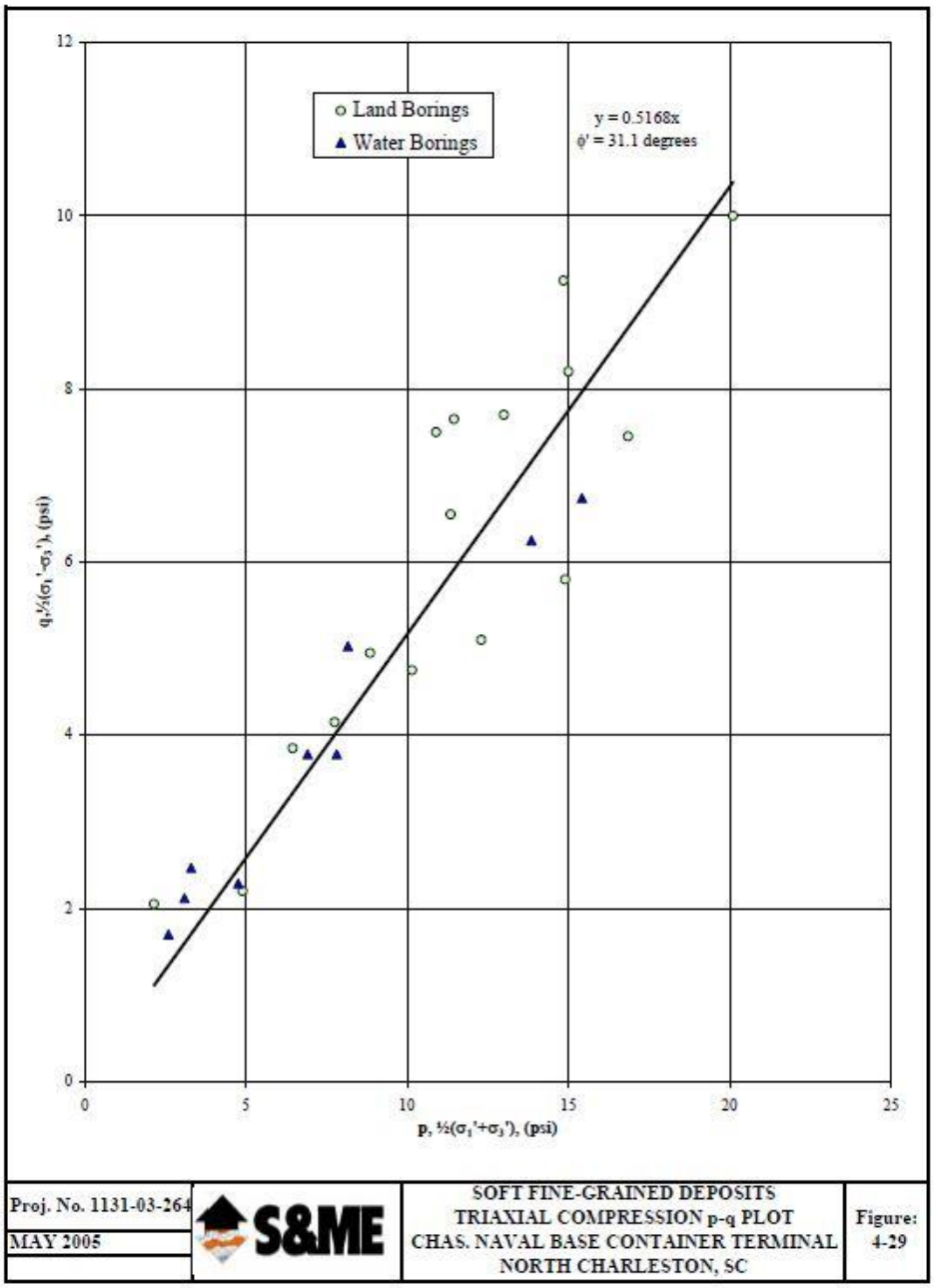

Nykirke, Norway

Data from Powell & Lunne (2006)

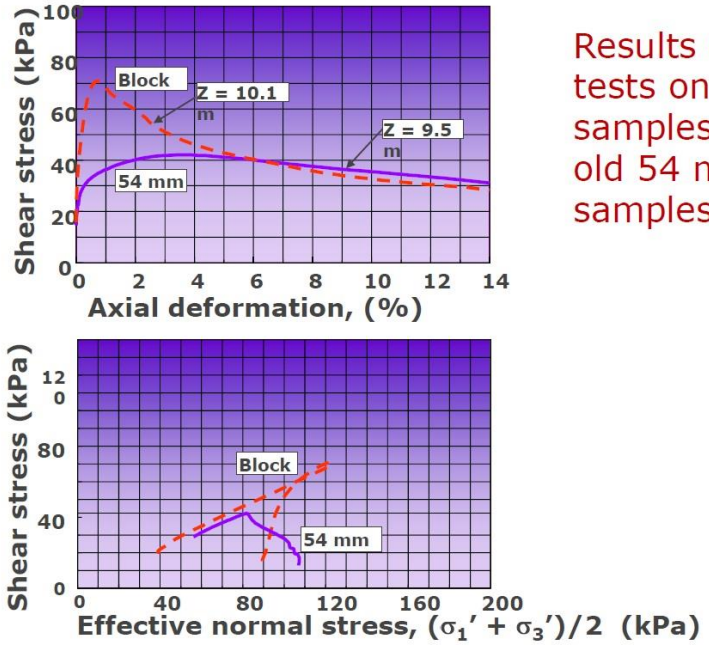

Results of CAUC triaxial tests on new block samples compared with old 54 mm piston samples

Onsoy, Norway

Data from Lunne et al. (2003)

Fig. 9. Results of CAUC and CAUE tests on Onsøy clay.

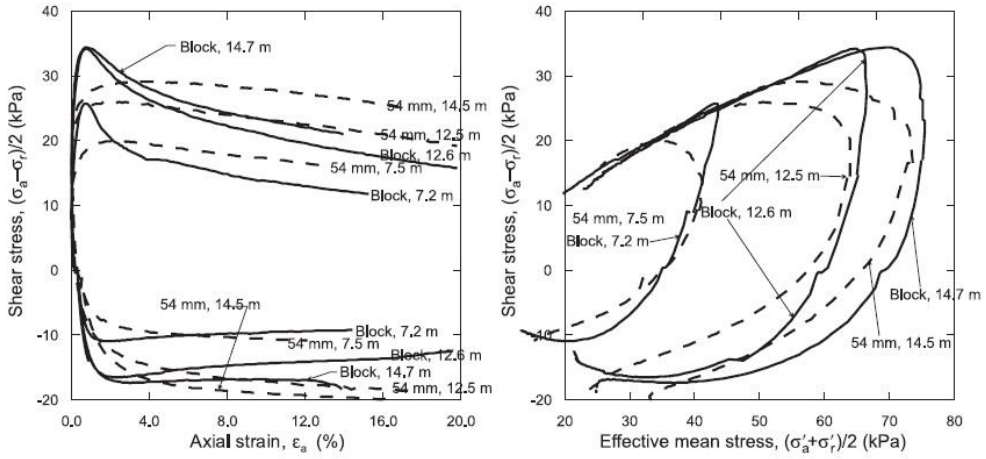

Pernio, Finland

Data from Lehtonenen 2015

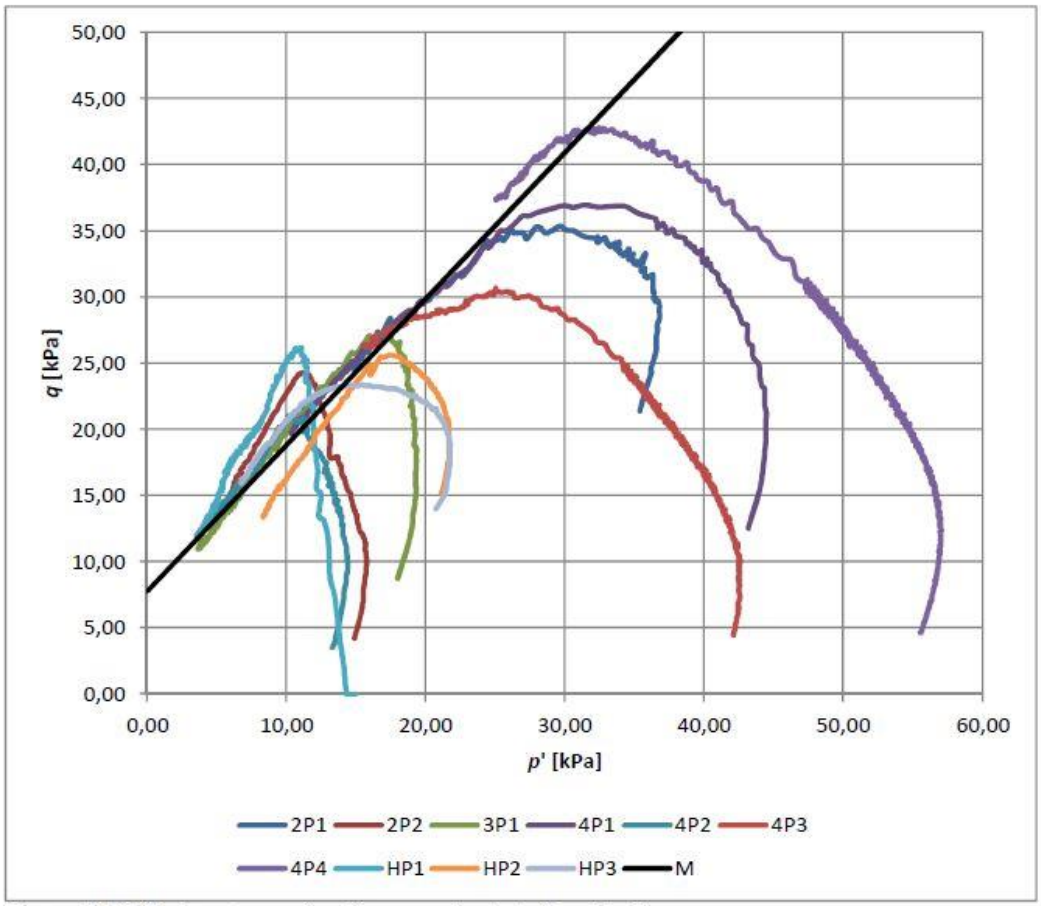

Figure 7.5. Effective stress paths of compression tests, Location B.

Figure 7.5 shows effective stress paths for tests from Location B. Additionally, the critical state M-line for M = 1.106, q_{int} = 7.76 kPa is shown. Overall, the visual fit between the assumed M-line and the tail parts of the stress paths is quite good.

Port Huron, MI

Data from Chen and Mayne (1994)

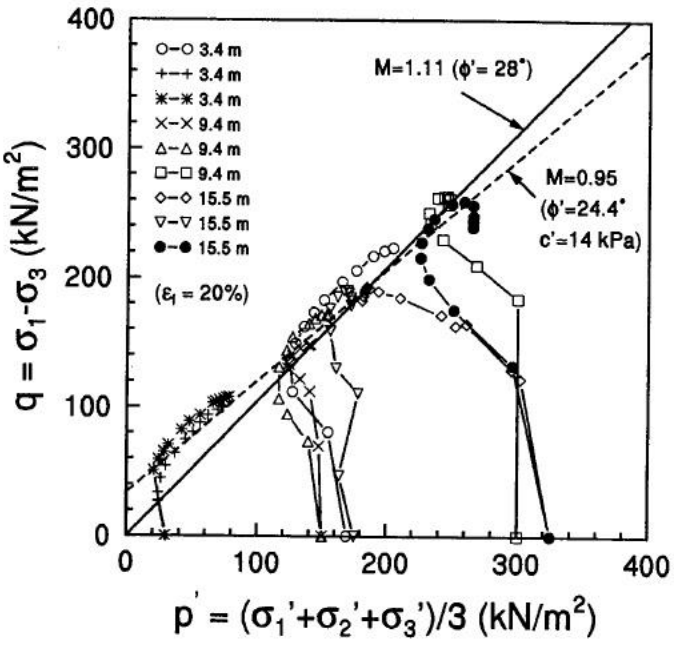

Figure 4.7. Summary Cambridge q-p' Stress Paths from Triaxial Tests on Specimens from Port Huron Site.

Queensborough Clay, UK

Data from Jardine 2003

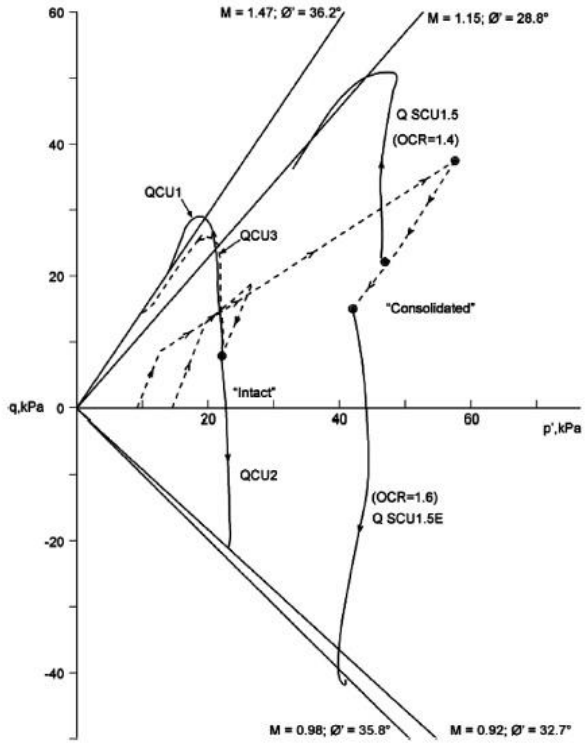

Figure 43. Effective stress paths followed in undrained extension and compression tests when sheared from (i) insitu 'intact' (ii) SHANSEP 'consolidated' conditions with OCR = 1.4 to 1.6.

Santa Cruz, Brazil

Data from Hosseinpour Almeida 2017

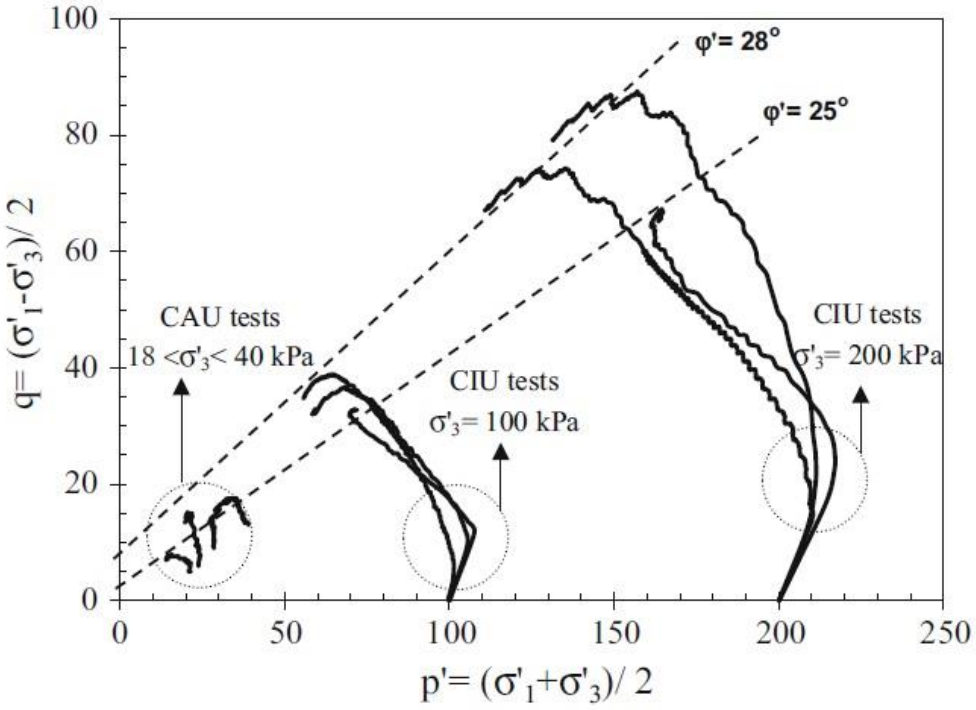

Fig. 11 Stress paths and failure envelopes of the soft clay studied

St. Hilaire, Canada

Data from Lafleur et al 1988

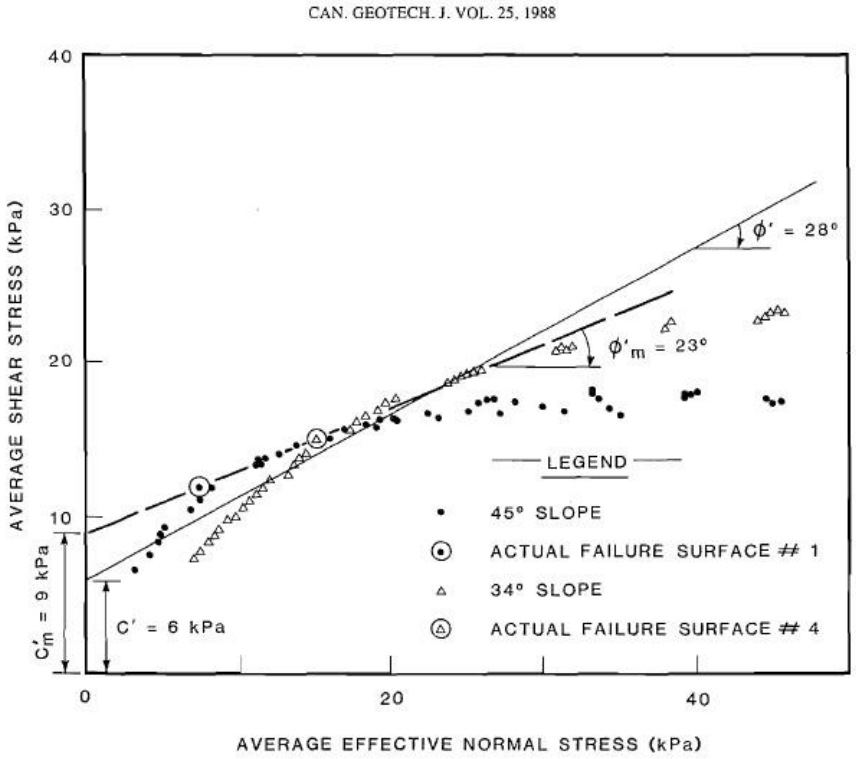

FIG. 12. Resistance envelopes—effective stress analyses.

Torpa, Sweden

Data from (Lofroth 2012)

ly than the stress paths of the piston samples. The scatter in estimated undrained shear strength between the three specimens is about the same for the piston samples and the block samples.

Looking at the tests at 8 m depth on the normally sensitive clay, there are both higher and lower values of the undrained shear strength from the tests on block samples than from the tests on piston samples. Also an equal difference of the stress paths can be noted for both the tests on block samples and the piston samples.

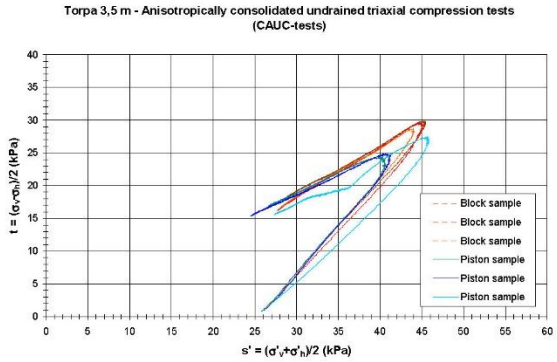

Figure 6-9: Stress paths for the CAUC triaxial tests on block samples and standard piston samples at 3.5 m depth.

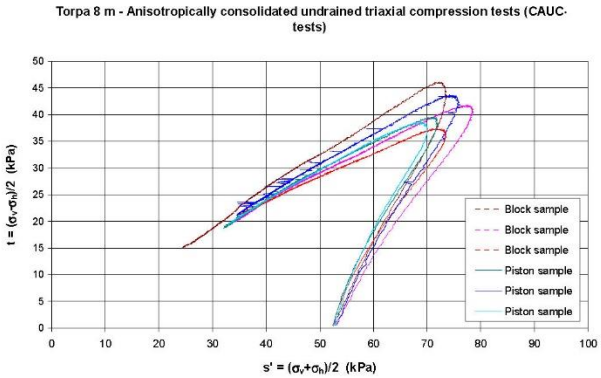

Figure 6-10: Stress paths for the CAUC triaxial tests on block samples and standard piston samples at 8 m depth.

Vassfjellet, Norway

Data from Paniagua et al (2016)

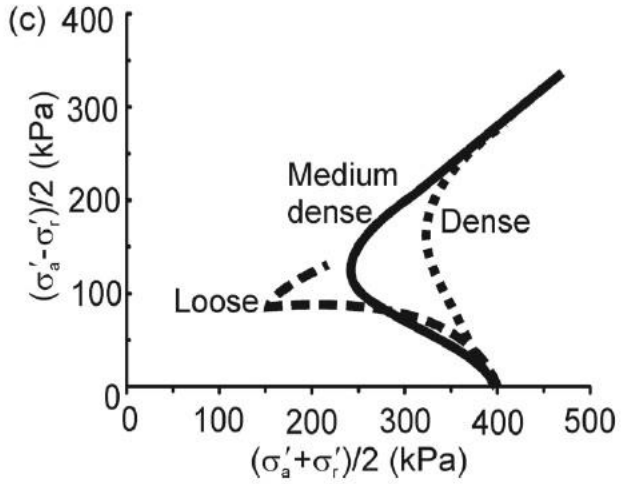

REFERENCES

Agaiby, S., Ouyang, Z., and Mayne, P.W. 2018. Helical probe tests in residual soils of the Appalachian Piedmont. *Geomechanics & Geoengineering: An International Journal*. Taylor & Francis Group, London; published online 05 Feb 2018: 1-9. https://doi.org/10.1080/17486025.2018.1434244.

Agaiby, S.S. 2018 *Advancements in the interpretation of seismic piezocone tests in clays and other geomaterials*. PhD Thesis, Civil & Environmental Engrg., Georgia Institute of Technology, Atlanta, GA: 457 p.

Agaiby, S.S. and Mayne, P.W. 2016. Use of shear wave velocity to estimate stress history and undrained shear strength of clays. *Proc. 5th Intl. Conf. on Geotechnical & Geophysical Site Characterization* (ISC-5), Jupiters - Gold Coast Australia. www.isc5.com.au

Agaiby, S.S. and Mayne, P.W. 2018. Evaluating undrained rigidity index of clays from piezocone data. *Proc. 4th Intl. Symposium on Cone Penetration Testing*, TU Delft, Taylor & Francis, CRC Press, 65-72.

Åhnberg, H. 1995. Use of CPT tests in very soft soils. *Proceedings, International Symposium on Cone Penetration Testing*, Vol. 2, (CPT'95, Linkoping), Swedish Geotechnical Institute: 619-624

Allman, M.A. and Atkinson, J.H. 1992. Mechanical properties of reconstituted Bothkennar soil. *Géotechnique* 42 (2): 289–301.

Almeida, M. and Parry, R. 1985. Small cone penetrometer tests and piezocone tests in laboratory consolidated clays. *Geotechnical Testing Journal*, Vol. 8, No. 1, ASTM: 14-24.

Almeida, M.S.S. and Marques, M.E.S. 2003. The behaviour of Sarapuí soft clay. *Characterisation & engineering properties of natural soils*, Vol. 1 (Singapore), Swets & Zeitlinger, Lisse, pp. 395–427.

Almeida, M.S.S. and Marques, M.E.S. 2013. *Design and Performance of Embankments on Very Soft Soils*. CRC Press, Leiden, the Netherlands. 228 pp.

Altaee, A., and Fellenius, B.H. 2002. *Evaluation and Analysis of Results of Static Loading Test US95 Sandpoint North and South, Sandpoint, Idaho*. Report No. 0005CS193, prepared for CH2M Hill, Boise, ID by Urkkada, Ottawa, ON: 69p.

Amoroso, S., 2011. *G-γ Decay Curves by Seismic Dilatometer (SDMT)*. Ph.D. dissertation, University of L'Aquila, L'Aquila, Italy.

Amundsen, H.A. and Thakur, V. 2017. Effects of storage on 54 mm piston samples of soft sensitive clay. *Proceedings of 19th ICSMGE*, Seoul, Korean Geotechnical Society, pp. 309–312. Available from www.issmge.org.

Amundsen, H.A., Emdal, A., Sandven, R., & Thakur, V. 2015, On engineering characterisation of a low plastic sensitive soft clay. *Proceeding GeoQuébec 2015*, Québec, Canada, Canadian Geotechnical Society: www.cgs.ca

Amundsen, H.A., Jønland, J., Emdal, A., & Thakur, V., 2017. An attempt to monitor pore pressure changes in a block sample during and after sampling. *Géotechnique Letters*, Vol. 7, No. 2, pp. 119–128, https://doi.org/10.1680/jgele.16.00176

Amundsen, H.A., Thakur, V., & Emdal, A. 2015. Comparison of two sample quality assessment methods applied to oedometer test results. *Proceeding of the Sixth International Symposium on Deformation Characteristics of Geomaterials*, Buenos Aires, Argentina, IOS Press, Amsterdam, the Netherlands, pp. 923–930.

Andersen, K.H. & Stenhamar, P. 1982. Static plate loading tests on overconsolidated clay. *Journal of the Geotechnical Engineering Division*, ASCE, 108(7): 918–934.

Andresen, A. & Kolstad, P. 1979. NGI 54 mm Samplers for undisturbed sampling of clays and representative sampling of coarser materials. *Proceeding of International Symposium of Soil Sampling*, Singapore, pp. 13–21.

Arman, A. & McManis, K.L. 1976. Effect of storage and extrusion on sample properties. soil specimen preparation for laboratory testing, ASTM STP 599, American Society for Standards & Materials International, West Conshohocken, PA, pp. 66–87.

ASTM D 3080. 2002. Standard test method for direct shear test of soils under consolidated drained conditions. *ASTM Book of Standards*. Vol. 04.08. ASTM International. West Conshohocken. PA.

ASTM D 4186. 2006, Standard test method for one-dimensional consolidation properties of saturated cohesive soils using controlled-strain loading. *ASTM Book of Standards* Vol. 04.08, ASTM International, West Conshohocken, PA, www.astm.org

ASTM D 4767-11. 2011. Standard test method for consolidated undrained triaxial compression test for cohesive soils. *ASTM Book of Standards.* Vol. 04.08, ASTM International, West Conshohocken, PA, www.astm.org. doi:10.1520/D4767-11.

ASTM D 5778. 2012. Standard test method for performing electronic friction cone and piezocone penetration testing of soils. *ASTM Book of Standards,* Vol. 04.08, American Society of Testing & Materials, West Conshohocken, PA. doi:10.1520/D5778-12.

ASTM D 6635. 2001. Standard test method for performing the flat plate dilatometer. *ASTM Book of Standards.* Vol. 04.08, ASTM International, West Conshohocken, PA: www.astm.org

Azzouz, A.S. and Baligh, M.M. 1984. Behavior of friction piles in plastic Empire clays, Vol. 2, *Report No. R84-14*. Constructed Facilities Division, Department of Civil Engineering, Massachusetts Institute of Technology. 619 pp.

Baligh, M. M., 1975. *Theory of Deep Static Cone Penetration Resistance.* Publication No. R75-56, Order No. 517, Massachusetts Institute of Technology, Cambridge, MA, 133p.

Baligh, M.M. 1984. The simple-pile approach to pile installation in clay. *Proceedings, Analysis and Design of Pile Foundations, San Francisco,* ASCE, Reston: 310-330.

Baligh, M.M. 1985. Strain path method. *Journal of Geotechnical Engineering*, 111(9), 1108-1136.

Baligh, M.M. 1986. Undrained deep penetration: pore pressures. *Geotechnique* 36 (4): 487-501.

Baligh, M.M., Azzouz, A.S., and Chin, C.-T. 1987. Disturbances due to 'Ideal' Tube Sampling. *J. Geotech. Eng.*, Vol. 113, No. 7, pp. 739–757, https://doi.org/10.1061/(ASCE)0733-9410(1987)113:7(739)

Bay, J.A., Anderson, L.R., Colocino, T.M., and Budge, A.S. 2005. Evaluation of SHANSEP parameters for soft Bonneville clays (No. UT-03.13). Utah State University, Department of Civil and Environmental Engineering: 45 pp.

Benoît, J., NeJame, L. A., Atwood, M. J., & Findlay, R. C.1990. Dilatometer lateral stress measurements in soft sensitive clays. *Transportation Research Record*, (1278). 150-155.

Berre, T., Schjetne, K., and Sollie, S., 1969. Sampling disturbance of soft marine clays. *Proceedings of the Seventh International Conference on Soil Mechanics and Foundation Engineering*, Special Session, Mexico City, Mexico, Sociedad Mexicana de Mecanica, Mexico City, Mexico, pp. 21–24.

Bihs, A., Long, M., Marchetti, D., and Ward, D. 2010. Interpretation of CPTU and SDMT in Organic, Irish Soils. *Second International Symposium on Cone Penetration Testing*, Huntington Beach, CA, Omnipress, Madison, WI, pp. 257–264.

Bishop, A.W. and Henkel, D.J. 1962. *The Measurement of Soil Properties in the Triaxial Test*. 2nd edition, Edward Arnold Publishers Ltd., London. 227 p.

Bjerrum, L. & Simons, N.E. 1960. Comparison of shear strength characteristics of normally consolidated clays. *Proceedings of the Research Conference on Shear Strength of Cohesive Soils*, (Boulder, CO), ASCE, Reston/VA: 711–726.

Bjerrum, L. 1973. Problems of soil mechanics and construction on soft clays and structurally unstable soils (collapsible, expansive and others) *Proceedings of the Eighth International Conference on Soil Mechanics and Foundation Engineering*, Moscow, USSR, Session 4, pp. 111–159.

Bonaparte, R. and Mitchell, J.K. 1979. The properties of San Francisco Bay mud at Hamilton Air Force Base, California. Report by Dept. of Civil Engineering, University of California, Berkeley, Calif. 179 pp.

Bozozuk, M. 1972. Downdrag measurements on a 160-ft floating pipe test pile in marine clay. *Canadian Geotechnical Journal*, 9(2): 127–136. doi:10.1139/t72-014.

Bozozuk, M., 1971. Effect of sampling, size, and storage on test results for marine clay. sampling of soil and rock, ASTM STP 483, ASTM International, West Conshohocken, PA, pp. 121–131, https://doi.org/10. 1520/STP26663S

Bruzzi, D., and Battaglio, M. 1987. Pore pressure measurements during cone penetration tests. *Report No. 229*, I quaderni dell'ISMES, Experimental Institute for Models and Structures, Milan, Italy, 265p.

Burland, J.B., Jamiolkowski, M., & Viggiani, C. 2003. The stabilisation of the Leaning Tower of Pisa. *Soils and Foundations*, 43(5), 63-80.

Burns, S.E. and Mayne, P.W. 2002. Analytical cavity expansion-critical state model for piezocone dissipation in fine-grained soils. *Soils & Foundations* 42 (2): 131-137.

Camp, W.M. 2004. Drilled and driven foundation behavior in a calcareous clay. *GeoSupport 2004: Drilled Shafts, Micropiling, Deep Mixing*, (GSP 124, Proceedings, GeoCongress, Orlando), ASCE, Reston, VA, pp. 1–18.

Camp, W.M., Brown, D.A., and Mayne, P.W. 2002a. Construction method effects on axial drilled shaft performance. *Deep Foundations 2002*, Vol. 2, GSP No. 116, ASCE, Reston, VA, pp. 193–208. doi:10.1061/40601(256)14.

Camp, W.M., Mayne, P.W., and Brown, D.A. 2002b. Drilled shaft axial design values in calcareous clay. *Deep Foundations 2002*, Vol. 2, GSP 116, ASCE, Reston, VA, pp. 1518–1532. doi:10.1061/40601(256)108.

Campanella, R.G. and Robertson, P.K. (1988). Current status of the piezocone test. *Penetration Testing 1988*, Vol. 1 (Proc. ISOPT-1, Orlando), Balkema, Rotterdam: 93-116.

Campanella, R.G., Robertson, P.K., and Gillespie, D. 1986. Factors affecting the pore water pressures and its measurement around a penetrating cone. *Proceedings of the 39th Canadian Geotechnical Conference*, Ottawa, Ontario: pp. 291–299.

Cao, L. F. 1997. *Interpretation of in-situ tests in clay with particular reference to reclaimed sites*. PhD thesis. Nanyang Technological University, Singapore. 356 pages.

Cao, L.F. 2003. Soil investigation in land reclamation. *Proceedings of the 1st World Forum of Chinese Scholars in Geotechnical Engineering*, (Geo-WCS 200), Shanghai, China, pp. 334–360.

Cargill, P.E. (2015). Personal Communication. ConeTec Investigations Inc. of Richmond, Virginia. www.conetec.com

Carroll, R., Long, M., & Ward, D. (2012). Use of CPTU and SDMT to characterize silty soil. *Geotechnical and Geophysical Site Characterization 4*, (ISC-4, Pernambuco), CRC Press-Taylor & Francis Group, London: 241-249.

Casagrande, A., 1932. The structure of clay and its importance in foundation engineering. *J. Boston Soc. Civ. Eng*., Vol. 19, No. 4, pp. 168–209.

Casey, B., 2014, *The consolidation and strength behavior of mechanically compressed fine-grained sediments*. Ph.D. thesis, Massachusetts Institute of Technology, Cambridge, MA. 259 pages.

Cavallaro, A., Ferraro, A., Grasso, S., and Maugeri, M., 2013. Site Response Analysis in the STM-M6 Industrial Area of the City of Catania (Italy). *Seventh International Conference on Case Histories in Geotechnical Engineering*, Chicago, IL, Missouri University of Science and Technology, Rolla, MO.

Ceccato, F., Beuth, L., Vermeer, P. A., & Simonini, P. 2016. Two-phase material point method applied to the study of cone penetration. *Computers and Geotechnics*, *80*, 440-452.

Chai, J. and Carter, J. P., 2009. Simulation of the Progressive Failure of an Embankment on Soft Soil," *Comput. Geotech*., Vol. 36, No. 6, pp. 1024–1038, https://doi.org/10.1016/j. compgeo.2009.03.010

Chandler, R. J. 1988. The in-situ measurement of the undrained shear strength of clays using the field vane. *Vane Shear Strength Testing In Soils: Field and Laboratory Studies, STP 1014*, American Society for Testing and Materials, West Conshohocken, PA: 13-44.

Charles, J. E. and Barnhill, S. A., 1987. *Report of Geotechnical Exploration, Group F, Route 17 Roadway Improvements Chesapeake, Virginia, Law Engineering Project NK7-1580,* Norfolk, VA.

Chen, B.S.-Y., and Mayne, P.W. 1994. Profiling the overconsolidation ratio of clays by piezocone tests. Report GIT-CEE-GEO-94-1, submitted to National Science Foundation, Civil & Environmental Engineering, Georgia Institute of Technology, Atlanta, GA: 280 pp. Download from: http://geosystems.ce.gatech.edu

Chew, V.C. 1993. Underfoot: a geologic guide to the Appalachian Trail. second edition, *Proc. Appalachian Trail Conference*, Harpers Ferry, West Virginia, 237 p.

Choo, H., Lee, W., Hong, S.-J., and Lee, C. 2016. Application of the Dilatometer Test for Estimating Undrained Shear Strength of Busan New Port Clay. *Ocean Eng.*, Vol. 115, pp. 39–47, https://doi.org/10.1016/j.oceaneng.2015.11.017

Chung, C.K. and Finno, R.J. 1992. Influence of depositional processes on the geotechnical parameters of Chicago glacial clays. *Engineering Geology*, 32(4): 225–242. doi:10.1016/0013-7952(92)90050-9.

Chung, S.G., Hong, Y.P., Lee, J.M., and Min, S.C. 2012. Evaluation of the undrained shear strength of Busan clay. *KSCE Journal of Civil Engineering*, 16(5): 733– 741. doi:10.1007/s12205-012-1583-8.

Cinicioglu, O. 2005. *In-Situ Shear Strength by Centrifuge Modelling*. Ph.D. thesis, Civil Engineering Dept., University of Colorado at Boulder: 281p.

Cinicioglu, O., Znidarčić, D., & Ko, H. Y. 2006. A new centrifugal testing method: Descending gravity test. ASTM *Geotechnical Testing Journal*, 29(5): 355-364

Cinicioglu, O., Znidarcic, D., & Ko, H.Y. 2007. New structure-based model for estimating undrained shear strength. *Journal of Geotechnical & Geoenvironmental Engrg*, 133(10), 1290-1301.

Clayton, C. R. I., Matthews, M. C., and Simons, N. E., 1995, *Site Investigation, 2nd Edition*, Blackwell Science, Oxford, United Kingdom, 584 p. www.geotechnique.info

Clayton, C.R.I. and Siddique, A., 1999. Tube sampling, disturbance-forgotten truths, and new perspectives. *Proc. Inst. Civil Engineers - Geotechnical Engineering* Vol. 137, No. 3, London: pp. 127–135.

Colliat, J. L., Dendani, H., Puech, A., & Nauroy, J. F. 2011. Gulf of Guinea deepwater sediments: geotechnical properties, design issues and installation experiences. *Proceedings of the 2nd International Symposium on Frontiers in Offshore Geotechnics* (ISFOG), Perth, Australia: 59-86.

Coutinho, R.Q. 2007. Characterization and engineering properties of Recife soft clays-Brazil. *Characterization and Engineering Properties of Natural Soils*. Vol. 4 (Singapore). Taylor & Francis, London: 2049-2099.

Crawford, C.B. & Campanella, R.G. 1991. Comparison of field consolidation with laboratory and in situ tests. *Canadian Geotechnical Journal* 28 (1): 103-112.

Cruz, I.R. 2009. *An evaluation of seismic flat dilatometer and lateral seismic piezocone*, MS Thesis, Dept of Civil Engineering, University of British Columbia.180 p.

Cruz, I.R. and Mayne, P.W. 2006. Interpretation of CPTU tests carried out in lacustrine Mexico City. *Clay, Site & Geomaterial Characterization (GSP 149),* Proceedings, GeoShanghai, ASCE, Reston, VA: pp. 24–31.

Dan, G., Sultan, N., and Savoye, B. 2007. The 1979 Nice Harbor catastrophe revisited: trigger mechanism inferred from Geotechnical measurements and numerical modelling. *Marine Geology*, 245(1–4): 40–64. doi: 10.1016/j.margeo.2007.06.011.

Danziger, F.A.B. 2007. In-situ testing of soft Brazilian soils. *Studia Geotechnica et Mechanica*, 29(1–2): 5–22.

DeGroot, D.J. and Landon, M.M. 2007. Laboratory testing of undisturbed soft clay samples to determine engineering design parameters. *Studia Geotechnica et Mechanica* 29, Nos. 1–2, pp. 23–37.

DeGroot, D.J., and Lutenegger, A.J. 2003. Geology and engineering properties of Connecticut Valley varved clay. *Characterisation and Engineering Properties of Natural Soils*. Vol. 1, Balkema, Rotterdam, pp. 695–724.

DeGroot, D.J., Poirier, S.E., and Landon, M.M., 2005. Sample disturbance of soft clays. *Studia Geotechnica et Mechanica* 27, Nos. 3–4, pp. 91–105.

DeJong, J.D., Jaeger, R.A., Boulanger, R.W., Randolph, M.F. & Wahl, D.A.J. 2013. Variable penetration rate cone testing for characterization of intermediate soils. *Geotechnical & Geophysical Site Characterization 4*, Vol. 1 (Proc. ISC-4, Pernambuco 2012), Taylor & Francis Group, London: 25-42.

DeJong, J.T., Jaeger, R.A., Boulanger, R.W., Randolph, M.F., and Wahl, D.A.J. 2012. Variable penetration rate cone testing for characterization of intermediate soils. *Geotechnical and Geophysical Site Characterization 4*. Vol. 1, Taylor and Francis, London: 25-42.

Demers, D. 2001. *Contribution au developement de l'usage du piezocone dans les sols argileux*. Ph.D. thesis, Universite Laval, Quebec, Canada: 435 p.

Demers, D., Leroueil, S., and d'Astous, J. 1999. Investigation of a landslide in Maskinonge, Quebec. *Canadian Geotechnical Journal*, 36(6): 1001–1014. doi: 10.1139/t99-069.

Diaz-Rodriguez, J.A., Leroueil, S., and Aleman, J.D. 1992. Yielding of Mexico City clay and other natural clays. *Journal of Geotechnical Engineering*, 118(7): 981–995. doi:10.1061/(ASCE)0733-9410(1992)118:7(981).

Dientmann, G., Schnaid, F., Maghous, S., & DeJong, J. 2017. Piezocone penetration rate effects in transient gold tailings. *Journal of Geotechnical and Geoenvironmental Engineering*, *144* (2), 04017116.

Donaghe, R.T., and Townsend, F.C. 1978. Effects of anisotropic versus isotropic consolidation in consolidated undrained triaxial compression tests of cohesive soils. ASTM *Geotechnical Testing Journal,* 1(4): 173–189. doi:10.1520/GTJ10868J.

Donohue, S. and Long, M. 2010. Assessment of sample quality in soft clay using shear wave velocity and suction measurements. *Géotechnique*, Vol. 60, No. 11, pp. 883–889, https://doi.org/10.1680/geot.8.T.007.3741

Donohue, S. and Long, M., 2009. Suction measurements as indicators of sample quality in soft clay. ASTM *Geotechnical Testing Journal* 32, No. 3, pp. 1–11, https://doi.org/10.1520/GTJ101416

Edil, T. B., and Wang, X. 2000. Shear strength and K_o of peats and organic soils. *Geotechnics of high water content materials, ASTM STP 1374*, West Conshohocken, Pa., 209–225.

El Howayek, A., Bobet, A., and Santagata, M. 2017. Geologic origin effects on mineralogy, index properties and fabric of a fine-grained carbonatic deposit. *Engineering Geology*, 216(1): 108–121. doi: 10.1016/j.enggeo.2016.11.017.

Emdal, A., Gylland, A., Amundsen, H.A., Kåsin, K., & Long, M. 2016. Mini-block sampler. *Canadian Geotechnical Journal*, 53(8), 1235-1245.

Esquivel, E.R. 1995. *Piezocone Testing: Centrifuge Modeling and Interpretation.* Ph.D. Thesis, University of Colorado at Boulder, Boulder, Colorado, USA, 260 pages.

Esquivel, E.R. and Silva, C.H. 2000. Miniature piezocone for use in centrifuge testing. *Innovations & Applications in Geotechnical Site Characterization*, GSP No. 97, ASCE, Reston/Virginia, 118-129.

Fellenius, B.H., Harris, D.E., and Anderson, D.G. 2004. Static loading test on a 45 m long pipe pile in Sandpoint, Idaho. *Canadian Geotechnical Journal*, 41(4): 613–628. doi:10.1139/t04-012.

Finnie, I. M. S., and Randolph, M. F. 1994. Punch-through and liquefaction induced failure of shallow foundations on calcareous sediments. *Proc. 17th Intl. Conf. on the Behavior of Offshore Structures*, Vol. 1, Massachusetts Institute of Technology, Boston, 217–230.

Finno, R.J. 1989. Subsurface conditions and pile installation data: Foundation Engineering Congress test section. *Predicted and Observed Axial Behavior of Piles*: (GSP 22), ASCE, Reston, VA: pp. 1–74.

Finno, R.J., and Chung, C.K. 1992. Stress-strain-strength responses of compressible Chicago glacial clays. *Journal of Geotechnical Engineering*, 118(10): 1607–1625. doi:10.1061/(ASCE)0733-9410(1992)118:10(1607).

Finno, R.J., Gassman, S.L., and Calvello, M. 2000. The NGES at Northwestern University. *National Geotechnical Experimentation Sites* (GSP 93), ASCE, Reston, VA: pp. 130–159.

Fitzgerald, M. R. 2009. Influence of drainage state on direct-push permeability profiling methods. *PhD Thesis*, College of Earth and Mineral Sciences, Pennsylvania State University, State College, PA: 140p

Frost, D. D. and Mayne, P. W. 1985. Report of Additional Geotechnical Studies, Smithsonian Museum Support Facilities, Suitland, Maryland, LETCO Project W5-4337, Washington, DC.

Garcia Martinez, M.F. 2014. *Geotechnical characterization of mixed sandy and silty soils using piezocone tests: Analysis of partial drainage phenomena and rate effects on the experimental soil response*. PhD Thesis, University of Bologna, Italy: 225 pages

Garner, M.P. 2007. Loading rate effects on axial pile capacity in clays. *Master thesis*, Department of Civil & Environmental Engineering, Brigham Young University, Provo, Utah. 122 p.

Gasparre, A., Nishimura, S., Coop, M.R., & Jardine, R.J. 2007. The influence of structure on the behaviour of London Clay. *Géotechnique, 57*(1), 19-31.

Germaine, J.T., and Germaine, A.V. 2009. *Geotechnical Laboratory Measurements for Engineers*. John Wiley & Sons, New York. 359 p.

Graham, J. and Lau, S. L. K., 1988. Influence of stress-release disturbance, storage, and reconsolidation procedures on the shear behaviour of reconstituted underwater clay. *Géotechnique* 38 (2): 279–300. https://doi.org/10.1680/geot.1988.38.2.279

Gylland, A. S., Jostad, H. P., and Nordal, S., 2014. Experimental Study of Strain Localization in Sensitive Clays. *Acta Geotech*., Vol. 9, No. 2, pp. 227–240, https://doi.org/10.1007/s11440-013-0217-8.

Gylland, A., Long, M., Emdal, A., and Sandven, R. 2013. Characterisation and engineering properties of Tiller clay. *Engineering Geology*, 164 (1) Elsevier: 86–100. doi: 10.1016/j.enggeo.2013.06.008.

Hamza, M., & Shahien, M. 2009. Effective stress shear strength parameters from piezocone. *Proc. 17th Intl. Conf. Soil Mech. and Geotechnical Engineering* (Alexandria): Vol. 5, 3451-3455. doi:10.3233/978-1-60750-031-5-3451

Hansbo, S., Jamiolkowski, M., and Kok, L. 1981. Consolidation by vertical drains. *Géotechnique,* 31(1): 45–66. doi:10.1680/geot.1981.31.1.45.

Hardison, M.A., and Landon, M. 2015. Correlation of engineering parameters of the Presumpscot Formation to the seismic cone penetration test (SCPTu), *Technical Report 15-12*, Department of Civil Engineering, University of Maine, submitted to Maine Dept. of Transportation: 393 p.

Hattab, M., Hammad, T., & Fleureau, J. M. 2015. Internal friction angle variation in a kaolin/montmorillonite clay mix and microstructural identification. *Géotechnique*, 65(1), 1-11.

Hegazy, Y.A. 1998. *Delineating geostratigraphy by cluster analysis*. PhD Thesis, Civil & Environmental Engrg., Georgia Institute of Technology, Atlanta, GA: 464 p.

Heil, H.M., Huder, J., and Amann, P. 1997. Determination of shear strength of soft lacustrine clays. *Proceedings, 14th ICSMFE (Hamburg)*, Balkema Rotterdam, Vol. 1, pp. 507–510.

Henriksson, M. and Carlsen, P., 1994. Lagringstidens inverkan på prover tagna med standardkolvprovtagare. *SGI Varia 430*, Statens Geotekniska Insitut, Linköping, Sweden, pp. 1–13.

Hight, D.W. 2001. Sampling effects in soft clay: an update on Ladd and Lambe (1963). *Proc. Symposium on Soil Behaviour and Soft Ground Construction Honoring Charles C. Ladd*, (GSP 119, Cambridge, MA), ASCE, Reston, VA, pp. 86–121.

Hight, D.W. and Jardine, R.J. 1993. Small-strain stiffness and strength characteristics of hard London tertiary clays. *Geotechnical Engineering of Hard Soils & Soft Rocks*, Balkema, Rotterdam: 533-552.

Hight, D.W. and Leroueil, S., 2003. Characterisation of soils for engineering purposes *Characterisation and Engineering Properties of Natural Soils*, Balkema, Rotterdam, Vol. 2, pp. 255–362.

Hight, D.W., Böese, R., Butcher, A.P., Clayton, C.R.I., & Smith, P.R. 1992. Disturbance of the Bothkennar clay prior to laboratory testing. *Géotechnique*, *42*(2), 199-217. https://doi.org/10.1680/geot.1992.42.2.199

Hight, D.W., McMillan, F., Powell, J.J.M., Jardine, R.J., & Allenou, C.P. 2003. Some characteristics of London clay. *Characterisation & Engineering Properties of Natural Soils*, Vol. 2 (Proc. Singapore), Swets & Zeitlinger, Lisse: 851-907.

Hight, D.W., Paul, M.A., Barras, B.F., Powell, J.J.M., Nash, D.F., Smith, P.R., Jardine, R.J. and Edwards, D.H. 2003. The characterisation of the Bothkennar clay. *Characterisation & Engineering Properties of Natural Soils*, Vol. 1 (Proc. Singapore), Swets & Zeitlinger, Lisse: 543-597.

Hird, C. and Sangtian, N. 2003. Experiments with a miniature piezocone in thinly layered soil. *Geotechnical Testing Journal*, Vol. 27, No. 1, ASTM: 1-11.

Hird, C. C., Johnson, P., and Sills, G. C. 2003. Performance of miniature piezocones in thinly layered soils. *Geotechnique*, 53(10), 885-900.

Hird, C.C. and Springman, S.M. 2006. Comparative performance of 5 cm^2 and 10 cm^2 piezocones in a lacustrine clay. *Géotechnique* 56 (6): 427-430.

Holtz, R.D., Kovacs, W.D., and Sheahan, T.C. 2010. *An Introduction to Geotechnical Engineering*, Second Edition, Prentice-Hall, Pearson, New Jersey: 864 pages.

Hosseinpour, I., Almeida, M.S.S., Riccio, M., and Baroni, M. 2017. Strength and compressibility characteristics of a soft clay subjected to ground treatment. *Geotechnical and Geological Engineering*, 35(3): 1051–1066. doi:10.1007/ s10706-017-0161-8.

Huang, A. B., Bunting, R. D., and Ahuja, A., 1990. *Fundamental Penetration Mechanisms of a Flat-Plate in Saturated* Clays, Report AFSOR-TR-90-1036, Clarkson University, Potsdam, NY, submitted to the U.S. Air Force Office of Scientific Research, Bolling AFB, Washington, DC, 249p.

Huang, A.B., Holtz, R.D., and Chameau, J.L. 1988. A calibration chamber for cohesive soils. *ASTM Geotechnical Testing Journal*, 11(1): 30-35.

Hunt, C. E. 2000. *Effect of Pile Installation on Static and Dynamic Soil Properties*. PhD dissertation, Dept. Civil and Environmental Engineering Univ. of California, Berkeley. 360p.

Hunt, C.E., Pestana, J.M., Bray, J.D., and Riemer, M. 2002. Effect of pile driving on static and dynamic properties of soft clay. *Journal of Geotechnical and Geoenvironmental Engineering*, 128(1): 13–24. doi:10.1061/(ASCE)1090-0241(2002) 128:1(13).

Hvorslev, H. J. 1960. Physical components of the shear strength of cohesive soils. *Proc. Conference on Shear Strength of Cohesive Soils*, (Boulder, Colorado), ASCE, Reston/VA: 169-273.

Hvorslev, M. J. 1949. *Subsurface Exploration and Sampling of Soils for Civil Engineering Purposes*, United States Army Waterways Experiment Station, Vicksburg, MS, 521p.

Iwasaki, K., & Kamei, T. 1994. Soil classification using the flat dilatometer in situ testing device and its reliability. Japan Society of Civil Engineers, *Journal of Geotechnical Engineering, Doboku Gakkai Ronbunshu*, 1994 (505), 239-247.

Jaeger, R. A. 2012. *Numerical and experimental study on cone penetration in sands and intermediate soils*. PhD thesis, Civil & Env. Engineering, University of California, Davis. 269 pages.

Jaeger, R.A., DeJong, J.T., Boulanger, R.W., Low, H.E., & Randolph, M.F. 2010. Variable penetration rate CPT in an intermediate soil. *Proceedings of the Second International Symposium on Cone Penetration Testing,* (CPT'10, Huntington Beach, California), Omnipress, Wisconsin. www.usucger.org

Jamiolkowski, M., & Pepe, M.C. 2001. Vertical yield stress of Pisa clay from piezocone tests. *Journal of Geotechnical and Geoenvironmental Engineering*, 127(10), 893-897.

Jamiolkowski, M., Ghionna, V.N., Lancellota, R., and Pasqualini, E. 1988. New correlations of penetration tests for design practice. *Penetration Testing 1988* (Proc. ISOPT-1, Orlando), Vol. 2, Balkema, Rotterdam: 263-296.

Jamiolkowski, M., Ladd, C.C., Germaine, J.T., and Lancellotta, R. 1985. New developments in field and laboratory testing of soils. *Proceedings of the 11th International Conference on Soil Mechanics & Foundation Engineering*, Vol. 1 (San Francisco), Balkema, Rotterdam, pp. 57–154. www.issmge.org

Janbu, N. 1963. Soil compressibility as determined by oedometer and triaxial tests, *Proceedings, European Conference on Soil Mechanics and Foundation Engineering*, Wiesbaden, Germany, Deutsche Gesellschaft für Erd-und Grundbau, Essen, Germany, pp. 19–25.

Janbu, N. and Senneset, K. 1974. Effective stress interpretation of in-situ static penetration tests. *Proceedings of the 1st European Symposium on Penetration Testing*, Vol. 2, Swedish Geotechnical Society, Stockholm: 181-193. Download available at: www.usucger.org

Jannuzzi, G.M.F., Danziger, F.A.B., & Martins, I. S. M. 2015. Geological–geotechnicalcharacterization of Sarapuí II clay. *Engineering Geology*, 190, 77-86.

Jardine, R.J., Smith, P.R., and Micholson, D.P. 2003. Properties of the soft Holocene Thames estuary clay from Queenborough, Kent. *Characterisation and Engineering Properties of Natural Soils*. Vol. 1, Balkema/Swets & Zeitlinger, Lisse, pp. 599–643.

Kallstenius, T., 1971. Secondary mechanical disturbance effects in cohesive soil samples. *Proceedings, Fourth Asian Conf. Soil Mechanics & Foundation Engineering, Special Session on Quality in Soil Sampling*, Bangkok, Thailand, International Group on Soil Sampling, Melbourne, Australia, pp. 30–39.

Kamei, T. & Iwasaki, K. 1995. Evaluation of undrained shear strength of cohesive soils using a flat dilatometer. *Soils and Foundations*, 35(2), 111-116.

Kanji, M.A. 1974. The relationship between drained friction angles and Atterberg limits of natural soils. *Géotechnique* 24 (4), 671–674, http://dx.doi.org/10.1680/geot.1974.24.4.671.

Karlsrud, K. and Hernandez-Martinez, F.G., 2013. Strength and deformation properties of norwegian clays from laboratory tests on high-quality block samples. *Canadian Geotechnical Journal* 50(12): 1273–1293, https://doi.org/10.1139/cgj-2013-0298

Karlsrud, K., Lunne, T., and Brattlien, K. 1996. Improved CPTU interpretations based on block samples. Publikasjon-Norges Geotekniske Institutt, 202, Oslo, pp. 195–201.

Karlsrud, K., Lunne, T., Kort, D.A. and Strandvik, S. 2005. CPTU correlations for clays. *Proc. 16th ICSMGE*, Vol. 2 (Osaka), Millpress, Rotterdam: 693-702.

Keaveny, J., 1985. *In-situ determination of drained and undrained soil strength using the cone penetration test*, Ph.D. Dissertation, University of California, Berkeley, 371p.

Keaveny, J.M. and Mitchell, J.K. 1986. Strength of fine-grained soils using the piezocone. *Use of In-Situ Tests in Geotechnical Engineering* (GSP 6), ASCE, Reston, VA: 668-699.

Kelly, R.B., Pineda, J.A., Bates, L., Suwal, L.P., and Fitzallen, A. 2017. Site characterization for the Ballina field testing facility. *Géotechnique*, 67(4): 279–300. doi:10.1680/jgeot.15. P.211.

Kim, D. & Tumay, M.T. 2007. Miniature piezocone penetration test results in cohesive soils. *Jordan Journal of Civil Engineering*, Vol. 1, No.1: 8-16

Kim, K. 2005. *Cone penetration test in clayey soil: rate effect and application to pile shaft resistance calculations*. PhD thesis, Civil & Environmental Engineering, Purdue University, West Lafayette, IN, USA.196pp.

Kim, K., Prezzi, M., Salgado, R. & Lee, W. 2008. Effect of penetration rate on cone penetration resistance in saturated clayey soils. *Journal of Geotechnical & Geoenvironmental Engineering ASCE* 134, No. 8: 1142–1153.

Kimball, W.P. 1936. Settlement records of the Mississippi River Bridge at New Orleans. *Proc. First International Conference on Soil Mechanics and Foundation Engineering*, Cambridge, MA, Harvard University, Cambridge, MA. www.issmge.org

Kirkpatrick, W.M. and Khan, A.J. 1984. The reaction of clays to sampling stress relief. *Géotechnique* 34 (1): 29–42, https://doi.org/10.1680/geot.1984. 34.1.29

Knappett, J. A., & Craig, R. F. 2012. *Craig's Soil Mechanics, 8th editionEdition*. London, UK: Spon Press: 570 pages. .

Konrad, J.-M. and Law, K. T. 1987. Undrained Shear Strength from Piezocone Tests. *Can. Geotech. J.*, Vol. 24, No. 3, pp. 392–405, https://doi.org/10.1139/t87-050

Koutsoftas, D.C., and Ladd, C.C. 1985. Design strengths for an offshore clay. *Journal of Geotechnical Engineering*, 111(3): 337–355. doi:10.1061/(ASCE)0733- 9410 (1985)111:3(337).

Koutsoftas, D.C., Foott, R., and Handfelt, L.D. 1987. Geotechnical investigations offshore Hong Kong. *Journal of Geotechnical Engineering*, 113(2): 87–105. doi:10.1061/(ASCE)0733-9410(1987)113:2(87).

Krage, C.P., DeJong, J.T., & Wilson, D.W. 2014. Variable penetration rate cone testing in sands with fines. *Geocharacterization and Modeling for Sustainability* (Proceedings Geo-Congress 2014, Atlanta), ASCE, Reston, VA: 170-179.

Kulhawy, F.H., and Mayne, P.W. 1990. Manual on estimating soil properties for foundation design. *EPRI Report EL-6800*, Electric Power Research Institute, Palo Alto, CA: 306 p. Available from www.epri.com.

Kurup, P., Voyiadjis, G., and Tumay, M. 1994. Calibration chamber studies of piezocone test in cohesive soils. *J. Geotechnical Engineering* 120 (1): 81-107.

L'Heureux, J. S. and Long, M. 2016. Correlations between shear wave velocity and geotechnical parameters in Norwegian clays. *Proc.17th Nordic Geotechnical Meeting (NGM 2016)*, Reykjavik, Iceland; 299-308.

L'Heureux, J.-S. and Paniagua, P., 2014. Effect of storage on sample quality-study on the 54 mm samples from Onsøy. Report NIFS - N.6.4.4, NGI, Oslo, Norway, pp. 1–20.

La Rochelle, P., Leroueil, S., and Tavenas, F. 1986. A technique for long-term storage of clay samples. *Canadian Geotechnical Journal*, Vol. 23, No. 4, pp. 602–605, https://doi.org/10.1139/t86-089

La Rochelle, P., Sarrailh, J., Roy, M., and Tavenas, F. A., 1976. Effect of storage and reconsolidation on the properties of Champlain clays. *Soil Specimen Preparation for Laboratory Testing*, ASTM STP 599, ASTM International, West Conshohocken, PA, pp. 126–146, https://doi.org/10.1520/STP39079S

La Rochelle, P., Sarrailh, J., Tavenas, F., Roy, M., and Leroueil, S. 1981. Causes of sampling disturbance and design of a new sampler for sensitive soils. *Canadian Geotechnical J.*, Vol. 18, No. 1, pp. 52–66, https://doi.org/10.1139/t81-006

Lacasse, S. & Lunne, T. 1982. Dilatometer tests in two soft marine clays. Oslo, N.G.I. Publ. No. 146: 1-8. (Also in Conference on "Updating Subsurface Sampling of Soils and Rocks and their In-Situ Testing", Engineering Foundation, Santa Barbara, California. Jan.)

Lacasse, S. and Berre, T. 1988. State-of-the-Art Paper: Triaxial testing methods for soils. *Advanced Triaxial Testing of Soil and Rock*, ASTM STP 977, R. T. Donaghe, R. C. Chaney, and M. L. Silver, Eds., ASTM International, West Conshohocken, PA, pp. 264–289, https://doi.org/10.1520/STP29081S

Lacasse, S., Berre, T., and Lefebvre, G. 1985. Block Sampling of Sensitive Clays. *Proc. 11th International Conference on Soil Mechanics and Foundation Engineering*, Vol. 1 (San Francisco), Balkema, Rotterdam, the Netherlands, pp. 887–892.

Ladanyi, B. 1967. Deep punching of sensitive clays. *Proceedings of 3rd Pan American Conference on Soil Mechanics and Foundation Engineering*, Caracas, Vol. 1: 533-546.

Ladanyi, B. and Johnston, G. H. 1974. Behavior of Circular Footings and Plate Anchors Embedded in Permafrost. *Can. Geotech. J.*, Vol. 11, No. 4, pp. 531–553, https://doi.org/10.1139/ t74-057

Ladd, C. C. 1991. Stability evaluation during staged construction. *Journal of Geotechnical Engineering*, *117*(4), 540-615.

Ladd, C.C. and Foott, R. 1974. New design procedure for stability of soft clays. *Journal of the Geotechnical Engineering Division, ASCE*, 100(7), pp. 763–786.

Ladd, C.C. and Lambe, T.W. 1963. The strength of 'undisturbed' clay determined from undrained tests. *Proc. Symposium on Laboratory Shear Testing of Soils*, Ottawa, Canada, ASTM Committee D-18, ASTM International, West Conshohocken, PA, pp. 342–371, https://doi.org/10.1520/STP30011S

Ladd, C.C., & DeGroot, D. J. 2003. Recommended practice for soft ground site characterization: Arthur Casagrande Lecture. *Proc.12th Panamerican Conference on Soil Mechanics and Geotechnical Engineering,* Vol. 1 (SARA, MIT). Verlag Glückauf, Essen: 3-57.

Lade, P.V. 2016. *Triaxial Testing of Soils*, Wiley & Sons, Ltd, Chichester, UK: 402 p.

Lafleur, J., Silvestri, V., Asselin, R., and Soulie, M. 1988. Behaviour of a test excavation in soft Champlain Sea clay. *Canadian Geotechnical Journal*, 25(4): 705–715. doi:10.1139/t88-081.

Lam, Y.C., Ganendra, D., and Prasad, K. 2016. Land reclamation & soil improvement works for a coal-fired power plant in Malaysia. *Japanese Geotechnical Society Special Publication*, 2(51): 1767–1772. doi: 10.3208/jgssp.SEA-12.

Lambe, T. W. 1964. Methods of estimating settlement. *Journal of Soil Mechanics & Foundations Division (ASCE)*, Vol. 90, Issue. 5, 43-68

Lambe, T.W. and Whitman, R.V. 1979. *Soil Mechanics, SI Version*, John Wiley & Sons, New York, 548 pages.

Lambson, M.D., Clare, D.G., Senner, D.W.F., and Semple, R.M. 1993. Investigation and interpretation of Pentre and Tilbrook Grange soil conditions. *Proceedings:*

Conference on Large Scale Pile Tests in Clay. Thomas Telford Publishing, London, pp. 134–196.

Landon, M.M. 2007. *Development of a non-destructive sample quality assessment method for soft clays*. Ph.D. dissertation, Department of Civil Engineering University of Massachusetts, Amherst. 701 p.

LaRochelle, P., Zebdi, M., Leroueil, S., Tavenas, F., and Virely, D. 1988. Piezocone tests in sensitive clays of Eastern Canada. *Penetration Testing 1988* (Proc. ISOPT-1, Orlando), Balkema, Rotterdam, Vol. 1, 831-841.

Larsson, R. 1997. Investigations and load tests in silty soils: results from a series of investigations in silty soils in Sweden. Rapport No. 54, Statens Geotekniska Institut, Linkoping. 257 pp.

Larsson, R., and Ahnberg, H. 2003. Long-term effects of excavations at crests of slopes. Report R-61, Swedish Geotechnical Institute, Linkoping. 368 pp.

Larsson, R., and Mulabdic´, M. 1991. Piezocone tests in clays. Report No. 42, Swedish Geotechnical Institute, Linkoping. 240 pp.

Larsson, R., Bergdahl, U., and Eriksson, L. 1987. Evaluation of Shear Strength in Cohesive Soils with Special Reference to Swedish Practice and Experience. *Geotech. Test. J*., Vol. 10, No. 3, pp. 105–112, https://doi.org/10.1520/GTJ10942J

Larsson, R., Westerberg, B., Albing, D., Knutsson, S., and Carlsson, E. 2007. Sulfidjord–geoteknisk klassificering och odranerad skjuvhallfasthet. [Sulphide soil—geotechnical classification and undrained shear strength.] *Report No. 69*, Swedish Geotechnical Institute, SGI, Linkoping. 135 pp. www.swedgeo.se

Lefebvre, G. and Poulin, C. 1979. A new method of sampling in sensitive clay. *Canadian Geotechnical J*., Vol. 16, No. 1, pp. 226–233, https://doi.org/10.1139/t79-019

Lefebvre, G., Leboeuf, D., Rahhal, M.E., Lacroix, A., Warde, J., and Stokoe II, K.H. 1994. Laboratory and field determinations of small-strain shear modulus for a structured Champlain clay. *Canadian Geotechnical Journal*, 31(1), 61-70.

Lehane, B.M. 2003. Vertically loaded shallow foundation on soft clayey silt. *Proceedings of the Institution of Civil Engineers - Geotechnical Engineering*, 156(1): 17–26. doi:10.1680/geng.2003.156.1.17.

Lehtonen, V.J. 2015. Modelling undrained shear strength and pore pressure based on an effective stress soil model in limit equilibrium method. *Publication 1337*. Tampereen teknillinen yliopisto. Julkaisu-Tampere University of Technology, Finland.

Leonards, G.A., & Frost, J.D. 1988. Settlement of shallow foundations on granular soils. *Journal of Geotechnical Engineering*, 114(7), 791-809.

Leroueil, S. 1992. A framework for the mechanical behavior of structured soils, from soft clays to weak rocks. *Proc.US-Brazil NSF Geotechnical Workshop on Applicability of Classical Soil Mechanics Principles to Structured Soils*, Belo Horizonte: 107–128.

Leroueil, S. and Hight, D.W. 2003. Behaviour and properties of natural soils and soft rocks. *Characterisation and Engineering Properties of Natural Soils* Workshop, Vol 1. (Singapore), Balkema, Rotterdam, the Netherlands, pp. 29–254.

Leroueil, S. and Vaughan, P.R. 1990. The general and congruent effects of structure in natural soils and weak rocks. *Géotechnique*, Vol. 40, No. 3, pp. 467–488, https://doi.org/10.1680/geot.1990.40.3.467

Leroueil, S., Demers, D., La Rochelle, P., Martel, G., and Virely, D. 1995. Practical use of the piezocone in eastern Canada clays. In CPT'95, *Proceedings of the International Symposium on Cone Penetration Testing*, Vol. 2, Swedish Geotechnical Society, Linköping, Sweden: 515-521.

Leroueil, S., Hamouche, K., Ravenasi, F., Boudali, M., Locat, J., and Virely, D. 2003. Geotechnical characterization and properties of a sensitive clay from Quebec. *Characterization and Engineering Properties of Natural* Soils, Vol. 1 (Singapore), Swets and Zeitlinger, Lisse, pp. 363–394.

Leroueil, S., Tavenas, F. A., Brucy, F., La Rochelle, P., and Roy, M., 1979. Behavior of destructured natural clays. *Journal of Geotechnical Engineering*, Vol. 105, No. 6, pp. 759–778.

Lessard, G. and Mitchell, J.K. 1985. The causes and effects of aging in quick clays. *Canadian Geotechnical J*. 22(3): 335–346, https://doi.org/10.1139/t85-046

Liu, S.Y., Shao, G.H., Du, Y.J., and Cai, G.J. 2011. Depositional and geotechnical properties of marine clays in Lianyungang, China. *Engineering Geology*, 121(1–2): 66–74. doi: 10.1016/j.enggeo.2011.04.014.

Liyanapathirana, D.S. 2016. Numerical simulation of deep penetration of a piezocone in a strain-softening clay, *International Journal of Geotechnical Engineering*, 10:2, 174-182.

Lo, K.Y., Bozozuk, M., and Law, K.T. 1976. Settlement analysis of the Gloucester test fill. *Canadian Geotechnical Journal*, 13(4): 339–354. doi:10.1139/t76-036.

Locat, A. 2012. *Rupture progressive et etalements dans les argiles sensibles*, Ph.D. dissertation, Universite Laval, Quebec. 216 p.

Locat, A., Leroueil, S., Bernander, S., Demers, D., Jostad, H.P., and Ouehb, L. 2011. Progressive failures in eastern Canadian and Scandinavian sensitive clays. *Canadian Geotechnical Journal*, 48(11): 1696–1712. doi:10.1139/t11-059.

Locat, J., Tanaka, H., Tan, T. S., Dasari, G. R., and Lee, H. 2003. Natural soils, geotechnical behavior and geological knowledge. *Characterization and Engineering Properties of Natural Soils,* Vol. 1, Swets & Zeitlinger, Lisse: pp. 3--28, (Swets &Zeitlinger, Lisse).

Löfroth, H. 2008. *Undrained shear strength in clay slopes-Influence of stress conditions. A model and field test study*. PhD dissertation, Chalmers University of Technology, Sweden.

Lofroth, H. 2012. Sampling in normal and high sensitive clay–a comparison of results from specimens taken with the SGI large-diameter sampler and the standard piston sampler. *Varia 637*, Swedish Geotechnical Institute, Linkoping. 26 pp.

Long, M. 2002. The quality of continuous soil samples. *Geotech. Test. J*., Vol. 25, No. 3, ASTM, pp. 234–253, https://doi.org/10.1520/GTJ11091J

Long, M. 2006. Use of a downhole block sampler for very soft organic soils. *Geotechnical Testing Journal* 29(5), ASTM: pp. 426–438, https://doi.org/10.1520/GTJ100201

Long, M., 2003. Sampling disturbance effects in soft laminated clays. *Proc. Inst. Civ. Eng. Geotechnical Engineering*, Vol. 156, No. 4, London: pp. 213–224, https://doi.org/10.1680/geng.2003.156.4.213

Long, M., El Hadj, N., and Hagberg, K. 2009. Quality of conventional fixed piston samples of Norwegian soft clay. *Journal of Geotechnical and Geoenvironmental Engineering*, 135(2): 185–198. doi:10.1061/(ASCE)1090-0241(2009)135: 2(185).

Long, M., Gudjonsson, G., Donohue, S., and Hagberg, K. 2010. Engineering characterization of Norwegian glaciomarine silt. *Engineering Geology*, 110(3–4): 51–65. doi: 10.1016/j.enggeo.2009.11.002.

Long, M.M. and O'Riordan, N.J. 2001. Field behavior of very soft clays at the Athlone embankments. *Géotechnique*, 51(4): 293–309. doi:10.1680/geot.2001. 51.4.293.

LoPresti, D.L., Jamiolkowski, M., and Pepe, M. 2003. Geotechnical characterization of the subsoil of Pisa Tower. *Characterisation & Engineering Properties of Natural Soils*. Vol. 2, Balkema, Rotterdam, pp. 909–946.

Low, H.E., Lunne, T., Andersen, K.H., Sjursen, M.A., Li, X. and Randolph, M.F. 2010. Estimation of intact and remoulded undrained shear strengths from penetration tests in soft clays. *Geotechnique* 60 (11): 843-859.

Low, H.E., Maynard, M.L., Randolph, M.F., and DeGroot, D.J. 2011. Geotechnical characterisation and engineering properties of Burswood clay. *Geotechnique*, 61(7): 575–591. doi:10.1680/geot.9. P.035.

Lu, Q., Randolph, M.F., Hu, Y., Bugarski, L.C. 2004. A numerical study of cone penetration in clay. *Geotechnique*; 54(4):257–267.

Lunne, T. (2010). The CPT in offshore soil investigations - a historic perspective. *Proceedings, 2nd Intl. Symp. on Cone Penetration Testing*, Vol. 1, Huntington Beach, CA; Omnipress: 71-113.

Lunne, T., and Lacasse, S. 1999. Geotechnical characteristics of low plasticity Drammen clay. *Proceedings of the International Symposium on Characterisation of Soft Marine Clays*, Yokosuka, Japan, February 1997. *Edited by* Tsuchida and Nakase. Balkema, Rotterdam. pp. 33–56.

Lunne, T., Andersen, K.H., Yang, S.L., Tjelta, T.I., and Strom, P.J. 2012. Undrained shear strength for foundation design at the Luva deep water field in the Norwegian Sea. *Geotechnical and Geophysical site Characterization 4, Vol. 1* (Proceedings, ISC-4, Pernambuco):1105-1114

Lunne, T., Berre, T., and Strandvik, S., 1997. Sample disturbance effects in soft low plastic norwegian clay. *Proc. Symposium on Recent Development in Soil and Pavement Mechanics*, Rio de Janeiro, Brazil, A. A. Balkema, Rotterdam, the Netherlands, pp. 81–102.

Lunne, T., Berre, T., Andersen, K. H., Strandvik, S., & Sjursen, M. 2006. Effects of sample disturbance and consolidation procedures on measured shear strength of soft marine Norwegian clays. *Canadian Geotechnical Journal*, 43(7), 726-750

Lunne, T., Christoffersen, H. P., and Tjelta, T. I. 1985. Engineering use of piezocone data in North Sea clays. *Proc., 11th Intl. Conf. on Soil Mechanics and Foundation Engrg*. (San Francisco), Vol. 2, A.A. Balkema, Rotterdam, The Netherlands, 907-912.

Lunne, T., Eidsmoen, T., Gillespie, D., and Howland, J.D. 1986*a*. Laboratory and field Evaluation of cone penetrometers. *Use of In-Situ Tests in Geotechnical Engineering (GSP 6)*, ASCE, Reston, VA: pp. 714–729.

Lunne, T., Eidsmoen, T., Powell, J. and Quarterman, R. 1986. Piezocone testing in overconsolidated clays. *Proceedings, 39th Canadian Geotechnical Conference: In-Situ Testing and Field Behavior*, Ottawa, 209-218.

Lunne, T., Long, M., and Forsberg, C.F. (2003). Characterization and engineering properties of Onsøy clay. *Characterisation & Engineering Properties of Natural Soils*, Vol. 1 (Singapore), Swets & Zeitlinger, Lisse: 395- 427.

Lunne, T., Long, M., and Uzielli, M. 2006. Characterisation and engineering properties of Troll clay. *Characterisation and Engineering Properties of Natural Soils II*, Singapore Vol. 3, Taylor & Francis Group, London, pp. 1939–1972.

Lunne, T., Randolph, M.F., Chung, S.F., Andersen, K.H. & Sjursen, M. 2005. Comparison of cone and t-bar factors in two onshore and one offshore clay sediments. *Frontiers in Offshore Geotechnics* (Proc. ISFOG-1, Perth), Taylor & Francis Group, London: 981-989.

Lunne, T., Robertson, P.K., and Powell, J.J.M. 1997. *Cone Penetration Testing in Geotechnical Practice*. Blackie Academic/Chapman-Hall Publishers, U.K., 312 pages.

Macedo, E.O. 2004. *Investigacao da resistencia nao drenada in situ atraves de ensaios de penetracao de cilindro,* Doctoral dissertation, *Dissertacao de mestrado,* COPPE/UFRJ, Rio de Janeiro.105 pages

Mahmoodzadeh, H. & Randolph, M.F. 2014. Penetrometer testing: effect of partial consolidation on subsequent dissipation-response. *Journal of Geotechnical & Geoenvironmental Engrg*. Vol. 140 (6), 04014022, 1-12

Marchetti, D., Marchetti, S., Monaco, P., and Totani, G. 2008. Experience with the Seismic Dilatometer (SDMT) in Various Soil Types. *Third International Conference on Site Characterization*, Taipei, Taiwan, Taylor & Francis Group, London, United Kingdom.

Marchetti, S. 1980. In-situ tests by flat dilatometer. *Journal of the Geotechnical Engineering Division* ASCE 106 (GT3): 299-321.

Marchetti, S. 2015. Some 2015 updates to the TC16 DMT report 2001. *Proc. 3rd Int. Conf. on the Flat Dilatometer DMT'15.* Rome, Italy. www.dmt15.com

Marchetti, S. and Totani, G. 1989. C_h Evaluations from DMTA Dissipation Curves. *12th International Conference on Soil Mechanics and Foundation Engineering*, Rio de Janeiro, Brazil, CRC Press, Boca Raton, FL, pp. 281–286.

Marchetti, S., Monaco, P., Calabrese, M., & Totani, G. 2006. Comparison of moduli determined by DMT and back figured from local strain measurements under a 40 m diameter circular test load in the Venice area. *Proc. 2nd Int. Conf. on the Flat Dilatometer,* Washington DC: pp. 220-230.

Marchetti, S., Monaco, P., Totani, G. & Calabrese, M. 2001. The flat dilatometer test (DMT) in soil investigations. *Proc. Intl. Conf. on In-Situ Measurement of Soil Properties and Case Histories*, Bali, Indonesia: 95-131.

Marchetti, S., Monaco, P., Totani, G., and Calabrese, M. 2006. The Flat Dilatometer Test (DMT) in Soil Investigations: A Report by the ISSMGE Committee TC16. *Second International Flat Dilatometer Conference,* Washington, DC, In-Situ Soil Testing, Fredericksburg, VA, pp. 7–48.

Masood, T., Mitchell, J.K., Lunne, T., and Hauge, E.A. 1988, In-situ testing at Hamilton Air Force Base and Bay Farm Island, CA, Joint Report NGI-UCB, University of California, Berkeley and Norwegian Geotechnical Institute, Oslo. 56 p.

May, R. E. 1987. *A study of the piezocone penetrometer in normally consolidated clay*. PhD dissertation, University of Oxford, UK.

Mayne, P. W., Kulhawy, F. H., and Trautmann, C. H. *1992 The Behavior of Drilled Shaft Foundations in Clay under Static and Cyclic Lateral Loading*, Report No. TR-100221, Electric Power Research Institute, Palo Alto, CA, 390p.

Mayne, P.W. 1980. Cam Clay predictions of undrained strength. *Journal of Geotechnical Engineering, ASCE,* Vol. 106, No. GT11: pp. 1219-1242.

Mayne, P.W. 1985. A review of undrained shear strength in direct simple shear. *Soils and Foundations*, 25 (3): 64-72.

Mayne, P.W. 1987. Determining preconsolidation stress and penetration pore pressures from DMT contact pressures. *ASTM Geotechnical Testing Journal*, 10(3): 146–150. doi:10.1520/GTJ10947J.

Mayne, P.W. 1988. Determining OCR in clays from laboratory strength. *Journal of Geotechnical Engineering* 114 (GT 1), 76-92.

Mayne, P.W. 1989. Site Characterization of Yorktown Formation for New Accelerator. *Foundation Engineering: Principles & Practices* (GSP No. 22), Vol. 1, ASCE, Reston, VA, pp. 1–15.

Mayne, P.W. 1991. Determination of OCR in clays by piezocone tests using cavity expansion and critical-state concepts. *Soils & Foundations* 31 (2), Japanese Geotechnical Society: 65-76.

Mayne, P.W. 1993. In-situ determination of clay stress history by piezocone tests, *Predictive Soil Mechanics*, (Proc. Wroth Memorial Symposium, Oxford), Thomas Telford, London: 361-373.

Mayne, P.W. 2005. Keynote: Integrated ground behavior: in-situ and lab tests. *Deformation Characteristics of Geomaterials*, Vol. 2. (Proc. IS-Lyon), Taylor and Francis Group, London: 155-177.

Mayne, P.W. 2006a Interrelationships of DMT and CPT readings in soft clays. *Flat Dilatometer Testing* (Proc. 2nd Intl. Conf. on DMT, Washington D.C.): 231-236.

Mayne, P.W. 2006b. *James K. Mitchell Lecture:* Undisturbed sand strength from seismic cone tests. *Geomechanics and GeoEngineering* Vol. 1 (4), Taylor & Francis Group, London: 239-257.

Mayne, P.W. 2007a. *Synthesis 368 on Cone Penetration Test*. National Cooperative Highway Research Program (NCHRP), Transportation Research Board, National Academies Press, Washington, DC: 118 pages: www.trb.org

Mayne, P.W. 2007b. In-situ test calibrations for evaluating soil parameters. *Characterization & Engineering Properties of Natural Soils*, Vol. 3, Taylor & Francis, London: 1602-1652.

Mayne, P.W. 2007c. In-situ test calibrations for evaluating soil parameters. *Characterization & Engineering Properties of Natural Soils*, Vol. 3 (Proc. Singapore 2006), Taylor & Francis Group, London, pp. 1602–1652.

Mayne, P.W. 2008. Keynote paper: Piezocone profiling of clays for maritime site investigations. *Geotechnics in Maritime Engineering*, Vol. 1, Proc., 11th Baltic Sea Geotechnical Conference, Gdansk, Polish Committee on Geotechnics: 333-350.

Mayne, P.W. 2012. Invited keynote: Quandary in geomaterial characterization: new vs. old. *Shaking the Foundations of GeoEngineering Education* (Proc. IC-Univ. of Ireland - Galway), Taylor & Francis Group, London: 15-26.

Mayne, P.W. 2013a. Geotechnics 2013 in the Atlantic Piedmont Province. *The 16th George F. Sowers Lecture*, ASCE Georgia Geotechnical Section, Atlanta, GA

Mayne, P.W. 2013b. Updating our geotechnical curricula via a balanced approach of in-situ, laboratory, and geophysical testing of soil. *Proceedings, 61st Annual Geotechnical Conference*, Minnesota Geotechnical Society, University of Minnesota, St. Paul, pp. 65–86.

Mayne, P.W. 2014 Interpretation of geotechnical parameters from seismic piezocone tests. *Proceedings, 3rd International Symposium on Cone Penetration Testing*, (CPT'14, Las Vegas), pp. 47–73. Available from www.usucger.org

Mayne, P.W. 2016. Evaluating effective stress parameters and undrained shear strengths of soft-firm clays from CPT and DMT. *Australian Geomechanics Journal* 51 (4): 27-55.

Mayne, P.W. and Bachus, R.C. 1989. Penetration porewater pressures in clays by CPTU, DMT, and SBP. *Proc. 13th Intl. Conf. Soil Mechanics & Foundation Engrg.* (1), Rio de Janeiro: 291-294.

Mayne, P.W. and Pearce, R.A. 2005. Site characterization of Bootlegger Cove Formation clay for Port of Anchorage. *Frontiers in Offshore Geotechnics (Proc. ISFOG, Perth),* Taylor & Francis, London: 951-955.

Mayne, P.W. and Peuchen, J. 2018. Evaluation of CPTU N_{kt} cone factor for undrained strength of clays. *Proc. 4th Intl. Symposium on Cone Penetration Testing* (CPT'18, Delft), CRC Press/Balkema.

Mayne, P.W. and Stewart, H.E. 1988. Pore pressure response of K_0-consolidated clays. *Journal of Geotechnical Engineering*, Vol. 114 (11): 1340-1346.

Mayne, P.W., & Martin, G.K. 1998. Commentary on Marchetti flat dilatometer correlations in soils. *Geotechnical Testing Journal*, 21(3), 222-239.

Mayne, P.W., and Schneider, J.A. 2001. Evaluating drilled shaft response by seismic cone. *Foundations and Ground Improvement*, Geotechnical Special Publication no. 113, American Society of Civil Engineers, Reston, VA: 655-669.

Mayne, P.W., Christopher, B., Berg, R., and DeJong, J. 2002. *Subsurface Investigations - Geotechnical Site Characterization.* Publication No. FHWA-NHI-01-031, National Highway Institute, Federal Highway Administration, Washington, D.C., 301 pages.

Mayne, P.W., Coop, M.R., Springman, S., Huang, A-B., and Zornberg, J. 2009. State-of-the-Art Paper (SOA-1): Geomaterial behavior and testing. *Proc. 17th Intl. Conf. Soil Mechanics & Geotechnical Engineering*, Vol. 4 (ICSMGE, Alexandria, Egypt), Millpress/IOS Press Rotterdam: 2777-2872.

Mayne, P.W., Greig, J, & Agaiby, S. 2018. Evaluating CPTu in sensitive Haney clay using a modified SCE-CSSM solution. *Proc. GeoEdmonton 2018*, (71st Canadian Geotechnical Conference), Canadian Geotechnical Society: www.cgs.ca

Mayne, P.W., Kulhawy, F.H., and Kay, J.N. 1990. Observations on the development of porewater stresses during piezocone penetration in clays. *Canadian Geotechnical Journal*, 27(4): 418–428. doi:10.1139/t90-058.

Mayne, P.W., Paniagua, P., L'Heureux, J-S., Lindgård, A., & Emdal, A. 2019. Analytical CPTu model for sensitive clay at Tiller-Flotten site, Norway. *Proceedings of the XVII ECSMGE 2019*, Reykjavik, Iceland.

Mayne, P.W., Peuchen, J. and Baltoukas, D. 2015. Piezocone evaluation of undrained strength in soft to firm offshore clays. *Frontiers in Offshore Geotechnics III*, Vol. 2 (Proc. ISFOG, Oslo), Taylor & Francis Group, London: 1091-1096.

McConnell, A. 2015. Personal Communication. In-Situ Research Group, Brisbane, Australia.

McManus, K. and Kulhawy, F.H. 1991. A cohesive soil for large-size laboratory deposits. *Geotechnical Testing Journal*, Vol. 14, No. 1, ASTM: 26-34.

McQueen, W., Miller, B., Mayne, P.W., and Agaiby, S. 2016. Piezocone dissipation tests at the Canadian Test Site No. 1, Gloucester, Ontario. *Canadian Geotechnical Journal*, 53(5): 884–888. doi:10.1139/cgj-2015-0090.

McRostie, G.C., and Crawford, C.B. 2001. Canadian Geotechnical Research Site No. 1 at Gloucester. *Canadian Geotechnical Journal*, 38(5): 1134–1141. doi:10.1139/t01-025.

Mesri, G. & Abdel-Ghaffar, M.E.M. 1993. Cohesion intercept in effective stress-stability analysis. *Journal of Geotechnical Engineering* 119 (8): 1229-1249.

Mesri, G., Rokshar, A., & Bohar, B.F., 1975. Composition and compressibility of typical samples of Mexico City clay. *Géotechnique*, 25: 527–574.

Messerklinger, S., Kahr, G., Plotze, M., Giudici Trausch, J., Springman, S.M., and Lojander, M. 2003. Mineralogical and mechanical behaviour of soft Finnish and Swiss clays. *Proceedings of the International Workshop on Geotechnics of Soft Soils—Theory and Practice*, Noordwijkerhout, the Netherlands, pp. 17–19.

Mitchell, J.K., & Soga, K. 2005. *Fundamentals of Soil Behavior*, Third Edition, John Wiley & Sons, New York. 558 pages.

Nagaraj, T. S., Miura, N., Chung, S. G., and Prasad, K. N., 2003. Analysis and Assessment of Sampling Disturbance of Soft Sensitive Clays. *Géotechnique*, Vol. 53, No. 7, pp. 679–683, https://doi.org/10.1680/geot.2003.53.7.679

Nash, D.F.T., Powell, J.J.M., and Lloyd, I.M. 1992. Initial investigations of the soft clay test site at Bothkennar, UK. *Geotechnique*, 42(2): 163–181. doi:10.1680/ geot.1992.42.2.163.

Nyirenda, Z. M. 1989. Piezocone studies in lightly overconsolidated clay, *PhD thesis*, Dept. of Engineering Mechanics, Oxford University, UK.

O'Neill, M.W., and Yoon, G. 1995. Engineering properties of overconsolidated Pleistocene soils of Texas Gulf Coast. *Transportation Research Record 1479*, Transportation Res. Board, Washington, DC, 81–88.

Olson, R. E. 1976. Shearing strengths of kaolinite, illite, and montmorillonite. *Journal of Geotechnical and Geoenvironmental Engineering*, 102(GT2). 180-182

Ouyang, Z. and Mayne, P. W. 2018a. Calibration of NTH method for friction angle using centrifuge CPTUs in clays. *Proceedings 4th International Symposium on Cone Penetration Testing* (CPT'18, Delft), Taylor & Francis Group, London: www.cpt18.org

Ouyang, Z. and Mayne, P.W. 2017. Spherical cavity expansion nexus between CPTu and DMT in soft-firm clays. *Proceedings of the 19th International Conference on Soil Mechanics and Geotechnical Engineering*, Vol. 1, Korean Geotechnical Society, Seoul: 631-634. www.issmge.org

Ouyang, Z. and Mayne, P.W. 2018b. Effective friction angle of clays and silts from cone piezocone penetration tests. *Canadian Geotechnical Journal 55(9): 1230–1247:* https://doi.org/10.1139/cgj-2017-0451

Ouyang, Z. and Mayne, P.W. 2018c. Effective stress strength parameters of clays from DMT. *ASTM Geotechnical Testing Journal.* Vol. 41, No. 5: 851-867: https://doi.org/10.1520/GTJ20170379. ISSN 0149-6115.

Ouyang, Z. and Mayne, P.W. 2019a. Evaluating rigidity index, OCR, and s_u from dilatometer data in soft to firm clays. *Proceedings, 16th Panamerican Conference on Soil Mechanics and Geotechnical Engineering*, Cancun. Mexican Geotechnical Society, (in review): www.issmge.org

Ouyang, Z. and Mayne, P.W. 2019c. Modified NTH method for assessing the effective friction angle of normally-consolidated and overconsolidated clays from piezocone tests. *ASCE Journal of Geotechnical and Geoenvironmental Engineering* (accepted for publication by ASCE JGGE on 03 Feb 2019: GTENG-7251R2)

Ouyang, Z., Mayne, P.W. & Sharp, J. 2016. Review of clay chamber tests using miniature cone and piezocone penetrometers, *Proc. GeoVancouver 2016*, (69th Canadian Geotechnical Conference): www.cgs.ca

Ouyang, Z., Mayne, P.W. 2017. Effective friction angle of soft to firm clays from flat dilatometer tests. *Geotechnical Engineering.* Vol. 170 (2) Proc. Institution of Civil Engineers, London: 137-147. DOI 10.1680/jgeen.16.00073.

Ozkul, Z.H., Remmes, B., and Bik, M. 2013. Piezocone profiling of a deepwater clay site in the Gulf of Guinea. *Proceedings of the Offshore Technology Conference*, Houston, Texas. Paper number: OTC24136

Paniagua-López, P., Carroll, R., Blaker, Ø., L'Heureux, J. S., & Nordal, S. 2016. Monotonic and dilatory excess porewater dissipations in silt following CPTU at variable penetration rate, *Geotechnical and Geophysical Site Characterisation*, (Proc. ISC-5, Gold Coast): australiangeomechanics.org

Perić, D., Znidarcic, D., Sture, S., and Schiffman, R. L. 1988. *Experimental and Numerical Modeling of a Strip Footing on Clay*. US Army Engineer Waterways Report, University of Colorado, Boulder. 164 pp

Persson, J. 2004. *The unloading modulus of soft soil: a field and laboratory study*. Licentiate thesis, Chalmers tekniska hogskola.

Pestana, J.M., Hunt, C.E., & Bray, J.D. 2002. Soil deformation and excess pore pressure field around a closed-ended pile. *Journal of Geotechnical and Geoenvironmental Engineering* 128(1): 1-12.

Pestana, J.M., Hunt, C.E., and Bray, J.D. 2002. Soil deformation and excess pore pressure field around a closed-ended pile. *Journal of Geotechnical and Geoenvironmental Engineering*, 128(1): 1–12. doi:10.1061/(ASCE)1090-0241(2002) 128:1(1).

Pineda, J.A., McConnell, A., and Kelly, R.B. 2014. Performance of an innovative direct-push piston sampler in soft clay. *Proceedings, 3rd International Symposium on*

Cone Penetration Testing (CPT'14, Las Vegas), pp. 279–288. Available from www.cpt14.com.

Poulsen, R., Nielsen, B.N., & Ibsen, L.B. 2013. Correlation between cone penetration rate and measured cone penetration parameters in silty soils. *Proceedings of the 18th International Conference on Soil Mechanics and Geotechnical Engineering. Paris*: pp. 603-606. www.issmge.org

Powell, J.J.M. & Quarterman, R.S.T. 1988. The interpretation of cone penetration tests in clays with particular reference to rate effects. *Penetration Testing 1988,* Vol. 2 (Proc. ISOPT, Orlando), Balkema, Rotterdam: 903 – 910.

Powell, J.J.M. and Lunne, T. 2005. A comparison of different sized piezocones in UK clays. *Proc. 16th Intl. Conf. on Soil Mechanics & Geot. Engineering*, (Osaka), Millpress/IOS Press, Amsterdam: 729-734.

Powell, J.J.M., and Lunne, T. 2005. Use of CPTU data in clays/fine grained soils. *Studia Geotechnica et Mechanica*, 27(3–4): 29–66.

Pytten, E., Flobak, T., and Ottesen, H. B., 2017. Fv. 287 Strandgata: Kjøreplass bru. Road Construction in Quick Clay. *Landslides in Sensitive Clays-from Research to Practice*, Springer, New York, NY, pp. 373–383.

Ramalho-Ortigao, A.J., Costa-Filho, L.M. 1982. Discussion: Cam Clay predictions of undrained strength. *Journal of Geotechnical Engineering, ASCE,* Vol. 108, No. GT1 pp. 181-183.

Randolph, M. F., and Hope, S. 2004. Effect of cone velocity on cone resistance and excess pore pressures. *Proc., International Symposium on Engineering Practice and Performance of Soft Deposits*, Yodogawa Kogisha, Osaka, 147–152.

Randolph, M. F., Jewell, R. J., and Stone, K. J. L. 1991. Establishing a new centrifuge facility. *Proc., Intl. Conf. on Centrifuge Modelling, Centrifuge 91*, Balkema, Rotterdam, Netherlands, 3–9.

Randolph, M.F. 2004. Characterization of soft sediments for offshore applications. *Geotechnical & Geophysical Site Characterization*, Vol. 1 (Proc. ISC-2, Porto), Millpress, Rotterdam: 209-232.

Reite, A. J., Selnes, H., and Sveian, H., 1982. A proposed deglaciation chronology for the Trondheimsfjord Area, Central Norway. *Geol. Surv. Norway Bull*., Vol. 375, pp. 75–84.

Robertson, P. K., Campanella, R. G., Gillespie, D., and Grieg, J. 1986. Use of piezometer cone data. *Use of In-Situ Tests in Geotechnical Engineering* (GSP No. 6), ASCE, Reston, VA: 1263 - 1280.

Robertson, P.K. 1990. Soil classification using the cone penetration test. *Canadian Geotechnical Journal*, 27(1): 151-158.

Robertson, P.K. 1991. Closure to: Soil classification using the CPT. *Canadian Geotechnical Journal* 28 (1): 173-178.

Robertson, P.K. 2009. Interpretation of cone penetration tests – a unified approach. *Canadian Geotechnical Journal*, Vol. 46 (11): 1337 - 1355.

Robertson, P.K. 2016. Cone penetration test (CPT)-based soil behaviour type (SBT) classification system - an update. *Canadian Geotechnical Journal*, 53(12): 1910–1927. doi:10.1139/cgj-2016-0044.

Robertson, P.K. and Campanella, R.G. 1983. Interpretation of cone penetration tests: Part I (sands), *Canadian Geotechnical Journal*, Vol. 20 (4): 718-733.

Robertson, P.K., and Cabal, K.L. 2016. Guide to cone penetration testing for geotechnical engineering. 6th Edition, *Gregg Drilling and Testing Inc*., USA,143p.

Robertson, P.K., and Wride, C.E. 1998. Evaluating cyclic liquefaction potential using the cone penetration test. *Canadian Geotechnical Journal*, 35(3): 442–459.

Robertson, P.K., Sully, J.P., Woeller, D.J., Lunne, T., Powell, J.J.M., and Gillespie, D.G. 1992. Estimating coefficient of consolidation from piezocone tests. *Canadian Geotechnical Journal*, 29(4): 539–550. doi:10.1139/t92-061.

Robinson, K.E. and Taylor, H., 1969. Selection and performance of anchors for guyed transmission towers. *Canadian Geotechnical Journal*, 6 (1), 119-137.

Roche, J. 2006. *Modeling of a soft sensitive marine silty clay deposit for a landfill expansion study*, MS Thesis, Dept of Civil Engineering, University of New Hampshire.

Rømoen, M., 2005. Evaluation of Ground Conditions and Stability of the Berg Area in Trondheim. *Project thesis*, Norwegian University of Science and Technology (NTNU), Trondheim, Norway.

Roque, R., Janbu, N., and Senneset, K., 1988. Basic Interpretation Procedures of Flat Dilatometer Tests. *Proceeding: First International Symposium on Penetration Testing*, Orlando, FL, Balkema, Rotterdam, the Netherlands, pp. 577–587.

Rossato, G., Ninis, N., and Jardine, R. 1992. Properties of some kaolin-based model clay soils. *Geotechnical Testing Journal, ASTM*, 15(2): 166–179. doi:10. 1520/GTJ10238J.

Rowe, P. W., 1972. The relevance of soil fabric to site investigation practice. *Géotechnique* Vol. 22, No. 2, pp. 195–300, https://doi.org/10.1680/geot.1972.22.2.195

Sambhandharaksa, S. 1977. *Stress-strain-strength anisotropy of varved clays*. Sc.D. dissertation, Massachusetts Institute of Technology, Cambridge, Mass.

Sandbækken, G., Berre, T., and Lacasse, S., 1986. Oedometer Testing at the Norwegian Geotechnical Institute. *Consolidation of Soils: Testing and Evaluation*, ASTM STP892, R.N. Yong and F.C. Townsend, Eds., ASTM International, West Conshohocken, PA, pp. 329–353, https://doi.org/10.1520/STP34622S

Sandroni, S., Barreto, E., and Leroueil, S. 2015. The Santana Port accident: Could it be a sensitive clay flowslide under the Equator? *Proceedings, GeoQuebec 2015*, (68th Canadian Geotechnical Conference), Canadian Geotechnical Society, Ottawa.

Sandven, R. 1990. *Strength and deformation properties obtained from piezocone tests.* PhD Thesis, Norwegian University of Science & Technology, Trondheim: 342 pages

Sandven, R. and Watn, A. 1995. Theme lecture: interpretation of test results. Soil classification and parameter evaluation from piezocone tests. *Proc. Intl. Symposium on Cone Penetration Testing*, Vol. 3, Swedish Geotechnical Society Report SGF 3:95, Linköping: 35-55.

Sandven, R., Gylland, A., Montafia, A., Kåsin, K., Pfaffhuber, A. A., & Long, M. 2015 Detection of brittle materials. Summary report with recommendations. NIFS project final report. Document code: 415559-2-RIG-RAP-004rev01, prepared by MULTICONSUL, Trondheim: 149 pages

Sandven, R., Gylland, A., Montafia, A., Kåsin, K., Pfaffhuber, A. A., & Long, M. 2016. In situ detection of sensitive clays, Part II: results. *Proceedings of the 17th Nordic Geotechnical Meeting: Challenges in Nordic Geotechnics*, Reykjavik, Iceland, pp 113–123

Sandven, R., Ørbech, T., and Lunne, T. 2004. Sample disturbance in highly sensitive clay. *Geotechnical & Geophysical Site Characterization* (*ISC-2*, A. Viana da Fonseca and P. W. Mayne, Eds., Porto, Portugal), Millpress, Rotterdam, the Netherlands, Vol. 2, pp. 1861–1868.

Santamarina, J. and Diaz-Rodriguez, J. 2003. Friction in soils: Micro and Macroscale Observations. *12th Pan American Conference on Soil Mechanics & Geotechnical Engineering*, Vol. 1, (Proc. SARA, MIT), Verlag, Essen: 633-638.

Saxena, S.K., Hedberg, J., & Ladd, C.C. 1978. Geotechnical properties of Hackensack Valley varved clays of New Jersey. *Geotechnical Testing Journal*, 1 (3), 148-161.

Schjetne, K., 1971. The measurement of pore pressure during sampling. *Fourth Asian ISSMFE, Special Session on Quality in Soil Sampling*, Bangkok, Thailand, International Society for Soil Mechanics and Geotechnical Engineering, London, United Kingdom, pp. 12–16.

Schmertmann, J. H., 1991, *DMT Digest*, No. 12, GPE, Inc., 4509 NW 23rd Avenue, Suite 19, Gainesville, FL 32601.

Schmertmann, J.H. 1986. Dilatometer to compute foundation settlement. *Use of In - Situ Tests in Geotechnical Engineering*, (Proc. In-Situ'86, Virginia Tech, Blacksburg, VA), GSP 6, ASCE, Reston, Virginia: 303-321.

Schnaid, F. 2009. *In-Situ Testing in Geomechanics: The Main Tests*. Taylor & Francis Group, London. 330 pp.

Schnaid, F., Odebrecht, E., Sosnoski, J., and Robertson, P. K. 2016 Effects of Test Procedure on Flat Dilatometer Test (DMT) Results in Intermediate Soils. *Can. Geotech. J.*, Vol. 53, No. 8, pp. 1270–1280, https://doi.org/10.1139/cgj-2015-0463

Schneider, J.A. 2008. *Analysis of piezocone data for displacement pile design*. Doctoral Dissertation, Civil & Mining Engineering, University of Western Australia: 340 pages.

Schneider, J.A., and Hotstream, J.N. 2011. *Cone Penetrometer Comparison Testing, Report No. WHRP0092-10-10,* University of Wisconsin – Madison, Dept. of Civil and Environmental Engineering. 298 p.

Schneider, J.A., Hotstream, J.N., Mayne, P.W., & Randolph, M.F. 2012. Comparing CPTU Q–F and Q–$\Delta u_2/\sigma_{v0}'$ soil classification charts. *Géotechnique Letters*, 2(4), 209-215.

Schneider, J.A., Randolph, M.F., Mayne, P.W. & Ramsey, N.R. 2008. Analysis of factors influencing soil classification using normalized piezocone tip resistance and pore pressure parameters, *J. of Geotechnical and GeoEnvironmental Engineering, ASCE*, 134(11): 1567–1586.

Schofield, A. and Wroth, P. (1968) *Critical State Soil Mechanics*. McGraw-Hill, London, 310 p. www.geotechnique.info

Schofield, A.N. 1980. Cambridge geotechnical centrifuge operations. *Geotechnique*, 30(3), 227-268.

Seed, R.B., Bea, R.G., Abdelmalak, R.I., Athanasopoulos, A.G., Boutwell, G.P., Jr., Bray, J.D., et al. 2006. Final Report: Investigation of the performance of the New Orleans Flood Protection System in Hurricane Katrina on August 29, 2005: Volume 2. Independent Levee Investigation Team: National Science Foundation under Grants No. CMS-0413327 and CMS-0611632.

Seed, R.B., Bea, R.G., Athanasopoulos-Zekkos, A., Boutwell, G.P., Bray, J.D., Cheung, C., et al. 2008. New Orleans and Hurricane Katrina. II: the central region and the lower Ninth Ward. *Journal of Geotechnical and Geoenvironmental Engineering*, 134(5): 718–739.

Sellountou, E.A., Vipulanandan, C. and O'Neill, M.W. 2004. Estimation of drained shear strength parameters of Beaumont overconsolidated clay from piezocone data. *Proc. Center for Innovative Grouting Materials and Technology* (CIGMAT), Dept. of Civil and Environmental Engineering, University of Houston.

Senneset, K. & Janbu, N. 1985. Shear strength parameters obtained from static cone penetration tests. *Strength Testing of Marine Sediments*. Special Technical Publication No. 883, ASTM, West Conshohocken, PA: 41-54.

Senneset, K., Janbu, N., and Svaniø, G. 1982. Strength and deformation parameters from cone penetration tests *Proceedings, European Symposium on Penetration Testing*, Vol. 2, Balkema, Amsterdam, 1982, pp. 863-870.

Senneset, K., Sandven, R., and Janbu, N. 1989. Evaluation of soil parameters from piezocone tests. *Transportation Research* Record 1235, National Academy Press, Washington, D.C., pp. 24–37.

SESI. 2006. Personal communication. Southern Earth Sciences Incorporated, Mobile, Ala.

Shibuya, S., Tamrakar, S. B., & Manakul, W. 2003. Geotechnical hazards in Bangkok—present and future. *Lowland Technology International*, *5*(1), 1-13.

Silva, M.F. and Bolton, M.D., 2005. Interpretation of centrifuge piezocone tests in dilatants, low plasticity silts. *Proc., Int. Conf. on Problematic Soils*. Vol. 3, Eastern Mediterra-nean University Press, Cyprus: pp. 1277-1284.

Sjursen, M.A., Low, H.E., Gue, C.S., Li, X., Lunne, T., and Randoph, M. 2006. Shear strength parameters determined by in-situ tests for deep water soft soil. Joint NGI-UWA Industry Project by Norwegian Geotechnical Institute (NGI, Oslo) and University of Western Australia (UWA, Perth). 558 p.

Skempton, A. W. and Sowa, V. A., 1963. The behaviour of saturated clays during sampling and testing. *Géotechnique*, Vol. 13, No. 4, Thomas Telford, London: pp. 269–290, https://doi.org/10.1680/geot.1963.13.4.269

Skempton, A.W. 1961. Horizontal stresses in an overconsolidated Eocene clay. *Proc. 5th ICSMGE*, Vol. 3, Paris: 351-357.

Smith, M. G. 1993. *A laboratory study of the Marchetti dilatometer*. Doctoral dissertation, University of Oxford, UK: 264p.

So, T.C. 2009. Engineering Behaviour of Hong Kong Marine Clay during Vacuum Preloading. *Ph.D. thesis*, University of Hong Kong, Pok Fu Lam, Hong Kong.

Soccodato, F.M. 2002. Geotechnical properties of Fucino clayey soil. *Characterisation & Engineering Properties of Natural Soils*. Vol. 1 (Singapore), Swets & Zeitlinger, Lisse, pp. 791–807.

Soleimanbeigi, A. 2013. Undrained shear strength of normally consolidated and overconsolidated clays from pressuremeter tests: a case study. *Geotechnical and Geological Engineering,* **31**(5): 1511–1524. doi:10.1007/s10706-013-9675-x.

Sorensen, K. K., & Okkels, N. 2013. Correlation between drained shear strength and plasticity index of undisturbed overconsolidated clays. *Proceedings of the 18th International Conference on Soil Mechanics and Geotechnical Engineering*, Paris, Vol. 1, pp. 423-428.

Springman, S., (Ed.), Laue, J. (Ed.), Seward, L. (Ed.) 2010. *Physical Modelling in Geotechnics*, (Proc. 7th IC on Physical Modeling in Geotechnics, Zurich), Two Volume Set. CRC Press/Taylor & Francis, London: 1552 p.

Springman, S., Trausch, J., Heil, H., and Heim, R. 1999. Strength of soft Swiss lacustrine clay: Cone penetration and triaxial test data. *Transportation Research Record* 1675, National Academy Press, Washington, D.C., pp. 1–9.

Stuedlein, A.W., Kramer, S.L., Arduino, P., and Holtz, R.D. 2012. Geotechnical characterization and random field modeling of desiccated clay. *Journal of Geotechnical and Geoenvironmental Engineering,* 138(11): 1301–1313. doi:10. 1061/(ASCE)GT.1943-5606.0000723.

Styler, M.A. and Mayne, P.W. 2013. Site investigation using continuous shear wave velocity measurements during cone penetration testing at Gloucester, Ontario. *GeoMontreal 2013*, 66th Canadian Geotechnical Conf., Paper 345

Su, P.C., Chen, Y.C., Sun, C.Y., and Wang, G.S. 1993. The flat dilatometer tests in clay," *Proceedings, 11th Southeast Asian Geotechnical Conference,* Singapore, pp. 205-210.

Sultan, N., Cattaneo, A., Urgeles, R., Lee, H., Locat, J., Trincardi, F., Berne, S., Canals, M., and Lafuerza, S. 2008. A geomechanical approach for the genesis of sediment undulations on the Adriatic shelf. *Geochemistry, Geophysics, Geosystems*, 9(4): 1–25. doi:10.1029/2007GC001822.

Sultan, N., Cochonat, P., Canals, M., Cattaneo, A., Dennielou, B., Haflidason, H., Laberg, J.S., Long, D., Mienert, J., Trincardi, F., and Urgeles, R. 2004. Triggering mechanisms of slope instability processes and sediment failures on continental margins: a geotechnical approach. *Marine Geology*, 213(1): 291–321. doi: 10.1016/j.margeo.2004.10.011.

Sultan, N., Voisset, M., Marsset, B., Marsset, T., Cauquil, E., and Colliat, J.L. 2007. Potential role of compressional structures in generating submarine slope failures in the Niger Delta. *Marine Geology*, 237(3): 169–190. doi:10.1016/j. margeo.2006.11.002.

Suzuki, Y. 2015. *Investigation and interpretation of cone penetration rate effects.* PhD thesis, University of Western Australia, Crawley, Australia: 323 pages

Svaan, O., 1977. The Influence of Storage on Clay (in Norwegian). *Report F.74.7*, Des. 1977, Norwegian Institute of Technology (NTH), Trondheim, Norway, 40p.

Takai, A., Inui, T., & Katsumi, T. 2016. Evaluating the hydraulic barrier performance of soil-bentonite cutoff walls using the piezocone penetration test. *Soils and Foundations*, 56(2), 277-290.

Takemura, J., Watabe, Y., and Tanaka, M. 2006. Characterization of alluvial deposits in Mekong Delta. *Characterisation and Engineering Properties of Natural Soils II*, Singapore. Vol. 3, Taylor & Francis Group, London, pp. 1805–1829.

Takesue, K., and Isano, T. 2001. Development and application of a lateral stress cone. *In Proceedings, International Conference on In-Situ Measurements of Soil Properties* and Case Histories, Bali, Indonesia, pp. 623–629.

Tanaka, H. 1995. National report - The current state of CPT in Japan. *Proceedings, International Symposium on Cone Penetration Testing* (CPT '95), Vol. 1, Swedish Geotechnical Society, Linkoping, pp. 115–124.

Tanaka, H. 2006. Geotechnical properties of Hachirogata clay. *Characterisation and Engineering Properties of Natural Soils* (Singapore), Vol. 3, Taylor & Francis Group/CRC Press, London, pp. 1831–1852.

Tanaka, H. and Tanaka, M. 1996. *A Site Investigation Method Using Cone Penetration and Dilatometer Tests*. Technical Note No. 837 of the Port and Harbor Research Institute, Yokosuka, Japan, 54p.

Tanaka, H., 2000. Sample quality of cohesive soils: lessons from three sites, Ariake, Bothkennar and Drammen. *Soils & Foundations,* Vol. 40, No. 4, pp. 57–74, https://doi.org/10.3208/sandf.40.4_57

Tanaka, H., Locat, J., Shibuya, S., Soon, T.T., and Shiwakoti, D.R. 2001. Characterization of Singapore, Bangkok, and Ariake clays. *Canadian Geotechnical Journal,* 38(2): 378–400. doi:10.1139/t00-106.

Tanaka, H., Shiwakoti, D. R., & Tanaka, M. (2003. Applicability of SHANSEP method to six different natural clays, using triaxial and direct shear tests. *Soils and Foundations*, 43(3), 43-55.

Tanaka, H., Tanaka, M., Suzuki, S., and Sakagami, T. 2003. Development of a new cone penetrometer and its application to great depths of Pleistocene clays. *Soils and Foundations*, 43(6): 51–61.

Tavenas, F. and Leroueil, S., 1987. Laboratory and In situ stress-strain-time behaviour of soft clays. *Proc. Symposium on Geotechnical Engineering of Soft Clays*, Mexico City, Mexico, pp. 1–43.

Teh, C.I. and Houlsby, G.T. 1991. An analytical study of the cone penetration test in clay. *Geotechnique* Vol. 41 (1): 17-31.

Teh, K.L., Leung, C.F., & Chow, Y.K. 2006. Characterization of layered soil using miniature piezocone. *Proc. 6th Int. Conf. on Physical Modelling in Geotechnics*, Hong Kong: 209-304.

Teh, K.L., Leung, C.F., Chow, Y.K., Cassidy, M.J., & Foo, K.S. 2007. Miniature penetrometers responses in sand overlying clay. *Proc. 16th Southeast Asian Geotechnical Conference,* Kuala Lumpur, Malaysia: 405-410.

Terzaghi, K. 1925. *Erdbaumechanik auf Bodenphysikalischer Grundlage*, Deuticke, Vienna.

Terzaghi, K., Peck, R. B., & Mesri, G. 1996. *Soil mechanics in engineering practice*. John Wiley & Sons. 565 pages.

Tommasi, P., Chiocci, F. L., and Esu, F., 2008, Geotechnical properties of soft clayey sediments from the submerged Tiber river Delta, Italy. *Marine. Georesources & Geotechnology*. Vol.16, No.3, pp. 221–242

Torrance, J. K., 1976. Pore Water Extraction and the Effect of Sample Storage on the Pore Water Chemistry of Leda Clay. *Soil Specimen Preparation for Laboratory Testing*, ASTM STP 599, D. A. Sangrey and R. J. Mitchell, Eds., ASTM International, West Conshohocken, PA, pp. 147–157, https://doi.org/10.1520/STP39080S.

Totani, G., Marchetti, S., Calabrese, M., and Monaco, P., 1994. Field Studies of an Instrumented Full-Scale Pile Driven in Clay. *13th International Conference on Soil Mechanics and Foundation Engineering*, New Delhi, India, Oxford & IBH Publishing Co. Pvt. Ltd., New Delhi, India, pp. 695–698.

Tumay, M. T., & Kurup, P. U. 2001. Development of a continuous intrusion miniature cone penetration test system for subsurface explorations. *Soils and Foundations*, 41(6), 129-138.

Uzielli, M., Lacasse, S., Nadim, F., and Lunne, T. 2006. Uncertainty-based characterization of Troll marine clay. *Characterization and Engineering Properties of Natural Soils (Singapore)*, Vol. 4, Taylor & Francis Group, London, pp. 2753–2782.

Valls-Marquez, M. 2009. Evaluating the capabilities of some constitutive models in reproducing the experimental behaviour of stiff clay subjected to tunneling stress paths. PhD thesis, Department of Civil Engineering, The University of Birmingham, UK. 400p.

Van Helden, M.J. 2013. *Measurement and modeling of anisotropic spatial variability of soils for probabilistic stability analysis of earth slopes.* PhD thesis, Civil Engineering, University of Manitoba, Canada: 268 p.

Velosa, C.L., Remmes, B., and Bik, M. 2013. Strength characterization of soft marine deposits off East Africa using the CPT Stinger method. Report by TDI-Brooks International, Inc., 14391 S. Dowling RD, College Station, TX 77845, USA.

Vesić, A.S. 1972. Expansion of cavities in infinite soil mass. ASCE *J. Soil Mechanics & Foundations Division* 98 (SM3): 265-290.

Vesić, A.S. 1977. Design of Pile Foundations. *NCHRP Synthesis of Highway Practice 42*, National Cooperative Highway Research Project, Transportation Research Board, Washington, DC: 68 pages.

Walker, J. and Yu, H. S. 2006. Adaptive finite element analysis of cone penetration in clay, *Acta Geotecnica*, 1, 43–57.

Watabe, Y., Tanaka, M., and Takemura, J. 2004. Evaluation of in situ K_0 for Ariake, Bangkok and Hai-Phong clays. *Geotechnical & Geophysical Site Characterization*, Vol. 2, (Proc. ISC-2, Porto), Millpress, Rotterdam, 1765–1772

Watabe, Y., Tanaka, M., Tanaka, H., and Tsuchida, T. 2003. K_0-consolidation in a triaxial cell and evaluation of in-situ K_0 for marine clays with various characteristics. *Soils and Foundations*, 43(1): 1–20. doi:10.3208/sandf.43.1.

Waxse, J. 2008. personal communication. Terracon Corporation, Kansas City, Mo.

Weary, D.J. 2005. An Appalachian regional karst map and progress towards a new national karst map. *US Geological Survey Report 5160*-part A: 93-101: www.usgs.gov

Weech, C. 2002. Installation and load testing of helical piles in a sensitive fine-grained soil. *M.Sc. Thesis*, Department of Civil Engineering, University of British Columbia, Vancouver, BC, Canada. 349 pages.

Whittle, A.J. (1992). Constitutive modelling for deep penetration problems in clay. In *Proceedings of 3rd International Conference on Computational Plasticity: Fundamentals and Applications*, Barcelona, Vol. 2, 883–894.

Whittle, A.J., DeGroot, D.J., Ladd, C.C. and Seah, T-H. 1994. Model prediction of anisotropic behavior of Boston Blue Clay. *Journal of Geotechnical Engineering* 120(1): 199-224.

Whittle, A.J., Sutabutr, T., Germaine, J.T., and Varney, A. 2001. Prediction and interpretation of pore pressure dissipation for a tapered piezoprobe. *Geotechnique*, 51(7): 601–617. doi:10.1680/geot.2001.51.7.601.

Willman, D.A., Thornley, J.D., and Krzewinski, T.G. 2016. Port of Anchorage Test Pile Program. Geotechnical Data Report No. 1530824 submitted to Kiewit Infrastructure West Company by Golder Associates, Anchorage, Alaska. 534 pp.

Wissa, A.E.Z., Fuleihan, N.F., and Ingra, T.S. 1983. Evaluation of phosphatic clay disposal and reclamation methods. Vol. 5. Shear strength characteristics of phosphatic clays. Florida Institute of Phosphate Research, Research Project FIPR-80-02-002, prepared by Ardaman & Associates, Orlando. 187 p.

Wissa, A.E.Z., Fuleihan, N.F., and Ingra, T.S. 1991. Evaluation of phosphatic clay disposal and reclamation methods. Vol. 8. Predictive methodology applied to case histories. Florida Institute of Phosphate Research, Research Project FIPR- 87-02-073, prepared by Ardaman & Associates, Orlando. 134 p.

Wood, D. M. 1990. *Soil Behaviour and Critical State Soil Mechanics*, Cambridge University Press, Cambridge. 488 pages

Wood, T. 2016. *On the Small Strain Stiffness of Some Scandinavian Clays and Impact on Deep Excavation*. Ph.D. thesis, Chalmers University of Technology, Gothenburg, Sweden.

Yashima, A., Shigematsu, H., and Oka, F. 1998. Effect of internal structure as related to geotechnical properties of Osaka pleistocene clay. *Proceedings of the International Symposium on Problematic Soils*, IS-Tohoku'98, Sendai, Japan. *Edited by* Yanagisawa, Moroto, and Mitachi. pp. 571–574.

Yi, J. T., Goh, S. H., Lee, F. H., & Randolph, M. F. 2012. A numerical study of cone penetration in fine-grained soils allowing for consolidation effects. *Géotechnique*, *62*(8), 707.

Yokel, F. Y. and Mayne, P.W., 1986. *Helical Probe Tests for Shallow Soil Exploration*. Report NDSIR 86-3351, National Institute of Standards & Technology, Gaithersburg, MD: 51 pages.

Yokel, F. Y. and Mayne, P.W., 1988. Helical Probe Tests: Initial Test Calibration, *ASTM Geotechnical Testing Journal*, 11 (3), 179-186.

Yu, H. S., and Mitchell, J. K. 1998. Analysis of Cone Resistance: Review of Methods. *J. Geotech. Geoenviron. Eng*., Vol. 124, No. 2, pp. 140–149, https://doi.org/10.1061/(ASCE)1090- 0241(1998)124:2(140)

Zhou, Y.G., Liang, T., Chen, Y.M., Ling, D.S., Kong, L.G., Shamoto, Y., & Ishikawa, A. 2014. A two-dimensional miniature cone penetration test system for centrifuge

modelling. *Proceedings of the 8th International Conference on Physical Modelling in Geotechnics (ICPMG2014)*, Perth, Australia, 301-307.

Zwanenburg, C., & Jardine, R. J. 2015. Laboratory, in situ and full-scale load tests to assess flood embankment stability on peat. *Géotechnique*, 65(4), 309-326.